

Contract No:

This document was prepared in conjunction with work accomplished under Contract No. DE-AC09-08SR22470 with the U.S. Department of Energy (DOE) Office of Environmental Management (EM).

Disclaimer:

This work was prepared under an agreement with and funded by the U.S. Government. Neither the U. S. Government or its employees, nor any of its contractors, subcontractors or their employees, makes any express or implied:

- 1) warranty or assumes any legal liability for the accuracy, completeness, or for the use or results of such use of any information, product, or process disclosed; or
- 2) representation that such use or results of such use would not infringe privately owned rights; or
- 3) endorsement or recommendation of any specifically identified commercial product, process, or service.

Any views and opinions of authors expressed in this work do not necessarily state or reflect those of the United States Government, or its contractors, or subcontractors.

We put science to work.™



**Savannah River
National Laboratory™**

OPERATED BY SAVANNAH RIVER NUCLEAR SOLUTIONS

A U.S. DEPARTMENT OF ENERGY NATIONAL LABORATORY • SAVANNAH RIVER SITE • AIKEN, SC

Defense Waste Processing Facility (DWPF) Durability-Composition Models and the Applicability of the Associated Reduction of Constraints (ROC) Criteria for High TiO₂ Containing Glasses

C.M. Jantzen

T.B. Edwards

C.L. Trivelpiece

August 2016

SRNL-STI-2016-00372, Revision 0

DISCLAIMER

This work was prepared under an agreement with and funded by the U.S. Government. Neither the U.S. Government or its employees, nor any of its contractors, subcontractors or their employees, makes any express or implied:

1. warranty or assumes any legal liability for the accuracy, completeness, or for the use or results of such use of any information, product, or process disclosed; or
2. representation that such use or results of such use would not infringe privately owned rights; or
3. endorsement or recommendation of any specifically identified commercial product, process, or service.

Any views and opinions of authors expressed in this work do not necessarily state or reflect those of the United States Government, or its contractors, or subcontractors.

Printed in the United States of America

**Prepared for
U.S. Department of Energy**

Keywords: DWPF, process control, durability, Salt Waste Processing Facility, Monosodium Titanate, Crystalline Silicon Titanate

Retention: *Permanent*

Defense Waste Processing Facility (DWPF) Durability-Composition Models and the Applicability of the Associated Reduction of Constraints (ROC) Criteria for High TiO₂ Containing Glasses

C.M. Jantzen
T.B. Edwards
C.L. Trivelpiece

August 2016



OPERATED BY SAVANNAH RIVER NUCLEAR SOLUTIONS

Prepared for the U.S. Department of Energy under contract number DE-AC09-08SR22470.

REVIEWS AND APPROVALS

AUTHORS:

C.M. Jantzen, Engineering Process Development Date

T.B. Edwards, Engineering Process Development Date

C.L. Trivelpiece, Engineering Process Development Date

TECHNICAL REVIEW:

K.M. Fox, Hanford Mission Programs, Reviewed per E7 2.60 Date

D.L. McClane, Engineering Process Development Date

APPROVAL:

E.N. Hoffman, Manager Date
Engineering Process Development

D.E. Dooley, Director, Date
Environmental & Chemical Process Technology Research Programs

E.J. Freed, Manager Date
Waste Solidification Engineering

ACKNOWLEDGEMENTS

The research presented in this document was sponsored by the Savannah River Defense Waste Processing Facility (DWPF) in connection with work done under Contract No. DE-AC09-96SR18500 with the U.S. Department of Energy. The development of the 1995 durability models and accumulation of the associated validation data were completed from 1988 to present under DOE Contracts Nos. DE-AC09-89SR18035 with E.I. DuPont deNemours & Co., DE-AC09-96SR18500 with Westinghouse Savannah River Co. (WSRC) and Washington Group Inc. (WGI), and DE-AC09-08SR22470 with Savannah River Nuclear Solutions (SRNS). Special thanks are due to Charles Crawford and Madison Caldwell of SRNL for the density measurements on the Waste Compliance Plan (WCP), Environmental Assessment (EA) and Defense Waste Processing Facility (DWPF) startup frit glasses by buoyancy.

EXECUTIVE SUMMARY

Radioactive high level waste (HLW) at the Savannah River Site (SRS) has successfully been vitrified into borosilicate glass in the DWPF since 1996. Vitrification requires stringent product/process (P/P) constraints since the glass cannot be reworked once it has been poured into ten foot tall by two foot diameter canisters. A unique “feed forward” statistical process control (SPC) was developed for this control rather than relying on statistical quality control (SQC). In SPC, the feed composition to the DWPF melter is controlled prior to vitrification. In SQC, the glass product would be sampled after it is vitrified. Individual glass property-composition models form the basis for the “feed forward” SPC. The models transform constraints on the melt and glass properties into constraints on the feed composition going to the melter in order to determine, at the 95% confidence level, that the feed will be processable and that the durability of the resulting waste form will be acceptable to a geologic repository.

The DWPF SPC system is known as the Product Composition Control System (PCCS). One of the process models within PCCS is known as the Thermodynamic Hydration Energy Reaction MOdel (THERMOTM), which was developed in 1995 and utilizes data from the short term (7-day) durability test given in the ASTM standard C1285A. The DWPF durability model is based on a free energy of hydration function calculated from the molar glass compositions. An individual component free energy, ΔG_i , exists for each oxide in a HLW glass and the ΔG_i 's are weighted by the molar concentration of each oxide in the glass. This gives an overall preliminary hydration free energy, ΔG_p , for a given glass, which is predictive and independent of any leachate solution pH impacts. The less negative the ΔG_p the more durable the glass; the more negative the ΔG_p the less durable the glass.

The DWPF PCCS models are parsimonious in that the oxide terms in each model are only those which are necessary and sufficient to describe the glass property of interest. This approach excludes composition terms that are unnecessary to the implementation of the DWPF flowsheets, and helps to minimize the sources of error in the PCCS models. These parsimonious models have successfully operated the DWPF vitrification process over the last 20 years.

The DWPF will soon be receiving increased concentrations of TiO₂, Na₂O, and Cs₂O enriched wastes from the Salt Waste Processing Facility (SWPF). The SWPF has been built to pretreat the high-curie fraction of the salt waste to be removed from the HLW tanks in the F- and H-Area Tank Farms at the SRS. The SWPF contains unit operations that remove and concentrate the radioactive cesium (¹³⁷Cs), strontium (⁹⁰Sr), and actinides from the bulk salt solution feed. Separation processes planned at SRS include caustic side solvent extraction (CSSX), for ¹³⁷Cs removal, and ion exchange/sorption of ⁹⁰Sr and alpha-emitting radionuclides with monosodium titanate (MST which is NaHTi₂O₅•2.8H₂O). The predominant alpha-emitting radionuclides in the highly alkaline waste solutions include plutonium isotopes ²³⁸Pu, ²³⁹Pu and ²⁴⁰Pu. The MST is the source of the TiO₂ and Na₂O enriched wastes while the Cs₂O is derived from the CSSX stream that will be coming to the DWPF from the SWPF.

The SWPF process will replace the current Actinide Removal Process (ARP)/Modular CSSX Unit (MCU) process currently in use. The ARP already sends MST to the DWPF for vitrification but the volume of the ARP product, including the associated MST component, is less than the volume anticipated with the SWPF wastes. The 1995 THERMOTM model includes a TiO₂ term but since the DWPF has been operating under a TiO₂ solubility constraint of 2 weight percent (wt%) TiO₂ in the final glass, this TiO₂ term has not been validated at higher TiO₂ concentrations.

In order to validate the existing TiO₂ term in THERMOTM beyond 2.0 wt% in the DWPF, new durability data were developed over the target range of 2.00 to 6.00 wt% TiO₂ and evaluated against the 1995 durability model. The durability was measured by the 7-day Product Consistency Test (PCT described in

ASTM C1285A) for the SWPF study glasses which were designed to cover the anticipated concentrations of TiO₂, Na₂O, and Cs₂O based on the projected volumes of the SWPF wastes. These glasses were also designed to cover any gaps in TiO₂ content above the 2.0 wt% solubility limit and the 6.0 wt% maximum TiO₂ anticipated during coupled (sludge + SWPF) processing at DWPF. Although the 1995 DWPF durability model covers 6.42-16.80 wt% Na₂O and 0-1.16 wt% Cs₂O, the SWPF target range evaluated spanned 8 to 18 wt% Na₂O and 0.3 to 1.0 wt% Cs₂O (where Cs₂O measured was actually 1.62 wt%).

Alternate equations for various ΔG_i terms were calculated and evaluated for the THERMO™ models. This included the Al₂O₃, B₂O₃, Cs₂O, Fe₂O₃, K₂O, Li₂O, Na₂O, SiO₂ and TiO₂ ΔG_i terms singly and in groups. However, it was determined that all these terms adequately described HLW glass durability including the impact of SWPF concentrations on glass durability.

During the course of the DWPF durability modeling and the associated Reduction of Constraints (ROC) modeling, it was determined that for glasses with TiO₂≥2.0 wt% the ROC had to be moved to a 4.0 wt% Al₂O₃ restriction with uncertainties needing to be factored into these concentrations. For glasses with <2.0 wt% TiO₂ the original ROC of 3 wt% Al₂O₃ with an alkali constraint or 4 wt% Al₂O₃ without an alkali constraint would apply.

The revised ROC removed several SWPF glasses from the durability modeling and the model comparison ranges for TiO₂ became 1.9-5.85 wt% instead of the targeted 2-6 wt% TiO₂. Conversely, the analyzed SWPF glasses were higher in Na₂O and Cs₂O than the target concentrations, giving a range of 8.03-18.14 wt% Na₂O and 0.48-1.62 wt% Cs₂O.

This study documents the adequacy of the existing THERMO™ terms. Since the original ROC criteria were developed after the THERMO™ model was developed, there are some glasses in THERMO™ that fail the original ROC and DWPF REDuction/OXidation (REDOX) modeling criteria. These data points were removed from the viscosity model when it was revised in 2005 and from the liquidus model when it was developed in 2001. To make all the PCCS models consistent, these nine data points were removed from the THERMO™ durability database, and revised slopes and intercepts were fitted for boron, sodium, lithium and silicon release. These modified THERMO™ models have higher R² values and smaller root mean square errors (RMSEs). The associated ΔG_p for the Property Acceptance Region (PAR) in PCCS is slightly more negative than previously established, which opens up the DWPF PCCS durability window slightly for future processing. Since the PCCS durability window becomes slightly larger, all previous qualified DWPF glasses are still qualified. Therefore, the modified THERMO™ durability models in which ΔG_p is correlated to the response of a 7-day ASTM C1285A (PCT) take the following form:

$$\begin{aligned}\log_{10}[\text{NC}_B] \text{ (g/L)} &= -1.901602 - 0.180215 \Delta G_p & R^2 &= 0.80 & \text{RMSE} &= 0.195316 \\ \log_{10}[\text{NC}_{\text{Li}}] \text{ (g/L)} &= -1.541811 - 0.1453413 \Delta G_p & R^2 &= 0.80 & \text{RMSE} &= 0.161483 \\ \log_{10}[\text{NC}_{\text{Na}}] \text{ (g/L)} &= -1.803846 - 0.1704731 \Delta G_p & R^2 &= 0.83 & \text{RMSE} &= 0.168133\end{aligned}$$

compared to the 1995 THERMO™ models

$$\begin{aligned}\log_{10}[\text{NC}_B] \text{ (g/L)} &= -1.901447 - 0.1812039 \Delta G_p & R^2 &= 0.77 & \text{RMSE} &= 0.216264 \\ \log_{10}[\text{NC}_{\text{Li}}] \text{ (g/L)} &= -1.545942 - 0.1468048 \Delta G_p & R^2 &= 0.75 & \text{RMSE} &= 0.182722 \\ \log_{10}[\text{NC}_{\text{Na}}] \text{ (g/L)} &= -1.801158 - 0.1710066 \Delta G_p & R^2 &= 0.80 & \text{RMSE} &= 0.187881\end{aligned}$$

where ΔG_p is in kcal/100g glass and NC_i, where i is the ith elemental component in the glass, is in g/L.

Since the associated ΔG_p PAR limits are slightly more negative than previously established, this opens up the DWPF PCCS durability window slightly and does not impact the durability determinations of previously made DWPF canister glass. The modified THERMO™ models were validated with the SWPF data up to 5.85 wt% TiO₂. Additional SRNL high TiO₂ databases were used to perform additional validation studies of the modified THERMO™ models up to 6.62 wt% TiO₂. Validation limits are not model limits and they are not solubility limits.

The leachate data used in the 1995 durability model were also investigated to determine if glass density was a concern to the 1995 THERMO™ models, i.e. higher density glasses have a lower available surface area for every gram of glass leached. It was concluded that the RMSE's of the THERMO™ models encompassed any variation in NC_i due to the additional surface area since the ranges of the 1995 THERMO™ glasses overlap those of the SWPF glasses.

The 1995 THERMO™ model did not contain a ΔG_i for Nb₂O₅ but two ΔG_i 's were developed. The data presented in this report helped determine that an Nb₂O₅ ΔG_i of +13.20 kcal/mole should be used with the modified THERMO™ models presented in this study and the only additional changes that will be needed in PCCS are those associated with implementation of the Nb₂O₅ term, i.e. analytic and transfer errors. This Nb₂O₅ term has been added into THERMO™ for potential future use, should the DWPF ever need to process other titanate containing ion exchange materials, such as Crystalline SilicoTitanate (CST - Na_{1.5}Nb_{0.5}Ti_{1.5}O₃SiO₄•2H₂O). The ΔG_i for the Nb₂O₅ term is not being implemented currently, since the DWPF is not processing CST, nor does it appear likely that CST will be processed in the near future. Since CST contains Nb₂O₅, Nb could become an element in the glass that is reportable to the geologic repository if present at >0.5 wt% on an elemental basis. This would require a revision to the DWPF Waste Acceptance Product Specifications (WAPS). Additionally, the measurement uncertainty needed to implement an Nb term in PCCS is currently not available. Therefore, the ΔG_i for Nb₂O₅ is being provided for future use should the DWPF have to process CST. When CST processing becomes necessary, the other implementation requirements associated with a ΔG_i for Nb₂O₅ will be addressed. The use of the ΔG_i for Nb₂O₅ was fit to the same slope and intercept of the modified THERMO™ models and no other changes were found to be necessary. The modified THERMO™ model will cover future DWPF processing of MST alone, CST alone, or coupled CST-MST flowsheet additions.

It is recommended that the modified THERMO™ durability models and the modified PAR limits for the durability constraints be incorporated in the next revision of the technical bases for PCCS and then implemented into PCCS. It is also recommended that an ROC of 4 wt% Al₂O₃ be implemented with no restrictions on the amount of alkali in the glass for TiO₂ values \geq 2 wt%.

The ultimate limit on the amount of TiO₂ that can be accommodated from SWPF will be determined by the three PCCS models, the waste composition of a given sludge batch, the waste loading of the sludge batch, and the frit used for vitrification. Once a component like TiO₂ is present at larger concentrations than 1-2 wt%, the interactions of that component with other components in the melter feed must be considered simultaneously, i.e. an individual solubility limit cannot be defined to globally account for the interactions with all the remaining sludge/frit composition variables. It is known that Ti⁴⁺ competes with Al³⁺ for alkali bonding and it is known that Ti⁴⁺ and Fe³⁺ have a coupled impact on their joint solubility in a glass.

TABLE OF CONTENTS

| | |
|--|------|
| ACKNOWLEDGEMENTS | v |
| EXECUTIVE SUMMARY | vi |
| LIST OF TABLES..... | xi |
| LIST OF FIGURES | xii |
| LIST OF ABBREVIATIONS..... | xiii |
| 1.0 Introduction..... | 1 |
| 2.0 DWPF Durability P/P Models and Reduction of Constraints (ROC) Criteria..... | 2 |
| 2.1 Historical Perspective..... | 2 |
| 2.2 Modeling Constraints | 6 |
| 2.3 Homogeneity and Reduction of Constraints (ROC) Evolution..... | 7 |
| 2.3.1 <i>High P₂O₅ Constraint</i> | 10 |
| 2.3.2 <i>High B₂O₃ Constraint</i> | 10 |
| 2.3.3 <i>Crystallization Constraint</i> | 10 |
| 2.4 Calculation of Glass Durability | 11 |
| 3.0 Defining Future Coupled DWPF-SWPF Processing Ranges..... | 11 |
| 4.0 Experimental Measurement Data..... | 12 |
| 5.0 Quality Assurance..... | 13 |
| 6.0 Results and Discussion of SWPF PCT Measurements | 13 |
| 6.1 Leachate Measurements in Analytical Sequence | 14 |
| 6.2 Leachate Measurements by Glass Identifier..... | 14 |
| 6.3 Results for the Samples of the Multi-Element Solution Standard..... | 14 |
| 6.4 Normalization of the PCT Results..... | 15 |
| 6.5 Effects of Heat Treatments..... | 16 |
| 7.0 Results and Discussion: Density, Congruency, Durability Models, and ROC Criteria | 16 |
| 7.1 Internal Consistency of THERMO™ and SWPF Glass Durability Data | 17 |
| 7.2 Predicted versus Measured Durability of SWPF Glasses..... | 20 |
| 7.3 Reduction of Constraints (ROC) Criteria: Competition Between Al ₂ O ₃ and TiO ₂ for Alkali..... | 22 |
| 7.4 Exclusion of some SWPF glasses | 24 |
| 7.5 Exclusion of some THERMO™ glasses | 24 |
| 7.6 Assessment of Glass Density Effects | 24 |
| 7.7 Applicability of Modified PCCS THERMO™ Durability Models..... | 25 |
| 7.8 Uncertainties for the Modified THERMO™ Models Relative to those for the THERMO™ Models | 29 |

| | |
|---|-----|
| 7.9 Property Acceptance Region (PAR) Assessments for the Modified THERMO™ Models | 29 |
| 7.10 Validation of THERMO™ Using Additional High TiO ₂ Containing Glasses..... | 31 |
| 8.0 Modification of the Durability-Composition Models for CST Flowsheet..... | 33 |
| 8.1 Evaluation of a ΔG _i for Nb ₂ O ₅ With the Modified THERMO™ Models | 33 |
| 8.2 Development of ΔG _i for Nb ₂ O ₅ | 34 |
| 8.3 Applicability of Durability Models with ΔG _p Modified to Include Nb ₂ O ₅ Contribution | 35 |
| 8.4 Changes needed in PCCS for Nb ₂ O ₅ Contribution..... | 37 |
| 9.0 Conclusions..... | 37 |
| APPENDIX A. SWPF (TiO ₂ -only) Glass Database (wt% on a vitrified oxide basis indicated by “v”)...39 | 39 |
| APPENDIX B. Tables and Exhibits for the PCT Measurements of the High TiO ₂ Glass Study.44 | 44 |
| APPENDIX C. THERMO™ Database (Measured Bias Corrected wt% on a vitrified oxide basis indicated by “v”)...... | 132 |
| APPENDIX D. Uncertainties for THERMO™ Models | 138 |
| APPENDIX E. SRNL High TiO ₂ Glass Validation Data (Measured Bias Corrected wt% on a vitrified oxide basis indicated by “v”)...... | 146 |
| APPENDIX F. SRNL CST (TiO ₂ -Nb ₂ O ₅ -ZrO ₂) Glass Validation Database (Measured Bias Corrected wt% on a vitrified oxide basis indicated by “v”). | 148 |
| 10.0 References..... | 152 |

LIST OF TABLES

| | |
|---|-----------|
| Table 1. Waste Glass Product and Process (P/P) Constraints..... | 1 |
| Table 2. Species Included in THERMO TM or Subsequently Developed | 5 |
| Table 3. Oxide Intervals for Reduction of Constraints Study for Coupled Operations with ARP and MCU | 10 |
| Table 4. Oxide Intervals for SWPF Gap Analysis Study [79] | 12 |
| Table 5. Measurements of Solution Standards for PCT Analytical Blocks..... | 15 |
| Table 6. Reduction of Constraints (ROC) for SWPF High TiO ₂ Glasses..... | 22 |
| Table 7. Model Slopes, Intercepts and Statistical Fitting Information | 29 |
| Table 8. PCT Measurements Generated for the EA Standard Glass..... | 30 |
| Table 9. PAR Values for the THERMO TM Models Currently Utilized by PCCS..... | 30 |
| Table 10. PAR Values for the Modified THERMO TM Models..... | 30 |
| Table 11. Additional High TiO ₂ Validation Data | 32 |
| Table 12. CST Validation Data..... | 34 |

LIST OF FIGURES

| | |
|---|----|
| Figure 2-1. Graphical Representation of the Constraints Applied to the Choice of Model and Validation Data for the Durability, Viscosity, and Liquidus P/P Models for Glasses with 0-2.00 wt% TiO ₂ | 7 |
| Figure 2-2. Complications in Glass Durability Modeling from Composition Due to Phase Separated Glasses.[19,20] | 7 |
| Figure 2-3. Dependency of HLW Glass Phase Separation on the Al ₂ O ₃ Content of the Glasses.[19,20,51] | 8 |
| Figure 7-1. Internal Consistency of the THERMO™ Model Data Compared to the SWPF Glass Data... | 19 |
| Figure 7-2. Bivariate Fit of log ₁₀ [NC _B] (g/L) By ΔG _p Display=quenched/measured bc results. The green triangles are the EA glass standard responses and the red circles are the ARM-1 glass standard responses for the for the 13 SWPF ovens used to test the remaining SWPF glasses. | 21 |
| Figure 7-3. Bivariate Fit of log10[NC _B] (g/L) By ΔG _p Display=ccc/measured bc results. . The green triangles are the EA glass standard responses and the red circles are the ARM-1 glass standard responses for the for the 13 SWPF ovens used to test the remaining SWPF glasses. | 21 |
| Figure 7-4. Glasses in THERMO™ Model that Violate the original ROC are Indicated in the Circled Region..... | 23 |
| Figure 7-5. Revised Modeling Criteria and ROC for High Versus Low TiO ₂ Containing Glasses..... | 23 |
| Figure 7-6. The Range of Glass Densities for THERMO™ Versus SWPF Glasses. | 25 |
| Figure 7-7. Modified THERMO™ Models. | 27 |
| Figure 7-8. Comparison of the Modified Historic THERMO™ Models and the SWPF Data. | 28 |
| Figure 7-9. Internal Consistency of Additional TiO ₂ Validation Data from References 97 and 98 where Figure a compares B and Li leach data and Figure b compares B and Na leach data. | 32 |
| Figure 7-10. Additional Validation Data for the Modified THERMO™ Model..... | 33 |
| Figure 8-1. Internal Consistency of CST Validation Data from References 99-107. Open red squares are the CST data and the solid red symbols are the KT data. | 36 |
| Figure 8-2. Validation Data for Using the Modified THERMO™ Models for CST Containing Glasses. | 36 |

LIST OF ABBREVIATIONS

| | |
|---------|--|
| AD | Analytic Development |
| ANA-VSL | Atkins North America-Vitreous State Laboratory |
| ANOVA | Analysis of Variance |
| APS | Amorphous Phase Separation |
| ARM-1 | Approved Reference Material |
| ARP | Actinide Removal Process |
| ASME | American Society of Mechanical Engineers |
| ASTM | American Society for Testing and Materials |
| bc | bias corrected |
| CCC | Centerline Canister Cooling |
| CELS | Corning Engineering Laboratory Services |
| CPS | Crystalline Phase Separation |
| CSSX | Caustic-Side Solvent Extraction |
| CST | Crystalline SilicoTitanate |
| DCP | Direct Current Plasma Emission Spectrometry |
| DOE | Department of Energy |
| DWPF | Defense Waste Processing Facility |
| EPA | Environmental Protection Agency |
| GWB | Geochemists Work Bench |
| HLW | High Level Waste |
| L95 | Lower 95% confidence interval |
| LHS | Left Hand Side |
| MAR | Measurement Acceptance Region |
| MCU | Modular CSSX Unit |
| MFT | Melter Feed Tank |
| MRO | Medium Range Order |
| MST | MonoSodium Titanate |
| NQA | Nuclear Quality Assurance |
| OLS | Ordinary Least Squares |
| P/P | Product/Process |
| PAR | Property Acceptable Region |
| PCCS | Product Composition Control System |
| PCT | Product Consistency Test |
| QAP | Quality Assurance Program |
| RCRA | Resource Conservation and Recovery Act |
| REDOX | REDUction/OXidation |
| RHS | Right Hand Side |
| ROC | Reduction of Constraints |
| RMSE | Root Mean Square Error |
| SB | Sludge Batch |
| SA | Surface Area |

| | |
|---------|---|
| SATP | Standard Ambient Temperature and Pressure |
| SME | Slurry Mix Evaporator |
| SPC | Statistical Process Control |
| SQC | Statistical Quality Control |
| SRNL | Savannah River National Laboratory |
| SRNS | Savannah River Nuclear Solutions |
| SRS | Savannah River Site |
| SWPF | Salt Waste Processing Facility |
| TCLP | Toxicity Characteristic Leaching Procedure |
| THERMO™ | Thermodynamic Hydration Energy Reaction MOdel |
| TTQAP | Task Technical and Quality Assurance Plan |
| TTR | Technical Task Request |
| U95 | Upper 95% confidence interval |
| wt% | Weight Percent |
| WAPS | Waste Acceptance Product Specifications |
| WASRD | Waste Acceptance System Requirement Document |
| WCP | Waste Form Compliance Plan |
| WGI | Washington Group Inc. |
| WL | Waste Loading |
| WSRC | Westinghouse Savannah River Co. |
| XRD | X-ray Diffraction |
| XRF | X-ray Fluorescence |

1.0 Introduction

Borosilicate glasses have been used in the United States and in Europe to immobilize radioactive high level waste (HLW) for ultimate geologic disposal. Waste glass formulations should maximize the concentration of waste in the vitrified waste form so that waste glass volumes and the associated storage and disposal costs are reduced. Moreover, the optimization of HLW glass formulations [1,2,3] must simultaneously balance multiple product/process (P/P) constraints (Table 1).

Table 1. Waste Glass Product and Process (P/P) Constraints

| Product Constraints | Process Constraints |
|-----------------------|------------------------------|
| chemical durability | melt viscosity/resistivity |
| glass homogeneity | liquidus |
| thermal stability | waste solubility |
| regulatory compliance | melt temperature/corrosivity |
| mechanical stability | radionuclide volatility |
| | REDUction/Oxidation (REDOX)* |

- * controls foaming and thus improves melt rate, controls metal nodule formation improving melter longevity, and reducing conditions improve melter refractory longevity

The chemical durability, which includes glass homogeneity, melt viscosity, and the liquidus constraints from Table 1 are the only parameters controlled during HLW processing. Thermal and mechanical stability were measured during development of the HLW processing flowsheet.[4] Regulatory compliance using the Toxicity Characteristic Leaching Procedure (TCLP) was bounded by using 1X and 10X the Environmental Protection Agency (EPA) Resource Conservation and Recovery Act (RCRA) hazardous constituents anticipated to be in glasses made from the range of wastes found in the Savannah River Site (SRS) tank farm. [5,6] Melt temperature, was balanced against volatilization of radionuclides and materials of construction corrosivity during extensive pilot scale testing at the SRS before the Defense Waste Processing Facility (DWPF) startup. The melt temperature was optimized at 1150°C to minimize radionuclide volatility, afford an adequate viscosity to the melt for convection, and at the same time minimize corrosion of melter materials of construction, i.e. Inconel®690 and Monofrax™ K-3 refractory.[7,8,9] Melter REDOX is controlled at an $\text{Fe}^{2+}/\Sigma\text{Fe}$ target of ~0.2 and in the range of $\text{Fe}^{2+}/\Sigma\text{Fe} = 0.09-0.33$ where REDOX does not have a significant impact on glass durability.[10,11,12,13,14] Waste solubility is handled as limits of the individual species in weight percent (wt%) in the glass.[15]

Radioactive HLW has successfully been vitrified into borosilicate glass during HLW processing at the DWPF since 1996. The DWPF must measure melt/glass acceptability prior to the melter, since no remediation of the glass composition to ensure durability and processability is possible except in the vessel (i.e., in the Slurry Mix Evaporator (SME) vessel) in which frit and waste are blended. Therefore, the acceptability decision is made on the upstream process (specifically, at the SME), rather than on the downstream melt or glass product. That is, it is based on “feed forward” statistical *process control*[†] (SPC) rather than statistical *quality control* (SQC).^{††} The DWPF SPC control system is known as the Product Composition Control System (PCCS). Individual property-composition models enable the monitoring and process control strategies embedded in the DWPF PCCS.[16] These models transform constraints on the melt and glass properties such as viscosity, liquidus, and durability into constraints on feed composition.

[†] This controls the slurry feed to the melter *prior* to vitrification.

^{††} Which would adjudicate product release by sampling the glass *after* it's been made.

The DWPF property-composition models have been under development and validation since the late 1980's. The individual property models for each feed/glass constraint have been developed over wider property ranges than the glasses that were anticipated to be made in the DWPF. The property models that have been developed are mechanistic^t in nature, and depend on known relationships between glass structure/bonding (viscosity)[17, 18], thermodynamics of quasicrystalline melt structures and their hydration (durability) [19, 20], and interactions of quasicrystalline melt species at high temperatures (liquidus).[21, 22, 23]. The P/P models group terms with very similar effects so that each model only contains the terms that are necessary and sufficient (parsimonious) to model the P/P property of interest.

The Thermodynamic Hydration Energy Reaction MOdel™ (THERMO™) durability models currently in use at DWPF will be assessed in this document against newly generated data covering the future composition region defined by SWPF processing (see Section 2.4 for discussion). Specifically, this document will assess the impact of enriched TiO₂ waste streams from SWPF on the adequacy of the component hydration free energy for TiO₂, Na₂O, and Cs₂O. The TiO₂ and Na₂O enriched waste streams are generated by decontamination of the HLW salt waste stream using MonoSodiumTitanate (MST) to remove ⁹⁰Sr and ¹³⁷Cs. Since the THERMO™ durability models contain a TiO₂ term and alkali terms for Na₂O and Cs₂O, the adequacy of these terms at TiO₂ values \geq 2.0 wt% will be assessed. Note that the DWPF has been operating with a solubility limit of TiO₂ \leq 2.0 wt % since 2003 [24] and \leq 1.0 wt % TiO₂ between 1996-2003.[15]

In the future, the DWPF may also receive Crystalline SilicoTitanate (CST) that may be used to decontaminate the ¹³⁷Cs from the salt waste or from tank cleanout. The CST is remarkable for its ability to separate parts-per-million concentrations of cesium from highly alkaline solutions (pH>14) containing high sodium concentrations (>5M). It is also highly effective for removing cesium from neutral and acidic solutions, and for removing strontium from basic and neutral solutions.[25] The CST is comprised primarily of: Na, Si, Ti, and Nb (originally referred to as proprietary material one, or PM-1 and later as IE-911) plus an exchangeable monovalent cation. The binder is based on a technology that employs zirconium (formerly PM-2).[26] The THERMO™ durability models do not contain an Nb₂O₅ term but two potential terms were developed in 2010.[27] The adequacy of which Nb₂O₅ term to use in the THERMO™ durability models will also be assessed in this study.

2.0 DWPF Durability P/P Models and Reduction of Constraints (ROC) Criteria

2.1 Historical Perspective

The most important glass product property is the glass durability. The durability of a waste glass is the single most important variable controlling release of radionuclides and/or hazardous constituents. The intrusion of groundwater into, and passage through, a waste form burial site, in which the waste forms are emplaced, is the most likely mechanism by which constituents of concern may be removed from the waste glass and carried to the biosphere. Thus, it is important that waste glasses be stable in the presence of groundwater.

For homogeneous^f borosilicate high level waste (HLW) glasses, acceptable performance is defined as an acceptably low dissolution rate, which is controlled by maintaining the glass composition within an acceptable range. The approach can be represented in terms of linking several relationships:

^t Mechanistic models can be applied to composition regions outside of the regions for which they were developed. The DWPF mechanistic models allow more flexibility for process control than empirical models which are (1) restricted to the compositional region over which they were developed and (2) require glass formulations near the center of a pre-qualified glass composition region instead of in regions where waste loading can be maximized.

^f Glasses not exhibiting amorphous phase separation and not crystallized, i.e. the types of glasses used in the THERMO™ durability models.

Equation 1

**process control ↔ composition control ↔ dissolution rate control ↔ performance control
↔ acceptable performance**

The linkages expressed in Equation 1 are appropriate for HLW waste glasses because the radionuclides are incorporated within the glass structure and are released congruently as the glass dissolves. In general, for any waste form, it must be established that control of performance in a laboratory test predicts acceptable control of performance in a disposal system based on performance testing and modeling.

The Waste Acceptance System Requirement Document (WASRD) states that the durability and phase stability of vitrified HLW must be assessed [28], while geologic repository modeling requires the “maximum radionuclide release.” These are tied together by the linking relationships shown above, i.e. that process and composition control translates into acceptable performance. The “product quality constraint” on the HLW glass requires that the waste form producer demonstrate control of the waste form production by comparing production samples or process control information, separately or in combination to the Environmental Assessment (EA) benchmark glass [29, 30] using the Product Consistency Test (PCT also known as ASTM C1285) [31] or equivalent. For waste form acceptance^f, the mean concentrations of lithium, sodium, and boron in the leachate, after normalization for the concentrations in the glass, shall be 2σ less than those of the EA benchmark glass.

For borosilicate glass dissolution, the rate of release of a radionuclide from the waste form is proportional to both the dissolution rate of the waste form and the relative abundance of the radionuclide in the waste form.[32] Thus for borosilicate glass, ⁹⁹Tc is the radionuclide released at the fastest rate (¹³⁷Cs is released at a somewhat slower rate). However, extensive testing [33,34,35,36,37,38,39,40,41,42,43] has demonstrated that ⁹⁹Tc is released congruently at the same rate as Na, Li and B for homogeneous glasses.[§] This enables the Na, Li, and B to be measured in a glass durability test such as ASTM C1285 and be equated to the “maximum radionuclide release.” The Na, Li and B are not sequestered in precipitates that participate in surface alteration reactions and are also not solubility limited.

In vitreous waste forms, the molecular structure controls dissolution (contaminant release) by establishing the distribution of ion exchange sites, hydrolysis sites, and the access of water to those sites.[44,45] Thus the DWPF durability model, THERMO™ [19,20], estimates the relative durability of silicate and borosilicate glasses based on their compositions. THERMO™ calculates the thermodynamic driving force of each glass component to hydrate based on the mechanistic role of that component during dissolution, e.g. ion exchange, matrix dissolution, accelerated matrix dissolution, surface layer formation, and/or oxidative dissolution. The overall tendency of a given glass to hydrate is expressed as a preliminary glass dissolution estimator, i.e. the change in the free energy of hydration of a glass (ΔG_p) based solely on its composition expressed as ΔG_i for each “i” different silicate and oxide component in the glass.

^f The following is a quote from ASTM C1285. “The most important elements to be analyzed in the PCT leachate are those that best represent the extent of dissolution of the glass waste form. For example, elements that are not sequestered in alteration phases that participate in surface alteration reactions, and are also not solubility limited, are good indicators of glass waste form durability. Extensive testing of any glass waste form must be performed in order to determine what elements represent the extent of dissolution of the glass waste form. This bounds the extent of dissolution of the radioactive constituents. For example, in high level borosilicate waste glass, Tc⁹⁹, present at $\sim 4.1 \times 10^{-4}$ weight % in the waste form, has been shown to be released congruently (stoichiometrically) with boron, lithium, and sodium.” Therefore, for borosilicate glass waste forms, the leachates are routinely analyzed for boron, lithium, and sodium if these elements are present at > 1 mass % in the glass. Additional mechanistic information about high level borosilicate waste glass durability is gained by analyzing for other elements present in the glass, i.e. Si.”

[§] Na and Li can precipitate in long term ASTM C1285B testing as zeolitic phases but not in short term ASTM C1285A testing. B does not precipitate in either long or short term testing.

When the partial thermodynamic hydration free energies, ΔG_i 's, are weighted by the molar concentration of the silicate and oxide components present in a glass, then the overall hydration tendency of the glass can be represented by the additive contributions of the thermodynamic partial molar quantities as expressed in Equation 2:

Equation 2
$$\Delta G_p = \left[\sum (\Delta G_i \cdot f_i) \right]_{T,P}$$

where ΔG_p is the preliminary Gibbs free energy (G) glass dissolution estimator. The ΔG_p is based on equations that mechanistically represent glass dissolution as a process of ion exchange, matrix dissolution, and surface layer formation. The ΔG_i 's are the partial molar hydration free energies of the components i's, and f_i are the amounts of each species expressed in dimensionless molar fractions at constant temperature (T) and pressure (P), i.e. Standard Ambient Temperature and Pressure (SATP) of 25°C and 1 bar.

The partial molar free energies in THERMO™ are for the species listed in Table 2 along with the compositional range in wt% used during modeling. The bolded oxide species given in this table are for the DWPF pour stream samples from 1996 to present since each pour stream sample that has been leached using ASTM C1285 has been found to be acceptable. These DWPF pour stream samples are not included in the ComPro™ database [46,47]. Therefore, the pour stream data from References 48,49, and 50 are included in Table 2 for completeness.

Table 2. Species Included in THERMO™ or Subsequently Developed

| Oxide Species | THERMO™ “Model Data” Oxide Range (wt%) [19,20,48,49,50] | Ref. for ΔG_i | Oxide Species | THERMO™ “Model Data” Oxide Range (wt%) [19,20,48,49,50] | Ref. for ΔG_i |
|---------------------------|---|-----------------------|---------------------------|---|-----------------------|
| Al_2O_3 | 1.36 [‡] -13.90 | [19,20] | NpO_2 | 8.21E-04-3.08E-03 | [53] |
| AmO_2^* | 7.58E-05-4.95E-04 | [19,20] | Na_2O | 6.42-16.80 | [19,20] |
| As_2O_3 | Validation [§] | [19,20] | Nd_2O_3 | 0.00-5.96 | [19,20] |
| B_2O_3 | 6.10-13.30 | [19,20] | NiO | 0.00-2.97 | [19,20] |
| BaO | 0.00-0.66 | [19,20] | P_2O_5 | 0.00-0.65 | [19,20] |
| CaO | 0.38-2.23 | [19,20] | PbO | 0.00-0.25 | [19,20] |
| CdO | Validation [§] | [19,20] | PuO_2 | 4.01E-03-1.65E-02 | [19,20] |
| Ce_2O_3^* | 0.00-1.44 | [19,20] | Rb_2O | 0.00 | [19,20] |
| CoO | Validation [§] | [19,20] | RuO_2^* | 0.014-0.049 ^ξ | [19,20] |
| Cr_2O_3 | 0.00-0.55 | [19,20] | Sb_2O_3^* | Validation [§] | [19,20] |
| Cs_2O | 0.00-1.16 | [19,20] | SeO_2^* | Validation [§] | [19,20] |
| Cu_2O^* | 0.00-0.30 | [19,20] | SiO_2 | 39.80-59.80 | [19,20] |
| CuO^* | 0.00-0.33 | [19,20] | SnO_2^* | Validation [§] | [19,20] |
| FeO^* | 0.00-8.81 | [19,20] | SrO | 0.00-0.45 | [19,20] |
| Fe_2O_3^* | 0.00-14.30 | [19,20] | TcO_2^* | 5.54E-05-6.24E-04 | [19,20] |
| HfO_2^* | Validation [§] | [53] | TeO_2 | 0.00 | [19,20] |
| K_2O | 0.00-5.73 | [19,20] | ThO_2 | 0.68-1.00 | [19,20] |
| La_2O_3 | 0.00-0.42 | [19,20] | TiO_2 | 0.00-3.21 | [19,20] |
| Li_2O | 2.59-5.16 | [19,20] | U_3O_8^* | 0-3.51 | [19,20] |
| MgO | 0.00-3.24 | [19,20] | Y_2O_3 | Validation [§] | [19,20] |
| MnO^* | 0.00-3.36 | [19,20] | ZnO | 0.00-1.46 | [19,20] |
| MoO_3^* | 0.00-1.67 | [19,20] | ZrO_2 | 0.00-1.80 | [19,20] |
| Nb_2O_5 | Validation this study | [27] | | | |

*These are REDOX active species and the oxidation states of the species are predicted at the REDOX range over which DWPF processes.[19,20]

†During development of THERMO™, it was determined that a minimum of 3 wt% Al_2O_3 was necessary in high Fe_2O_3 containing and high Na_2O containing glasses to avoid phase separation [51]. This is consistent with the known miscibility gap in the $\text{Al}_2\text{O}_3\text{-Fe}_2\text{O}_3\text{-Na}_2\text{O}\text{-SiO}_2$ quaternary system that defines the crystallization of basalt [51].

ξ From the Waste Form Compliance Plan (WCP) glass ranges [52].

§ A ΔG_i term exists in THERMO™ and 7-day PCT data exist to assess the ΔG_i terms but such validations of the terms have not been performed.

Since 1995, when THERMO™ was developed, partial molar free energies have been developed for HfO_2 and NpO_2 .[53] Additionally, two potential partial molar free energy were developed for Nb_2O_5 .[27] While these partial free energies have been developed, they have not been assessed against the existing validation data for glasses high in HfO_2 , NpO_2 , and other species noted in Table 2 as yet. The Nb_2O_5 partial free energy will be validated in this study.

Note that Ag° and Au° are not oxides at the DWPF REDOX range and are not included in Table 2. They are metallic, and/or melt insoluble phases that do not have partial molar free energies associated with them in THERMO™.

Free energy is used rather than enthalpy because chemical durability is a chemical process, and the reaction progress is related to the free energy rather than the enthalpy of the overall reaction. The more negative the ΔG_p , the more readily the reaction will occur. The less negative the ΔG_p , the less readily the reaction will occur.

The ΔG_p is correlated to the response of a 7-day ASTM C1285A (PCT-A) in the 1995 PCCS THERMO™ References 19 and 20. For homogeneous glasses, the following equations are incorporated in PCCS:

| | | |
|------------|--|--------------|
| Equation 3 | $\log_{10}[\text{NC}_B] \text{ (g/L)} = -1.9014 - 0.1812 \Delta G_p$ | $R^2 = 0.77$ |
| Equation 4 | $\log_{10}[\text{NC}_{\text{Li}}] \text{ (g/L)} = -1.5459 - 0.1468 \Delta G_p$ | $R^2 = 0.75$ |
| Equation 5 | $\log_{10}[\text{NC}_{\text{Na}}] \text{ (g/L)} = -1.8012 - 0.1710 \Delta G_p$ | $R^2 = 0.80$ |

where ΔG_p is in kcal/100g glass and NC_i is in g/L for $i = \text{B}, \text{Li}$, and Na .

2.2 Modeling Constraints

For all models and validation data, various constraints are applied. The first requires that the chemical composition of the glass, on an oxide basis, be within 100 ± 5 wt%.[54] The “sum of oxides” constraint helps to minimize the impact of analytic errors during modeling and validation.

Moreover, a given glass must be homogeneous, i.e. not phase separated by liquid-liquid amorphous phase separation (APS). Glasses can be phase separated due to low Al_2O_3 (≤ 3.00 wt%), high P_2O_5 (≥ 2.25 wt%), or high B_2O_3 (≥ 15.00 wt%) concentrations (see discussion in Section 2.3).

Likewise, glasses for modeling should not be crystallized since phase separated and/or crystallized glasses can give anomalous durability [19,20,44,45,55], viscosity [56], and liquidus [57] responses. The potential impacts of crystallization on durability, i.e. a radionuclide vector from a crystal or from accelerated grain boundary dissolution, are shown in Equation 6.

Glasses should be homogeneous (not phase separated nor crystallized) because the glass durability can be influenced by any of the four terms given in Equation 6. In order to minimize or eliminate the last three terms, so that a model represents only the effects of glass composition on the first term: inhomogeneous glasses and crystallized glasses are excluded from modeling. Modeling does not include melt insoluble ($\text{Ag}^\circ, \text{Au}^\circ, \text{RuO}_2$, etc.) as these species do not impact glass durability [20] other than that they can act as nuclei and promote crystallization [58] that can impact glass durability (3rd and 4th terms) as shown in Equation 6.

Equation 6

$$\begin{aligned} \sum \text{Durability} = & \underbrace{\text{durability}_{(\text{homogeneous})}}_{1\text{st term}} + \underbrace{\text{durability}_{(\text{amorphous phase separation})}}_{2\text{nd term}} + \underbrace{\text{durability}_{(\text{crystallization})}}_{3\text{rd term}} \\ & + \underbrace{\text{durability}_{(\text{accelerated grain boundary})}}_{4\text{th term}} \end{aligned}$$

The glass REDOX, expressed as the $\text{Fe}^{2+}/\Sigma\text{Fe}$ ratio, must be < 0.33 , which is the upper limit of processability in the DWPF melter. REDOX values < 0.33 have been shown not to impact glass durability [59,60,61], glass viscosity, or glass liquidus values, while higher REDOX ratios (more reducing values) can impact these properties. The sum of the alkali ($\Sigma\text{R}_2\text{O}$ where $\text{R}_2\text{O} = \text{Cs}_2\text{O} + \text{K}_2\text{O} + \text{Li}_2\text{O} + \text{Na}_2\text{O}$) and Al_2O_3 constraints shown in Figure 2-1 were developed after the THERMO™ model was implemented in PCCS.[62,63] The impacts of the ROC and REDOX criteria on the glasses selected for modeling are discussed in Sections 7.3, 7.4, and 7.7.

The constraints, without the uncertainties factored into the values shown, are summarized graphically in the figure below. These constraints are applied so that model accuracy is maximized and model error is minimized by ensuring complete glass analyses and no anomalous property responses.

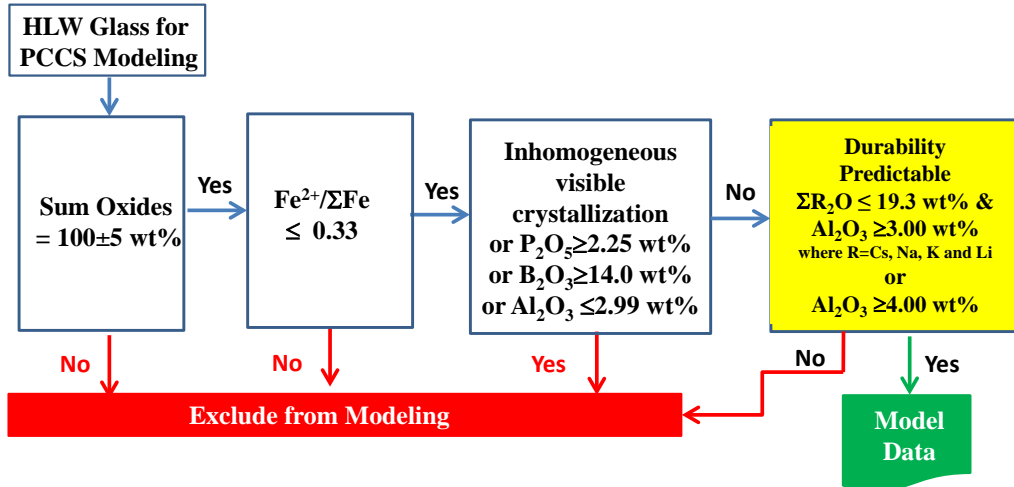


Figure 2-1. Graphical Representation of the Constraints Applied to the Choice of Model and Validation Data for the Durability, Viscosity, and Liquidus P/P Models for Glasses with 0-2.00 wt% TiO₂.

The Al₂O₃ term in the inhomogeneous by visible crystallization is 2.99 wt% to accommodate the WCP Purex glass which contains 2.99 wt% Al₂O₃.

2.3 Homogeneity and Reduction of Constraints (ROC) Evolution

A homogeneity constraint was developed as part of THERMO™ to ensure that DWPF glasses were homogeneous and not phase separated.[19,20] The homogeneity constraint ensured that the glasses modeled were homogeneous and not in the phase separation continuum space shown in Figure 2-2. It was noted during the development of THERMO™ that a minimum of 3 wt% Al₂O₃ was necessary in high Fe₂O₃ containing and high Na₂O containing glasses to avoid amorphous phase separation.[19,20,51] The data used to determine these limits are shown in Figure 2-3. Amorphous phase separation in low Al₂O₃ containing glasses is consistent with the known immiscibility gap in the Al₂O₃-Fe₂O₃-Na₂O-SiO₂ quaternary system that defines the melt surface and crystallization of molten basalt magmas.[64] It is also consistent with known phase separation in Na₂O-Al₂O₃-SiO₂ glasses that are known to phase separate when the glasses contain less than ~ 3 wt% Al₂O₃.[65,66]

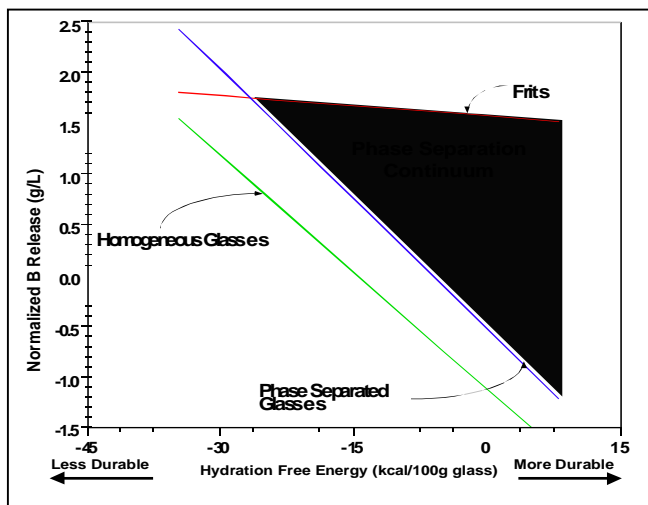


Figure 2-2. Complications in Glass Durability Modeling from Composition Due to Phase Separated Glasses.[19,20]

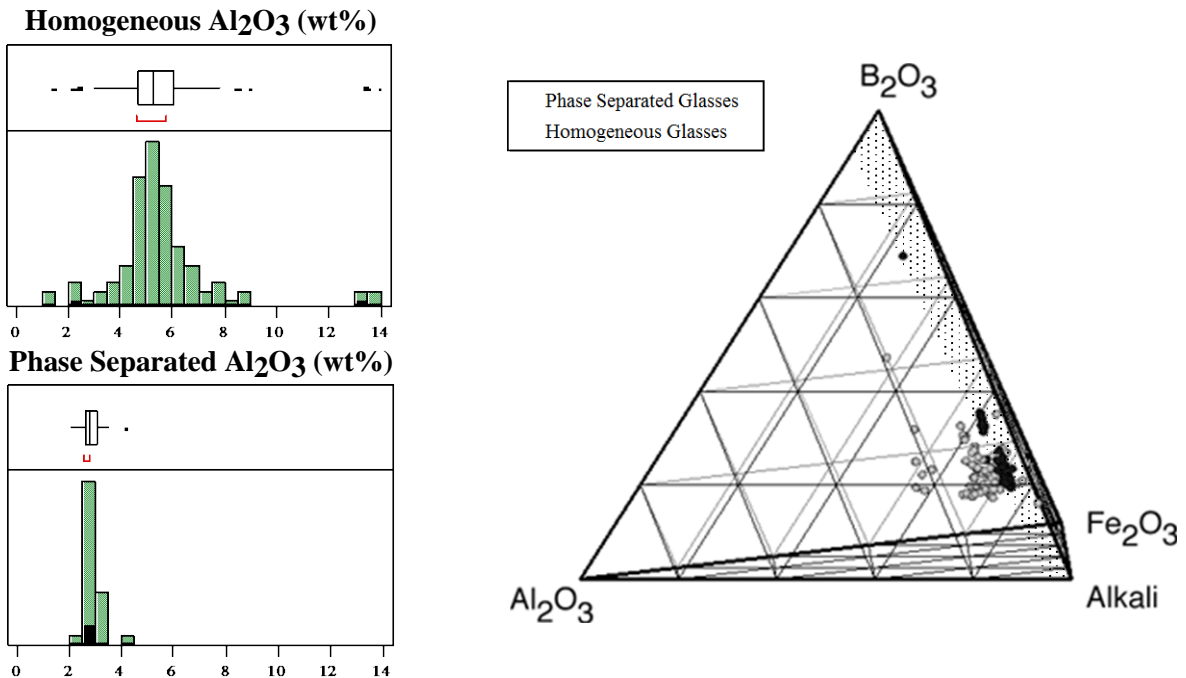


Figure 2-3. Dependency of HLW Glass Phase Separation on the Al_2O_3 Content of the Glasses.[19,20,51]

The homogeneity constraint was implemented in the DWPF PCCS to avoid the possible production of glasses that could be phase separated (liquid-liquid phase separation) and not predictable by the durability models. While the homogeneity constraint was typically an issue at lower waste loadings (WLs), it may impact the operating windows[§] for DWPF operations, where the glass forming systems may be limited to lower waste loadings based on fissile or heat load limits. In the Sludge Batch 1b (SB1b) variability study, application of the homogeneity constraint at the Measurement Acceptable Region (MAR) limit eliminated much of the potential operating window for DWPF.[62] As a result, Edwards and Brown [63] developed criteria that allowed DWPF to relax the homogeneity constraint from the MAR to the Property Acceptable Region (PAR), which opened up the operating window for DWPF operations. These criteria are defined as:

- (1) use the alumina constraint as currently implemented in PCCS ($\text{Al}_2\text{O}_3 \geq 3$ wt%) and add a sum of alkali constraint with an upper limit of 19.3 wt% ($\sum \text{R}_2\text{O} < 19.3$ wt%), or
- (2) adjust the lower limit on the Al_2O_3 constraint to 4 wt% ($\text{Al}_2\text{O}_3 \geq 4$ wt%) and no sum of alkali constraint.

where $\sum \text{R}_2\text{O}$ is the sum of the concentrations of the alkali oxides, i.e. $\text{Cs}_2\text{O} + \text{K}_2\text{O} + \text{Li}_2\text{O} + \text{Na}_2\text{O}$. The alkali and alumina limits in criterion 1 above are those of the WCP Purex glass and the criteria are not only to ensure that glasses are not phase separated but to ensure that the glass durability stays well below that of the benchmark EA glass. Recent studies on the long term durability of high alkali versus low alkali glasses have shown that high alkali glasses return to the undesirable accelerated rate of dissolution preferentially to low alkali glasses but the relationship to the alumina content of the glass is still under study.[67,68] Therefore, the implementation of an alkali/alumina constraint for DWPF glasses was prudent.

[§] The waste loading interval over which a particular glass system is considered to be acceptable based on model predictions.

Historical glasses of interest to DWPF meeting criteria 1 and 2 above were found to be acceptable using a normalized boron release [NC_B] of 10 g/L as a benchmark. This value was chosen in order to be certain that the boron releases of the study glasses were well below that of the EA glass with measurement and analytical uncertainties considered. It should be emphasized that this limit was not empirically derived and was only used as a guide to develop the Al_2O_3 and/or sum or alkali criteria. Herman et al. [69] later demonstrated that these criteria could be used to replace the homogeneity constraint for future sludge-only batches.

In addition to the sludge only studies cited above, another study [70] was conducted to better understand the homogeneity-composition relationship for coupled operations. Specifically, the initiation of the Actinide Removal Process (ARP) and MCU (Modular CSSX Unit where CSSX is Caustic-Side Solvent Extraction) at SRS in 2008 required a need to revisit the DWPF homogeneity constraint shown in Figure 2-1 and discussed in Section 2.2 for coupled operations. This constraint was specifically addressed through the variability study for Sludge Batch 5 (SB5) which contained ARP/MCU.[70] However, additional benefit was gained for ARP/MCU processing if the homogeneity constraint could be replaced by the Al_2O_3 and sum of alkali constraints for future fully coupled operations composition projections as was done for sludge only processing in DWPF. Raszewski and Edwards [70] conducted this ROC study for coupled operations. The compositional region covered by this study is provided in Table 3. The “Others” component in this table includes: BaO, CdO, Ce_2O_3 , La_2O_3 , PbO, SO_4 , ZnO, and ZrO_2 . PCTs were conducted and evaluated for the glasses tested as part of this study on coupled feeds with ARP/MCU. This led to the replacement of the homogeneity constraint, in its entirety, for coupled operations with TiO_2 levels up to 2 wt% in glass [70] with the same ROC criteria given above for sludge-only processing.

Table 3. Oxide Intervals for Reduction of Constraints Study for Coupled Operations with ARP and MCU

| Oxide | Minimum (wt%) | Maximum (wt%) |
|--------------------------------|---------------|---------------|
| Al ₂ O ₃ | 3.25 | 18 |
| B ₂ O ₃ | 4.5 | 14 |
| CaO | 0 | 4 |
| Cr ₂ O ₃ | 0 | 0.2 |
| Fe ₂ O ₃ | 5 | 21 |
| Li ₂ O | 4 | 7 |
| MgO | 0 | 1.5 |
| MnO | 0.3 | 5.5 |
| Na ₂ O | 10 | 18 |
| NiO | 0 | 2.5 |
| SiO ₂ | 30 | 55 |
| TiO ₂ | 0.5 | 2.0 |
| U ₃ O ₈ | 0 | 9.5 |
| Others | 0 | 2.0 |

2.3.1 High P₂O₅ Constraint

Glasses can also be phase separated due to high P₂O₅ content; therefore glasses are screened (Figure 2-1) and are not used for modeling if they contain >2.25 wt% P₂O₅. This is also the P₂O₅ solubility limit in PCCS. Glasses with P₂O₅>2.25 wt% have been shown to cause lithium phosphate phase separation and compromise glass durability.[71, 72, 73] High P₂O₅ (>2.25 wt%) concentration creates crystalline phosphate phases by crystalline phase separation (CPS). In CPS the two phases, one phosphate rich, co-exist as liquid phases in the melt and the glass cannot be quenched rapidly enough to prevent the phosphate rich liquid from crystallizing.[72,73]

2.3.2 High B₂O₃ Constraint

Glasses can also be phase separated due to high B₂O₃ content.[74] In 1994 Tovena, et. al. [55] demonstrated that various glass durability models, whether based on thermodynamics, enthalpy or structural concepts, did not predict waste glass durability accurately when the composition of the waste glass contained >15% B₂O₃ with little or no Al₂O₃. For these glasses, all the models predicted the glass durability to be significantly better than the measured values, i.e. the models said the glasses were more durable than the measured durability. Tovena, et. al. [55] attributed the under prediction to phase separation and complete dissolution of a borate rich phase in the glass when the Al₂O₃ content was insufficient. This was confirmed by SRNL researchers in 1995 [19,20,51] and a B₂O₃ constraint of 14 wt% is imposed during modeling to be conservative. An upper B₂O₃ limit is not currently in PCCS because DWPF glasses do not contain high concentrations of B₂O₃ due to the high concentrations of other melt fluxes, i.e. alkali, in the DWPF wastes, i.e. high B₂O₃ in the presence of high Na₂O and Cs₂O oxides would violate the PCCS low viscosity limit. In addition, the ROC maintains a sufficiently high Al₂O₃ content such that the exact B₂O₃/Al₂O₃ ratio need not be defined for DWPF glasses to avoid a compositional space in which phase separation may be of concern.

2.3.3 Crystallization Constraint

Crystallization can impact durability in several ways as shown in Equation 6. For homogeneous glasses, it has been shown that B release is congruent with the ⁹⁹Tc dissolution.[33-43] As long as ⁹⁹Tc does not

partition into a given crystalline phase, this relationship will hold. If ^{99}Tc partially partitions into a crystalline phase, then there would be a durability vector from both the glass and the crystal. In addition, one would have to consider whether the release of ^{99}Tc from the glass was accelerated from the grain boundary around the crystal since the crystal can deplete the surrounding glass of certain glass forming components. If ^{99}Tc partitioned completely into a crystalline phase, then there would be a durability vector only from the crystal. If ^{99}Tc would partially or completely partition to a crystalline phase then the congruency of the ^{99}Tc release to B release would no longer hold.

Spinel crystallization has been found not to accelerate grain boundary dissolution because it is isotropic and so is the waste glass. Spinel is not allowed to form in the melter and forms on cooling of the glass within the canister. Spinel does not sequester any radionuclides nor glass formers and so spinel crystallization impacts on glass durability are virtually non-existent.[45,75] Therefore, no constraint exists for spinel crystallization.

Nepheline has been found to have a strong impact on durability and acmite has a moderate impact on durability.[75] Nepheline and acmite both form during canister cooling. Acmite sequesters mostly transition metals from the waste and minimal glass formers (Si and not Al) and hence no acmite constraint exists. However, nepheline sequesters glass formers (both Si and Al) from the matrix glass, and thus, accelerates grain boundary dissolution (see Equation 6). While nepheline does not sequester ^{99}Tc , it may sequester ^{137}Cs and nepheline crystallization in a nuclear waste glass canister is, therefore, minimized during processing by processing glass compositions that are unfavorable to nepheline formation. This additional constraint, the nepheline constraint, was defined by Li et. al. [76,77] and implemented in DWPF by Edwards, Peeler, and Fox [78].

2.4 Calculation of Glass Durability

The 2014 revision of the PCT procedure [31] requires that the density of a glass be used to calculate the surface area (SA) term in the denominator of the normalized release formula, NL_i , for any element released from a glass. The formalism is $\text{SA} = (6 * \text{mass}) / (\text{density} * \text{diameter of particle}) (\text{m}^2)$. If the mass and particle size are constants, then a denser glass gives a smaller SA. Since the SA appears in the denominator of the normalized release calculation, the resulting normalized release for the element of interest would be higher than the value determined for a less dense glass (all other things being equal). The DWPF THERMO™ models use the NC_i release which is not dependent on the SA as is the NL_i parameter. The impact of ignoring density effects by using NC_i can only be evaluated indirectly by investigating the effects of density on NL_i . During the 1995 THERMO™ model development, the glass densities were all assumed to be very similar and the impact of a varying SA on the leachate concentrations was not examined. Therefore, the impact of ignoring density on the DWPF THERMO™ models is assessed two different ways in this document. First, the range of densities used during THERMO™ development is assessed against the SWPF glass densities given in Appendix A. Secondly, the effects of variations in glass density on the value of NL_i relative to the effects of model uncertainty are to be investigated.

3.0 Defining Future Coupled DWPF-SWPF Processing Ranges

The information in Table 3, from the ROC evaluation for coupled operations involving ARP and MCU, was used to support an effort to define any potential gaps in the compositional range of the current PCCS models when compared to the compositional region projected for the SWPF flowsheet. In addition to addressing this issue for the PCCS models, the SWPF gap analysis study [79,80,81] extended the reduction of constraints coverage to the glass composition region anticipated for the DWPF and SWPF coupled flowsheet. From Reference 79, the compositional region of interest is defined by the oxides and wt% intervals given in Table 4. In this table, the shaded oxide rows define the “others” component for this compositional region.

Thus, one may look to the glass regions of Table 3 and Table 4 to define the region of interest for assessing the applicability of the PCCS THERMO™ models for SWPF processing. The PCCS THERMO™ data [19,20], augmented by select validation data given in ComPro™ [46,47] for high TiO₂ glasses, were used to investigate the applicability of the existing durability models to the SWPF space defined by Table 3 and Table 4.

Table 4. Oxide Intervals for SWPF Gap Analysis Study [79]

| Oxide | Minimum (wt%) | Maximum (wt%) |
|--------------------------------|---------------|---------------|
| Al ₂ O ₃ | 3.5 | 13 |
| B ₂ O ₃ | 4.5 | 10 |
| BaO | 0 | 0.25 |
| CaO | 0.2 | 2 |
| Ce ₂ O ₃ | 0 | 0.2 |
| CoO | 0 | 0.1 |
| Cr ₂ O ₃ | 0 | 0.2 |
| Cs ₂ O | 0.3 | 1 |
| CuO | 0 | 0.1 |
| Fe ₂ O ₃ | 5 | 16 |
| K ₂ O | 0 | 0.2 |
| La ₂ O ₃ | 0 | 0.1 |
| Li ₂ O | 1 | 7 |
| MgO | 0 | 2 |
| MnO | 0.2 | 4 |
| Na ₂ O | 8 | 18 |
| NiO | 0 | 2 |
| PbO | 0 | 0.25 |
| SO ₄ | 0 | 0.3 |
| SiO ₂ | 40 | 55 |
| ThO ₂ | 0 | 1 |
| TiO ₂ | 2 | 6 |
| U ₃ O ₈ | 0 | 6 |
| ZnO | 0 | 0.2 |
| ZrO ₂ | 0 | 0.25 |

4.0 Experimental Measurement Data

The SWPF glasses were made and analyzed by Atkins North America-Vitreous State Laboratory (ANA-VSL). The details of the glass fabrication are given in Reference 82. The chemical compositions were measured by X-ray Fluorescence (XRF) and other methods. Since XRF cannot measure light elements such as B and Li, the glasses were dissolved and analyzed by Direct Current Plasma Emission Spectrometry (DCP) for these two elements. For each glass, two XRF and two DCP preparations were performed and two measurements were performed on each on different days. Therefore, each glass had four replicate measurements. The SRNL EA glass was used as a glass standard. The EA glass had been manufactured and analyzed by Corning Engineering Laboratory Services (CELS) and the analyses were validated by SRNL Analytic Development (AD).[29,30] The details of the SWPF glass measurements and bias correction to the EA glass standards are discussed elsewhere.[83] The measured biased

corrected (bc) glass compositions used in this study for modeling are given in Appendix A for completeness.

The ANA-VSL conducted the PCTs for this study under the auspices of an analytical plan [84]. The glasses tested included quenched glasses and glasses that had been subjected to centerline canister cooling (ccc). No data were provided by ANA-VSL as to what phases had crystallized during the ccc treatment. The ccc treated samples are not used in THERMOTM model assessments because they may be crystallized (see Figure 2-1). The ccc treated samples are used as supporting data since no evaluation can be made as to whether the ccc leachate responses were caused by crystallization of spinel, acmite, nepheline, etc. The ANA-VSL provided the measurements of glass durability in Reference 85 (see also Appendix B). The Approved Reference Material-1 (ARM-1) and EA glasses were also subjected to durability testing to demonstrate that the PCT-A procedure was in control and those data are also provided in Appendix B. This report presents and evaluates the durability data provided by ANA-VSL against the 1995 THERMOTM model data given in Reference 20 and Appendix C.

5.0 Quality Assurance

All of the model assessments presented in this study were performed in accordance with DOE/RW-0333P and a Quality Assurance Program (QAP) that meets the Quality Assurance criteria specified in DOE O. 414.1, *Quality Assurance*, 10 CFR 830, *Nuclear Safety Management*, Subpart A, “*Quality Assurance Requirements*”, paragraph 830.122 and also meets the requirements of ASME Nuclear Quality Assurance (NQA)-1, *Quality Assurance Requirements for Nuclear Facility Applications*.

The customer for this work is DWPF/SALTSTONE Facility Engineering. The point of contact is E.W. Holtzscheiter. The request is detailed in X-TTR-S-00012 and is in accordance with the Task Technical and Quality Assurance Plan (TTQAP) given in Reference 80. This work involved research and development that is considered technical baseline. The TTR requires DOE/RW-0333P to be invoked for specific tasks associated with waste form affecting properties (such as glass durability).

Requirements for performing reviews of technical reports and the extent of review are established in manual E7 2.60. SRNL documents the extent and type of review using the SRNL Technical Report Design Checklist contained in WSRC-IM-2002-00011, Rev. 2. All of the durability property-composition models presented in this report were conducted using JMP Version 11.1.1 (CMJ), validated using JMP Pro Version 11.2.1 (TBE), and checked by E7 2.60 using JMP Version 11.2.0 (CLT).[86]

6.0 Results and Discussion of SWPF PCT Measurements

Table B1 in Appendix B provides the elemental leachate concentration measurements for the solution samples generated by the PCTs for the study glasses. The values for these measurements are given as received by SRNL. All of the measurements for the blanks associated with this testing were below the detection limit of the analytical process. These measurements (indicated by a “<”) were replaced by their detection limits in subsequent analyses. Based on weight measurements of the test vessels before and after the 7-day procedures, there was no water-loss issue with any vessel during any of the PCT testing. Table B2 in Appendix B provides the summary for each glass and each standard glass (by oven used) in terms of the average of the common logarithm of the PCT leachate compositions. These values are used in conjunction with the bc measured glass composition data to generate the durability plots provided in the rest of this document. Table B3 in Appendix B provides the initial and final pH values for each of the test solutions.

In the sections that follow, the analytical sequences of the measurements are explored, the measurements for each glass are reviewed, the measurements of the multi-element solution standard are investigated, the normalized PCTs for each glass are determined, comparisons are made between the PCTs for the two heat

treatments of each glass, and the predictability of the PCT responses of the study glasses by the PCCS THERMO™ durability models is explored. JMP Pro Version 11.2.1 [86] was used to support these analyses.

6.1 Leachate Measurements in Analytical Sequence

Exhibit B1 in Appendix B provides plots of the common logarithms of the leachate concentrations (expressed in parts per million (ppm), which is equivalent in this testing to mg/L) in analytical sequence by analytical block in groups of three blocks. Each of these groups corresponds to a pair of oven runs that were used to conduct the complete set of PCT measurements needed to support this study. No issues were observed in these plots.

6.2 Leachate Measurements by Glass Identifier

Exhibit B2 in Appendix B provides plots of the leachate concentrations as common logarithms of the ppm values for both the quenched and ccc version of each of the high TiO₂ study glasses. These plots allow for the assessment of the repeatability of the measurements and any differences between the quenched and ccc versions of a given glass. For some of the glasses, scatter in the triplicate values of some analytes is observed; however, these results do not affect the evaluation of the THERMO™ model and the ROC. There are slight differences between the quenched and ccc versions of the glass releases as anticipated for crystallized or phase separated glasses; the ccc versions of a couple of the glasses (see SWPF-01 and SWPF-12) appear to be less durable (i.e., they have a larger ppm release value) than their quenched counterparts. A closer look at the quenched and ccc outcomes is provided below although the ccc data are not used in the evaluation of the THERMO™ models.

6.3 Results for the Samples of the Multi-Element Solution Standard

Exhibit B3 in Appendix B provides analyses of the measurements of the multi-element solution standard by analytical block including analysis of variance (ANOVA) investigations for each element of interest. The reference value of the solution standard for each element of interest is also provided as part of the information in this header.

A statistically significant difference (at a 5% level) among the averages of analytical blocks for these measurements was indicated for all of the analytes: B, Li, Na, and Si. Similar differences have been observed in previous DWPF variability studies (for example, see [87]). No attempt was made to bias correct for the statistically significant effects since averaging the ppm values for each set of triplicates (i.e., over three of the analytical blocks) tends to lessen the impact of these effects. Table 5 provides the block averages, the reference values, and the percent differences between the overall averages and reference values for these measurements. Based on these results no issues are seen with the reported data.

Table 5. Measurements of Solution Standards for PCT Analytical Blocks

| Analytical Block | Avg B (ppm) | Avg Li (ppm) | Avg Na (ppm) | Avg Si (ppm) |
|------------------|-------------|--------------|--------------|--------------|
| A | 19.88 | 10.34 | 82.69 | 49.18 |
| B | 19.76 | 9.93 | 80.95 | 49.51 |
| C | 20.14 | 10.42 | 80.98 | 49.62 |
| D | 19.96 | 10.06 | 80.09 | 49.90 |
| E | 20.24 | 10.17 | 81.07 | 51.57 |
| F | 20.31 | 10.09 | 80.13 | 51.41 |
| G | 20.53 | 10.53 | 81.42 | 50.42 |
| H | 20.88 | 10.54 | 81.17 | 50.72 |
| I | 20.39 | 10.43 | 81.07 | 50.34 |
| J | 20.11 | 10.47 | 80.86 | 50.39 |
| K | 20.02 | 10.31 | 80.95 | 50.04 |
| L | 20.13 | 10.26 | 81.14 | 50.32 |
| M | 20.30 | 10.36 | 80.60 | 50.45 |
| N | 20.23 | 10.42 | 81.23 | 50.25 |
| O | 20.22 | 10.32 | 80.99 | 50.20 |
| P | 20.20 | 10.29 | 80.87 | 50.29 |
| Q | 20.18 | 10.26 | 80.89 | 50.19 |
| R | 20.20 | 10.24 | 80.75 | 50.48 |
| S | 20.21 | 10.22 | 80.68 | 50.26 |
| T | 20.20 | 10.15 | 80.55 | 50.22 |
| U | 20.21 | 10.15 | 80.91 | 50.20 |
| Grand Average | 20.20 | 10.28 | 80.95 | 50.28 |
| Reference Value | 20 | 10 | 81 | 50 |
| % Difference | 1.02% | 2.84% | -0.06% | 0.57% |

6.4 Normalization of the PCT Results

The PCT leachate data were used to determine normalized concentrations for each element of interest using the targeted, measured, and measured bc compositions of the glasses following the expression given in ASTM C1285:

Equation 7

$$NC_i = \frac{c_i(\text{sample})}{f_i}$$

where NC_i is the normalized concentration in units of $\text{g}_{\text{waste form}}/\text{L}_{\text{leachant}}$, c_i is the concentration of element “ i ” in the leachate in units of g_i/L , and f_i is the mass fraction of element “ i ” in the unleached glass in units of $\text{g}_i/\text{g}_{\text{glass}}$.

An equation was developed to allow for calculation of the NC_i values using the units of measurement provided with the analytical results for this study, and to accommodate the triplicate leachate measurements for each of the study glasses. Note that the symbols in this second equation were kept consistent with those used in ASTM C1285, but the units of measurement differ. The common logarithm of the normalized concentration for each element “ i ” (NC_i) for each of the study glasses was determined using the equation:

Equation 8
$$\log_{10}(NC_i) = \overline{\log_{10} c_i} - [1 + \log_{10} f_i]$$

where NC_i remains in units of $\text{g}_{\text{waste form}}/\text{L}_{\text{leachant}}$, $\overline{\log_{10} c_i}$ is the average of the common logarithms of the measured concentrations of element “ i ” in the triplicate leachates in units of mg/L, and $\log_{10} f_i$ is either the common logarithm of the targeted concentration of element “ i ” in the glass in units of wt %, or the common logarithm of the average measured concentration of element “ i ” in the glass in units of wt %, or the common logarithm of the average measured bc concentrations of element “ i ” in the glass in units of wt % (i.e., the values from Reference 83 or converted from Appendix A oxide values of wt%).

The results for the normalized concentrations are provided in Table B4 in Appendix B. The values are provided in grams per liter (g/L) as well as the common logarithms of the g/L values. The durabilities of all of these glasses (both quenched and ccc) are acceptable when compared to the durability of the EA glass. Specifically for boron, the worst durability is for the SWPF-01 ccc glass (targeted composition), with a value ~8.8 g/L, which is still much better than the reference value for EA for this element of 16.7 g/L [29,30].

Exhibit B4 in Appendix B provides scatter plots that contain normalized concentrations for both the quenched and ccc version of the study glasses based on the three compositional views although only the measured bc view will be used to evaluate THERMO™. The EA and ARM results are not included in this analysis. These plots offer an opportunity to investigate the consistency in the leaching across the elements for the glasses of this study. Consistency in the leaching across the elements is typically demonstrated by a high degree of linear correlation among the values for pairs of these elements. The smallest correlation is in the plot for Li and Na based upon the measured bc compositional view; the correlation for this pair of analytes is ~85.98%, which demonstrates a good consistency of the results among all four of the analytes.

6.5 Effects of Heat Treatments

Exhibit B5 in Appendix B provides plots of the normalized PCT responses between the two heat treatments for the study glasses as well as the responses for ARM and EA. The results are grouped by compositional view. These plots provide a basis for judging the impact of differences in the PCT response due to the heat treatment of the glass. For most of the glasses except those already discussed in Section 6.2, there is no difference between the quenched and ccc versions of the study glasses, indicating that the thermal heat treatment had very little (if any) impact on the PCT responses. However, this is not true for SWPF-01. Regardless of the compositional view, the PCT response for the ccc version indicates a much less durable glass than the response for the quenched version of SWPF-01. As stated above, the normalized concentration for the boron response for the ccc version of SWPF-01 (based upon the targeted composition for this glass) is ~8.8 g/L, while the durability of the quenched counterpart is ~0.9 g/L, almost an order of magnitude smaller.

7.0 Results and Discussion: Density, Congruency, Durability Models, and ROC Criteria

The discussions above indicate that all of the PCT responses for the study glasses are better than those of the EA glass for the analytes of interest. Certainly, glass performance better than the EA glass was a desirable outcome for the PCT results for the SWPF glasses; however, another desired outcome of the SWPF study was that the glass performance be predictable. The assessment of the predictability of the PCT responses by DWPF’s current models in PCCS is made from two perspectives: (1) the predictability of the PCT responses for the high TiO₂ glasses by the current PCCS models for boron, lithium, and sodium, and (2) the viability of the reduction of constraints (ROC) approach (which was applied for glass systems with TiO₂ up to 2 wt%) to be extended to glass systems with TiO₂ at higher concentrations.

The homogeneity constraint was implemented as part of PCCS to help ensure that the current durability models would be applicable to the glass compositions (i.e., homogenous glasses) being processed during DWPF operations. ROC studies were conducted to eliminate the dependence of PCCS on the homogeneity constraint. An ROC study for coupled operations with TiO₂ up to 2 wt% [70] led to the replacement of the homogeneity constraint, in its entirety, by the following criteria:

- (1) use the alumina constraint as currently implemented in PCCS ($\text{Al}_2\text{O}_3 \geq 3$ wt%) and add a sum of alkali constraint with an upper limit of 19.3 wt% ($\sum \text{R}_2\text{O} = \text{Cs}_2\text{O} + \text{K}_2\text{O} + \text{Li}_2\text{O} + \text{Na}_2\text{O} < 19.3$ wt%), or
- (2) adjust the lower limit on the Al₂O₃ constraint to 4 wt% ($\text{Al}_2\text{O}_3 \geq 4$ wt%) and no sum of alkali constraint.

The structure of this section will be the following:

- Assess the congruency/internal consistency of the raw leachate values in THERMO™ and SWPF datasets (Section 7.1)
- Compare THERMO™ and SWPF modeling datasets (Section 7.2)
- Revise ROC for high TiO₂ containing glasses due to the known structural competition between alumina and titania for alkali in silica and borosilicate glasses (Section 7.3)
- Apply the revised ROC for glasses containing ≥ 2.0 wt% TiO₂ to the SWPF glasses: glasses failing the new ROC must be removed from the SWPF glass dataset (Section 7.4).
- Apply the original ROC for glasses containing ≤ 2.0 wt% TiO₂ and the REDOX criteria from Figure 2-1 to the 1995 THERMO™ models which exclude several glasses and refit the slopes and intercepts of the THERMO™ models creating modified THERMO™ models (Section 7.5)
- Assess the impact of glass density effects, if any, on the PCT response for the THERMO™ and SWPF glasses (Section 7.6)
- Assess the SWPF glass durabilities to the modified THERMO™ models which validates the existing THERMO™ ΔG_i values (Section 7.7)
- Assess the impact of the modified THERMO™ models on the DWPF operating window (Sections 7.8 and 7.9)
- Validate the existing THERMO™ ΔG_i values with other high TiO₂ glass durability data from ComPro™ (Section 7.10).

7.1 Internal Consistency of THERMO™ and SWPF Glass Durability Data

Boron, sodium, and lithium releases from glass are considered to be the most conservative indicators of glass durability since these elements are leached from glass more rapidly than other elements. In addition, boron is considered to be the best indicator of glass durability because boron does not saturate in the leachate and does not participate in precipitation reactions caused by supersaturation. The consistency of the leachate data can, therefore, be evaluated by plotting the release of any leachate element against the release of boron. The internal consistency of both the leachate data and the glass composition analyses can be evaluated simultaneously (Figure 7-1) by plotting the normalized concentration of boron, NC_B, against the normalized concentration of the other constituents, e.g., NC_{Li}, NC_{Na}, and NC_{Si}.[§] Information

[§] The following is a quote from ASTM C1285. “The most important elements to be analyzed in the PCT leachate are those that best represent the extent of dissolution of the glass waste form. For example, elements that are not sequestered in alteration phases that participate in surface alteration reactions, and are also not solubility limited, are good indicators of glass waste form durability. Extensive testing of any glass waste form must be performed in order to determine what elements represent the extent of dissolution of the glass waste form.. This bounds the extent of dissolution of the radioactive constituents. For example, in high level borosilicate waste glass, Tc⁹⁹, present at $\sim 4.1 \times 10^{-4}$ weight % in the waste form, has been shown to be released congruently (stoichiometrically) with boron, lithium, and sodium. Therefore, for borosilicate glass waste forms, the leachates are routinely analyzed for boron, lithium, and sodium if these elements are present at > 1 mass % in

was provided in THERMOTM for NC_B, NC_{Li}, NC_{Na}, and NC_{Si} and these same concentrations are evaluated in this study.

Since the normalized release concentrations are the leachate concentrations divided by the glass compositions in element wt%, consistency in the log₁₀[NC_B] versus log₁₀[NC_i] plots provides a simultaneous check on both the leachate and glass composition analyses. Use of the normalized release units compensates for the glass chemistry, e.g., if a high Li containing glass releases more Li than a low Li containing glass then this effect is accounted for by normalization relative to the concentration of Li in the glass.

Therefore, correlations of log₁₀[NC_{Li}], log₁₀[NC_{Na}], and log₁₀[NC_{Si}], with log₁₀[NC_B] were used in THERMOTM to determine leachate congruency and consistency.[20] This same approach is used below to compare the THERMOTM correlations to the SWPF correlations. All of the correlations in THERMOTM [20] indicated a high degree of internal consistency of both the leachate analyses and the glass chemical analyses. In addition these plots demonstrated the following:

- R² values of approximately 0.99 for the elements of concern for the DWPF WAPS, i.e., the log₁₀[NC_{Li}] vs. log₁₀[NC_B] and the log₁₀[NC_{Na}] vs. log₁₀[NC_B] plots
- slopes of ~1 and intercepts of ~0 for the elements of concern for the DWPF WAPS for homogeneous glasses, e.g., the log₁₀[NC_{Li}] vs. log₁₀[NC_B] and the log₁₀[NC_{Na}] vs. log₁₀[NC_B] plots, which indicate that B and the alkalis are released at similar rates, i.e. congruently^f
- R² value of 0.95 for the log₁₀[NC_{Si}] vs. log₁₀[NC_B] plot showing analytic consistency but potential incongruity (see next item)
- slopes of <1 for log₁₀[NC_{Si}] vs. log₁₀[NC_B] indicating that Si is released to solution at a slower rate than B, Na, and Li and/or precipitates out of the leachates, forms colloids that may not get measured in solution analyses, or is sequestered in the glass leached layer, i.e., it participates in condensation reactions.

Figure 7-1 compares the THERMOTM model leachate consistency to the current SWPF leachate consistency. The leachate consistency for the log₁₀[NC_{Na}] vs. log₁₀[NC_B] plots for the SWPF glasses has a similar slope and intercept to the leachate data for log₁₀[NC_{Na}] vs. log₁₀[NC_B] for the THERMOTM model data (Figure 7-1a). While the SWPF data and the THERMOTM data are quite close, the THERMOTM leachates are more internally consistent, i.e. have a higher R² and a lower RMSE, which means there is less scatter in the data. Less scatter can be a function of many factors such as the analytic instrumentation used for analysis of the leachate and the glass or slight variations in the way in which the test is performed in each laboratory.

The leachate consistency for the log₁₀[NC_{Li}] vs. log₁₀[NC_B] plot for the SWPF glasses has a similar slope and intercept to the leachate data for log₁₀[NC_{Li}] vs. log₁₀[NC_B] for the THERMOTM model data (Figure 7-1b). While the SWPF data and the THERMOTM data are quite close, the THERMOTM leachates are more internally consistent, i.e. have a higher R² and a lower RMSE, which means there is less scatter in the data.

The leachate consistency for the log₁₀[NC_{Si}] vs. log₁₀[NC_B] plot for the SWPF glasses is quite different than the leachate data for log₁₀[NC_{Si}] vs. log₁₀[NC_B] plot for the THERMOTM model data (Figure 7-1c). Since log₁₀[NC_{Si}] is not of great importance to the WAPS acceptability, this will not be discussed further.

the glass. Additional mechanistic information about high level borosilicate waste glass durability is gained by analyzing for other elements present in the glass, i.e. Si.”

^f The slopes are slightly different because the release of each element is slightly different depending on its local bonding and coordination in the glass structure.

Given that, in general, the THERMO™ leachates are more internally consistent, i.e. have a higher R² and a lower RMSE (less scatter in the data), the SWPF data will be overlain on the THERMO™ model for comparison. This comparison is performed because the SWPF data have larger scatter than the THERMO™ model data and overlaying the SWPF data validates the alkali and TiO₂ ΔG_i terms in the THERMO™ model without refitting the model and compromising the THERMO™ model's R² and RMSE values.

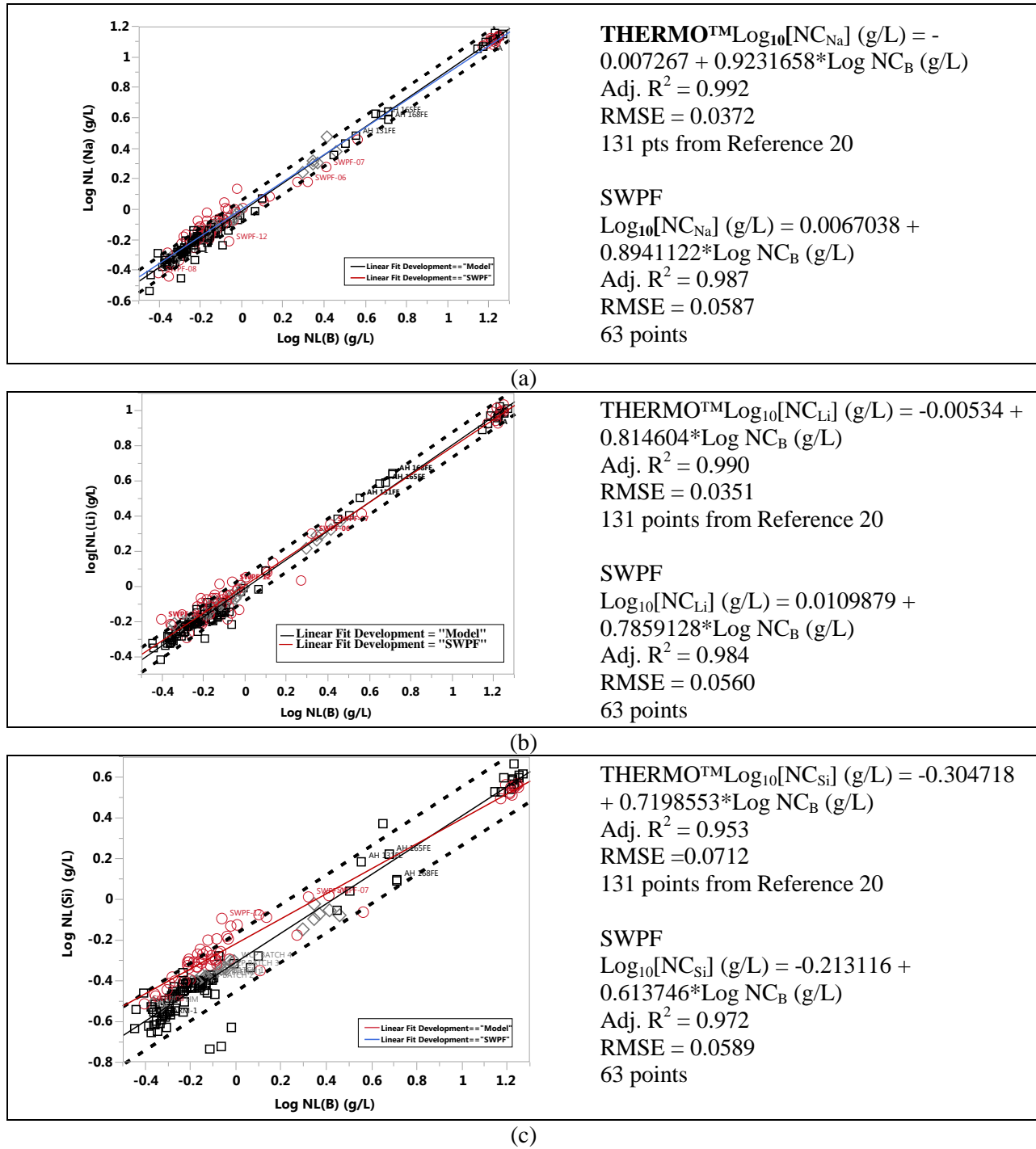


Figure 7-1. Internal Consistency of the THERMO™ Model Data Compared to the SWPF Glass Data.

7.2 Predicted versus Measured Durability of SWPF Glasses

Exhibit B6 in Appendix B provides plots of the THERMO™ durability models [20] for B, Li, Na, and Si that relate the logarithm of the normalized PCT (for each element of interest) to the linear function of the free energy of hydration term (ΔG_p , kcal/100g glass) derived for the targeted, measured, and measured bc compositional views for the study glasses. The results for both heat treatments (quenched and ccc) and the compositional perspectives (targeted, measured, and measured bc) are shown on each plot. Prediction limits, at a 95% confidence level for an individual PCT result, are also plotted with the linear fit. The EA and ARM results are also indicated on each of these plots.

Two of the $\log_{10}[\text{NC}_B]$ plots from Appendix B Exhibit B6 are repeated in Figure 7-2 (quenched/measured bc) and Figure 7-3 (ccc/measured bc) with only the unpredictable glass durability results shown and labeled. This is done to help identify the glasses that are unpredictable which lie mostly above the upper 95% (U95) confidence interval. From the THERMO™ model perspective Figure 7-2 for quenched glasses is more important than Figure 7-3 for ccc heat treated glasses since crystallized glasses are not modeled in THERMO™ (Figure 2-1).

Comparisons of Figure 7-2 and Figure 7-3, shows that the ccc versions of the glasses above the U95 have more unpredictable results than their quenched counterparts with SWPF-01 being the prime example. For Figure 7-3 and Figure 7-2 only those glasses whose PCT responses are under predicted are shown (along with the EA and ARM-1 glass results). The unpredictability of several of the glasses, whose ΔG_p values fall to the less negative side of the x-axis, would not be seen as an issue since the measured bc PCT response for glasses that demonstrate this behavior indicate that the glasses are durable and very acceptable relative to the EA glass. It should be noted that the ccc and quenched versions of glasses SWPF-03, -06, and -07 demonstrate similar PCT response behavior during comparisons of Figure 7-2 and Figure 7-3.

The quenched glasses that exhibit unpredictability in Figure 7-2, those glasses where the ΔG_p values fall to the more positive side of the x-axis, may be phase separated, as this is the region in which phase separation was determined to exist for some glasses during THERMO™ modeling (see Figure 2-2). Since the SWPF glass dataset is being used to validate the terms in the THERMO™ model, the cause of the anomalous behavior had to be accounted for. Glasses exhibiting anomalous behavior, were the primary reason that the ROC was developed and applied in PCCS after the THERMO™ model was developed.

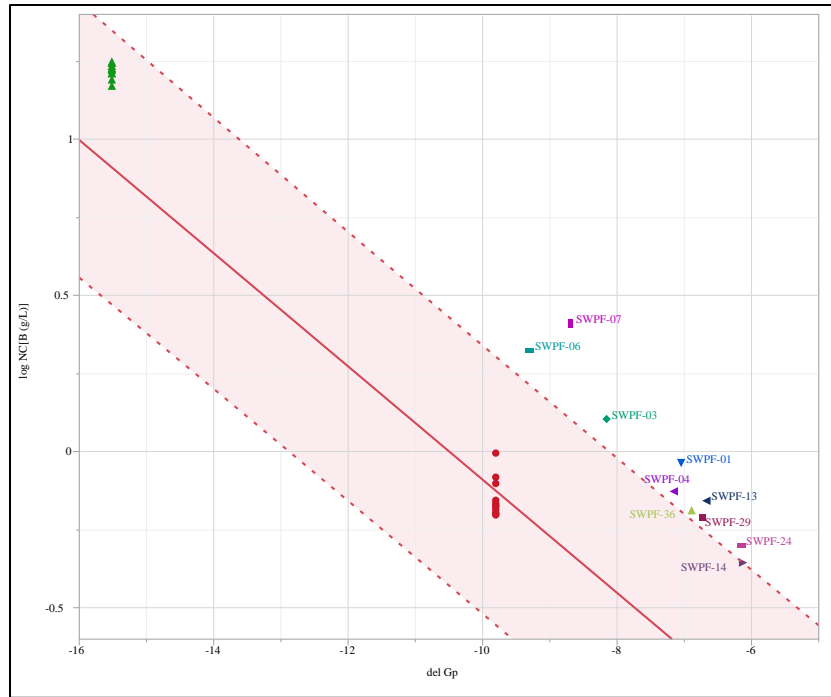


Figure 7-2. Bivariate Fit of $\log_{10}[\text{NC}_\text{B}]$ (g/L) By ΔG_p Display=quenched/measured bc results. The green triangles are the EA glass standard responses and the red circles are the ARM-1 glass standard responses for the 13 SWPF oven runs used to test the remaining SWPF glasses. Only the under predictable SWPF glasses are shown.

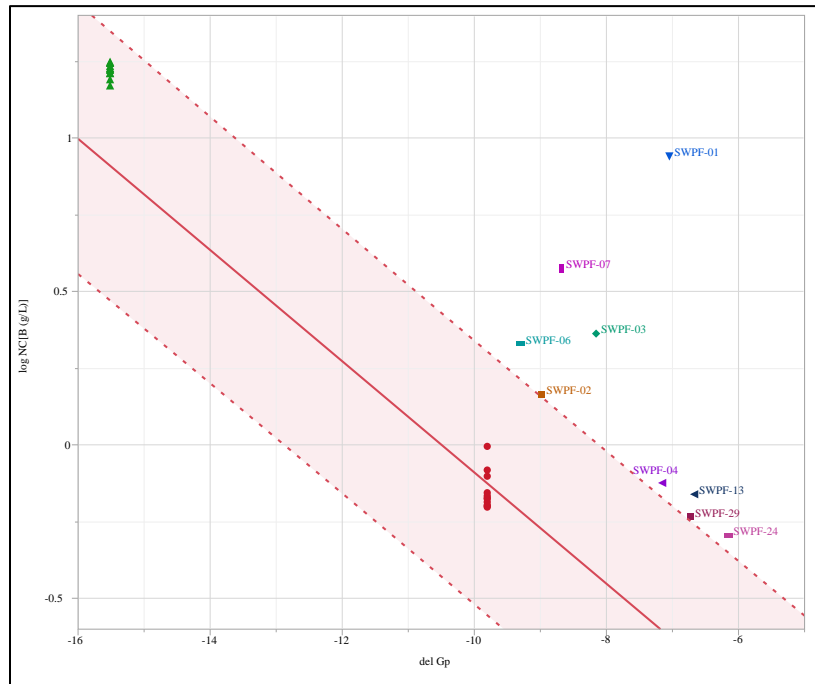


Figure 7-3. Bivariate Fit of $\log_{10}[\text{NC}_\text{B}]$ (g/L) By ΔG_p Display=ccc/measured bc results. The green triangles are the EA glass standard responses and the red circles are the ARM-1 glass standard responses for the 13 SWPF oven runs used to test the remaining SWPF glasses. Only the under predictable SWPF glasses are shown.

7.3 Reduction of Constraints (ROC) Criteria: Competition Between Al₂O₃ and TiO₂ for Alkali

A closer look at the compositions of the under predictable glasses in Figure 7-2 and Figure 7-3, i.e. SWPF-01, -03, -06, and 07, in the alkali-alumina compositional space of interest to the ROC (see Section 2.3) is provided in

Table 6. These glasses meet the ≥ 3.0 Al₂O₃ plus $\Sigma R_2 O$ constraint in Figure 2-1 but show anomalous leaching behavior.

Table 6. Reduction of Constraints (ROC) for SWPF High TiO₂ Glasses

| SRNL ID | Heat Treatment | Compositional View | Al ₂ O ₃ wt% | $\Sigma R_2 O$ wt% | [NC _B] (g/L) | [NC _{Li}] (g/L) | [NC _{Na}] (g/L) | [NC _{Si}] (g/L) |
|---------|----------------|--------------------|------------------------------------|--------------------|--------------------------|---------------------------|---------------------------|---------------------------|
| SWPF-01 | quenched | Measured | 3.670 | 16.485 | 0.917 | 0.953 | 0.802 | 0.663 |
| SWPF-03 | quenched | Measured | 3.623 | 15.461 | 1.269 | 1.215 | 1.126 | 0.848 |
| SWPF-06 | quenched | Measured | 3.625 | 16.905 | 2.100 | 2.005 | 1.446 | 1.039 |
| SWPF-07 | quenched | Measured | 3.626 | 15.407 | 2.570 | 2.269 | 1.805 | 1.042 |
| SWPF-01 | quenched | targeted | 3.500 | 16.200 | 0.924 | 0.947 | 0.814 | 0.665 |
| SWPF-03 | quenched | targeted | 3.500 | 15.300 | 1.282 | 1.193 | 1.145 | 0.850 |
| SWPF-06 | quenched | targeted | 3.500 | 17.100 | 2.105 | 1.956 | 1.431 | 1.033 |
| SWPF-07 | quenched | targeted | 3.500 | 15.500 | 2.572 | 2.219 | 1.780 | 1.042 |
| SWPF-01 | quenched | Measured bc | 3.903 | 16.152 | 0.917 | 0.953 | 0.836 | 0.661 |
| SWPF-03 | quenched | Measured bc | 3.853 | 15.127 | 1.269 | 1.215 | 1.174 | 0.845 |
| SWPF-06 | quenched | Measured bc | 3.854 | 16.507 | 2.100 | 2.005 | 1.508 | 1.035 |
| SWPF-07 | quenched | Measured bc | 3.856 | 15.084 | 2.570 | 2.269 | 1.882 | 1.038 |

The SWPF anomalous glass responses correlate with low targeted Al₂O₃ content in these glasses, i.e. the current PCCS constraint for Al₂O₃ is:

$$Al_2O_3 \text{ (wt\%)} \geq 3.0$$

before accounting for measurement uncertainty. The PCCS limit of ≥ 3.0 wt% Al₂O₃ was developed by looking at sludge-only DWPF glasses and MCU/ARP coupled DWPF glasses [62,63,69,70] but it is well known that in the natural analog quaternary system Na₂O-Al₂O₃-Fe₂O₃-SiO₂ that a region of amorphous phase separation occurs in glasses with ≤ 4 wt% Al₂O₃.[64] In addition, glasses in the Na₂O-Al₂O₃-SiO₂ system are known to undergo amorphous phase separation when the glasses contain ≤ 3 wt% Al₂O₃.[65,66] A discussion of the exact Al₂O₃ limit to avoid amorphous phase separation, lying somewhere between 3-4 wt% Al₂O₃, can be found in Reference 51.

The measured Al₂O₃ content of the SWPF glasses (Appendix A) is ~4.0 wt% Al₂O₃. This indicates that there is a need for an adjustment to the Al₂O₃ constraint in PCCS based on the following rationale:

- Determination of the homogeneity of these SWPF glasses was not an objective of the SWPF task plan and hence no data were available regarding the glass homogeneity.
- The measured Al₂O₃ content of the anomalous SWPF glasses (in weight percent) are ~4.0 wt%.
- Knowledge from natural analog systems that the exact Al₂O₃ limit to avoid amorphous phase separation is somewhere between 3-4 wt% Al₂O₃ depending on glass composition.
- Knowledge that a competition exists between Al and Ti in glasses when medium range order (MRO) alkali aluminate and alkali titanyl complexes like LiAlO₂ and LiTiO₂ form.[88,89]
- The coordination of Ti decreases from 5-fold in glass, to 4-fold, with the addition of Al₂O₃ as tetrahedral (4-fold) alkali groups such as NaAlO₂, NaTiO₂ and their Li or K analog form.[89]

- The impact of the TiO_2 on glass-in-glass phase separation could come from the competition between the Al and Ti in $(\text{Na},\text{Li})\text{AlO}_2$ and $(\text{Na},\text{Li})\text{TiO}_2$ MRO groups or from the fact that Al and Ti compete for these alkali since the alkali and alumina terms are linked in the ROC.

Therefore it is recommended that for glasses with $\text{TiO}_2 \geq 2.0$ wt% that the ROC be changed from ≥ 3.0 wt% Al_2O_3 with an alkali constraint to ≥ 4.0 wt% Al_2O_3 with no restriction on the alkali content (see Figure 7-4). This would change Figure 2-1 to Figure 7-5 for all DWPF P/P models.

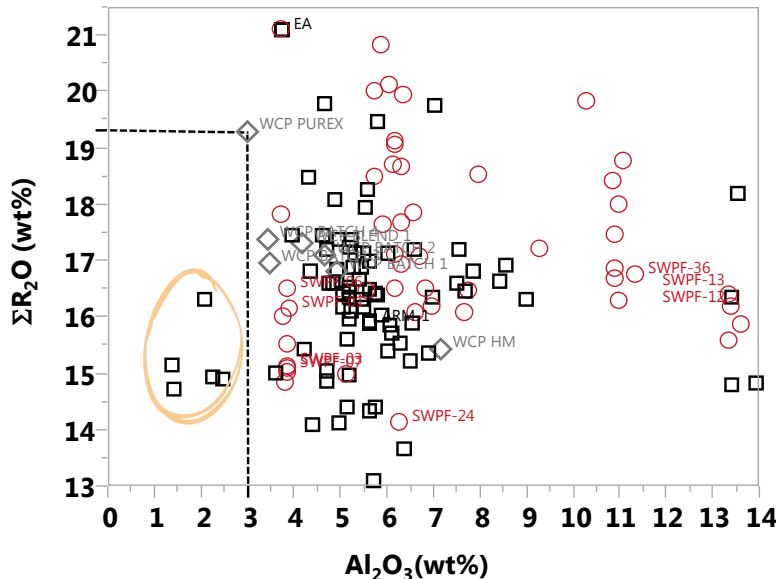


Figure 7-4. Glasses in THERMO™ Model that Violate the original ROC are Indicated in the Circled Region.

SWPF glasses are indicated by small red circles and the THERMO™ model glasses are indicated by all the remaining black symbols.

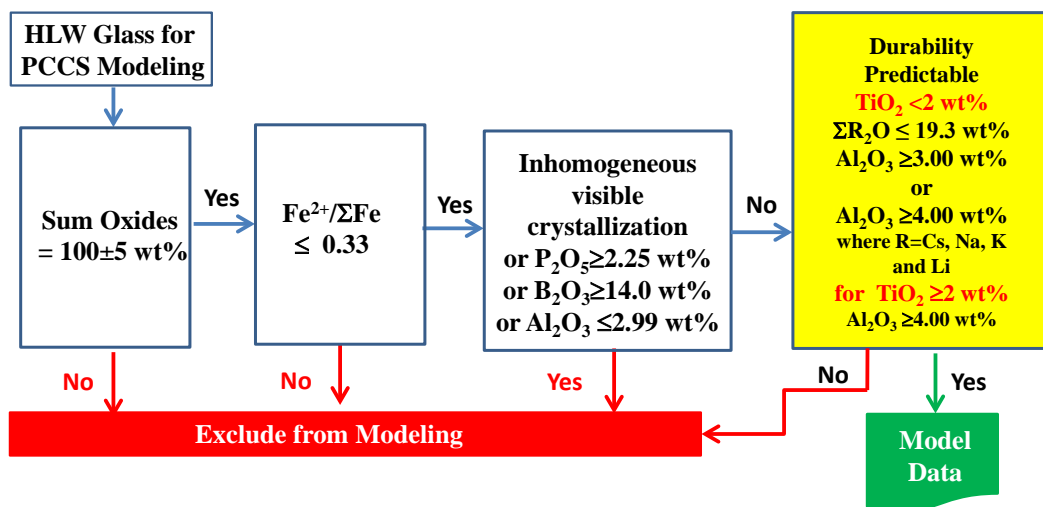


Figure 7-5. Revised Modeling Criteria and ROC for High Versus Low TiO_2 Containing Glasses.

7.4 Exclusion of some SWPF glasses

Applying the new ROC criteria given in Figure 7-5 to the SWPF glasses eliminates glasses SWPF-01 through SWPF-09 as having anomalous durability responses as a consequence of potential amorphous phase separation. Glass SWPF-08 and glass SWPF-12 were found to contain unreacted Fe₂O₃ during XRD of as quenched glasses for the liquidus study.[90] Therefore, SWPF-01 through SWPF-09 and SWPF-12 were not used in SWPF modeling for viscosity [91] and are not used in this study. These glass data are shaded out in Appendix A, an indication that they are not being used in modeling.

7.5 Exclusion of some THERMO™ glasses

As discussed above, the historic ROC was developed [62,63,69,70] after the THERMO™ model was developed and implemented in PCCS. Therefore, several glasses in THERMO™ fail the ROC shown in Figure 2-1 and circled in Figure 7-4. Several glasses in THERMO™ also do not adhere to the REDOX guidelines [59-61] set up after the THERMO™ model was developed. Removing the glasses circled in Figure 7-4 from THERMO™ makes all the PCCS models (durability, viscosity, and liquidus) consistent regarding the modeling criteria given in Figure 2-1.

The glasses that violate the original ROC that were eliminated from the THERMO™ model are 131Fe, 165Fe, 168Fe, 200Fe, and 202Fe, where the numbers indicate the frit used with high Fe containing wastes. These same five glasses also fail the REDOX criteria. An additional four data points (SHUM-8, SHUM-9, SHUM-13, and SHUM-14) also violate the REDOX criteria. A total of nine data points were removed from the THERMO™ model dataset before a comparison of the modified THERMO™ model could be made against the SWPF dataset in Section 7.7. Assessments of density (Sections 7.6) also use the modified THERMO™ database.

7.6 Assessment of Glass Density Effects

The THERMO™ models report the PCT leachate concentrations in units of NC_i as defined by Equation 7. These units of g_{waste form}/L_{leachant} assume a near constant density for the waste glasses tested since density is not part of the calculation of NC_i from leachate concentration and glass composition. The ASTM C1285 (PCT) procedure allows for calculation of NC_i PCT leachate concentrations. The NL_i takes into account the density of the glass as shown in Equation 9.

Equation 9

$$NL_i = \frac{NC_i}{SA/V}$$

Where SA/V is the surface area of the glass particles exposed to the leachate divided by the leachate volume. The SA/V is expressed in units of m²/L and the NL_i in g_{waste form}/m² which is grams of waste form dissolved per meter square of exposed glass surface area (SA). The SA is dependent on the mass of glass used in the test, the particle diameter, and the density of the glass as shown in Equation 10.

Equation 10

$$SA = \frac{6 \text{ mass}}{\rho d}$$

where

| | | |
|--------|---|----------------------------------|
| ρ | = | density in g/m ³ |
| d | = | particle size diameter in m |
| mass | = | mass in g |
| SA | = | surface area in m ² . |

The impact of the glass density is mathematically accounted for in the NL_i parameter, but not in the NC_i parameter.

Many, but not all, densities were measured for those glasses included in the THERMO™ model in 1995. Those that were experimentally determined are given in Appendix C. The densities for the SWPF glasses are given in Reference 83. The Schumacher density model used during SB1 [92] is being modified for radioactive glasses [93] so that the densities of the missing THERMO™ model glasses can eventually be filled in.

In general, the THERMO™ glass densities cover the region from 2.52-2.75 g/cc with the ARM-1 glass being 2.75 g/cc as shown in Figure 7-6. The SWPF data cover a range from 2.57-2.88 g/cc (SWPF-14 and SWPF-10) as shown in Figure 7-6, i.e. there are only a few SWPF glasses in the 2.75-2.88 density range. The SWPF glasses are denser glasses since TiO_2 is a heavy oxide, but in general the density ranges of the THERMO™ model data and the SWPF data overlap, and the full interval of values, which covers 2.52 to 2.88 g/cc, is only 6.7% above and below the midpoint of this interval (i.e. 2.70 g/cc). Thus, for a glass with a density of 2.70 g/cc, its NL_i value for an element of interest would change by $\pm 6.7\%$ (or in common logarithms of the NL_i value by only ± 0.03) if the density was instead at one of the endpoints of this interval. It should be noted, for example, that the RMSE for the modified THERMO™ model for boron (see the next section) has a value of 0.1953 as a common logarithm of the NC_i value. Thus, the impact of density is small when compared to the uncertainty of the durability-composition models for all the elements of interest.

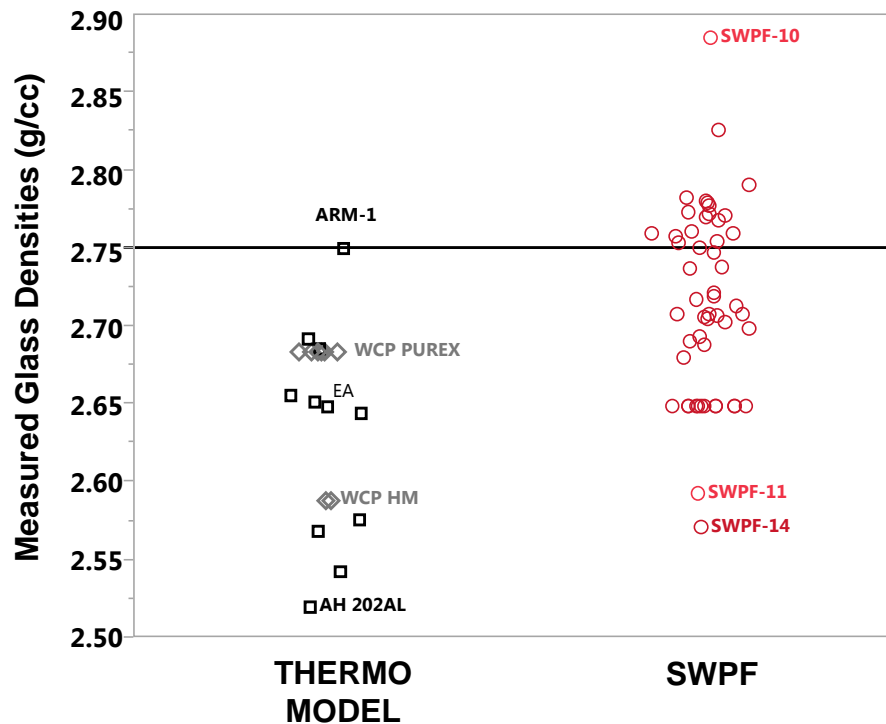


Figure 7-6. The Range of Glass Densities for THERMO™ Versus SWPF Glasses.

7.7 Applicability of Modified PCCS THERMO™ Durability Models

The PCCS THERMO™ model from 1995 has 131 data points. By removing the nine data points that violate the constraints shown in Figure 2-1, a modeling pool of 122 glasses remain. Removing these nine points makes all of the PCCS models consistent, since they all follow the constraints in Figure 2-1. The regressions from the 122 data point modified THERMO™ models, when refitted to the original ΔG_i values, give the following ordinary least squares (OLS) equations:

$$\begin{aligned}\log_{10}[\text{NC}_B] \text{ (g/L)} &= -1.901602 - 0.180215 \Delta G_p & R^2 &= 0.80 & \text{RMSE} &= 0.195316 \\ \log_{10}[\text{NC}_{\text{Li}}] \text{ (g/L)} &= -1.541811 - 0.1453413 \Delta G_p & R^2 &= 0.80 & \text{RMSE} &= 0.161483 \\ \log_{10}[\text{NC}_{\text{Na}}] \text{ (g/L)} &= -1.803846 - 0.1704731 \Delta G_p & R^2 &= 0.83 & \text{RMSE} &= 0.168133\end{aligned}$$

which gives an almost imperceptible change in the slopes and intercepts from the original 1995 OLS of

$$\begin{aligned}\log_{10}[\text{NC}_B] \text{ (g/L)} &= -1.901447 - 0.1812039 \Delta G_p & R^2 &= 0.77 & \text{RMSE} &= 0.216264 \\ \log_{10}[\text{NC}_{\text{Li}}] \text{ (g/L)} &= -1.545942 - 0.1468048 \Delta G_p & R^2 &= 0.75 & \text{RMSE} &= 0.182722 \\ \log_{10}[\text{NC}_{\text{Na}}] \text{ (g/L)} &= -1.801158 - 0.1710066 \Delta G_p & R^2 &= 0.80 & \text{RMSE} &= 0.187881\end{aligned}$$

The newly generated regressions do have better R^2 values than the original THERMO™ OLS and smaller RMSE's which translate to less model error and a slightly larger DWPF PCCS durability operating window.

The refit THERMO™ OLS models, designated as the modified THERMO™ models, are shown in Figure 7-7a-d including one for silicon release since this was also shown in Reference 20. The impact of this refit on the PCCS durability operating window is discussed in Section 7.8.

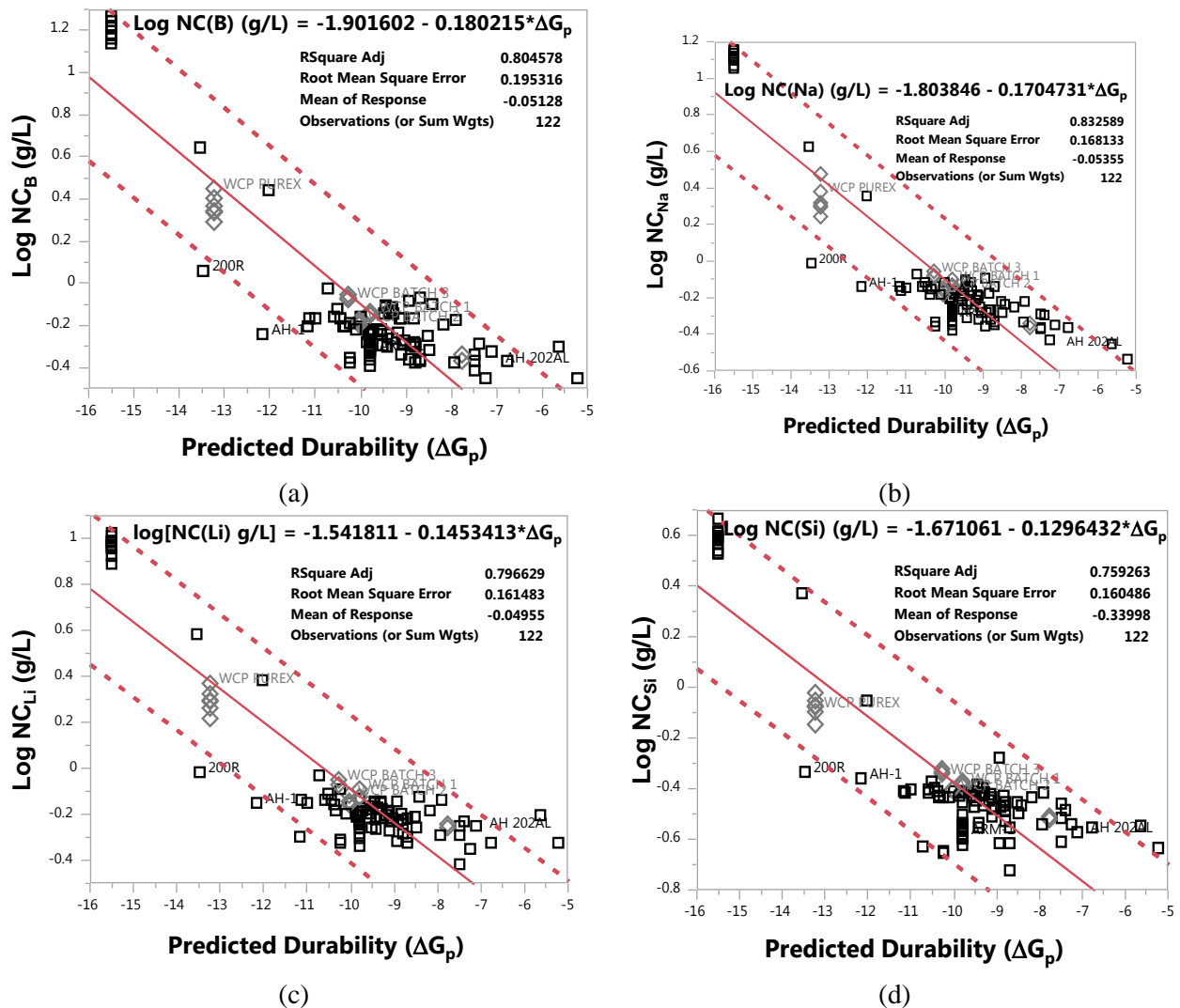


Figure 7-7. Modified THERMO™ Models.

Once the modified THERMO™ models had been defined above, the SWPF durability data as described in Section 7.4 for homogeneous glasses that adhere to the constraints in Figure 7-5 was overlaid on the modified models as shown in Figure 7-8a-d. The THERMO™ model is indicated by the OLS fit (solid lower lines in each figure), and the 95% upper and lower confidence bands (dashed lines in each figure). When modeled against the same ΔG_p on the x-axis, the SWPF data fell along an OLS fit (upper solid line in each figure) that is slightly biased above the THERMO™ OLS, but within the upper 95% confidence bands. This type of bias is within the precision and bias reported for the PCT procedure which was determined by numerous inter-laboratory and intra-laboratory round robins, i.e. the standard deviation divided by the consensus mean and multiplied by 100 is in the range of 7.5-9.5%. [31]

In Figure 7-8a-d most of the THERMO™ data points have been hidden and only the EA glass, ARM-1 glass and some WCP glass data points are shown for the modified THERMO™ models. Comparison between the SWPF EA and ARM-1 standard glass data to the THERMO™ EA and ARM-1 glass data demonstrates that for the ARM-1 standard glass the SWPF leachate concentration data are biased high compared to the THERMO™ data. The THERMO™ data for the ARM-1 glass data are shown by the black boxes and the SWPF ARM-1 glass data are shown by the orange solid triangles. Bias during PCT

analyses can occur due to differences in the amount of sieving or the amount of sample washing between laboratories.[31,94]

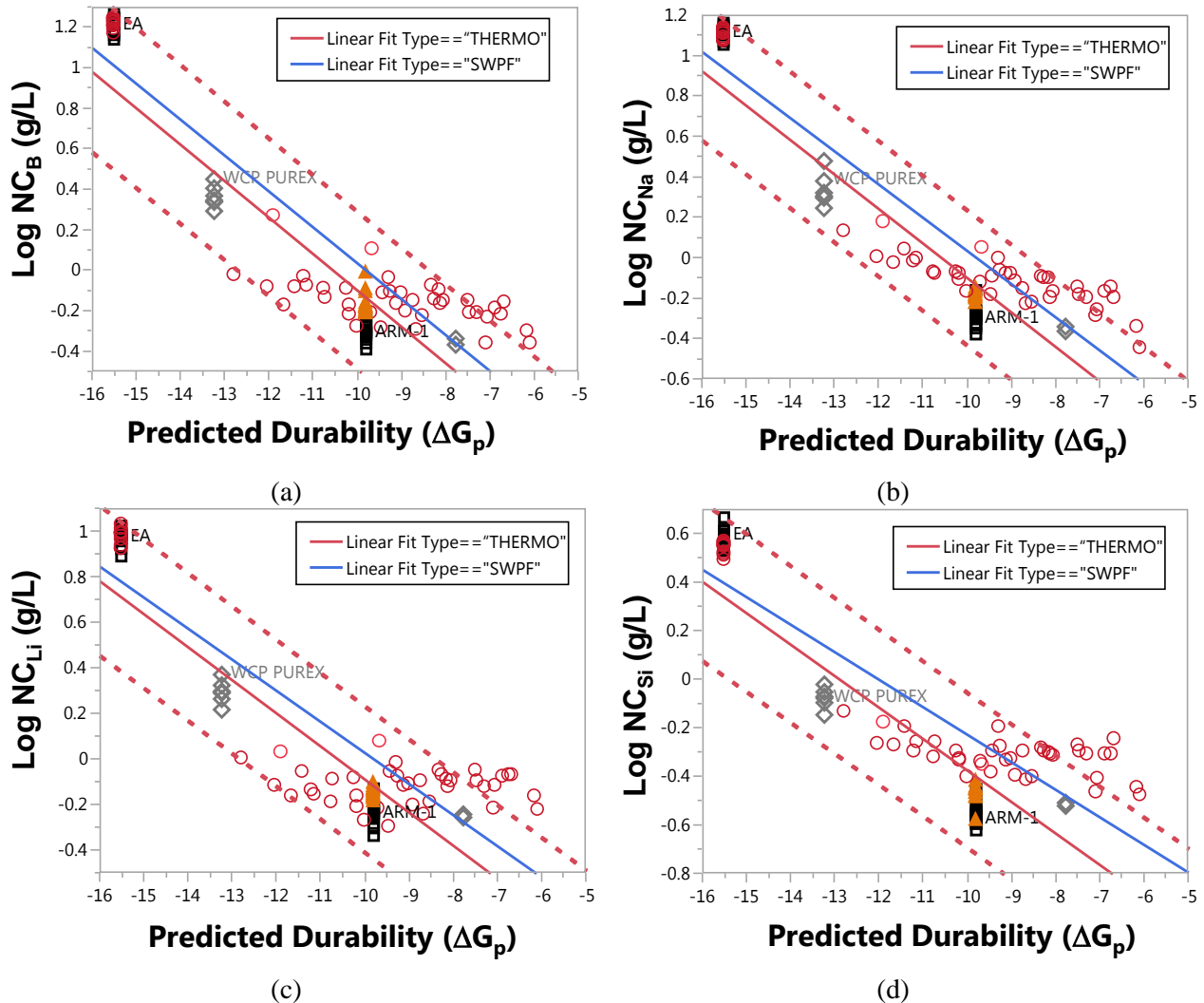


Figure 7-8. Comparison of the Modified THERMO™ Models and the SWPF Data.

The SWPF ARM-1 glass data are shown by the orange solid triangles. The SWPF TiO₂ glasses and EA glass are shown by the open circles. Most THERMO™ data points are hidden except the black boxes indicating the THERMO™ ARM-1 and EA glasses and the open diamonds indicating the THERMO™ WCP glass data.

Moreover, the RMSE of the SWPF data is larger than the RMSE of the THERMO™ model for all elements (Table 7). For some elements the R² of the SWPF data fits are slightly better than the modified THERMO™ model but this does not hold true for all elements. Due to the high leachate bias of the SWPF standard glasses, which would alter the slope and intercept of any model fit to this data significantly (Table 7) and to the large RMSE of the SWPF dataset, the SWPF data are overlaid onto the modified THERMO™ models but the models were not refit with the combined SWPF and THERMO™ datasets.

The adequacy of the ΔG_i terms in the THERMO™ model was examined based on new leachate speciation calculated from Geochemists Workbench (GWB) to see if improvements could be made in the THERMO™ models, i.e., alternate ΔG_i terms were calculated for all the alkalis, Al₂O₃, B₂O₃, SiO₂ and

TiO_2 . None of the revised ΔG_i terms, alone or together, improved the THERMO™ model or the SWPF data fits, indicating that the 1995 THERMO™ model and ΔG_i terms are adequate and do not need to be changed for the modified THERMO™ model or for the SWPF data. All of the original THERMO™ ΔG_i terms appear adequate for SWPF glasses over the compositional ranges studied, i.e. TiO_2 concentrations of 5.85 wt%, Cs_2O values of 1.62 wt%, and Na_2O values of 18.14 wt% (Appendix A).

Table 7. Model Slopes, Intercepts and Statistical Fitting Information

| Log NC _i | Dataset | OLS Intercept/Slope | Adj. R ² | RMSE | # Data Points |
|----------------------|---------|---------------------|---------------------|--------|---------------|
| Log NC _B | THERMO™ | -1.9016/-0.1802 | 0.80 | 0.1953 | 122 |
| | SWPF | -1.7455/-0.1777 | 0.82 | 0.2352 | 66 |
| Log NC _{Li} | THERMO™ | -1.5418/-0.1453 | 0.80 | 0.1615 | 122 |
| | SWPF | -1.3412/-0.1367 | 0.76 | 0.2195 | 66 |
| Log NC _{Na} | THERMO™ | -1.8038/-0.1705 | 0.83 | 0.1681 | 122 |
| | SWPF | -1.6115/-0.1643 | 0.86 | 0.1922 | 66 |
| Log NC _{Si} | THERMO™ | -1.6711/-0.1296 | 0.76 | 0.1605 | 122 |
| | SWPF | -1.3659/-0.1136 | 0.77 | 0.1760 | 66 |

7.8 Uncertainties for the Modified THERMO™ Models Relative to those for the THERMO™ Models

Exhibit D1 in Appendix D provides a graphical representation of and summary information for the fitted lines for the THERMO™ and modified THERMO™ models for each of the elements of interest. For each element, the metrics from the fit for the modified THERMO™ model are better (i.e., the R^2 value is higher and the RMSE is smaller) than the corresponding metrics from the fit for the THERMO™ model. This outcome leads to less model error for the modified THERMO™ models relative to the THERMO™ models. This is demonstrated in the graphic of Exhibit D1 by the 95% confidence limits for an individual prediction (i.e., the dashed lines) in each of the plots. The dashed lines for the modified THERMO™ models fall within those of the THERMO™ models. A closer look at how these uncertainties impact PCCS is provided in the next section.

7.9 Property Acceptance Region (PAR) Assessments for the Modified THERMO™ Models

This section provides a closer look at how the durability-composition models are integrated into DWPF's PCCS [95] and the information that is necessary to complete that process for the modified THERMO™ durability models. The current PAR limits employed in PCCS [95] were determined as a limit on ΔG_p [96] for each of the THERMO™ durability models based upon PCT measurements of the EA standard glass [29,30]. The durability of the EA is the accepted durability standard for HLW glass. The PAR is that portion of the glass composition region that satisfies the property constraint after model uncertainties have been addressed.

The development of the PAR limits for the THERMO™ models [96] is illustrated in Exhibit D2 in Appendix D for boron. This exhibit is a repeat of Figure 2 from Reference [96], and shows ΔG_p on the x-axis and $\log_{10}[\text{NC}_B(\text{g/L})]$ on the y-axis. The green line is the prediction line for the THERMO™ model for boron. The red **x**'s on the plot indicate the PCT boron data used for fitting the THERMO™ model. Note the vertical cluster of **x** symbols in the top left portion of the plot. These plotted EA points provided the "basis" for durability comparisons for boron. A 95%/95% upper tolerance bound (the blue line) shown in the exhibit provides the upper limit for 95% of the boron PCT responses anticipated for any given ΔG_p value with a 95% confidence. A horizontal line is shown in the exhibit (i.e., the "Critical Limit for $\log_{10}[\text{NC}_B]$ "), and it corresponds to the "2 sigma" limit for NC_B provided in the last line of Table 8 (i.e., $\text{NC}_B = 14.251 \text{ g/L}$ or $\log_{10}[\text{NC}_B] = 1.153845 \text{ g/L}$).

Table 8. PCT Measurements Generated for the EA Standard Glass

| Descriptor | B (g/L) | Li (g/L) | Na (g/L) |
|-------------------------------|----------|----------|----------|
| Mean | 16.695 | 9.565 | 13.346 |
| Standard Deviation (s) | 1.222 | 0.735 | 0.902 |
| “2 sigma” limit = Mean - 2 s | 14.251 | 8.095 | 11.542 |
| \log_{10} (“2 sigma” limit) | 1.153845 | 0.908217 | 1.062281 |

The information in Table 8 was determined based upon the results from a series of PCTs (42 replicate durability assessments) that were conducted on the EA glass and reported by Jantzen et al.[29,30]. Table 8 provides the averages of the EA normalized PCT responses as well as the standard deviations of these responses. For reference, the mean minus 2 times the standard deviation is provided for each of the three elements.

The vertical line at the intersection of this horizontal line with the 95%/95% upper tolerance bound provides a lower limit (-14.1058 kcal/mol) for the values of ΔG_p . One can say that 95% of the PCT boron releases as normalized concentrations will fall below the 14.251 g/L value with 95% confidence for glass compositions whose values for ΔG_p are larger than -14.1058 kcal/mol. The value of -14.1058, is the PAR value in PCCS for the THERMO™ boron durability-composition model [95]. A similar approach was utilized to develop corresponding PAR values for the THERMO™ models for lithium and sodium [96]. These values, which are shown in Table 9, serve to define the PAR limits for the durability constraints currently implemented by PCCS [95].

Table 9. PAR Values for the THERMO™ Models Currently Utilized by PCCS

| Durability Model | B (g/L) | Li (g/L) | Na (g/L) |
|---------------------------------|----------|----------|----------|
| PCCS PAR Value for ΔG_p | -14.1058 | -13.8695 | -14.1991 |

Exhibit D3 in Appendix D repeats the graphical depiction of the development of each of the PAR values of Table 9 but the plot for each element also provides the depiction of the development of the PAR value for the modified THERMO™ model for that element. The resulting PAR values for the modified models are provided in Table 10. Note that for each element the PAR value for the modified THERMO™ model is more negative than the corresponding value for the historic model. Thus, the modified THERMO™ models expand the DWPF operating window relative to the durability constraints, and all previous SME batches processed at the DWPF which satisfied the PAR constraints for the historic models for durability (i.e., had ΔG_p values that were more positive than the values of Table 9) would also satisfy the PAR constraints for the modified THERMO™ models.

Table 10. PAR Values for the Modified THERMO™ Models

| Modified THERMO™ Durability Model | B (g/L) | Li (g/L) | Na (g/L) |
|-----------------------------------|----------|----------|----------|
| PCCS PAR Value for ΔG_p | -14.3952 | -14.2481 | -14.4765 |

PCCS also integrates the effect of measurement uncertainty into the SME acceptability decision [95]. A measured SME composition that is within the MAR for each of the applicable constraints is said to be within the acceptable operating window of the DWPF (the result is a transfer of the SME batch to the Melter Feed Tank (MFT) and ultimately to the melter). The MAR limits are to be computed in the same manner as currently implemented in PCCS [95].

It recommended that the modified THERMO™ models and these proposed PAR limits for the durability constraints be incorporated in the next revision of the technical bases for PCCS (i.e., into the SME acceptability report of Brown, Postles, and Edwards [95]) and then implemented into PCCS.

7.10 Validation of THERMO™ Using Additional High TiO₂ Containing Glasses

References 97 and 98, two studies which maximized waste loadings in defense waste glasses were used to validate the SWPF TiO₂-only viscosity model [91] and these two databases will also be used as additional validation for the modified THERMO™ models over higher TiO₂ composition ranges. The acceptable glasses from these studies span TiO₂ compositions from 1.25 to 6.76 wt% TiO₂. The acceptable SWPF TiO₂ data (minus the revised ROC excluded glasses) spanned 1.90 to 5.85 wt% TiO₂ (Appendix A) and the THERMO™ database (minus the ROC and REDOX excluded glasses) spanned 0-1.78 wt% TiO₂ (Appendix C). Since the SWPF database was overlain on the modified THERMO™ models, the validated ranges of TiO₂ covered in the modified THERMO™ models are 0-5.85 wt%.

Two high waste loaded glass databases were used for additional validation of the modified THERMO™ models. These two databases span TiO₂ values of 1.25-6.13 wt% in the absence of Nb₂O₅ and minimal ZrO₂, i.e., 0.01-0.86 wt% ZrO₂ (Appendix E). The high waste loaded glasses in References 97 and 98 are, therefore, used in this study as a second validation of the TiO₂ ΔG_i term in the modified THERMO™ models. The high TiO₂ glass validation database is given in Appendix E. Glasses that were omitted from the high TiO₂ validation data included the following:

- HLW-01 through HLW-06 and FY09EM21-03 which were crystallized
- HLW-15, HLW-18, FY09EM21-05, FY09EM21-08, FY09EM21-11, FY09EM21-14 and FY09EM21-15 which contained >2.00 wt% TiO₂ and Al₂O₃<4.00 wt%
- FY09EM21-14 which also had over 14 wt% B₂O₃

Using the two high waste loaded glass databases for additional durability validation entails looking at the consistency of the leachate data for the Reference 97 and 98 studies. While Reference study 97 was not performed to RW-0333P standards, Reference study 98 is RW-0333P compliant. However, both studies had inconsistent leachate responses as shown by the circled data in Figure 7-9. There were eleven inconsistent leachate responses in the two high TiO₂ databases (Appendix E) and these data were not used and are shaded in Appendix E. Another fourteen glasses had been reported to be crystallized, failed the high TiO₂ ROC, and/or had B₂O₃ concentrations >14.0 wt% (see bulleted list above), and the data from these glasses were not used. This left a validation dataset of 16 glasses, out of the 41 glasses in the two studies. Glasses that were included in the additional high TiO₂ validation are given in Table 11. The fit of these sixteen glasses to the modified THERMO™ models is shown in Figure 7-10. The 16 additional high TiO₂ data from Reference 97 and 98 studies fit the modified THERMO™ models well (Figure 7-10a-d). This additional SRNL dataset validates the modified THERMO™ model from 1.25-6.13 wt% TiO₂.

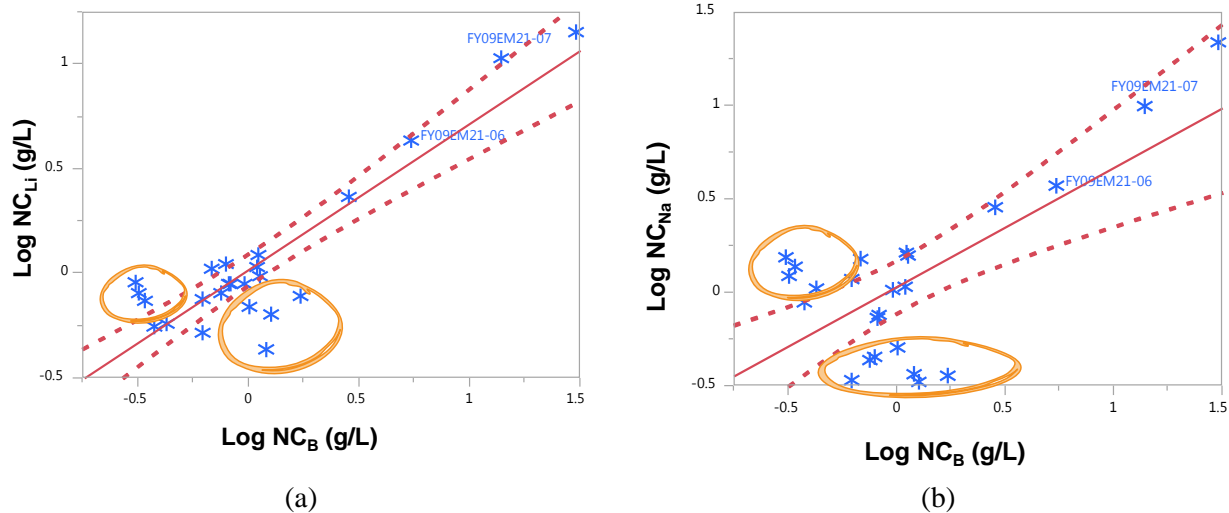


Figure 7-9. Internal Consistency of Additional TiO₂ Validation Data from References 97 and 98 where Figure a compares B and Li leach data and Figure b compares B and Na leach data.

Table 11. Additional High TiO₂ Validation Data

| High TiO ₂ Validation Data Sample Identifications |
|--|
| HWL-07 |
| HWL-11 |
| HWL-13 |
| HWL-14 |
| HWL-19 |
| HWL-21 |
| HWL-22 |
| FY09EM21-09 |
| FY09EM21-12 |
| FY09EM21-16 |
| FY09EM21-17 |
| FY09EM21-18 |
| FY09EM21-19 |
| FY09EM21-20 |
| FY09EM21-25 |
| FY09EM21-27 |
| TiO ₂ = 1.25-6.13 wt% |

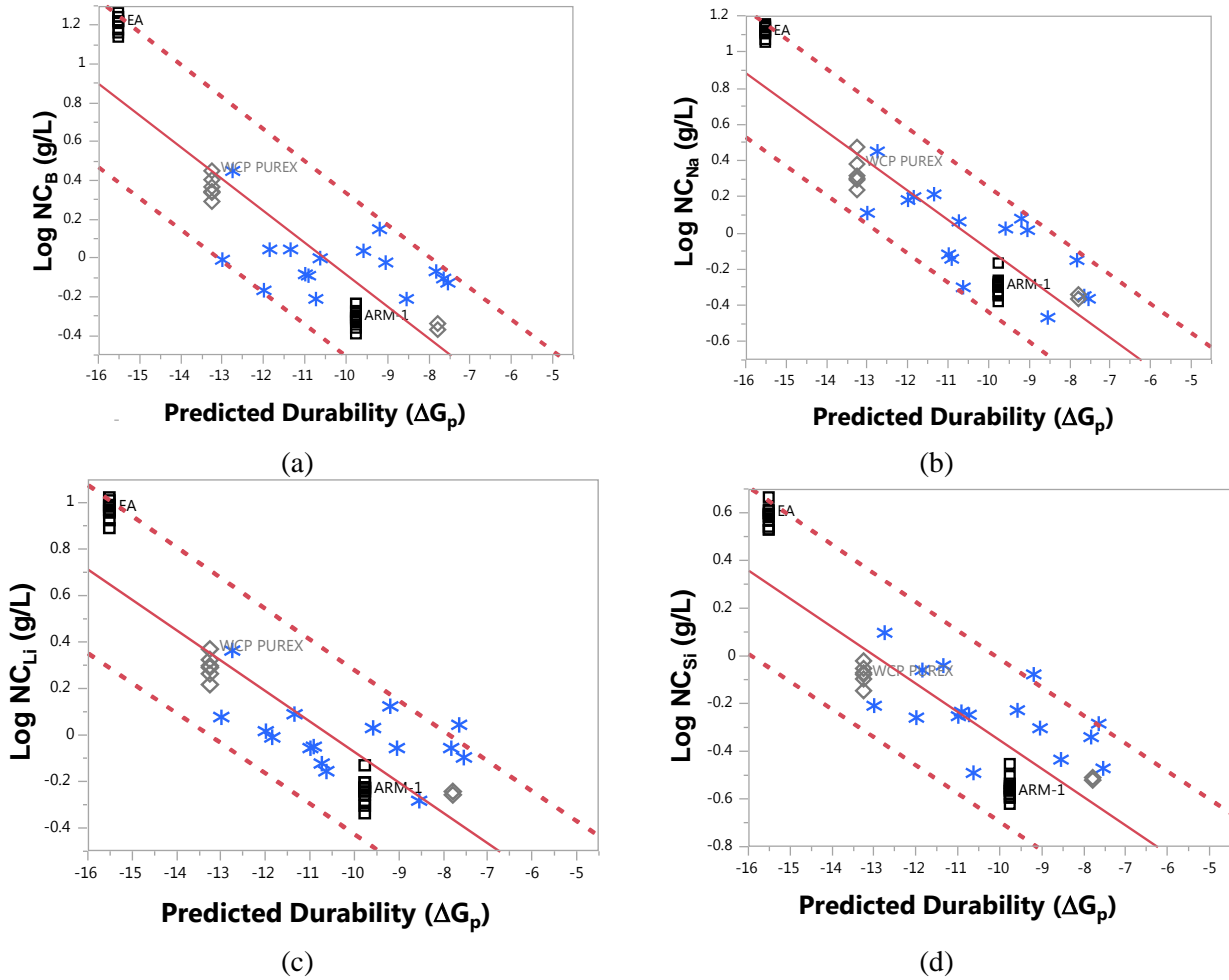


Figure 7-10. Additional Validation Data for the Modified THERMO™ Model.

8.0 Modification of the Durability-Composition Models for CST Flowsheet

8.1 Evaluation of a ΔG_i for Nb₂O₅ With the Modified THERMO™ Models

The SRNL CST durability data from References 99, 100, 101, 102, and 103 were used to validate which of the two Nb₂O₅ ΔG_i terms developed in 2010 [27] fit the high Nb₂O₅ data the best. In addition, this CST data provided additional validation of the THERMO™ model for the ΔG_{TiO_2} and ΔG_{ZrO_2} terms (all species found in Crystalline SilicoTitanate). Many of the CST glasses from References 99-103 failed the ROC limits for glasses with ≤ 2.00 wt% TiO₂ and Al₂O₃<3.00 wt%, and many more failed the higher ROC limits for glasses with >2.00 wt% TiO₂ and Al₂O₃<4.00 wt% defined in this study. This left a four glass population from these CST studies which is insufficient to validate a $\Delta G_{Nb_2O_5}$ term.

An additional dataset of 116 glasses was available in References 104, 105, 106, and 107 for validation of the $\Delta G_{Nb_2O_5}$ term. The KT studies in References 104-107 were designed to maximize the amount of TiO₂ in a glass if the DWPF vitrified combinations of CST and MST. The combined glasses from References

99-107 that fit the ROC criteria and are not crystallized are listed in Table 12 and Appendix F and span TiO₂ compositions from 0.00 to 6.62 wt% TiO₂.

For validating the Nb₂O₅ ΔG_i, studies KT-01 through KT-03 were not used as their compositions were outside the range of any glasses that might be processed in the DWPF in the future. This left a validation dataset of 58 KT study glasses and 4 CST study glasses to validate the Nb₂O₅ ΔG_i term. The CST THERMO™ validation spans TiO₂ = 0.00–6.62 wt%, Nb₂O₅ concentrations of 0-2.30 wt% and ZrO₂ concentrations of 0-2.90 wt% and 8.64-15.43 wt% Na₂O.

Table 12. CST Validation Data

| CST Validation Data Sample Identifications | |
|--|---------|
| CST 15 | KT06-18 |
| CST 20 | KT07-01 |
| CST 26 | KT07-02 |
| CST 32 | KT07-03 |
| KT04-01 | KT07-04 |
| KT04-02 | KT07-05 |
| KT04-03 | KT07-06 |
| KT04-04 | KT07-07 |
| KT04-05 | KT07-08 |
| KT04-06 | KT07-09 |
| KT04-07 | KT07-10 |
| KT04-08 | KT08-01 |
| KT04-09 | KT08-02 |
| KT04-10 | KT08-03 |
| KT06-01 | KT08-04 |
| KT06-02 | KT08-05 |
| KT06-03 | KT08-06 |
| KT06-04 | KT08-07 |
| KT06-05 | KT08-08 |
| KT06-06 | KT08-09 |
| KT06-07 | KT08-10 |
| KT06-08 | KT10-01 |
| KT06-09 | KT10-02 |
| KT06-10 | KT10-03 |
| KT06-11 | KT10-04 |
| KT06-12 | KT10-05 |
| KT06-13 | KT10-06 |
| KT06-14 | KT10-07 |
| KT06-15 | KT10-08 |
| KT06-16 | KT10-09 |
| KT06-17 | KT10-10 |
| TiO ₂ = 0.00-6.62 wt% | |

8.2 Development of ΔG_i for Nb₂O₅

Reference 27 describes the derivation of the ΔG_i for Nb₂O₅. During the derivation it was assumed that Nb is +5 in the glass and that +5 is also the most stable oxidation state of Nb in natural waters. The +5

aqueous species used in Reference 27 was $\text{Nb}(\text{OH})_6^-$ instead of $\text{Nb}(\text{OH})_5^{(\text{aq})}$. The $\text{Nb}(\text{OH})_6^-$ was chosen as $\text{Nb}(\text{OH})_5^{(\text{aq})}$ can continue to hydrolyze to $\text{Nb}(\text{OH})_6^-$. Using $\text{Nb}(\text{OH})_6^-$ on the RHS of Equation 11 gives a ΔG_i term for Nb_2O_5 of +33.18 kcal/mole.

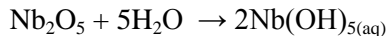
Equation 11



$$\begin{aligned}\Delta G_{(\text{products})} - \Delta G_{(\text{reactants})} &= (2*(-392.85)) - (-422.05 + 7*(-56.69)) = \\ -785.7 + 818.88 &= +\mathbf{33.18} \text{ kcal/mole}\end{aligned}$$

Using $\text{Nb}(\text{OH})_5^{(\text{aq})}$ on the RHS of Equation 12 gave a ΔG_i for Nb_2O_5 of +13.20 kcal/mole.

Equation 12



The overall dissolution of Nb_2O_5 to $\text{Nb}(\text{OH})_5^{(\text{aq})}$ at pH>7 can then be written as shown in Equation 12 and evaluated as

$$\begin{aligned}\Delta G_{(\text{products})} - \Delta G_{(\text{reactants})} &= (2*(-346.15)) - (-422.05 + 5*(-56.69)) = \\ -692.3 + 705.5 &= +\mathbf{13.20} \text{ kcal/mole}\end{aligned}$$

Using $\text{Nb}(\text{OH})_5^{(\text{aq})}$ on the RHS of Equation 12 gave a ΔG_i for Nb_2O_5 of +13.20 kcal/mole.

In 2010, PCT data from the available CST studies were inconclusive as to which ΔG_i gave a better fit to the durability data for these high Nb_2O_5 containing glasses due to the fact that many of the CST glasses violated the 3.0 wt% Al_2O_3 ROC for glasses with ≤ 2.0 wt% TiO_2 and many more were found to violate the 4.0 wt% Al_2O_3 ROC for glasses with > 2.0 wt% TiO_2 defined in this study. This left a smaller pool of CST validation data, but between late 2010 and 2011, the 116 KT glasses became available for additional validation of the high TiO_2 and Nb_2O_5 containing glasses. The pooled CST and KT validation glasses are given in Table 12 and were used to determine which of these ΔG_i data fit the THERMO™ models better.

8.3 Applicability of Durability Models with ΔG_p Modified to Include Nb_2O_5 Contribution

In a similar fashion to the manner in which the SWPF durability dataset and the high TiO_2 containing glass datasets were handled, the CST leachates were checked for the consistency of the B versus Li and Na responses compared to the consistency of the original THERMO™ leachate datasets. A slight bias to higher Li leachate values compared to B leachate values is found for all the datasets but especially for the CST glasses as shown in the circled region of Figure 8-1a. Likewise, there is a low Na leachate bias for these same CST glasses as shown in the circled region of Figure 8-1b.

Even with these leachate biases included in the validation dataset of sixty-two glasses, the data fit the modified THERMO™ models well using an Nb_2O_5 ΔG_i of +13.20 kcal/mole (see Figure 8-2a-d). When the alternate ΔG_i of +33.18 kcal/mole was used it also fit the modified THERMO™ models but the points were slightly skewed to more positive ΔG_p values. Discrimination between these two ΔG_i values is difficult because the concentrations of Nb_2O_5 on a molar basis, the basis used in the calculation of ΔG_p , are in the third decimal place and the Nb_2O_5 concentrations dominate the calculation of ΔG_p instead of the ΔG_i term. However, the Nb_2O_5 ΔG_i of +13.20 kcal/mole appears to fit the data better and is recommended for use in the modified THERMO™ models. No additional changes will be needed in PCCS other than the implementation of the Nb_2O_5 ΔG_i term. This additional dataset also validates the TiO_2 ΔG_i term up to 6.62 wt%.

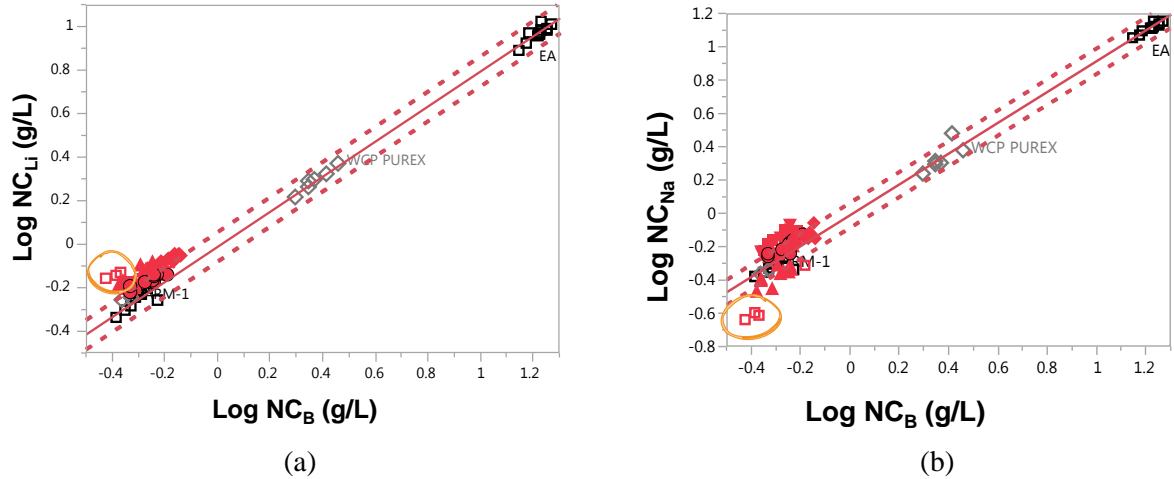


Figure 8-1. Internal Consistency of CST Validation Data from References 99-107. Open red squares are the CST data and the solid red symbols are the KT data.

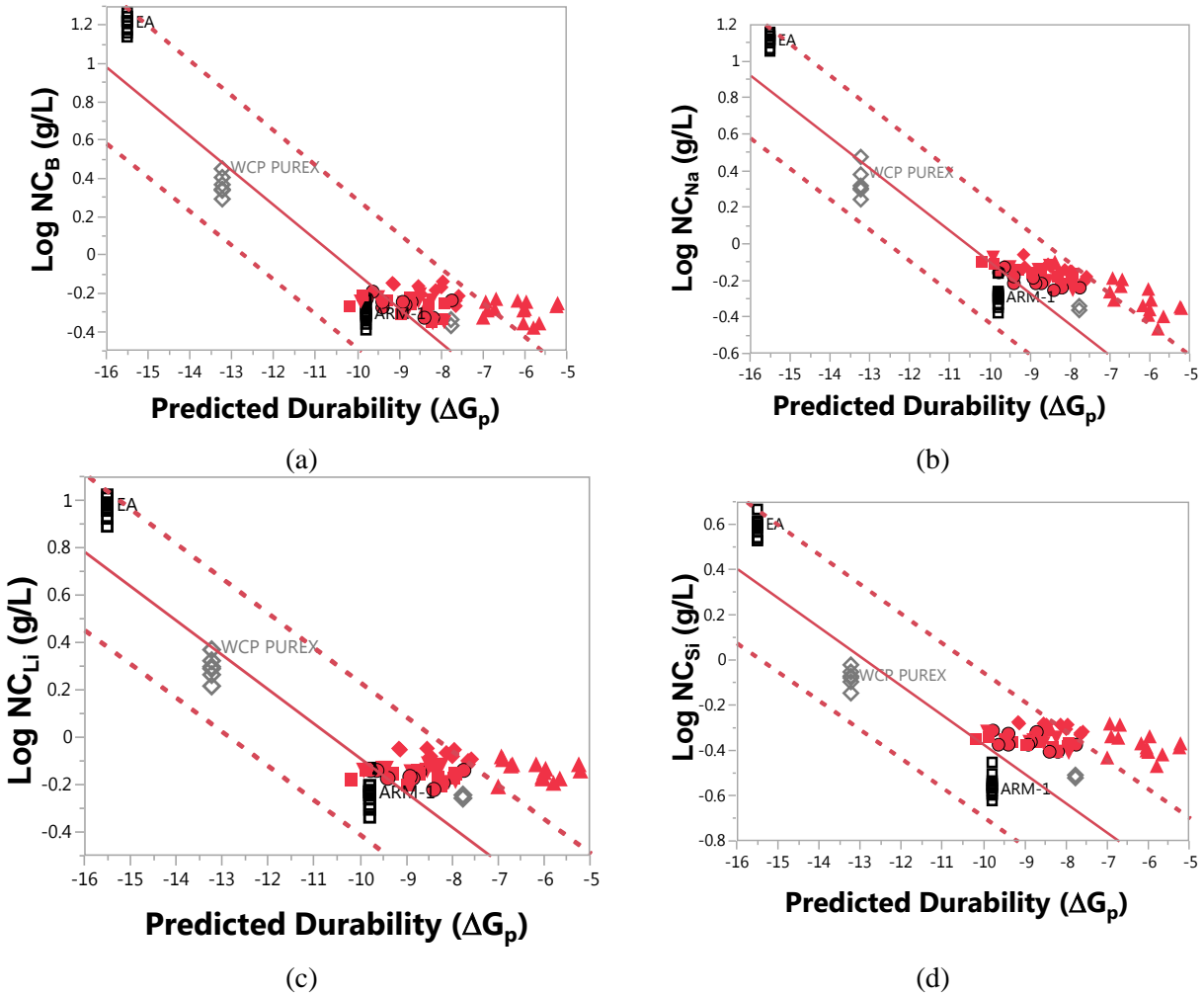


Figure 8-2. Validation Data for Using the Modified THERMO™ Models for CST Containing Glasses.

8.4 Changes needed in PCCS for Nb₂O₅ Contribution

The ΔG_i for Nb₂O₅ term is not being implemented currently as the DWPF is not processing CST. Since the CST contains Nb₂O₅ then Nb would then become an element in the glass that is reportable to the geologic repository if present at >0.5 wt% on an elemental basis. This would require a revision to the DWPF Waste Acceptance Product Specifications (WAPS).[28] In addition, there is no data to support the analytic measurement uncertainty needed to implement an Nb term in PCCS. Therefore, the ΔG_i for Nb₂O₅ is being provided for future use should the DWPF have to process CST. When CST processing becomes necessary, the other implementation requirements associated with a ΔG_i for Nb₂O₅ will be addressed. The use of the ΔG_i for Nb₂O₅ fits the modified THERMO™ model and no other changes are necessary.

9.0 Conclusions

In order to validate the existing TiO₂ term in the 1995 THERMO™ models beyond 2.0 wt% in the DWPF, new durability data were developed over the target range of 2.00 to 6.00 wt% TiO₂ and evaluated against the models. At the same time, the Na₂O and Cs₂O durability terms were evaluated over the SWPF measured composition range, i.e. 8.03 to 18.14 wt% Na₂O and 0.48 to 1.62 wt% Cs₂O (where Cs₂O measured was actually 1.62 wt%) even though the THERMO™ DWPF durability model covered 6.42-16.80 wt% Na₂O and 0-1.16 wt% Cs₂O. It was determined that the Na₂O, Cs₂O, and TiO₂ terms adequately described the impact of higher MST concentrations on glass durability.

During the course of the DWPF durability modeling and the associated ROC modeling, it was determined that for glasses with TiO₂>2.0 wt% the ROC had to be moved to a 4.0 wt% Al₂O₃ restriction. Several SWPF glasses were removed from durability modeling due to the revised ROC restriction and the ranges for TiO₂ validation became 1.90-5.85 wt% instead of the targeted 2-6 wt% TiO₂ originally planned for model validation. These are not model limits, as mechanistic models can be used over wider ranges than they are developed or validated for.

This study documents the adequacy of the existing THERMO™ terms. Since the original ROC criteria were developed after the THERMO™ model was developed, there were some glasses in THERMO™ that failed the original ROC and the DWPF REDOX modeling criteria. These data points were removed from the other PCCS models between 2001 and 2005. To make all the PCCS models consistent these nine data points were removed and the revised slopes and intercepts were fitted for boron, sodium, and lithium release. These modified THERMO™ models have higher R² values and smaller RMSEs which opens the PCCS durability window slightly for future processing. Since the PCCS durability window becomes slightly larger with the modified THERMO™ models all previous qualified DWPF glasses are still qualified.

The modified durability models in which ΔG_p is correlated to the response of a 7-day ASTM C1285 (PCT) take the following form:

| | | |
|---|--------------|--------------------------|
| $\log_{10}[\text{NC}_B] \text{ (g/L)} = -1.901602 - 0.180215 \Delta G_p$ | $R^2 = 0.80$ | $\text{RMSE} = 0.195316$ |
| $\log_{10}[\text{NC}_{\text{Li}}] \text{ (g/L)} = -1.541811 - 0.1453413 \Delta G_p$ | $R^2 = 0.80$ | $\text{RMSE} = 0.161483$ |
| $\log_{10}[\text{NC}_{\text{Na}}] \text{ (g/L)} = -1.803846 - 0.1704731 \Delta G_p$ | $R^2 = 0.83$ | $\text{RMSE} = 0.168133$ |

compared to the 1995 THERMO™ models

| | | |
|---|--------------|--------------------------|
| $\log_{10}[\text{NC}_B] \text{ (g/L)} = -1.901447 - 0.1812039 \Delta G_p$ | $R^2 = 0.77$ | $\text{RMSE} = 0.216264$ |
| $\log_{10}[\text{NC}_{\text{Li}}] \text{ (g/L)} = -1.545942 - 0.1468048 \Delta G_p$ | $R^2 = 0.75$ | $\text{RMSE} = 0.182722$ |
| $\log_{10}[\text{NC}_{\text{Na}}] \text{ (g/L)} = -1.801158 - 0.1710066 \Delta G_p$ | $R^2 = 0.80$ | $\text{RMSE} = 0.187881$ |

where ΔG_p is in kcal/100g glass and NC_i , where i is the i^{th} elemental component in the glass, is in g/L. Since the associated ΔG_p PAR limits are slightly more negative than previously established, this opens up the DWPF PCCS durability window slightly and does not impact the durability determinations of previously made DWPF canister glass. The modified THERMO™ models were validated with the SWPF data up to 5.85 wt% TiO_2 . Additional SRNL high TiO_2 databases were used to perform additional validation studies of the modified THERMO™ models up to 6.62 wt% TiO_2 . Validation limits are not model limits and they are not solubility limits.

It is recommended that the modified THERMO™ durability models and the modified PAR limits for the durability constraints be incorporated in the next revision of the technical bases for PCCS and then implemented into PCCS. It is also recommended that an ROC of 4 wt% Al_2O_3 be implemented with no restrictions on the amount of alkali in the glass for TiO_2 values ≥ 2 wt%. For glasses with < 2.0 wt% TiO_2 the original ROC of 3 wt% Al_2O_3 with an alkali constraint or 4 wt% Al_2O_3 without an alkali constraint would apply.

The leachate data used in the THERMO™ durability model were also investigated to determine if glass density was a concern to the THERMO™ models, i.e. higher density glasses have a lower available surface area for every gram of glass leached. It was concluded that the RMSE's of the modified THERMO™ models encompassed any PCT variation due to the additional surface area since the ranges of the THERMO™ glass densities overlap those of the SWPF glasses.

The 1995 THERMO™ model did not contain a ΔG_i for Nb_2O_5 but two estimates for ΔG_{Nb} were developed in 2010. The data presented in this report helped determine that an $Nb_2O_5 \Delta G_i$ of +13.20 kcal/mole should be used with the modified THERMO™ models presented in this study and the only additional changes that will be needed in PCCS are those associated with implementation of the Nb_2O_5 term, i.e. changes in the WAPS and determination of the Nb measurement errors. This Nb_2O_5 term was added into THERMO™ for potential future use, should the DWPF ever need to process other titanate containing ion exchange materials, such as Crystalline SilicoTitanate (CST - $Na_{1.5}Nb_{0.5}Ti_{1.5}O_3SiO_4 \bullet 2H_2O$).

The ultimate limit on the amount of TiO_2 that can be accommodated from SWPF will be determined by the three PCCS models, the waste composition of a given sludge batch, the waste loading of the sludge batch, and the frit used for vitrification. Once a component like TiO_2 is present at larger concentrations than 1-2 wt%, the interactions of that component with other components in the melter feed must be considered simultaneously, i.e. an individual solubility limit cannot be defined to globally account for the interactions with all the remaining sludge/frit composition variables. It is known that Ti^{4+} competes with Al^{3+} for alkali bonding and it is known that Ti^{4+} and Fe^{3+} have a coupled impact on their joint solubility in a glass.

APPENDIX A. SWPF (TiO₂-only) Glass Database (wt% on a vitrified oxide basis indicated by “v”)

| Sample ID | Density (g/cc) from Ref 83 | Al ₂ O ₃ (v) | B ₂ O ₃ (v) | BaO(v) | CaO(v) | CeO ₂ (v) | CoO(v) | Cr ₂ O ₃ (v) | Cs ₂ O(v) | CuO(v) | Fe ₂ O ₃ (v) | K ₂ O(v) | La ₂ O ₃ (v) | Li ₂ O(v) | MgO(v) | MnO(v) | NiO(v) | PbO(v) | RuO ₂ (v) | SO ₄ (v) | SiO ₂ (v) | ThO ₂ (v) | TiO ₂ (v) | U ₃ O ₈ (v) | ZnO(v) | ZrO ₂ (v) | Sum Oxides | |
|-----------|-------------------------------|------------------------------------|-----------------------------------|--------|--------|----------------------|--------|------------------------------------|----------------------|--------|------------------------------------|---------------------|------------------------------------|----------------------|--------|--------|--------|--------|----------------------|---------------------|----------------------|----------------------|----------------------|-----------------------------------|--------|----------------------|------------|--------|
| SWPF-01 | 2.682 | 3.90 | 4.54 | 0.23 | 0.23 | 0.19 | 0.11 | 0.19 | 1.19 | 0.11 | 13.27 | 0.22 | 0.09 | 6.95 | 1.85 | 0.21 | 7.78 | 0.00 | 0.22 | 0.11 | 0.39 | 55.34 | 0.95 | 2.05 | 0.00 | 0.18 | 0.24 | 100.53 |
| SWPF-02 | 2.761 | 3.87 | 4.50 | 0.00 | 2.11 | 0.00 | 0.00 | 0.00 | 0.36 | 0.00 | 4.98 | 0.00 | 0.00 | 6.91 | 0.00 | 4.20 | 7.76 | 2.00 | 0.00 | 0.09 | 0.00 | 55.49 | 0.86 | 1.99 | 4.97 | 0.00 | 0.00 | 100.09 |
| SWPF-03 | 2.688 | 3.85 | 4.55 | 0.00 | 2.04 | 0.00 | 0.00 | 0.00 | 0.45 | 0.00 | 7.54 | 0.00 | 0.00 | 6.87 | 1.85 | 4.07 | 7.81 | 0.00 | 0.00 | 0.11 | 0.00 | 55.32 | 0.00 | 6.03 | 0.00 | 0.00 | 0.00 | 100.49 |
| SWPF-04 | 2.717 | 3.86 | 4.54 | 0.20 | 2.11 | 0.30 | 0.05 | 0.19 | 0.69 | 0.10 | 4.96 | 0.24 | 0.06 | 6.84 | 0.00 | 0.21 | 7.75 | 0.00 | 0.23 | 0.11 | 0.32 | 55.62 | 0.00 | 5.90 | 5.51 | 0.19 | 0.21 | 100.20 |
| SWPF-05 | 2.867 | 3.72 | 10.22 | 0.21 | 0.25 | 0.31 | 0.05 | 0.19 | 0.33 | 0.12 | 5.12 | 0.24 | 0.05 | 1.06 | 1.80 | 4.14 | 16.18 | 2.12 | 0.23 | 0.09 | 0.33 | 39.90 | 1.00 | 6.09 | 6.23 | 0.20 | 0.23 | 100.41 |
| SWPF-06 | 2.658 | 3.85 | 10.03 | 0.00 | 0.24 | 0.00 | 0.00 | 0.00 | 0.38 | 0.00 | 5.09 | 0.00 | 0.00 | 6.83 | 0.00 | 0.21 | 9.30 | 0.00 | 0.00 | 0.12 | 0.00 | 54.89 | 0.96 | 1.99 | 6.03 | 0.00 | 0.00 | 99.92 |
| SWPF-07 | 2.686 | 3.86 | 10.01 | 0.30 | 0.22 | 0.40 | 0.05 | 0.18 | 0.45 | 0.10 | 4.89 | 0.22 | 0.07 | 6.84 | 0.00 | 4.03 | 7.56 | 2.00 | 0.22 | 0.13 | 0.32 | 52.06 | 0.00 | 5.96 | 0.00 | 0.18 | 0.23 | 100.29 |
| SWPF-08 | 2.818 | 3.92 | 10.12 | 0.00 | 0.24 | 0.00 | 0.00 | 0.00 | 1.15 | 0.00 | 15.34 | 0.00 | 0.00 | 0.98 | 1.84 | 0.21 | 8.07 | 0.00 | 0.00 | 0.13 | 0.00 | 45.57 | 0.97 | 5.86 | 6.15 | 0.00 | 0.00 | 100.54 |
| SWPF-09 | 2.76 | 3.75 | 9.99 | 0.00 | 2.00 | 0.00 | 0.00 | 0.00 | 1.24 | 0.00 | 4.84 | 0.00 | 0.00 | 6.81 | 1.87 | 0.22 | 7.96 | 1.94 | 0.00 | 0.10 | 0.00 | 47.39 | 0.00 | 5.69 | 5.76 | 0.00 | 0.00 | 99.56 |
| SWPF-10 | 2.884 | 3.81 | 10.02 | 0.20 | 2.05 | 0.18 | 0.08 | 0.19 | 1.11 | 0.12 | 15.51 | 0.25 | 0.07 | 1.05 | 0.00 | 4.06 | 12.43 | 0.00 | 0.22 | 0.11 | 0.37 | 40.00 | 0.00 | 1.96 | 5.94 | 0.19 | 0.21 | 100.12 |

| Sample ID | Density (g/cc) from Ref. 83 | Al2O3(v) | B2O3(v) | BaO(v) | CaO(v) | Ce2O3(v) | CoO(v) | Cr2O3(v) | Cs2O(v) | CuO(v) | Fe2O3(v) | K2O(v) | La2O3(v) | Li2O(v) | MgO(v) | MnO(v) | Na2O(v) | NiO(v) | PbO(v) | RuO2(v) | SO4(v) | SiO2(v) | ThO2(v) | TiO2(v) | U3O8(v) | ZnO(v) | ZrO2(v) | Sum Oxides |
|-----------|-----------------------------|----------|---------|--------|--------|----------|--------|----------|---------|--------|----------|--------|----------|---------|--------|--------|---------|--------|--------|---------|--------|---------|---------|---------|---------|--------|---------|------------|
| SWPF-11 | 2.592 | 5.85 | 10.31 | 0.00 | 0.23 | 0.00 | 0.00 | 0.00 | 1.62 | 0.00 | 4.91 | 0.00 | 0.00 | 1.07 | 0.00 | 0.21 | 18.14 | 1.99 | 0.00 | 0.14 | 0.00 | 53.72 | 0.00 | 1.90 | 0.00 | 0.00 | 100.08 | |
| SWPF-12 | 2.813 | 13.63 | 4.51 | 0.00 | 0.23 | 0.00 | 0.00 | 0.00 | 0.33 | 0.00 | 14.94 | 0.00 | 0.00 | 7.13 | 0.00 | 0.21 | 8.42 | 0.00 | 0.00 | 0.12 | 0.00 | 40.67 | 0.00 | 4.63 | 5.66 | 0.00 | 0.00 | 100.47 |
| SWPF-13 | 2.750 | 13.38 | 4.57 | 0.21 | 0.22 | 0.19 | 0.05 | 0.19 | 1.11 | 0.11 | 4.98 | 0.23 | 0.12 | 6.81 | 1.92 | 4.08 | 8.03 | 0.00 | 0.23 | 0.14 | 0.32 | 45.15 | 0.00 | 1.95 | 6.24 | 0.20 | 0.22 | 100.65 |
| SWPF-14 | 2.570 | 13.34 | 10.21 | 0.31 | 1.94 | 0.42 | 0.04 | 0.17 | 0.48 | 0.09 | 4.84 | 0.22 | 0.06 | 6.77 | 1.94 | 0.19 | 8.11 | 0.00 | 0.23 | 0.16 | 0.33 | 48.36 | 0.00 | 1.93 | 0.00 | 0.19 | 0.24 | 100.57 |
| SWPF-15 | 2.706 | 13.35 | 10.14 | 0.23 | 1.98 | 0.24 | 0.05 | 0.19 | 1.26 | 0.10 | 4.83 | 0.22 | 0.15 | 6.76 | 0.00 | 3.99 | 8.18 | 0.00 | 0.22 | 0.11 | 0.30 | 40.10 | 0.95 | 5.85 | 0.86 | 0.19 | 0.23 | 100.46 |
| SWPF-16 | 2.717 | 6.62 | 7.96 | 0.11 | 1.04 | 0.10 | 0.06 | 0.11 | 0.72 | 0.07 | 7.64 | 0.14 | 0.06 | 5.46 | 0.95 | 1.96 | 9.75 | 0.65 | 0.11 | 0.13 | 0.23 | 49.30 | 0.37 | 3.96 | 2.92 | 0.10 | 0.11 | 100.64 |
| SWPF-17 | 2.679 | 6.31 | 5.93 | 0.06 | 0.66 | 0.06 | 0.04 | 0.05 | 1.09 | 0.04 | 7.51 | 0.09 | 0.03 | 2.64 | 1.41 | 1.17 | 14.84 | 0.51 | 0.06 | 0.12 | 0.16 | 51.02 | 0.24 | 4.90 | 1.52 | 0.06 | 0.06 | 100.56 |
| SWPF-18 | 2.698 | 6.24 | 5.89 | 0.06 | 0.65 | 0.06 | 0.05 | 0.05 | 1.09 | 0.04 | 7.49 | 0.08 | 0.03 | 5.68 | 0.47 | 1.17 | 15.42 | 1.47 | 0.06 | 0.12 | 0.18 | 48.88 | 0.71 | 2.92 | 1.52 | 0.05 | 0.05 | 100.43 |
| SWPF-19 | 2.704 | 6.28 | 5.91 | 0.18 | 1.55 | 0.14 | 0.06 | 0.14 | 0.62 | 0.09 | 7.50 | 0.19 | 0.04 | 2.65 | 0.48 | 3.08 | 14.23 | 0.49 | 0.16 | 0.13 | 0.28 | 51.12 | 0.24 | 2.98 | 1.52 | 0.14 | 0.17 | 100.37 |
| SWPF-20 | 2.780 | 6.31 | 5.79 | 0.19 | 1.54 | 0.15 | 0.10 | 0.14 | 0.66 | 0.08 | 12.75 | 0.17 | 0.04 | 5.57 | 1.40 | 1.16 | 10.53 | 0.50 | 0.16 | 0.12 | 0.34 | 45.12 | 0.71 | 4.96 | 1.48 | 0.15 | 0.17 | 100.31 |
| SWPF-21 | 2.825 | 6.18 | 5.78 | 0.06 | 1.56 | 0.06 | 0.05 | 0.05 | 1.02 | 0.05 | 8.09 | 0.09 | 0.03 | 2.57 | 0.47 | 3.16 | 15.39 | 1.50 | 0.05 | 0.13 | 0.18 | 43.46 | 0.71 | 4.97 | 4.57 | 0.05 | 0.05 | 100.27 |

| Sample ID | Density (g/cc) from Ref. 83 | Al2O3(v) | B2O3(v) | BaO(v) | CaO(v) | Ce2O3(v) | CoO(v) | Cr2O3(v) | Cs2O(v) | CuO(v) | Fe2O3(v) | K2O(v) | La2O3(v) | Li2O(v) | MgO(v) | MnO(v) | Na2O(v) | NiO(v) | PbO(v) | RuO2(v) | SO4(v) | SiO2(v) | ThO2(v) | TiO2(v) | U3O8(v) | ZnO(v) | ZrO2(v) | Sum Oxides |
|-----------|--------------------------------|----------|---------|--------|--------|----------|--------|----------|---------|--------|----------|--------|----------|---------|--------|--------|---------|--------|--------|---------|--------|---------|---------|---------|---------|--------|---------|------------|
| SWPF-22 | 2.767 | 6.18 | 7.10 | 0.06 | 1.54 | 0.05 | 0.04 | 0.05 | 1.09 | 0.04 | 12.84 | 0.09 | 0.03 | 2.61 | 0.48 | 3.10 | 15.33 | 0.50 | 0.06 | 0.12 | 0.24 | 43.67 | 0.27 | 3.00 | 1.52 | 0.05 | 0.05 | 100.12 |
| SWPF-23 | 2.771 | 6.14 | 8.35 | 0.17 | 0.68 | 0.11 | 0.06 | 0.14 | 0.54 | 0.10 | 7.57 | 0.19 | 0.09 | 2.53 | 1.26 | 1.20 | 15.44 | 0.50 | 0.17 | 0.12 | 0.28 | 43.70 | 0.83 | 4.90 | 4.53 | 0.14 | 0.17 | 99.90 |
| SWPF-24 | 2.753 | 6.25 | 8.55 | 0.06 | 0.67 | 0.06 | 0.04 | 0.05 | 0.99 | 0.04 | 12.80 | 0.10 | 0.03 | 2.56 | 0.46 | 1.17 | 10.48 | 0.50 | 0.05 | 0.13 | 0.20 | 46.96 | 0.80 | 2.93 | 4.46 | 0.06 | 0.05 | 100.45 |
| SWPF-25 | 2.782 | 6.17 | 8.64 | 0.06 | 1.61 | 0.06 | 0.04 | 0.06 | 0.55 | 0.03 | 7.48 | 0.09 | 0.03 | 5.52 | 0.46 | 3.11 | 10.34 | 0.50 | 0.06 | 0.11 | 0.15 | 45.36 | 0.81 | 4.82 | 4.43 | 0.05 | 0.05 | 100.60 |
| SWPF-26 | 2.779 | 6.16 | 8.66 | 0.06 | 1.55 | 0.06 | 0.04 | 0.06 | 1.02 | 0.05 | 7.51 | 0.09 | 0.03 | 5.61 | 1.40 | 3.13 | 10.38 | 1.47 | 0.06 | 0.11 | 0.17 | 45.23 | 0.26 | 2.93 | 4.45 | 0.06 | 0.05 | 100.58 |
| SWPF-27 | 2.769 | 10.88 | 5.74 | 0.06 | 0.69 | 0.07 | 0.05 | 0.05 | 0.59 | 0.05 | 7.54 | 0.10 | 0.03 | 5.47 | 0.49 | 3.13 | 10.53 | 1.45 | 0.05 | 0.13 | 0.17 | 43.94 | 0.27 | 4.86 | 4.03 | 0.06 | 0.05 | 100.47 |
| SWPF-28 | 2.759 | 10.88 | 5.85 | 0.06 | 0.68 | 0.06 | 0.04 | 0.06 | 1.00 | 0.04 | 7.71 | 0.09 | 0.03 | 5.29 | 1.41 | 3.17 | 11.09 | 0.50 | 0.05 | 0.13 | 0.16 | 43.76 | 0.82 | 2.96 | 4.59 | 0.06 | 0.05 | 100.53 |
| SWPF-29 | 2.757 | 10.90 | 5.69 | 0.18 | 1.58 | 0.17 | 0.08 | 0.14 | 1.00 | 0.08 | 7.73 | 0.18 | 0.12 | 5.35 | 0.47 | 1.19 | 10.31 | 0.51 | 0.17 | 0.12 | 0.29 | 43.89 | 0.27 | 4.91 | 4.52 | 0.15 | 0.16 | 100.16 |
| SWPF-30 | 2.707 | 10.96 | 8.64 | 0.18 | 0.67 | 0.20 | 0.07 | 0.14 | 1.07 | 0.09 | 7.49 | 0.17 | 0.07 | 2.61 | 0.46 | 3.05 | 12.43 | 0.49 | 0.16 | 0.13 | 0.28 | 43.88 | 0.82 | 4.93 | 1.52 | 0.15 | 0.17 | 100.83 |
| SWPF-31 | 2.693 | 10.98 | 8.77 | 0.06 | 1.55 | 0.07 | 0.04 | 0.04 | 0.65 | 0.03 | 7.52 | 0.08 | 0.03 | 2.47 | 1.36 | 1.17 | 14.81 | 1.50 | 0.05 | 0.14 | 0.18 | 43.72 | 0.84 | 3.00 | 1.53 | 0.05 | 0.05 | 100.69 |
| SWPF-32 | 2.719 | 6.95 | 5.90 | 0.11 | 1.10 | 0.10 | 0.04 | 0.08 | 0.89 | 0.06 | 7.08 | 0.13 | 0.03 | 5.11 | 0.80 | 1.85 | 10.06 | 0.96 | 0.10 | 0.13 | 0.22 | 50.74 | 0.52 | 4.68 | 2.63 | 0.09 | 0.10 | 100.44 |

| Sample ID | Density (g/cc) from Ref. 83 | Al2O3(v) | B2O3(v) | BaO(v) | CaO(v) | Ce2O3(v) | CoO(v) | Cr2O3(v) | Cs2O(v) | CuO(v) | Fe2O3(v) | K2O(v) | La2O3(v) | Li2O(v) | MgO(v) | MnO(v) | Na2O(v) | NiO(v) | PbO(v) | RuO2(v) | SO4(v) | SiO2(v) | ThO2(v) | TiO2(v) | U3O8(v) | ZnO(v) | ZrO2(v) | Sum Oxides |
|-----------|--------------------------------|----------|---------|--------|--------|----------|--------|----------|---------|--------|----------|--------|----------|---------|--------|--------|---------|--------|--------|---------|--------|---------|---------|---------|---------|--------|---------|------------|
| SWPF-33 | 2.777 | 7.67 | 8.38 | 0.11 | 1.07 | 0.11 | 0.05 | 0.09 | 0.75 | 0.08 | 8.52 | 0.15 | 0.03 | 4.88 | 0.90 | 1.89 | 10.30 | 0.98 | 0.11 | 0.12 | 0.25 | 44.80 | 0.53 | 3.91 | 4.66 | 0.10 | 0.11 | 100.55 |
| SWPF-34 | 2.690 | 10.30 | 6.43 | 0.10 | 0.98 | 0.10 | 0.05 | 0.08 | 0.82 | 0.06 | 6.46 | 0.12 | 0.06 | 3.09 | 1.02 | 1.92 | 15.81 | 0.99 | 0.10 | 0.13 | 0.21 | 45.65 | 0.55 | 3.67 | 1.58 | 0.09 | 0.11 | 100.48 |
| SWPF-35 | 2.754 | 7.77 | 8.87 | 0.10 | 1.08 | 0.11 | 0.04 | 0.08 | 0.83 | 0.07 | 10.58 | 0.12 | 0.03 | 5.32 | 1.08 | 2.49 | 10.18 | 0.90 | 0.11 | 0.11 | 0.25 | 43.62 | 0.54 | 4.31 | 1.92 | 0.09 | 0.10 | 100.69 |
| SWPF-36 | 2.688 | 11.34 | 6.53 | 0.13 | 1.10 | 0.10 | 0.06 | 0.08 | 0.90 | 0.06 | 7.00 | 0.13 | 0.04 | 5.37 | 1.05 | 2.02 | 10.37 | 1.09 | 0.10 | 0.13 | 0.23 | 46.39 | 0.56 | 4.13 | 1.27 | 0.11 | 0.11 | 100.40 |
| SWPF-37 | 2.737 | 5.13 | 7.81 | 0.11 | 1.10 | 0.11 | 0.05 | 0.10 | 0.79 | 0.07 | 9.63 | 0.13 | 0.04 | 4.63 | 0.93 | 1.84 | 9.43 | 1.04 | 0.11 | 0.13 | 0.23 | 49.68 | 0.52 | 3.82 | 2.78 | 0.09 | 0.11 | 100.41 |
| SWPF-38 | 2.790 | 5.54 | 7.63 | 0.10 | 1.05 | 0.10 | 0.04 | 0.09 | 0.75 | 0.07 | 11.28 | 0.13 | 0.03 | 2.26 | 1.00 | 2.27 | 13.32 | 0.99 | 0.10 | 0.13 | 0.25 | 44.93 | 0.56 | 4.02 | 3.63 | 0.09 | 0.09 | 100.43 |
| SWPF-39 | 2.707 | 6.04 | 5.88 | 0.10 | 1.07 | 0.09 | 0.06 | 0.09 | 0.81 | 0.05 | 7.03 | 0.12 | 0.04 | 4.95 | 0.93 | 1.74 | 14.24 | 0.96 | 0.09 | 0.12 | 0.21 | 49.39 | 0.52 | 3.90 | 1.76 | 0.08 | 0.09 | 100.37 |
| SWPF-40 | 2.736 | 10.85 | 7.73 | 0.13 | 1.19 | 0.13 | 0.04 | 0.10 | 0.85 | 0.07 | 9.42 | 0.14 | 0.03 | 4.55 | 1.02 | 2.72 | 12.87 | 0.92 | 0.11 | 0.11 | 0.26 | 41.65 | 0.55 | 3.86 | 1.40 | 0.11 | 0.13 | 100.96 |
| SWPF-41 | 2.705 | 5.75 | 8.36 | 0.11 | 1.07 | 0.10 | 0.05 | 0.10 | 0.86 | 0.06 | 6.38 | 0.12 | 0.07 | 5.99 | 0.95 | 2.37 | 11.53 | 0.99 | 0.11 | 0.13 | 0.22 | 48.64 | 0.56 | 4.06 | 1.82 | 0.10 | 0.11 | 100.61 |
| SWPF-42 | 2.707 | 5.91 | 6.78 | 0.09 | 1.00 | 0.11 | 0.04 | 0.08 | 0.78 | 0.06 | 6.21 | 0.12 | 0.04 | 2.26 | 0.96 | 1.73 | 14.48 | 0.91 | 0.09 | 0.13 | 0.21 | 50.58 | 0.58 | 3.75 | 3.25 | 0.09 | 0.10 | 100.36 |
| SWPF-43 | 2.773 | 6.57 | 5.86 | 0.09 | 1.14 | 0.09 | 0.05 | 0.09 | 0.75 | 0.06 | 11.08 | 0.12 | 0.06 | 5.38 | 1.01 | 1.97 | 11.60 | 0.99 | 0.10 | 0.11 | 0.25 | 45.68 | 0.57 | 3.97 | 2.68 | 0.09 | 0.10 | 100.46 |

| Sample ID | Density (g/cc) from Ref. 83 | Al2O3(v) | B2O3(v) | BaO(v) | CaO(v) | Ce2O3(v) | CoO(v) | Cr2O3(v) | Cs2O(v) | CuO(v) | Fe2O3(v) | K2O(v) | La2O3(v) | Li2O(v) | MgO(v) | MnO(v) | NiO(v) | PbO(v) | RuO2(v) | SO4(v) | SiO2(v) | ThO2(v) | TiO2(v) | U3O8(v) | ZnO(v) | ZrO2(v) | Sum Oxides | |
|-----------|-----------------------------|----------|---------|--------|--------|----------|--------|----------|---------|--------|----------|--------|----------|---------|--------|--------|--------|--------|---------|--------|---------|---------|---------|---------|--------|---------|------------|--------|
| SWPF-44 | 2.760 | 6.83 | 7.24 | 0.10 | 1.21 | 0.11 | 0.05 | 0.08 | 0.76 | 0.08 | 6.67 | 0.13 | 0.07 | 5.02 | 0.96 | 2.37 | 10.59 | 1.01 | 0.11 | 0.12 | 0.23 | 47.61 | 0.57 | 3.98 | 4.40 | 0.10 | 0.11 | 100.50 |
| SWPF-45 | 2.721 | 6.67 | 6.56 | 0.11 | 1.09 | 0.08 | 0.06 | 0.08 | 0.79 | 0.06 | 10.26 | 0.13 | 0.03 | 2.35 | 1.03 | 1.73 | 13.83 | 0.90 | 0.10 | 0.13 | 0.24 | 48.47 | 0.49 | 3.67 | 1.36 | 0.09 | 0.11 | 100.42 |
| SWPF-46 | 2.770 | 6.32 | 6.05 | 0.10 | 1.10 | 0.14 | 0.06 | 0.10 | 0.76 | 0.08 | 6.95 | 0.13 | 0.05 | 3.46 | 0.91 | 1.81 | 15.57 | 1.09 | 0.11 | 0.12 | 0.23 | 46.22 | 0.54 | 3.71 | 4.52 | 0.10 | 0.11 | 100.34 |
| SWPF-47 | 2.746 | 7.98 | 7.80 | 0.10 | 1.14 | 0.10 | 0.04 | 0.09 | 0.76 | 0.07 | 6.68 | 0.13 | 0.05 | 4.41 | 1.14 | 2.10 | 13.22 | 1.09 | 0.12 | 0.12 | 0.23 | 43.35 | 0.62 | 4.76 | 4.16 | 0.10 | 0.11 | 100.49 |
| SWPF-48 | 2.702 | 9.28 | 8.04 | 0.11 | 1.13 | 0.10 | 0.04 | 0.06 | 0.87 | 0.06 | 7.18 | 0.11 | 0.06 | 3.75 | 1.06 | 2.37 | 12.47 | 1.12 | 0.10 | 0.13 | 0.22 | 46.11 | 0.59 | 3.84 | 1.49 | 0.09 | 0.10 | 100.49 |
| SWPF-49 | 2.712 | 5.74 | 8.27 | 0.13 | 1.07 | 0.11 | 0.06 | 0.10 | 0.87 | 0.06 | 7.22 | 0.13 | 0.04 | 3.56 | 0.85 | 1.75 | 15.44 | 0.92 | 0.12 | 0.12 | 0.24 | 47.29 | 0.57 | 3.38 | 2.10 | 0.10 | 0.13 | 100.37 |
| SWPF-50 | 2.759 | 11.06 | 6.23 | 0.12 | 1.11 | 0.09 | 0.05 | 0.10 | 0.76 | 0.07 | 6.90 | 0.14 | 0.06 | 5.67 | 0.97 | 2.22 | 12.22 | 0.89 | 0.12 | 0.11 | 0.24 | 42.58 | 0.55 | 3.66 | 4.40 | 0.10 | 0.11 | 100.54 |
| MAX* | 2.884 | 13.38 | 10.31 | 0.31 | 2.05 | 0.42 | 0.10 | 0.19 | 1.62 | 0.12 | 15.51 | 0.25 | 0.15 | 6.81 | 1.94 | 4.08 | 18.14 | 1.99 | 0.23 | 0.16 | 0.37 | 53.72 | 0.95 | 5.85 | 6.24 | 0.20 | 0.24 | 100.96 |
| MIN* | 2.570 | 3.81 | 4.57 | 0.00 | 0.22 | 0.00 | 0.00 | 0.00 | 0.48 | 0.00 | 4.83 | 0.00 | 0.00 | 1.05 | 0.00 | 0.19 | 8.03 | 0.00 | 0.00 | 0.11 | 0.00 | 40.00 | 0.00 | 1.90 | 0.00 | 0.00 | 0.00 | 99.90 |

*Where max and min refer to the glasses used for modeling and not the glasses excluded.

Table B1. PCT Measurements for High TiO₂ Glasses (continued)**APPENDIX B. Tables and Exhibits for the PCT Measurements of the High TiO₂ Glass Study.****Table B1. PCT Measurements for High TiO₂ Glasses**

| Oven Run | SRNL ID | VSL Sample ID | Block | Seq | Lab ID | Values As Received (ar) | | | | Below Detects Set to Detection Limit | | | |
|----------|----------|---------------|-------|-----|-------------|-------------------------|----------|----------|----------|--------------------------------------|----------|----------|----------|
| | | | | | | B (ppm) | Li (ppm) | Na (ppm) | Si (ppm) | B (ppm) | Li (ppm) | Na (ppm) | Si (ppm) |
| . | soln std | | A | 1 | std-A1 | 20.13 | 10.70 | 81.40 | 49.92 | 20.13 | 10.70 | 81.400 | 49.92 |
| 1 | SWPF-04 | GAP-31 | A | 2 | GAP-pct-201 | 10.13 | 34.11 | 43.29 | 166.31 | 10.13 | 34.11 | 43.290 | 166.31 |
| 2 | SWPF-08 | GAP-37 | A | 3 | GAP-pct-046 | 11.01 | 3.18 | 22.98 | 64.50 | 11.01 | 3.18 | 22.980 | 64.50 |
| 1 | SWPF-03 | GAP-43 | A | 4 | GAP-pct-080 | 17.73 | 39.83 | 70.08 | 220.63 | 17.73 | 39.83 | 70.080 | 220.63 |
| 2 | SWPF-05 | GAP-33ccc | A | 5 | GAP-pct-307 | 111.41 | 12.32 | 338.40 | 161.86 | 111.41 | 12.32 | 338.400 | 161.86 |
| 2 | SWPF-05 | GAP-33ccc | A | 6 | GAP-pct-398 | 101.47 | 11.10 | 305.54 | 156.74 | 101.47 | 11.10 | 305.540 | 156.74 |
| 1 | SWPF-02 | GAP-22ccc | A | 7 | GAP-pct-380 | 20.76 | 50.49 | 75.96 | 231.13 | 20.76 | 50.49 | 75.960 | 231.13 |
| 2 | SWPF-07 | GAP-21ccc | A | 8 | GAP-pct-287 | 121.65 | 110.81 | 159.53 | 357.37 | 121.65 | 110.81 | 159.530 | 357.37 |
| 2 | ARM-1 | ARM-1 | A | 9 | GAP-pct-131 | 27.34 | 17.88 | 50.56 | 75.59 | 27.34 | 17.88 | 50.560 | 75.59 |
| 1 | SWPF-02 | GAP-22 | A | 10 | GAP-pct-320 | 13.80 | 35.86 | 57.47 | 195.70 | 13.80 | 35.86 | 57.470 | 195.70 |
| 1 | SWPF-04 | GAP-31ccc | A | 11 | GAP-pct-011 | 10.62 | 32.72 | 42.99 | 168.55 | 10.62 | 32.72 | 42.990 | 168.55 |
| 1 | SWPF-01 | GAP-15 | A | 12 | GAP-pct-085 | 12.25 | 30.87 | 48.49 | 169.40 | 12.25 | 30.87 | 48.490 | 169.40 |
| . | soln std | | A | 13 | std-A2 | 20.05 | 10.29 | 83.72 | 50.12 | 20.05 | 10.29 | 83.720 | 50.12 |
| 1 | blank | blank | A | 14 | GAP-pct-341 | < 4.20 | < 1.05 | < 0.21 | < 0.84 | 4.20 | 1.05 | 0.210 | 0.84 |
| 2 | EA | EA | A | 15 | GAP-pct-277 | 567.49 | 178.66 | 1683.60 | 744.05 | 567.49 | 178.66 | 1683.600 | 744.05 |
| 1 | SWPF-03 | GAP-43ccc | A | 16 | GAP-pct-289 | 32.86 | 95.82 | 105.77 | 351.68 | 32.86 | 95.82 | 105.770 | 351.68 |
| 2 | SWPF-06 | GAP-38ccc | A | 17 | GAP-pct-396 | 62.81 | 59.49 | 98.99 | 257.14 | 62.81 | 59.49 | 98.990 | 257.14 |
| 2 | SWPF-07 | GAP-21 | A | 18 | GAP-pct-010 | 73.99 | 66.12 | 97.56 | 241.19 | 73.99 | 66.12 | 97.560 | 241.19 |
| 2 | SWPF-08 | GAP-37ccc | A | 19 | GAP-pct-281 | 12.64 | 3.01 | 23.50 | 66.12 | 12.64 | 3.01 | 23.500 | 66.12 |
| 2 | SWPF-06 | GAP-38 | A | 20 | GAP-pct-356 | 64.14 | 63.51 | 104.30 | 266.76 | 64.14 | 63.51 | 104.300 | 266.76 |
| 1 | EA | EA | A | 21 | GAP-pct-212 | 577.55 | 165.40 | 1501.30 | 726.18 | 577.55 | 165.40 | 1501.300 | 726.18 |
| 1 | ARM-1 | ARM-1 | A | 22 | GAP-pct-157 | 20.87 | 16.80 | 46.40 | 72.98 | 20.87 | 16.80 | 46.400 | 72.98 |
| 1 | SWPF-01 | GAP-15ccc | A | 23 | GAP-pct-327 | 118.49 | 216.94 | 372.29 | 698.56 | 118.49 | 216.94 | 372.290 | 698.56 |
| . | soln std | | A | 24 | std-A3 | 19.45 | 10.04 | 82.96 | 47.51 | 19.45 | 10.04 | 82.960 | 47.51 |
| . | soln std | | B | 1 | std-B1 | 19.95 | 10.24 | 80.70 | 50.28 | 19.95 | 10.24 | 80.700 | 50.28 |
| 2 | SWPF-07 | GAP-21ccc | B | 2 | GAP-pct-381 | 118.80 | 101.81 | 154.76 | 330.59 | 118.80 | 101.81 | 154.760 | 330.59 |
| 2 | SWPF-06 | GAP-38 | B | 3 | GAP-pct-317 | 64.21 | 61.19 | 103.69 | 258.47 | 64.21 | 61.19 | 103.690 | 258.47 |
| 1 | SWPF-02 | GAP-22ccc | B | 4 | GAP-pct-384 | 21.86 | 49.88 | 74.53 | 231.73 | 21.86 | 49.88 | 74.530 | 231.73 |
| 1 | SWPF-01 | GAP-15 | B | 5 | GAP-pct-116 | 13.78 | 30.73 | 48.36 | 174.19 | 13.78 | 30.73 | 48.360 | 174.19 |
| 2 | SWPF-08 | GAP-37ccc | B | 6 | GAP-pct-379 | 13.24 | 2.66 | 23.48 | 69.71 | 13.24 | 2.66 | 23.480 | 69.71 |
| 2 | SWPF-08 | GAP-37 | B | 7 | GAP-pct-199 | 13.35 | 2.89 | 22.89 | 67.80 | 13.35 | 2.89 | 22.890 | 67.80 |
| 1 | EA | EA | B | 8 | GAP-pct-322 | 588.77 | 166.38 | 1509.20 | 778.04 | 588.77 | 166.38 | 1509.200 | 778.04 |
| 2 | EA | EA | B | 9 | GAP-pct-078 | 581.81 | 190.52 | 1668.20 | 749.78 | 581.81 | 190.52 | 1668.200 | 749.78 |
| 2 | SWPF-07 | GAP-21 | B | 10 | GAP-pct-342 | 80.43 | 77.96 | 116.08 | 259.57 | 80.43 | 77.96 | 116.080 | 259.57 |
| 1 | SWPF-04 | GAP-31ccc | B | 11 | GAP-pct-090 | 11.21 | 31.30 | 41.59 | 162.65 | 11.21 | 31.30 | 41.590 | 162.65 |
| 1 | SWPF-03 | GAP-43 | B | 12 | GAP-pct-054 | 18.91 | 38.70 | 67.98 | 222.40 | 18.91 | 38.70 | 67.980 | 222.40 |
| . | soln std | | B | 13 | std-B2 | 19.67 | 9.76 | 79.81 | 49.46 | 19.67 | 9.76 | 79.810 | 49.46 |
| 1 | SWPF-03 | GAP-43ccc | B | 14 | GAP-pct-072 | 34.69 | 94.99 | 107.46 | 356.82 | 34.69 | 94.99 | 107.460 | 356.82 |

Table B1. PCT Measurements for High TiO₂ Glasses (continued)

| Oven Run | SRNL ID | VSL Sample ID | Block | Seq | Lab ID | Values As Received (ar) | | | | Below Detects Set to Detection Limit | | | |
|----------|----------|---------------|-------|-----|-------------|-------------------------|----------|----------|----------|--------------------------------------|----------|----------|----------|
| | | | | | | B (ppm) | Li (ppm) | Na (ppm) | Si (ppm) | B (ppm) | Li (ppm) | Na (ppm) | Si (ppm) |
| 1 | SWPF-04 | GAP-31 | B | 15 | GAP-pct-353 | 10.48 | 31.94 | 41.36 | 165.06 | 10.48 | 31.94 | 41.360 | 165.06 |
| 1 | ARM-1 | ARM-1 | B | 16 | GAP-pct-283 | 23.71 | 16.12 | 46.30 | 79.38 | 23.71 | 16.12 | 46.300 | 79.38 |
| 2 | blank | blank | B | 17 | GAP-pct-081 | < 4.20 | < 1.05 | < 0.21 | < 0.84 | 4.20 | 1.05 | 0.210 | 0.84 |
| 1 | SWPF-02 | GAP-22 | B | 18 | GAP-pct-404 | 14.40 | 35.22 | 57.32 | 193.44 | 14.40 | 35.22 | 57.320 | 193.44 |
| 2 | ARM-1 | ARM-1 | B | 19 | GAP-pct-173 | 28.01 | 18.20 | 50.93 | 74.84 | 28.01 | 18.20 | 50.930 | 74.84 |
| 2 | SWPF-05 | GAP-33 | B | 20 | GAP-pct-314 | 119.27 | 12.36 | 350.44 | 161.45 | 119.27 | 12.36 | 350.440 | 161.45 |
| 2 | SWPF-06 | GAP-38ccc | B | 21 | GAP-pct-205 | 68.26 | 61.53 | 104.83 | 267.04 | 68.26 | 61.53 | 104.830 | 267.04 |
| 1 | SWPF-01 | GAP-15ccc | B | 22 | GAP-pct-112 | 117.88 | 229.62 | 376.93 | 699.12 | 117.88 | 229.62 | 376.930 | 699.12 |
| 1 | blank | blank | B | 23 | GAP-pct-346 | < 4.20 | < 1.05 | < 0.21 | < 0.84 | 4.20 | 1.05 | 0.210 | 0.84 |
| 2 | SWPF-05 | GAP-33ccc | B | 24 | GAP-pct-147 | 104.74 | 10.85 | 311.24 | 162.62 | 104.74 | 10.85 | 311.240 | 162.62 |
| . | soln std | | B | 25 | std-B3 | 19.67 | 9.78 | 82.33 | 48.78 | 19.67 | 9.78 | 82.330 | 48.78 |
| . | soln std | | C | 1 | std-C1 | 20.33 | 10.54 | 80.00 | 50.17 | 20.33 | 10.54 | 80.000 | 50.17 |
| 2 | SWPF-05 | GAP-33 | C | 2 | GAP-pct-197 | 118.46 | 13.61 | 337.30 | 159.03 | 118.46 | 13.61 | 337.300 | 159.03 |
| 1 | SWPF-03 | GAP-43 | C | 3 | GAP-pct-088 | 17.16 | 37.87 | 65.88 | 212.64 | 17.16 | 37.87 | 65.880 | 212.64 |
| 2 | blank | blank | C | 4 | GAP-pct-104 | < 4.20 | < 1.05 | < 0.21 | < 0.84 | 4.20 | 1.05 | 0.210 | 0.84 |
| 2 | SWPF-08 | GAP-37ccc | C | 5 | GAP-pct-188 | 13.32 | 3.01 | 23.35 | 68.26 | 13.32 | 3.01 | 23.350 | 68.26 |
| 2 | EA | EA | C | 6 | GAP-pct-187 | 568.84 | 179.13 | 1629.50 | 769.68 | 568.84 | 179.13 | 1629.500 | 769.68 |
| 1 | SWPF-01 | GAP-15ccc | C | 7 | GAP-pct-180 | 132.23 | 212.73 | 374.79 | 727.35 | 132.23 | 212.73 | 374.790 | 727.35 |
| 2 | SWPF-06 | GAP-38ccc | C | 8 | GAP-pct-119 | 68.79 | 63.82 | 104.26 | 260.59 | 68.79 | 63.82 | 104.260 | 260.59 |
| 1 | EA | EA | C | 9 | GAP-pct-394 | 584.49 | 165.96 | 1510.80 | 728.15 | 584.49 | 165.96 | 1510.800 | 728.15 |
| 2 | SWPF-05 | GAP-33ccc | C | 10 | GAP-pct-263 | 109.01 | 11.84 | 321.15 | 162.32 | 109.01 | 11.84 | 321.150 | 162.32 |
| 1 | SWPF-04 | GAP-31 | C | 11 | GAP-pct-073 | 11.13 | 32.82 | 41.65 | 162.87 | 11.13 | 32.82 | 41.650 | 162.87 |
| 1 | ARM-1 | ARM-1 | C | 12 | GAP-pct-224 | 26.41 | 16.98 | 49.31 | 83.29 | 26.41 | 16.98 | 49.310 | 83.29 |
| . | soln std | | C | 13 | std-C2 | 20.18 | 10.35 | 81.11 | 49.34 | 20.18 | 10.35 | 81.110 | 49.34 |
| 2 | SWPF-07 | GAP-21 | C | 14 | GAP-pct-376 | 85.63 | 72.84 | 104.03 | 257.54 | 85.63 | 72.84 | 104.030 | 257.54 |
| 1 | SWPF-02 | GAP-22 | C | 15 | GAP-pct-315 | 14.43 | 37.68 | 61.92 | 194.27 | 14.43 | 37.68 | 61.920 | 194.27 |
| 1 | SWPF-04 | GAP-31ccc | C | 16 | GAP-pct-285 | 10.06 | 33.44 | 45.19 | 167.30 | 10.06 | 33.44 | 45.190 | 167.30 |
| 2 | SWPF-08 | GAP-37 | C | 17 | GAP-pct-017 | 12.75 | 2.84 | 22.76 | 63.25 | 12.75 | 2.84 | 22.760 | 63.25 |
| 1 | SWPF-01 | GAP-15 | C | 18 | GAP-pct-015 | 12.76 | 30.75 | 48.02 | 169.04 | 12.76 | 30.75 | 48.020 | 169.04 |
| 2 | SWPF-07 | GAP-21ccc | C | 19 | GAP-pct-251 | 109.62 | 94.00 | 138.56 | 294.07 | 109.62 | 94.00 | 138.560 | 294.07 |
| 2 | ARM-1 | ARM-1 | C | 20 | GAP-pct-019 | 27.73 | 17.20 | 47.85 | 73.53 | 27.73 | 17.20 | 47.850 | 73.53 |
| 1 | SWPF-02 | GAP-22ccc | C | 21 | GAP-pct-182 | 18.64 | 46.63 | 71.78 | 213.93 | 18.64 | 46.63 | 71.780 | 213.93 |
| 2 | SWPF-06 | GAP-38 | C | 22 | GAP-pct-252 | 67.87 | 66.21 | 104.01 | 271.93 | 67.87 | 66.21 | 104.010 | 271.93 |
| 1 | SWPF-03 | GAP-43ccc | C | 23 | GAP-pct-203 | 30.49 | 94.81 | 104.64 | 336.44 | 30.49 | 94.81 | 104.640 | 336.44 |
| . | soln std | | C | 24 | std-C3 | 19.91 | 10.38 | 81.83 | 49.34 | 19.91 | 10.38 | 81.830 | 49.34 |
| . | soln std | | D | 1 | std-D1 | 19.98 | 10.02 | 80.03 | 50.00 | 19.98 | 10.02 | 80.030 | 50.00 |
| 4 | EA | EA | D | 2 | GAP-pct-208 | 507.81 | 164.31 | 1432.40 | 706.89 | 507.81 | 164.31 | 1432.400 | 706.89 |
| 4 | ARM-1 | ARM-1 | D | 3 | GAP-pct-086 | 24.23 | 17.28 | 48.51 | 80.47 | 24.23 | 17.28 | 48.510 | 80.47 |
| 4 | SWPF-16 | GAP-26 | D | 4 | GAP-pct-043 | 17.65 | 19.47 | 47.40 | 115.47 | 17.65 | 19.47 | 47.400 | 115.47 |
| 3 | SWPF-09 | GAP-44 | D | 5 | GAP-pct-297 | 44.05 | 44.06 | 73.41 | 181.99 | 44.05 | 44.06 | 73.410 | 181.99 |
| 3 | SWPF-12 | GAP-34 | D | 6 | GAP-pct-121 | 12.06 | 35.53 | 39.44 | 149.31 | 12.06 | 35.53 | 39.440 | 149.31 |

Table B1. PCT Measurements for High TiO₂ Glasses (continued)

| Oven Run | SRNL ID | VSL Sample ID | Block | Seq | Lab ID | Values As Received (ar) | | | | Below Detects Set to Detection Limit | | | |
|----------|----------|---------------|-------|-----|-------------|-------------------------|----------|----------|----------|--------------------------------------|----------|----------|----------|
| | | | | | | B (ppm) | Li (ppm) | Na (ppm) | Si (ppm) | B (ppm) | Li (ppm) | Na (ppm) | Si (ppm) |
| 4 | SWPF-15 | GAP-14ccc | D | 7 | GAP-pct-340 | 16.13 | 18.54 | 29.04 | 70.68 | 16.13 | 18.54 | 29.040 | 70.68 |
| 4 | SWPF-13 | GAP-19 | D | 8 | GAP-pct-002 | 10.12 | 26.63 | 37.71 | 116.94 | 10.12 | 26.63 | 37.710 | 116.94 |
| 3 | SWPF-11 | GAP-10ccc | D | 9 | GAP-pct-365 | 37.02 | 3.89 | 139.74 | 134.40 | 37.02 | 3.89 | 139.740 | 134.40 |
| 4 | SWPF-14 | GAP-12 | D | 10 | GAP-pct-140 | 12.63 | 19.11 | 21.81 | 71.96 | 12.63 | 19.11 | 21.810 | 71.96 |
| 4 | SWPF-15 | GAP-14 | D | 11 | GAP-pct-150 | 17.22 | 24.25 | 33.95 | 69.10 | 17.22 | 24.25 | 33.950 | 69.10 |
| 3 | SWPF-10 | GAP-47 | D | 12 | GAP-pct-227 | 37.95 | 5.67 | 104.84 | 78.93 | 37.95 | 5.67 | 104.840 | 78.93 |
| . | soln std | | D | 13 | std-D2 | 19.98 | 10.13 | 80.09 | 49.88 | 19.98 | 10.13 | 80.090 | 49.88 |
| 3 | SWPF-10 | GAP-47ccc | D | 14 | GAP-pct-303 | 24.48 | 3.79 | 73.31 | 75.46 | 24.48 | 3.79 | 73.310 | 75.46 |
| 3 | EA | EA | D | 15 | GAP-pct-367 | 598.52 | 188.52 | 1659.10 | 774.13 | 598.52 | 188.52 | 1659.100 | 774.13 |
| 4 | SWPF-13 | GAP-19ccc | D | 16 | GAP-pct-071 | 11.09 | 26.70 | 37.06 | 112.52 | 11.09 | 26.70 | 37.060 | 112.52 |
| 3 | SWPF-11 | GAP-10 | D | 17 | GAP-pct-316 | 58.49 | 5.36 | 210.07 | 165.42 | 58.49 | 5.36 | 210.070 | 165.42 |
| 3 | blank | blank | D | 18 | GAP-pct-136 | < 4.20 | < 1.05 | < 0.21 | < 0.84 | 4.20 | 1.05 | 0.210 | 0.84 |
| 4 | SWPF-16 | GAP-26ccc | D | 19 | GAP-pct-168 | 13.27 | 17.00 | 43.54 | 103.30 | 13.27 | 17.00 | 43.540 | 103.30 |
| 3 | ARM-1 | ARM-1 | D | 20 | GAP-pct-132 | 23.06 | 17.68 | 51.04 | 73.58 | 23.06 | 17.68 | 51.040 | 73.58 |
| 3 | SWPF-12 | GAP-34ccc | D | 21 | GAP-pct-278 | 26.22 | 92.81 | 72.28 | 265.92 | 26.22 | 92.81 | 72.280 | 265.92 |
| 3 | SWPF-09 | GAP-44ccc | D | 22 | GAP-pct-308 | 29.71 | 35.61 | 59.73 | 145.20 | 29.71 | 35.61 | 59.730 | 145.20 |
| 4 | SWPF-14 | GAP-12ccc | D | 23 | GAP-pct-134 | 11.41 | 16.69 | 21.14 | 64.60 | 11.41 | 16.69 | 21.140 | 64.60 |
| . | soln std | | D | 24 | std-D3 | 19.92 | 10.02 | 80.16 | 49.81 | 19.92 | 10.02 | 80.160 | 49.81 |
| . | soln std | | E | 1 | std-E1 | 19.98 | 10.23 | 80.98 | 51.67 | 19.98 | 10.23 | 80.980 | 51.67 |
| 3 | ARM-1 | ARM-1 | E | 2 | GAP-pct-336 | 24.11 | 17.21 | 49.16 | 79.59 | 24.11 | 17.21 | 49.160 | 79.59 |
| 4 | SWPF-13 | GAP-19 | E | 3 | GAP-pct-155 | 11.16 | 26.79 | 37.29 | 123.18 | 11.16 | 26.79 | 37.290 | 123.18 |
| 3 | blank | blank | E | 4 | GAP-pct-111 | < 4.20 | < 1.05 | < 0.21 | < 0.84 | 4.20 | 1.05 | 0.210 | 0.84 |
| 3 | SWPF-10 | GAP-47ccc | E | 5 | GAP-pct-068 | 25.05 | 3.80 | 73.28 | 80.87 | 25.05 | 3.80 | 73.280 | 80.87 |
| 3 | SWPF-12 | GAP-34 | E | 6 | GAP-pct-098 | 11.13 | 33.76 | 37.01 | 153.09 | 11.13 | 33.76 | 37.010 | 153.09 |
| 4 | EA | EA | E | 7 | GAP-pct-337 | 526.58 | 163.49 | 1419.40 | 707.73 | 526.58 | 163.49 | 1419.400 | 707.73 |
| 4 | SWPF-14 | GAP-12 | E | 8 | GAP-pct-253 | 13.88 | 18.05 | 20.67 | 74.18 | 13.88 | 18.05 | 20.670 | 74.18 |
| 4 | SWPF-13 | GAP-19ccc | E | 9 | GAP-pct-370 | 9.34 | 26.77 | 35.62 | 121.16 | 9.34 | 26.77 | 35.620 | 121.16 |
| 4 | ARM-1 | ARM-1 | E | 10 | GAP-pct-108 | 23.89 | 16.45 | 46.01 | 75.10 | 23.89 | 16.45 | 46.010 | 75.10 |
| 4 | SWPF-16 | GAP-26 | E | 11 | GAP-pct-130 | 15.83 | 18.45 | 43.71 | 110.86 | 15.83 | 18.45 | 43.710 | 110.86 |
| 3 | SWPF-09 | GAP-44 | E | 12 | GAP-pct-294 | 41.45 | 41.30 | 68.33 | 176.29 | 41.45 | 41.30 | 68.330 | 176.29 |
| . | soln std | | E | 13 | std-E2 | 20.05 | 10.08 | 81.30 | 51.01 | 20.05 | 10.08 | 81.300 | 51.01 |
| 4 | SWPF-15 | GAP-14ccc | E | 14 | GAP-pct-032 | 15.25 | 17.98 | 27.26 | 69.42 | 15.25 | 17.98 | 27.260 | 69.42 |
| 4 | blank | blank | E | 15 | GAP-pct-373 | < 4.20 | < 1.05 | < 0.21 | < 0.84 | 4.20 | 1.05 | 0.210 | 0.84 |
| 3 | SWPF-12 | GAP-34ccc | E | 16 | GAP-pct-324 | 26.53 | 89.17 | 68.01 | 263.30 | 26.53 | 89.17 | 68.010 | 263.30 |
| 4 | SWPF-14 | GAP-12ccc | E | 17 | GAP-pct-051 | 11.79 | 15.89 | 20.02 | 70.10 | 11.79 | 15.89 | 20.020 | 70.10 |
| 3 | SWPF-10 | GAP-47 | E | 18 | GAP-pct-325 | 40.89 | 5.79 | 103.07 | 84.15 | 40.89 | 5.79 | 103.070 | 84.15 |
| 4 | SWPF-15 | GAP-14 | E | 19 | GAP-pct-007 | 19.90 | 24.24 | 33.55 | 75.73 | 19.90 | 24.24 | 33.550 | 75.73 |
| 3 | SWPF-11 | GAP-10ccc | E | 20 | GAP-pct-114 | 37.05 | 3.88 | 141.74 | 139.04 | 37.05 | 3.88 | 141.740 | 139.04 |
| 3 | SWPF-09 | GAP-44ccc | E | 21 | GAP-pct-185 | 31.88 | 34.62 | 56.99 | 158.71 | 31.88 | 34.62 | 56.990 | 158.71 |
| 4 | SWPF-16 | GAP-26ccc | E | 22 | GAP-pct-139 | 13.83 | 16.41 | 40.78 | 106.16 | 13.83 | 16.41 | 40.780 | 106.16 |
| 3 | EA | EA | E | 23 | GAP-pct-091 | 651.82 | 195.97 | 1740.30 | 836.15 | 651.82 | 195.97 | 1740.300 | 836.15 |

Table B1. PCT Measurements for High TiO₂ Glasses (continued)

| Oven Run | SRNL ID | VSL Sample ID | Block | Seq | Lab ID | Values As Received (ar) | | | | Below Detects Set to Detection Limit | | | |
|----------|----------|---------------|-------|-----|-------------|-------------------------|----------|----------|----------|--------------------------------------|----------|----------|----------|
| | | | | | | B (ppm) | Li (ppm) | Na (ppm) | Si (ppm) | B (ppm) | Li (ppm) | Na (ppm) | Si (ppm) |
| 3 | SWPF-11 | GAP-10 | E | 24 | GAP-pct-330 | 60.32 | 5.19 | 202.27 | 167.74 | 60.32 | 5.19 | 202.270 | 167.74 |
| . | soln std | | E | 25 | std-E3 | 20.68 | 10.19 | 80.92 | 52.03 | 20.68 | 10.19 | 80.920 | 52.03 |
| . | soln std | | F | 1 | std-F1 | 20.43 | 9.82 | 80.01 | 51.29 | 20.43 | 9.82 | 80.010 | 51.29 |
| 4 | SWPF-14 | GAP-12 | F | 2 | GAP-pct-160 | 15.61 | 20.04 | 22.40 | 81.03 | 15.61 | 20.04 | 22.400 | 81.03 |
| 4 | SWPF-14 | GAP-12ccc | F | 3 | GAP-pct-198 | 12.41 | 16.99 | 21.33 | 72.84 | 12.41 | 16.99 | 21.330 | 72.84 |
| 4 | SWPF-13 | GAP-19ccc | F | 4 | GAP-pct-189 | 9.22 | 27.43 | 36.62 | 121.17 | 9.22 | 27.43 | 36.620 | 121.17 |
| 4 | SWPF-15 | GAP-14 | F | 5 | GAP-pct-029 | 18.93 | 24.10 | 33.28 | 76.08 | 18.93 | 24.10 | 33.280 | 76.08 |
| 4 | SWPF-13 | GAP-19 | F | 6 | GAP-pct-052 | 8.61 | 27.50 | 38.49 | 118.95 | 8.61 | 27.50 | 38.490 | 118.95 |
| 3 | SWPF-09 | GAP-44 | F | 7 | GAP-pct-213 | 41.03 | 43.38 | 72.15 | 183.16 | 41.03 | 43.38 | 72.150 | 183.16 |
| 3 | EA | EA | F | 8 | GAP-pct-350 | 610.59 | 199.66 | 1662.10 | 832.94 | 610.59 | 199.66 | 1662.100 | 832.94 |
| 3 | SWPF-11 | GAP-10 | F | 9 | GAP-pct-334 | 59.62 | 5.66 | 202.40 | 168.54 | 59.62 | 5.66 | 202.400 | 168.54 |
| 4 | EA | EA | F | 10 | GAP-pct-142 | 530.27 | 175.22 | 1537.80 | 713.02 | 530.27 | 175.22 | 1537.800 | 713.02 |
| 4 | SWPF-16 | GAP-26ccc | F | 11 | GAP-pct-042 | 16.61 | 18.77 | 45.33 | 113.08 | 16.61 | 18.77 | 45.330 | 113.08 |
| 3 | SWPF-12 | GAP-34 | F | 12 | GAP-pct-351 | 13.35 | 36.38 | 38.85 | 155.71 | 13.35 | 36.38 | 38.850 | 155.71 |
| . | soln std | | F | 13 | std-F2 | 20.67 | 10.35 | 79.27 | 52.36 | 20.67 | 10.35 | 79.270 | 52.36 |
| 4 | SWPF-16 | GAP-26 | F | 14 | GAP-pct-079 | 17.48 | 19.93 | 46.28 | 113.47 | 17.48 | 19.93 | 46.280 | 113.47 |
| 3 | SWPF-10 | GAP-47 | F | 15 | GAP-pct-206 | 41.23 | 6.12 | 106.09 | 87.61 | 41.23 | 6.12 | 106.090 | 87.61 |
| 4 | blank | blank | F | 16 | GAP-pct-167 | < 4.20 | < 1.05 | < 0.21 | < 0.84 | 4.20 | 1.05 | 0.210 | 0.84 |
| 4 | SWPF-15 | GAP-14ccc | F | 17 | GAP-pct-335 | 15.06 | 19.78 | 29.37 | 71.65 | 15.06 | 19.78 | 29.370 | 71.65 |
| 3 | SWPF-10 | GAP-47ccc | F | 18 | GAP-pct-191 | 25.29 | 4.11 | 75.49 | 79.18 | 25.29 | 4.11 | 75.490 | 79.18 |
| 4 | ARM-1 | ARM-1 | F | 19 | GAP-pct-014 | 20.41 | 16.42 | 44.96 | 74.57 | 20.41 | 16.42 | 44.960 | 74.57 |
| 3 | SWPF-09 | GAP-44ccc | F | 20 | GAP-pct-184 | 32.76 | 37.19 | 60.64 | 160.71 | 32.76 | 37.19 | 60.640 | 160.71 |
| 3 | SWPF-11 | GAP-10ccc | F | 21 | GAP-pct-105 | 39.15 | 4.59 | 149.21 | 146.06 | 39.15 | 4.59 | 149.210 | 146.06 |
| 3 | ARM-1 | ARM-1 | F | 22 | GAP-pct-245 | 26.07 | 19.92 | 54.03 | 86.00 | 26.07 | 19.92 | 54.030 | 86.00 |
| 3 | SWPF-12 | GAP-34ccc | F | 23 | GAP-pct-255 | 26.96 | 97.86 | 73.61 | 271.35 | 26.96 | 97.86 | 73.610 | 271.35 |
| . | soln std | | F | 24 | std-F3 | 19.82 | 10.11 | 81.12 | 50.59 | 19.82 | 10.11 | 81.120 | 50.59 |
| . | soln std | | G | 1 | std-G1 | 20.57 | 10.46 | 81.78 | 50.61 | 20.57 | 10.46 | 81.780 | 50.61 |
| 5 | blank | blank | G | 2 | GAP-pct-279 | < 4.20 | < 1.05 | < 0.21 | < 0.84 | 4.20 | 1.05 | 0.210 | 0.84 |
| 5 | SWPF-19 | GAP-35 | G | 3 | GAP-pct-055 | 10.21 | 6.93 | 72.32 | 98.88 | 10.21 | 6.93 | 72.320 | 98.88 |
| 6 | SWPF-23 | GAP-23ccc | G | 4 | GAP-pct-235 | 19.88 | 8.44 | 96.37 | 100.08 | 19.88 | 8.44 | 96.370 | 100.08 |
| 6 | SWPF-21 | GAP-41ccc | G | 5 | GAP-pct-025 | 12.73 | 9.18 | 111.49 | 111.80 | 12.73 | 9.18 | 111.490 | 111.80 |
| 5 | SWPF-19 | GAP-35ccc | G | 6 | GAP-pct-127 | 9.30 | 6.82 | 67.47 | 93.66 | 9.30 | 6.82 | 67.470 | 93.66 |
| 5 | SWPF-20 | GAP-46ccc | G | 7 | GAP-pct-141 | 11.07 | 19.30 | 57.03 | 104.01 | 11.07 | 19.30 | 57.030 | 104.01 |
| 5 | SWPF-17 | GAP-05 | G | 8 | GAP-pct-239 | 9.65 | 6.28 | 73.47 | 99.61 | 9.65 | 6.28 | 73.470 | 99.61 |
| 5 | SWPF-17 | GAP-05ccc | G | 9 | GAP-pct-166 | 8.18 | 7.26 | 73.62 | 105.21 | 8.18 | 7.26 | 73.620 | 105.21 |
| 5 | SWPF-18 | GAP-29 | G | 10 | GAP-pct-269 | 17.53 | 27.78 | 155.39 | 168.47 | 17.53 | 27.78 | 155.390 | 168.47 |
| 5 | ARM-1 | ARM-1 | G | 11 | GAP-pct-402 | 22.54 | 15.72 | 43.46 | 72.16 | 22.54 | 15.72 | 43.460 | 72.16 |
| 6 | EA | EA | G | 12 | GAP-pct-175 | 595.32 | 196.09 | 1550.10 | 819.39 | 595.32 | 196.09 | 1550.100 | 819.39 |
| . | soln std | | G | 13 | std-G2 | 20.46 | 10.59 | 81.09 | 50.27 | 20.46 | 10.59 | 81.090 | 50.27 |
| 5 | SWPF-18 | GAP-29ccc | G | 14 | GAP-pct-280 | 16.82 | 27.97 | 149.95 | 165.76 | 16.82 | 27.97 | 149.950 | 165.76 |
| 6 | SWPF-22 | GAP-20 | G | 15 | GAP-pct-156 | 22.22 | 8.94 | 108.00 | 100.15 | 22.22 | 8.94 | 108.000 | 100.15 |

Table B1. PCT Measurements for High TiO₂ Glasses (continued)

| Oven Run | SRNL ID | VSL Sample ID | Block | Seq | Lab ID | Values As Received (ar) | | | | Below Detects Set to Detection Limit | | | |
|----------|----------|---------------|-------|-----|-------------|-------------------------|----------|----------|----------|--------------------------------------|----------|----------|----------|
| | | | | | | B (ppm) | Li (ppm) | Na (ppm) | Si (ppm) | B (ppm) | Li (ppm) | Na (ppm) | Si (ppm) |
| 6 | SWPF-21 | GAP-41 | G | 16 | GAP-pct-301 | 14.98 | 8.30 | 112.88 | 111.69 | 14.98 | 8.30 | 112.880 | 111.69 |
| 6 | ARM-1 | ARM-1 | G | 17 | GAP-pct-056 | 24.29 | 17.39 | 46.33 | 72.09 | 24.29 | 17.39 | 46.330 | 72.09 |
| 6 | SWPF-23 | GAP-23 | G | 18 | GAP-pct-093 | 22.99 | 8.04 | 99.04 | 100.37 | 22.99 | 8.04 | 99.040 | 100.37 |
| 6 | SWPF-24 | GAP-42ccc | G | 19 | GAP-pct-143 | 13.18 | 7.64 | 34.35 | 82.06 | 13.18 | 7.64 | 34.350 | 82.06 |
| 6 | SWPF-22 | GAP-20ccc | G | 20 | GAP-pct-257 | 17.78 | 8.89 | 97.42 | 98.51 | 17.78 | 8.89 | 97.420 | 98.51 |
| 5 | SWPF-20 | GAP-46 | G | 21 | GAP-pct-107 | 14.66 | 21.96 | 62.07 | 107.42 | 14.66 | 21.96 | 62.070 | 107.42 |
| 5 | EA | EA | G | 22 | GAP-pct-345 | 600.13 | 191.47 | 1594.30 | 801.85 | 600.13 | 191.47 | 1594.300 | 801.85 |
| 6 | SWPF-24 | GAP-42 | G | 23 | GAP-pct-026 | 13.67 | 7.98 | 33.41 | 74.74 | 13.67 | 7.98 | 33.410 | 74.74 |
| . | soln std | | G | 24 | std-G3 | 20.57 | 10.53 | 81.39 | 50.38 | 20.57 | 10.53 | 81.390 | 50.38 |
| . | soln std | | H | 1 | std-H1 | 20.33 | 10.66 | 81.38 | 49.93 | 20.33 | 10.66 | 81.380 | 49.93 |
| 6 | SWPF-21 | GAP-41 | H | 2 | GAP-pct-183 | 15.40 | 8.41 | 114.67 | 112.37 | 15.40 | 8.41 | 114.670 | 112.37 |
| 5 | SWPF-20 | GAP-46ccc | H | 3 | GAP-pct-084 | 10.44 | 18.67 | 57.84 | 104.76 | 10.44 | 18.67 | 57.840 | 104.76 |
| 5 | SWPF-17 | GAP-05ccc | H | 4 | GAP-pct-288 | 10.00 | 6.93 | 75.51 | 105.72 | 10.00 | 6.93 | 75.510 | 105.72 |
| 6 | ARM-1 | ARM-1 | H | 5 | GAP-pct-243 | 23.13 | 17.31 | 48.17 | 77.29 | 23.13 | 17.31 | 48.170 | 77.29 |
| 5 | SWPF-19 | GAP-35ccc | H | 6 | GAP-pct-237 | 8.62 | 6.74 | 66.88 | 94.48 | 8.62 | 6.74 | 66.880 | 94.48 |
| 5 | SWPF-20 | GAP-46 | H | 7 | GAP-pct-371 | 14.08 | 21.30 | 64.13 | 104.11 | 14.08 | 21.30 | 64.130 | 104.11 |
| 6 | SWPF-22 | GAP-20ccc | H | 8 | GAP-pct-284 | 16.18 | 9.00 | 105.87 | 103.22 | 16.18 | 9.00 | 105.870 | 103.22 |
| 6 | SWPF-22 | GAP-20 | H | 9 | GAP-pct-282 | 20.97 | 9.33 | 114.72 | 110.20 | 20.97 | 9.33 | 114.720 | 110.20 |
| 6 | SWPF-21 | GAP-41ccc | H | 10 | GAP-pct-382 | 12.55 | 9.56 | 113.63 | 117.81 | 12.55 | 9.56 | 113.630 | 117.81 |
| 6 | SWPF-24 | GAP-42 | H | 11 | GAP-pct-268 | 13.68 | 8.92 | 39.20 | 85.95 | 13.68 | 8.92 | 39.200 | 85.95 |
| 6 | blank | blank | H | 12 | GAP-pct-240 | < 4.20 | < 1.05 | < 0.21 | < 0.84 | 4.20 | 1.05 | 0.210 | 0.84 |
| . | soln std | | H | 13 | std-H2 | 21.27 | 10.65 | 80.76 | 51.71 | 21.27 | 10.65 | 80.760 | 51.71 |
| 6 | EA | EA | H | 14 | GAP-pct-306 | 582.76 | 195.27 | 1533.90 | 828.38 | 582.76 | 195.27 | 1533.900 | 828.38 |
| 5 | SWPF-18 | GAP-29 | H | 15 | GAP-pct-030 | 17.47 | 26.06 | 157.27 | 169.41 | 17.47 | 26.06 | 157.270 | 169.41 |
| 6 | SWPF-23 | GAP-23ccc | H | 16 | GAP-pct-292 | 22.94 | 8.40 | 97.22 | 101.22 | 22.94 | 8.40 | 97.220 | 101.22 |
| 6 | SWPF-24 | GAP-42ccc | H | 17 | GAP-pct-057 | 14.67 | 7.69 | 37.99 | 89.66 | 14.67 | 7.69 | 37.990 | 89.66 |
| 5 | SWPF-19 | GAP-35 | H | 18 | GAP-pct-082 | 10.46 | 6.55 | 73.66 | 97.52 | 10.46 | 6.55 | 73.660 | 97.52 |
| 6 | SWPF-23 | GAP-23 | H | 19 | GAP-pct-087 | 19.66 | 7.67 | 99.99 | 97.56 | 19.66 | 7.67 | 99.990 | 97.56 |
| 5 | SWPF-18 | GAP-29ccc | H | 20 | GAP-pct-250 | 16.59 | 27.71 | 148.99 | 165.49 | 16.59 | 27.71 | 148.990 | 165.49 |
| 5 | ARM-1 | ARM-1 | H | 21 | GAP-pct-310 | 22.60 | 15.78 | 43.65 | 72.32 | 22.60 | 15.78 | 43.650 | 72.32 |
| 5 | EA | EA | H | 22 | GAP-pct-067 | 614.51 | 192.50 | 1595.50 | 804.41 | 614.51 | 192.50 | 1595.500 | 804.41 |
| 5 | SWPF-17 | GAP-05 | H | 23 | GAP-pct-053 | 9.49 | 6.12 | 72.21 | 98.74 | 9.49 | 6.12 | 72.210 | 98.74 |
| 5 | blank | blank | H | 24 | GAP-pct-385 | < 4.20 | < 1.05 | < 0.21 | < 0.84 | 4.20 | 1.05 | 0.210 | 0.84 |
| . | soln std | | H | 25 | std-H3 | 21.03 | 10.31 | 81.38 | 50.52 | 21.03 | 10.31 | 81.380 | 50.52 |
| . | soln std | | I | 1 | std-II | 20.57 | 10.52 | 81.21 | 50.66 | 20.57 | 10.52 | 81.210 | 50.66 |
| 6 | SWPF-21 | GAP-41ccc | I | 2 | GAP-pct-165 | 13.21 | 9.04 | 110.50 | 114.26 | 13.21 | 9.04 | 110.500 | 114.26 |
| 6 | SWPF-23 | GAP-23ccc | I | 3 | GAP-pct-161 | 22.16 | 7.93 | 94.11 | 100.58 | 22.16 | 7.93 | 94.110 | 100.58 |
| 6 | SWPF-22 | GAP-20ccc | I | 4 | GAP-pct-339 | 18.19 | 8.27 | 97.24 | 100.55 | 18.19 | 8.27 | 97.240 | 100.55 |
| 6 | SWPF-23 | GAP-23 | I | 5 | GAP-pct-249 | 21.47 | 7.39 | 92.93 | 97.76 | 21.47 | 7.39 | 92.930 | 97.76 |
| 6 | SWPF-22 | GAP-20 | I | 6 | GAP-pct-034 | 19.22 | 8.60 | 109.50 | 102.65 | 19.22 | 8.60 | 109.500 | 102.65 |
| 6 | ARM-1 | ARM-1 | I | 7 | GAP-pct-329 | 23.10 | 16.37 | 45.55 | 74.04 | 23.10 | 16.37 | 45.550 | 74.04 |

Table B1. PCT Measurements for High TiO₂ Glasses (continued)

| Oven Run | SRNL ID | VSL Sample ID | Block | Seq | Lab ID | Values As Received (ar) | | | | Below Detects Set to Detection Limit | | | |
|----------|----------|---------------|-------|-----|-------------|-------------------------|----------|----------|----------|--------------------------------------|----------|----------|----------|
| | | | | | | B (ppm) | Li (ppm) | Na (ppm) | Si (ppm) | B (ppm) | Li (ppm) | Na (ppm) | Si (ppm) |
| 5 | SWPF-19 | GAP-35ccc | I | 8 | GAP-pct-065 | 8.47 | 6.11 | 63.40 | 89.89 | 8.47 | 6.11 | 63.400 | 89.89 |
| 5 | SWPF-17 | GAP-05ccc | I | 9 | GAP-pct-387 | 8.86 | 6.45 | 68.19 | 96.72 | 8.86 | 6.45 | 68.190 | 96.72 |
| 6 | SWPF-21 | GAP-41 | I | 10 | GAP-pct-077 | 15.54 | 8.38 | 115.33 | 113.49 | 15.54 | 8.38 | 115.330 | 113.49 |
| 5 | EA | EA | I | 11 | GAP-pct-389 | 596.97 | 197.81 | 1599.30 | 825.41 | 596.97 | 197.81 | 1599.300 | 825.41 |
| 6 | EA | EA | I | 12 | GAP-pct-038 | 609.76 | 197.69 | 1539.10 | 829.44 | 609.76 | 197.69 | 1539.100 | 829.44 |
| . | soln std | | I | 13 | std-I2 | 20.14 | 10.14 | 80.91 | 50.05 | 20.14 | 10.14 | 80.910 | 50.05 |
| 5 | SWPF-17 | GAP-05 | I | 14 | GAP-pct-403 | 9.78 | 6.18 | 72.55 | 99.68 | 9.78 | 6.18 | 72.550 | 99.68 |
| 6 | SWPF-24 | GAP-42ccc | I | 15 | GAP-pct-291 | 12.61 | 7.24 | 34.53 | 82.09 | 12.61 | 7.24 | 34.530 | 82.09 |
| 6 | blank | blank | I | 16 | GAP-pct-137 | < 4.20 | < 1.05 | < 0.21 | < 0.84 | 4.20 | 1.05 | 0.210 | 0.84 |
| 5 | SWPF-18 | GAP-29 | I | 17 | GAP-pct-196 | 17.39 | 27.01 | 155.18 | 168.99 | 17.39 | 27.01 | 155.180 | 168.99 |
| 5 | SWPF-19 | GAP-35 | I | 18 | GAP-pct-006 | 8.86 | 6.35 | 69.81 | 89.44 | 8.86 | 6.35 | 69.810 | 89.44 |
| 5 | ARM-1 | ARM-1 | I | 19 | GAP-pct-400 | 20.69 | 15.43 | 42.61 | 71.97 | 20.69 | 15.43 | 42.610 | 71.97 |
| 5 | SWPF-20 | GAP-46ccc | I | 20 | GAP-pct-033 | 10.39 | 17.51 | 53.76 | 96.26 | 10.39 | 17.51 | 53.760 | 96.26 |
| 6 | SWPF-24 | GAP-42 | I | 21 | GAP-pct-158 | 12.56 | 7.93 | 34.74 | 77.20 | 12.56 | 7.93 | 34.740 | 77.20 |
| 5 | SWPF-20 | GAP-46 | I | 22 | GAP-pct-170 | 14.94 | 20.59 | 62.20 | 105.21 | 14.94 | 20.59 | 62.200 | 105.21 |
| 5 | SWPF-18 | GAP-29ccc | I | 23 | GAP-pct-244 | 16.97 | 27.84 | 148.72 | 164.52 | 16.97 | 27.84 | 148.720 | 164.52 |
| . | soln std | | I | 24 | std-I3 | 20.45 | 10.62 | 81.09 | 50.30 | 20.45 | 10.62 | 81.090 | 50.30 |
| . | soln std | | J | 1 | std-J1 | 20.15 | 10.48 | 81.13 | 50.52 | 20.15 | 10.48 | 81.130 | 50.52 |
| 7 | ARM-1 | ARM-1 | J | 2 | GAP-pct-162 | 25.24 | 16.45 | 46.20 | 76.62 | 25.24 | 16.45 | 46.200 | 76.62 |
| 8 | EA | EA | J | 3 | GAP-pct-273 | 599.42 | 191.65 | 1564.50 | 817.35 | 599.42 | 191.65 | 1564.500 | 817.35 |
| 8 | SWPF-31 | GAP-30 | J | 4 | GAP-pct-366 | 19.03 | 6.93 | 82.71 | 81.93 | 19.03 | 6.93 | 82.710 | 81.93 |
| 7 | SWPF-25 | GAP-17ccc | J | 5 | GAP-pct-270 | 19.16 | 19.68 | 53.88 | 102.34 | 19.16 | 19.68 | 53.880 | 102.34 |
| 8 | SWPF-31 | GAP-30ccc | J | 6 | GAP-pct-372 | 18.21 | 7.26 | 77.12 | 81.25 | 18.21 | 7.26 | 77.120 | 81.25 |
| 8 | ARM-1 | ARM-1 | J | 7 | GAP-pct-286 | 22.16 | 16.55 | 46.16 | 75.26 | 22.16 | 16.55 | 46.160 | 75.26 |
| 7 | SWPF-26 | GAP-06ccc | J | 8 | GAP-pct-115 | 20.05 | 20.16 | 58.28 | 105.60 | 20.05 | 20.16 | 58.280 | 105.60 |
| 7 | SWPF-25 | GAP-17 | J | 9 | GAP-pct-028 | 20.71 | 21.17 | 59.51 | 103.98 | 20.71 | 21.17 | 59.510 | 103.98 |
| 7 | SWPF-28 | GAP-50 | J | 10 | GAP-pct-358 | 12.91 | 20.86 | 65.40 | 106.00 | 12.91 | 20.86 | 65.400 | 106.00 |
| 7 | SWPF-27 | GAP-24ccc | J | 11 | GAP-pct-242 | 10.58 | 18.03 | 47.81 | 104.32 | 10.58 | 18.03 | 47.810 | 104.32 |
| 7 | SWPF-28 | GAP-50ccc | J | 12 | GAP-pct-070 | 12.42 | 20.77 | 61.46 | 106.74 | 12.42 | 20.77 | 61.460 | 106.74 |
| . | soln std | | J | 13 | std-J2 | 20.06 | 10.34 | 80.56 | 50.57 | 20.06 | 10.34 | 80.560 | 50.57 |
| 7 | SWPF-27 | GAP-24 | J | 14 | GAP-pct-375 | 12.29 | 18.16 | 47.04 | 102.25 | 12.29 | 18.16 | 47.040 | 102.25 |
| 8 | SWPF-29 | GAP-32ccc | J | 15 | GAP-pct-022 | 10.16 | 17.72 | 48.10 | 101.04 | 10.16 | 17.72 | 48.100 | 101.04 |
| 7 | SWPF-26 | GAP-06 | J | 16 | GAP-pct-313 | 23.14 | 21.58 | 65.73 | 113.73 | 23.14 | 21.58 | 65.730 | 113.73 |
| 8 | SWPF-32 | GAP-09 | J | 17 | GAP-pct-222 | 11.29 | 18.30 | 46.54 | 122.70 | 11.29 | 18.30 | 46.540 | 122.70 |
| 8 | SWPF-30 | GAP-16ccc | J | 18 | GAP-pct-008 | 11.66 | 6.06 | 42.68 | 73.90 | 11.66 | 6.06 | 42.680 | 73.90 |
| 7 | blank | blank | J | 19 | GAP-pct-102 | < 4.20 | < 1.05 | < 0.21 | < 0.84 | 4.20 | 1.05 | 0.210 | 0.84 |
| 8 | SWPF-30 | GAP-16 | J | 20 | GAP-pct-120 | 12.94 | 7.52 | 50.17 | 72.32 | 12.94 | 7.52 | 50.170 | 72.32 |
| 7 | EA | EA | J | 21 | GAP-pct-045 | 603.02 | 195.25 | 1628.00 | 834.05 | 603.02 | 195.25 | 1628.000 | 834.05 |
| 8 | SWPF-32 | GAP-09ccc | J | 22 | GAP-pct-296 | 10.21 | 18.47 | 48.28 | 111.66 | 10.21 | 18.47 | 48.280 | 111.66 |
| 8 | SWPF-29 | GAP-32 | J | 23 | GAP-pct-152 | 11.40 | 20.62 | 53.41 | 100.42 | 11.40 | 20.62 | 53.410 | 100.42 |
| . | soln std | | J | 24 | std-J3 | 20.12 | 10.59 | 80.89 | 50.07 | 20.12 | 10.59 | 80.890 | 50.07 |

Table B1. PCT Measurements for High TiO₂ Glasses (continued)

| Oven Run | SRNL ID | VSL Sample ID | Block | Seq | Lab ID | Values As Received (ar) | | | | Below Detects Set to Detection Limit | | | |
|----------|----------|---------------|-------|-----|-------------|-------------------------|----------|----------|----------|--------------------------------------|----------|----------|----------|
| | | | | | | B (ppm) | Li (ppm) | Na (ppm) | Si (ppm) | B (ppm) | Li (ppm) | Na (ppm) | Si (ppm) |
| . | soln std | | K | 1 | std-K1 | 19.90 | 10.37 | 80.89 | 49.97 | 19.90 | 10.37 | 80.890 | 49.97 |
| 7 | SWPF-27 | GAP-24ccc | K | 2 | GAP-pct-179 | 10.83 | 19.39 | 51.51 | 111.20 | 10.83 | 19.39 | 51.510 | 111.20 |
| 8 | blank | blank | K | 3 | GAP-pct-233 | < 4.20 | < 1.05 | < 0.21 | < 0.84 | 4.20 | 1.05 | 0.210 | 0.84 |
| 7 | SWPF-28 | GAP-50 | K | 4 | GAP-pct-266 | 13.71 | 21.25 | 64.08 | 104.66 | 13.71 | 21.25 | 64.080 | 104.66 |
| 8 | EA | EA | K | 5 | GAP-pct-151 | 591.25 | 187.46 | 1616.40 | 814.89 | 591.25 | 187.46 | 1616.400 | 814.89 |
| 7 | SWPF-26 | GAP-06ccc | K | 6 | GAP-pct-209 | 21.78 | 24.00 | 67.47 | 120.83 | 21.78 | 24.00 | 67.470 | 120.83 |
| 8 | SWPF-31 | GAP-30ccc | K | 7 | GAP-pct-144 | 17.98 | 8.52 | 82.94 | 85.72 | 17.98 | 8.52 | 82.940 | 85.72 |
| 8 | SWPF-31 | GAP-30 | K | 8 | GAP-pct-092 | 16.58 | 7.57 | 84.74 | 84.07 | 16.58 | 7.57 | 84.740 | 84.07 |
| 7 | SWPF-25 | GAP-17 | K | 9 | GAP-pct-397 | 20.85 | 23.59 | 63.81 | 112.14 | 20.85 | 23.59 | 63.810 | 112.14 |
| 7 | ARM-1 | ARM-1 | K | 10 | GAP-pct-101 | 22.76 | 17.56 | 46.49 | 74.33 | 22.76 | 17.56 | 46.490 | 74.33 |
| 8 | SWPF-29 | GAP-32 | K | 11 | GAP-pct-295 | 10.37 | 22.04 | 55.79 | 102.85 | 10.37 | 22.04 | 55.790 | 102.85 |
| 7 | blank | blank | K | 12 | GAP-pct-352 | < 4.20 | < 1.05 | < 0.21 | < 0.84 | 4.20 | 1.05 | 0.210 | 0.84 |
| . | soln std | | K | 13 | std-K2 | 20.05 | 10.26 | 80.65 | 50.06 | 20.05 | 10.26 | 80.650 | 50.06 |
| 8 | SWPF-30 | GAP-16 | K | 14 | GAP-pct-074 | 11.71 | 7.62 | 46.70 | 70.17 | 11.71 | 7.62 | 46.700 | 70.17 |
| 8 | SWPF-30 | GAP-16ccc | K | 15 | GAP-pct-302 | 10.67 | 6.38 | 46.07 | 73.86 | 10.67 | 6.38 | 46.070 | 73.86 |
| 7 | SWPF-27 | GAP-24 | K | 16 | GAP-pct-044 | 10.51 | 19.94 | 50.04 | 104.37 | 10.51 | 19.94 | 50.040 | 104.37 |
| 7 | EA | EA | K | 17 | GAP-pct-262 | 618.55 | 193.38 | 1687.70 | 821.12 | 618.55 | 193.38 | 1687.700 | 821.12 |
| 7 | SWPF-26 | GAP-06 | K | 18 | GAP-pct-190 | 20.77 | 20.99 | 63.24 | 101.47 | 20.77 | 20.99 | 63.240 | 101.47 |
| 8 | SWPF-29 | GAP-32ccc | K | 19 | GAP-pct-202 | 10.47 | 19.17 | 50.57 | 97.48 | 10.47 | 19.17 | 50.570 | 97.48 |
| 8 | SWPF-32 | GAP-09ccc | K | 20 | GAP-pct-354 | 10.23 | 20.04 | 50.27 | 121.98 | 10.23 | 20.04 | 50.270 | 121.98 |
| 8 | SWPF-32 | GAP-09 | K | 21 | GAP-pct-110 | 11.52 | 19.77 | 50.08 | 121.29 | 11.52 | 19.77 | 50.080 | 121.29 |
| 7 | SWPF-28 | GAP-50ccc | K | 22 | GAP-pct-258 | 13.89 | 21.67 | 63.73 | 110.73 | 13.89 | 21.67 | 63.730 | 110.73 |
| 8 | ARM-1 | ARM-1 | K | 23 | GAP-pct-305 | 22.92 | 17.84 | 49.52 | 79.73 | 22.92 | 17.84 | 49.520 | 79.73 |
| 7 | SWPF-25 | GAP-17ccc | K | 24 | GAP-pct-128 | 19.72 | 20.94 | 60.67 | 109.18 | 19.72 | 20.94 | 60.670 | 109.18 |
| . | soln std | | K | 25 | std-K3 | 20.11 | 10.29 | 81.31 | 50.09 | 20.11 | 10.29 | 81.310 | 50.09 |
| . | soln std | | L | 1 | std-L1 | 20.02 | 10.27 | 80.96 | 50.44 | 20.02 | 10.27 | 80.960 | 50.44 |
| 7 | EA | EA | L | 2 | GAP-pct-248 | 628.51 | 195.58 | 1686.10 | 841.04 | 628.51 | 195.58 | 1686.100 | 841.04 |
| 8 | EA | EA | L | 3 | GAP-pct-094 | 584.36 | 187.96 | 1697.20 | 819.18 | 584.36 | 187.96 | 1697.200 | 819.18 |
| 8 | ARM-1 | ARM-1 | L | 4 | GAP-pct-220 | 24.92 | 19.02 | 52.32 | 79.36 | 24.92 | 19.02 | 52.320 | 79.36 |
| 7 | SWPF-28 | GAP-50ccc | L | 5 | GAP-pct-348 | 13.56 | 22.28 | 65.19 | 110.52 | 13.56 | 22.28 | 65.190 | 110.52 |
| 7 | SWPF-25 | GAP-17ccc | L | 6 | GAP-pct-332 | 17.51 | 20.70 | 56.06 | 100.45 | 17.51 | 20.70 | 56.060 | 100.45 |
| 8 | SWPF-30 | GAP-16ccc | L | 7 | GAP-pct-194 | 11.73 | 6.33 | 46.92 | 75.64 | 11.73 | 6.33 | 46.920 | 75.64 |
| 7 | SWPF-25 | GAP-17 | L | 8 | GAP-pct-390 | 21.11 | 23.07 | 62.72 | 106.74 | 21.11 | 23.07 | 62.720 | 106.74 |
| 8 | SWPF-29 | GAP-32ccc | L | 9 | GAP-pct-312 | 10.28 | 19.40 | 52.44 | 98.06 | 10.28 | 19.40 | 52.440 | 98.06 |
| 8 | SWPF-31 | GAP-30ccc | L | 10 | GAP-pct-133 | 16.99 | 8.19 | 83.52 | 81.29 | 16.99 | 8.19 | 83.520 | 81.29 |
| 7 | SWPF-26 | GAP-06ccc | L | 11 | GAP-pct-319 | 20.40 | 23.63 | 68.28 | 115.20 | 20.40 | 23.63 | 68.280 | 115.20 |
| 7 | SWPF-26 | GAP-06 | L | 12 | GAP-pct-207 | 21.74 | 22.43 | 68.45 | 109.86 | 21.74 | 22.43 | 68.450 | 109.86 |
| . | soln std | | L | 13 | std-L2 | 20.10 | 10.21 | 81.23 | 50.39 | 20.10 | 10.21 | 81.230 | 50.39 |
| 8 | SWPF-29 | GAP-32 | L | 14 | GAP-pct-149 | 10.87 | 21.23 | 54.62 | 99.48 | 10.87 | 21.23 | 54.620 | 99.48 |
| 7 | SWPF-27 | GAP-24ccc | L | 15 | GAP-pct-261 | 10.28 | 18.91 | 50.29 | 106.73 | 10.28 | 18.91 | 50.290 | 106.73 |
| 8 | SWPF-30 | GAP-16 | L | 16 | GAP-pct-214 | 10.60 | 7.15 | 47.44 | 68.18 | 10.60 | 7.15 | 47.440 | 68.18 |

Table B1. PCT Measurements for High TiO₂ Glasses (continued)

| Oven Run | SRNL ID | VSL Sample ID | Block | Seq | Lab ID | Values As Received (ar) | | | | Below Detects Set to Detection Limit | | | |
|----------|----------|---------------|-------|-----|-------------|-------------------------|----------|----------|----------|--------------------------------------|----------|----------|----------|
| | | | | | | B (ppm) | Li (ppm) | Na (ppm) | Si (ppm) | B (ppm) | Li (ppm) | Na (ppm) | Si (ppm) |
| 8 | SWPF-32 | GAP-09ccc | L | 17 | GAP-pct-063 | 10.30 | 19.58 | 50.09 | 119.55 | 10.30 | 19.58 | 50.090 | 119.55 |
| 8 | SWPF-32 | GAP-09 | L | 18 | GAP-pct-215 | 11.20 | 19.76 | 50.80 | 119.03 | 11.20 | 19.76 | 50.800 | 119.03 |
| 7 | SWPF-28 | GAP-50 | L | 19 | GAP-pct-369 | 12.92 | 21.57 | 67.41 | 103.49 | 12.92 | 21.57 | 67.410 | 103.49 |
| 7 | ARM-1 | ARM-1 | L | 20 | GAP-pct-122 | 23.48 | 18.07 | 49.75 | 73.78 | 23.48 | 18.07 | 49.750 | 73.78 |
| 8 | SWPF-31 | GAP-30 | L | 21 | GAP-pct-123 | 15.78 | 7.26 | 87.94 | 81.54 | 15.78 | 7.26 | 87.940 | 81.54 |
| 7 | SWPF-27 | GAP-24 | L | 22 | GAP-pct-254 | 10.63 | 19.93 | 51.34 | 99.11 | 10.63 | 19.93 | 51.340 | 99.11 |
| 8 | blank | blank | L | 23 | GAP-pct-338 | < 4.20 | < 1.05 | < 0.21 | < 0.84 | 4.20 | 1.05 | 0.210 | 0.84 |
| . | soln std | | L | 24 | std-L3 | 20.26 | 10.29 | 81.24 | 50.13 | 20.26 | 10.29 | 81.240 | 50.13 |
| . | soln std | | M | 1 | std-M1 | 20.18 | 10.34 | 80.91 | 50.51 | 20.18 | 10.34 | 80.910 | 50.51 |
| 9 | SWPF-35 | GAP-03ccc | M | 2 | GAP-pct-177 | 20.83 | 20.10 | 55.93 | 108.70 | 20.83 | 20.10 | 55.930 | 108.70 |
| 9 | SWPF-34 | GAP-36 | M | 3 | GAP-pct-264 | 12.16 | 8.89 | 98.87 | 100.48 | 12.16 | 8.89 | 98.870 | 100.48 |
| 10 | SWPF-39 | GAP-49 | M | 4 | GAP-pct-300 | 15.14 | 20.23 | 117.22 | 147.75 | 15.14 | 20.23 | 117.220 | 147.75 |
| 9 | SWPF-34 | GAP-36ccc | M | 5 | GAP-pct-003 | 11.68 | 9.76 | 96.13 | 100.89 | 11.68 | 9.76 | 96.130 | 100.89 |
| 9 | ARM-1 | ARM-1 | M | 6 | GAP-pct-236 | 28.44 | 18.07 | 48.72 | 80.92 | 28.44 | 18.07 | 48.720 | 80.92 |
| 9 | SWPF-36 | GAP-11 | M | 7 | GAP-pct-401 | 13.42 | 21.11 | 53.52 | 108.29 | 13.42 | 21.11 | 53.520 | 108.29 |
| 10 | SWPF-37 | GAP-07ccc | M | 8 | GAP-pct-361 | 16.27 | 18.61 | 48.19 | 122.73 | 16.27 | 18.61 | 48.190 | 122.73 |
| 10 | SWPF-37 | GAP-07 | M | 9 | GAP-pct-290 | 17.73 | 19.57 | 51.37 | 125.63 | 17.73 | 19.57 | 51.370 | 125.63 |
| 9 | SWPF-36 | GAP-11ccc | M | 10 | GAP-pct-388 | 10.95 | 17.62 | 46.25 | 98.59 | 10.95 | 17.62 | 46.250 | 98.59 |
| 10 | SWPF-40 | GAP-48 | M | 11 | GAP-pct-096 | 16.43 | 16.32 | 80.81 | 91.77 | 16.43 | 16.32 | 80.810 | 91.77 |
| 9 | SWPF-33 | GAP-40 | M | 12 | GAP-pct-145 | 18.70 | 18.75 | 52.02 | 102.23 | 18.70 | 18.75 | 52.020 | 102.23 |
| . | soln std | | M | 13 | std-M2 | 20.30 | 10.39 | 80.43 | 50.31 | 20.30 | 10.39 | 80.430 | 50.31 |
| 10 | SWPF-38 | GAP-13 | M | 14 | GAP-pct-219 | 18.52 | 7.78 | 80.70 | 99.36 | 18.52 | 7.78 | 80.700 | 99.36 |
| 10 | SWPF-38 | GAP-13ccc | M | 15 | GAP-pct-364 | 15.50 | 7.42 | 74.87 | 100.71 | 15.50 | 7.42 | 74.870 | 100.71 |
| 10 | ARM-1 | ARM-1 | M | 16 | GAP-pct-075 | 34.96 | 18.78 | 51.51 | 84.72 | 34.96 | 18.78 | 51.510 | 84.72 |
| 9 | blank | blank | M | 17 | GAP-pct-226 | < 4.20 | < 1.05 | < 0.21 | < 0.84 | 4.20 | 1.05 | 0.210 | 0.84 |
| 9 | SWPF-33 | GAP-40ccc | M | 18 | GAP-pct-018 | 17.55 | 17.55 | 50.53 | 106.71 | 17.55 | 17.55 | 50.530 | 106.71 |
| 9 | SWPF-35 | GAP-03 | M | 19 | GAP-pct-378 | 23.64 | 22.36 | 61.52 | 105.59 | 23.64 | 22.36 | 61.520 | 105.59 |
| 10 | SWPF-39 | GAP-49ccc | M | 20 | GAP-pct-395 | 15.28 | 22.60 | 117.82 | 153.53 | 15.28 | 22.60 | 117.820 | 153.53 |
| 9 | EA | EA | M | 21 | GAP-pct-047 | 610.27 | 209.16 | 1725.70 | 832.42 | 610.27 | 209.16 | 1725.700 | 832.42 |
| 10 | EA | EA | M | 22 | GAP-pct-192 | 564.80 | 201.35 | 1613.40 | 801.06 | 564.80 | 201.35 | 1613.400 | 801.06 |
| 10 | SWPF-40 | GAP-48ccc | M | 23 | GAP-pct-311 | 31.93 | 24.15 | 99.97 | 109.27 | 31.93 | 24.15 | 99.970 | 109.27 |
| . | soln std | | M | 24 | std-M3 | 20.41 | 10.34 | 80.47 | 50.54 | 20.41 | 10.34 | 80.470 | 50.54 |
| . | soln std | | N | 1 | std-N1 | 20.17 | 10.39 | 80.99 | 50.28 | 20.17 | 10.39 | 80.990 | 50.28 |
| 9 | ARM-1 | ARM-1 | N | 2 | GAP-pct-223 | 29.15 | 17.57 | 47.18 | 77.74 | 29.15 | 17.57 | 47.180 | 77.74 |
| 10 | SWPF-40 | GAP-48ccc | N | 3 | GAP-pct-021 | 31.09 | 24.85 | 99.09 | 107.37 | 31.09 | 24.85 | 99.090 | 107.37 |
| 10 | SWPF-38 | GAP-13ccc | N | 4 | GAP-pct-391 | 15.21 | 7.89 | 74.54 | 100.04 | 15.21 | 7.89 | 74.540 | 100.04 |
| 9 | SWPF-33 | GAP-40 | N | 5 | GAP-pct-069 | 18.10 | 18.19 | 51.84 | 102.02 | 18.10 | 18.19 | 51.840 | 102.02 |
| 9 | EA | EA | N | 6 | GAP-pct-265 | 601.47 | 209.77 | 1679.00 | 839.60 | 601.47 | 209.77 | 1679.000 | 839.60 |
| 10 | SWPF-39 | GAP-49 | N | 7 | GAP-pct-309 | 15.21 | 20.65 | 117.79 | 148.14 | 15.21 | 20.65 | 117.790 | 148.14 |
| 10 | SWPF-37 | GAP-07ccc | N | 8 | GAP-pct-089 | 15.33 | 17.60 | 45.67 | 117.93 | 15.33 | 17.60 | 45.670 | 117.93 |
| 9 | SWPF-34 | GAP-36 | N | 9 | GAP-pct-221 | 12.09 | 8.99 | 99.73 | 100.09 | 12.09 | 8.99 | 99.730 | 100.09 |

Table B1. PCT Measurements for High TiO₂ Glasses (continued)

| Oven Run | SRNL ID | VSL Sample ID | Block | Seq | Lab ID | Values As Received (ar) | | | | Below Detects Set to Detection Limit | | | |
|----------|----------|---------------|-------|-----|-------------|-------------------------|----------|----------|----------|--------------------------------------|----------|----------|----------|
| | | | | | | B (ppm) | Li (ppm) | Na (ppm) | Si (ppm) | B (ppm) | Li (ppm) | Na (ppm) | Si (ppm) |
| 10 | SWPF-38 | GAP-13 | N | 10 | GAP-pct-020 | 18.14 | 8.23 | 84.86 | 99.68 | 18.14 | 8.23 | 84.860 | 99.68 |
| 10 | SWPF-40 | GAP-48 | N | 11 | GAP-pct-229 | 16.20 | 16.03 | 80.02 | 91.28 | 16.20 | 16.03 | 80.020 | 91.28 |
| 9 | SWPF-34 | GAP-36ccc | N | 12 | GAP-pct-377 | 11.24 | 9.66 | 95.54 | 100.57 | 11.24 | 9.66 | 95.540 | 100.57 |
| . | soln std | | N | 13 | std-N2 | 20.28 | 10.37 | 81.03 | 50.38 | 20.28 | 10.37 | 81.030 | 50.38 |
| 9 | SWPF-36 | GAP-11ccc | N | 14 | GAP-pct-138 | 10.04 | 17.32 | 45.46 | 94.30 | 10.04 | 17.32 | 45.460 | 94.30 |
| 10 | blank | blank | N | 15 | GAP-pct-357 | < 4.20 | < 1.05 | < 0.21 | < 0.84 | 4.20 | 1.05 | 0.210 | 0.84 |
| 9 | blank | blank | N | 16 | GAP-pct-217 | < 4.20 | < 1.05 | < 0.21 | < 0.84 | 4.20 | 1.05 | 0.210 | 0.84 |
| 9 | SWPF-35 | GAP-03ccc | N | 17 | GAP-pct-024 | 19.97 | 20.05 | 54.99 | 107.16 | 19.97 | 20.05 | 54.990 | 107.16 |
| 10 | SWPF-39 | GAP-49ccc | N | 18 | GAP-pct-181 | 13.49 | 21.68 | 111.81 | 148.83 | 13.49 | 21.68 | 111.810 | 148.83 |
| 9 | SWPF-36 | GAP-11 | N | 19 | GAP-pct-118 | 13.14 | 20.96 | 52.80 | 107.98 | 13.14 | 20.96 | 52.800 | 107.98 |
| 9 | SWPF-33 | GAP-40ccc | N | 20 | GAP-pct-231 | 17.00 | 17.43 | 50.18 | 105.76 | 17.00 | 17.43 | 50.180 | 105.76 |
| 10 | EA | EA | N | 21 | GAP-pct-005 | 575.70 | 203.95 | 1569.40 | 803.12 | 575.70 | 203.95 | 1569.400 | 803.12 |
| 9 | SWPF-35 | GAP-03 | N | 22 | GAP-pct-399 | 22.59 | 22.45 | 61.63 | 106.68 | 22.59 | 22.45 | 61.630 | 106.68 |
| 10 | SWPF-37 | GAP-07 | N | 23 | GAP-pct-218 | 16.90 | 19.43 | 50.73 | 126.03 | 16.90 | 19.43 | 50.730 | 126.03 |
| 10 | ARM-1 | ARM-1 | N | 24 | GAP-pct-186 | 34.33 | 18.71 | 50.31 | 84.16 | 34.33 | 18.71 | 50.310 | 84.16 |
| . | soln std | | N | 25 | std-N3 | 20.23 | 10.49 | 81.67 | 50.10 | 20.23 | 10.49 | 81.670 | 50.10 |
| . | soln std | | O | 1 | std-O1 | 20.24 | 10.21 | 80.87 | 50.33 | 20.24 | 10.21 | 80.870 | 50.33 |
| 9 | SWPF-34 | GAP-36 | O | 2 | GAP-pct-293 | 12.21 | 8.80 | 98.02 | 100.15 | 12.21 | 8.80 | 98.020 | 100.15 |
| 9 | SWPF-35 | GAP-03 | O | 3 | GAP-pct-267 | 23.54 | 22.17 | 61.04 | 105.60 | 23.54 | 22.17 | 61.040 | 105.60 |
| 10 | SWPF-39 | GAP-49ccc | O | 4 | GAP-pct-386 | 13.97 | 21.88 | 112.49 | 148.14 | 13.97 | 21.88 | 112.490 | 148.14 |
| 10 | SWPF-38 | GAP-13ccc | O | 5 | GAP-pct-095 | 15.13 | 7.61 | 74.60 | 100.01 | 15.13 | 7.61 | 74.600 | 100.01 |
| 9 | SWPF-35 | GAP-03ccc | O | 6 | GAP-pct-368 | 17.95 | 17.59 | 49.61 | 94.11 | 17.95 | 17.59 | 49.610 | 94.11 |
| 9 | SWPF-36 | GAP-11ccc | O | 7 | GAP-pct-247 | 10.96 | 18.50 | 47.51 | 99.89 | 10.96 | 18.50 | 47.510 | 99.89 |
| 10 | ARM-1 | ARM-1 | O | 8 | GAP-pct-343 | 34.24 | 18.95 | 50.65 | 84.02 | 34.24 | 18.95 | 50.650 | 84.02 |
| 10 | SWPF-37 | GAP-07 | O | 9 | GAP-pct-076 | 17.38 | 19.28 | 50.08 | 124.30 | 17.38 | 19.28 | 50.080 | 124.30 |
| 9 | ARM-1 | ARM-1 | O | 10 | GAP-pct-344 | 29.16 | 17.35 | 48.19 | 77.16 | 29.16 | 17.35 | 48.190 | 77.16 |
| 10 | SWPF-39 | GAP-49 | O | 11 | GAP-pct-323 | 14.98 | 20.39 | 117.87 | 146.33 | 14.98 | 20.39 | 117.870 | 146.33 |
| 10 | SWPF-40 | GAP-48 | O | 12 | GAP-pct-234 | 16.55 | 16.27 | 80.06 | 90.94 | 16.55 | 16.27 | 80.060 | 90.94 |
| . | soln std | | O | 13 | std-O2 | 20.14 | 10.33 | 81.01 | 50.23 | 20.14 | 10.33 | 81.010 | 50.23 |
| 9 | SWPF-34 | GAP-36ccc | O | 14 | GAP-pct-210 | 10.96 | 8.78 | 89.25 | 93.51 | 10.96 | 8.78 | 89.250 | 93.51 |
| 9 | EA | EA | O | 15 | GAP-pct-298 | 663.12 | 218.68 | 1793.20 | 867.30 | 663.12 | 218.68 | 1793.200 | 867.30 |
| 9 | SWPF-33 | GAP-40 | O | 16 | GAP-pct-083 | 18.41 | 18.28 | 51.91 | 101.98 | 18.41 | 18.28 | 51.910 | 101.98 |
| 10 | blank | blank | O | 17 | GAP-pct-200 | < 4.20 | < 1.05 | < 0.21 | < 0.84 | 4.20 | 1.05 | 0.210 | 0.84 |
| 9 | SWPF-33 | GAP-40ccc | O | 18 | GAP-pct-171 | 16.94 | 17.25 | 50.02 | 103.48 | 16.94 | 17.25 | 50.020 | 103.48 |
| 10 | SWPF-38 | GAP-13 | O | 19 | GAP-pct-230 | 18.26 | 8.53 | 85.69 | 100.99 | 18.26 | 8.53 | 85.690 | 100.99 |
| 10 | SWPF-37 | GAP-07ccc | O | 20 | GAP-pct-064 | 15.82 | 18.36 | 47.91 | 123.32 | 15.82 | 18.36 | 47.910 | 123.32 |
| 10 | EA | EA | O | 21 | GAP-pct-035 | 578.62 | 203.57 | 1650.30 | 811.97 | 578.62 | 203.57 | 1650.300 | 811.97 |
| 10 | SWPF-40 | GAP-48ccc | O | 22 | GAP-pct-274 | 31.04 | 24.95 | 101.00 | 109.94 | 31.04 | 24.95 | 101.000 | 109.94 |
| 9 | SWPF-36 | GAP-11 | O | 23 | GAP-pct-153 | 13.08 | 21.07 | 52.36 | 106.11 | 13.08 | 21.07 | 52.360 | 106.11 |
| . | soln std | | O | 24 | std-O3 | 20.29 | 10.42 | 81.08 | 50.05 | 20.29 | 10.42 | 81.080 | 50.05 |
| . | soln std | | P | 1 | std-P1 | 20.23 | 10.46 | 80.98 | 50.38 | 20.23 | 10.46 | 80.980 | 50.38 |

Table B1. PCT Measurements for High TiO₂ Glasses (continued)

| Oven Run | SRNL ID | VSL Sample ID | Block | Seq | Lab ID | Values As Received (ar) | | | | Below Detects Set to Detection Limit | | | |
|----------|----------|---------------|-------|-----|-------------|-------------------------|----------|----------|----------|--------------------------------------|----------|----------|----------|
| | | | | | | B (ppm) | Li (ppm) | Na (ppm) | Si (ppm) | B (ppm) | Li (ppm) | Na (ppm) | Si (ppm) |
| 11 | SWPF-41 | GAP-04ccc | P | 2 | GAP-pct-216 | 20.65 | 25.35 | 76.20 | 138.14 | 20.65 | 25.35 | 76.200 | 138.14 |
| 11 | blank | blank | P | 3 | GAP-pct-041 | < 4.20 | < 1.05 | < 0.21 | < 0.84 | 4.20 | 1.05 | 0.210 | 0.84 |
| 11 | EA | EA | P | 4 | GAP-pct-326 | 555.63 | 198.61 | 1560.70 | 824.99 | 555.63 | 198.61 | 1560.700 | 824.99 |
| 11 | SWPF-43 | GAP-28 | P | 5 | GAP-pct-333 | 16.47 | 24.81 | 87.34 | 138.46 | 16.47 | 24.81 | 87.340 | 138.46 |
| 11 | SWPF-42 | GAP-27 | P | 6 | GAP-pct-109 | 12.78 | 6.52 | 82.07 | 109.90 | 12.78 | 6.52 | 82.070 | 109.90 |
| 12 | SWPF-46 | GAP-39ccc | P | 7 | GAP-pct-211 | 13.07 | 11.67 | 105.66 | 117.53 | 13.07 | 11.67 | 105.660 | 117.53 |
| 11 | SWPF-44 | GAP-01ccc | P | 8 | GAP-pct-331 | 12.58 | 17.51 | 51.71 | 112.81 | 12.58 | 17.51 | 51.710 | 112.81 |
| 12 | SWPF-46 | GAP-39 | P | 9 | GAP-pct-349 | 12.44 | 11.46 | 113.13 | 122.31 | 12.44 | 11.46 | 113.130 | 122.31 |
| 12 | EA | EA | P | 10 | GAP-pct-276 | 624.26 | 197.81 | 1686.70 | 849.87 | 624.26 | 197.81 | 1686.700 | 849.87 |
| 12 | SWPF-45 | GAP-08 | P | 11 | GAP-pct-099 | 10.04 | 6.27 | 60.67 | 88.31 | 10.04 | 6.27 | 60.670 | 88.31 |
| 11 | ARM-1 | ARM-1 | P | 12 | GAP-pct-066 | 21.84 | 15.94 | 43.12 | 74.96 | 21.84 | 15.94 | 43.120 | 74.96 |
| . | soln std | | P | 13 | std-P2 | 20.21 | 10.26 | 80.73 | 50.14 | 20.21 | 10.26 | 80.730 | 50.14 |
| 11 | SWPF-42 | GAP-27ccc | P | 14 | GAP-pct-031 | 12.05 | 7.02 | 79.04 | 107.76 | 12.05 | 7.02 | 79.040 | 107.76 |
| 12 | SWPF-45 | GAP-08ccc | P | 15 | GAP-pct-103 | 9.90 | 6.21 | 60.00 | 90.47 | 9.90 | 6.21 | 60.000 | 90.47 |
| 11 | SWPF-44 | GAP-01 | P | 16 | GAP-pct-154 | 15.92 | 18.89 | 55.43 | 113.80 | 15.92 | 18.89 | 55.430 | 113.80 |
| 11 | SWPF-43 | GAP-28ccc | P | 17 | GAP-pct-359 | 14.88 | 24.67 | 84.19 | 141.04 | 14.88 | 24.67 | 84.190 | 141.04 |
| 11 | SWPF-41 | GAP-04 | P | 18 | GAP-pct-004 | 18.62 | 21.84 | 70.97 | 123.41 | 18.62 | 21.84 | 70.970 | 123.41 |
| 12 | ARM-1 | ARM-1 | P | 19 | GAP-pct-174 | 20.97 | 15.65 | 42.31 | 72.03 | 20.97 | 15.65 | 42.310 | 72.03 |
| 12 | SWPF-47 | GAP-45 | P | 20 | GAP-pct-059 | 15.99 | 13.98 | 75.94 | 93.93 | 15.99 | 13.98 | 75.940 | 93.93 |
| 12 | SWPF-47 | GAP-45ccc | P | 21 | GAP-pct-241 | 14.02 | 13.57 | 70.49 | 94.44 | 14.02 | 13.57 | 70.490 | 94.44 |
| . | soln std | | P | 22 | std-P3 | 20.17 | 10.14 | 80.91 | 50.35 | 20.17 | 10.14 | 80.910 | 50.35 |
| . | soln std | | Q | 1 | std-Q1 | 20.30 | 10.36 | 81.19 | 50.28 | 20.30 | 10.36 | 81.190 | 50.28 |
| 12 | SWPF-46 | GAP-39ccc | Q | 2 | GAP-pct-148 | 13.28 | 11.85 | 106.82 | 118.78 | 13.28 | 11.85 | 106.820 | 118.78 |
| 12 | blank | blank | Q | 3 | GAP-pct-393 | < 4.20 | < 1.05 | < 0.21 | < 0.84 | 4.20 | 1.05 | 0.210 | 0.84 |
| 11 | SWPF-42 | GAP-27ccc | Q | 4 | GAP-pct-304 | 11.87 | 6.91 | 76.67 | 106.58 | 11.87 | 6.91 | 76.670 | 106.58 |
| 12 | SWPF-46 | GAP-39 | Q | 5 | GAP-pct-100 | 12.94 | 10.85 | 107.77 | 113.22 | 12.94 | 10.85 | 107.770 | 113.22 |
| 11 | blank | blank | Q | 6 | GAP-pct-113 | < 4.20 | < 1.05 | < 0.21 | < 0.84 | 4.20 | 1.05 | 0.210 | 0.84 |
| 11 | SWPF-43 | GAP-28ccc | Q | 7 | GAP-pct-392 | 15.34 | 24.04 | 81.35 | 136.14 | 15.34 | 24.04 | 81.350 | 136.14 |
| 12 | EA | EA | Q | 8 | GAP-pct-023 | 611.45 | 196.86 | 1699.20 | 849.24 | 611.45 | 196.86 | 1699.200 | 849.24 |
| 12 | SWPF-45 | GAP-08ccc | Q | 9 | GAP-pct-256 | 9.86 | 6.50 | 61.68 | 91.37 | 9.86 | 6.50 | 61.680 | 91.37 |
| 11 | SWPF-44 | GAP-01ccc | Q | 10 | GAP-pct-009 | 14.20 | 17.99 | 52.74 | 111.57 | 14.20 | 17.99 | 52.740 | 111.57 |
| 12 | SWPF-47 | GAP-45ccc | Q | 11 | GAP-pct-060 | 14.75 | 14.00 | 72.67 | 97.69 | 14.75 | 14.00 | 72.670 | 97.69 |
| 11 | EA | EA | Q | 12 | GAP-pct-260 | 542.12 | 193.24 | 1521.00 | 832.87 | 542.12 | 193.24 | 1521.000 | 832.87 |
| . | soln std | | Q | 13 | std-Q2 | 20.08 | 10.25 | 80.64 | 50.12 | 20.08 | 10.25 | 80.640 | 50.12 |
| 12 | SWPF-47 | GAP-45 | Q | 14 | GAP-pct-232 | 16.34 | 14.23 | 78.20 | 94.89 | 16.34 | 14.23 | 78.200 | 94.89 |
| 11 | SWPF-44 | GAP-01 | Q | 15 | GAP-pct-049 | 15.80 | 19.19 | 56.47 | 113.60 | 15.80 | 19.19 | 56.470 | 113.60 |
| 11 | SWPF-42 | GAP-27 | Q | 16 | GAP-pct-097 | 13.41 | 6.65 | 81.33 | 109.84 | 13.41 | 6.65 | 81.330 | 109.84 |
| 11 | ARM-1 | ARM-1 | Q | 17 | GAP-pct-050 | 22.19 | 16.44 | 43.84 | 74.89 | 22.19 | 16.44 | 43.840 | 74.89 |
| 12 | ARM-1 | ARM-1 | Q | 18 | GAP-pct-146 | 22.75 | 16.46 | 44.99 | 72.34 | 22.75 | 16.46 | 44.990 | 72.34 |
| 11 | SWPF-41 | GAP-04ccc | Q | 19 | GAP-pct-228 | 20.64 | 25.68 | 76.39 | 136.58 | 20.64 | 25.68 | 76.390 | 136.58 |
| 11 | SWPF-41 | GAP-04 | Q | 20 | GAP-pct-159 | 19.67 | 23.36 | 73.54 | 127.42 | 19.67 | 23.36 | 73.540 | 127.42 |

Table B1. PCT Measurements for High TiO₂ Glasses (continued)

| Oven Run | SRNL ID | VSL Sample ID | Block | Seq | Lab ID | Values As Received (ar) | | | | Below Detects Set to Detection Limit | | | |
|----------|----------|---------------|-------|-----|-------------|-------------------------|----------|----------|----------|--------------------------------------|----------|----------|----------|
| | | | | | | B (ppm) | Li (ppm) | Na (ppm) | Si (ppm) | B (ppm) | Li (ppm) | Na (ppm) | Si (ppm) |
| 12 | SWPF-45 | GAP-08 | Q | 21 | GAP-pct-383 | 10.44 | 6.27 | 60.71 | 87.65 | 10.44 | 6.27 | 60.710 | 87.65 |
| 11 | SWPF-43 | GAP-28 | Q | 22 | GAP-pct-259 | 16.67 | 24.52 | 85.41 | 136.25 | 16.67 | 24.52 | 85.410 | 136.25 |
| . | soln std | | Q | 23 | std-Q3 | 20.15 | 10.18 | 80.83 | 50.16 | 20.15 | 10.18 | 80.830 | 50.16 |
| . | soln std | | R | 1 | std-R1 | 20.31 | 10.40 | 80.97 | 50.50 | 20.31 | 10.40 | 80.970 | 50.50 |
| 12 | SWPF-45 | GAP-08ccc | R | 2 | GAP-pct-106 | 9.98 | 6.17 | 60.55 | 90.39 | 9.98 | 6.17 | 60.550 | 90.39 |
| 11 | EA | EA | R | 3 | GAP-pct-027 | 543.29 | 193.05 | 1515.40 | 835.12 | 543.29 | 193.05 | 1515.400 | 835.12 |
| 12 | EA | EA | R | 4 | GAP-pct-062 | 607.59 | 195.63 | 1672.60 | 848.36 | 607.59 | 195.63 | 1672.600 | 848.36 |
| 11 | SWPF-42 | GAP-27ccc | R | 5 | GAP-pct-225 | 11.96 | 6.94 | 77.11 | 108.39 | 11.96 | 6.94 | 77.110 | 108.39 |
| 11 | SWPF-41 | GAP-04 | R | 6 | GAP-pct-040 | 19.28 | 22.90 | 71.99 | 125.08 | 19.28 | 22.90 | 71.990 | 125.08 |
| 11 | SWPF-44 | GAP-01 | R | 7 | GAP-pct-318 | 16.10 | 18.63 | 55.86 | 112.34 | 16.10 | 18.63 | 55.860 | 112.34 |
| 11 | SWPF-43 | GAP-28 | R | 8 | GAP-pct-238 | 17.30 | 23.88 | 84.91 | 135.04 | 17.30 | 23.88 | 84.910 | 135.04 |
| 12 | SWPF-45 | GAP-08 | R | 9 | GAP-pct-246 | 10.82 | 6.16 | 60.44 | 87.31 | 10.82 | 6.16 | 60.440 | 87.31 |
| 12 | ARM-1 | ARM-1 | R | 10 | GAP-pct-321 | 22.16 | 15.95 | 44.11 | 72.83 | 22.16 | 15.95 | 44.110 | 72.83 |
| 11 | SWPF-42 | GAP-27 | R | 11 | GAP-pct-036 | 13.11 | 6.24 | 80.95 | 108.11 | 13.11 | 6.24 | 80.950 | 108.11 |
| 11 | SWPF-41 | GAP-04ccc | R | 12 | GAP-pct-355 | 20.02 | 24.83 | 73.57 | 132.59 | 20.02 | 24.83 | 73.570 | 132.59 |
| . | soln std | | R | 13 | std-R2 | 20.18 | 10.19 | 80.58 | 50.55 | 20.18 | 10.19 | 80.580 | 50.55 |
| 11 | SWPF-43 | GAP-28ccc | R | 14 | GAP-pct-193 | 15.96 | 23.81 | 81.18 | 135.42 | 15.96 | 23.81 | 81.180 | 135.42 |
| 11 | SWPF-44 | GAP-01ccc | R | 15 | GAP-pct-129 | 14.98 | 18.44 | 53.57 | 113.90 | 14.98 | 18.44 | 53.570 | 113.90 |
| 12 | SWPF-47 | GAP-45ccc | R | 16 | GAP-pct-013 | 14.59 | 13.79 | 70.90 | 93.91 | 14.59 | 13.79 | 70.900 | 93.91 |
| 12 | blank | blank | R | 17 | GAP-pct-178 | < 4.20 | < 1.05 | < 0.21 | < 0.84 | 4.20 | 1.05 | 0.210 | 0.84 |
| 12 | SWPF-46 | GAP-39ccc | R | 18 | GAP-pct-125 | 13.14 | 11.74 | 105.68 | 117.49 | 13.14 | 11.74 | 105.680 | 117.49 |
| 11 | ARM-1 | ARM-1 | R | 19 | GAP-pct-058 | 22.53 | 16.30 | 43.82 | 75.26 | 22.53 | 16.30 | 43.820 | 75.26 |
| 12 | SWPF-46 | GAP-39 | R | 20 | GAP-pct-016 | 12.91 | 11.23 | 108.54 | 114.52 | 12.91 | 11.23 | 108.540 | 114.52 |
| 12 | SWPF-47 | GAP-45 | R | 21 | GAP-pct-135 | 16.69 | 14.22 | 77.48 | 94.59 | 16.69 | 14.22 | 77.480 | 94.59 |
| . | soln std | | R | 22 | std-R3 | 20.10 | 10.13 | 80.69 | 50.38 | 20.10 | 10.13 | 80.690 | 50.38 |
| . | soln std | | S | 1 | std-S1 | 20.22 | 10.26 | 81.01 | 50.51 | 20.22 | 10.26 | 81.010 | 50.51 |
| 13 | SWPF-50 | GAP-18 | S | 2 | GAP-pct-117 | 14.97 | 22.34 | 79.88 | 107.67 | 14.97 | 22.34 | 79.880 | 107.67 |
| 13 | SWPF-48 | GAP-25ccc | S | 3 | GAP-pct-176 | 12.29 | 10.92 | 52.65 | 83.09 | 12.29 | 10.92 | 52.650 | 83.09 |
| 13 | SWPF-49 | GAP-02ccc | S | 4 | GAP-pct-328 | 22.23 | 14.00 | 115.51 | 125.40 | 22.23 | 14.00 | 115.510 | 125.40 |
| 13 | SWPF-48 | GAP-25 | S | 5 | GAP-pct-362 | 14.25 | 11.41 | 57.27 | 85.25 | 14.25 | 11.41 | 57.270 | 85.25 |
| 13 | ARM-1 | ARM-1 | S | 6 | GAP-pct-164 | 21.75 | 16.65 | 44.98 | 77.20 | 21.75 | 16.65 | 44.980 | 77.20 |
| . | soln std | | S | 7 | std-S2 | 20.38 | 10.26 | 80.70 | 50.13 | 20.38 | 10.26 | 80.700 | 50.13 |
| 13 | SWPF-50 | GAP-18ccc | S | 8 | GAP-pct-363 | 26.94 | 35.75 | 100.18 | 136.23 | 26.94 | 35.75 | 100.180 | 136.23 |
| 13 | blank | blank | S | 9 | GAP-pct-001 | < 4.20 | < 1.05 | < 0.21 | < 0.84 | 4.20 | 1.05 | 0.210 | 0.84 |
| 13 | EA | EA | S | 10 | GAP-pct-271 | 569.04 | 175.39 | 1593.20 | 754.22 | 569.04 | 175.39 | 1593.200 | 754.22 |
| 13 | SWPF-49 | GAP-02 | S | 11 | GAP-pct-347 | 20.88 | 12.67 | 115.80 | 119.77 | 20.88 | 12.67 | 115.800 | 119.77 |
| . | soln std | | S | 12 | std-S3 | 20.03 | 10.14 | 80.34 | 50.15 | 20.03 | 10.14 | 80.340 | 50.15 |
| . | soln std | | T | 13 | std-T1 | 20.30 | 10.29 | 81.20 | 50.42 | 20.30 | 10.29 | 81.200 | 50.42 |
| 13 | ARM-1 | ARM-1 | T | 14 | GAP-pct-275 | 22.63 | 16.84 | 46.00 | 78.79 | 22.63 | 16.84 | 46.000 | 78.79 |
| 13 | SWPF-50 | GAP-18ccc | T | 15 | GAP-pct-360 | 26.51 | 35.31 | 99.24 | 132.22 | 26.51 | 35.31 | 99.240 | 132.22 |
| 13 | SWPF-49 | GAP-02ccc | T | 16 | GAP-pct-048 | 22.48 | 13.72 | 111.07 | 121.52 | 22.48 | 13.72 | 111.070 | 121.52 |

Table B1. PCT Measurements for High TiO₂ Glasses (continued)

| Oven Run | SRNL ID | VSL Sample ID | Block | Seq | Lab ID | Values As Received (ar) | | | | Below Detects Set to Detection Limit | | | |
|----------|----------|---------------|-------|-----|-------------|-------------------------|----------|----------|----------|--------------------------------------|----------|----------|----------|
| | | | | | | B (ppm) | Li (ppm) | Na (ppm) | Si (ppm) | B (ppm) | Li (ppm) | Na (ppm) | Si (ppm) |
| 13 | SWPF-48 | GAP-25ccc | T | 17 | GAP-pct-124 | 13.82 | 10.83 | 52.77 | 85.18 | 13.82 | 10.83 | 52.770 | 85.18 |
| 13 | SWPF-49 | GAP-02 | T | 18 | GAP-pct-126 | 22.83 | 12.98 | 117.52 | 123.90 | 22.83 | 12.98 | 117.520 | 123.90 |
| . | soln std | | T | 19 | std-T2 | 20.18 | 10.13 | 80.05 | 50.02 | 20.18 | 10.13 | 80.050 | 50.02 |
| 13 | EA | EA | T | 20 | GAP-pct-299 | 570.76 | 173.48 | 1594.80 | 772.55 | 570.76 | 173.48 | 1594.800 | 772.55 |
| 13 | SWPF-50 | GAP-18 | T | 21 | GAP-pct-374 | 15.06 | 21.78 | 76.67 | 103.22 | 15.06 | 21.78 | 76.670 | 103.22 |
| 13 | SWPF-48 | GAP-25 | T | 22 | GAP-pct-272 | 15.57 | 11.23 | 54.61 | 85.48 | 15.57 | 11.23 | 54.610 | 85.48 |
| . | soln std | | T | 23 | std-T3 | 20.13 | 10.02 | 80.39 | 50.23 | 20.13 | 10.02 | 80.390 | 50.23 |
| . | soln std | | U | 1 | std-U1 | 20.22 | 10.16 | 80.65 | 50.07 | 20.22 | 10.16 | 80.650 | 50.07 |
| 13 | SWPF-49 | GAP-02ccc | U | 2 | GAP-pct-195 | 22.17 | 13.84 | 111.90 | 121.32 | 22.17 | 13.84 | 111.900 | 121.32 |
| 13 | SWPF-50 | GAP-18 | U | 3 | GAP-pct-169 | 15.62 | 22.25 | 79.18 | 105.19 | 15.62 | 22.25 | 79.180 | 105.19 |
| 13 | EA | EA | U | 4 | GAP-pct-172 | 572.22 | 171.98 | 1599.20 | 755.13 | 572.22 | 171.98 | 1599.200 | 755.13 |
| 13 | blank | blank | U | 5 | GAP-pct-163 | < 4.20 | < 1.05 | < 0.21 | < 0.84 | 4.20 | 1.05 | 0.210 | 0.84 |
| 13 | SWPF-49 | GAP-02 | U | 6 | GAP-pct-012 | 20.75 | 12.44 | 113.86 | 118.53 | 20.75 | 12.44 | 113.860 | 118.53 |
| . | soln std | | U | 7 | std-U2 | 20.23 | 10.17 | 80.88 | 50.27 | 20.23 | 10.17 | 80.880 | 50.27 |
| 13 | ARM-1 | ARM-1 | U | 8 | GAP-pct-039 | 22.65 | 16.33 | 45.42 | 77.05 | 22.65 | 16.33 | 45.420 | 77.05 |
| 13 | SWPF-48 | GAP-25 | U | 9 | GAP-pct-061 | 14.75 | 11.19 | 56.61 | 86.39 | 14.75 | 11.19 | 56.610 | 86.39 |
| 13 | SWPF-50 | GAP-18ccc | U | 10 | GAP-pct-037 | 27.14 | 35.70 | 101.00 | 134.44 | 27.14 | 35.70 | 101.000 | 134.44 |
| 13 | SWPF-48 | GAP-25ccc | U | 11 | GAP-pct-204 | 12.11 | 10.64 | 51.85 | 82.96 | 12.11 | 10.64 | 51.850 | 82.96 |
| . | soln std | | U | 12 | std-U3 | 20.18 | 10.12 | 81.19 | 50.27 | 20.18 | 10.12 | 81.190 | 50.27 |

Table B2. Average of the Common Logarithm of the PCT Measurements

| Desc | SRNL ID | Heat Treatment | log[B(ppm)] | log[Li(ppm)] | log[Na(ppm)] | log[Si(ppm)] |
|----------|---------|----------------|-------------|--------------|--------------|--------------|
| Oven 1 | ARM | ref | 1.3721 | 1.2209 | 1.6750 | 1.8945 |
| Oven 2 | ARM | ref | 1.4424 | 1.2493 | 1.6969 | 1.8730 |
| Oven 3 | ARM | ref | 1.3871 | 1.2609 | 1.7107 | 1.9007 |
| Oven 4 | ARM | ref | 1.3575 | 1.2230 | 1.6672 | 1.8846 |
| Oven 5 | ARM | ref | 1.3409 | 1.1943 | 1.6359 | 1.8582 |
| Oven 6 | ARM | ref | 1.3711 | 1.2309 | 1.6690 | 1.8718 |
| Oven 7 | ARM | ref | 1.3767 | 1.2392 | 1.6763 | 1.8745 |
| Oven 8 | ARM | ref | 1.3674 | 1.2498 | 1.6926 | 1.8926 |
| Oven 9 | ARM | ref | 1.4611 | 1.2470 | 1.6815 | 1.8954 |
| Oven 10 | ARM | ref | 1.5379 | 1.2745 | 1.7060 | 1.9258 |
| Oven 11 | ARM | ref | 1.3461 | 1.2102 | 1.6394 | 1.8753 |
| Oven 12 | ARM | ref | 1.3414 | 1.2046 | 1.6414 | 1.8597 |
| Oven 13 | ARM | ref | 1.3491 | 1.2202 | 1.6577 | 1.8903 |
| Oven 1 | EA | ref | 2.7661 | 2.2199 | 3.1781 | 2.8714 |
| Oven 2 | EA | ref | 2.7579 | 2.2617 | 3.2202 | 2.8776 |
| Oven 3 | EA | ref | 2.7923 | 2.2893 | 3.2271 | 2.9106 |
| Oven 4 | EA | ref | 2.7172 | 2.2242 | 3.1650 | 2.8508 |
| Oven 5 | EA | ref | 2.7809 | 2.2876 | 3.2031 | 2.9087 |
| Oven 6 | EA | ref | 2.7751 | 2.2930 | 3.1878 | 2.9168 |
| Oven 7 | EA | ref | 2.7900 | 2.2894 | 3.2219 | 2.9201 |
| Oven 8 | EA | ref | 2.7721 | 2.2765 | 3.2109 | 2.9123 |
| Oven 9 | EA | ref | 2.7954 | 2.3273 | 3.2385 | 2.9275 |
| Oven 10 | EA | ref | 2.7582 | 2.3074 | 3.2070 | 2.9060 |
| Oven 11 | EA | ref | 2.7380 | 2.2899 | 3.1853 | 2.9196 |
| Oven 12 | EA | ref | 2.7884 | 2.2939 | 3.2269 | 2.9290 |
| Oven 13 | EA | ref | 2.7564 | 2.2396 | 3.2030 | 2.8811 |
| D-Opt OL | SWPF-01 | ccc | 2.0888 | 2.3417 | 2.5736 | 2.8502 |
| D-Opt OL | SWPF-02 | ccc | 1.3091 | 1.6899 | 1.8696 | 2.3530 |
| D-Opt OL | SWPF-03 | ccc | 1.5137 | 1.9787 | 2.0251 | 2.5418 |
| D-Opt OL | SWPF-04 | ccc | 1.0261 | 1.5115 | 1.6358 | 2.2205 |
| D-Opt OL | SWPF-05 | ccc | 2.0213 | 1.0514 | 2.4950 | 2.2056 |
| D-Opt OL | SWPF-06 | ccc | 1.8232 | 1.7895 | 2.0114 | 2.4176 |
| D-Opt OL | SWPF-07 | ccc | 2.0666 | 2.0085 | 2.1780 | 2.5136 |
| D-Opt OL | SWPF-08 | ccc | 1.1160 | 0.4607 | 1.3700 | 1.8326 |
| D-Opt OL | SWPF-09 | ccc | 1.4973 | 1.5538 | 1.7716 | 2.1895 |
| D-Opt OL | SWPF-10 | ccc | 1.3969 | 0.5908 | 1.8693 | 1.8947 |
| D-Opt OL | SWPF-11 | ccc | 1.5767 | 0.6135 | 2.1569 | 2.1454 |
| D-Opt OL | SWPF-12 | ccc | 1.4244 | 1.9695 | 1.8528 | 2.4262 |
| D-Opt OL | SWPF-13 | ccc | 0.9933 | 1.4308 | 1.5614 | 2.0727 |
| D-Opt OL | SWPF-14 | ccc | 1.0742 | 1.2179 | 1.3185 | 1.8394 |
| D-Opt OL | SWPF-15 | ccc | 1.1896 | 1.2730 | 1.4555 | 1.8487 |
| centroid | SWPF-16 | ccc | 1.1614 | 1.2397 | 1.6352 | 2.0311 |
| D-Opt IL | SWPF-17 | ccc | 0.9534 | 0.8371 | 1.8596 | 2.0106 |
| D-Opt IL | SWPF-18 | ccc | 1.2251 | 1.4447 | 2.1738 | 2.2182 |
| D-Opt IL | SWPF-19 | ccc | 0.9440 | 0.8162 | 1.8188 | 1.9669 |
| D-Opt IL | SWPF-20 | ccc | 1.0265 | 1.2667 | 1.7496 | 2.0069 |
| D-Opt IL | SWPF-21 | ccc | 1.1081 | 0.9665 | 2.0487 | 2.0592 |
| D-Opt IL | SWPF-22 | ccc | 1.2396 | 0.9402 | 2.0004 | 2.0032 |
| D-Opt IL | SWPF-23 | ccc | 1.3349 | 0.9166 | 1.9818 | 2.0027 |
| D-Opt IL | SWPF-24 | ccc | 1.1290 | 0.8763 | 1.5513 | 1.9270 |
| D-Opt IL | SWPF-25 | ccc | 1.2735 | 1.3103 | 1.7544 | 2.0167 |
| D-Opt IL | SWPF-26 | ccc | 1.3166 | 1.3527 | 1.8096 | 2.0558 |
| D-Opt IL | SWPF-27 | ccc | 1.0237 | 1.2734 | 1.6976 | 2.0309 |
| D-Opt IL | SWPF-28 | ccc | 1.1230 | 1.3337 | 1.8024 | 2.0387 |
| D-Opt IL | SWPF-29 | ccc | 1.0129 | 1.2730 | 1.7019 | 1.9950 |
| D-Opt IL | SWPF-30 | ccc | 1.0547 | 0.7962 | 1.6550 | 1.8719 |
| D-Opt IL | SWPF-31 | ccc | 1.2484 | 0.9016 | 1.9092 | 1.9176 |
| SF | SWPF-32 | ccc | 1.0106 | 1.2867 | 1.6949 | 2.0706 |
| SF | SWPF-33 | ccc | 1.2345 | 1.2408 | 1.7011 | 2.0225 |
| SF | SWPF-34 | ccc | 1.0527 | 0.9726 | 1.9712 | 1.9924 |
| SF | SWPF-35 | ccc | 1.2910 | 1.2835 | 1.7278 | 2.0133 |
| SF | SWPF-36 | ccc | 1.0270 | 1.2506 | 1.6665 | 1.9893 |
| SF | SWPF-37 | ccc | 1.1987 | 1.2597 | 1.6743 | 2.0839 |
| SF | SWPF-38 | ccc | 1.1841 | 0.8830 | 1.8731 | 2.0011 |

Table B2. PCT Measurements for High TiO₂ Glasses (continued)

| Desc | SRNL ID | Heat Treatment | log[B(ppm)] | log[Li(ppm)] | log[Na(ppm)] | log[Si(ppm)] |
|----------|---------|----------------|-------------|--------------|--------------|--------------|
| SF | SWPF-39 | ccc | 1.1531 | 1.3434 | 2.0569 | 2.1765 |
| SF | SWPF-40 | ccc | 1.4962 | 1.3918 | 2.0001 | 2.0368 |
| SF | SWPF-41 | ccc | 1.3104 | 1.4028 | 1.8772 | 2.1327 |
| SF | SWPF-42 | ccc | 1.0777 | 0.8424 | 1.8899 | 2.0317 |
| SF | SWPF-43 | ccc | 1.1872 | 1.3833 | 1.9150 | 2.1383 |
| SF | SWPF-44 | ccc | 1.1425 | 1.2547 | 1.7215 | 2.0521 |
| SF | SWPF-45 | ccc | 0.9962 | 0.7988 | 1.7835 | 1.9578 |
| SF | SWPF-46 | ccc | 1.1194 | 1.0702 | 2.0255 | 2.0716 |
| SF | SWPF-47 | ccc | 1.1599 | 1.1394 | 1.8534 | 1.9792 |
| SF | SWPF-48 | ccc | 1.1044 | 1.0333 | 1.7195 | 1.9229 |
| SF | SWPF-49 | ccc | 1.3482 | 1.1415 | 2.0523 | 2.0890 |
| SF | SWPF-50 | ccc | 1.4291 | 1.5513 | 2.0006 | 2.1280 |
| D-Opt OL | SWPF-01 | quenched | 1.1111 | 1.4883 | 1.6839 | 2.2326 |
| D-Opt OL | SWPF-02 | quenched | 1.1525 | 1.5592 | 1.7699 | 2.2888 |
| D-Opt OL | SWPF-03 | quenched | 1.2533 | 1.5887 | 1.8322 | 2.3395 |
| D-Opt OL | SWPF-04 | quenched | 1.0242 | 1.5178 | 1.6242 | 2.2168 |
| D-Opt OL | SWPF-05 | quenched | 2.0657 | 1.1055 | 2.5340 | 2.2062 |
| D-Opt OL | SWPF-06 | quenched | 1.8155 | 1.8035 | 2.0170 | 2.4243 |
| D-Opt OL | SWPF-07 | quenched | 1.9024 | 1.8582 | 2.0237 | 2.4025 |
| D-Opt OL | SWPF-08 | quenched | 1.0909 | 0.4722 | 1.3594 | 1.8139 |
| D-Opt OL | SWPF-09 | quenched | 1.6249 | 1.6324 | 1.8529 | 2.2564 |
| D-Opt OL | SWPF-10 | quenched | 1.6020 | 0.7677 | 2.0198 | 1.9216 |
| D-Opt OL | SWPF-11 | quenched | 1.7743 | 0.7324 | 2.3115 | 2.2233 |
| D-Opt OL | SWPF-12 | quenched | 1.0844 | 1.5466 | 1.5845 | 2.1838 |
| D-Opt OL | SWPF-13 | quenched | 0.9959 | 1.4309 | 1.5778 | 2.0780 |
| D-Opt OL | SWPF-14 | quenched | 1.1457 | 1.2799 | 1.3347 | 1.8787 |
| D-Opt OL | SWPF-15 | quenched | 1.2707 | 1.3838 | 1.5262 | 1.8667 |
| centroid | SWPF-16 | quenched | 1.2296 | 1.2850 | 1.6606 | 2.0540 |
| D-Opt IL | SWPF-17 | quenched | 0.9840 | 0.7919 | 1.8618 | 1.9971 |
| D-Opt IL | SWPF-18 | quenched | 1.2421 | 1.4304 | 2.1930 | 2.2278 |
| D-Opt IL | SWPF-19 | quenched | 0.9920 | 0.8199 | 1.8568 | 1.9786 |
| D-Opt IL | SWPF-20 | quenched | 1.1630 | 1.3279 | 1.7979 | 2.0235 |
| D-Opt IL | SWPF-21 | quenched | 1.1848 | 0.9224 | 2.0580 | 2.0512 |
| D-Opt IL | SWPF-22 | quenched | 1.3174 | 0.9519 | 2.0442 | 2.0181 |
| D-Opt IL | SWPF-23 | quenched | 1.3290 | 0.8862 | 1.9880 | 1.9937 |
| D-Opt IL | SWPF-24 | quenched | 1.1236 | 0.9172 | 1.5527 | 1.8985 |
| D-Opt IL | SWPF-25 | quenched | 1.3199 | 1.3538 | 1.7923 | 2.0317 |
| D-Opt IL | SWPF-26 | quenched | 1.3397 | 1.3356 | 1.8180 | 2.0344 |
| D-Opt IL | SWPF-27 | quenched | 1.0459 | 1.2861 | 1.6941 | 2.0081 |
| D-Opt IL | SWPF-28 | quenched | 1.1197 | 1.3268 | 1.8170 | 2.0200 |
| D-Opt IL | SWPF-29 | quenched | 1.0363 | 1.3282 | 1.7372 | 2.0039 |
| D-Opt IL | SWPF-30 | quenched | 1.0686 | 0.8708 | 1.6820 | 1.8464 |
| D-Opt IL | SWPF-31 | quenched | 1.2324 | 0.8603 | 1.9299 | 1.9165 |
| SF | SWPF-32 | quenched | 1.0545 | 1.2847 | 1.6911 | 2.0828 |
| SF | SWPF-33 | quenched | 1.2649 | 1.2649 | 1.7154 | 2.0089 |
| SF | SWPF-34 | quenched | 1.0847 | 0.9490 | 1.9951 | 2.0010 |
| SF | SWPF-35 | quenched | 1.3665 | 1.3488 | 1.7881 | 2.0251 |
| SF | SWPF-36 | quenched | 1.1210 | 1.3232 | 1.7234 | 2.0312 |
| SF | SWPF-37 | quenched | 1.2389 | 1.2884 | 1.7052 | 2.0980 |
| SF | SWPF-38 | quenched | 1.2626 | 0.9124 | 1.9228 | 2.0000 |
| SF | SWPF-39 | quenched | 1.1793 | 1.3101 | 2.0705 | 2.1685 |
| SF | SWPF-40 | quenched | 1.2147 | 1.2097 | 1.9047 | 1.9606 |
| SF | SWPF-41 | quenched | 1.2830 | 1.3559 | 1.8583 | 2.0979 |
| SF | SWPF-42 | quenched | 1.1172 | 0.8108 | 1.9109 | 2.0385 |
| SF | SWPF-43 | quenched | 1.2256 | 1.3874 | 1.9339 | 2.1354 |
| SF | SWPF-44 | quenched | 1.2025 | 1.2765 | 1.7476 | 2.0540 |
| SF | SWPF-45 | quenched | 1.0182 | 0.7947 | 1.7825 | 1.9433 |
| SF | SWPF-46 | quenched | 1.1059 | 1.0483 | 2.0406 | 2.0668 |
| SF | SWPF-47 | quenched | 1.2132 | 1.1505 | 1.8876 | 1.9753 |
| SF | SWPF-48 | quenched | 1.1716 | 1.0522 | 1.7494 | 1.9330 |
| SF | SWPF-49 | quenched | 1.3318 | 1.1036 | 2.0634 | 2.0817 |
| SF | SWPF-50 | quenched | 1.1822 | 1.3448 | 1.8952 | 2.0226 |

Table B3. Initial and Final pH Values for the PCTs of the High TiO₂ Glasses

| SRNL ID | Oven Run | Working Glass ID (w HT) | Block | Seq | Lab ID | Initial pH | Final pH |
|----------|----------|-------------------------|-------|-----|-------------|------------|----------|
| soln std | . | soln std | A | 1 | std-A1 | . | . |
| SWPF-04 | 1 | GAP-31 | A | 2 | GAP-pct-201 | 6.71 | 10.68 |
| SWPF-08 | 2 | GAP-37 | A | 3 | GAP-pct-046 | 5.98 | 9.19 |
| SWPF-03 | 1 | GAP-43 | A | 4 | GAP-pct-080 | 6.71 | 10.61 |
| SWPF-05 | 2 | GAP-33 | A | 5 | GAP-pct-307 | 5.98 | 10.74 |
| SWPF-05 | 2 | GAP-33ccc | A | 6 | GAP-pct-398 | 5.98 | 10.67 |
| SWPF-02 | 1 | GAP-22ccc | A | 7 | GAP-pct-380 | 6.71 | 10.89 |
| SWPF-07 | 2 | GAP-21ccc | A | 8 | GAP-pct-287 | 5.98 | 10.65 |
| ARM-1 | 2 | ARM-1 | A | 9 | GAP-pct-131 | 5.98 | 10.12 |
| SWPF-02 | 1 | GAP-22 | A | 10 | GAP-pct-320 | 6.71 | 10.8 |
| SWPF-04 | 1 | GAP-31ccc | A | 11 | GAP-pct-011 | 6.71 | 10.58 |
| SWPF-01 | 1 | GAP-15 | A | 12 | GAP-pct-085 | 6.71 | 10.58 |
| soln std | . | soln std | A | 13 | std-A2 | . | . |
| blank | 1 | blank | A | 14 | GAP-pct-341 | 6.71 | 6.54 |
| EA | 2 | EA | A | 15 | GAP-pct-277 | 5.98 | 11.97 |
| SWPF-03 | 1 | GAP-43ccc | A | 16 | GAP-pct-289 | 6.71 | 11.26 |
| SWPF-06 | 2 | GAP-38ccc | A | 17 | GAP-pct-396 | 5.98 | 10.48 |
| SWPF-07 | 2 | GAP-21 | A | 18 | GAP-pct-010 | 5.98 | 10.53 |
| SWPF-08 | 2 | GAP-37ccc | A | 19 | GAP-pct-281 | 5.98 | 9.18 |
| SWPF-06 | 2 | GAP-38 | A | 20 | GAP-pct-356 | 5.98 | 10.51 |
| EA | 1 | EA | A | 21 | GAP-pct-212 | 6.71 | 11.79 |
| ARM-1 | 1 | ARM-1 | A | 22 | GAP-pct-157 | 6.71 | 10.27 |
| SWPF-01 | 1 | GAP-15ccc | A | 23 | GAP-pct-327 | 6.71 | 11.68 |
| soln std | . | soln std | A | 24 | std-A3 | . | . |
| soln std | . | soln std | B | 1 | std-B1 | . | . |
| SWPF-07 | 2 | GAP-21ccc | B | 2 | GAP-pct-381 | 5.98 | 10.63 |
| SWPF-06 | 2 | GAP-38 | B | 3 | GAP-pct-317 | 5.98 | 10.5 |
| SWPF-02 | 1 | GAP-22ccc | B | 4 | GAP-pct-384 | 6.71 | 10.92 |
| SWPF-01 | 1 | GAP-15 | B | 5 | GAP-pct-116 | 6.71 | 10.6 |
| SWPF-08 | 2 | GAP-37ccc | B | 6 | GAP-pct-379 | 5.98 | 9.19 |
| SWPF-08 | 2 | GAP-37 | B | 7 | GAP-pct-199 | 5.98 | 9.17 |
| EA | 1 | EA | B | 8 | GAP-pct-322 | 6.71 | 11.71 |
| EA | 2 | EA | B | 9 | GAP-pct-078 | 5.98 | 11.94 |
| SWPF-07 | 2 | GAP-21 | B | 10 | GAP-pct-342 | 5.98 | 10.55 |
| SWPF-04 | 1 | GAP-31ccc | B | 11 | GAP-pct-090 | 6.71 | 10.65 |
| SWPF-03 | 1 | GAP-43 | B | 12 | GAP-pct-054 | 6.71 | 10.58 |
| soln std | . | soln std | B | 13 | std-B2 | . | . |
| SWPF-03 | 1 | GAP-43ccc | B | 14 | GAP-pct-072 | 6.71 | 11.29 |
| SWPF-04 | 1 | GAP-31 | B | 15 | GAP-pct-353 | 6.71 | 10.65 |
| ARM-1 | 1 | ARM-1 | B | 16 | GAP-pct-283 | 6.71 | 10.24 |
| blank | 2 | blank | B | 17 | GAP-pct-081 | 5.98 | 6.38 |
| SWPF-02 | 1 | GAP-22 | B | 18 | GAP-pct-404 | 6.71 | 10.69 |
| ARM-1 | 2 | ARM-1 | B | 19 | GAP-pct-173 | 5.98 | 10.16 |
| SWPF-05 | 2 | GAP-33 | B | 20 | GAP-pct-314 | 5.98 | 10.8 |
| SWPF-06 | 2 | GAP-38ccc | B | 21 | GAP-pct-205 | 5.98 | 10.49 |
| SWPF-01 | 1 | GAP-15ccc | B | 22 | GAP-pct-112 | 6.71 | 11.7 |
| blank | 1 | blank | B | 23 | GAP-pct-346 | 6.71 | 6.5 |
| SWPF-05 | 2 | GAP-33ccc | B | 24 | GAP-pct-147 | 5.98 | 10.64 |
| soln std | . | soln std | B | 25 | std-B3 | . | . |
| soln std | . | soln std | C | 1 | std-C1 | . | . |
| SWPF-05 | 2 | GAP-33 | C | 2 | GAP-pct-197 | 5.98 | 10.64 |
| SWPF-03 | 1 | GAP-43 | C | 3 | GAP-pct-088 | 6.71 | 10.58 |
| blank | 2 | blank | C | 4 | GAP-pct-104 | 5.98 | 6.64 |
| SWPF-08 | 2 | GAP-37ccc | C | 5 | GAP-pct-188 | 5.98 | 9.17 |
| EA | 2 | EA | C | 6 | GAP-pct-187 | 5.98 | 11.97 |
| SWPF-01 | 1 | GAP-15ccc | C | 7 | GAP-pct-180 | 6.71 | 11.68 |
| SWPF-06 | 2 | GAP-38ccc | C | 8 | GAP-pct-119 | 5.98 | 10.48 |
| EA | 1 | EA | C | 9 | GAP-pct-394 | 6.71 | 11.72 |
| SWPF-05 | 2 | GAP-33ccc | C | 10 | GAP-pct-263 | 5.98 | 10.68 |
| SWPF-04 | 1 | GAP-31 | C | 11 | GAP-pct-073 | 6.71 | 10.65 |
| ARM-1 | 1 | ARM-1 | C | 12 | GAP-pct-224 | 6.71 | 10.14 |
| soln std | . | soln std | C | 13 | std-C2 | . | . |
| SWPF-07 | 2 | GAP-21 | C | 14 | GAP-pct-376 | 5.98 | 10.58 |

**Table B3. Initial and Final pH Values for the PCTs of the High TiO₂ Glasses
(continued)**

| SRNL ID | Oven Run | Working Glass ID (w HT) | Block | Seq | Lab ID | Initial pH | Final pH |
|----------|----------|-------------------------|-------|-----|-------------|------------|----------|
| SWPF-02 | 1 | GAP-22 | C | 15 | GAP-pct-315 | 6.71 | 10.73 |
| SWPF-04 | 1 | GAP-31ccc | C | 16 | GAP-pct-285 | 6.71 | 10.65 |
| SWPF-08 | 2 | GAP-37 | C | 17 | GAP-pct-017 | 5.98 | 9.32 |
| SWPF-01 | 1 | GAP-15 | C | 18 | GAP-pct-015 | 6.71 | 10.67 |
| SWPF-07 | 2 | GAP-21ccc | C | 19 | GAP-pct-251 | 5.98 | 10.66 |
| ARM-1 | 2 | ARM-1 | C | 20 | GAP-pct-019 | 5.98 | 10.19 |
| SWPF-02 | 1 | GAP-22ccc | C | 21 | GAP-pct-182 | 6.71 | 10.9 |
| SWPF-06 | 2 | GAP-38 | C | 22 | GAP-pct-252 | 5.98 | 10.48 |
| SWPF-03 | 1 | GAP-43ccc | C | 23 | GAP-pct-203 | 6.71 | 11.27 |
| soln std | . | soln std | C | 24 | std-C3 | . | . |
| soln std | . | soln std | D | 1 | std-D1 | . | . |
| EA | 4 | EA | D | 2 | GAP-pct-208 | 6.27 | 11.65 |
| ARM-1 | 4 | ARM-1 | D | 3 | GAP-pct-086 | 6.27 | 10.24 |
| SWPF-16 | 4 | GAP-26 | D | 4 | GAP-pct-043 | 6.27 | 10.41 |
| SWPF-09 | 3 | GAP-44 | D | 5 | GAP-pct-297 | 6.36 | 10.74 |
| SWPF-12 | 3 | GAP-34 | D | 6 | GAP-pct-121 | 6.36 | 11.13 |
| SWPF-15 | 4 | GAP-14ccc | D | 7 | GAP-pct-340 | 6.27 | 10.48 |
| SWPF-13 | 4 | GAP-19 | D | 8 | GAP-pct-002 | 6.27 | 10.78 |
| SWPF-11 | 3 | GAP-10ccc | D | 9 | GAP-pct-365 | 6.36 | 10.41 |
| SWPF-14 | 4 | GAP-12 | D | 10 | GAP-pct-140 | 6.27 | 10.36 |
| SWPF-15 | 4 | GAP-14 | D | 11 | GAP-pct-150 | 6.27 | 10.67 |
| SWPF-10 | 3 | GAP-47 | D | 12 | GAP-pct-227 | 6.36 | 10.21 |
| soln std | . | soln std | D | 13 | std-D2 | . | . |
| SWPF-10 | 3 | GAP-47ccc | D | 14 | GAP-pct-303 | 6.36 | 10.08 |
| EA | 3 | EA | D | 15 | GAP-pct-367 | 6.36 | 11.85 |
| SWPF-13 | 4 | GAP-19ccc | D | 16 | GAP-pct-071 | 6.27 | 10.8 |
| SWPF-11 | 3 | GAP-10 | D | 17 | GAP-pct-316 | 6.36 | 10.59 |
| blank | 3 | blank | D | 18 | GAP-pct-136 | 6.36 | 6.07 |
| SWPF-16 | 4 | GAP-26ccc | D | 19 | GAP-pct-168 | 6.27 | 10.38 |
| ARM-1 | 3 | ARM-1 | D | 20 | GAP-pct-132 | 6.36 | 10.44 |
| SWPF-12 | 3 | GAP-34ccc | D | 21 | GAP-pct-278 | 6.36 | 11.67 |
| SWPF-09 | 3 | GAP-44ccc | D | 22 | GAP-pct-308 | 6.36 | 10.73 |
| SWPF-14 | 4 | GAP-12ccc | D | 23 | GAP-pct-134 | 6.27 | 10.37 |
| soln std | . | soln std | D | 24 | std-D3 | . | . |
| soln std | . | soln std | E | 1 | std-E1 | . | . |
| ARM-1 | 3 | ARM-1 | E | 2 | GAP-pct-336 | 6.36 | 10.46 |
| SWPF-13 | 4 | GAP-19 | E | 3 | GAP-pct-155 | 6.27 | 10.8 |
| blank | 3 | blank | E | 4 | GAP-pct-111 | 6.36 | 6.17 |
| SWPF-10 | 3 | GAP-47ccc | E | 5 | GAP-pct-068 | 6.36 | 10.09 |
| SWPF-12 | 3 | GAP-34 | E | 6 | GAP-pct-098 | 6.36 | 11.12 |
| EA | 4 | EA | E | 7 | GAP-pct-337 | 6.27 | 11.65 |
| SWPF-14 | 4 | GAP-12 | E | 8 | GAP-pct-253 | 6.27 | 10.39 |
| SWPF-13 | 4 | GAP-19ccc | E | 9 | GAP-pct-370 | 6.27 | 10.8 |
| ARM-1 | 4 | ARM-1 | E | 10 | GAP-pct-108 | 6.27 | 10.3 |
| SWPF-16 | 4 | GAP-26 | E | 11 | GAP-pct-130 | 6.27 | 10.4 |
| SWPF-09 | 3 | GAP-44 | E | 12 | GAP-pct-294 | 6.36 | 10.71 |
| soln std | . | soln std | E | 13 | std-E2 | . | . |
| SWPF-15 | 4 | GAP-14ccc | E | 14 | GAP-pct-032 | 6.27 | 10.45 |
| blank | 4 | blank | E | 15 | GAP-pct-373 | 6.27 | 5.13 |
| SWPF-12 | 3 | GAP-34ccc | E | 16 | GAP-pct-324 | 6.36 | 11.63 |
| SWPF-14 | 4 | GAP-12ccc | E | 17 | GAP-pct-051 | 6.27 | 10.35 |
| SWPF-10 | 3 | GAP-47 | E | 18 | GAP-pct-325 | 6.36 | 10.22 |
| SWPF-15 | 4 | GAP-14 | E | 19 | GAP-pct-007 | 6.27 | 10.65 |
| SWPF-11 | 3 | GAP-10ccc | E | 20 | GAP-pct-114 | 6.36 | 10.42 |
| SWPF-09 | 3 | GAP-44ccc | E | 21 | GAP-pct-185 | 6.36 | 10.72 |
| SWPF-16 | 4 | GAP-26ccc | E | 22 | GAP-pct-139 | 6.27 | 10.37 |
| EA | 3 | EA | E | 23 | GAP-pct-091 | 6.36 | 11.89 |
| SWPF-11 | 3 | GAP-10 | E | 24 | GAP-pct-330 | 6.36 | 10.53 |
| soln std | . | soln std | E | 25 | std-E3 | . | . |
| soln std | . | soln std | F | 1 | std-F1 | . | . |
| SWPF-14 | 4 | GAP-12 | F | 2 | GAP-pct-160 | 6.27 | 10.4 |

**Table B3. Initial and Final pH Values for the PCTs of the High TiO₂ Glasses
(continued)**

| SRNL ID | Oven Run | Working Glass ID (w HT) | Block | Seq | Lab ID | Initial pH | Final pH |
|----------|----------|-------------------------|-------|-----|-------------|------------|----------|
| SWPF-14 | 4 | GAP-12ccc | F | 3 | GAP-pct-198 | 6.27 | 10.29 |
| SWPF-13 | 4 | GAP-19ccc | F | 4 | GAP-pct-189 | 6.27 | 10.78 |
| SWPF-15 | 4 | GAP-14 | F | 5 | GAP-pct-029 | 6.27 | 10.62 |
| SWPF-13 | 4 | GAP-19 | F | 6 | GAP-pct-052 | 6.27 | 10.79 |
| SWPF-09 | 3 | GAP-44 | F | 7 | GAP-pct-213 | 6.36 | 10.72 |
| EA | 3 | EA | F | 8 | GAP-pct-350 | 6.36 | 11.99 |
| SWPF-11 | 3 | GAP-10 | F | 9 | GAP-pct-334 | 6.36 | 10.55 |
| EA | 4 | EA | F | 10 | GAP-pct-142 | 6.27 | 11.62 |
| SWPF-16 | 4 | GAP-26ccc | F | 11 | GAP-pct-042 | 6.27 | 10.37 |
| SWPF-12 | 3 | GAP-34 | F | 12 | GAP-pct-351 | 6.36 | 11.14 |
| soln std | . | soln std | F | 13 | std-F2 | . | . |
| SWPF-16 | 4 | GAP-26 | F | 14 | GAP-pct-079 | 6.27 | 10.42 |
| SWPF-10 | 3 | GAP-47 | F | 15 | GAP-pct-206 | 6.36 | 10.23 |
| blank | 4 | blank | F | 16 | GAP-pct-167 | 6.27 | 5.09 |
| SWPF-15 | 4 | GAP-14ccc | F | 17 | GAP-pct-335 | 6.27 | 10.49 |
| SWPF-10 | 3 | GAP-47ccc | F | 18 | GAP-pct-191 | 6.36 | 10.11 |
| ARM-1 | 4 | ARM-1 | F | 19 | GAP-pct-014 | 6.27 | 10.22 |
| SWPF-09 | 3 | GAP-44ccc | F | 20 | GAP-pct-184 | 6.36 | 10.73 |
| SWPF-11 | 3 | GAP-10ccc | F | 21 | GAP-pct-105 | 6.36 | 10.39 |
| ARM-1 | 3 | ARM-1 | F | 22 | GAP-pct-245 | 6.36 | 10.35 |
| SWPF-12 | 3 | GAP-34ccc | F | 23 | GAP-pct-255 | 6.36 | 11.65 |
| soln std | . | soln std | F | 24 | std-F3 | . | . |
| soln std | . | soln std | G | 1 | std-G1 | . | . |
| blank | 5 | blank | G | 2 | GAP-pct-279 | 6.5 | 5.15 |
| SWPF-19 | 5 | GAP-35 | G | 3 | GAP-pct-055 | 6.5 | 10.43 |
| SWPF-23 | 6 | GAP-23ccc | G | 4 | GAP-pct-235 | 5.85 | 10.54 |
| SWPF-21 | 6 | GAP-41ccc | G | 5 | GAP-pct-025 | 5.85 | 10.83 |
| SWPF-19 | 5 | GAP-35ccc | G | 6 | GAP-pct-127 | 6.5 | 10.39 |
| SWPF-20 | 5 | GAP-46ccc | G | 7 | GAP-pct-141 | 6.5 | 10.59 |
| SWPF-17 | 5 | GAP-05 | G | 8 | GAP-pct-239 | 6.5 | 10.52 |
| SWPF-17 | 5 | GAP-05ccc | G | 9 | GAP-pct-166 | 6.5 | 10.46 |
| SWPF-18 | 5 | GAP-29 | G | 10 | GAP-pct-269 | 6.5 | 11.18 |
| ARM-1 | 5 | ARM-1 | G | 11 | GAP-pct-402 | 6.5 | 10.24 |
| EA | 6 | EA | G | 12 | GAP-pct-175 | 5.85 | 11.58 |
| soln std | . | soln std | G | 13 | std-G2 | . | . |
| SWPF-18 | 5 | GAP-29ccc | G | 14 | GAP-pct-280 | 6.5 | 11.18 |
| SWPF-22 | 6 | GAP-20 | G | 15 | GAP-pct-156 | 5.85 | 10.75 |
| SWPF-21 | 6 | GAP-41 | G | 16 | GAP-pct-301 | 5.85 | 10.83 |
| ARM-1 | 6 | ARM-1 | G | 17 | GAP-pct-056 | 5.85 | 10.19 |
| SWPF-23 | 6 | GAP-23 | G | 18 | GAP-pct-093 | 5.85 | 10.58 |
| SWPF-24 | 6 | GAP-42ccc | G | 19 | GAP-pct-143 | 5.85 | 9.8 |
| SWPF-22 | 6 | GAP-20ccc | G | 20 | GAP-pct-257 | 5.85 | 10.7 |
| SWPF-20 | 5 | GAP-46 | G | 21 | GAP-pct-107 | 6.5 | 10.68 |
| EA | 5 | EA | G | 22 | GAP-pct-345 | 6.5 | 11.83 |
| SWPF-24 | 6 | GAP-42 | G | 23 | GAP-pct-026 | 5.85 | 9.78 |
| soln std | . | soln std | G | 24 | std-G3 | . | . |
| soln std | . | soln std | H | 1 | std-H1 | . | . |
| SWPF-21 | 6 | GAP-41 | H | 2 | GAP-pct-183 | 5.85 | 10.81 |
| SWPF-20 | 5 | GAP-46ccc | H | 3 | GAP-pct-084 | 6.5 | 10.58 |
| SWPF-17 | 5 | GAP-05ccc | H | 4 | GAP-pct-288 | 6.5 | 10.47 |
| ARM-1 | 6 | ARM-1 | H | 5 | GAP-pct-243 | 5.85 | 10.16 |
| SWPF-19 | 5 | GAP-35ccc | H | 6 | GAP-pct-237 | 6.5 | 10.34 |
| SWPF-20 | 5 | GAP-46 | H | 7 | GAP-pct-371 | 6.5 | 10.68 |
| SWPF-22 | 6 | GAP-20ccc | H | 8 | GAP-pct-284 | 5.85 | 10.66 |
| SWPF-22 | 6 | GAP-20 | H | 9 | GAP-pct-282 | 5.85 | 10.82 |
| SWPF-21 | 6 | GAP-41ccc | H | 10 | GAP-pct-382 | 5.85 | 10.8 |
| SWPF-24 | 6 | GAP-42 | H | 11 | GAP-pct-268 | 5.85 | 9.79 |
| blank | 6 | blank | H | 12 | GAP-pct-240 | 5.85 | 5.29 |
| soln std | . | soln std | H | 13 | std-H2 | . | . |
| EA | 6 | EA | H | 14 | GAP-pct-306 | 5.85 | 11.57 |
| SWPF-18 | 5 | GAP-29 | H | 15 | GAP-pct-030 | 6.5 | 11.2 |

**Table B3. Initial and Final pH Values for the PCTs of the High TiO₂ Glasses
(continued)**

| SRNL ID | Oven Run | Working Glass ID (w HT) | Block | Seq | Lab ID | Initial pH | Final pH |
|----------|----------|-------------------------|-------|-----|-------------|------------|----------|
| SWPF-23 | 6 | GAP-23ccc | H | 16 | GAP-pct-292 | 5.85 | 10.49 |
| SWPF-24 | 6 | GAP-42ccc | H | 17 | GAP-pct-057 | 5.85 | 9.78 |
| SWPF-19 | 5 | GAP-35 | H | 18 | GAP-pct-082 | 6.5 | 10.41 |
| SWPF-23 | 6 | GAP-23 | H | 19 | GAP-pct-087 | 5.85 | 10.54 |
| SWPF-18 | 5 | GAP-29ccc | H | 20 | GAP-pct-250 | 6.5 | 11.15 |
| ARM-1 | 5 | ARM-1 | H | 21 | GAP-pct-310 | 6.5 | 10.21 |
| EA | 5 | EA | H | 22 | GAP-pct-067 | 6.5 | 11.84 |
| SWPF-17 | 5 | GAP-05 | H | 23 | GAP-pct-053 | 6.5 | 10.54 |
| blank | 5 | blank | H | 24 | GAP-pct-385 | 6.5 | 5.26 |
| soln std | . | soln std | H | 25 | std-H3 | . | . |
| soln std | . | soln std | I | 1 | std-I1 | . | . |
| SWPF-21 | 6 | GAP-41ccc | I | 2 | GAP-pct-165 | 5.85 | 10.8 |
| SWPF-23 | 6 | GAP-23ccc | I | 3 | GAP-pct-161 | 5.85 | 10.51 |
| SWPF-22 | 6 | GAP-20ccc | I | 4 | GAP-pct-339 | 5.85 | 10.68 |
| SWPF-23 | 6 | GAP-23 | I | 5 | GAP-pct-249 | 5.85 | 10.52 |
| SWPF-22 | 6 | GAP-20 | I | 6 | GAP-pct-034 | 5.85 | 10.78 |
| ARM-1 | 6 | ARM-1 | I | 7 | GAP-pct-329 | 5.85 | 10.19 |
| SWPF-19 | 5 | GAP-35ccc | I | 8 | GAP-pct-065 | 6.5 | 10.31 |
| SWPF-17 | 5 | GAP-05ccc | I | 9 | GAP-pct-387 | 6.5 | 10.42 |
| SWPF-21 | 6 | GAP-41 | I | 10 | GAP-pct-077 | 5.85 | 10.8 |
| EA | 5 | EA | I | 11 | GAP-pct-389 | 6.5 | 11.83 |
| EA | 6 | EA | I | 12 | GAP-pct-038 | 5.85 | 11.6 |
| soln std | . | soln std | I | 13 | std-I2 | . | . |
| SWPF-17 | 5 | GAP-05 | I | 14 | GAP-pct-403 | 6.5 | 10.5 |
| SWPF-24 | 6 | GAP-42ccc | I | 15 | GAP-pct-291 | 5.85 | 9.79 |
| blank | 6 | blank | I | 16 | GAP-pct-137 | 5.85 | 5.36 |
| SWPF-18 | 5 | GAP-29 | I | 17 | GAP-pct-196 | 6.5 | 11.19 |
| SWPF-19 | 5 | GAP-35 | I | 18 | GAP-pct-006 | 6.5 | 10.41 |
| ARM-1 | 5 | ARM-1 | I | 19 | GAP-pct-400 | 6.5 | 10.24 |
| SWPF-20 | 5 | GAP-46ccc | I | 20 | GAP-pct-033 | 6.5 | 10.56 |
| SWPF-24 | 6 | GAP-42 | I | 21 | GAP-pct-158 | 5.85 | 9.81 |
| SWPF-20 | 5 | GAP-46 | I | 22 | GAP-pct-170 | 6.5 | 10.65 |
| SWPF-18 | 5 | GAP-29ccc | I | 23 | GAP-pct-244 | 6.5 | 11.16 |
| soln std | . | soln std | I | 24 | std-I3 | . | . |
| soln std | . | soln std | J | 1 | std-J1 | . | . |
| ARM-1 | 7 | ARM-1 | J | 2 | GAP-pct-162 | 5.78 | 10.19 |
| EA | 8 | EA | J | 3 | GAP-pct-273 | 5.38 | 11.56 |
| SWPF-31 | 8 | GAP-30 | J | 4 | GAP-pct-366 | 5.38 | 10.48 |
| SWPF-25 | 7 | GAP-17ccc | J | 5 | GAP-pct-270 | 5.78 | 10.49 |
| SWPF-31 | 8 | GAP-30ccc | J | 6 | GAP-pct-372 | 5.38 | 10.48 |
| ARM-1 | 8 | ARM-1 | J | 7 | GAP-pct-286 | 5.38 | 10.18 |
| SWPF-26 | 7 | GAP-06ccc | J | 8 | GAP-pct-115 | 5.78 | 10.56 |
| SWPF-25 | 7 | GAP-17 | J | 9 | GAP-pct-028 | 5.78 | 10.56 |
| SWPF-28 | 7 | GAP-50 | J | 10 | GAP-pct-358 | 5.78 | 10.76 |
| SWPF-27 | 7 | GAP-24ccc | J | 11 | GAP-pct-242 | 5.78 | 10.56 |
| SWPF-28 | 7 | GAP-50ccc | J | 12 | GAP-pct-070 | 5.78 | 10.74 |
| soln std | . | soln std | J | 13 | std-J2 | . | . |
| SWPF-27 | 7 | GAP-24 | J | 14 | GAP-pct-375 | 5.78 | 10.58 |
| SWPF-29 | 8 | GAP-32ccc | J | 15 | GAP-pct-022 | 5.38 | 10.67 |
| SWPF-26 | 7 | GAP-06 | J | 16 | GAP-pct-313 | 5.78 | 10.63 |
| SWPF-32 | 8 | GAP-09 | J | 17 | GAP-pct-222 | 5.38 | 10.51 |
| SWPF-30 | 8 | GAP-16ccc | J | 18 | GAP-pct-008 | 5.38 | 10.01 |
| blank | 7 | blank | J | 19 | GAP-pct-102 | 5.78 | 5.12 |
| SWPF-30 | 8 | GAP-16 | J | 20 | GAP-pct-120 | 5.38 | 10.11 |
| EA | 7 | EA | J | 21 | GAP-pct-045 | 5.78 | 11.77 |
| SWPF-32 | 8 | GAP-09ccc | J | 22 | GAP-pct-296 | 5.38 | 10.47 |
| SWPF-29 | 8 | GAP-32 | J | 23 | GAP-pct-152 | 5.38 | 10.7 |
| soln std | . | soln std | J | 24 | std-J3 | . | . |
| soln std | . | soln std | K | 1 | std-K1 | . | . |
| SWPF-27 | 7 | GAP-24ccc | K | 2 | GAP-pct-179 | 5.78 | 10.58 |
| blank | 8 | blank | K | 3 | GAP-pct-233 | 5.38 | 5.29 |

**Table B3. Initial and Final pH Values for the PCTs of the High TiO₂ Glasses
(continued)**

| SRNL ID | Oven Run | Working Glass ID (w HT) | Block | Seq | Lab ID | Initial pH | Final pH |
|----------|----------|-------------------------|-------|-----|-------------|------------|----------|
| SWPF-28 | 7 | GAP-50 | K | 4 | GAP-pct-266 | 5.78 | 10.73 |
| EA | 8 | EA | K | 5 | GAP-pct-151 | 5.38 | 11.79 |
| SWPF-26 | 7 | GAP-06ccc | K | 6 | GAP-pct-209 | 5.78 | 10.57 |
| SWPF-31 | 8 | GAP-30ccc | K | 7 | GAP-pct-144 | 5.38 | 10.47 |
| SWPF-31 | 8 | GAP-30 | K | 8 | GAP-pct-092 | 5.38 | 10.53 |
| SWPF-25 | 7 | GAP-17 | K | 9 | GAP-pct-397 | 5.78 | 10.54 |
| ARM-1 | 7 | ARM-1 | K | 10 | GAP-pct-101 | 5.78 | 10.16 |
| SWPF-29 | 8 | GAP-32 | K | 11 | GAP-pct-295 | 5.38 | 10.68 |
| blank | 7 | blank | K | 12 | GAP-pct-352 | 5.78 | 5.09 |
| soln std | . | soln std | K | 13 | std-K2 | . | . |
| SWPF-30 | 8 | GAP-16 | K | 14 | GAP-pct-074 | 5.38 | 10.12 |
| SWPF-30 | 8 | GAP-16ccc | K | 15 | GAP-pct-302 | 5.38 | 10.03 |
| SWPF-27 | 7 | GAP-24 | K | 16 | GAP-pct-044 | 5.78 | 10.58 |
| EA | 7 | EA | K | 17 | GAP-pct-262 | 5.78 | 11.82 |
| SWPF-26 | 7 | GAP-06 | K | 18 | GAP-pct-190 | 5.78 | 10.57 |
| SWPF-29 | 8 | GAP-32ccc | K | 19 | GAP-pct-202 | 5.38 | 10.65 |
| SWPF-32 | 8 | GAP-09ccc | K | 20 | GAP-pct-354 | 5.38 | 10.42 |
| SWPF-32 | 8 | GAP-09 | K | 21 | GAP-pct-110 | 5.38 | 10.44 |
| SWPF-28 | 7 | GAP-50ccc | K | 22 | GAP-pct-258 | 5.78 | 10.73 |
| ARM-1 | 8 | ARM-1 | K | 23 | GAP-pct-305 | 5.38 | 10.18 |
| SWPF-25 | 7 | GAP-17ccc | K | 24 | GAP-pct-128 | 5.78 | 10.52 |
| soln std | . | soln std | K | 25 | std-K3 | . | . |
| soln std | . | soln std | L | 1 | std-L1 | . | . |
| EA | 7 | EA | L | 2 | GAP-pct-248 | 5.78 | 11.85 |
| EA | 8 | EA | L | 3 | GAP-pct-094 | 5.38 | 11.76 |
| ARM-1 | 8 | ARM-1 | L | 4 | GAP-pct-220 | 5.38 | 10.11 |
| SWPF-28 | 7 | GAP-50ccc | L | 5 | GAP-pct-348 | 5.78 | 10.72 |
| SWPF-25 | 7 | GAP-17ccc | L | 6 | GAP-pct-332 | 5.78 | 10.45 |
| SWPF-30 | 8 | GAP-16ccc | L | 7 | GAP-pct-194 | 5.38 | 10.05 |
| SWPF-25 | 7 | GAP-17 | L | 8 | GAP-pct-390 | 5.78 | 10.56 |
| SWPF-29 | 8 | GAP-32ccc | L | 9 | GAP-pct-312 | 5.38 | 10.67 |
| SWPF-31 | 8 | GAP-30ccc | L | 10 | GAP-pct-133 | 5.38 | 10.45 |
| SWPF-26 | 7 | GAP-06ccc | L | 11 | GAP-pct-319 | 5.78 | 10.57 |
| SWPF-26 | 7 | GAP-06 | L | 12 | GAP-pct-207 | 5.78 | 10.66 |
| soln std | . | soln std | L | 13 | std-L2 | . | . |
| SWPF-29 | 8 | GAP-32 | L | 14 | GAP-pct-149 | 5.38 | 10.72 |
| SWPF-27 | 7 | GAP-24ccc | L | 15 | GAP-pct-261 | 5.78 | 10.52 |
| SWPF-30 | 8 | GAP-16 | L | 16 | GAP-pct-214 | 5.38 | 10.09 |
| SWPF-32 | 8 | GAP-09ccc | L | 17 | GAP-pct-063 | 5.38 | 10.43 |
| SWPF-32 | 8 | GAP-09 | L | 18 | GAP-pct-215 | 5.38 | 10.52 |
| SWPF-28 | 7 | GAP-50 | L | 19 | GAP-pct-369 | 5.78 | 10.74 |
| ARM-1 | 7 | ARM-1 | L | 20 | GAP-pct-122 | 5.78 | 10.14 |
| SWPF-31 | 8 | GAP-30 | L | 21 | GAP-pct-123 | 5.38 | 10.5 |
| SWPF-27 | 7 | GAP-24 | L | 22 | GAP-pct-254 | 5.78 | 10.56 |
| blank | 8 | blank | L | 23 | GAP-pct-338 | 5.38 | 5.22 |
| soln std | . | soln std | L | 24 | std-L3 | . | . |
| soln std | . | soln std | M | 1 | std-M1 | . | . |
| SWPF-35 | 9 | GAP-03ccc | M | 2 | GAP-pct-177 | 5.76 | 10.53 |
| SWPF-34 | 9 | GAP-36 | M | 3 | GAP-pct-264 | 5.76 | 10.8 |
| SWPF-39 | 10 | GAP-49 | M | 4 | GAP-pct-300 | 5.75 | 10.96 |
| SWPF-34 | 9 | GAP-36ccc | M | 5 | GAP-pct-003 | 5.76 | 10.8 |
| ARM-1 | 9 | ARM-1 | M | 6 | GAP-pct-236 | 5.76 | 10.26 |
| SWPF-36 | 9 | GAP-11 | M | 7 | GAP-pct-401 | 5.76 | 10.7 |
| SWPF-37 | 10 | GAP-07ccc | M | 8 | GAP-pct-361 | 5.75 | 10.23 |
| SWPF-37 | 10 | GAP-07 | M | 9 | GAP-pct-290 | 5.75 | 10.21 |
| SWPF-36 | 9 | GAP-11ccc | M | 10 | GAP-pct-388 | 5.76 | 10.61 |
| SWPF-40 | 10 | GAP-48 | M | 11 | GAP-pct-096 | 5.75 | 10.73 |
| SWPF-33 | 9 | GAP-40 | M | 12 | GAP-pct-145 | 5.76 | 10.45 |
| soln std | . | soln std | M | 13 | std-M2 | . | . |
| SWPF-38 | 10 | GAP-13 | M | 14 | GAP-pct-219 | 5.75 | 10.33 |
| SWPF-38 | 10 | GAP-13ccc | M | 15 | GAP-pct-364 | 5.75 | 10.26 |

**Table B3. Initial and Final pH Values for the PCTs of the High TiO₂ Glasses
(continued)**

| SRNL ID | Oven Run | Working Glass ID (w HT) | Block | Seq | Lab ID | Initial pH | Final pH |
|----------|----------|-------------------------|-------|-----|-------------|------------|----------|
| ARM-1 | 10 | ARM-1 | M | 16 | GAP-pct-075 | 5.75 | 10.17 |
| blank | 9 | blank | M | 17 | GAP-pct-226 | 5.76 | 5.43 |
| SWPF-33 | 9 | GAP-40ccc | M | 18 | GAP-pct-018 | 5.76 | 10.43 |
| SWPF-35 | 9 | GAP-03 | M | 19 | GAP-pct-378 | 5.76 | 10.65 |
| SWPF-39 | 10 | GAP-49ccc | M | 20 | GAP-pct-395 | 5.75 | 10.98 |
| EA | 9 | EA | M | 21 | GAP-pct-047 | 5.76 | 11.68 |
| EA | 10 | EA | M | 22 | GAP-pct-192 | 5.75 | 11.79 |
| SWPF-40 | 10 | GAP-48ccc | M | 23 | GAP-pct-311 | 5.75 | 10.84 |
| soln std | . | soln std | M | 24 | std-M3 | . | . |
| soln std | . | soln std | N | 1 | std-N1 | . | . |
| ARM-1 | 9 | ARM-1 | N | 2 | GAP-pct-223 | 5.76 | 10.24 |
| SWPF-40 | 10 | GAP-48ccc | N | 3 | GAP-pct-021 | 5.75 | 10.83 |
| SWPF-38 | 10 | GAP-13ccc | N | 4 | GAP-pct-391 | 5.75 | 10.27 |
| SWPF-33 | 9 | GAP-40 | N | 5 | GAP-pct-069 | 5.76 | 10.43 |
| EA | 9 | EA | N | 6 | GAP-pct-265 | 5.76 | 11.77 |
| SWPF-39 | 10 | GAP-49 | N | 7 | GAP-pct-309 | 5.75 | 10.95 |
| SWPF-37 | 10 | GAP-07ccc | N | 8 | GAP-pct-089 | 5.75 | 10.21 |
| SWPF-34 | 9 | GAP-36 | N | 9 | GAP-pct-221 | 5.76 | 10.8 |
| SWPF-38 | 10 | GAP-13 | N | 10 | GAP-pct-020 | 5.75 | 10.33 |
| SWPF-40 | 10 | GAP-48 | N | 11 | GAP-pct-229 | 5.75 | 10.73 |
| SWPF-34 | 9 | GAP-36ccc | N | 12 | GAP-pct-377 | 5.76 | 10.8 |
| soln std | . | soln std | N | 13 | std-N2 | . | . |
| SWPF-36 | 9 | GAP-11ccc | N | 14 | GAP-pct-138 | 5.76 | 10.59 |
| blank | 10 | blank | N | 15 | GAP-pct-357 | 5.75 | 5.32 |
| blank | 9 | blank | N | 16 | GAP-pct-217 | 5.76 | 5.19 |
| SWPF-35 | 9 | GAP-03ccc | N | 17 | GAP-pct-024 | 5.76 | 10.53 |
| SWPF-39 | 10 | GAP-49ccc | N | 18 | GAP-pct-181 | 5.75 | 10.92 |
| SWPF-36 | 9 | GAP-11 | N | 19 | GAP-pct-118 | 5.76 | 10.72 |
| SWPF-33 | 9 | GAP-40ccc | N | 20 | GAP-pct-231 | 5.76 | 10.41 |
| EA | 10 | EA | N | 21 | GAP-pct-005 | 5.75 | 11.8 |
| SWPF-35 | 9 | GAP-03 | N | 22 | GAP-pct-399 | 5.76 | 10.65 |
| SWPF-37 | 10 | GAP-07 | N | 23 | GAP-pct-218 | 5.75 | 10.23 |
| ARM-1 | 10 | ARM-1 | N | 24 | GAP-pct-186 | 5.75 | 10.16 |
| soln std | . | soln std | N | 25 | std-N3 | . | . |
| soln std | . | soln std | O | 1 | std-O1 | . | . |
| SWPF-34 | 9 | GAP-36 | O | 2 | GAP-pct-293 | 5.76 | 10.83 |
| SWPF-35 | 9 | GAP-03 | O | 3 | GAP-pct-267 | 5.76 | 10.58 |
| SWPF-39 | 10 | GAP-49ccc | O | 4 | GAP-pct-386 | 5.75 | 10.95 |
| SWPF-38 | 10 | GAP-13ccc | O | 5 | GAP-pct-095 | 5.75 | 10.28 |
| SWPF-35 | 9 | GAP-03ccc | O | 6 | GAP-pct-368 | 5.76 | 10.5 |
| SWPF-36 | 9 | GAP-11ccc | O | 7 | GAP-pct-247 | 5.76 | 10.6 |
| ARM-1 | 10 | ARM-1 | O | 8 | GAP-pct-343 | 5.75 | 10.17 |
| SWPF-37 | 10 | GAP-07 | O | 9 | GAP-pct-076 | 5.75 | 10.23 |
| ARM-1 | 9 | ARM-1 | O | 10 | GAP-pct-344 | 5.76 | 10.26 |
| SWPF-39 | 10 | GAP-49 | O | 11 | GAP-pct-323 | 5.75 | 10.97 |
| SWPF-40 | 10 | GAP-48 | O | 12 | GAP-pct-234 | 5.75 | 10.73 |
| soln std | . | soln std | O | 13 | std-O2 | . | . |
| SWPF-34 | 9 | GAP-36ccc | O | 14 | GAP-pct-210 | 5.76 | 10.77 |
| EA | 9 | EA | O | 15 | GAP-pct-298 | 5.76 | 11.68 |
| SWPF-33 | 9 | GAP-40 | O | 16 | GAP-pct-083 | 5.76 | 10.44 |
| blank | 10 | blank | O | 17 | GAP-pct-200 | 5.75 | 5.73 |
| SWPF-33 | 9 | GAP-40ccc | O | 18 | GAP-pct-171 | 5.76 | 10.4 |
| SWPF-38 | 10 | GAP-13 | O | 19 | GAP-pct-230 | 5.75 | 10.35 |
| SWPF-37 | 10 | GAP-07ccc | O | 20 | GAP-pct-064 | 5.75 | 10.2 |
| EA | 10 | EA | O | 21 | GAP-pct-035 | 5.75 | 11.66 |
| SWPF-40 | 10 | GAP-48ccc | O | 22 | GAP-pct-274 | 5.75 | 10.85 |
| SWPF-36 | 9 | GAP-11 | O | 23 | GAP-pct-153 | 5.76 | 10.72 |
| soln std | . | soln std | O | 24 | std-O3 | . | . |
| soln std | . | soln std | P | 1 | std-P1 | . | . |
| SWPF-41 | 11 | GAP-04ccc | P | 2 | GAP-pct-216 | 5.47 | 10.75 |
| blank | 11 | blank | P | 3 | GAP-pct-041 | 5.47 | 5.8 |

**Table B3. Initial and Final pH Values for the PCTs of the High TiO₂ Glasses
(continued)**

| SRNL ID | Oven Run | Working Glass ID (w HT) | Block | Seq | Lab ID | Initial pH | Final pH |
|----------|----------|-------------------------|-------|-----|-------------|------------|----------|
| EA | 11 | EA | P | 4 | GAP-pct-326 | 5.47 | 11.83 |
| SWPF-43 | 11 | GAP-28 | P | 5 | GAP-pct-333 | 5.47 | 10.88 |
| SWPF-42 | 11 | GAP-27 | P | 6 | GAP-pct-109 | 5.47 | 10.46 |
| SWPF-46 | 12 | GAP-39ccc | P | 7 | GAP-pct-211 | 5.47 | 10.94 |
| SWPF-44 | 11 | GAP-01ccc | P | 8 | GAP-pct-331 | 5.47 | 10.54 |
| SWPF-46 | 12 | GAP-39 | P | 9 | GAP-pct-349 | 5.47 | 11.03 |
| EA | 12 | EA | P | 10 | GAP-pct-276 | 5.47 | 11.89 |
| SWPF-45 | 12 | GAP-08 | P | 11 | GAP-pct-099 | 5.47 | 10.44 |
| ARM-1 | 11 | ARM-1 | P | 12 | GAP-pct-066 | 5.47 | 10.16 |
| soln std | . | soln std | P | 13 | std-P2 | . | . |
| SWPF-42 | 11 | GAP-27ccc | P | 14 | GAP-pct-031 | 5.47 | 10.42 |
| SWPF-45 | 12 | GAP-08ccc | P | 15 | GAP-pct-103 | 5.47 | 10.41 |
| SWPF-44 | 11 | GAP-01 | P | 16 | GAP-pct-154 | 5.47 | 10.62 |
| SWPF-43 | 11 | GAP-28ccc | P | 17 | GAP-pct-359 | 5.47 | 10.79 |
| SWPF-41 | 11 | GAP-04 | P | 18 | GAP-pct-004 | 5.47 | 10.69 |
| ARM-1 | 12 | ARM-1 | P | 19 | GAP-pct-174 | 5.47 | 10.31 |
| SWPF-47 | 12 | GAP-45 | P | 20 | GAP-pct-059 | 5.47 | 10.83 |
| SWPF-47 | 12 | GAP-45ccc | P | 21 | GAP-pct-241 | 5.47 | 10.76 |
| soln std | . | soln std | P | 22 | std-P3 | . | . |
| soln std | . | soln std | Q | 1 | std-Q1 | . | . |
| SWPF-46 | 12 | GAP-39ccc | Q | 2 | GAP-pct-148 | 5.47 | 11 |
| blank | 12 | blank | Q | 3 | GAP-pct-393 | 5.47 | 5.56 |
| SWPF-42 | 11 | GAP-27ccc | Q | 4 | GAP-pct-304 | 5.47 | 10.38 |
| SWPF-46 | 12 | GAP-39 | Q | 5 | GAP-pct-100 | 5.47 | 10.95 |
| blank | 11 | blank | Q | 6 | GAP-pct-113 | 5.47 | 5.3 |
| SWPF-43 | 11 | GAP-28ccc | Q | 7 | GAP-pct-392 | 5.47 | 10.84 |
| EA | 12 | EA | Q | 8 | GAP-pct-023 | 5.47 | 11.87 |
| SWPF-45 | 12 | GAP-08ccc | Q | 9 | GAP-pct-256 | 5.47 | 10.46 |
| SWPF-44 | 11 | GAP-01ccc | Q | 10 | GAP-pct-009 | 5.47 | 10.47 |
| SWPF-47 | 12 | GAP-45ccc | Q | 11 | GAP-pct-060 | 5.47 | 10.78 |
| EA | 11 | EA | Q | 12 | GAP-pct-260 | 5.47 | 11.75 |
| soln std | . | soln std | Q | 13 | std-Q2 | . | . |
| SWPF-47 | 12 | GAP-45 | Q | 14 | GAP-pct-232 | 5.47 | 10.81 |
| SWPF-44 | 11 | GAP-01 | Q | 15 | GAP-pct-049 | 5.47 | 10.62 |
| SWPF-42 | 11 | GAP-27 | Q | 16 | GAP-pct-097 | 5.47 | 10.45 |
| ARM-1 | 11 | ARM-1 | Q | 17 | GAP-pct-050 | 5.47 | 10.22 |
| ARM-1 | 12 | ARM-1 | Q | 18 | GAP-pct-146 | 5.47 | 10.31 |
| SWPF-41 | 11 | GAP-04ccc | Q | 19 | GAP-pct-228 | 5.47 | 10.71 |
| SWPF-41 | 11 | GAP-04 | Q | 20 | GAP-pct-159 | 5.47 | 10.75 |
| SWPF-45 | 12 | GAP-08 | Q | 21 | GAP-pct-383 | 5.47 | 10.48 |
| SWPF-43 | 11 | GAP-28 | Q | 22 | GAP-pct-259 | 5.47 | 10.89 |
| soln std | . | soln std | Q | 23 | std-Q3 | . | . |
| soln std | . | soln std | R | 1 | std-R1 | . | . |
| SWPF-45 | 12 | GAP-08ccc | R | 2 | GAP-pct-106 | 5.47 | 10.41 |
| EA | 11 | EA | R | 3 | GAP-pct-027 | 5.47 | 11.64 |
| EA | 12 | EA | R | 4 | GAP-pct-062 | 5.47 | 11.89 |
| SWPF-42 | 11 | GAP-27ccc | R | 5 | GAP-pct-225 | 5.47 | 10.4 |
| SWPF-41 | 11 | GAP-04 | R | 6 | GAP-pct-040 | 5.47 | 10.7 |
| SWPF-44 | 11 | GAP-01 | R | 7 | GAP-pct-318 | 5.47 | 10.58 |
| SWPF-43 | 11 | GAP-28 | R | 8 | GAP-pct-238 | 5.47 | 10.83 |
| SWPF-45 | 12 | GAP-08 | R | 9 | GAP-pct-246 | 5.47 | 10.44 |
| ARM-1 | 12 | ARM-1 | R | 10 | GAP-pct-321 | 5.47 | 10.4 |
| SWPF-42 | 11 | GAP-27 | R | 11 | GAP-pct-036 | 5.47 | 10.46 |
| SWPF-41 | 11 | GAP-04ccc | R | 12 | GAP-pct-355 | 5.47 | 10.7 |
| soln std | . | soln std | R | 13 | std-R2 | . | . |
| SWPF-43 | 11 | GAP-28ccc | R | 14 | GAP-pct-193 | 5.47 | 10.85 |
| SWPF-44 | 11 | GAP-01ccc | R | 15 | GAP-pct-129 | 5.47 | 10.6 |
| SWPF-47 | 12 | GAP-45ccc | R | 16 | GAP-pct-013 | 5.47 | 10.76 |
| blank | 12 | blank | R | 17 | GAP-pct-178 | 5.47 | 5.7 |
| SWPF-46 | 12 | GAP-39ccc | R | 18 | GAP-pct-125 | 5.47 | 11 |
| ARM-1 | 11 | ARM-1 | R | 19 | GAP-pct-058 | 5.47 | 10.18 |

Table B3. Initial and Final pH Values for the PCTs of the High TiO₂ Glasses (continued)

| SRNL ID | Oven Run | Working Glass ID (w HT) | Block | Seq | Lab ID | Initial pH | Final pH |
|----------|----------|-------------------------|-------|-----|-------------|------------|----------|
| SWPF-46 | 12 | GAP-39 | R | 20 | GAP-pct-016 | 5.47 | 11.01 |
| SWPF-47 | 12 | GAP-45 | R | 21 | GAP-pct-135 | 5.47 | 10.83 |
| soln std | . | soln std | R | 22 | std-R3 | . | . |
| soln std | . | soln std | S | 1 | std-S1 | . | . |
| SWPF-50 | 13 | GAP-18 | S | 2 | GAP-pct-117 | 5.48 | 11.12 |
| SWPF-48 | 13 | GAP-25ccc | S | 3 | GAP-pct-176 | 5.48 | 10.54 |
| SWPF-49 | 13 | GAP-02ccc | S | 4 | GAP-pct-328 | 5.48 | 10.99 |
| SWPF-48 | 13 | GAP-25 | S | 5 | GAP-pct-362 | 5.48 | 10.61 |
| ARM-1 | 13 | ARM-1 | S | 6 | GAP-pct-164 | 5.48 | 10.41 |
| soln std | . | soln std | S | 7 | std-S2 | . | . |
| SWPF-50 | 13 | GAP-18ccc | S | 8 | GAP-pct-363 | 5.48 | 11.25 |
| blank | 13 | blank | S | 9 | GAP-pct-001 | 5.48 | 5.2 |
| EA | 13 | EA | S | 10 | GAP-pct-271 | 5.48 | 11.71 |
| SWPF-49 | 13 | GAP-02 | S | 11 | GAP-pct-347 | 5.48 | 10.94 |
| soln std | . | soln std | S | 12 | std-S3 | . | . |
| soln std | . | soln std | T | 13 | std-T1 | . | . |
| ARM-1 | 13 | ARM-1 | T | 14 | GAP-pct-275 | 5.48 | 10.41 |
| SWPF-50 | 13 | GAP-18ccc | T | 15 | GAP-pct-360 | 5.48 | 11.24 |
| SWPF-49 | 13 | GAP-02ccc | T | 16 | GAP-pct-048 | 5.48 | 10.95 |
| SWPF-48 | 13 | GAP-25ccc | T | 17 | GAP-pct-124 | 5.48 | 10.53 |
| SWPF-49 | 13 | GAP-02 | T | 18 | GAP-pct-126 | 5.48 | 11 |
| soln std | . | soln std | T | 19 | std-T2 | . | . |
| EA | 13 | EA | T | 20 | GAP-pct-299 | 5.48 | 11.71 |
| SWPF-50 | 13 | GAP-18 | T | 21 | GAP-pct-374 | 5.48 | 11.11 |
| SWPF-48 | 13 | GAP-25 | T | 22 | GAP-pct-272 | 5.48 | 10.61 |
| soln std | . | soln std | T | 23 | std-T3 | . | . |
| soln std | . | soln std | U | 1 | std-U1 | . | . |
| SWPF-49 | 13 | GAP-02ccc | U | 2 | GAP-pct-195 | 5.48 | 10.89 |
| SWPF-50 | 13 | GAP-18 | U | 3 | GAP-pct-169 | 5.48 | 11.12 |
| EA | 13 | EA | U | 4 | GAP-pct-172 | 5.48 | 11.7 |
| blank | 13 | blank | U | 5 | GAP-pct-163 | 5.48 | 5.2 |
| SWPF-49 | 13 | GAP-02 | U | 6 | GAP-pct-012 | 5.48 | 11 |
| soln std | . | soln std | U | 7 | std-U2 | . | . |
| ARM-1 | 13 | ARM-1 | U | 8 | GAP-pct-039 | 5.48 | 10.42 |
| SWPF-48 | 13 | GAP-25 | U | 9 | GAP-pct-061 | 5.48 | 10.6 |
| SWPF-50 | 13 | GAP-18ccc | U | 10 | GAP-pct-037 | 5.48 | 11.25 |
| SWPF-48 | 13 | GAP-25ccc | U | 11 | GAP-pct-204 | 5.48 | 10.52 |
| soln std | . | soln std | U | 12 | std-U3 | . | . |

Table B4. PCT Normalized Concentrations for the Study Glasses by Compositional View and Heat Treatment

| Desc | SRNL ID | Heat Treatment | Comp View | log NC [B (g/L)] | log NC [Li(g/L)] | log NC [Na (g/L)] | log NC [Si (g/L)] | NC B(g/L) | NC Li (g/L) | NC Na (g/L) | NC Si (g/L) |
|----------|---------|----------------|-----------|------------------|------------------|-------------------|-------------------|-----------|-------------|-------------|-------------|
| Oven 1 | ARM | ref | ref | -0.1732 | -0.1520 | -0.1807 | -0.4427 | 0.671 | 0.705 | 0.660 | 0.361 |
| Oven 2 | ARM | ref | ref | -0.1029 | -0.1235 | -0.1588 | -0.4642 | 0.789 | 0.752 | 0.694 | 0.343 |
| Oven 3 | ARM | ref | ref | -0.1582 | -0.1120 | -0.1450 | -0.4365 | 0.695 | 0.773 | 0.716 | 0.366 |
| Oven 4 | ARM | ref | ref | -0.1878 | -0.1498 | -0.1886 | -0.4526 | 0.649 | 0.708 | 0.648 | 0.353 |
| Oven 5 | ARM | ref | ref | -0.2043 | -0.1785 | -0.2199 | -0.4789 | 0.625 | 0.663 | 0.603 | 0.332 |
| Oven 6 | ARM | ref | ref | -0.1742 | -0.1420 | -0.1867 | -0.4654 | 0.670 | 0.721 | 0.651 | 0.342 |
| Oven 7 | ARM | ref | ref | -0.1686 | -0.1336 | -0.1795 | -0.4627 | 0.678 | 0.735 | 0.661 | 0.345 |
| Oven 8 | ARM | ref | ref | -0.1778 | -0.1230 | -0.1632 | -0.4446 | 0.664 | 0.753 | 0.687 | 0.359 |
| Oven 9 | ARM | ref | ref | -0.0841 | -0.1258 | -0.1743 | -0.4418 | 0.824 | 0.748 | 0.669 | 0.362 |
| Oven 10 | ARM | ref | ref | -0.0073 | -0.0984 | -0.1497 | -0.4114 | 0.983 | 0.797 | 0.708 | 0.388 |
| Oven 11 | ARM | ref | ref | -0.1992 | -0.1626 | -0.2163 | -0.4619 | 0.632 | 0.688 | 0.608 | 0.345 |
| Oven 12 | ARM | ref | ref | -0.2039 | -0.1683 | -0.2144 | -0.4774 | 0.625 | 0.679 | 0.610 | 0.333 |
| Oven 13 | ARM | ref | ref | -0.1962 | -0.1526 | -0.1981 | -0.4469 | 0.637 | 0.704 | 0.634 | 0.357 |
| Oven 1 | EA | ref | ref | 1.2209 | 0.9235 | 1.0825 | 0.5139 | 16.629 | 8.385 | 12.093 | 3.265 |
| Oven 2 | EA | ref | ref | 1.2127 | 0.9653 | 1.1246 | 0.5201 | 16.318 | 9.233 | 13.322 | 3.312 |
| Oven 3 | EA | ref | ref | 1.2471 | 0.9929 | 1.1314 | 0.5530 | 17.664 | 9.838 | 13.534 | 3.573 |
| Oven 4 | EA | ref | ref | 1.1720 | 0.9279 | 1.0694 | 0.4932 | 14.859 | 8.470 | 11.733 | 3.114 |
| Oven 5 | EA | ref | ref | 1.2357 | 0.9912 | 1.1075 | 0.5512 | 17.206 | 9.800 | 12.809 | 3.558 |
| Oven 6 | EA | ref | ref | 1.2299 | 0.9966 | 1.0922 | 0.5593 | 16.978 | 9.923 | 12.365 | 3.625 |
| Oven 7 | EA | ref | ref | 1.2448 | 0.9931 | 1.1263 | 0.5626 | 17.570 | 9.841 | 13.376 | 3.653 |
| Oven 8 | EA | ref | ref | 1.2268 | 0.9801 | 1.1153 | 0.5548 | 16.859 | 9.552 | 13.040 | 3.587 |
| Oven 9 | EA | ref | ref | 1.2502 | 1.0310 | 1.1429 | 0.5700 | 17.791 | 10.739 | 13.897 | 3.715 |
| Oven 10 | EA | ref | ref | 1.2129 | 1.0110 | 1.1114 | 0.5485 | 16.328 | 10.257 | 12.924 | 3.536 |
| Oven 11 | EA | ref | ref | 1.1927 | 0.9935 | 1.0897 | 0.5621 | 15.586 | 9.852 | 12.294 | 3.648 |
| Oven 12 | EA | ref | ref | 1.2432 | 0.9976 | 1.1313 | 0.5715 | 17.507 | 9.944 | 13.529 | 3.728 |
| Oven 13 | EA | ref | ref | 1.2112 | 0.9432 | 1.1073 | 0.5236 | 16.261 | 8.774 | 12.804 | 3.339 |
| D-Opt OL | SWPF-01 | ccc | Measured | 0.9521 | 0.8398 | 0.7940 | 0.4390 | 8.956 | 6.915 | 6.223 | 2.748 |
| D-Opt OL | SWPF-02 | ccc | Measured | 0.1759 | 0.1907 | 0.0915 | -0.0593 | 1.499 | 1.551 | 1.234 | 0.872 |
| D-Opt OL | SWPF-03 | ccc | Measured | 0.3761 | 0.4819 | 0.2442 | 0.1308 | 2.377 | 3.033 | 1.755 | 1.352 |
| D-Opt OL | SWPF-04 | ccc | Measured | -0.1111 | 0.0168 | -0.1422 | -0.1929 | 0.774 | 1.039 | 0.721 | 0.641 |
| D-Opt OL | SWPF-05 | ccc | Measured | 0.5319 | 0.3665 | 0.3974 | -0.0635 | 3.404 | 2.326 | 2.497 | 0.864 |
| D-Opt OL | SWPF-06 | ccc | Measured | 0.3423 | 0.2955 | 0.1546 | 0.0099 | 2.199 | 1.975 | 1.428 | 1.023 |
| D-Opt OL | SWPF-07 | ccc | Measured | 0.5865 | 0.5136 | 0.4108 | 0.1290 | 3.859 | 3.263 | 2.575 | 1.346 |
| D-Opt OL | SWPF-08 | ccc | Measured | -0.3688 | -0.1908 | -0.4251 | -0.4942 | 0.428 | 0.644 | 0.376 | 0.320 |
| D-Opt OL | SWPF-09 | ccc | Measured | 0.0106 | 0.0615 | -0.0037 | -0.1567 | 1.025 | 1.152 | 0.991 | 0.697 |
| D-Opt OL | SWPF-10 | ccc | Measured | -0.0914 | -0.0903 | -0.0996 | -0.3778 | 0.810 | 0.812 | 0.795 | 0.419 |
| D-Opt OL | SWPF-11 | ccc | Measured | 0.0762 | -0.0759 | 0.0237 | -0.2553 | 1.192 | 0.840 | 1.056 | 0.556 |
| D-Opt OL | SWPF-12 | ccc | Measured | 0.2883 | 0.4671 | 0.0531 | 0.1464 | 1.942 | 2.932 | 1.130 | 1.401 |
| D-Opt OL | SWPF-13 | ccc | Measured | -0.1540 | -0.0613 | -0.2176 | -0.2525 | 0.702 | 0.868 | 0.606 | 0.559 |
| D-Opt OL | SWPF-14 | ccc | Measured | -0.4221 | -0.2717 | -0.4648 | -0.5156 | 0.378 | 0.535 | 0.343 | 0.305 |
| D-Opt OL | SWPF-15 | ccc | Measured | -0.3036 | -0.2159 | -0.3321 | -0.4250 | 0.497 | 0.608 | 0.466 | 0.376 |
| centroid | SWPF-16 | ccc | Measured | -0.2210 | -0.1463 | -0.2345 | -0.3304 | 0.601 | 0.714 | 0.583 | 0.467 |

Table B4. PCT Normalized Concentrations for the Study Glasses by Compositional View and Heat Treatment (continued)

| Desc | SRNL ID | Heat Treatment | Comp View | log NC [B (g/L)] | log NC [Li(g/L)] | log NC [Na (g/L)] | log NC [Si (g/L)] | NC B(g/L) | NC Li (g/L) | NC Na (g/L) | NC Si (g/L) |
|----------|---------|----------------|-----------|------------------|------------------|-------------------|-------------------|-----------|-------------|-------------|-------------|
| D-Opt IL | SWPF-17 | ccc | Measured | -0.3068 | -0.2435 | -0.1927 | -0.3659 | 0.493 | 0.571 | 0.642 | 0.431 |
| D-Opt IL | SWPF-18 | ccc | Measured | -0.0263 | 0.0412 | 0.1048 | -0.1396 | 0.941 | 1.100 | 1.273 | 0.725 |
| D-Opt IL | SWPF-19 | ccc | Measured | -0.3092 | -0.2556 | -0.2154 | -0.4104 | 0.491 | 0.555 | 0.609 | 0.389 |
| D-Opt IL | SWPF-20 | ccc | Measured | -0.2176 | -0.1285 | -0.1535 | -0.3162 | 0.606 | 0.744 | 0.702 | 0.483 |
| D-Opt IL | SWPF-21 | ccc | Measured | -0.1391 | -0.0991 | -0.0194 | -0.2476 | 0.726 | 0.796 | 0.956 | 0.565 |
| D-Opt IL | SWPF-22 | ccc | Measured | -0.0972 | -0.1328 | -0.0659 | -0.3056 | 0.799 | 0.737 | 0.859 | 0.495 |
| D-Opt IL | SWPF-23 | ccc | Measured | -0.0722 | -0.1422 | -0.0927 | -0.3066 | 0.847 | 0.721 | 0.808 | 0.494 |
| D-Opt IL | SWPF-24 | ccc | Measured | -0.2888 | -0.1874 | -0.3550 | -0.4137 | 0.514 | 0.649 | 0.442 | 0.386 |
| D-Opt IL | SWPF-25 | ccc | Measured | -0.1487 | -0.0878 | -0.1462 | -0.3088 | 0.710 | 0.817 | 0.714 | 0.491 |
| D-Opt IL | SWPF-26 | ccc | Measured | -0.1023 | -0.0450 | -0.0922 | -0.2685 | 0.790 | 0.902 | 0.809 | 0.539 |
| D-Opt IL | SWPF-27 | ccc | Measured | -0.2207 | -0.1200 | -0.2107 | -0.2808 | 0.602 | 0.759 | 0.616 | 0.524 |
| D-Opt IL | SWPF-28 | ccc | Measured | -0.1226 | -0.0561 | -0.1283 | -0.2713 | 0.754 | 0.879 | 0.744 | 0.535 |
| D-Opt IL | SWPF-29 | ccc | Measured | -0.2283 | -0.1116 | -0.1970 | -0.3163 | 0.591 | 0.773 | 0.635 | 0.483 |
| D-Opt IL | SWPF-30 | ccc | Measured | -0.3635 | -0.2692 | -0.3216 | -0.4383 | 0.433 | 0.538 | 0.477 | 0.365 |
| D-Opt IL | SWPF-31 | ccc | Measured | -0.1736 | -0.1572 | -0.1435 | -0.3910 | 0.671 | 0.696 | 0.719 | 0.406 |
| SF | SWPF-32 | ccc | Measured | -0.2391 | -0.0881 | -0.1896 | -0.3027 | 0.577 | 0.816 | 0.646 | 0.498 |
| SF | SWPF-33 | ccc | Measured | -0.1617 | -0.1047 | -0.1940 | -0.2968 | 0.689 | 0.786 | 0.640 | 0.505 |
| SF | SWPF-34 | ccc | Measured | -0.2285 | -0.1742 | -0.1097 | -0.3350 | 0.591 | 0.670 | 0.777 | 0.462 |
| SF | SWPF-35 | ccc | Measured | -0.1356 | -0.1093 | -0.1622 | -0.2944 | 0.732 | 0.778 | 0.688 | 0.508 |
| SF | SWPF-36 | ccc | Measured | -0.2669 | -0.1461 | -0.2314 | -0.3451 | 0.541 | 0.714 | 0.587 | 0.452 |
| SF | SWPF-37 | ccc | Measured | -0.1727 | -0.0728 | -0.1830 | -0.2806 | 0.672 | 0.846 | 0.656 | 0.524 |
| SF | SWPF-38 | ccc | Measured | -0.1770 | -0.1370 | -0.1344 | -0.3196 | 0.665 | 0.729 | 0.734 | 0.479 |
| SF | SWPF-39 | ccc | Measured | -0.0894 | -0.0076 | 0.0203 | -0.1854 | 0.814 | 0.983 | 1.048 | 0.653 |
| SF | SWPF-40 | ccc | Measured | 0.1350 | 0.0764 | 0.0077 | -0.2510 | 1.365 | 1.192 | 1.018 | 0.561 |
| SF | SWPF-41 | ccc | Measured | -0.0847 | -0.0314 | -0.0679 | -0.2225 | 0.823 | 0.930 | 0.855 | 0.599 |
| SF | SWPF-42 | ccc | Measured | -0.2295 | -0.1658 | -0.1539 | -0.3405 | 0.590 | 0.683 | 0.702 | 0.457 |
| SF | SWPF-43 | ccc | Measured | -0.0568 | -0.0015 | -0.0322 | -0.1896 | 0.877 | 0.996 | 0.929 | 0.646 |
| SF | SWPF-44 | ccc | Measured | -0.1903 | -0.1030 | -0.1882 | -0.2925 | 0.645 | 0.789 | 0.648 | 0.510 |
| SF | SWPF-45 | ccc | Measured | -0.2964 | -0.2256 | -0.2422 | -0.3946 | 0.505 | 0.595 | 0.573 | 0.403 |
| SF | SWPF-46 | ccc | Measured | -0.1385 | -0.1226 | -0.0518 | -0.2601 | 0.727 | 0.754 | 0.888 | 0.549 |
| SF | SWPF-47 | ccc | Measured | -0.2082 | -0.1592 | -0.1528 | -0.3247 | 0.619 | 0.693 | 0.703 | 0.473 |
| SF | SWPF-48 | ccc | Measured | -0.2765 | -0.1947 | -0.2614 | -0.4078 | 0.529 | 0.639 | 0.548 | 0.391 |
| SF | SWPF-49 | ccc | Measured | -0.0427 | -0.0668 | -0.0211 | -0.2528 | 0.906 | 0.857 | 0.953 | 0.559 |
| SF | SWPF-50 | ccc | Measured | 0.1590 | 0.1439 | 0.0287 | -0.1681 | 1.442 | 1.393 | 1.068 | 0.679 |
| D-Opt OL | SWPF-01 | quenched | Measured | -0.0256 | -0.0136 | -0.0958 | -0.1785 | 0.943 | 0.969 | 0.802 | 0.663 |
| D-Opt OL | SWPF-02 | quenched | Measured | 0.0193 | 0.0599 | -0.0083 | -0.1235 | 1.045 | 1.148 | 0.981 | 0.752 |
| D-Opt OL | SWPF-03 | quenched | Measured | 0.1157 | 0.0919 | 0.0514 | -0.0715 | 1.305 | 1.236 | 1.126 | 0.848 |
| D-Opt OL | SWPF-04 | quenched | Measured | -0.1130 | 0.0231 | -0.1538 | -0.1966 | 0.771 | 1.055 | 0.702 | 0.636 |
| D-Opt OL | SWPF-05 | quenched | Measured | 0.5763 | 0.4207 | 0.4365 | -0.0628 | 3.770 | 2.634 | 2.732 | 0.865 |
| D-Opt OL | SWPF-06 | quenched | Measured | 0.3345 | 0.3095 | 0.1603 | 0.0167 | 2.160 | 2.040 | 1.446 | 1.039 |
| D-Opt OL | SWPF-07 | quenched | Measured | 0.4223 | 0.3633 | 0.2565 | 0.0179 | 2.644 | 2.308 | 1.805 | 1.042 |
| D-Opt OL | SWPF-08 | quenched | Measured | -0.3940 | -0.1793 | -0.4358 | -0.5129 | 0.404 | 0.662 | 0.367 | 0.307 |

Table B4. PCT Normalized Concentrations for the Study Glasses by Compositional View and Heat Treatment (continued)

| Desc | SRNL ID | Heat Treatment | Comp View | log NC [B (g/L)] | log NC [Li(g/L)] | log NC [Na (g/L)] | log NC [Si (g/L)] | NC B(g/L) | NC Li (g/L) | NC Na (g/L) | NC Si (g/L) |
|----------|---------|----------------|-----------|------------------|------------------|-------------------|-------------------|-----------|-------------|-------------|-------------|
| D-Opt OL | SWPF-09 | quenched | Measured | 0.1382 | 0.1402 | 0.0776 | -0.0899 | 1.375 | 1.381 | 1.196 | 0.813 |
| D-Opt OL | SWPF-10 | quenched | Measured | 0.1138 | 0.0866 | 0.0508 | -0.3509 | 1.300 | 1.221 | 1.124 | 0.446 |
| D-Opt OL | SWPF-11 | quenched | Measured | 0.2739 | 0.0430 | 0.1783 | -0.1774 | 1.879 | 1.104 | 1.508 | 0.665 |
| D-Opt OL | SWPF-12 | quenched | Measured | -0.0517 | 0.0443 | -0.2152 | -0.0960 | 0.888 | 1.107 | 0.609 | 0.802 |
| D-Opt OL | SWPF-13 | quenched | Measured | -0.1513 | -0.0612 | -0.2013 | -0.2472 | 0.706 | 0.869 | 0.629 | 0.566 |
| D-Opt OL | SWPF-14 | quenched | Measured | -0.3505 | -0.2098 | -0.4486 | -0.4764 | 0.446 | 0.617 | 0.356 | 0.334 |
| D-Opt OL | SWPF-15 | quenched | Measured | -0.2225 | -0.1052 | -0.2613 | -0.4070 | 0.599 | 0.785 | 0.548 | 0.392 |
| centroid | SWPF-16 | quenched | Measured | -0.1528 | -0.1010 | -0.2091 | -0.3075 | 0.703 | 0.792 | 0.618 | 0.493 |
| D-Opt IL | SWPF-17 | quenched | Measured | -0.2762 | -0.2887 | -0.1905 | -0.3793 | 0.529 | 0.514 | 0.645 | 0.418 |
| D-Opt IL | SWPF-18 | quenched | Measured | -0.0092 | 0.0270 | 0.1239 | -0.1300 | 0.979 | 1.064 | 1.330 | 0.741 |
| D-Opt IL | SWPF-19 | quenched | Measured | -0.2612 | -0.2519 | -0.1774 | -0.3987 | 0.548 | 0.560 | 0.665 | 0.399 |
| D-Opt IL | SWPF-20 | quenched | Measured | -0.0810 | -0.0673 | -0.1052 | -0.2995 | 0.830 | 0.856 | 0.785 | 0.502 |
| D-Opt IL | SWPF-21 | quenched | Measured | -0.0624 | -0.1432 | -0.0101 | -0.2556 | 0.866 | 0.719 | 0.977 | 0.555 |
| D-Opt IL | SWPF-22 | quenched | Measured | -0.0195 | -0.1211 | -0.0222 | -0.2908 | 0.956 | 0.757 | 0.950 | 0.512 |
| D-Opt IL | SWPF-23 | quenched | Measured | -0.0780 | -0.1726 | -0.0865 | -0.3157 | 0.836 | 0.672 | 0.819 | 0.483 |
| D-Opt IL | SWPF-24 | quenched | Measured | -0.2942 | -0.1465 | -0.3536 | -0.4422 | 0.508 | 0.714 | 0.443 | 0.361 |
| D-Opt IL | SWPF-25 | quenched | Measured | -0.1023 | -0.0442 | -0.1083 | -0.2939 | 0.790 | 0.903 | 0.779 | 0.508 |
| D-Opt IL | SWPF-26 | quenched | Measured | -0.0792 | -0.0620 | -0.0838 | -0.2899 | 0.833 | 0.867 | 0.825 | 0.513 |
| D-Opt IL | SWPF-27 | quenched | Measured | -0.1985 | -0.1073 | -0.2143 | -0.3036 | 0.633 | 0.781 | 0.611 | 0.497 |
| D-Opt IL | SWPF-28 | quenched | Measured | -0.1259 | -0.0630 | -0.1137 | -0.2900 | 0.748 | 0.865 | 0.770 | 0.513 |
| D-Opt IL | SWPF-29 | quenched | Measured | -0.2049 | -0.0564 | -0.1617 | -0.3073 | 0.624 | 0.878 | 0.689 | 0.493 |
| D-Opt IL | SWPF-30 | quenched | Measured | -0.3496 | -0.1946 | -0.2946 | -0.4639 | 0.447 | 0.639 | 0.507 | 0.344 |
| D-Opt IL | SWPF-31 | quenched | Measured | -0.1896 | -0.1985 | -0.1228 | -0.3921 | 0.646 | 0.633 | 0.754 | 0.405 |
| SF | SWPF-32 | quenched | Measured | -0.1953 | -0.0901 | -0.1935 | -0.2905 | 0.638 | 0.813 | 0.641 | 0.512 |
| SF | SWPF-33 | quenched | Measured | -0.1314 | -0.0806 | -0.1797 | -0.3104 | 0.739 | 0.831 | 0.661 | 0.489 |
| SF | SWPF-34 | quenched | Measured | -0.1965 | -0.1978 | -0.0859 | -0.3263 | 0.636 | 0.634 | 0.821 | 0.472 |
| SF | SWPF-35 | quenched | Measured | -0.0601 | -0.0440 | -0.1019 | -0.2825 | 0.871 | 0.904 | 0.791 | 0.522 |
| SF | SWPF-36 | quenched | Measured | -0.1729 | -0.0734 | -0.1745 | -0.3032 | 0.672 | 0.844 | 0.669 | 0.498 |
| SF | SWPF-37 | quenched | Measured | -0.1325 | -0.0441 | -0.1521 | -0.2664 | 0.737 | 0.903 | 0.705 | 0.541 |
| SF | SWPF-38 | quenched | Measured | -0.0985 | -0.1075 | -0.0847 | -0.3207 | 0.797 | 0.781 | 0.823 | 0.478 |
| SF | SWPF-39 | quenched | Measured | -0.0633 | -0.0409 | 0.0339 | -0.1934 | 0.864 | 0.910 | 1.081 | 0.641 |
| SF | SWPF-40 | quenched | Measured | -0.1466 | -0.1057 | -0.0877 | -0.3272 | 0.714 | 0.784 | 0.817 | 0.471 |
| SF | SWPF-41 | quenched | Measured | -0.1121 | -0.0784 | -0.0868 | -0.2573 | 0.772 | 0.835 | 0.819 | 0.553 |
| SF | SWPF-42 | quenched | Measured | -0.1900 | -0.1975 | -0.1328 | -0.3337 | 0.646 | 0.635 | 0.736 | 0.464 |
| SF | SWPF-43 | quenched | Measured | -0.0184 | 0.0026 | -0.0133 | -0.1925 | 0.958 | 1.006 | 0.970 | 0.642 |
| SF | SWPF-44 | quenched | Measured | -0.1303 | -0.0812 | -0.1622 | -0.2906 | 0.741 | 0.829 | 0.688 | 0.512 |
| SF | SWPF-45 | quenched | Measured | -0.2744 | -0.2296 | -0.2432 | -0.4091 | 0.532 | 0.589 | 0.571 | 0.390 |
| SF | SWPF-46 | quenched | Measured | -0.1519 | -0.1445 | -0.0367 | -0.2650 | 0.705 | 0.717 | 0.919 | 0.543 |
| SF | SWPF-47 | quenched | Measured | -0.1549 | -0.1481 | -0.1185 | -0.3286 | 0.700 | 0.711 | 0.761 | 0.469 |
| SF | SWPF-48 | quenched | Measured | -0.2093 | -0.1758 | -0.2316 | -0.3977 | 0.618 | 0.667 | 0.587 | 0.400 |
| SF | SWPF-49 | quenched | Measured | -0.0591 | -0.1047 | -0.0101 | -0.2600 | 0.873 | 0.786 | 0.977 | 0.550 |
| SF | SWPF-50 | quenched | Measured | -0.0878 | -0.0625 | -0.0767 | -0.2735 | 0.817 | 0.866 | 0.838 | 0.533 |

Table B4. PCT Normalized Concentrations for the Study Glasses by Compositional View and Heat Treatment (continued)

| Desc | SRNL ID | Heat Treatment | Comp View | log NC [B (g/L)] | log NC [Li(g/L)] | log NC [Na (g/L)] | log NC [Si (g/L)] | NC B(g/L) | NC Li (g/L) | NC Na (g/L) | NC Si (g/L) |
|----------|---------|----------------|-----------|------------------|------------------|-------------------|-------------------|-----------|-------------|-------------|-------------|
| D-Opt OL | SWPF-01 | ccc | targeted | 0.9434 | 0.8297 | 0.8002 | 0.4401 | 8.779 | 6.755 | 6.313 | 2.755 |
| D-Opt OL | SWPF-02 | ccc | targeted | 0.1637 | 0.1779 | 0.0962 | -0.0571 | 1.458 | 1.506 | 1.248 | 0.877 |
| D-Opt OL | SWPF-03 | ccc | targeted | 0.3683 | 0.4666 | 0.2517 | 0.1317 | 2.335 | 2.928 | 1.785 | 1.354 |
| D-Opt OL | SWPF-04 | ccc | targeted | -0.1193 | -0.0005 | -0.1376 | -0.1896 | 0.760 | 0.999 | 0.728 | 0.646 |
| D-Opt OL | SWPF-05 | ccc | targeted | 0.5291 | 0.3844 | 0.3980 | -0.0662 | 3.382 | 2.423 | 2.501 | 0.859 |
| D-Opt OL | SWPF-06 | ccc | targeted | 0.3311 | 0.2774 | 0.1499 | 0.0075 | 2.143 | 1.894 | 1.412 | 1.017 |
| D-Opt OL | SWPF-07 | ccc | targeted | 0.5744 | 0.4964 | 0.4046 | 0.1291 | 3.754 | 3.136 | 2.539 | 1.346 |
| D-Opt OL | SWPF-08 | ccc | targeted | -0.3761 | -0.2063 | -0.4034 | -0.4913 | 0.421 | 0.622 | 0.395 | 0.323 |
| D-Opt OL | SWPF-09 | ccc | targeted | 0.0051 | 0.0417 | -0.0018 | -0.1551 | 1.012 | 1.101 | 0.996 | 0.700 |
| D-Opt OL | SWPF-10 | ccc | targeted | -0.0953 | -0.0762 | -0.0926 | -0.3771 | 0.803 | 0.839 | 0.808 | 0.420 |
| D-Opt OL | SWPF-11 | ccc | targeted | 0.0845 | -0.0534 | 0.0313 | -0.2647 | 1.215 | 0.884 | 1.075 | 0.544 |
| D-Opt OL | SWPF-12 | ccc | targeted | 0.2790 | 0.4574 | 0.0794 | 0.1545 | 1.901 | 2.867 | 1.201 | 1.427 |
| D-Opt OL | SWPF-13 | ccc | targeted | -0.1520 | -0.0813 | -0.2120 | -0.2517 | 0.705 | 0.829 | 0.614 | 0.560 |
| D-Opt OL | SWPF-14 | ccc | targeted | -0.4180 | -0.2941 | -0.4549 | -0.5147 | 0.382 | 0.508 | 0.351 | 0.306 |
| D-Opt OL | SWPF-15 | ccc | targeted | -0.3026 | -0.2390 | -0.3179 | -0.4231 | 0.498 | 0.577 | 0.481 | 0.377 |
| centroid | SWPF-16 | ccc | targeted | -0.2229 | -0.1597 | -0.2204 | -0.3245 | 0.599 | 0.692 | 0.602 | 0.474 |
| D-Opt IL | SWPF-17 | ccc | targeted | -0.3078 | -0.2278 | -0.1821 | -0.3688 | 0.492 | 0.592 | 0.657 | 0.428 |
| D-Opt IL | SWPF-18 | ccc | targeted | -0.0360 | 0.0373 | 0.1132 | -0.1425 | 0.920 | 1.090 | 1.298 | 0.720 |
| D-Opt IL | SWPF-19 | ccc | targeted | -0.3172 | -0.2488 | -0.2072 | -0.4126 | 0.482 | 0.564 | 0.621 | 0.387 |
| D-Opt IL | SWPF-20 | ccc | targeted | -0.2347 | -0.1407 | -0.1419 | -0.3157 | 0.583 | 0.723 | 0.721 | 0.483 |
| D-Opt IL | SWPF-21 | ccc | targeted | -0.1530 | -0.0984 | -0.0119 | -0.2515 | 0.703 | 0.797 | 0.973 | 0.560 |
| D-Opt IL | SWPF-22 | ccc | targeted | -0.1226 | -0.1247 | -0.0602 | -0.3075 | 0.754 | 0.750 | 0.871 | 0.493 |
| D-Opt IL | SWPF-23 | ccc | targeted | -0.0931 | -0.1483 | -0.0789 | -0.3080 | 0.807 | 0.711 | 0.834 | 0.492 |
| D-Opt IL | SWPF-24 | ccc | targeted | -0.2989 | -0.1887 | -0.3402 | -0.4133 | 0.502 | 0.648 | 0.457 | 0.386 |
| D-Opt IL | SWPF-25 | ccc | targeted | -0.1544 | -0.0970 | -0.1371 | -0.3051 | 0.701 | 0.800 | 0.729 | 0.495 |
| D-Opt IL | SWPF-26 | ccc | targeted | -0.1113 | -0.0546 | -0.0819 | -0.2675 | 0.774 | 0.882 | 0.828 | 0.540 |
| D-Opt IL | SWPF-27 | ccc | targeted | -0.2375 | -0.1339 | -0.1939 | -0.2798 | 0.579 | 0.735 | 0.640 | 0.525 |
| D-Opt IL | SWPF-28 | ccc | targeted | -0.1381 | -0.0736 | -0.1167 | -0.2720 | 0.728 | 0.844 | 0.764 | 0.535 |
| D-Opt IL | SWPF-29 | ccc | targeted | -0.2482 | -0.1344 | -0.1896 | -0.3157 | 0.565 | 0.734 | 0.646 | 0.483 |
| D-Opt IL | SWPF-30 | ccc | targeted | -0.3732 | -0.2687 | -0.3074 | -0.4388 | 0.423 | 0.539 | 0.493 | 0.364 |
| D-Opt IL | SWPF-31 | ccc | targeted | -0.1795 | -0.1634 | -0.1310 | -0.3931 | 0.661 | 0.686 | 0.740 | 0.405 |
| SF | SWPF-32 | ccc | targeted | -0.2454 | -0.1007 | -0.1799 | -0.3064 | 0.568 | 0.793 | 0.661 | 0.494 |
| SF | SWPF-33 | ccc | targeted | -0.1764 | -0.1195 | -0.1817 | -0.2962 | 0.666 | 0.759 | 0.658 | 0.506 |
| SF | SWPF-34 | ccc | targeted | -0.2457 | -0.1820 | -0.0961 | -0.3390 | 0.568 | 0.658 | 0.801 | 0.458 |
| SF | SWPF-35 | ccc | targeted | -0.1435 | -0.1103 | -0.1507 | -0.2941 | 0.719 | 0.776 | 0.707 | 0.508 |
| SF | SWPF-36 | ccc | targeted | -0.2855 | -0.1641 | -0.2242 | -0.3466 | 0.518 | 0.685 | 0.597 | 0.450 |
| SF | SWPF-37 | ccc | targeted | -0.1790 | -0.0824 | -0.1757 | -0.2817 | 0.662 | 0.827 | 0.667 | 0.523 |
| SF | SWPF-38 | ccc | targeted | -0.1834 | -0.1420 | -0.1266 | -0.3219 | 0.656 | 0.721 | 0.747 | 0.477 |
| SF | SWPF-39 | ccc | targeted | -0.1060 | -0.0123 | 0.0302 | -0.1897 | 0.783 | 0.972 | 1.072 | 0.646 |
| SF | SWPF-40 | ccc | targeted | 0.1265 | 0.0773 | 0.0206 | -0.2527 | 1.338 | 1.195 | 1.049 | 0.559 |
| SF | SWPF-41 | ccc | targeted | -0.0924 | -0.0371 | -0.0598 | -0.2244 | 0.808 | 0.918 | 0.871 | 0.597 |
| SF | SWPF-42 | ccc | targeted | -0.2393 | -0.1816 | -0.1451 | -0.3442 | 0.576 | 0.658 | 0.716 | 0.453 |

Table B4. PCT Normalized Concentrations for the Study Glasses by Compositional View and Heat Treatment (continued)

| Desc | SRNL ID | Heat Treatment | Comp View | log NC [B (g/L)] | log NC [Li(g/L)] | log NC [Na (g/L)] | log NC [Si (g/L)] | NC B(g/L) | NC Li (g/L) | NC Na (g/L) | NC Si (g/L) |
|----------|---------|----------------|-----------|------------------|------------------|-------------------|-------------------|-----------|-------------|-------------|-------------|
| SF | SWPF-43 | ccc | targeted | -0.0706 | -0.0144 | -0.0235 | -0.1925 | 0.850 | 0.967 | 0.947 | 0.642 |
| SF | SWPF-44 | ccc | targeted | -0.2055 | -0.1188 | -0.1758 | -0.2911 | 0.623 | 0.761 | 0.667 | 0.512 |
| SF | SWPF-45 | ccc | targeted | -0.3086 | -0.2417 | -0.2235 | -0.3965 | 0.491 | 0.573 | 0.598 | 0.401 |
| SF | SWPF-46 | ccc | targeted | -0.1497 | -0.1335 | -0.0424 | -0.2635 | 0.708 | 0.735 | 0.907 | 0.545 |
| SF | SWPF-47 | ccc | targeted | -0.2224 | -0.1710 | -0.1469 | -0.3274 | 0.599 | 0.675 | 0.713 | 0.471 |
| SF | SWPF-48 | ccc | targeted | -0.2956 | -0.2118 | -0.2449 | -0.4120 | 0.506 | 0.614 | 0.569 | 0.387 |
| SF | SWPF-49 | ccc | targeted | -0.0569 | -0.0728 | -0.0113 | -0.2577 | 0.877 | 0.846 | 0.974 | 0.553 |
| SF | SWPF-50 | ccc | targeted | 0.1408 | 0.1227 | 0.0456 | -0.1687 | 1.383 | 1.326 | 1.111 | 0.678 |
| D-Opt OL | SWPF-01 | quenched | targeted | -0.0343 | -0.0238 | -0.0895 | -0.1774 | 0.924 | 0.947 | 0.814 | 0.665 |
| D-Opt OL | SWPF-02 | quenched | targeted | 0.0071 | 0.0471 | -0.0035 | -0.1212 | 1.017 | 1.115 | 0.992 | 0.756 |
| D-Opt OL | SWPF-03 | quenched | targeted | 0.1079 | 0.0767 | 0.0588 | -0.0706 | 1.282 | 1.193 | 1.145 | 0.850 |
| D-Opt OL | SWPF-04 | quenched | targeted | -0.1212 | 0.0057 | -0.1492 | -0.1933 | 0.756 | 1.013 | 0.709 | 0.641 |
| D-Opt OL | SWPF-05 | quenched | targeted | 0.5735 | 0.4385 | 0.4371 | -0.0656 | 3.746 | 2.745 | 2.736 | 0.860 |
| D-Opt OL | SWPF-06 | quenched | targeted | 0.3233 | 0.2914 | 0.1555 | 0.0142 | 2.105 | 1.956 | 1.431 | 1.033 |
| D-Opt OL | SWPF-07 | quenched | targeted | 0.4102 | 0.3461 | 0.2503 | 0.0180 | 2.572 | 2.219 | 1.780 | 1.042 |
| D-Opt OL | SWPF-08 | quenched | targeted | -0.4012 | -0.1948 | -0.4140 | -0.5100 | 0.397 | 0.639 | 0.385 | 0.309 |
| D-Opt OL | SWPF-09 | quenched | targeted | 0.1327 | 0.1204 | 0.0795 | -0.0882 | 1.357 | 1.319 | 1.201 | 0.816 |
| D-Opt OL | SWPF-10 | quenched | targeted | 0.1099 | 0.1007 | 0.0578 | -0.3502 | 1.288 | 1.261 | 1.142 | 0.447 |
| D-Opt OL | SWPF-11 | quenched | targeted | 0.2822 | 0.0654 | 0.1859 | -0.1868 | 1.915 | 1.163 | 1.534 | 0.650 |
| D-Opt OL | SWPF-12 | quenched | targeted | -0.0609 | 0.0345 | -0.1889 | -0.0880 | 0.869 | 1.083 | 0.647 | 0.817 |
| D-Opt OL | SWPF-13 | quenched | targeted | -0.1494 | -0.0812 | -0.1956 | -0.2464 | 0.709 | 0.830 | 0.637 | 0.567 |
| D-Opt OL | SWPF-14 | quenched | targeted | -0.3464 | -0.2322 | -0.4387 | -0.4755 | 0.450 | 0.586 | 0.364 | 0.335 |
| D-Opt OL | SWPF-15 | quenched | targeted | -0.2215 | -0.1283 | -0.2472 | -0.4051 | 0.601 | 0.744 | 0.566 | 0.393 |
| centroid | SWPF-16 | quenched | targeted | -0.1547 | -0.1144 | -0.1950 | -0.3016 | 0.700 | 0.768 | 0.638 | 0.499 |
| D-Opt IL | SWPF-17 | quenched | targeted | -0.2771 | -0.2730 | -0.1799 | -0.3823 | 0.528 | 0.533 | 0.661 | 0.415 |
| D-Opt IL | SWPF-18 | quenched | targeted | -0.0190 | 0.0231 | 0.1323 | -0.1329 | 0.957 | 1.055 | 1.356 | 0.736 |
| D-Opt IL | SWPF-19 | quenched | targeted | -0.2692 | -0.2450 | -0.1692 | -0.4008 | 0.538 | 0.569 | 0.677 | 0.397 |
| D-Opt IL | SWPF-20 | quenched | targeted | -0.0981 | -0.0794 | -0.0936 | -0.2990 | 0.798 | 0.833 | 0.806 | 0.502 |
| D-Opt IL | SWPF-21 | quenched | targeted | -0.0763 | -0.1425 | -0.0026 | -0.2595 | 0.839 | 0.720 | 0.994 | 0.550 |
| D-Opt IL | SWPF-22 | quenched | targeted | -0.0448 | -0.1130 | -0.0165 | -0.2926 | 0.902 | 0.771 | 0.963 | 0.510 |
| D-Opt IL | SWPF-23 | quenched | targeted | -0.0989 | -0.1787 | -0.0727 | -0.3170 | 0.796 | 0.663 | 0.846 | 0.482 |
| D-Opt IL | SWPF-24 | quenched | targeted | -0.3043 | -0.1477 | -0.3388 | -0.4419 | 0.496 | 0.712 | 0.458 | 0.362 |
| D-Opt IL | SWPF-25 | quenched | targeted | -0.1080 | -0.0535 | -0.0992 | -0.2902 | 0.780 | 0.884 | 0.796 | 0.513 |
| D-Opt IL | SWPF-26 | quenched | targeted | -0.0882 | -0.0717 | -0.0735 | -0.2890 | 0.816 | 0.848 | 0.844 | 0.514 |
| D-Opt IL | SWPF-27 | quenched | targeted | -0.2153 | -0.1212 | -0.1974 | -0.3026 | 0.609 | 0.756 | 0.635 | 0.498 |
| D-Opt IL | SWPF-28 | quenched | targeted | -0.1414 | -0.0805 | -0.1021 | -0.2907 | 0.722 | 0.831 | 0.791 | 0.512 |
| D-Opt IL | SWPF-29 | quenched | targeted | -0.2249 | -0.0792 | -0.1543 | -0.3068 | 0.596 | 0.833 | 0.701 | 0.493 |
| D-Opt IL | SWPF-30 | quenched | targeted | -0.3593 | -0.1941 | -0.2805 | -0.4644 | 0.437 | 0.640 | 0.524 | 0.343 |
| D-Opt IL | SWPF-31 | quenched | targeted | -0.1955 | -0.2047 | -0.1103 | -0.3942 | 0.637 | 0.624 | 0.776 | 0.403 |
| SF | SWPF-32 | quenched | targeted | -0.2015 | -0.1026 | -0.1837 | -0.2942 | 0.629 | 0.790 | 0.655 | 0.508 |
| SF | SWPF-33 | quenched | targeted | -0.1461 | -0.0953 | -0.1674 | -0.3097 | 0.714 | 0.803 | 0.680 | 0.490 |
| SF | SWPF-34 | quenched | targeted | -0.2136 | -0.2056 | -0.0722 | -0.3303 | 0.611 | 0.623 | 0.847 | 0.467 |

Table B4. PCT Normalized Concentrations for the Study Glasses by Compositional View and Heat Treatment (continued)

| Desc | SRNL ID | Heat Treatment | Comp View | log NC [B (g/L)] | log NC [Li(g/L)] | log NC [Na (g/L)] | log NC [Si (g/L)] | NC B(g/L) | NC Li (g/L) | NC Na (g/L) | NC Si (g/L) |
|----------|---------|----------------|-------------|------------------|------------------|-------------------|-------------------|-----------|-------------|-------------|-------------|
| SF | SWPF-35 | quenched | targeted | -0.0681 | -0.0450 | -0.0904 | -0.2823 | 0.855 | 0.901 | 0.812 | 0.522 |
| SF | SWPF-36 | quenched | targeted | -0.1915 | -0.0915 | -0.1674 | -0.3047 | 0.643 | 0.810 | 0.680 | 0.496 |
| SF | SWPF-37 | quenched | targeted | -0.1388 | -0.0537 | -0.1448 | -0.2675 | 0.726 | 0.884 | 0.717 | 0.540 |
| SF | SWPF-38 | quenched | targeted | -0.1049 | -0.1125 | -0.0769 | -0.3230 | 0.785 | 0.772 | 0.838 | 0.475 |
| SF | SWPF-39 | quenched | targeted | -0.0798 | -0.0456 | 0.0437 | -0.1977 | 0.832 | 0.900 | 1.106 | 0.634 |
| SF | SWPF-40 | quenched | targeted | -0.1551 | -0.1048 | -0.0748 | -0.3290 | 0.700 | 0.786 | 0.842 | 0.469 |
| SF | SWPF-41 | quenched | targeted | -0.1198 | -0.0841 | -0.0787 | -0.2592 | 0.759 | 0.824 | 0.834 | 0.551 |
| SF | SWPF-42 | quenched | targeted | -0.1999 | -0.2132 | -0.1240 | -0.3373 | 0.631 | 0.612 | 0.752 | 0.460 |
| SF | SWPF-43 | quenched | targeted | -0.0322 | -0.0103 | -0.0046 | -0.1955 | 0.929 | 0.977 | 0.989 | 0.638 |
| SF | SWPF-44 | quenched | targeted | -0.1456 | -0.0970 | -0.1498 | -0.2892 | 0.715 | 0.800 | 0.708 | 0.514 |
| SF | SWPF-45 | quenched | targeted | -0.2866 | -0.2457 | -0.2245 | -0.4110 | 0.517 | 0.568 | 0.596 | 0.388 |
| SF | SWPF-46 | quenched | targeted | -0.1632 | -0.1553 | -0.0273 | -0.2684 | 0.687 | 0.699 | 0.939 | 0.539 |
| SF | SWPF-47 | quenched | targeted | -0.1691 | -0.1599 | -0.1127 | -0.3314 | 0.677 | 0.692 | 0.771 | 0.466 |
| SF | SWPF-48 | quenched | targeted | -0.2284 | -0.1929 | -0.2150 | -0.4019 | 0.591 | 0.641 | 0.609 | 0.396 |
| SF | SWPF-49 | quenched | targeted | -0.0733 | -0.1108 | -0.0002 | -0.2649 | 0.845 | 0.775 | 0.999 | 0.543 |
| SF | SWPF-50 | quenched | targeted | -0.1061 | -0.0838 | -0.0598 | -0.2741 | 0.783 | 0.825 | 0.871 | 0.532 |
| D-Opt OL | SWPF-01 | ccc | Measured bc | 0.9399 | 0.8325 | 0.8122 | 0.4374 | 8.708 | 6.799 | 6.489 | 2.738 |
| D-Opt OL | SWPF-02 | ccc | Measured bc | 0.1636 | 0.1833 | 0.1097 | -0.0609 | 1.458 | 1.525 | 1.287 | 0.869 |
| D-Opt OL | SWPF-03 | ccc | Measured bc | 0.3638 | 0.4745 | 0.2624 | 0.1292 | 2.311 | 2.982 | 1.830 | 1.347 |
| D-Opt OL | SWPF-04 | ccc | Measured bc | -0.1234 | 0.0094 | -0.1241 | -0.1945 | 0.753 | 1.022 | 0.751 | 0.639 |
| D-Opt OL | SWPF-05 | ccc | Measured bc | 0.5197 | 0.3591 | 0.4156 | -0.0651 | 3.309 | 2.286 | 2.604 | 0.861 |
| D-Opt OL | SWPF-06 | ccc | Measured bc | 0.3300 | 0.2882 | 0.1728 | 0.0083 | 2.138 | 1.942 | 1.489 | 1.019 |
| D-Opt OL | SWPF-07 | ccc | Measured bc | 0.5742 | 0.5062 | 0.4290 | 0.1274 | 3.751 | 3.207 | 2.686 | 1.341 |
| D-Opt OL | SWPF-08 | ccc | Measured bc | -0.3811 | -0.1983 | -0.4069 | -0.4958 | 0.416 | 0.633 | 0.392 | 0.319 |
| D-Opt OL | SWPF-09 | ccc | Measured bc | 0.0058 | 0.0536 | 0.0006 | -0.1559 | 1.013 | 1.131 | 1.001 | 0.698 |
| D-Opt OL | SWPF-10 | ccc | Measured bc | -0.0962 | -0.0984 | -0.0953 | -0.3770 | 0.801 | 0.797 | 0.803 | 0.420 |
| D-Opt OL | SWPF-11 | ccc | Measured bc | 0.0715 | -0.0840 | 0.0280 | -0.2545 | 1.179 | 0.824 | 1.067 | 0.557 |
| D-Opt OL | SWPF-12 | ccc | Measured bc | 0.2776 | 0.4491 | 0.0573 | 0.1472 | 1.895 | 2.813 | 1.141 | 1.404 |
| D-Opt OL | SWPF-13 | ccc | Measured bc | -0.1587 | -0.0693 | -0.2134 | -0.2517 | 0.694 | 0.853 | 0.612 | 0.560 |
| D-Opt OL | SWPF-14 | ccc | Measured bc | -0.4269 | -0.2797 | -0.4606 | -0.5148 | 0.374 | 0.525 | 0.346 | 0.306 |
| D-Opt OL | SWPF-15 | ccc | Measured bc | -0.3084 | -0.2239 | -0.3278 | -0.4242 | 0.492 | 0.597 | 0.470 | 0.376 |
| centroid | SWPF-16 | ccc | Measured bc | -0.2317 | -0.1643 | -0.2239 | -0.3314 | 0.587 | 0.685 | 0.597 | 0.466 |
| D-Opt IL | SWPF-17 | ccc | Measured bc | -0.3116 | -0.2514 | -0.1821 | -0.3669 | 0.488 | 0.561 | 0.658 | 0.430 |
| D-Opt IL | SWPF-18 | ccc | Measured bc | -0.0369 | 0.0232 | 0.1154 | -0.1407 | 0.919 | 1.055 | 1.304 | 0.723 |
| D-Opt IL | SWPF-19 | ccc | Measured bc | -0.3199 | -0.2736 | -0.2047 | -0.4114 | 0.479 | 0.533 | 0.624 | 0.388 |
| D-Opt IL | SWPF-20 | ccc | Measured bc | -0.2282 | -0.1465 | -0.1429 | -0.3172 | 0.591 | 0.714 | 0.720 | 0.482 |
| D-Opt IL | SWPF-21 | ccc | Measured bc | -0.1456 | -0.1105 | -0.0088 | -0.2487 | 0.715 | 0.775 | 0.980 | 0.564 |
| D-Opt IL | SWPF-22 | ccc | Measured bc | -0.1036 | -0.1441 | -0.0553 | -0.3067 | 0.788 | 0.718 | 0.880 | 0.494 |
| D-Opt IL | SWPF-23 | ccc | Measured bc | -0.0787 | -0.1534 | -0.0772 | -0.3075 | 0.834 | 0.702 | 0.837 | 0.493 |
| D-Opt IL | SWPF-24 | ccc | Measured bc | -0.2953 | -0.1987 | -0.3395 | -0.4145 | 0.507 | 0.633 | 0.458 | 0.385 |
| D-Opt IL | SWPF-25 | ccc | Measured bc | -0.1551 | -0.0990 | -0.1307 | -0.3096 | 0.700 | 0.796 | 0.740 | 0.490 |
| D-Opt IL | SWPF-26 | ccc | Measured bc | -0.1129 | -0.0630 | -0.0767 | -0.2693 | 0.771 | 0.865 | 0.838 | 0.538 |

Table B4. PCT Normalized Concentrations for the Study Glasses by Compositional View and Heat Treatment (continued)

| Desc | SRNL ID | Heat Treatment | Comp View | log NC [B (g/L)] | log NC [Li(g/L)] | log NC [Na (g/L)] | log NC [Si (g/L)] | NC B(g/L) | NC Li (g/L) | NC Na (g/L) | NC Si (g/L) |
|----------|---------|----------------|-------------|------------------|------------------|-------------------|-------------------|-----------|-------------|-------------|-------------|
| D-Opt IL | SWPF-27 | ccc | Measured bc | -0.2271 | -0.1312 | -0.1952 | -0.2816 | 0.593 | 0.739 | 0.638 | 0.523 |
| D-Opt IL | SWPF-28 | ccc | Measured bc | -0.1360 | -0.0566 | -0.1128 | -0.2722 | 0.731 | 0.878 | 0.771 | 0.534 |
| D-Opt IL | SWPF-29 | ccc | Measured bc | -0.2347 | -0.1228 | -0.1815 | -0.3171 | 0.583 | 0.754 | 0.658 | 0.482 |
| D-Opt IL | SWPF-30 | ccc | Measured bc | -0.3741 | -0.2873 | -0.3098 | -0.4400 | 0.423 | 0.516 | 0.490 | 0.363 |
| D-Opt IL | SWPF-31 | ccc | Measured bc | -0.1869 | -0.1576 | -0.1316 | -0.3927 | 0.650 | 0.696 | 0.739 | 0.405 |
| SF | SWPF-32 | ccc | Measured bc | -0.2525 | -0.0885 | -0.1778 | -0.3045 | 0.559 | 0.816 | 0.664 | 0.496 |
| SF | SWPF-33 | ccc | Measured bc | -0.1807 | -0.1150 | -0.1821 | -0.2986 | 0.660 | 0.767 | 0.657 | 0.503 |
| SF | SWPF-34 | ccc | Measured bc | -0.2475 | -0.1845 | -0.0979 | -0.3367 | 0.566 | 0.654 | 0.798 | 0.461 |
| SF | SWPF-35 | ccc | Measured bc | -0.1489 | -0.1097 | -0.1503 | -0.2961 | 0.710 | 0.777 | 0.707 | 0.506 |
| SF | SWPF-36 | ccc | Measured bc | -0.2803 | -0.1465 | -0.2195 | -0.3469 | 0.524 | 0.714 | 0.603 | 0.450 |
| SF | SWPF-37 | ccc | Measured bc | -0.1861 | -0.0732 | -0.1703 | -0.2821 | 0.651 | 0.845 | 0.676 | 0.522 |
| SF | SWPF-38 | ccc | Measured bc | -0.1904 | -0.1374 | -0.1217 | -0.3211 | 0.645 | 0.729 | 0.756 | 0.477 |
| SF | SWPF-39 | ccc | Measured bc | -0.1083 | -0.0179 | 0.0330 | -0.1869 | 0.779 | 0.960 | 1.079 | 0.650 |
| SF | SWPF-40 | ccc | Measured bc | 0.1161 | 0.0662 | 0.0203 | -0.2525 | 1.306 | 1.165 | 1.048 | 0.559 |
| SF | SWPF-41 | ccc | Measured bc | -0.1037 | -0.0417 | -0.0551 | -0.2240 | 0.788 | 0.908 | 0.881 | 0.597 |
| SF | SWPF-42 | ccc | Measured bc | -0.2458 | -0.1792 | -0.1412 | -0.3420 | 0.568 | 0.662 | 0.722 | 0.455 |
| SF | SWPF-43 | ccc | Measured bc | -0.0731 | -0.0148 | -0.0196 | -0.1911 | 0.845 | 0.966 | 0.956 | 0.644 |
| SF | SWPF-44 | ccc | Measured bc | -0.2093 | -0.1133 | -0.1736 | -0.2953 | 0.618 | 0.770 | 0.671 | 0.507 |
| SF | SWPF-45 | ccc | Measured bc | -0.3127 | -0.2391 | -0.2276 | -0.3974 | 0.487 | 0.577 | 0.592 | 0.401 |
| SF | SWPF-46 | ccc | Measured bc | -0.1549 | -0.1361 | -0.0372 | -0.2629 | 0.700 | 0.731 | 0.918 | 0.546 |
| SF | SWPF-47 | ccc | Measured bc | -0.2246 | -0.1725 | -0.1382 | -0.3275 | 0.596 | 0.672 | 0.727 | 0.470 |
| SF | SWPF-48 | ccc | Measured bc | -0.2928 | -0.2080 | -0.2468 | -0.4106 | 0.510 | 0.619 | 0.566 | 0.389 |
| SF | SWPF-49 | ccc | Measured bc | -0.0617 | -0.0770 | -0.0065 | -0.2556 | 0.868 | 0.837 | 0.985 | 0.555 |
| SF | SWPF-50 | ccc | Measured bc | 0.1428 | 0.1307 | 0.0433 | -0.1709 | 1.389 | 1.351 | 1.105 | 0.675 |
| D-Opt OL | SWPF-01 | quenched | Measured bc | -0.0378 | -0.0209 | -0.0776 | -0.1801 | 0.917 | 0.953 | 0.836 | 0.661 |
| D-Opt OL | SWPF-02 | quenched | Measured bc | 0.0070 | 0.0526 | 0.0099 | -0.1251 | 1.016 | 1.129 | 1.023 | 0.750 |
| D-Opt OL | SWPF-03 | quenched | Measured bc | 0.1035 | 0.0846 | 0.0696 | -0.0731 | 1.269 | 1.215 | 1.174 | 0.845 |
| D-Opt OL | SWPF-04 | quenched | Measured bc | -0.1253 | 0.0157 | -0.1357 | -0.1982 | 0.749 | 1.037 | 0.732 | 0.634 |
| D-Opt OL | SWPF-05 | quenched | Measured bc | 0.5640 | 0.4132 | 0.4547 | -0.0644 | 3.665 | 2.589 | 2.849 | 0.862 |
| D-Opt OL | SWPF-06 | quenched | Measured bc | 0.3222 | 0.3022 | 0.1785 | 0.0151 | 2.100 | 2.005 | 1.508 | 1.035 |
| D-Opt OL | SWPF-07 | quenched | Measured bc | 0.4100 | 0.3559 | 0.2747 | 0.0163 | 2.570 | 2.269 | 1.882 | 1.038 |
| D-Opt OL | SWPF-08 | quenched | Measured bc | -0.4062 | -0.1867 | -0.4176 | -0.5145 | 0.392 | 0.651 | 0.382 | 0.306 |
| D-Opt OL | SWPF-09 | quenched | Measured bc | 0.1334 | 0.1322 | 0.0819 | -0.0891 | 1.359 | 1.356 | 1.207 | 0.815 |
| D-Opt OL | SWPF-10 | quenched | Measured bc | 0.1090 | 0.0785 | 0.0551 | -0.3501 | 1.285 | 1.198 | 1.135 | 0.447 |
| D-Opt OL | SWPF-11 | quenched | Measured bc | 0.2691 | 0.0349 | 0.1826 | -0.1766 | 1.858 | 1.084 | 1.523 | 0.666 |
| D-Opt OL | SWPF-12 | quenched | Measured bc | -0.0623 | 0.0263 | -0.2110 | -0.0952 | 0.866 | 1.062 | 0.615 | 0.803 |
| D-Opt OL | SWPF-13 | quenched | Measured bc | -0.1561 | -0.0692 | -0.1970 | -0.2464 | 0.698 | 0.853 | 0.635 | 0.567 |
| D-Opt OL | SWPF-14 | quenched | Measured bc | -0.3553 | -0.2177 | -0.4443 | -0.4756 | 0.441 | 0.606 | 0.359 | 0.335 |
| D-Opt OL | SWPF-15 | quenched | Measured bc | -0.2273 | -0.1132 | -0.2570 | -0.4062 | 0.592 | 0.771 | 0.553 | 0.392 |
| centroid | SWPF-16 | quenched | Measured bc | -0.1634 | -0.1191 | -0.1985 | -0.3086 | 0.686 | 0.760 | 0.633 | 0.491 |
| D-Opt IL | SWPF-17 | quenched | Measured bc | -0.2809 | -0.2966 | -0.1799 | -0.3804 | 0.524 | 0.505 | 0.661 | 0.417 |
| D-Opt IL | SWPF-18 | quenched | Measured bc | -0.0199 | 0.0090 | 0.1345 | -0.1311 | 0.955 | 1.021 | 1.363 | 0.740 |

Table B4. PCT Normalized Concentrations for the Study Glasses by Compositional View and Heat Treatment (continued)

| Desc | SRNL ID | Heat Treatment | Comp View | log NC [B (g/L)] | log NC [Li(g/L)] | log NC [Na (g/L)] | log NC [Si (g/L)] | NC B(g/L) | NC Li (g/L) | NC Na (g/L) | NC Si (g/L) |
|----------|---------|----------------|-------------|------------------|------------------|-------------------|-------------------|-----------|-------------|-------------|-------------|
| D-Opt IL | SWPF-19 | quenched | Measured bc | -0.2718 | -0.2699 | -0.1668 | -0.3997 | 0.535 | 0.537 | 0.681 | 0.398 |
| D-Opt IL | SWPF-20 | quenched | Measured bc | -0.0917 | -0.0853 | -0.0946 | -0.3006 | 0.810 | 0.822 | 0.804 | 0.500 |
| D-Opt IL | SWPF-21 | quenched | Measured bc | -0.0689 | -0.1547 | 0.0005 | -0.2566 | 0.853 | 0.700 | 1.001 | 0.554 |
| D-Opt IL | SWPF-22 | quenched | Measured bc | -0.0258 | -0.1324 | -0.0116 | -0.2918 | 0.942 | 0.737 | 0.974 | 0.511 |
| D-Opt IL | SWPF-23 | quenched | Measured bc | -0.0846 | -0.1838 | -0.0710 | -0.3165 | 0.823 | 0.655 | 0.849 | 0.483 |
| D-Opt IL | SWPF-24 | quenched | Measured bc | -0.3007 | -0.1577 | -0.3381 | -0.4430 | 0.500 | 0.695 | 0.459 | 0.361 |
| D-Opt IL | SWPF-25 | quenched | Measured bc | -0.1088 | -0.0555 | -0.0927 | -0.2947 | 0.778 | 0.880 | 0.808 | 0.507 |
| D-Opt IL | SWPF-26 | quenched | Measured bc | -0.0899 | -0.0801 | -0.0683 | -0.2908 | 0.813 | 0.832 | 0.855 | 0.512 |
| D-Opt IL | SWPF-27 | quenched | Measured bc | -0.2049 | -0.1185 | -0.1987 | -0.3044 | 0.624 | 0.761 | 0.633 | 0.496 |
| D-Opt IL | SWPF-28 | quenched | Measured bc | -0.1393 | -0.0635 | -0.0982 | -0.2909 | 0.726 | 0.864 | 0.798 | 0.512 |
| D-Opt IL | SWPF-29 | quenched | Measured bc | -0.2113 | -0.0676 | -0.1463 | -0.3082 | 0.615 | 0.856 | 0.714 | 0.492 |
| D-Opt IL | SWPF-30 | quenched | Measured bc | -0.3602 | -0.2127 | -0.2828 | -0.4656 | 0.436 | 0.613 | 0.521 | 0.342 |
| D-Opt IL | SWPF-31 | quenched | Measured bc | -0.2030 | -0.1989 | -0.1109 | -0.3939 | 0.627 | 0.633 | 0.775 | 0.404 |
| SF | SWPF-32 | quenched | Measured bc | -0.2086 | -0.0905 | -0.1816 | -0.2923 | 0.619 | 0.812 | 0.658 | 0.510 |
| SF | SWPF-33 | quenched | Measured bc | -0.1503 | -0.0908 | -0.1678 | -0.3121 | 0.707 | 0.811 | 0.679 | 0.487 |
| SF | SWPF-34 | quenched | Measured bc | -0.2155 | -0.2081 | -0.0740 | -0.3281 | 0.609 | 0.619 | 0.843 | 0.470 |
| SF | SWPF-35 | quenched | Measured bc | -0.0735 | -0.0444 | -0.0900 | -0.2843 | 0.844 | 0.903 | 0.813 | 0.520 |
| SF | SWPF-36 | quenched | Measured bc | -0.1863 | -0.0739 | -0.1626 | -0.3049 | 0.651 | 0.843 | 0.688 | 0.496 |
| SF | SWPF-37 | quenched | Measured bc | -0.1459 | -0.0445 | -0.1394 | -0.2679 | 0.715 | 0.903 | 0.725 | 0.540 |
| SF | SWPF-38 | quenched | Measured bc | -0.1119 | -0.1079 | -0.0721 | -0.3222 | 0.773 | 0.780 | 0.847 | 0.476 |
| SF | SWPF-39 | quenched | Measured bc | -0.0822 | -0.0512 | 0.0465 | -0.1949 | 0.828 | 0.889 | 1.113 | 0.638 |
| SF | SWPF-40 | quenched | Measured bc | -0.1655 | -0.1159 | -0.0751 | -0.3287 | 0.683 | 0.766 | 0.841 | 0.469 |
| SF | SWPF-41 | quenched | Measured bc | -0.1311 | -0.0887 | -0.0740 | -0.2588 | 0.739 | 0.815 | 0.843 | 0.551 |
| SF | SWPF-42 | quenched | Measured bc | -0.2063 | -0.2108 | -0.1201 | -0.3352 | 0.622 | 0.615 | 0.758 | 0.462 |
| SF | SWPF-43 | quenched | Measured bc | -0.0347 | -0.0107 | -0.0007 | -0.1941 | 0.923 | 0.976 | 0.998 | 0.640 |
| SF | SWPF-44 | quenched | Measured bc | -0.1493 | -0.0914 | -0.1476 | -0.2934 | 0.709 | 0.810 | 0.712 | 0.509 |
| SF | SWPF-45 | quenched | Measured bc | -0.2907 | -0.2432 | -0.2286 | -0.4119 | 0.512 | 0.571 | 0.591 | 0.387 |
| SF | SWPF-46 | quenched | Measured bc | -0.1684 | -0.1579 | -0.0221 | -0.2678 | 0.679 | 0.695 | 0.950 | 0.540 |
| SF | SWPF-47 | quenched | Measured bc | -0.1712 | -0.1614 | -0.1039 | -0.3314 | 0.674 | 0.690 | 0.787 | 0.466 |
| SF | SWPF-48 | quenched | Measured bc | -0.2256 | -0.1891 | -0.2170 | -0.4005 | 0.595 | 0.647 | 0.607 | 0.398 |
| SF | SWPF-49 | quenched | Measured bc | -0.0781 | -0.1150 | 0.0045 | -0.2628 | 0.835 | 0.767 | 1.010 | 0.546 |
| SF | SWPF-50 | quenched | Measured bc | -0.1041 | -0.0758 | -0.0621 | -0.2763 | 0.787 | 0.840 | 0.867 | 0.529 |

Exhibit B1. PCT Measurements in Analytical Sequence by Analytical Block

Analyte= $\log[B \text{ ppm}]$, Block Groupings=A-B-C

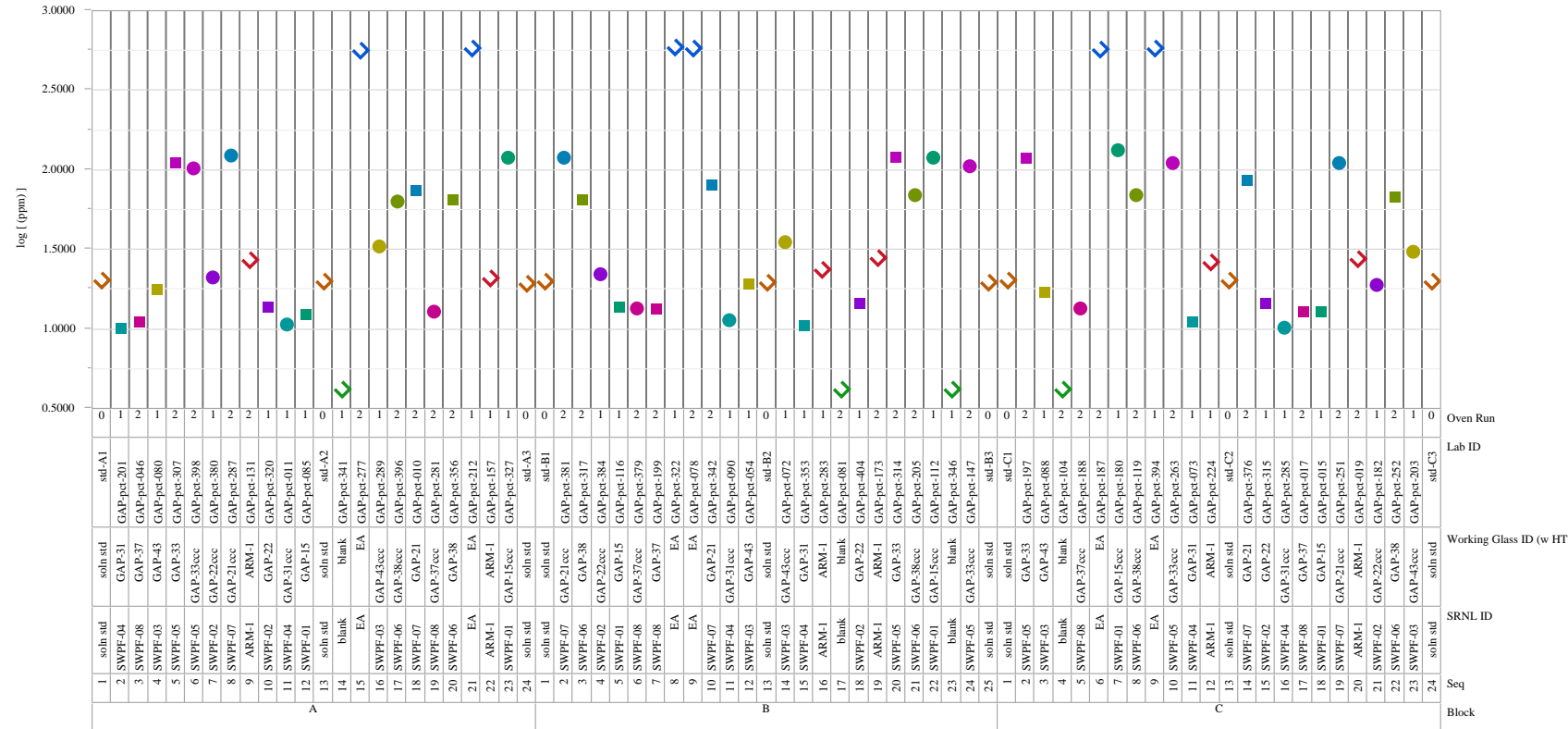


Exhibit B1. PCT Measurements in Analytical Sequence by Analytical Block (continued)

Analyte=log[B ppm], Block Groupings=D-E-F

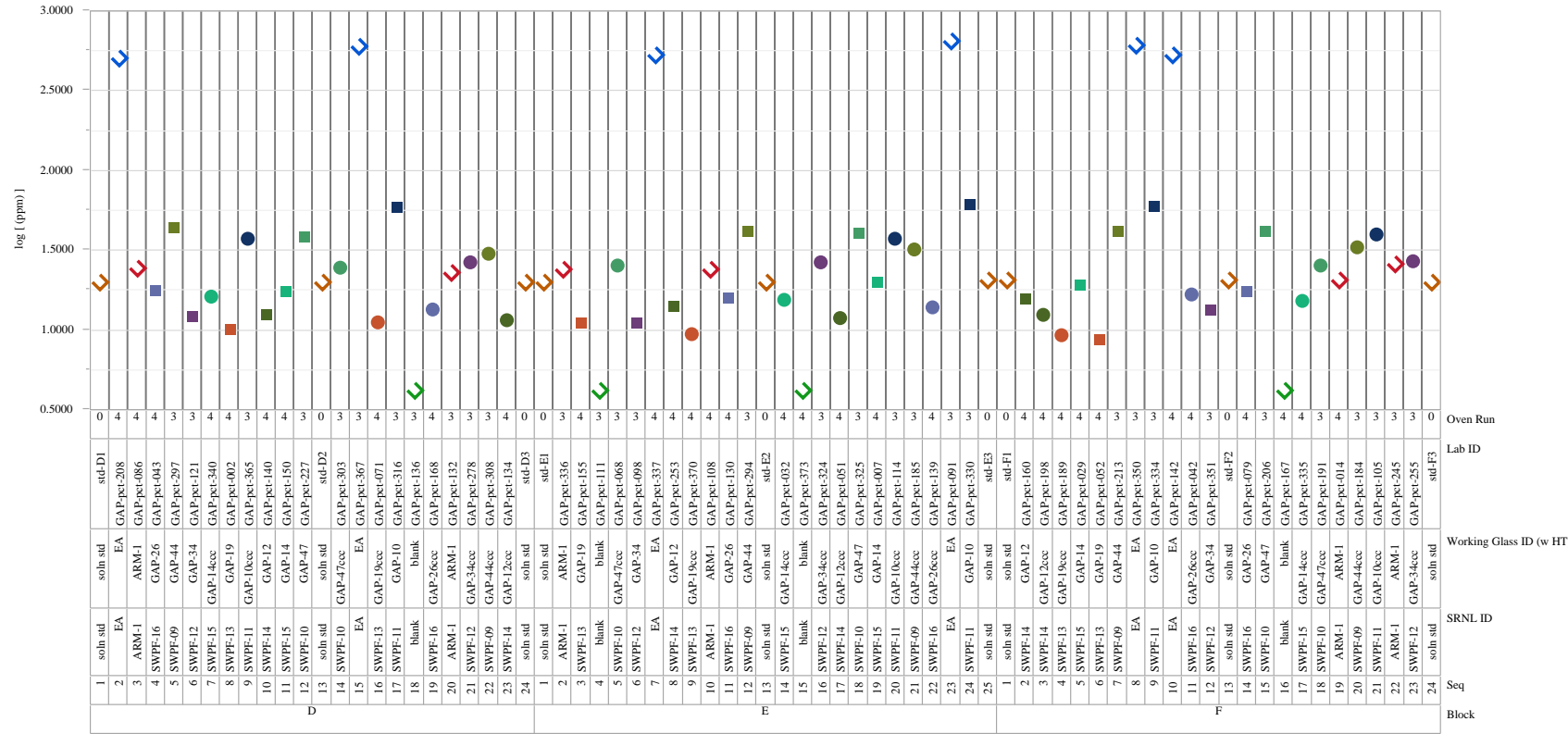


Exhibit B1. PCT Measurements in Analytical Sequence by Analytical Block (continued)

Analyte= $\log[B \text{ ppm}]$, Block Groupings=G-H-I

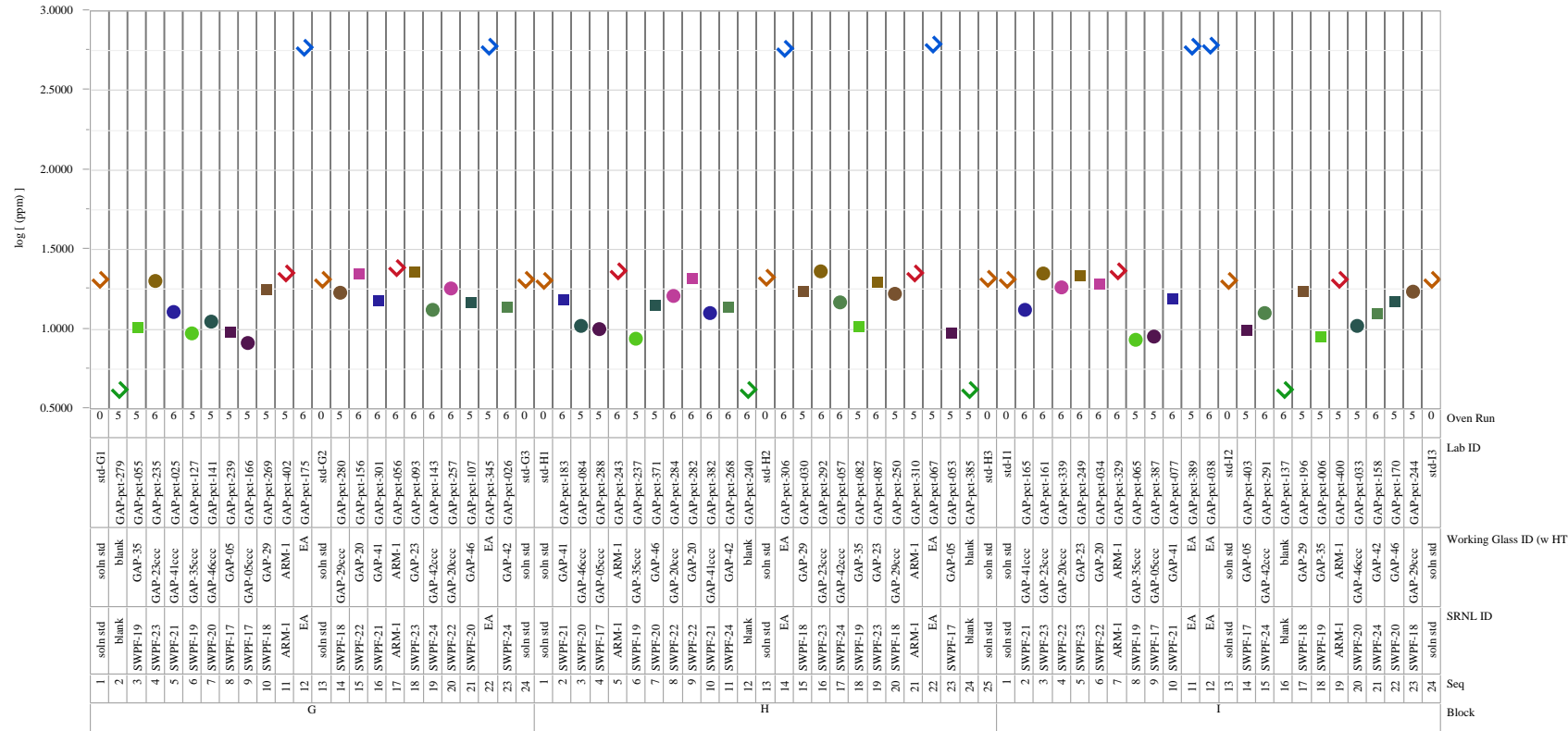


Exhibit B1. PCT Measurements in Analytical Sequence by Analytical Block (continued)

Analyte= $\log[B \text{ ppm}]$, Block Groupings=J-K-L

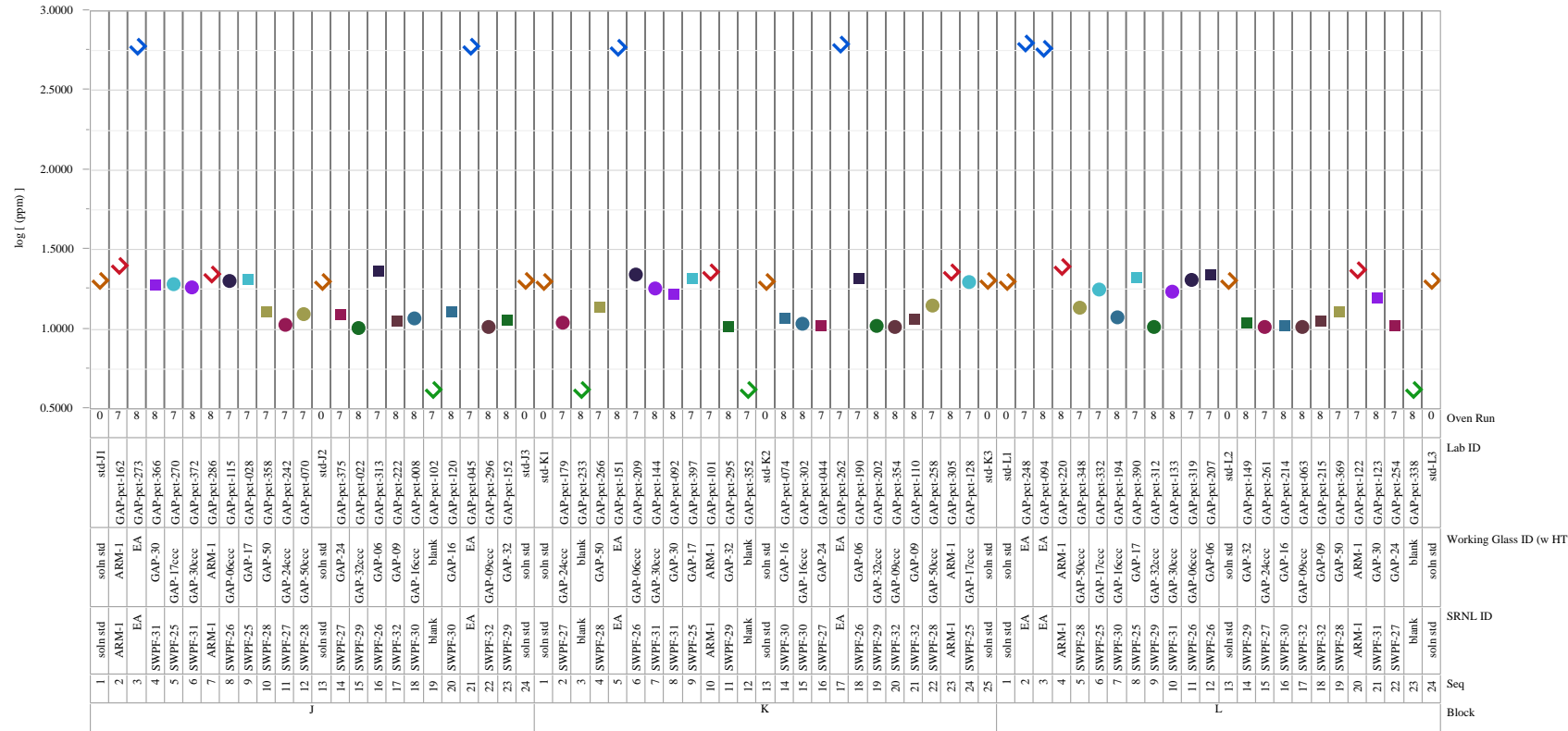


Exhibit B1. PCT Measurements in Analytical Sequence by Analytical Block (continued)

Analyte= $\log[B \text{ ppm}]$, Block Groupings=M-N-O

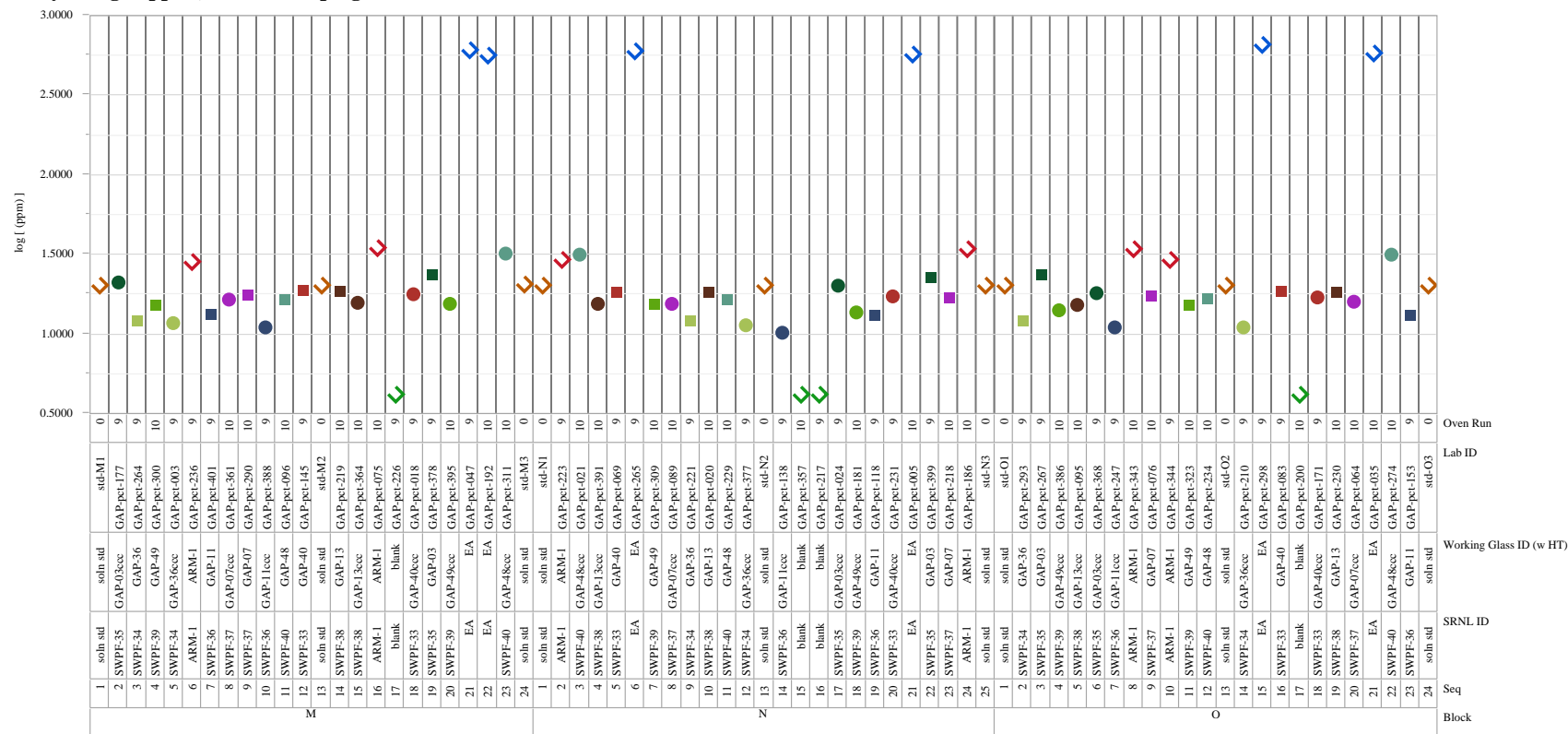


Exhibit B1. PCT Measurements in Analytical Sequence by Analytical Block (continued)

Analyte= $\log[B \text{ ppm}]$, Block Groupings=P-Q-R

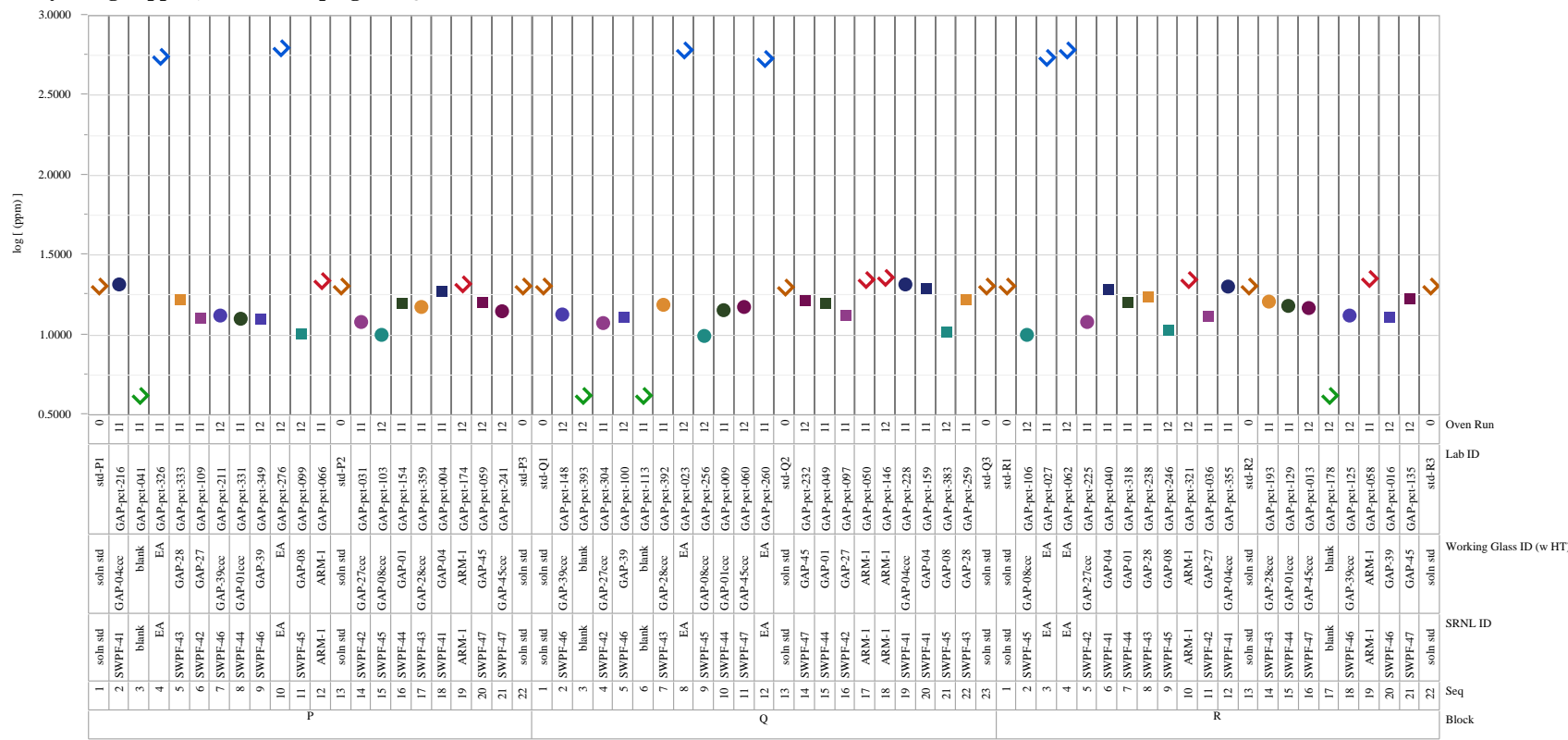


Exhibit B1. PCT Measurements in Analytical Sequence by Analytical Block (continued)

Analyte= $\log[B \text{ ppm}]$, Block Groupings=S-T-U

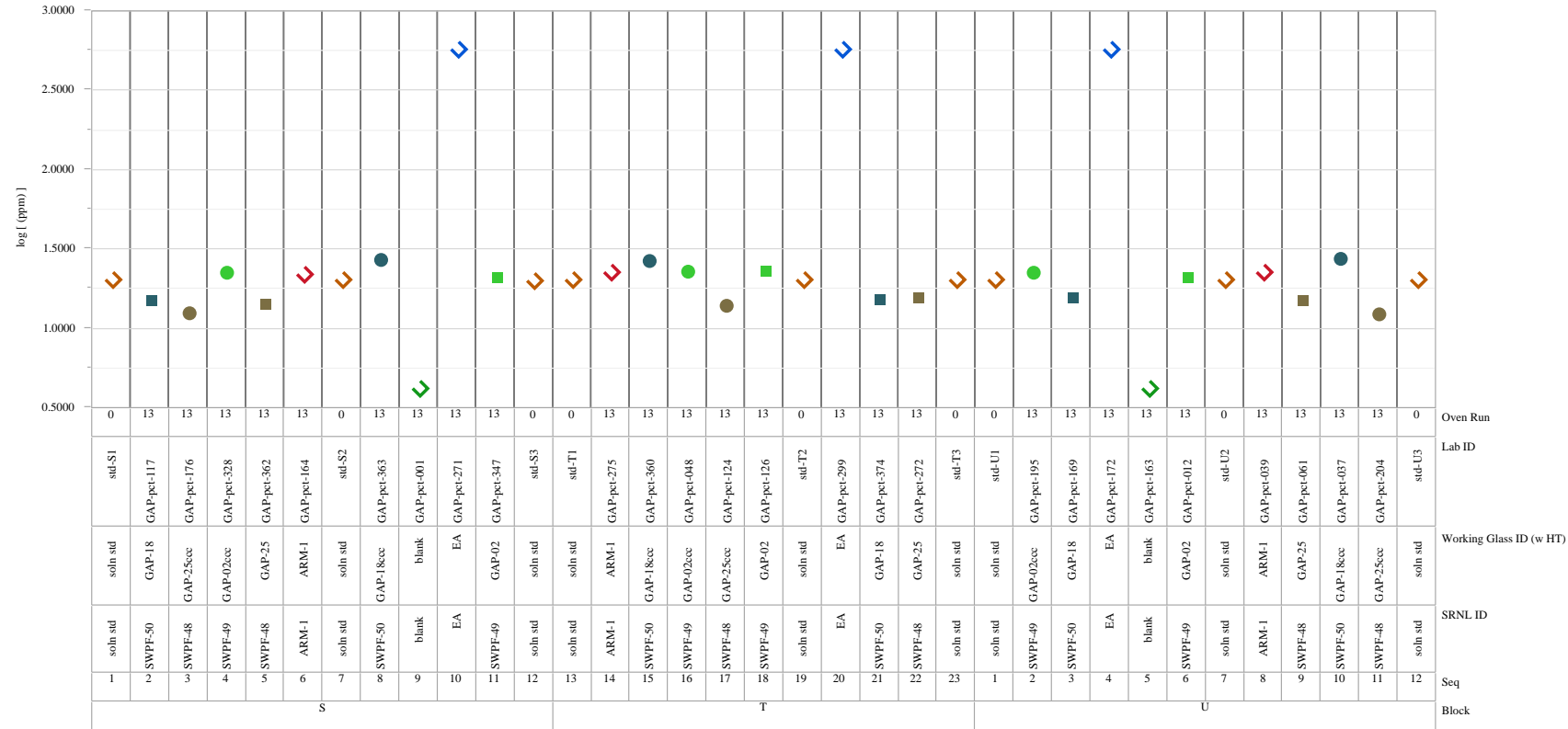


Exhibit B1. PCT Measurements in Analytical Sequence by Analytical Block (continued)

Analyte= $\log[\text{Li ppm}]$, Block Groupings=A-B-C

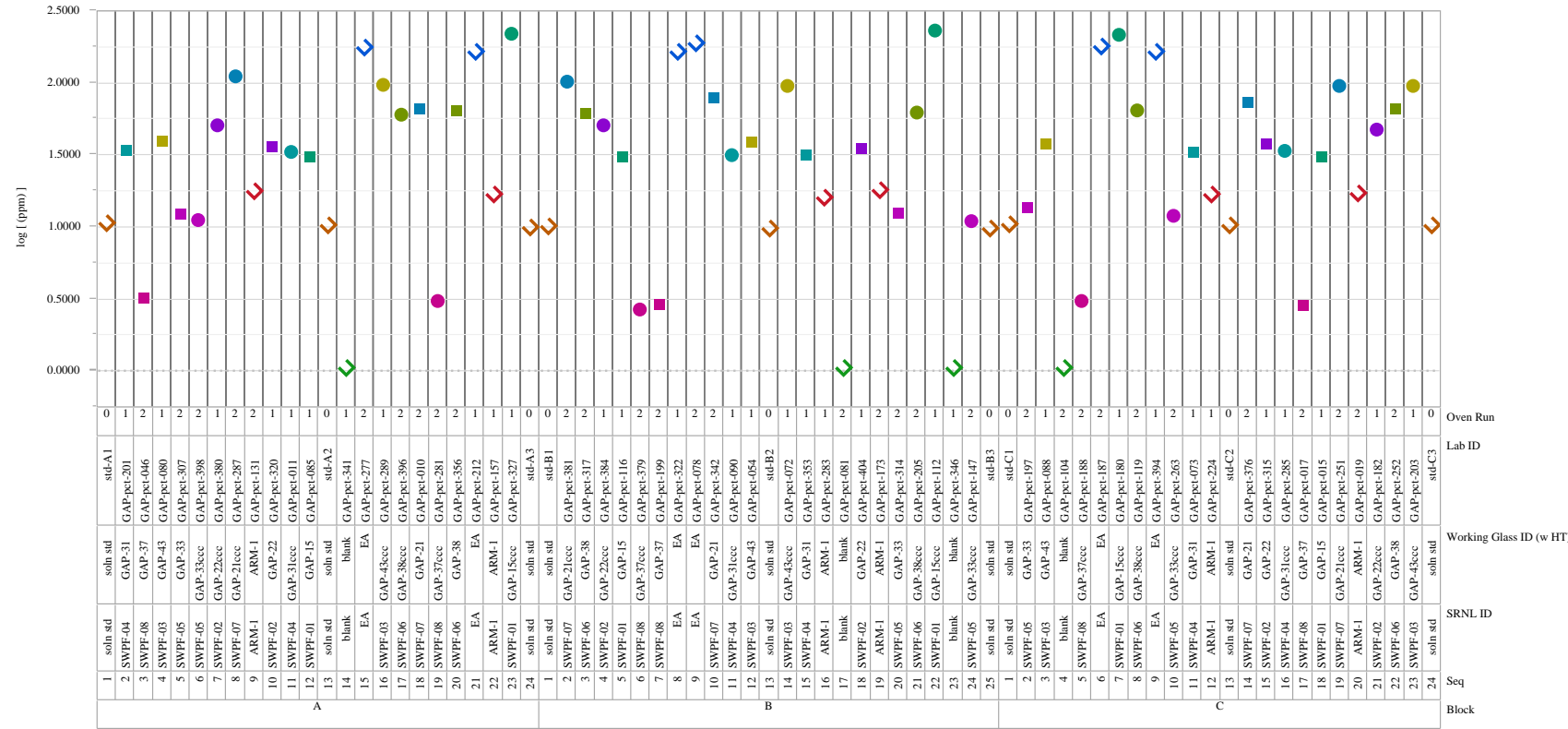


Exhibit B1. PCT Measurements in Analytical Sequence by Analytical Block (continued)

Analyte= $\log[\text{Li ppm}]$, Block Groupings=D-E-F

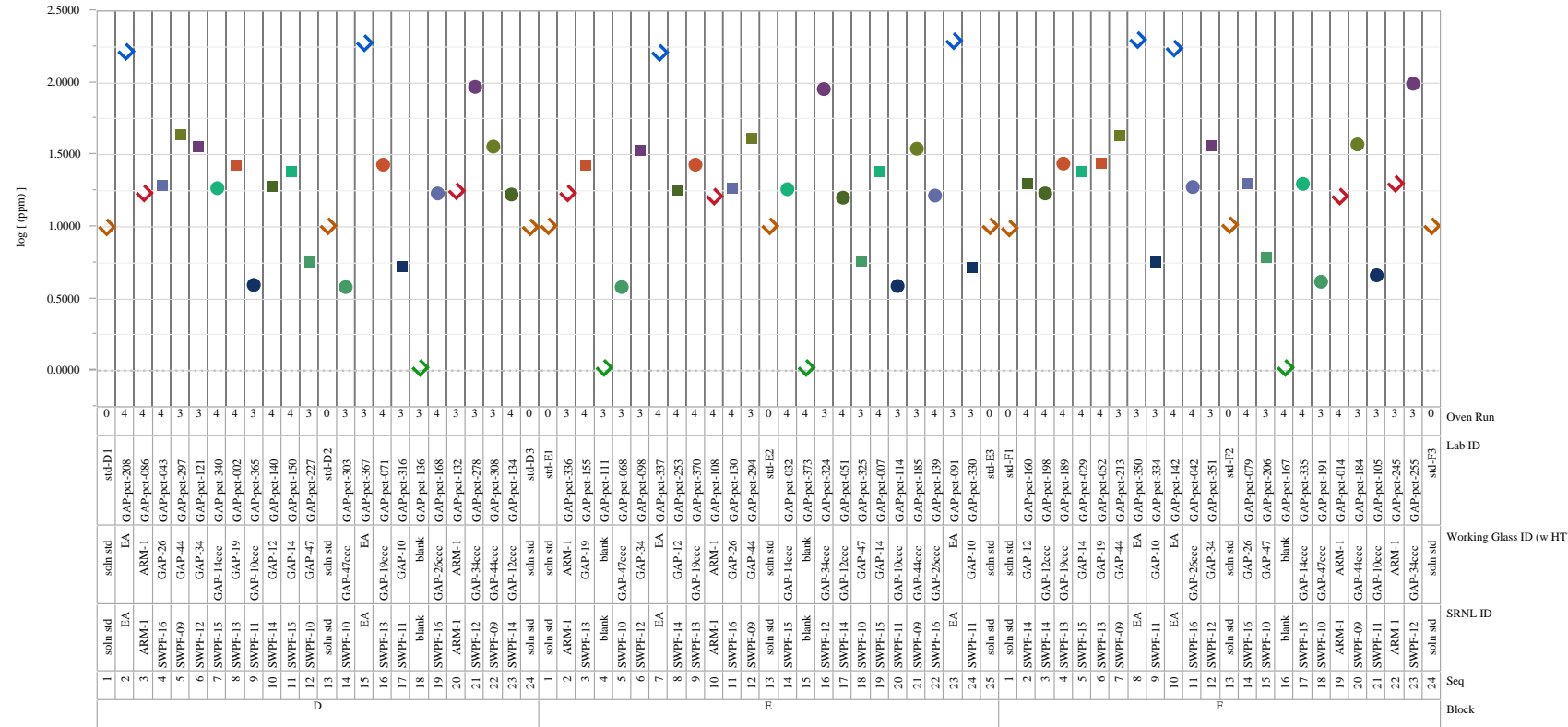


Exhibit B1. PCT Measurements in Analytical Sequence by Analytical Block (continued)

Analyte= $\log[\text{Li ppm}]$, Block Groupings=G-H-I

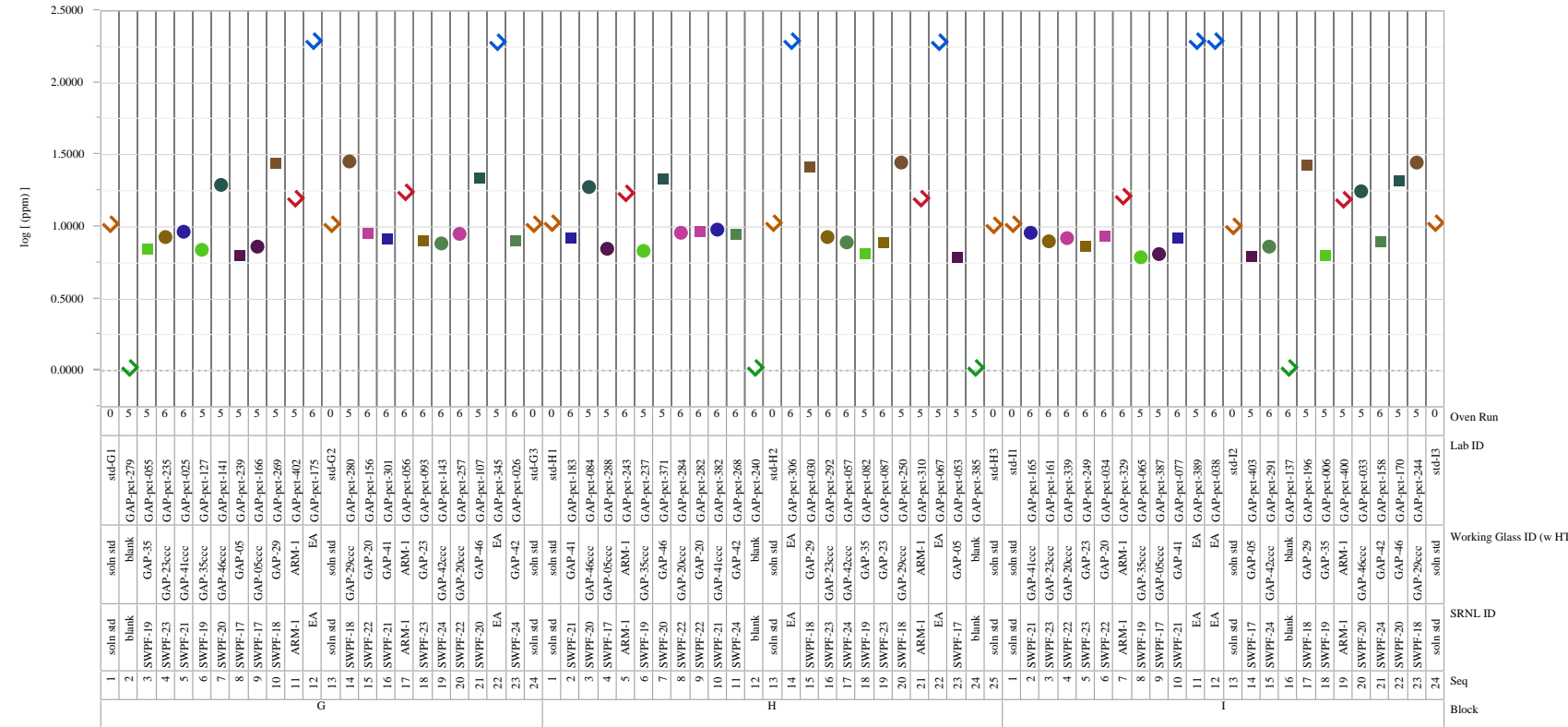


Exhibit B1. PCT Measurements in Analytical Sequence by Analytical Block (continued)

Analyte=log[Li ppm], Block Groupings=J-K-L

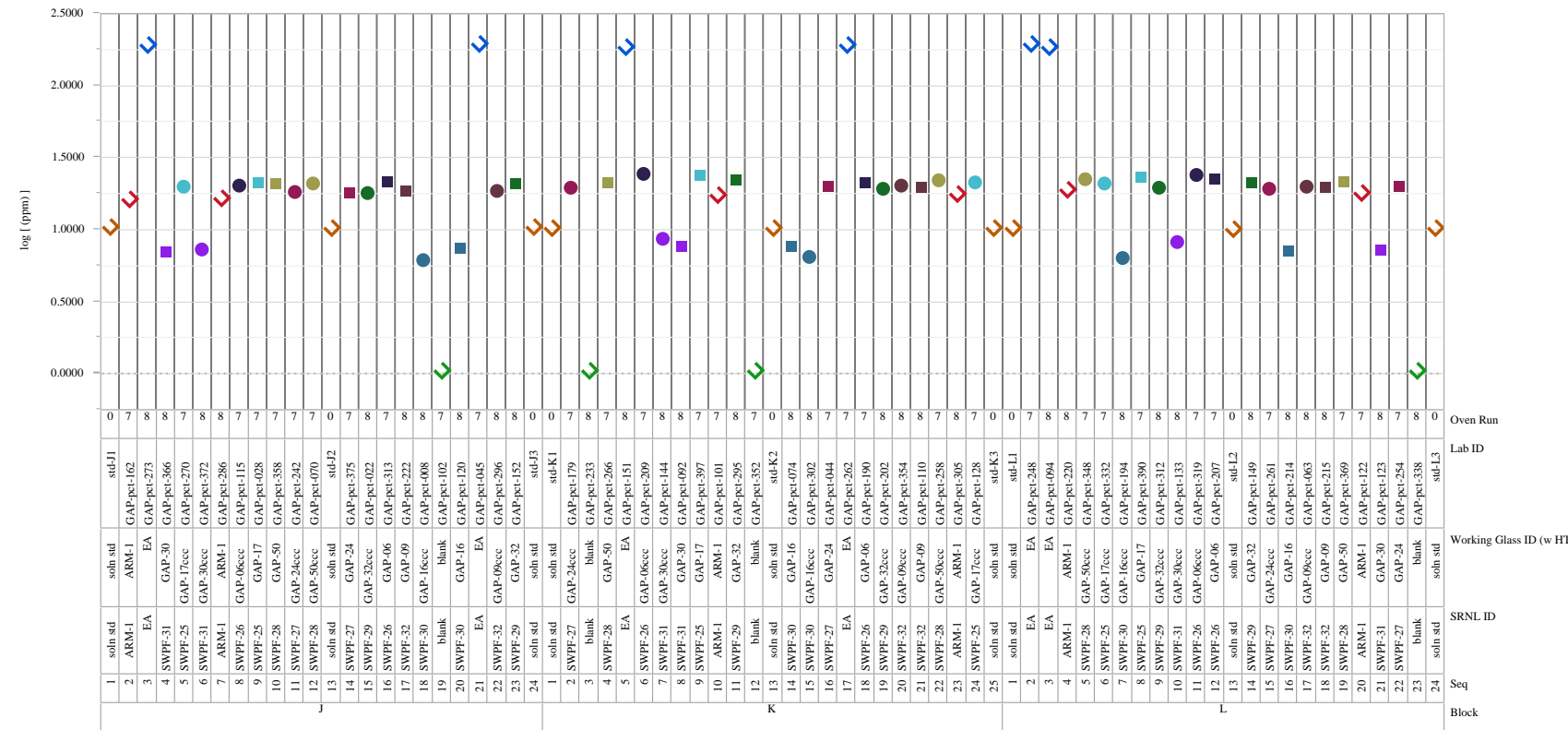


Exhibit B1. PCT Measurements in Analytical Sequence by Analytical Block (continued)

Analyte= $\log[\text{Li ppm}]$, Block Groupings=M-N-O

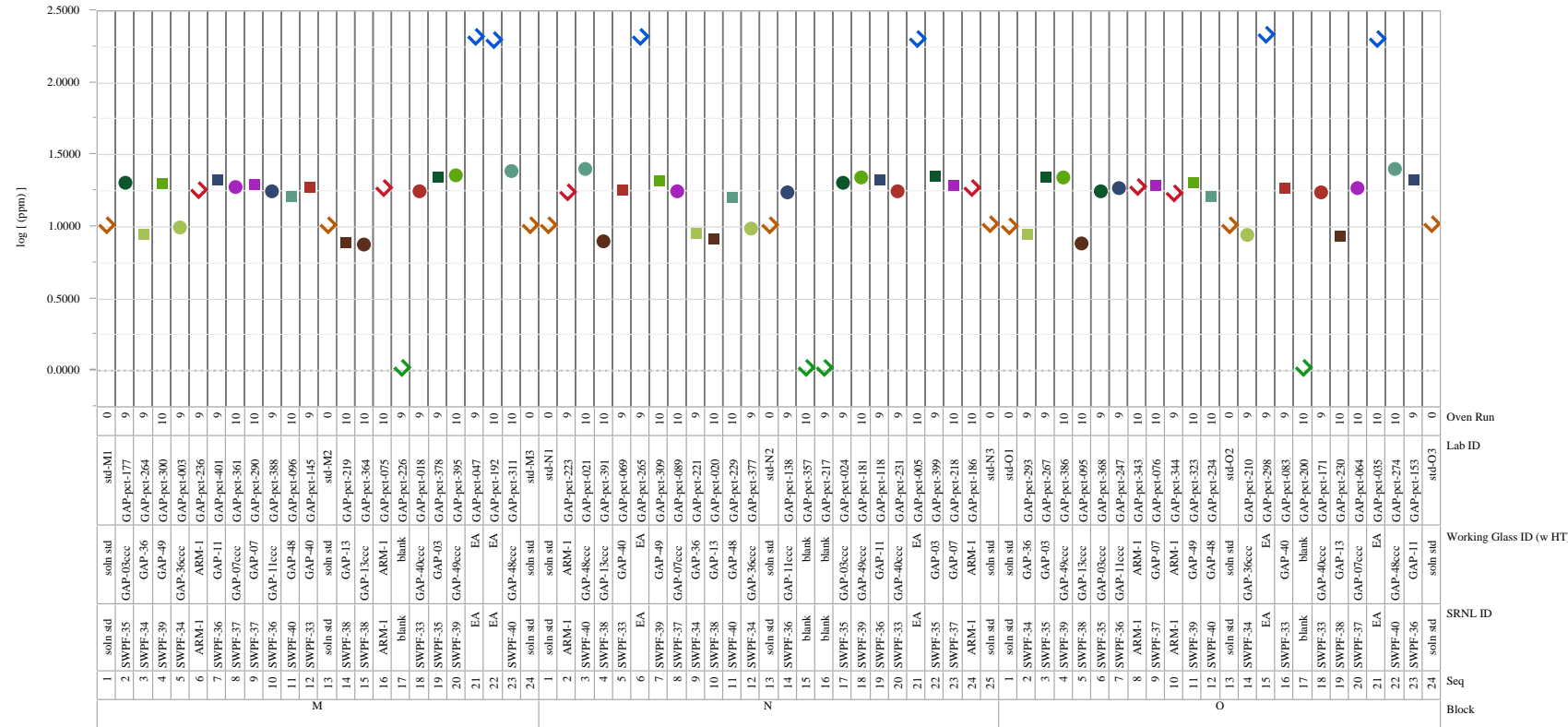


Exhibit B1. PCT Measurements in Analytical Sequence by Analytical Block (continued)

Analyte=log[Li ppm], Block Groupings=P-Q-R

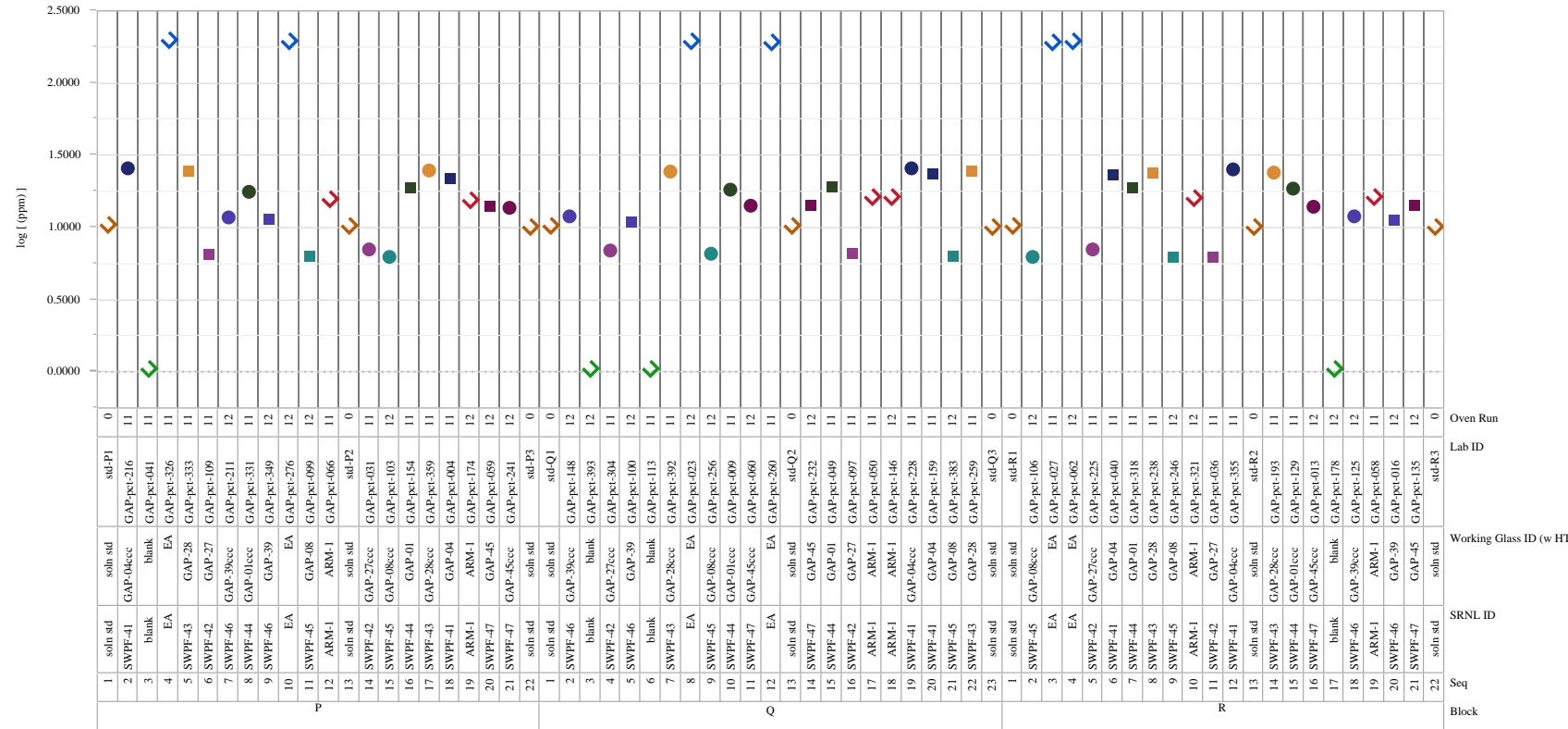


Exhibit B1. PCT Measurements in Analytical Sequence by Analytical Block (continued)

Analyte=log[Li ppm], Block Groupings=S-T-U

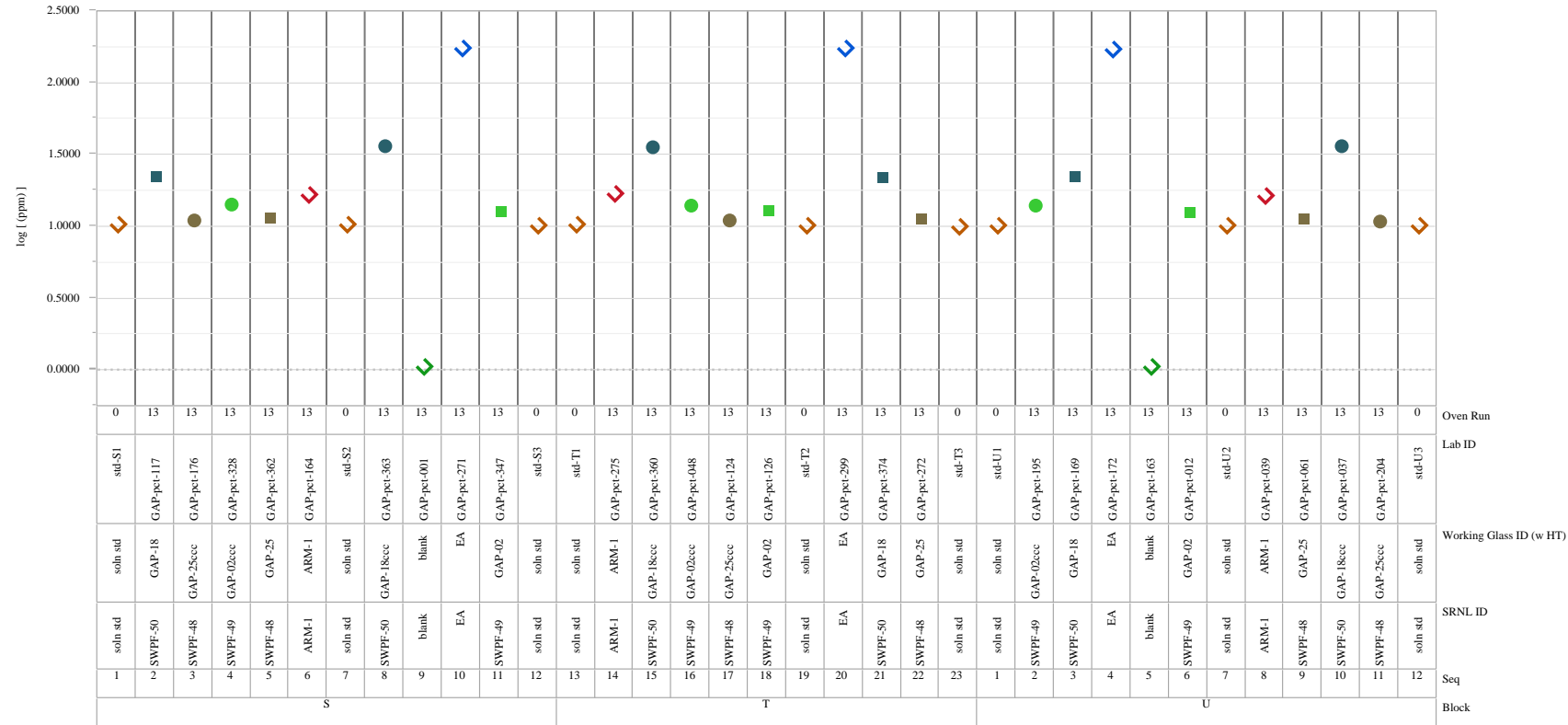


Exhibit B1. PCT Measurements in Analytical Sequence by Analytical Block (continued)

Analyte= $\log[\text{Na ppm}]$, Block Groupings=A-B-C

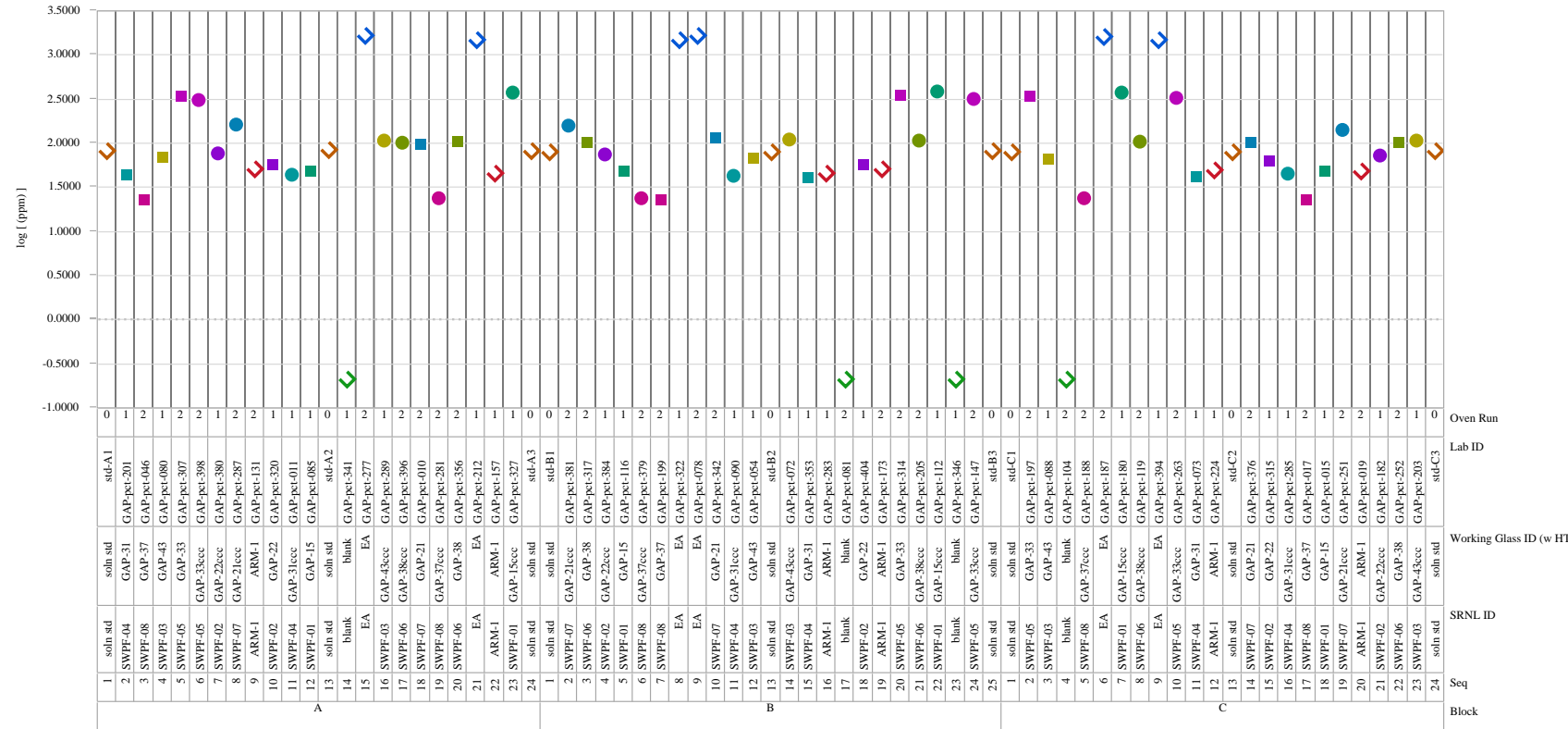


Exhibit B1. PCT Measurements in Analytical Sequence by Analytical Block (continued)

Analyte= $\log[\text{Na ppm}]$, Block Groupings=D-E-F

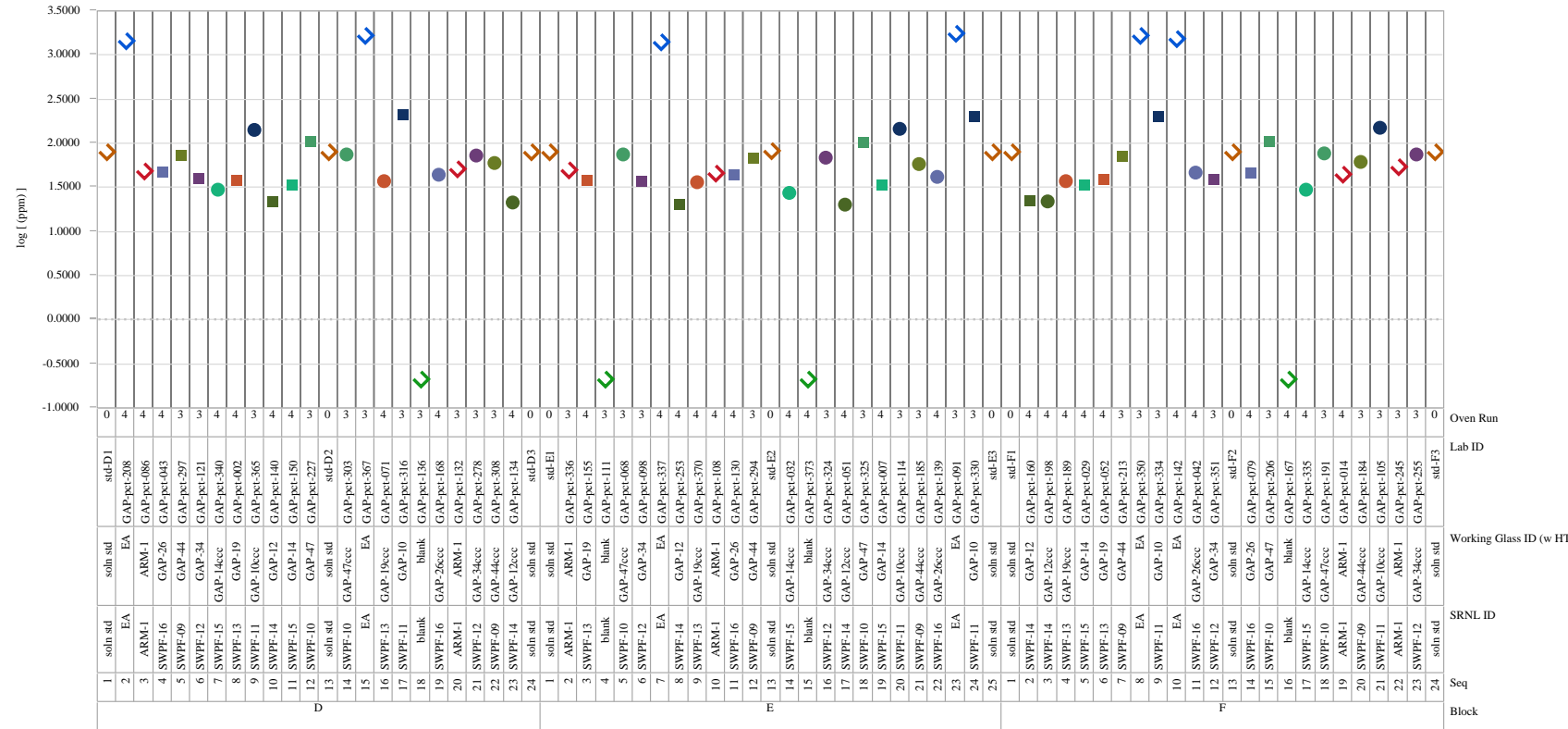


Exhibit B1. PCT Measurements in Analytical Sequence by Analytical Block (continued)

Analyte= $\log[\text{Na ppm}]$, Block Groupings=G-H-I

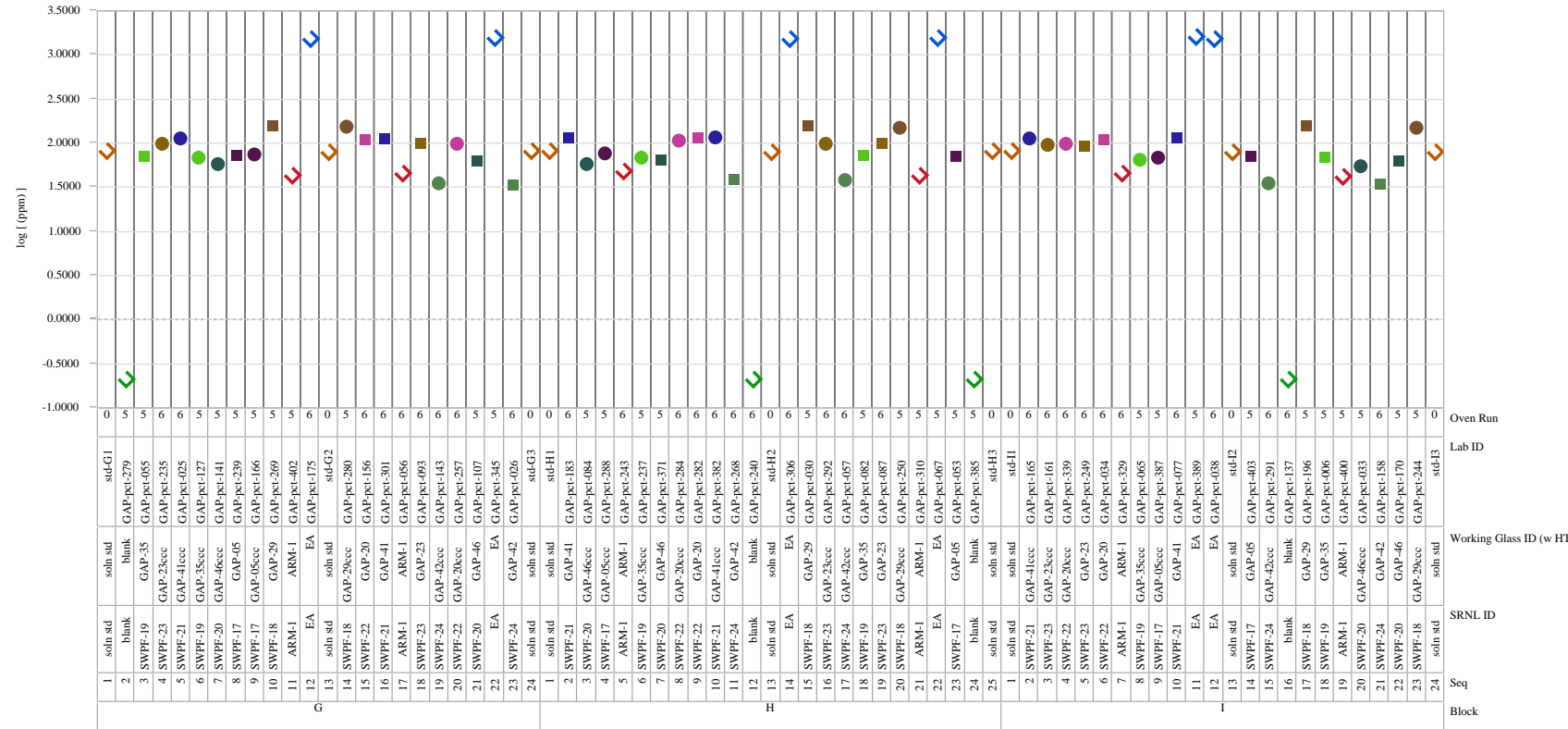


Exhibit B1. PCT Measurements in Analytical Sequence by Analytical Block (continued)

Analyte= $\log[\text{Na ppm}]$, Block Groupings=J-K-L

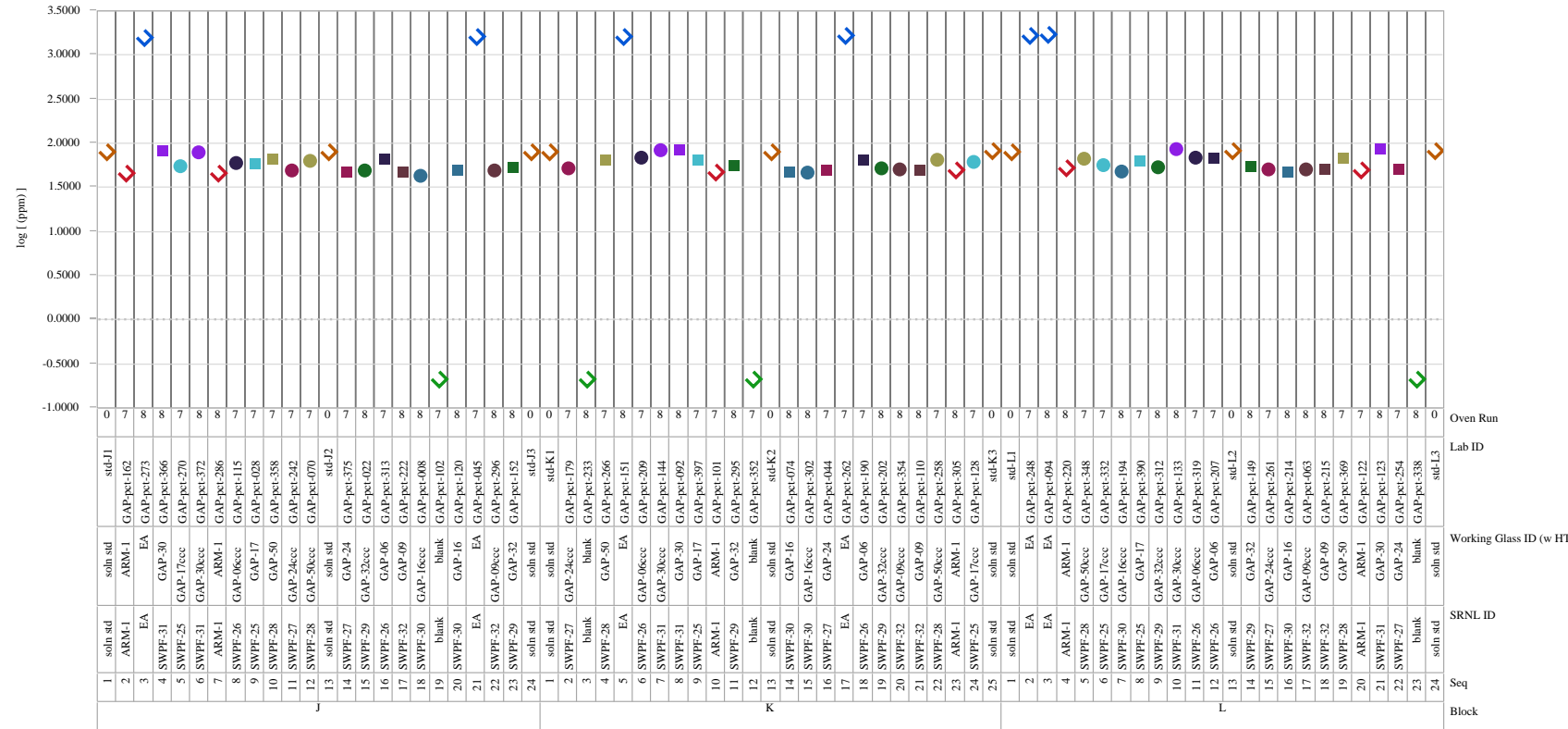


Exhibit B1. PCT Measurements in Analytical Sequence by Analytical Block (continued)

Analyte= $\log[\text{Na ppm}]$, Block Groupings=M-N-O

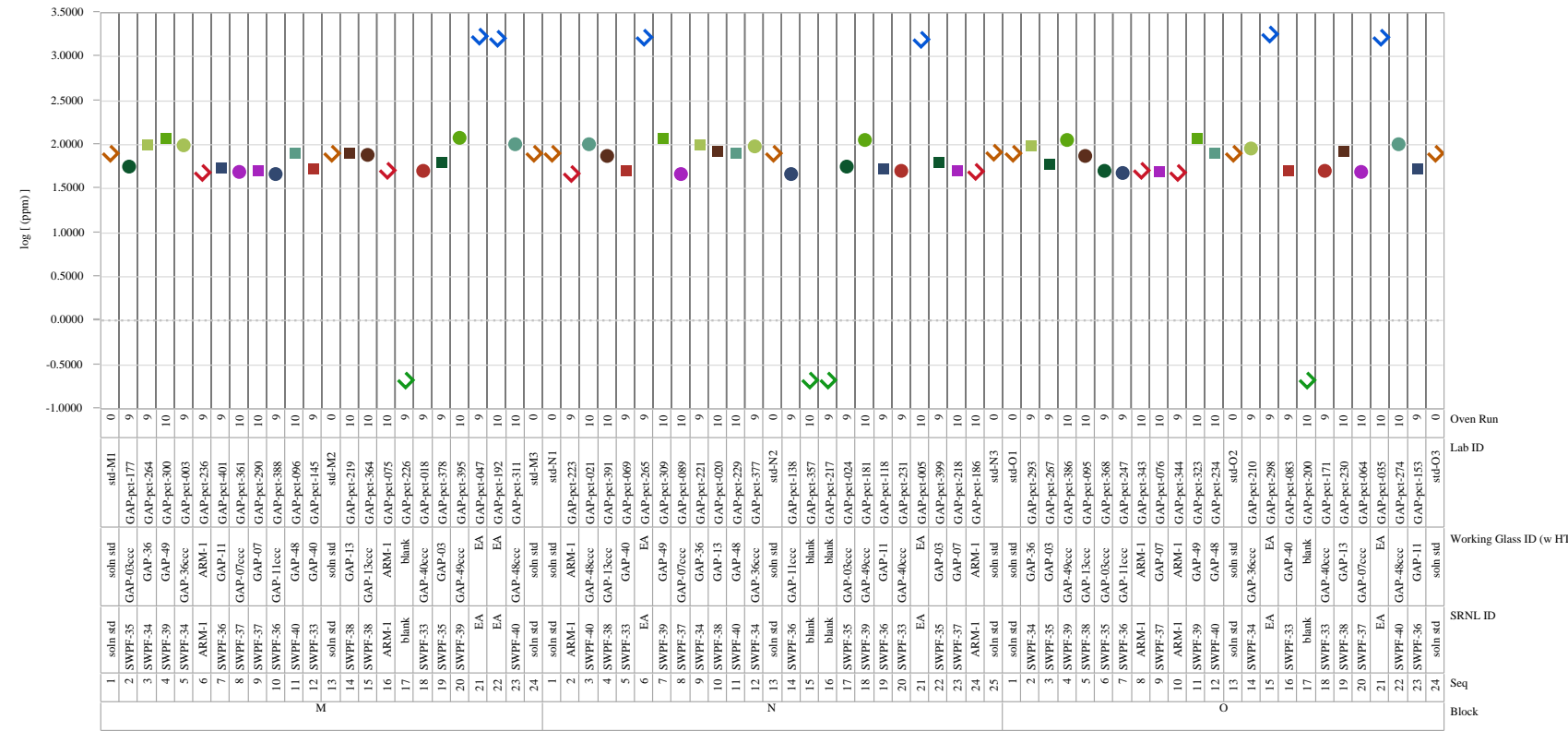


Exhibit B1. PCT Measurements in Analytical Sequence by Analytical Block (continued)

Analyte= $\log[\text{Na ppm}]$, Block Groupings=P-Q-R

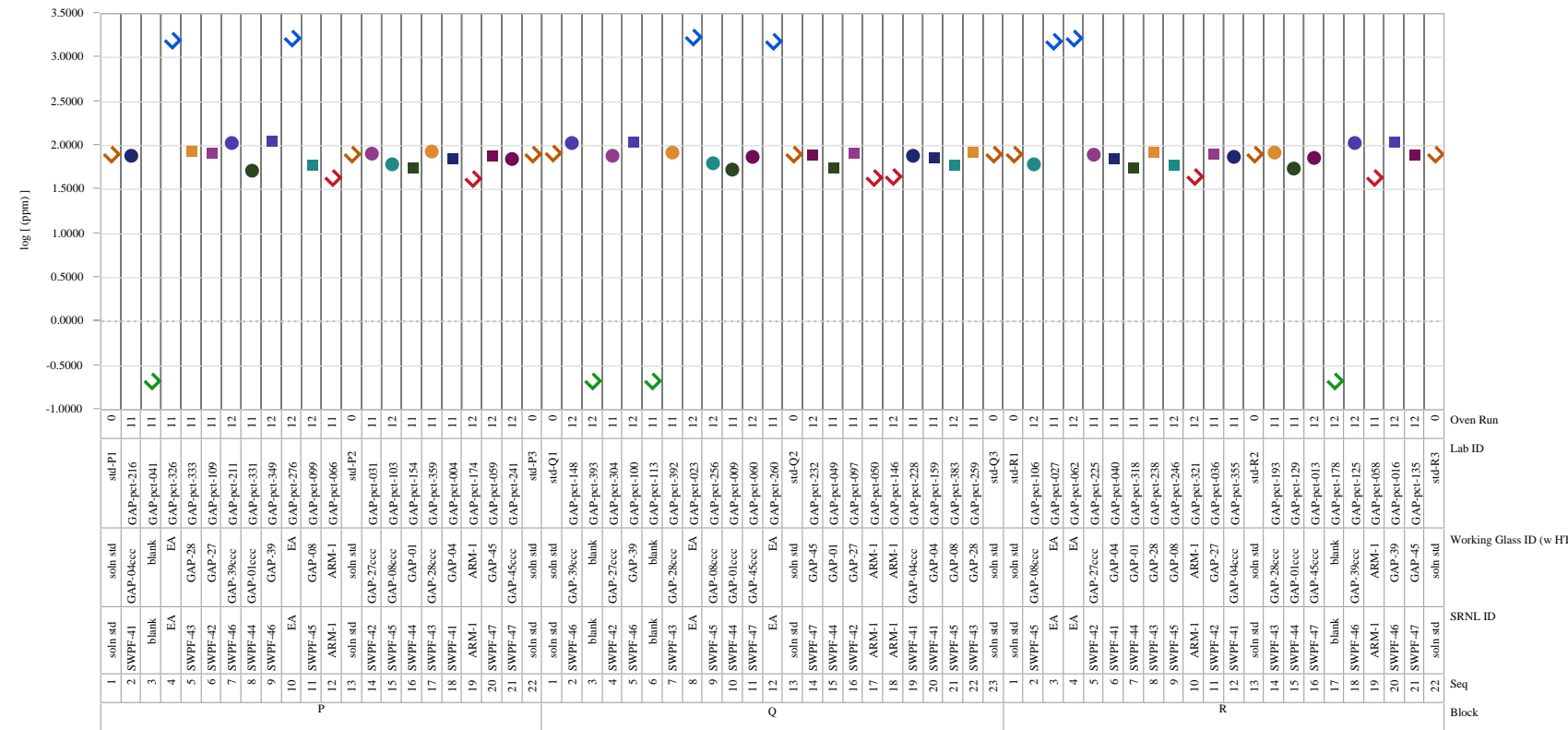


Exhibit B1. PCT Measurements in Analytical Sequence by Analytical Block (continued)

Analyte= $\log[\text{Na ppm}]$, Block Groupings=S-T-U

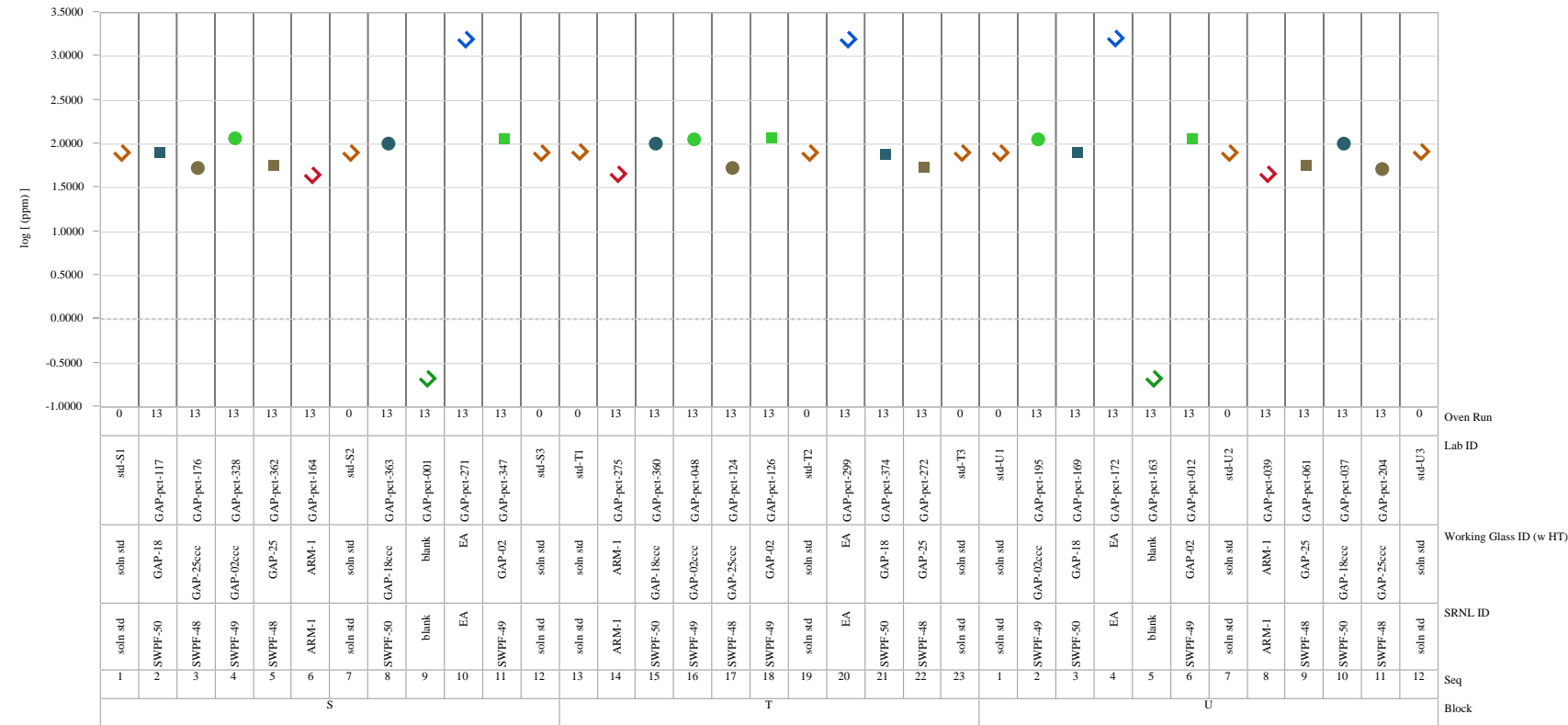


Exhibit B1. PCT Measurements in Analytical Sequence by Analytical Block (continued)

Analyte= $\log[\text{Si ppm}]$, Block Groupings=A-B-C

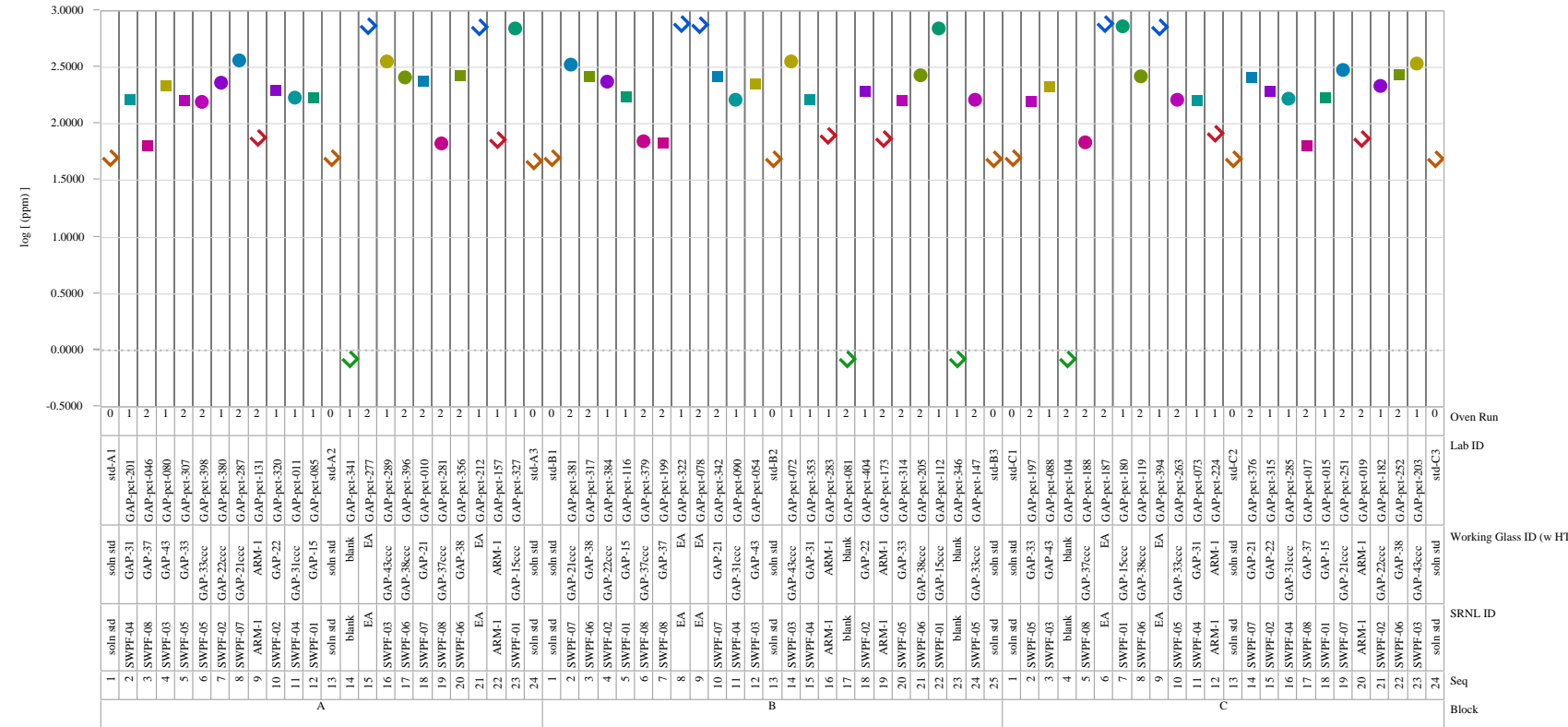


Exhibit B1. PCT Measurements in Analytical Sequence by Analytical Block (continued)

Analyte= $\log[\text{Si ppm}]$, Block Groupings=D-E-F

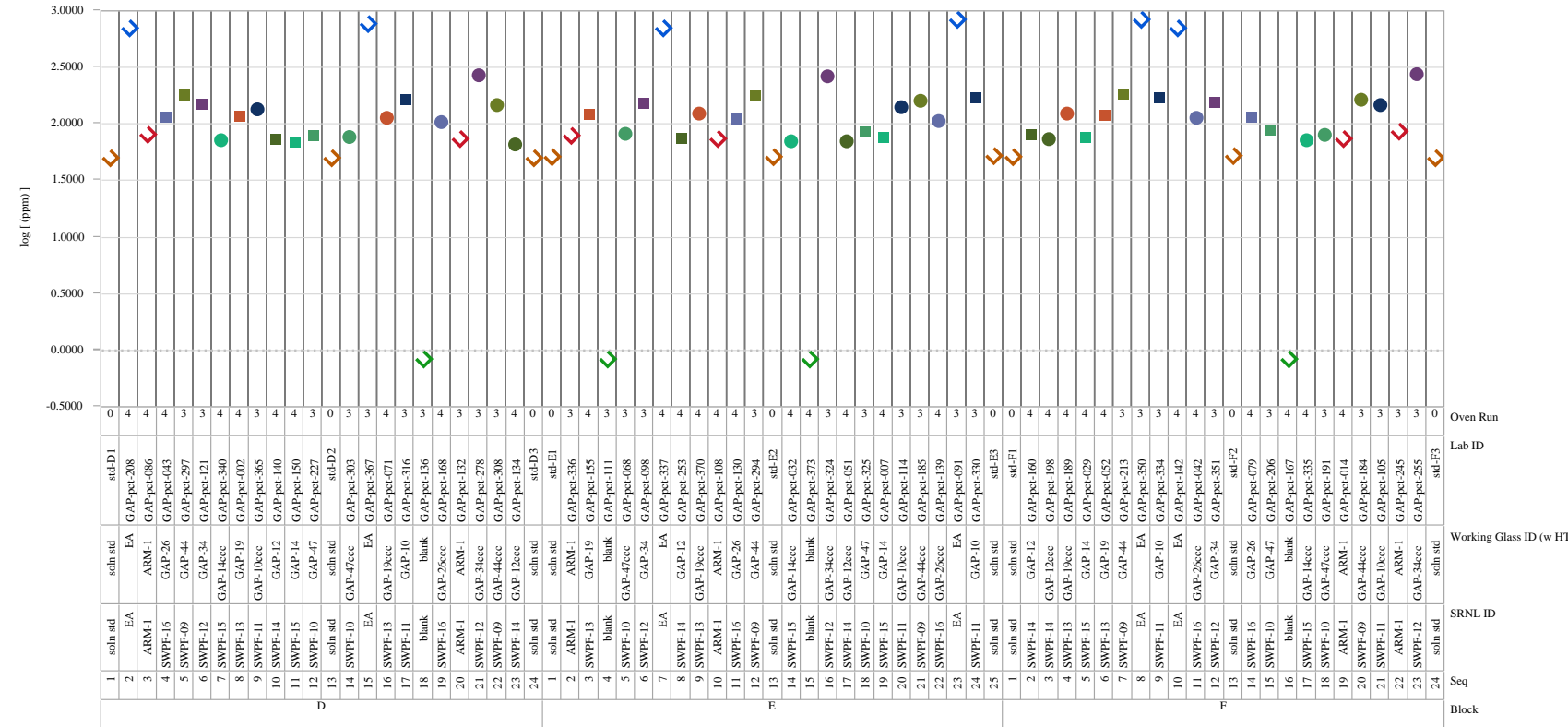


Exhibit B1. PCT Measurements in Analytical Sequence by Analytical Block (continued)

Analyte= $\log[\text{Si ppm}]$, Block Groupings=G-H-I

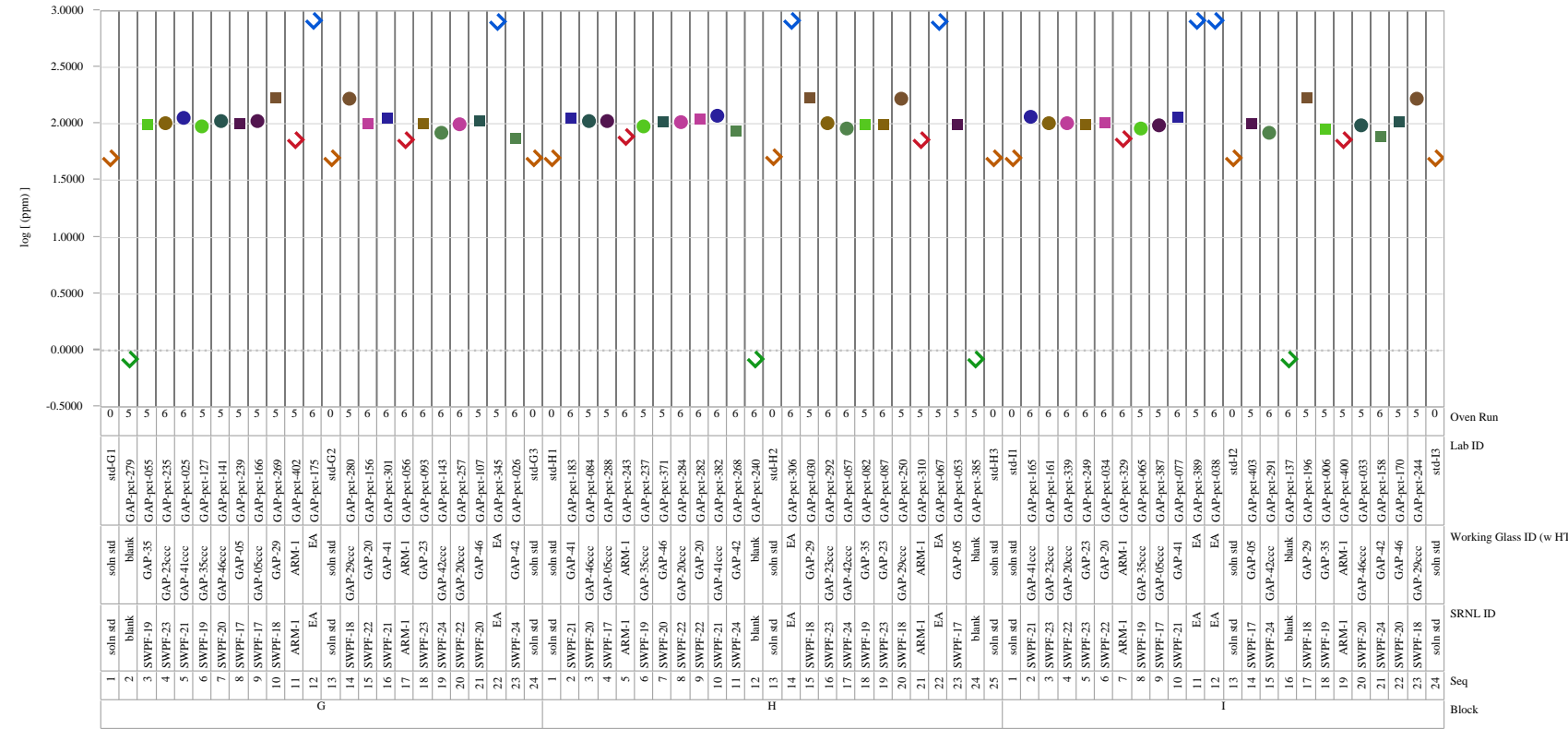


Exhibit B1. PCT Measurements in Analytical Sequence by Analytical Block (continued)

Analyte= $\log[\text{Si ppm}]$, Block Groupings=J-K-L

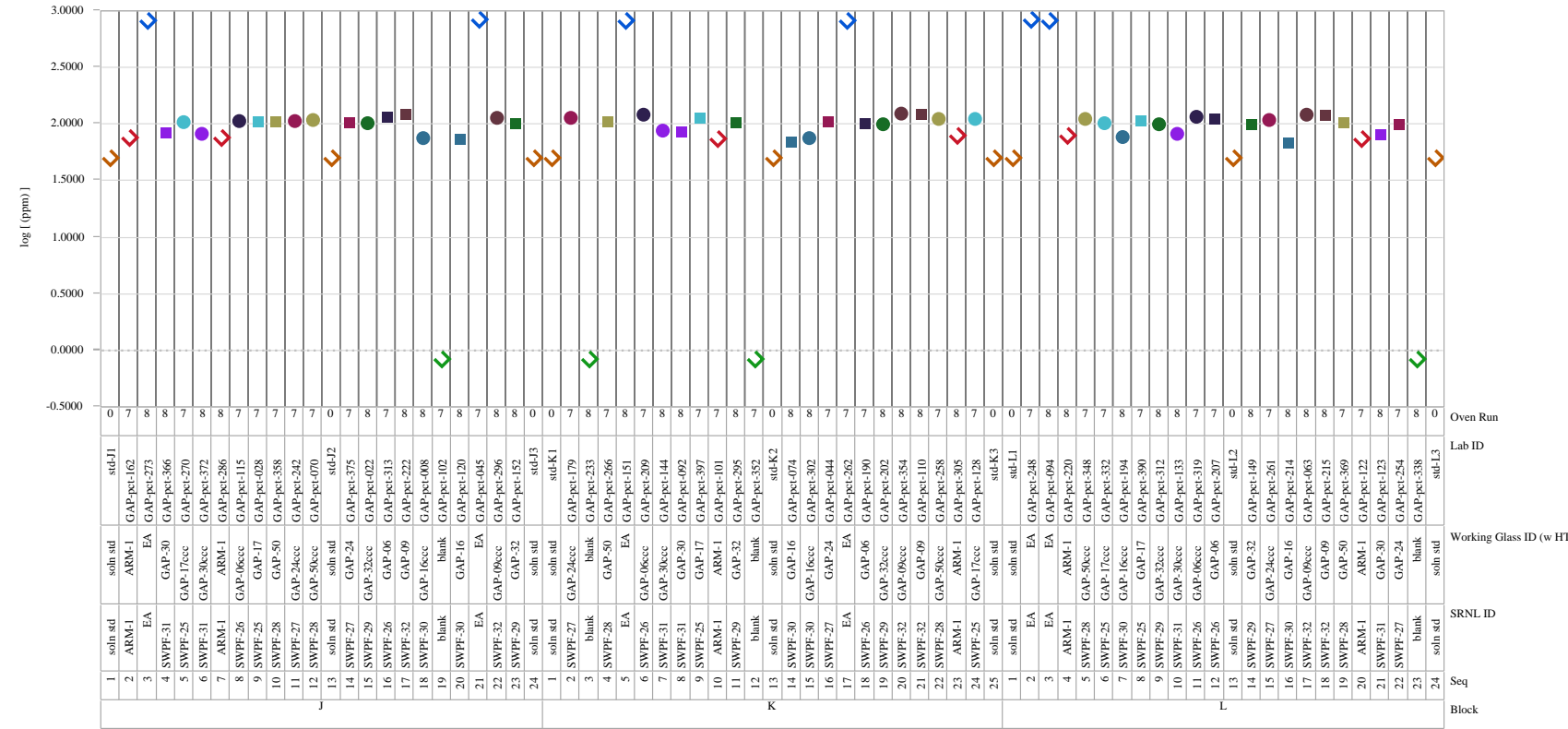


Exhibit B1. PCT Measurements in Analytical Sequence by Analytical Block (continued)

Analyte=log[Si ppm], Block Groupings=M-N-O

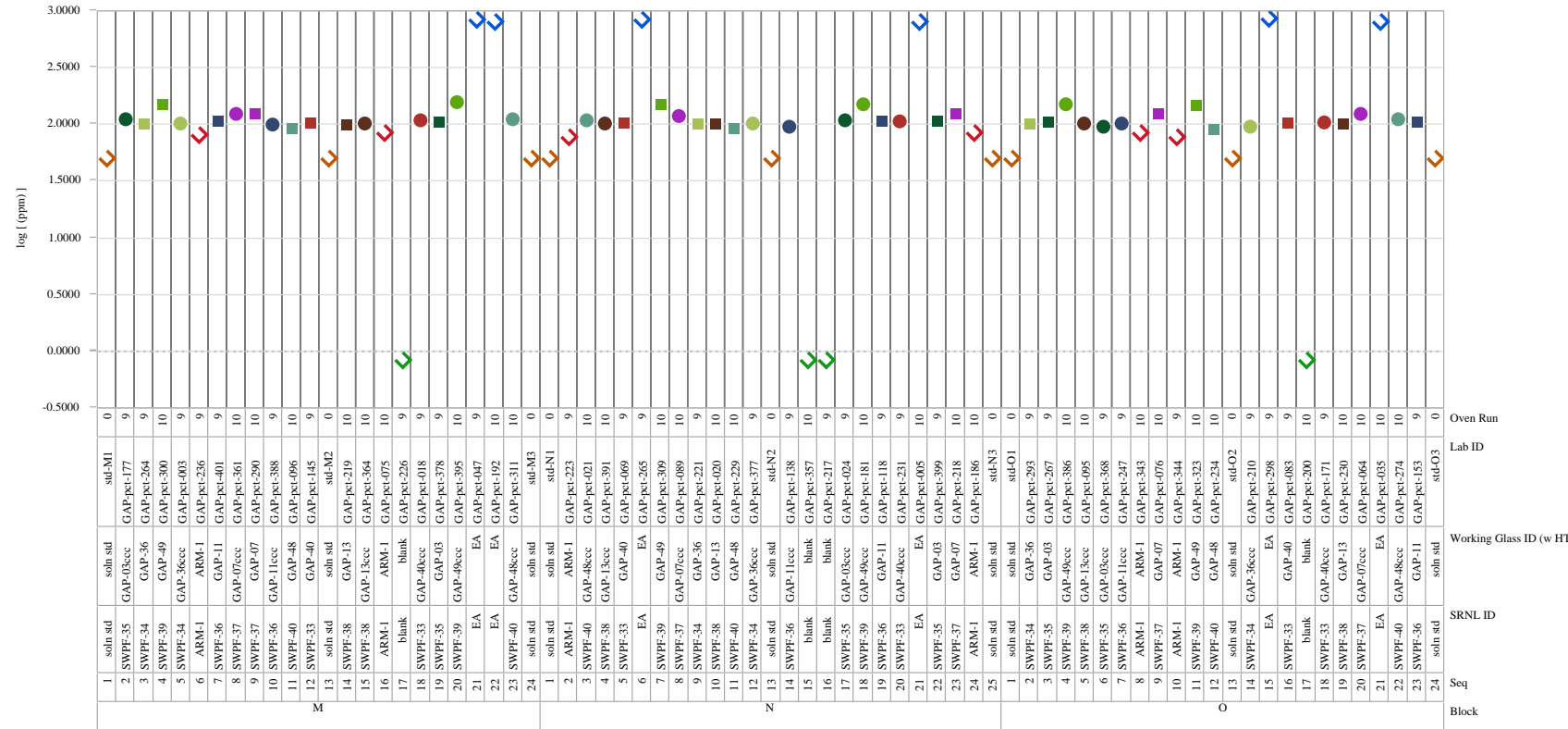


Exhibit B1. PCT Measurements in Analytical Sequence by Analytical Block (continued)

Analyte=log[Si ppm], Block Groupings=P-Q-R

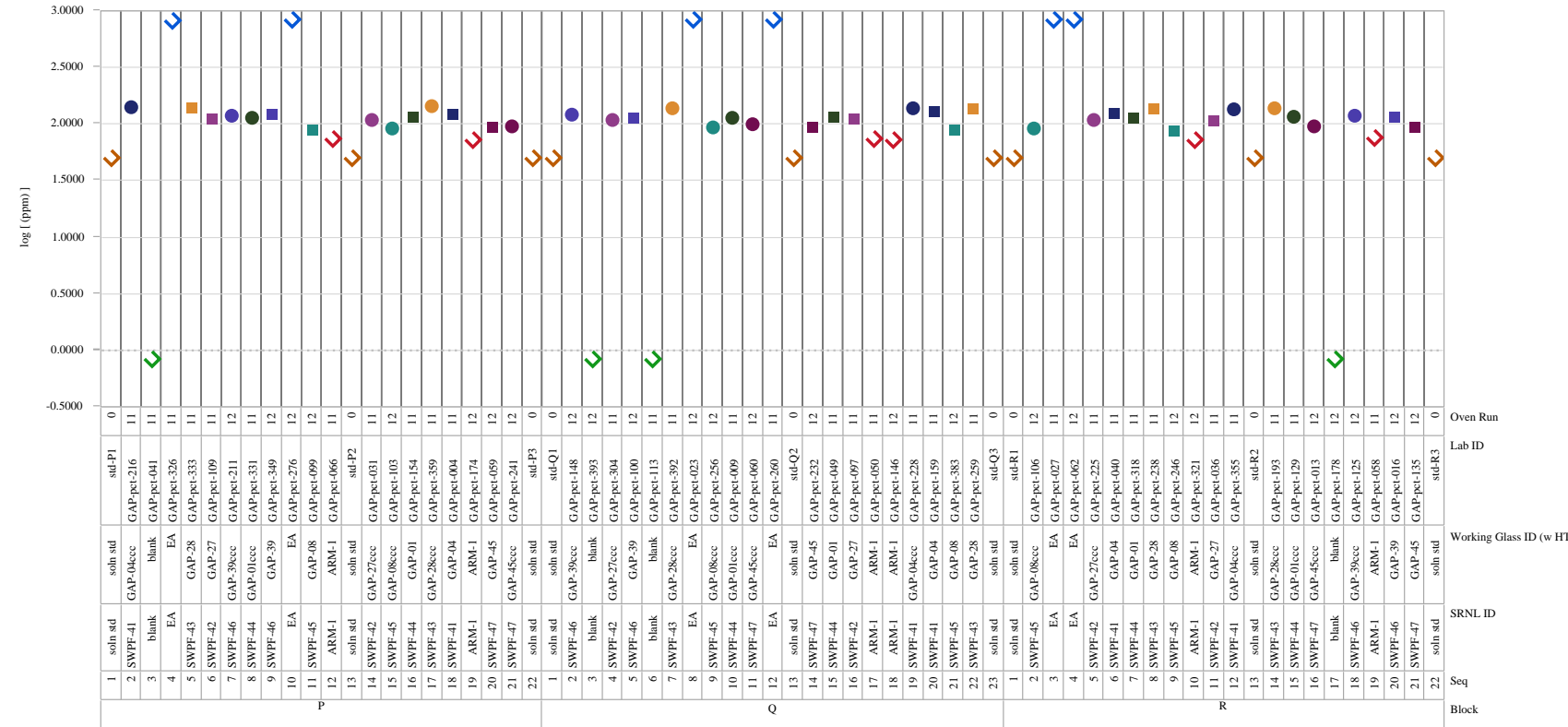


Exhibit B1. PCT Measurements in Analytical Sequence by Analytical Block (continued)

Analyte= $\log[\text{Si ppm}]$, Block Groupings=S-T-U

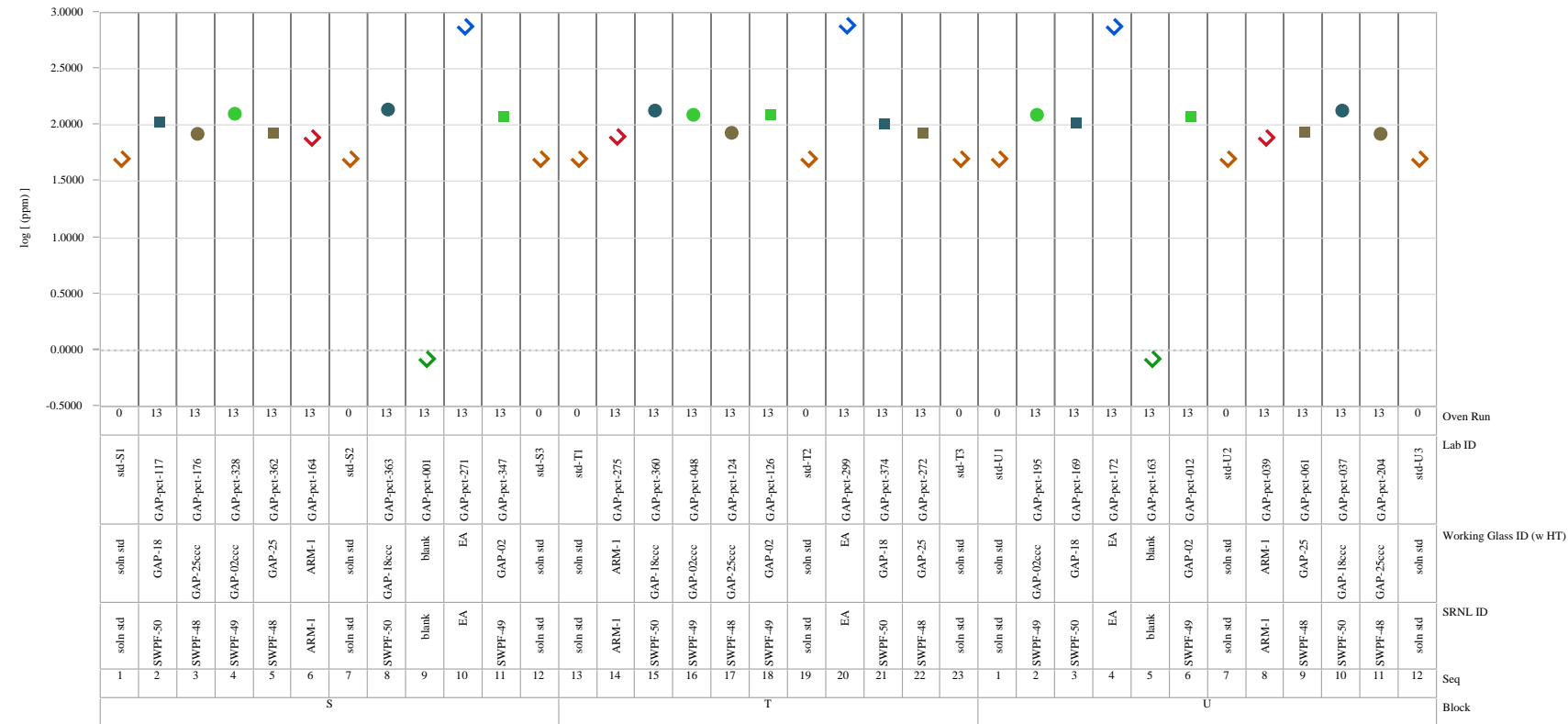


Exhibit B2. PCT Measurements by SRNL Glass ID and Heat Treatment

Analyte= $\log[B \text{ ppm}]$

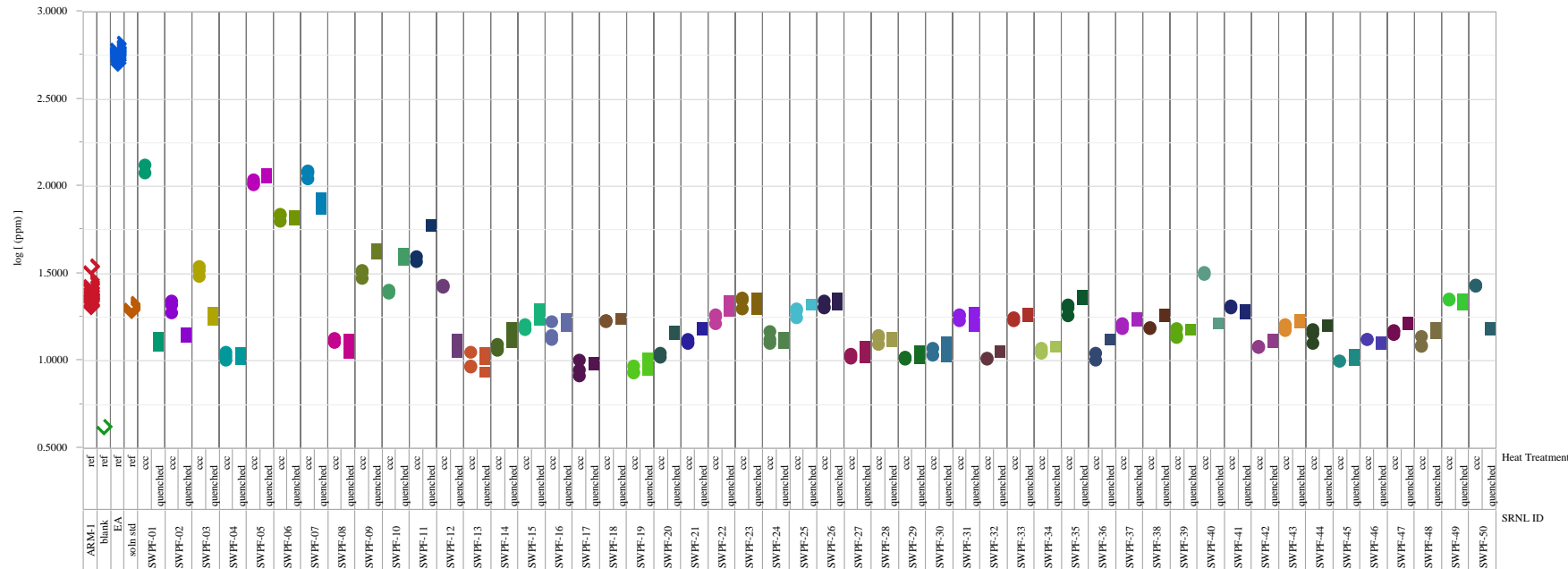


Exhibit B2. PCT Measurements by SRNL Glass ID and Heat Treatment (continued)

Analyte=log[Li ppm]

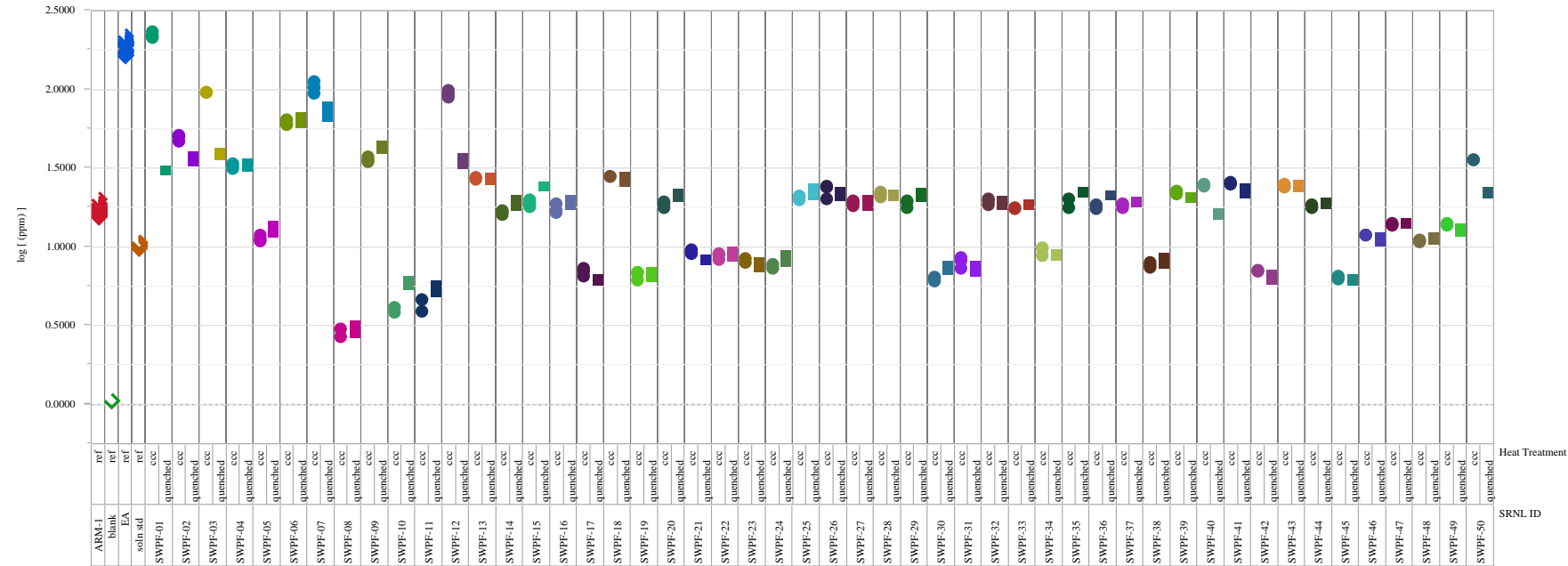


Exhibit B2. PCT Measurements by SRNL Glass ID and Heat Treatment (continued)

Analyte= $\log[\text{Na ppm}]$

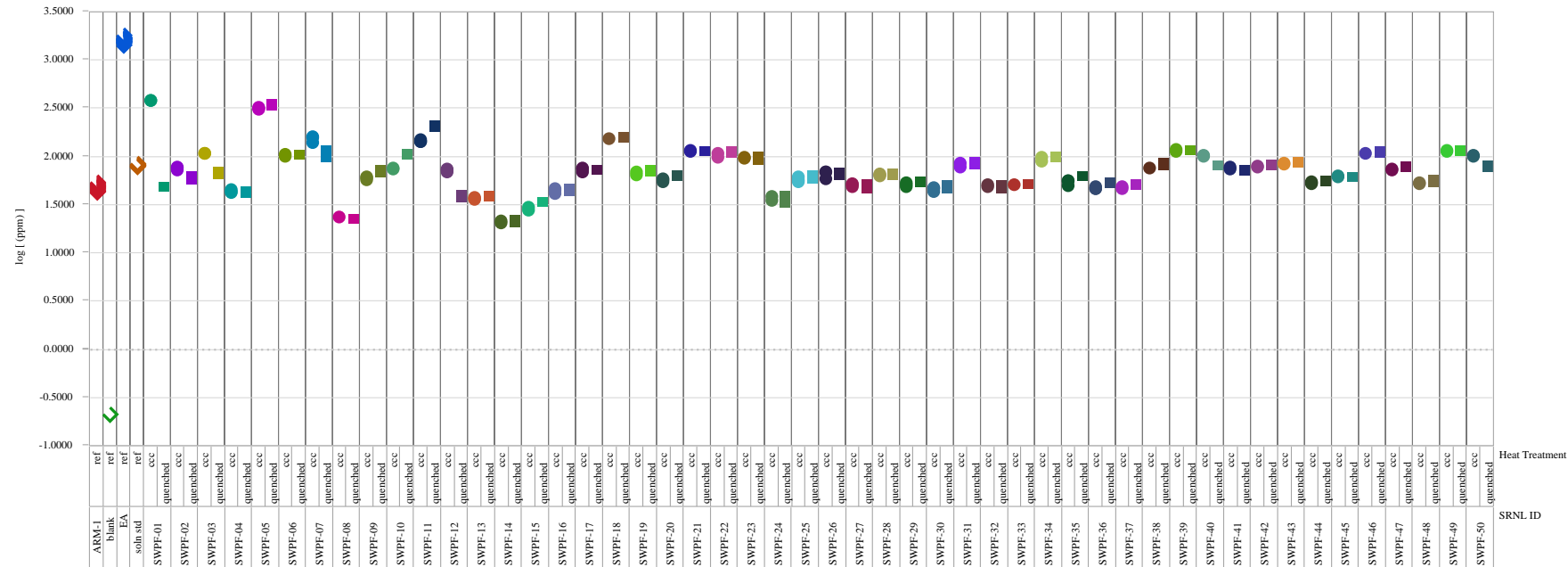


Exhibit B2. PCT Measurements by SRNL Glass ID and Heat Treatment (continued)

Analyte= $\log[\text{Si ppm}]$

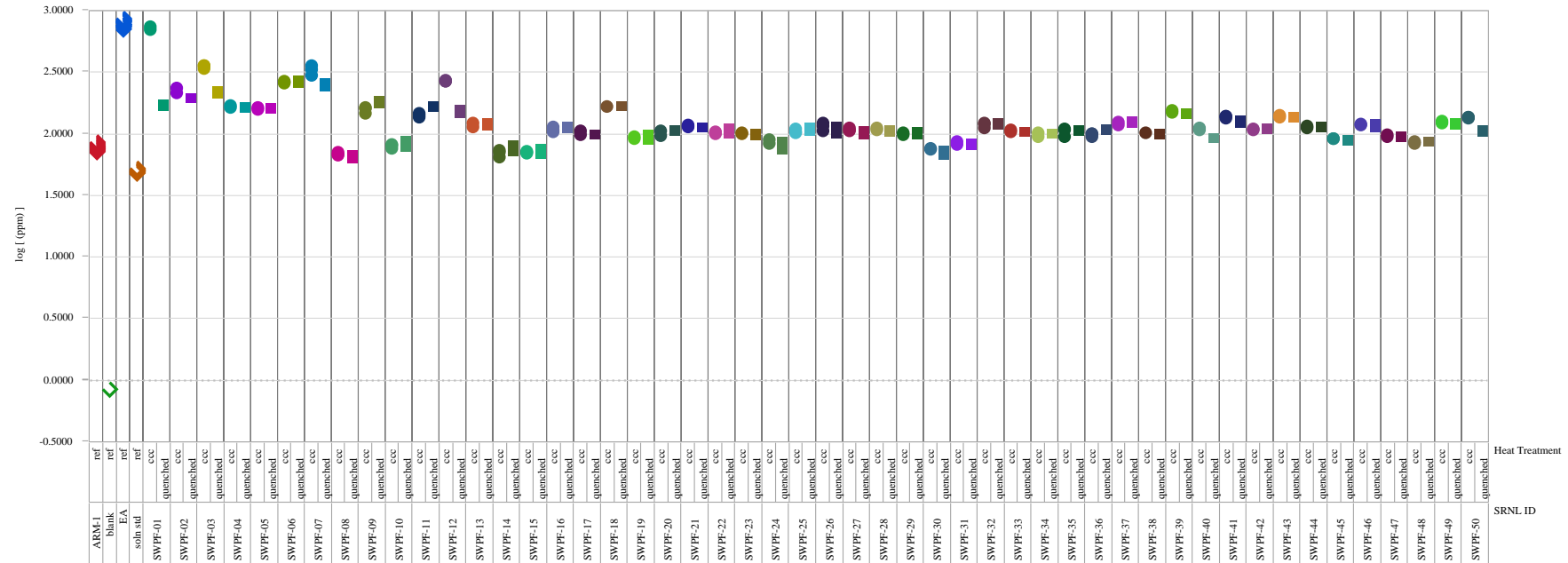
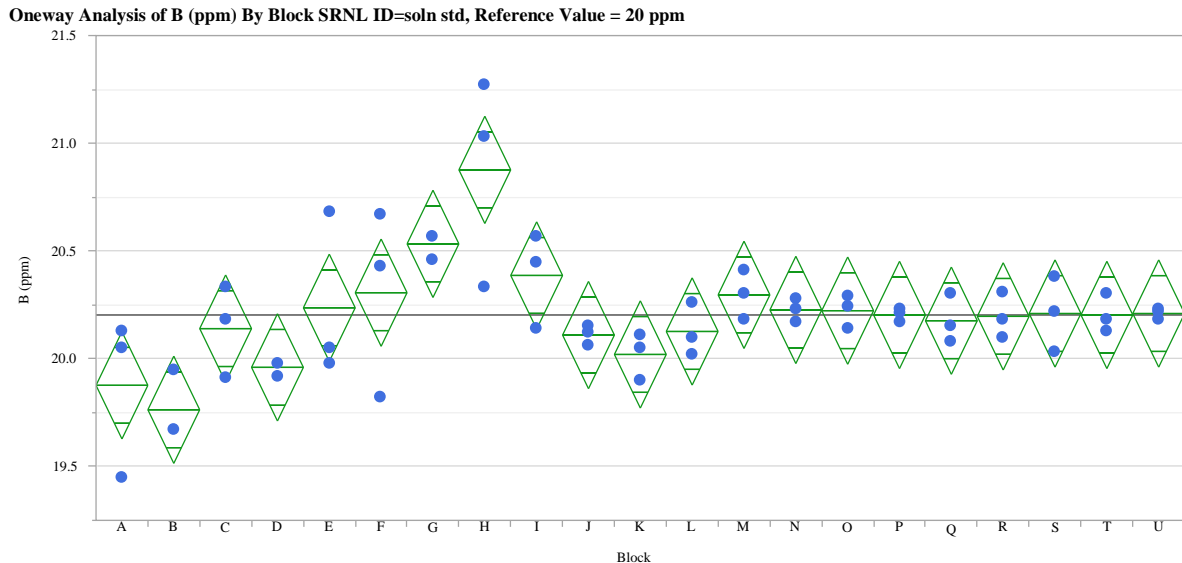


Exhibit B3. Measurements of the Solution Standard by Analytical Block.



Oneway Anova Summary of Fit

| | |
|----------------------------|----------|
| Rsquare | 0.617262 |
| Adj Rsquare | 0.435005 |
| Root Mean Square Error | 0.213575 |
| Mean of Response | 20.20397 |
| Observations (or Sum Wgts) | 63 |

Analysis of Variance

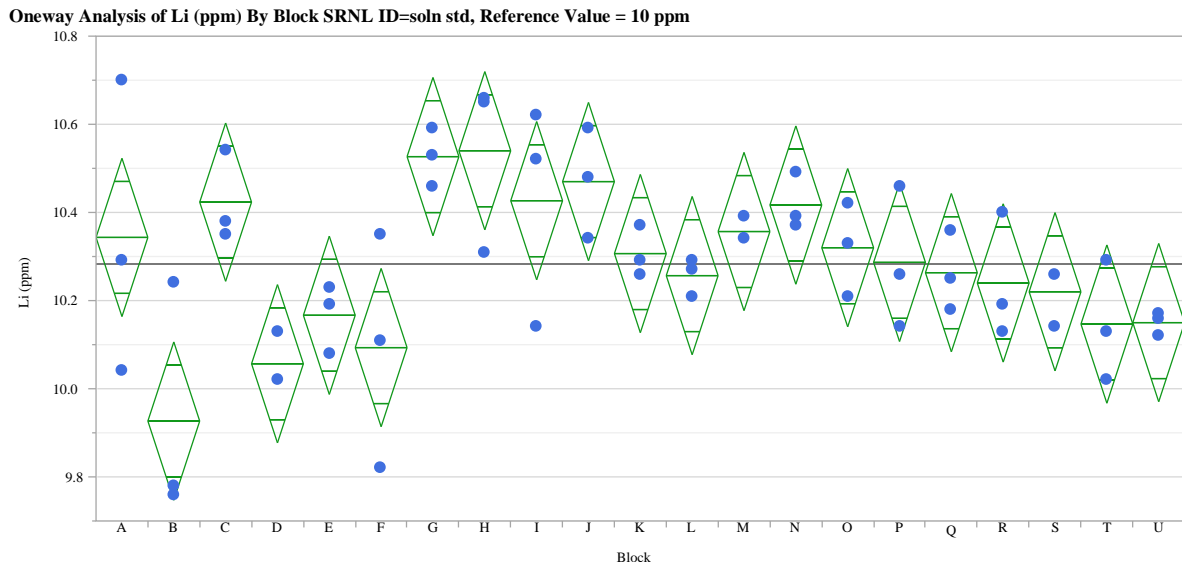
| Source | DF | Sum of Squares | Mean Square | F Ratio | Prob > F |
|----------|----|----------------|-------------|---------|----------|
| Block | 20 | 3.0897079 | 0.154485 | 3.3868 | 0.0004* |
| Error | 42 | 1.9158000 | 0.045614 | | |
| C. Total | 62 | 5.0055079 | | | |

Means for Oneway Anova

| Level | Number | Mean | Std Error | Lower 95% | Upper 95% |
|-------|--------|---------|-----------|-----------|-----------|
| A | 3 | 19.8767 | 0.12331 | 19.628 | 20.126 |
| B | 3 | 19.7633 | 0.12331 | 19.514 | 20.012 |
| C | 3 | 20.1400 | 0.12331 | 19.891 | 20.389 |
| D | 3 | 19.9600 | 0.12331 | 19.711 | 20.209 |
| E | 3 | 20.2367 | 0.12331 | 19.988 | 20.486 |
| F | 3 | 20.3067 | 0.12331 | 20.058 | 20.556 |
| G | 3 | 20.5333 | 0.12331 | 20.284 | 20.782 |
| H | 3 | 20.8767 | 0.12331 | 20.628 | 21.126 |
| I | 3 | 20.3867 | 0.12331 | 20.138 | 20.636 |
| J | 3 | 20.1100 | 0.12331 | 19.861 | 20.359 |
| K | 3 | 20.0200 | 0.12331 | 19.771 | 20.269 |
| L | 3 | 20.1267 | 0.12331 | 19.878 | 20.376 |
| M | 3 | 20.2967 | 0.12331 | 20.048 | 20.546 |
| N | 3 | 20.2267 | 0.12331 | 19.978 | 20.476 |
| O | 3 | 20.2233 | 0.12331 | 19.974 | 20.472 |
| P | 3 | 20.2033 | 0.12331 | 19.954 | 20.452 |
| Q | 3 | 20.1767 | 0.12331 | 19.928 | 20.426 |
| R | 3 | 20.1967 | 0.12331 | 19.948 | 20.446 |
| S | 3 | 20.2100 | 0.12331 | 19.961 | 20.459 |
| T | 3 | 20.2033 | 0.12331 | 19.954 | 20.452 |
| U | 3 | 20.2100 | 0.12331 | 19.961 | 20.459 |

Std Error uses a pooled estimate of error variance

**Exhibit B3. Measurements of the Solution Standard by Analytical Block.
(continued)**



**Oneway Anova
Summary of Fit**

| | |
|----------------------------|----------|
| Rsquare | 0.600759 |
| Adj Rsquare | 0.410644 |
| Root Mean Square Error | 0.154134 |
| Mean of Response | 10.2827 |
| Observations (or Sum Wgts) | 63 |

Analysis of Variance

| Source | DF | Sum of Squares | Mean Square | F Ratio | Prob > F |
|----------|----|----------------|-------------|---------|----------|
| Block | 20 | 1.5014413 | 0.075072 | 3.1600 | 0.0008* |
| Error | 42 | 0.9978000 | 0.023757 | | |
| C. Total | 62 | 2.4992413 | | | |

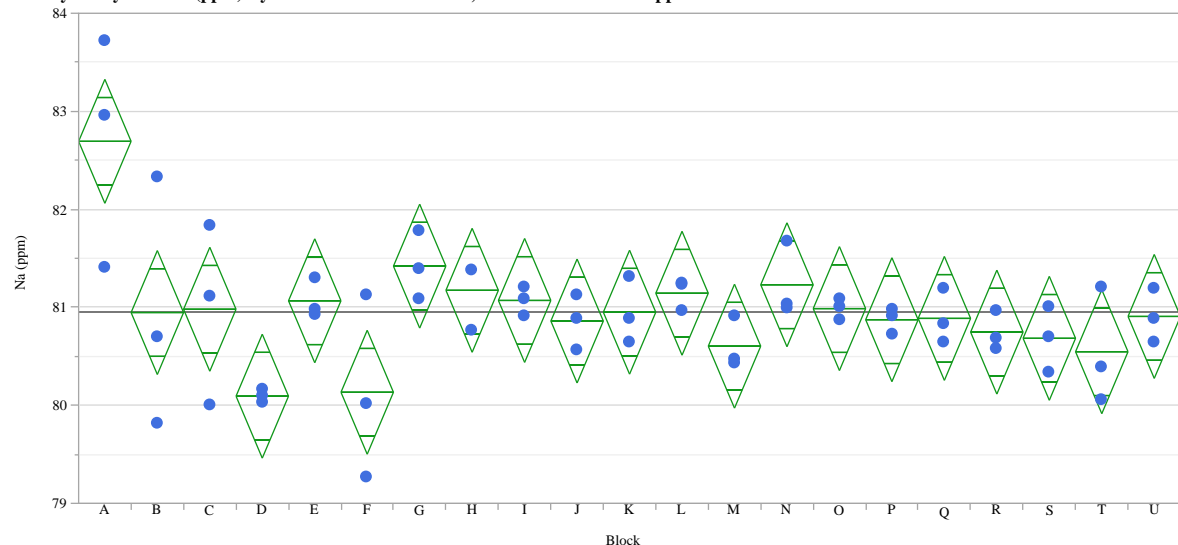
Means for Oneway Anova

| Level | Number | Mean | Std Error | Lower 95% | Upper 95% |
|-------|--------|---------|-----------|-----------|-----------|
| A | 3 | 10.3433 | 0.08899 | 10.164 | 10.523 |
| B | 3 | 9.9267 | 0.08899 | 9.747 | 10.106 |
| C | 3 | 10.4233 | 0.08899 | 10.244 | 10.603 |
| D | 3 | 10.0567 | 0.08899 | 9.877 | 10.236 |
| E | 3 | 10.1667 | 0.08899 | 9.987 | 10.346 |
| F | 3 | 10.0933 | 0.08899 | 9.914 | 10.273 |
| G | 3 | 10.5267 | 0.08899 | 10.347 | 10.706 |
| H | 3 | 10.5400 | 0.08899 | 10.360 | 10.720 |
| I | 3 | 10.4267 | 0.08899 | 10.247 | 10.606 |
| J | 3 | 10.4700 | 0.08899 | 10.290 | 10.650 |
| K | 3 | 10.3067 | 0.08899 | 10.127 | 10.486 |
| L | 3 | 10.2567 | 0.08899 | 10.077 | 10.436 |
| M | 3 | 10.3567 | 0.08899 | 10.177 | 10.536 |
| N | 3 | 10.4167 | 0.08899 | 10.237 | 10.596 |
| O | 3 | 10.3200 | 0.08899 | 10.140 | 10.500 |
| P | 3 | 10.2867 | 0.08899 | 10.107 | 10.466 |
| Q | 3 | 10.2633 | 0.08899 | 10.084 | 10.443 |
| R | 3 | 10.2400 | 0.08899 | 10.060 | 10.420 |
| S | 3 | 10.2200 | 0.08899 | 10.040 | 10.400 |
| T | 3 | 10.1467 | 0.08899 | 9.967 | 10.326 |
| U | 3 | 10.1500 | 0.08899 | 9.970 | 10.330 |

Std Error uses a pooled estimate of error variance

**Exhibit B3. Measurements of the Solution Standard by Analytical Block.
(continued)**

Oneway Analysis of Na (ppm) By Block SRNL ID=soln std, Reference Value = 81 ppm



**Oneway Anova
Summary of Fit**

| | |
|----------------------------|----------|
| Rsquare | 0.561231 |
| Adj Rsquare | 0.352293 |
| Root Mean Square Error | 0.542586 |
| Mean of Response | 80.95206 |
| Observations (or Sum Wgts) | 63 |

Analysis of Variance

| Source | DF | Sum of Squares | Mean Square | F Ratio | Prob > F |
|----------|----|----------------|-------------|---------|----------|
| Block | 20 | 15.815832 | 0.790792 | 2.6861 | 0.0035* |
| Error | 42 | 12.364800 | 0.294400 | | |
| C. Total | 62 | 28.180632 | | | |

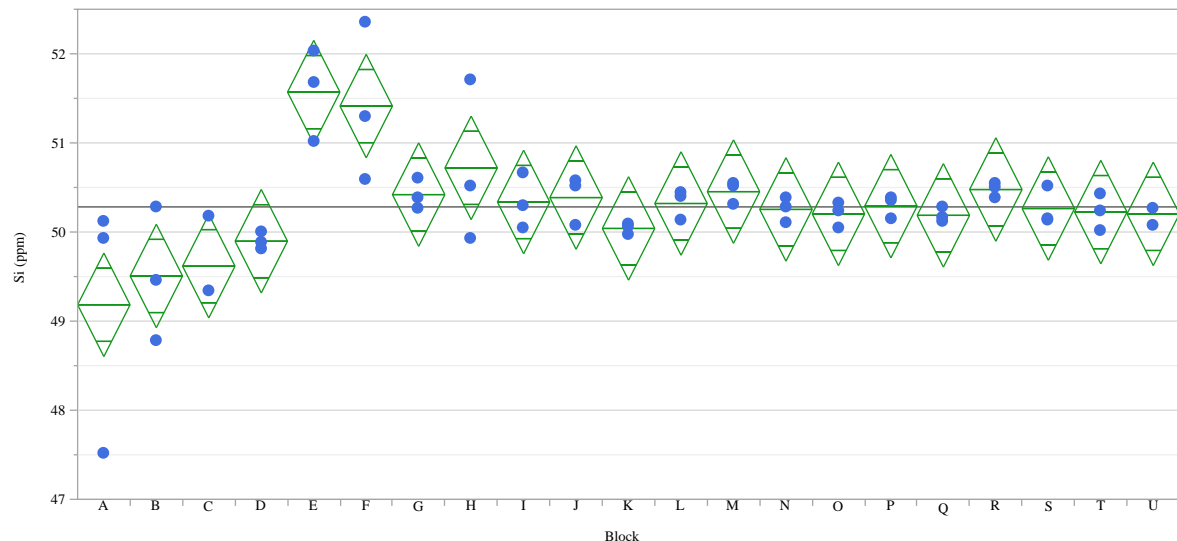
Means for Oneway Anova

| Level | Number | Mean | Std Error | Lower 95% | Upper 95% |
|-------|--------|---------|-----------|-----------|-----------|
| A | 3 | 82.6933 | 0.31326 | 82.061 | 83.326 |
| B | 3 | 80.9467 | 0.31326 | 80.314 | 81.579 |
| C | 3 | 80.9800 | 0.31326 | 80.348 | 81.612 |
| D | 3 | 80.0933 | 0.31326 | 79.461 | 80.726 |
| E | 3 | 81.0667 | 0.31326 | 80.434 | 81.699 |
| F | 3 | 80.1333 | 0.31326 | 79.501 | 80.766 |
| G | 3 | 81.4200 | 0.31326 | 80.788 | 82.052 |
| H | 3 | 81.1733 | 0.31326 | 80.541 | 81.806 |
| I | 3 | 81.0700 | 0.31326 | 80.438 | 81.702 |
| J | 3 | 80.8600 | 0.31326 | 80.228 | 81.492 |
| K | 3 | 80.9500 | 0.31326 | 80.318 | 81.582 |
| L | 3 | 81.1433 | 0.31326 | 80.511 | 81.776 |
| M | 3 | 80.6033 | 0.31326 | 79.971 | 81.236 |
| N | 3 | 81.2300 | 0.31326 | 80.598 | 81.862 |
| O | 3 | 80.9867 | 0.31326 | 80.354 | 81.619 |
| P | 3 | 80.8733 | 0.31326 | 80.241 | 81.506 |
| Q | 3 | 80.8867 | 0.31326 | 80.254 | 81.519 |
| R | 3 | 80.7467 | 0.31326 | 80.114 | 81.379 |
| S | 3 | 80.6833 | 0.31326 | 80.051 | 81.316 |
| T | 3 | 80.5467 | 0.31326 | 79.914 | 81.179 |
| U | 3 | 80.9067 | 0.31326 | 80.274 | 81.539 |

Std Error uses a pooled estimate of error variance

**Exhibit B3. Measurements of the Solution Standard by Analytical Block.
(continued)**

Oneway Analysis of Si (ppm) By Block SRNL ID=soln std, Reference Value = 50 ppm



**Oneway Anova
Summary of Fit**

| | |
|----------------------------|----------|
| Rsquare | 0.621788 |
| Adj Rsquare | 0.441687 |
| Root Mean Square Error | 0.498359 |
| Mean of Response | 50.28397 |
| Observations (or Sum Wgts) | 63 |

Analysis of Variance

| Source | DF | Sum of Squares | Mean Square | F Ratio | Prob > F |
|----------|----|----------------|-------------|---------|----------|
| Block | 20 | 17.149108 | 0.857455 | 3.4524 | 0.0004* |
| Error | 42 | 10.431200 | 0.248362 | | |
| C. Total | 62 | 27.580308 | | | |

Means for Oneway Anova

| Level | Number | Mean | Std Error | Lower 95% | Upper 95% |
|-------|--------|---------|-----------|-----------|-----------|
| A | 3 | 49.1833 | 0.28773 | 48.603 | 49.764 |
| B | 3 | 49.5067 | 0.28773 | 48.926 | 50.087 |
| C | 3 | 49.6167 | 0.28773 | 49.036 | 50.197 |
| D | 3 | 49.8967 | 0.28773 | 49.316 | 50.477 |
| E | 3 | 51.5700 | 0.28773 | 50.989 | 52.151 |
| F | 3 | 51.4133 | 0.28773 | 50.833 | 51.994 |
| G | 3 | 50.4200 | 0.28773 | 49.839 | 51.001 |
| H | 3 | 50.7200 | 0.28773 | 50.139 | 51.301 |
| I | 3 | 50.3367 | 0.28773 | 49.756 | 50.917 |
| J | 3 | 50.3867 | 0.28773 | 49.806 | 50.967 |
| K | 3 | 50.0400 | 0.28773 | 49.459 | 50.621 |
| L | 3 | 50.3200 | 0.28773 | 49.739 | 50.901 |
| M | 3 | 50.4533 | 0.28773 | 49.873 | 51.034 |
| N | 3 | 50.2533 | 0.28773 | 49.673 | 50.834 |
| O | 3 | 50.2033 | 0.28773 | 49.623 | 50.784 |
| P | 3 | 50.2900 | 0.28773 | 49.709 | 50.871 |
| Q | 3 | 50.1867 | 0.28773 | 49.606 | 50.767 |
| R | 3 | 50.4767 | 0.28773 | 49.896 | 51.057 |
| S | 3 | 50.2633 | 0.28773 | 49.683 | 50.844 |
| T | 3 | 50.2233 | 0.28773 | 49.643 | 50.804 |
| U | 3 | 50.2033 | 0.28773 | 49.623 | 50.784 |

Std Error uses a pooled estimate of error variance

**Exhibit B4. Correlations of Normalized PCT Responses by Compositional View
(continued)**

Values are in Common Logarithms

Multivariate Comp View=Measured
Correlations

| | log NC[B (g/L)] | log NC[Li(g/L)] | log NC[Na (g/L)] | log NC[Si (g/L)] |
|------------------|-----------------|-----------------|------------------|------------------|
| log NC[B (g/L)] | 1.0000 | 0.9467 | 0.9472 | 0.9062 |
| log NC[Li(g/L)] | 0.9467 | 1.0000 | 0.8592 | 0.9360 |
| log NC[Na (g/L)] | 0.9472 | 0.8592 | 1.0000 | 0.8742 |
| log NC[Si (g/L)] | 0.9062 | 0.9360 | 0.8742 | 1.0000 |

Scatterplot Matrix

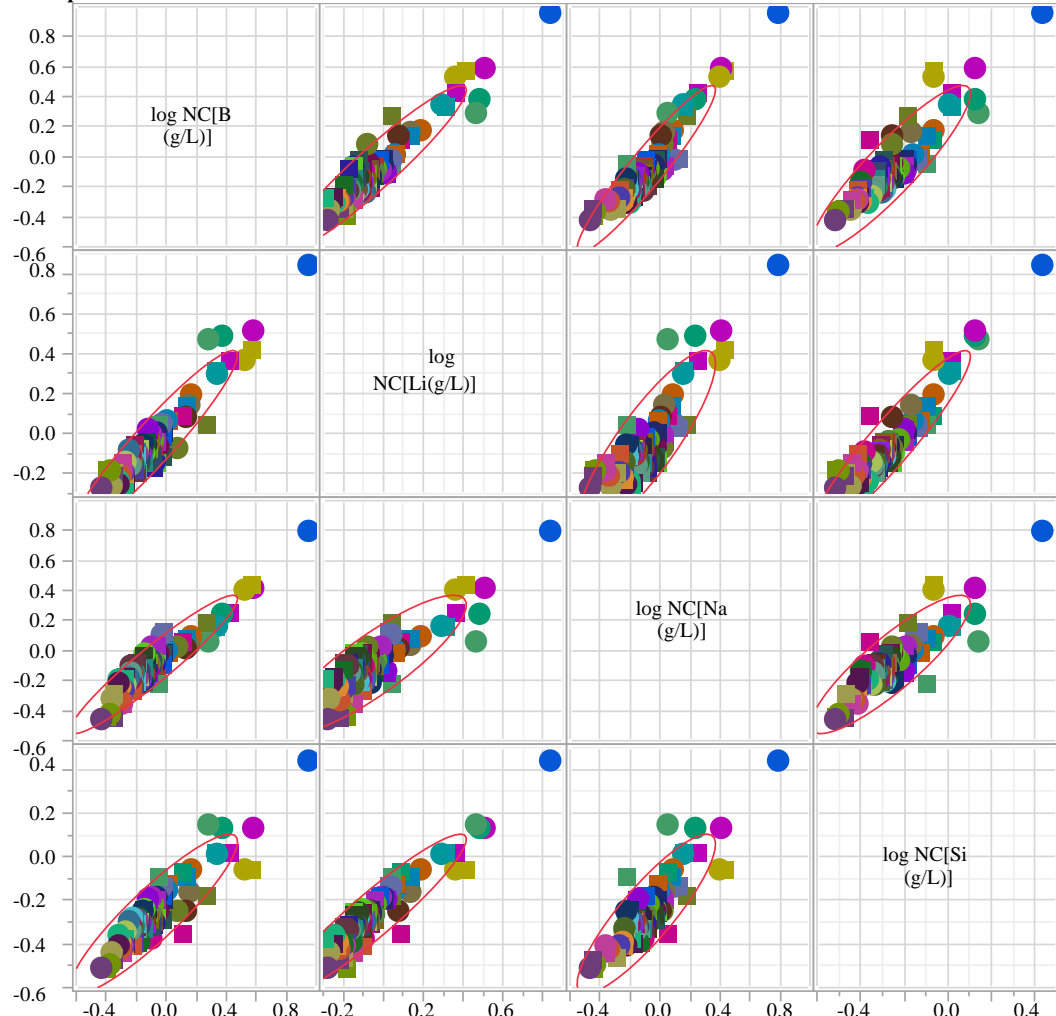


**Exhibit B4. Correlations of Normalized PCT Responses by Compositional View
(continued)**

Values are in Common Logarithms

Multivariate Comp View=Measured bc
Correlations

| | log NC[B (g/L)] | log NC[Li(g/L)] | log NC[Na (g/L)] | log NC[Si (g/L)] |
|------------------|-----------------|-----------------|------------------|------------------|
| log NC[B (g/L)] | 1.0000 | 0.9460 | 0.9449 | 0.9050 |
| log NC[Li(g/L)] | 0.9460 | 1.0000 | 0.8587 | 0.9345 |
| log NC[Na (g/L)] | 0.9449 | 0.8587 | 1.0000 | 0.8738 |
| log NC[Si (g/L)] | 0.9050 | 0.9345 | 0.8738 | 1.0000 |

Scatterplot Matrix

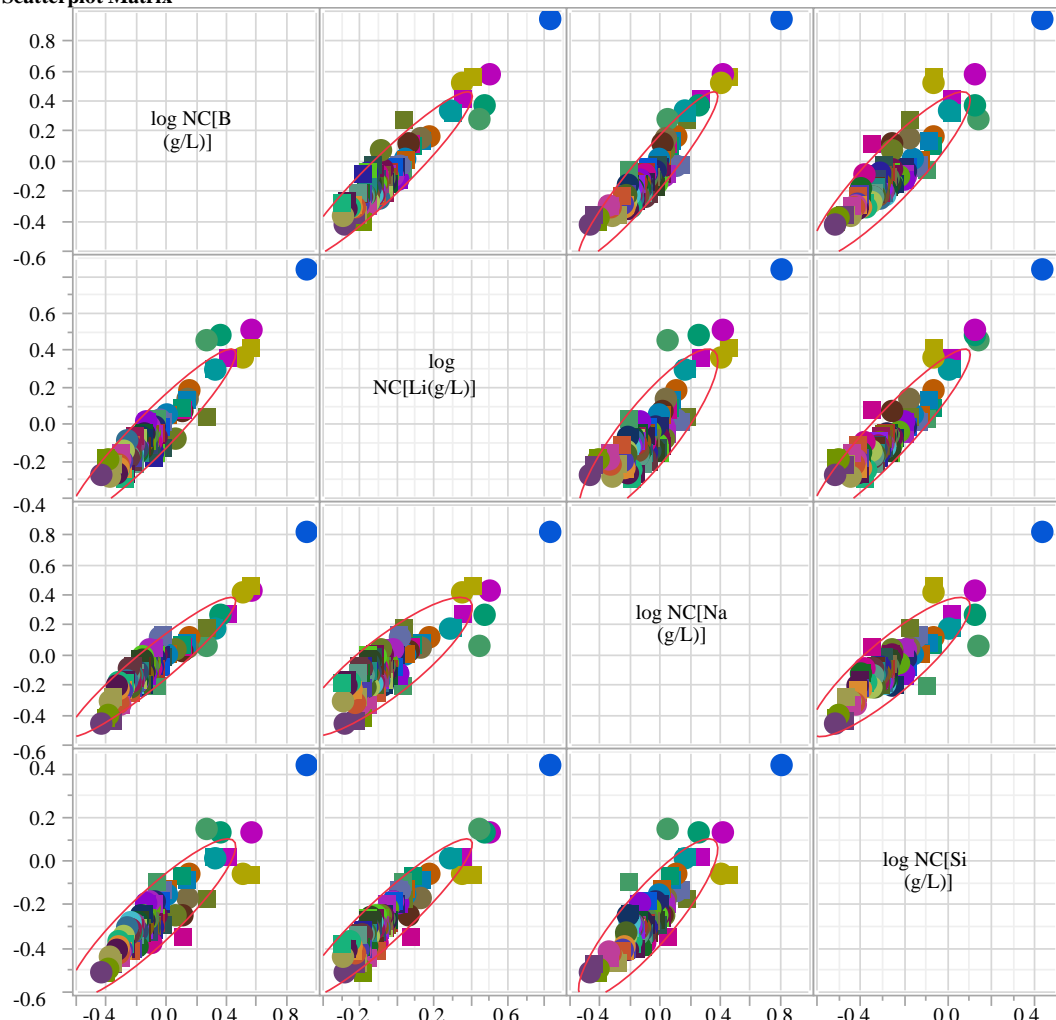


**Exhibit B4. Correlations of Normalized PCT Responses by Compositional View
(continued)**

Values are in Common Logarithms

Multivariate Comp View=targeted

Correlations

| | log NC[B (g/L)] | log NC[Li(g/L)] | log NC[Na (g/L)] | log NC[Si (g/L)] |
|------------------|-----------------|-----------------|------------------|------------------|
| log NC[B (g/L)] | 1.0000 | 0.9559 | 0.9444 | 0.9011 |
| log NC[Li(g/L)] | 0.9559 | 1.0000 | 0.8746 | 0.9343 |
| log NC[Na (g/L)] | 0.9444 | 0.8746 | 1.0000 | 0.8692 |
| log NC[Si (g/L)] | 0.9011 | 0.9343 | 0.8692 | 1.0000 |

Scatterplot Matrix

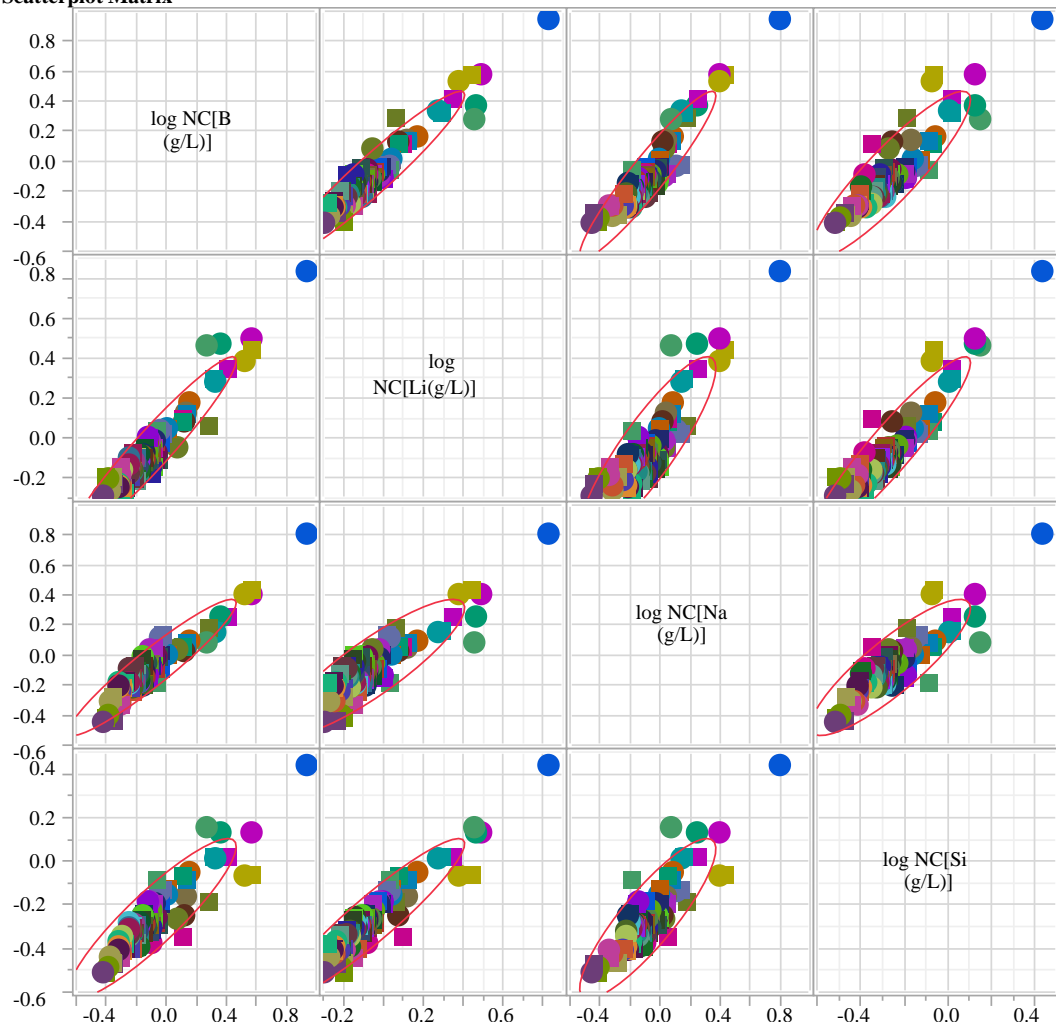


Exhibit B5. Normalized PCT Response by Glass ID and by Heat Treatment within Compositional View

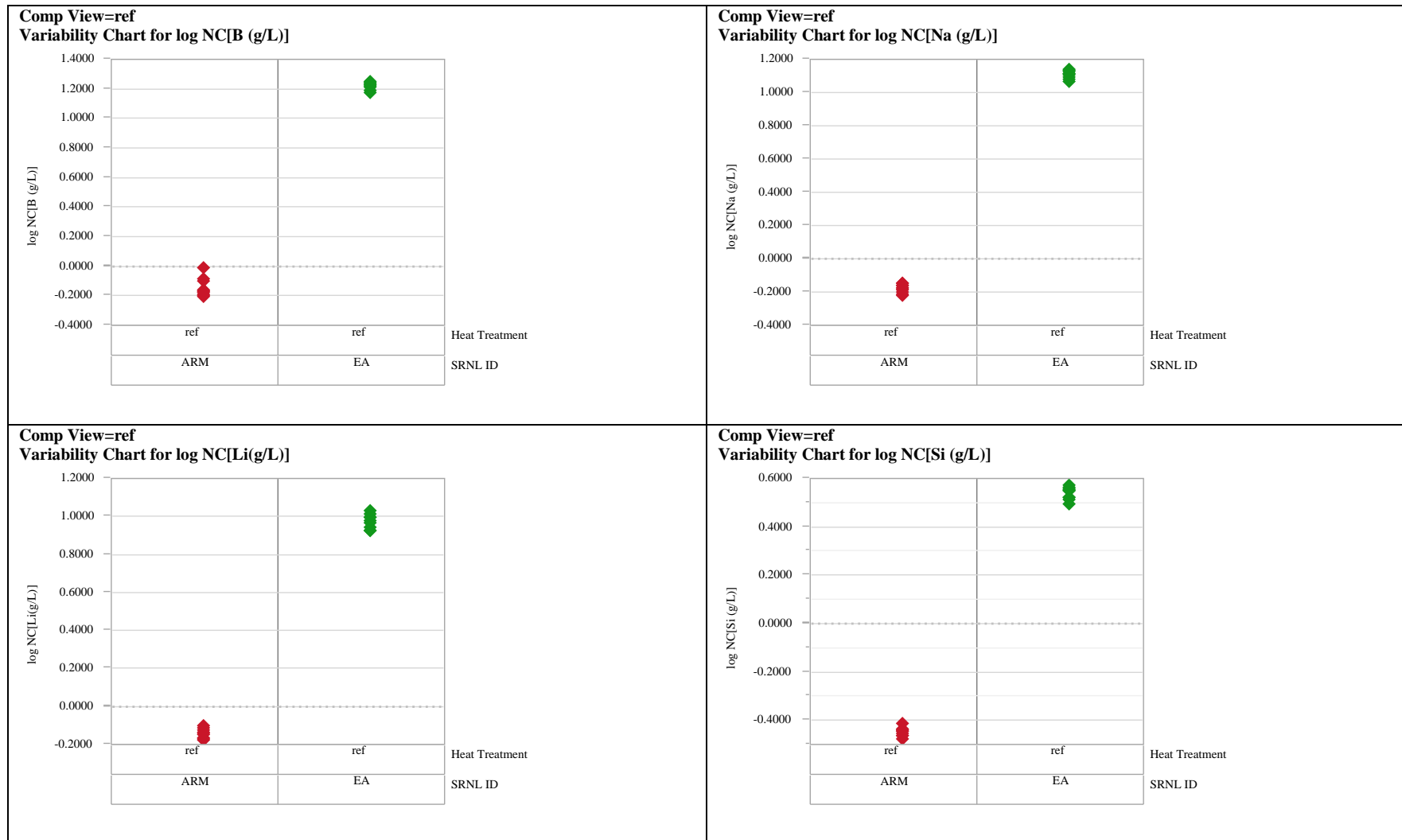


Exhibit B5. Normalized PCT Response by Glass ID and by Heat Treatment within Compositional View
 (continued)

Comp View=Measured
 Variability Chart for log NC[B (g/L)]

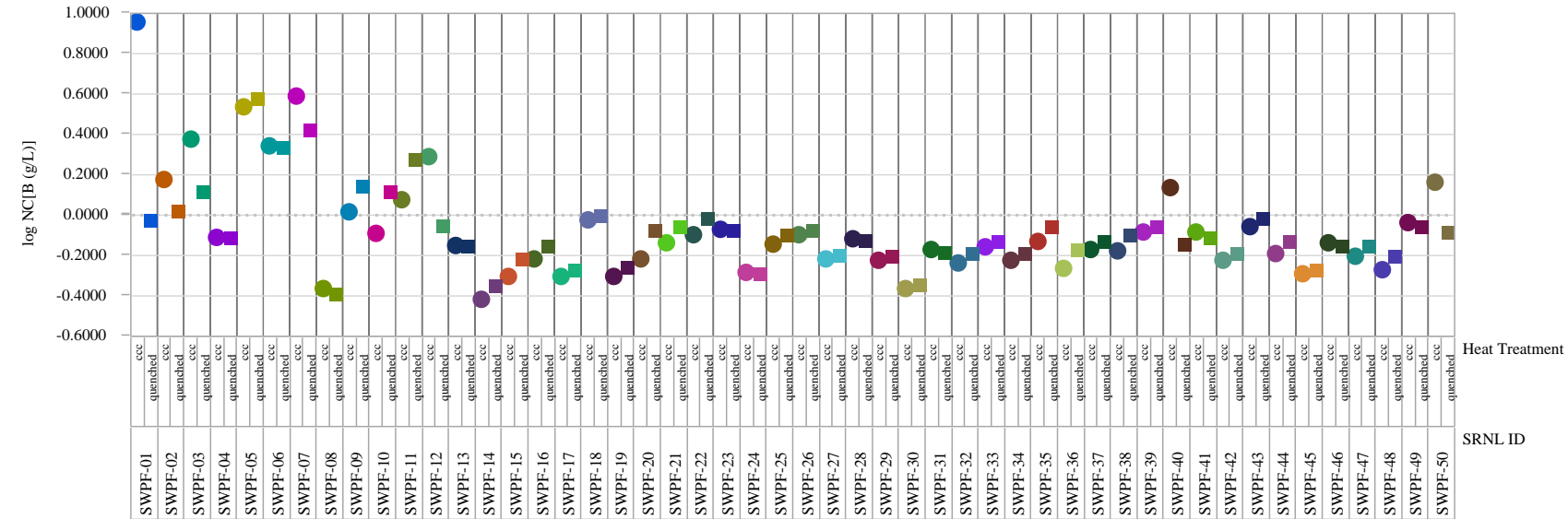


Exhibit B5. Normalized PCT Response by Glass ID and by Heat Treatment within Compositional View
(continued)

Comp View=Measured Variability Chart for log NC[Li(g/L)]

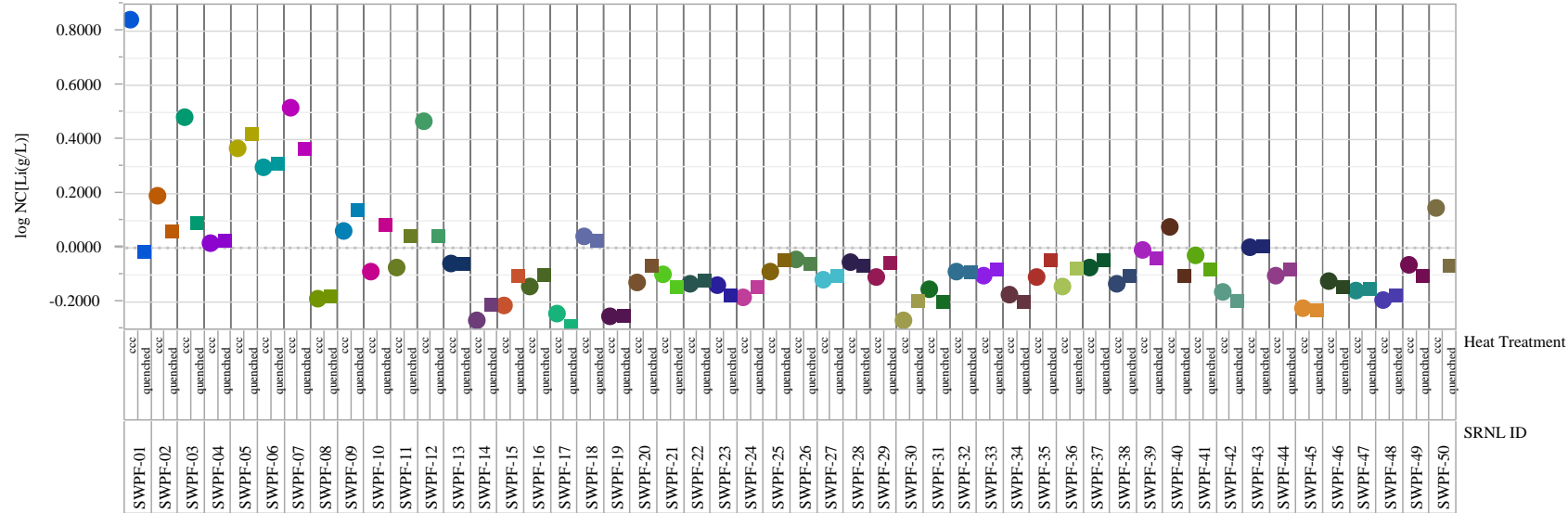


Exhibit B5. Normalized PCT Response by Glass ID and by Heat Treatment within Compositional View
 (continued)

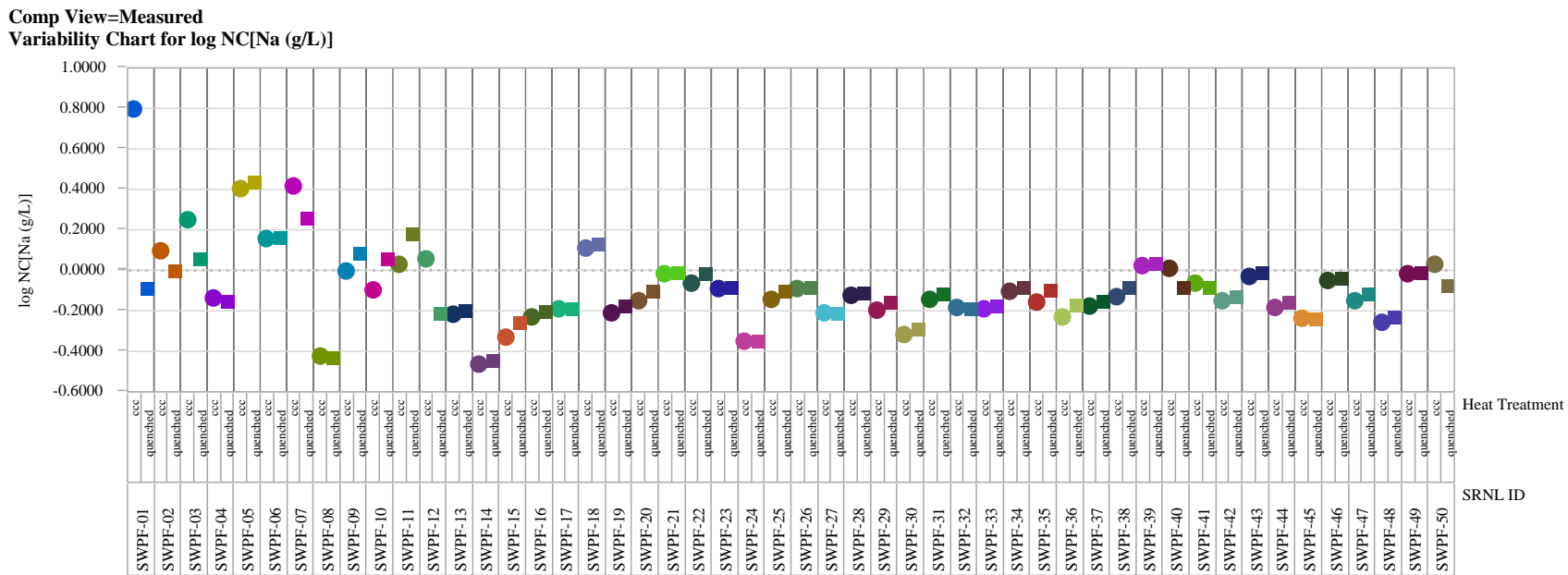


Exhibit B5. Normalized PCT Response by Glass ID and by Heat Treatment within Compositional View
 (continued)

Comp View=Measured
 Variability Chart for log NC[Si (g/L)]

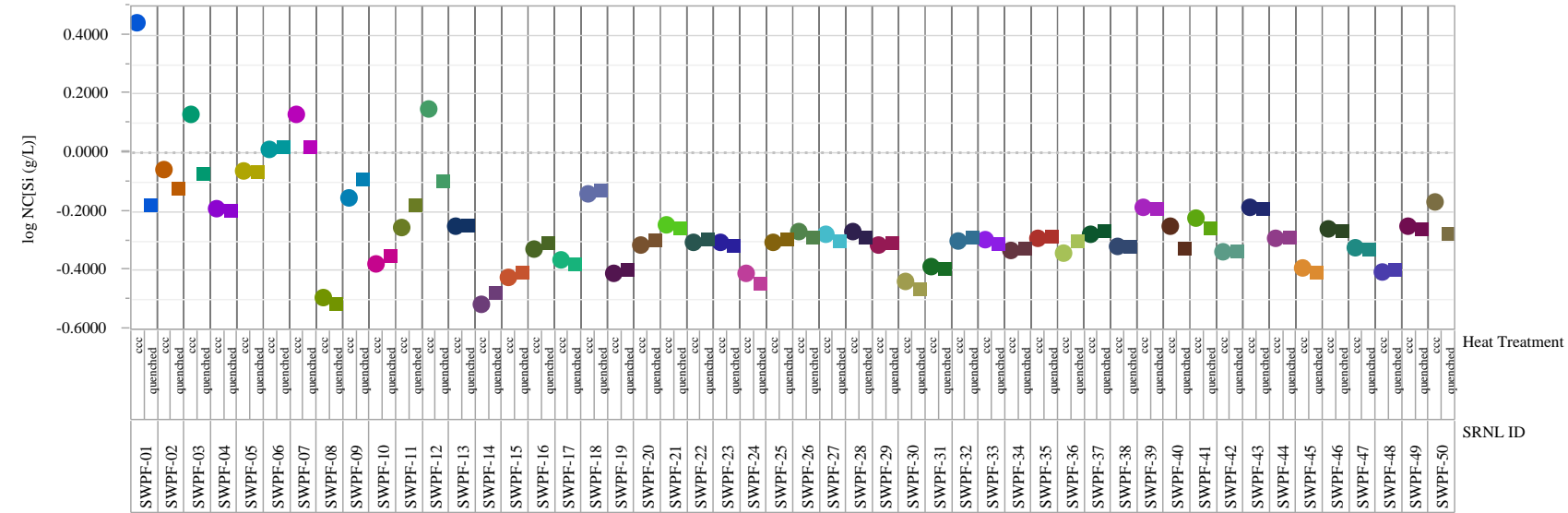


Exhibit B5. Normalized PCT Response by Glass ID and by Heat Treatment within Compositional View
(continued)

Comp View=Measured bc
Variability Chart for log NC[B (g/L)]

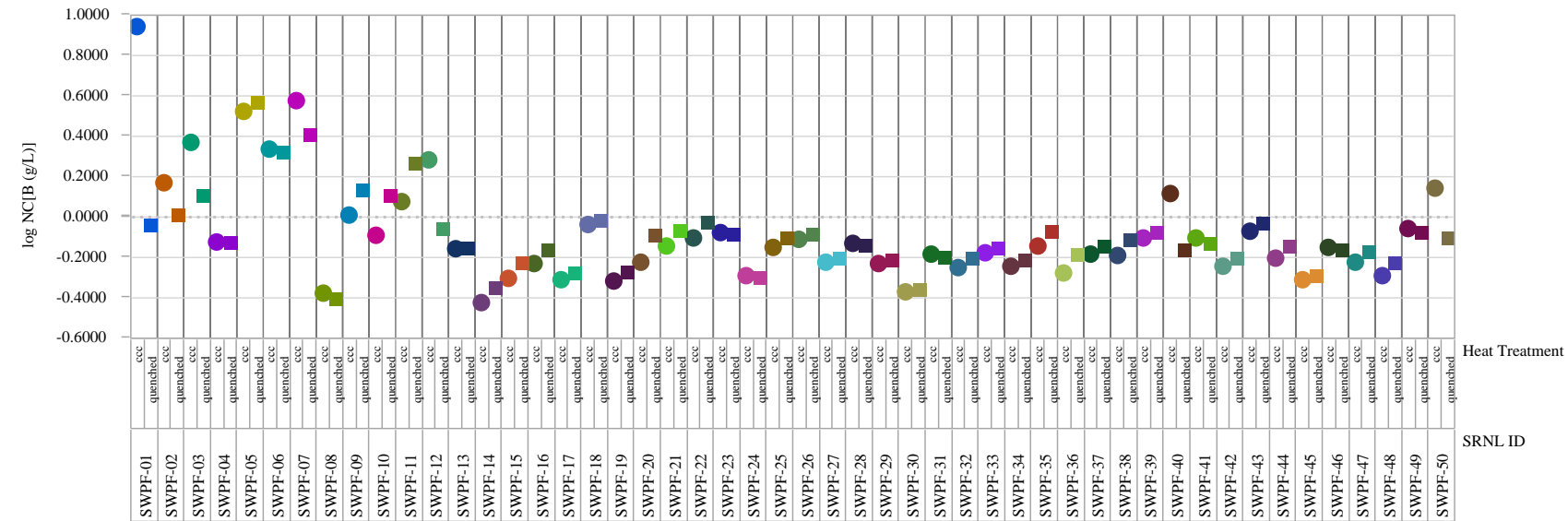


Exhibit B5. Normalized PCT Response by Glass ID and by Heat Treatment within Compositional View
 (continued)

Comp View=Measured bc
 Variability Chart for log NC[Li(g/L)]

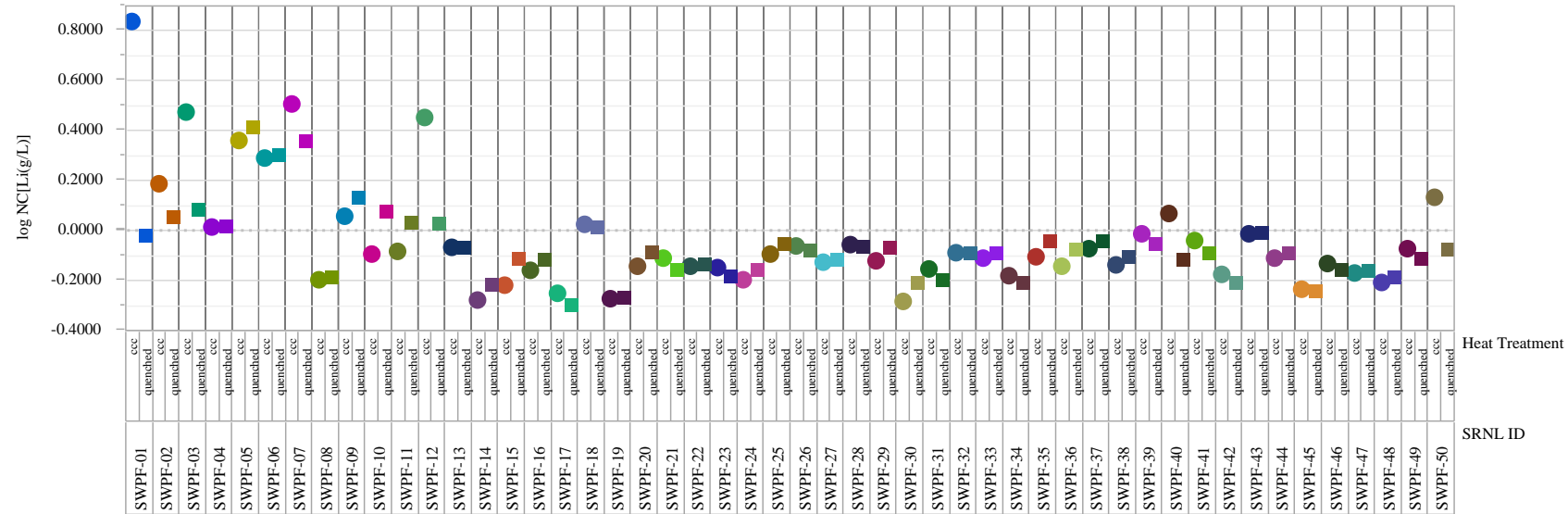


Exhibit B5. Normalized PCT Response by Glass ID and by Heat Treatment within Compositional View
 (continued)

Comp View=Measured bc
 Variability Chart for log NC[Na (g/L)]

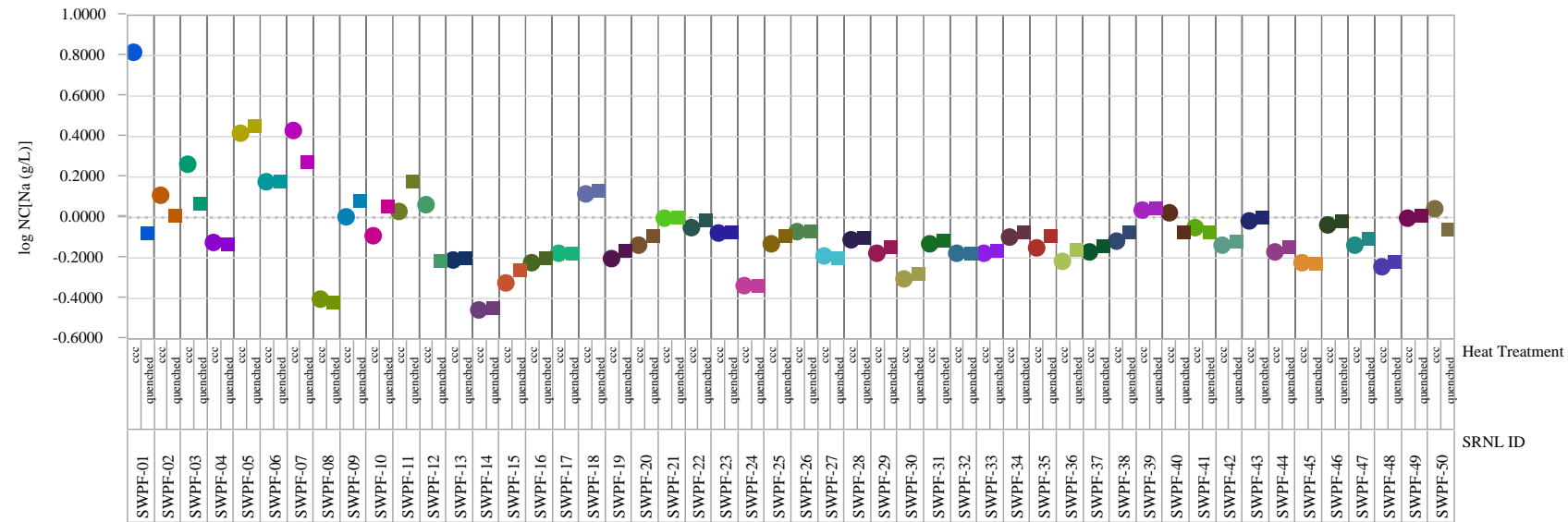


Exhibit B5. Normalized PCT Response by Glass ID and by Heat Treatment within Compositional View
 (continued)

Comp View=Measured bc
 Variability Chart for log NC[Si (g/L)]

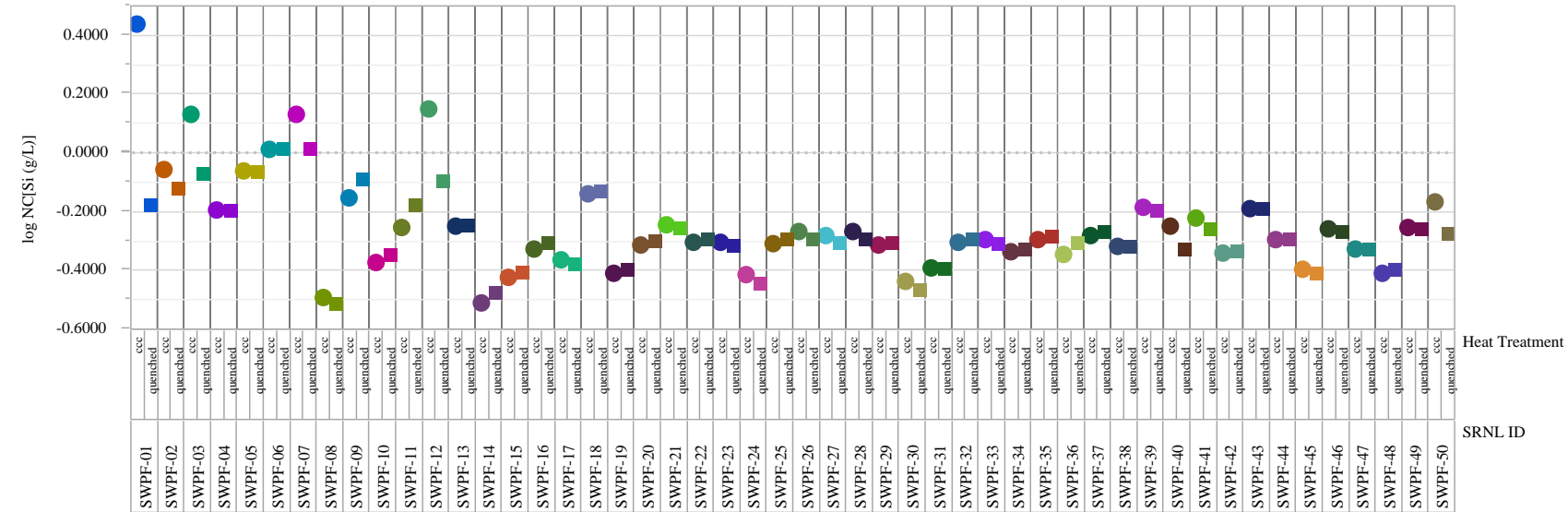


Exhibit B5. Normalized PCT Response by Glass ID and by Heat Treatment within Compositional View
(continued)

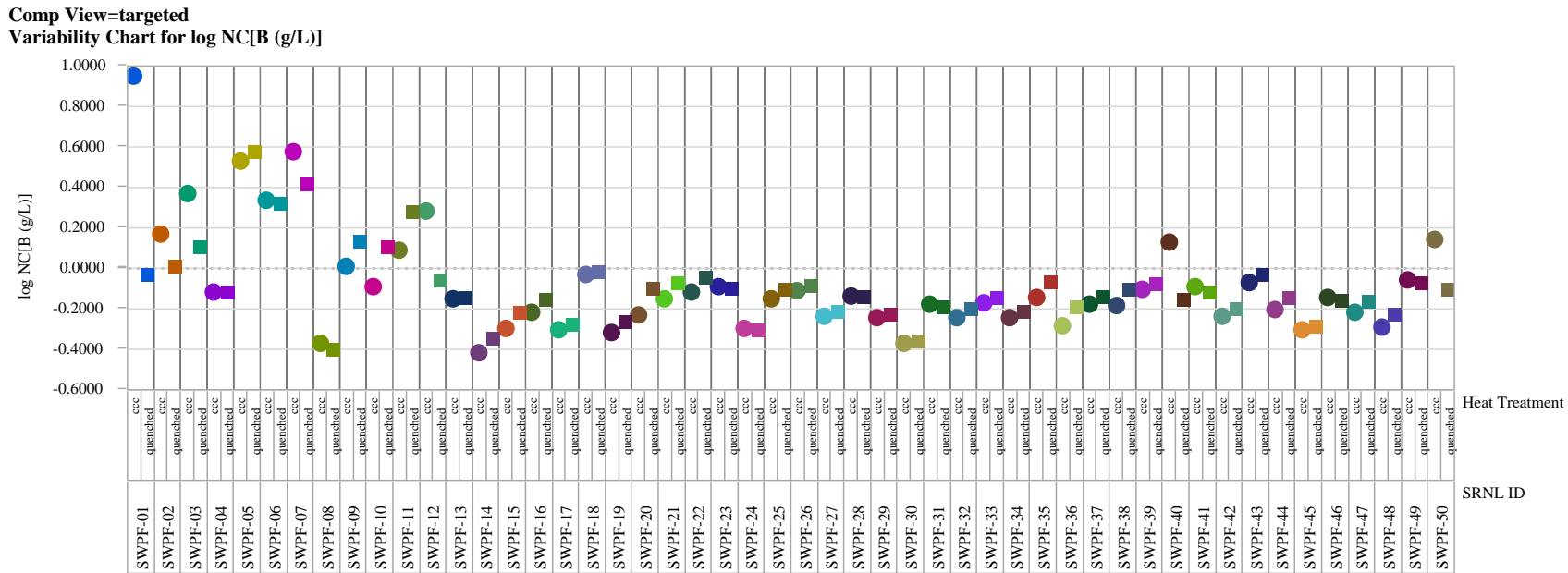


Exhibit B5. Normalized PCT Response by Glass ID and by Heat Treatment within Compositional View
(continued)

Comp View=targeted
Variability Chart for log NC[Li(g/L)]

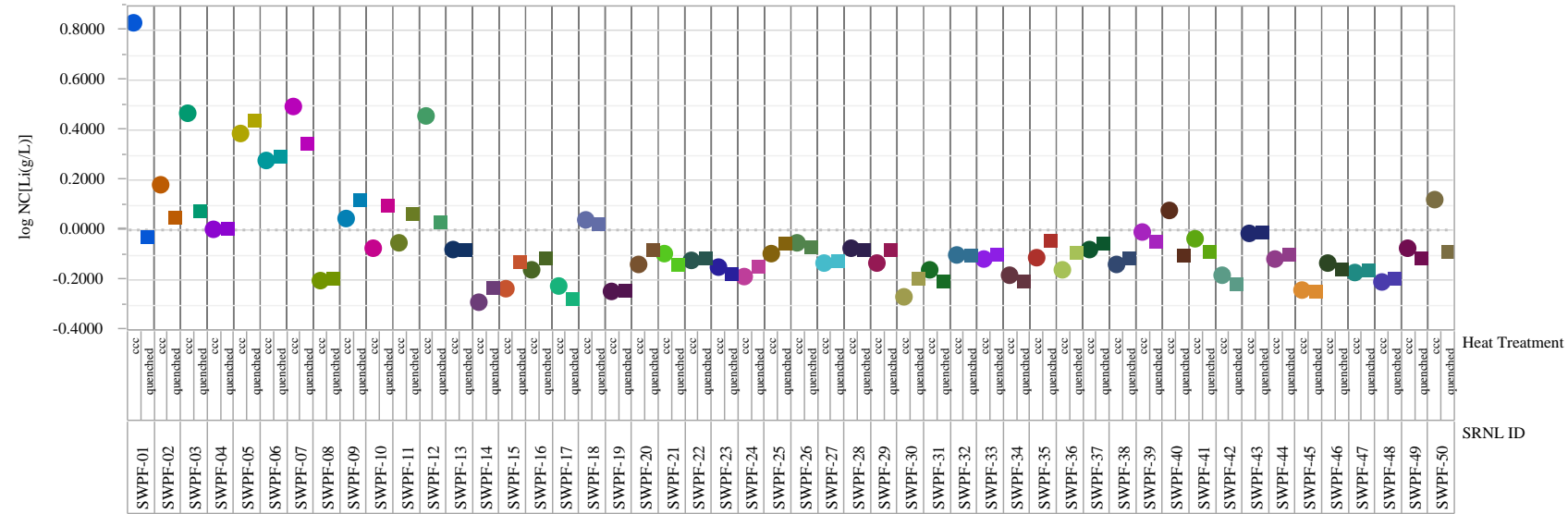


Exhibit B5. Normalized PCT Response by Glass ID and by Heat Treatment within Compositional View
(continued)

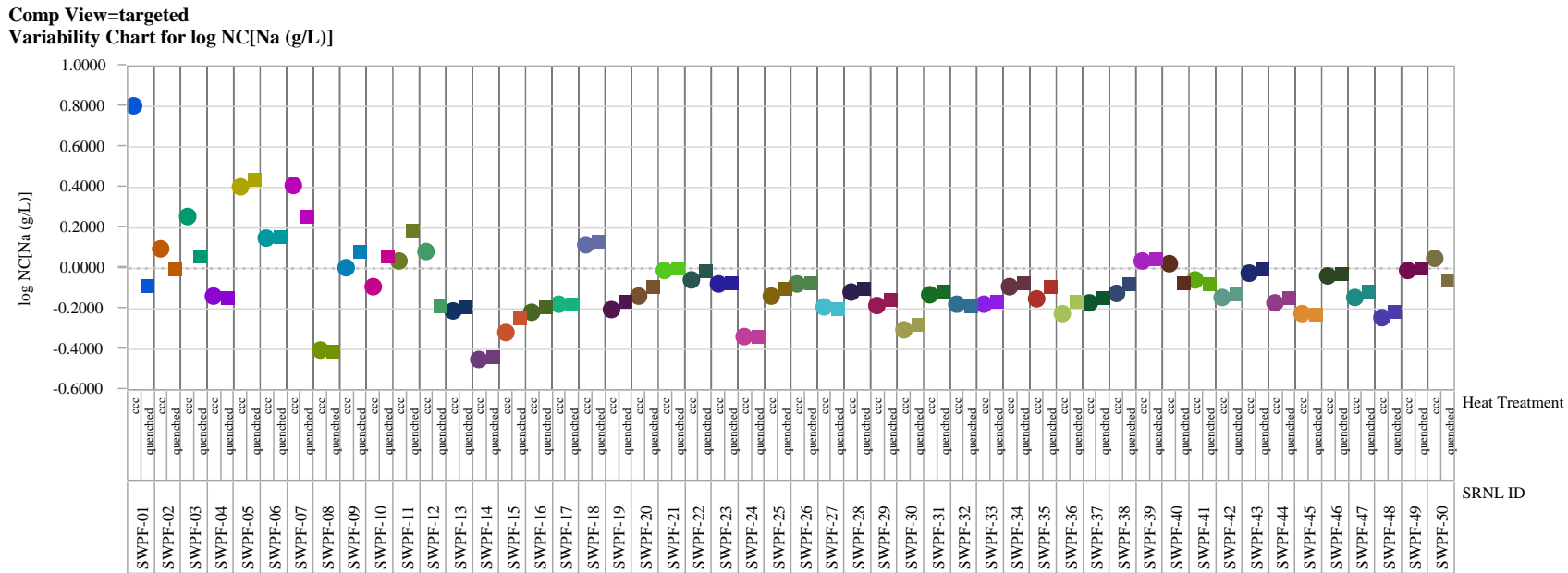


Exhibit B5. Normalized PCT Response by Glass ID and by Heat Treatment within Compositional View
(continued)

Comp View=targeted
Variability Chart for log NC[Si (g/L)]

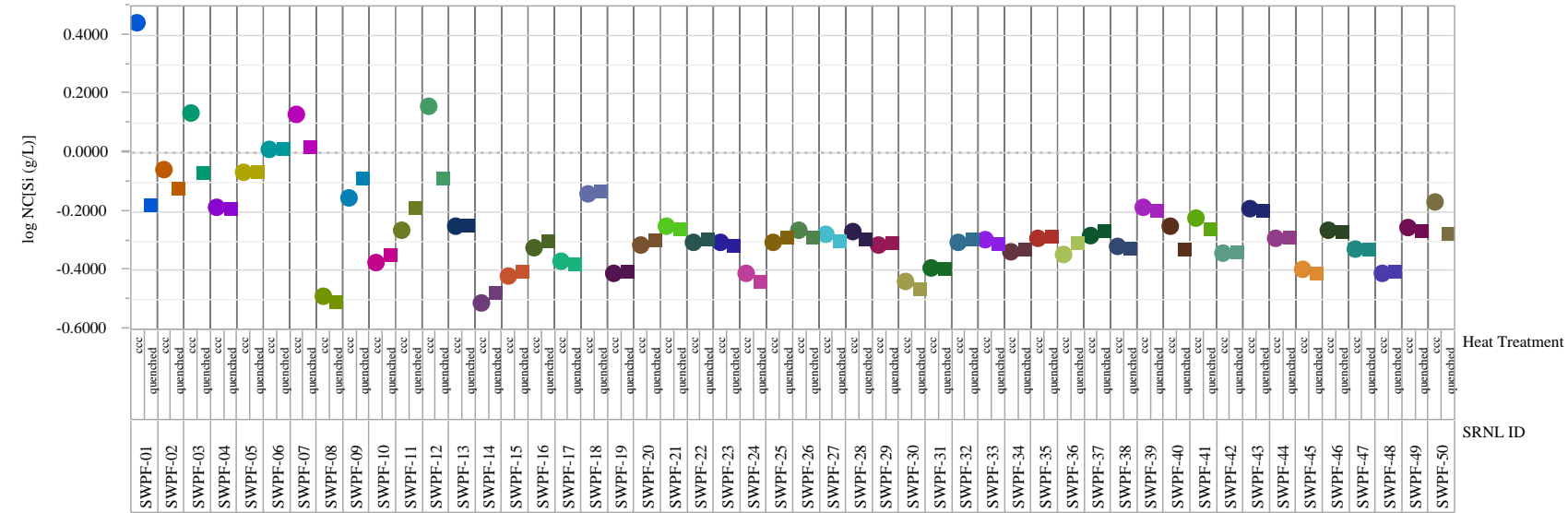
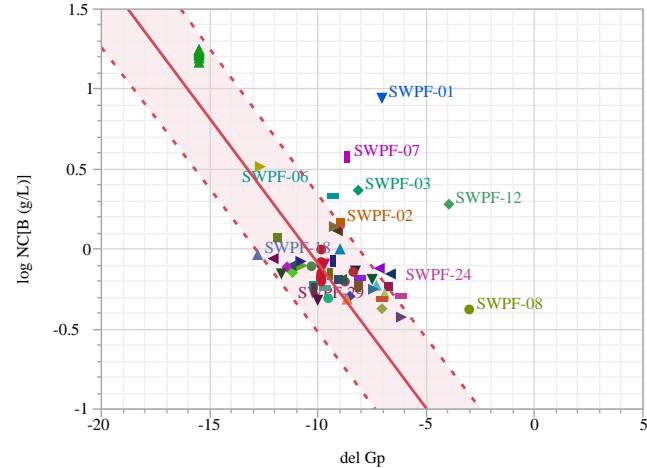
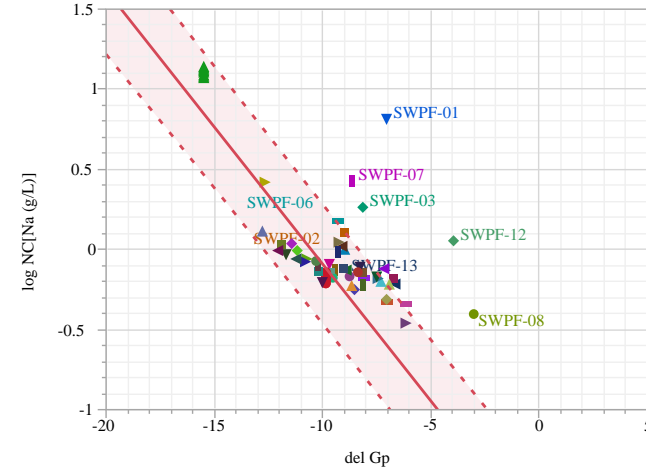


Exhibit B5. Normalized PCT Response by Glass ID and by Heat Treatment within Compositional View

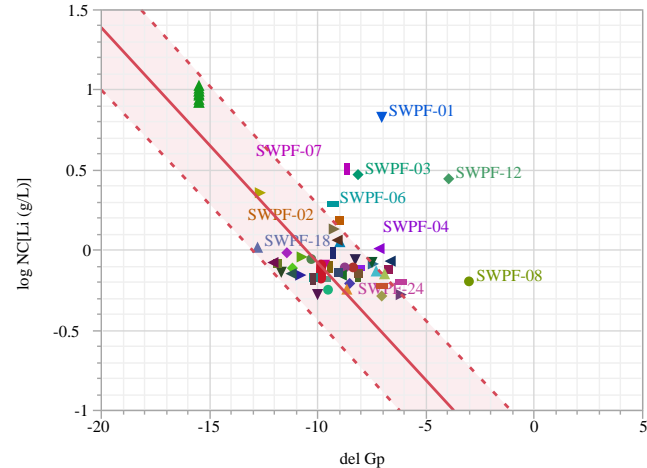
Bivariate Fit of log NC[B (g/L)] By del Gp Display=ccc/bias-corrected compositions



Bivariate Fit of log NC[Na (g/L)] By del Gp Display=ccc/bias-corrected compositions



Bivariate Fit of log NC[Li (g/L)] By del Gp Display=ccc/bias-corrected compositions



Bivariate Fit of log NC[Si (g/L)] By del Gp Display=ccc/bias-corrected compositions

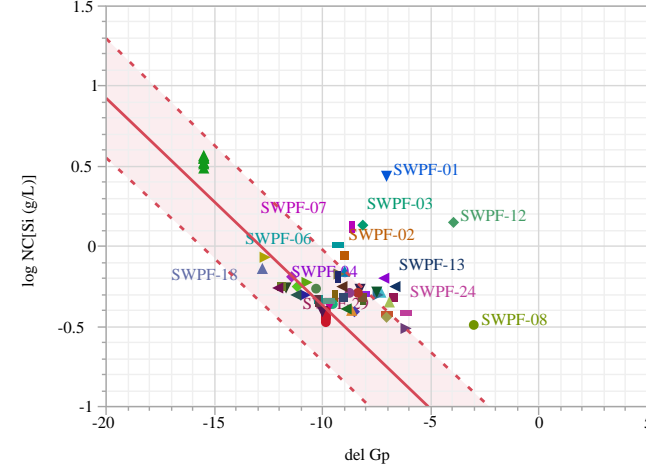
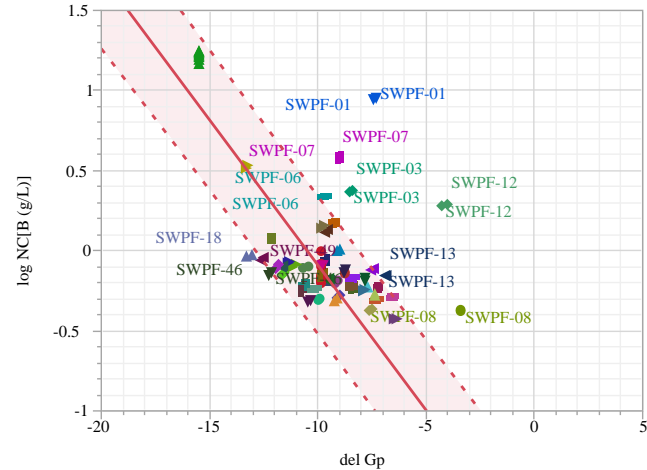
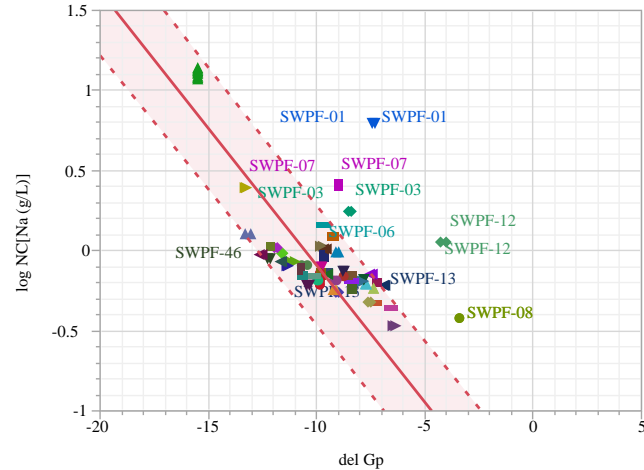


**Exhibit B5. Normalized PCT Response by Glass ID and by Heat Treatment within Compositional View
(continued)**

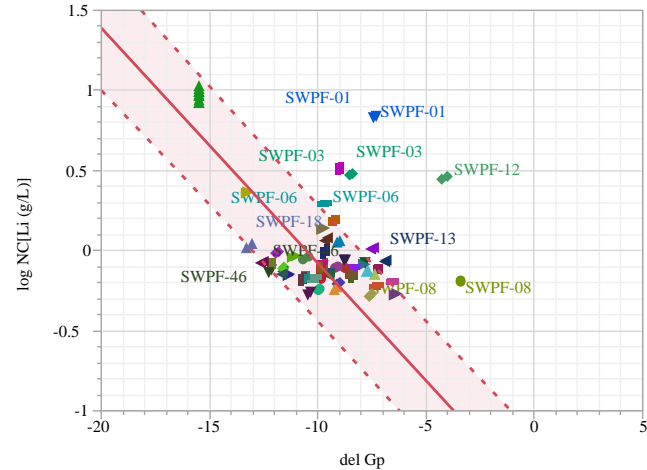
Bivariate Fit of log NC[B (g/L)] By del Gp Display=ccc/measured compositions



Bivariate Fit of log NC[Na (g/L)] By del Gp Display=ccc/measured compositions



Bivariate Fit of log NC[Li (g/L)] By del Gp Display=ccc/measured compositions



Bivariate Fit of log NC[Si (g/L)] By del Gp Display=ccc/measured compositions

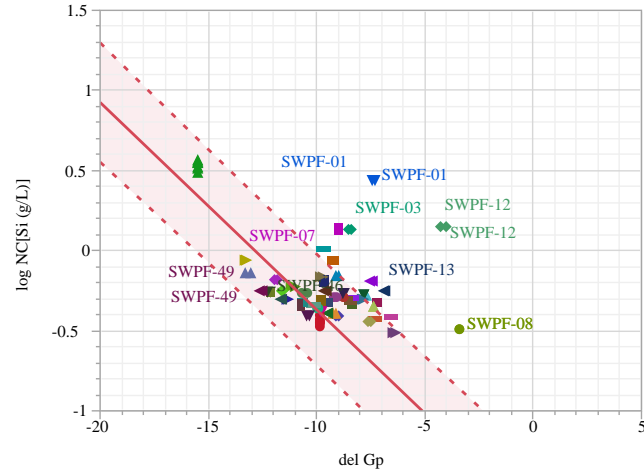
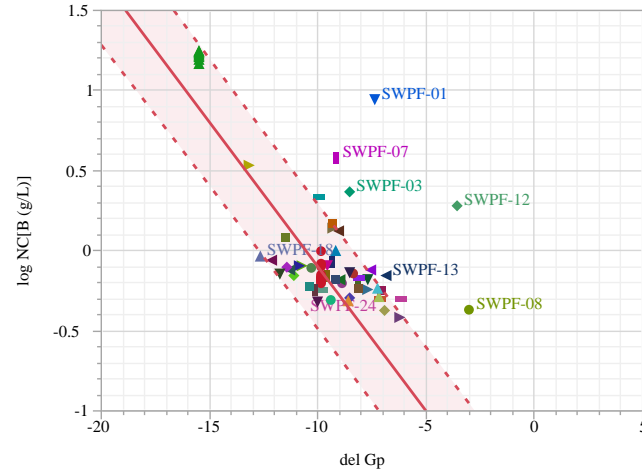
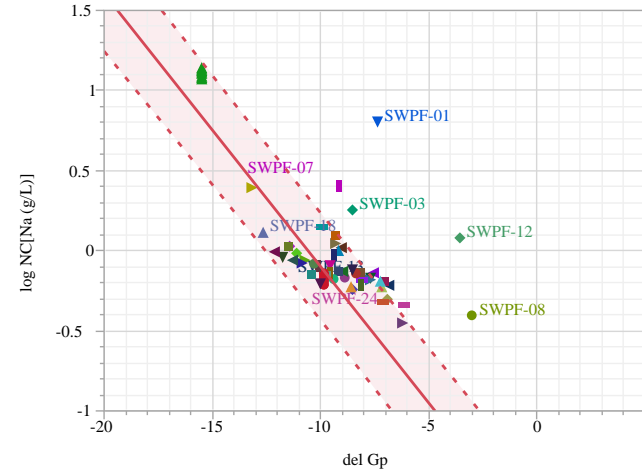


**Exhibit B5. Normalized PCT Response by Glass ID and by Heat Treatment within Compositional View
(continued)**

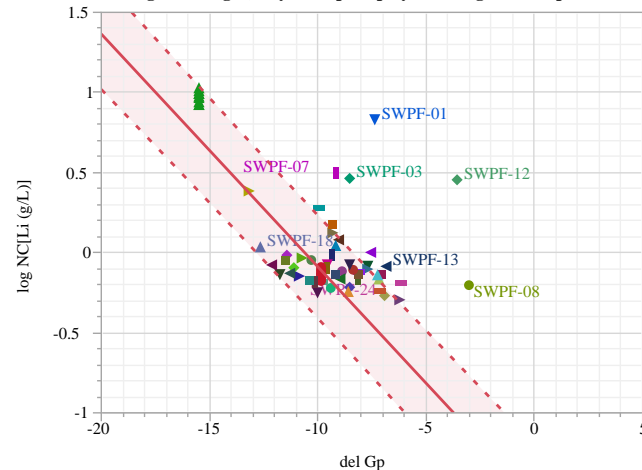
Bivariate Fit of log NC[B (g/L)] By del Gp Display=ccc/targeted compositions



Bivariate Fit of log NC[Na (g/L)] By del Gp Display=ccc/targeted compositions



Bivariate Fit of log NC[Li (g/L)] By del Gp Display=ccc/targeted compositions



Bivariate Fit of log NC[Si (g/L)] By del Gp Display=ccc/targeted compositions

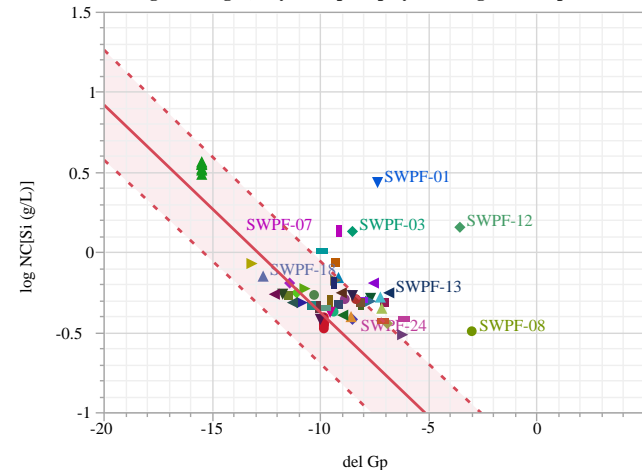
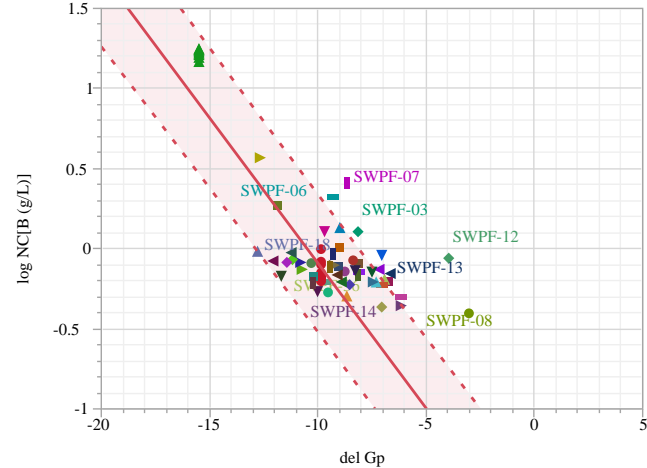
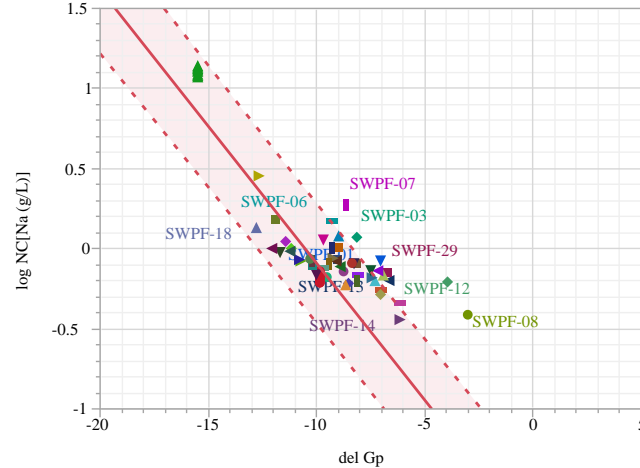


**Exhibit B5. Normalized PCT Response by Glass ID and by Heat Treatment within Compositional View
(continued)**

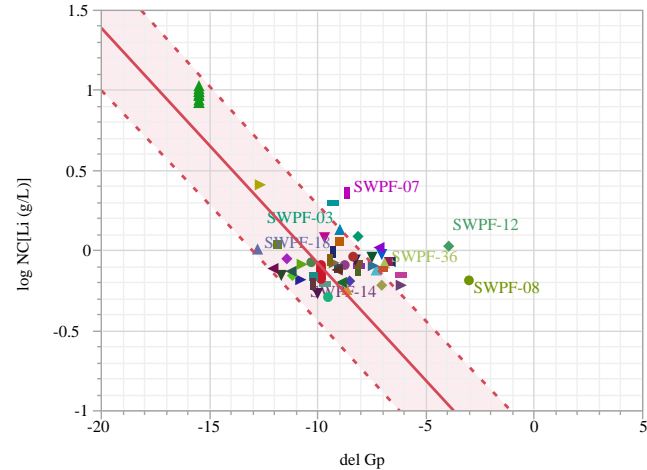
Bivariate Fit of log NC[B (g/L)] By del Gp Display=quenched/bias-corrected compositions



Bivariate Fit of log NC[Na (g/L)] By del Gp Display=quenched/bias-corrected compositions



Bivariate Fit of log NC[Li (g/L)] By del Gp Display=quenched/bias-corrected compositions



Bivariate Fit of log NC[Si (g/L)] By del Gp Display=quenched/bias-corrected compositions

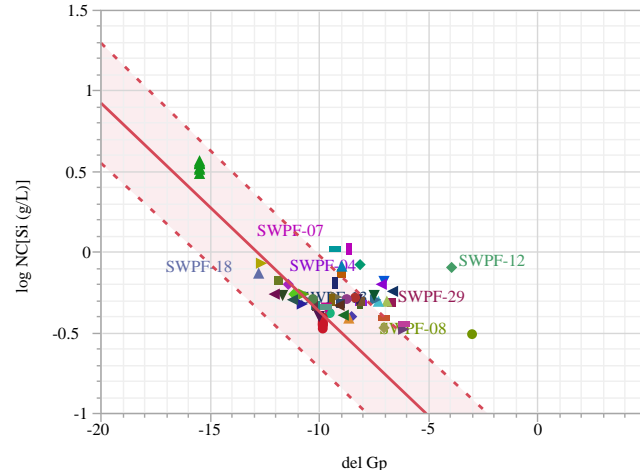
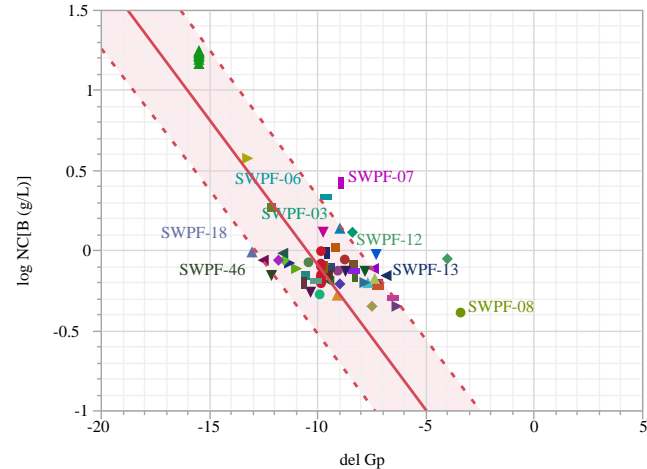
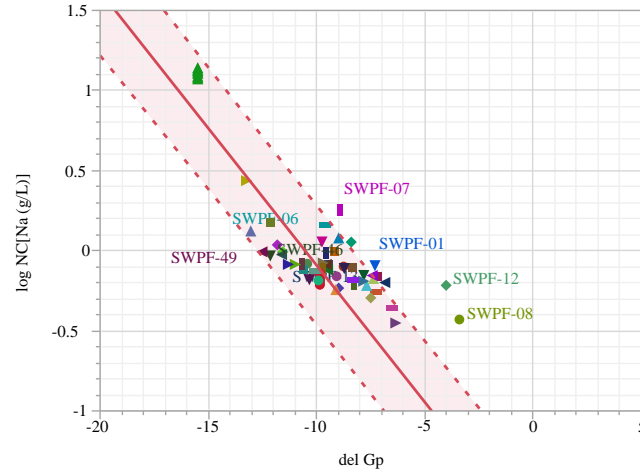


Exhibit B5. Normalized PCT Response by Glass ID and by Heat Treatment within Compositional View
 (continued)

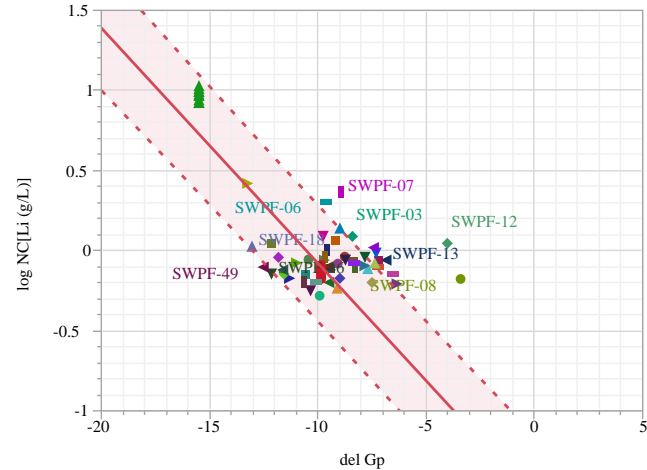
Bivariate Fit of log NC[B (g/L)] By del Gp Display=quenched/measured compositions



Bivariate Fit of log NC[Na (g/L)] By del Gp Display=quenched/measured compositions



Bivariate Fit of log NC[Li (g/L)] By del Gp Display=quenched/measured compositions



Bivariate Fit of log NC[Si (g/L)] By del Gp Display=quenched/measured compositions

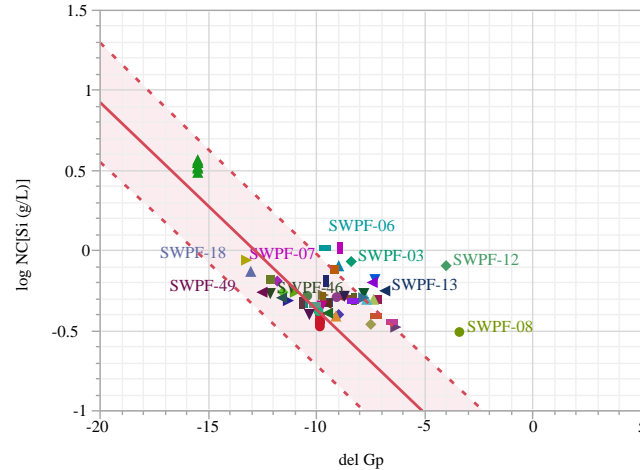
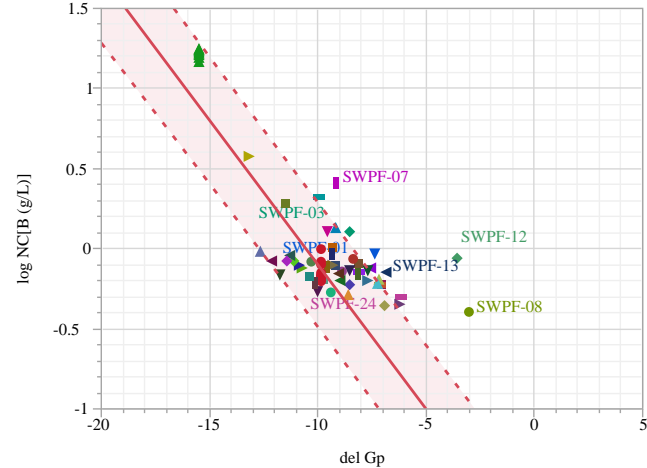
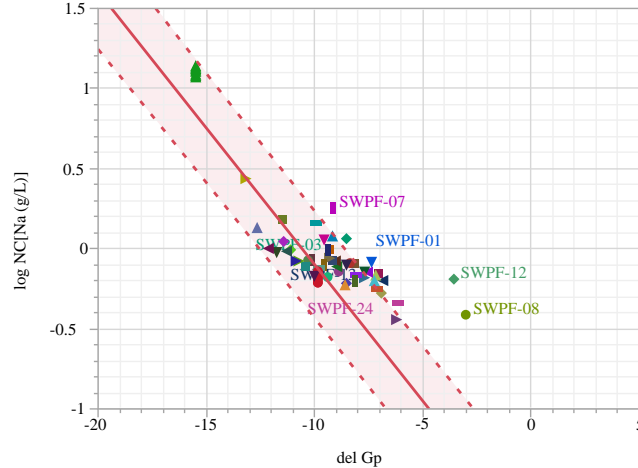


**Exhibit B5. Normalized PCT Response by Glass ID and by Heat Treatment within Compositional View
(continued)**

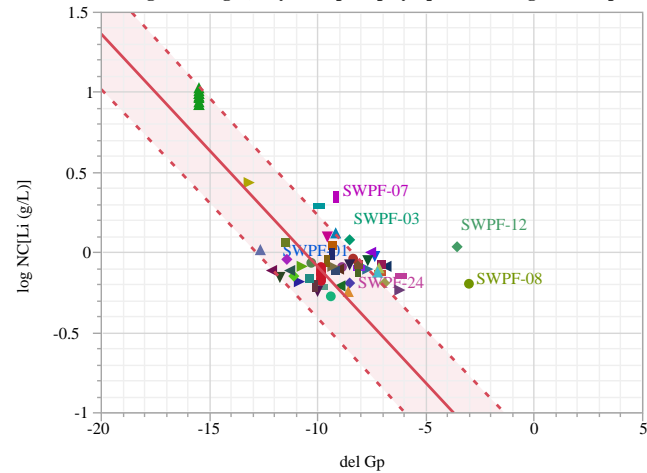
Bivariate Fit of log NC[B (g/L)] By del Gp Display=quenched/targeted compositions



Bivariate Fit of log NC[Na (g/L)] By del Gp Display=quenched/targeted compositions



Bivariate Fit of log NC[Li (g/L)] By del Gp Display=quenched/targeted compositions



Bivariate Fit of log NC[Si (g/L)] By del Gp Display=quenched/targeted compositions

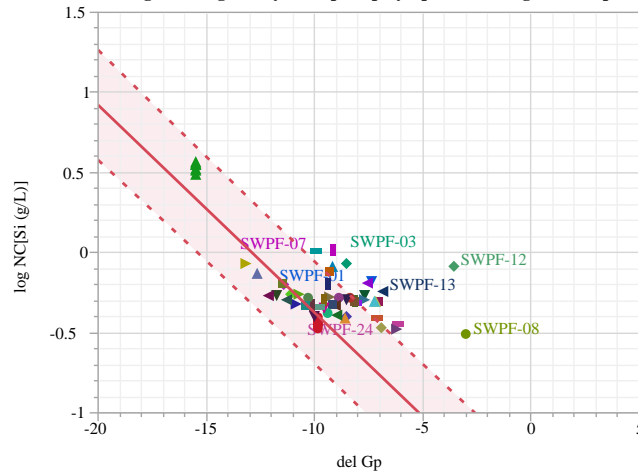


Exhibit B5. Normalized PCT Response by Glass ID and by Heat Treatment within Compositional View

APPENDIX C. THERMO™ Database (Measured Bias Corrected wt% on a vitrified oxide basis indicated by “v”).

| Sample ID | Measured Density (g/cc) | Measured pH | Mean(log(B (ppm))) | Mean(log(Li (ppm))) | Mean(log([Na (ppm)]) | Mean(log([Si (ppm)]) | FeII/FeIII | Al2O3(v) | B2O3(v) | BaO(v) | CaO(v) | Ce2O3(v) | Cr2O3(v) | Cs2O(v) | CuO(v) | Cu2O(v) | FeO(v) | Fe2O3(v) | K2O(v) | La2O3(v) | Li2O(v) | MgO(v) | MnO(v) | MnO2(v) | MoO3(v) | Na2O(v) | Nd2O3(v) | NiO(v) | P2O5(v) | PbO(v) | SiO2(v) | SrO(v) | TiO2(v) | Y2O3(v) | ZnO(v) | ZrO2(v) | ·Oxides(v) |
|-------------|-------------------------|-------------|--------------------|---------------------|----------------------|----------------------|------------|----------|---------|--------|--------|----------|----------|---------|--------|---------|--------|----------|--------|----------|---------|--------|--------|---------|---------|---------|----------|--------|---------|--------|---------|--------|---------|---------|--------|---------|------------|
| 165 CGW STD | 10.32 | 1.24 | 1.22 | 1.80 | 2.12 | 0.00 | 4.19 | 6.71 | 0.00 | 1.54 | 0.00 | 0.00 | 0.00 | 0.00 | 0.00 | 0.00 | 12.92 | 0.00 | 0.00 | 5.00 | 1.02 | 2.56 | 0.00 | 0.00 | 10.44 | 0.00 | 0.97 | 0.00 | 0.00 | 53.84 | 0.00 | 0.00 | 0.00 | 0.50 | 99.69 | | |
| 200R | 10.54 | 1.53 | 1.13 | 1.99 | 1.99 | 0.00 | 4.62 | 9.46 | 0.00 | 1.47 | 0.00 | 0.00 | 0.00 | 0.00 | 0.00 | 0.00 | 12.30 | 3.49 | 0.00 | 3.01 | 1.25 | 2.13 | 0.00 | 0.00 | 13.29 | 0.00 | 0.53 | 0.00 | 0.00 | 45.10 | 0.00 | 0.00 | 0.00 | 0.00 | 96.65 | | |
| 202G w/o Mn | 9.79 | 0.87 | 0.84 | 1.51 | 1.97 | 0.00 | 4.69 | 6.13 | 0.16 | 1.32 | 0.00 | 0.08 | 0.05 | 0.20 | 0.18 | 0.00 | 12.30 | 2.78 | 0.00 | 3.83 | 3.24 | 0.00 | 0.00 | 0.00 | 8.38 | 0.00 | 0.68 | 0.00 | 0.00 | 57.00 | 0.00 | 0.70 | 0.00 | 0.00 | 101.72 | | |
| 202P w/o Mn | 9.95 | 1.23 | 0.91 | 1.70 | 1.97 | 0.00 | 4.30 | 8.60 | 0.20 | 1.22 | 0.00 | 0.07 | 0.15 | 0.33 | 0.30 | 0.00 | 10.70 | 5.73 | 0.00 | 3.42 | 2.92 | 0.00 | 0.00 | 0.00 | 9.20 | 0.00 | 0.70 | 0.00 | 0.00 | 51.20 | 0.00 | 1.24 | 0.00 | 0.00 | 100.28 | | |
| AH 131AL | 2.58 | 10.21 | 1.38 | 1.12 | 1.86 | 1.89 | 0.02 | 13.50 | 10.80 | 0.00 | 0.38 | 0.00 | 0.00 | 0.00 | 0.00 | 0.00 | 0.09 | 4.57 | 0.00 | 0.36 | 4.09 | 1.38 | 2.51 | 0.00 | 0.00 | 14.10 | 0.00 | 0.63 | 0.00 | 0.00 | 46.40 | 0.00 | 0.72 | 0.00 | 0.00 | 99.87 | |
| AH 131AV | 2.69 | 9.85 | 1.20 | 1.16 | 1.65 | 2.00 | 0.07 | 4.39 | 7.60 | 0.00 | 0.76 | 0.00 | 0.00 | 0.00 | 0.00 | 0.00 | 0.70 | 11.13 | 0.00 | 0.00 | 4.25 | 0.67 | 2.59 | 0.00 | 0.00 | 9.86 | 0.00 | 1.04 | 0.00 | 0.00 | 55.00 | 0.00 | 0.06 | 0.00 | 0.00 | 98.93 | |
| AH 131FE | 2.77 | 10.22 | 1.91 | 1.78 | 2.39 | 2.57 | 1.29 | 2.25 | 7.33 | 0.00 | 1.01 | 0.00 | 0.00 | 0.00 | 0.00 | 0.00 | 8.81 | 7.61 | 0.00 | 0.00 | 4.06 | 0.66 | 0.93 | 0.00 | 0.00 | 10.90 | 0.00 | 2.56 | 0.00 | 0.00 | 51.40 | 0.00 | 0.01 | 0.00 | 0.00 | 98.40 | |
| AH 165AL | 2.57 | 9.92 | 1.06 | 1.09 | 1.45 | 1.85 | 0.06 | 13.40 | 7.34 | 0.00 | 0.51 | 0.00 | 0.00 | 0.00 | 0.00 | 0.00 | 0.24 | 4.57 | 0.00 | 0.00 | 4.20 | 0.66 | 2.62 | 0.00 | 0.00 | 10.60 | 0.00 | 0.67 | 0.00 | 0.00 | 53.60 | 0.00 | 0.00 | 0.00 | 0.00 | 99.20 | |
| AH 165AV | 2.69 | 10.05 | 1.12 | 1.19 | 1.62 | 1.98 | 0.05 | 5.17 | 6.57 | 0.00 | 1.04 | 0.00 | 0.00 | 0.00 | 0.00 | 0.00 | 0.47 | 11.08 | 0.00 | 0.00 | 5.02 | 0.66 | 2.57 | 0.00 | 0.00 | 9.96 | 0.00 | 1.01 | 0.00 | 0.00 | 55.30 | 0.00 | 0.00 | 0.00 | 0.00 | 99.61 | |
| AH 165FE | 2.80 | 10.53 | 2.03 | 1.87 | 2.52 | 2.61 | 0.87 | 1.42 | 7.28 | 0.00 | 1.40 | 0.00 | 0.00 | 0.00 | 0.00 | 0.00 | 7.14 | 9.07 | 0.00 | 0.00 | 4.05 | 0.65 | 1.07 | 0.00 | 0.00 | 10.70 | 0.00 | 2.97 | 0.00 | 0.00 | 52.00 | 0.00 | 0.00 | 0.00 | 0.00 | 98.60 | |
| AH 168AV | 2.655 | 9.72 | 1.42 | 1.17 | 1.65 | 1.92 | 0.06 | 5.58 | 10.60 | 0.00 | 0.68 | 0.00 | 0.00 | 0.00 | 0.00 | 0.00 | 0.61 | 10.51 | 0.00 | 0.00 | 4.24 | 0.74 | 2.64 | 0.00 | 0.00 | 10.10 | 0.00 | 1.02 | 0.00 | 0.00 | 51.60 | 0.00 | 0.00 | 0.00 | 0.00 | 99.01 | |
| AH 168FE | 2.73 | 10.11 | 2.26 | 1.93 | 2.49 | 2.45 | 0.74 | 2.47 | 11.40 | 0.00 | 1.35 | 0.00 | 0.00 | 0.00 | 0.00 | 0.00 | 6.22 | 9.39 | 0.00 | 0.00 | 4.12 | 0.71 | 0.98 | 0.00 | 0.00 | 10.80 | 0.00 | 2.82 | 0.00 | 0.00 | 48.30 | 0.00 | 0.00 | 0.00 | 0.00 | 99.23 | |
| AH 200AL | 2.542 | 9.68 | 1.16 | 0.84 | 1.54 | 1.75 | 0.02 | 13.40 | 10.20 | 0.00 | 0.54 | 0.00 | 0.00 | 0.00 | 0.00 | 0.00 | 0.07 | 4.39 | 3.12 | 0.00 | 2.65 | 1.25 | 2.49 | 0.00 | 0.00 | 10.60 | 0.00 | 0.61 | 0.00 | 0.00 | 48.40 | 0.00 | 1.70 | 0.00 | 0.00 | 99.45 | |
| AH 200AV | 2.651 | 9.62 | 1.27 | 0.89 | 1.63 | 1.81 | 0.04 | 5.14 | 10.30 | 0.00 | 0.63 | 0.00 | 0.00 | 0.00 | 0.00 | 0.00 | 0.39 | 11.47 | 3.18 | 0.00 | 2.68 | 1.24 | 2.55 | 0.00 | 0.00 | 9.77 | 0.00 | 1.02 | 0.00 | 0.00 | 49.50 | 0.00 | 1.41 | 0.00 | 0.00 | 99.30 | |
| AH 200FE | 2.784 | 10.15 | 2.20 | 1.72 | 2.54 | 2.44 | 0.67 | 2.07 | 10.10 | 0.00 | 0.92 | 0.00 | 0.00 | 0.00 | 0.00 | 0.00 | 5.94 | 9.80 | 3.15 | 0.00 | 2.59 | 1.21 | 0.95 | 0.00 | 0.00 | 10.60 | 0.00 | 2.57 | 0.00 | 0.00 | 47.40 | 0.00 | 1.78 | 0.00 | 0.00 | 99.10 | |
| AH 202AL | 2.520 | 9.69 | 0.91 | 0.97 | 1.20 | 1.76 | 0.02 | 13.90 | 7.42 | 0.00 | 0.41 | 0.00 | 0.00 | 0.00 | 0.00 | 0.00 | 0.08 | 4.31 | 3.32 | 0.00 | 4.18 | 1.28 | 2.51 | 0.00 | 0.00 | 7.34 | 0.00 | 0.62 | 0.00 | 0.00 | 52.40 | 0.00 | 1.71 | 0.00 | 0.00 | 99.51 | |
| AH 202AV | 2.64 | 9.68 | 1.08 | 1.07 | 1.40 | 1.92 | 0.03 | 4.96 | 7.44 | 0.00 | 0.72 | 0.00 | 0.00 | 0.00 | 0.00 | 0.00 | 0.31 | 11.56 | 3.33 | 0.00 | 4.27 | 1.30 | 2.59 | 0.00 | 0.00 | 6.55 | 0.00 | 1.00 | 0.00 | 0.00 | 54.10 | 0.00 | 1.37 | 0.00 | 0.00 | 99.53 | |
| AH 202FE | 2.74 | 10.12 | 1.84 | 1.70 | 2.18 | 2.43 | 0.73 | 1.36 | 7.08 | 0.00 | 0.96 | 0.00 | 0.00 | 0.00 | 0.00 | 0.00 | 6.28 | 9.62 | 3.28 | 0.00 | 4.27 | 1.26 | 0.95 | 0.00 | 0.00 | 7.62 | 0.00 | 2.73 | 0.00 | 0.00 | 52.55 | 0.00 | 1.72 | 0.00 | 0.00 | 99.70 | |
| AH-1 | | 10.61 | 1.27 | 1.17 | 1.81 | 1.96 | 0.00 | 6.98 | 10.30 | 0.00 | 0.96 | 0.00 | 0.03 | 0.07 | 0.00 | 0.00 | 0.00 | 12.00 | 3.31 | 0.00 | 4.47 | 0.66 | 2.31 | 0.00 | 0.00 | 11.90 | 0.00 | 0.94 | 0.00 | 0.00 | 44.08 | 0.04 | 1.33 | 0.00 | 0.00 | 99.03 | |
| AH-10 | | 10.07 | 1.01 | 1.03 | 1.33 | 1.89 | 0.00 | 5.14 | 7.59 | 0.00 | 0.68 | 0.00 | 0.01 | 0.06 | 0.00 | 0.00 | 0.00 | 11.30 | 3.09 | 0.00 | 4.44 | 1.11 | 2.67 | 0.00 | 0.00 | 6.83 | 0.00 | 0.96 | 0.00 | 0.00 | 54.20 | 0.05 | 1.30 | 0.00 | 0.00 | 99.44 | |
| AH-11 | | 9.80 | 1.25 | 0.98 | 1.34 | 1.80 | 0.00 | 5.70 | 12.00 | 0.00 | 0.65 | 0.00 | 0.01 | 0.06 | 0.00 | 0.00 | 0.00 | 11.00 | 2.99 | 0.00 | 3.62 | 1.11 | 2.63 | 0.00 | 0.00 | 6.42 | 0.00 | 0.93 | 0.00 | 0.00 | 50.40 | 0.04 | 1.29 | 0.00 | 0.00 | 98.86 | |
| AH-12 | | 10.12 | 1.37 | 1.00 | 1.70 | 1.66 | 0.00 | 6.04 | 8.75 | 0.00 | 0.69 | 0.00 | 0.00 | 0.06 | 0.00 | 0.00 | 0.00 | 11.60 | 3.13 | 0.00 | 3.47 | 0.58 | 2.64 | 0.00 | 0.00 | 9.20 | 0.00 | 0.97 | 0.00 | 0.00 | 50.90 | 0.05 | 1.33 | 0.00 | 0.00 | 99.42 | |

| Sample ID | Measured Density (g/cc) | | Chemical Compositions (ppm) by Element | | | | | | | | | | | | | | | | | | | | | | | | | | Oxides (%) | | | | | | | | | | | | |
|-------------------|-------------------------|-------------|--|--|------|---|------|--|-------|---|------------|----------|---------|--------|--------|----------|----------|---------|--------|---------|--------|----------|--------|----------|---------|--------|--------|---------|------------|---------|----------|--------|---------|--------|---------|--------|---------|---------|--------|---------|------------|
| | Mean | Measured pH | Mean | Mean <log[b(ppm)])< th=""><th>Mean</th><th>Mean<log[li(ppm)])< th=""><th>Mean</th><th>Mean<log[na(ppm)])< th=""><th>Mean</th><th>Mean<log[si(ppm)])< th=""><th>FeII/FeIII</th><th>Al2O3(v)</th><th>B2O3(v)</th><th>BaO(v)</th><th>CaO(v)</th><th>Ce2O3(v)</th><th>Cr2O3(v)</th><th>Cs2O(v)</th><th>CuO(v)</th><th>Eu2O(v)</th><th>FeO(v)</th><th>Fe2O3(v)</th><th>K2O(v)</th><th>La2O3(v)</th><th>Li2O(v)</th><th>MgO(v)</th><th>MnO(v)</th><th>MnO2(v)</th><th>MoO3(v)</th><th>Na2O(v)</th><th>Nd2O3(v)</th><th>NiO(v)</th><th>P2O5(v)</th><th>PhO(v)</th><th>SiO2(v)</th><th>SrO(v)</th><th>TiO2(v)</th><th>Y2O3(v)</th><th>ZnO(v)</th><th>ZrO2(v)</th><th>*Oxides(v)</th></log[si(ppm)])<></th></log[na(ppm)])<></th></log[li(ppm)])<></th></log[b(ppm)])<> | Mean | Mean <log[li(ppm)])< th=""><th>Mean</th><th>Mean<log[na(ppm)])< th=""><th>Mean</th><th>Mean<log[si(ppm)])< th=""><th>FeII/FeIII</th><th>Al2O3(v)</th><th>B2O3(v)</th><th>BaO(v)</th><th>CaO(v)</th><th>Ce2O3(v)</th><th>Cr2O3(v)</th><th>Cs2O(v)</th><th>CuO(v)</th><th>Eu2O(v)</th><th>FeO(v)</th><th>Fe2O3(v)</th><th>K2O(v)</th><th>La2O3(v)</th><th>Li2O(v)</th><th>MgO(v)</th><th>MnO(v)</th><th>MnO2(v)</th><th>MoO3(v)</th><th>Na2O(v)</th><th>Nd2O3(v)</th><th>NiO(v)</th><th>P2O5(v)</th><th>PhO(v)</th><th>SiO2(v)</th><th>SrO(v)</th><th>TiO2(v)</th><th>Y2O3(v)</th><th>ZnO(v)</th><th>ZrO2(v)</th><th>*Oxides(v)</th></log[si(ppm)])<></th></log[na(ppm)])<></th></log[li(ppm)])<> | Mean | Mean <log[na(ppm)])< th=""><th>Mean</th><th>Mean<log[si(ppm)])< th=""><th>FeII/FeIII</th><th>Al2O3(v)</th><th>B2O3(v)</th><th>BaO(v)</th><th>CaO(v)</th><th>Ce2O3(v)</th><th>Cr2O3(v)</th><th>Cs2O(v)</th><th>CuO(v)</th><th>Eu2O(v)</th><th>FeO(v)</th><th>Fe2O3(v)</th><th>K2O(v)</th><th>La2O3(v)</th><th>Li2O(v)</th><th>MgO(v)</th><th>MnO(v)</th><th>MnO2(v)</th><th>MoO3(v)</th><th>Na2O(v)</th><th>Nd2O3(v)</th><th>NiO(v)</th><th>P2O5(v)</th><th>PhO(v)</th><th>SiO2(v)</th><th>SrO(v)</th><th>TiO2(v)</th><th>Y2O3(v)</th><th>ZnO(v)</th><th>ZrO2(v)</th><th>*Oxides(v)</th></log[si(ppm)])<></th></log[na(ppm)])<> | Mean | Mean <log[si(ppm)])< th=""><th>FeII/FeIII</th><th>Al2O3(v)</th><th>B2O3(v)</th><th>BaO(v)</th><th>CaO(v)</th><th>Ce2O3(v)</th><th>Cr2O3(v)</th><th>Cs2O(v)</th><th>CuO(v)</th><th>Eu2O(v)</th><th>FeO(v)</th><th>Fe2O3(v)</th><th>K2O(v)</th><th>La2O3(v)</th><th>Li2O(v)</th><th>MgO(v)</th><th>MnO(v)</th><th>MnO2(v)</th><th>MoO3(v)</th><th>Na2O(v)</th><th>Nd2O3(v)</th><th>NiO(v)</th><th>P2O5(v)</th><th>PhO(v)</th><th>SiO2(v)</th><th>SrO(v)</th><th>TiO2(v)</th><th>Y2O3(v)</th><th>ZnO(v)</th><th>ZrO2(v)</th><th>*Oxides(v)</th></log[si(ppm)])<> | FeII/FeIII | Al2O3(v) | B2O3(v) | BaO(v) | CaO(v) | Ce2O3(v) | Cr2O3(v) | Cs2O(v) | CuO(v) | Eu2O(v) | FeO(v) | Fe2O3(v) | K2O(v) | La2O3(v) | Li2O(v) | MgO(v) | MnO(v) | MnO2(v) | MoO3(v) | Na2O(v) | Nd2O3(v) | NiO(v) | P2O5(v) | PhO(v) | SiO2(v) | SrO(v) | TiO2(v) | Y2O3(v) | ZnO(v) | ZrO2(v) | *Oxides(v) |
| AH-13 | 10.33 | 0.93 | 0.90 | 1.49 | 1.83 | 0.00 | 6.48 | 6.41 | 0.00 | 1.25 | 0.00 | 0.01 | 0.05 | 0.00 | 0.00 | 0.00 | 0.00 | 0.00 | 0.00 | 0.00 | 13.60 | 3.06 | 0.00 | 3.32 | 0.49 | 3.25 | 0.00 | 0.00 | 8.80 | 0.00 | 1.14 | 0.00 | 0.00 | 49.00 | 0.05 | 1.29 | 0.00 | 0.00 | 0.03 | 98.23 | |
| AH-15 | 10.18 | 1.09 | 0.79 | 1.50 | 1.72 | 0.00 | 6.87 | 9.20 | 0.00 | 1.27 | 0.00 | 0.01 | 0.05 | 0.00 | 0.00 | 0.00 | 0.00 | 0.00 | 0.00 | 0.00 | 13.60 | 3.10 | 0.00 | 2.80 | 1.02 | 3.26 | 0.00 | 0.00 | 9.41 | 0.00 | 1.13 | 0.00 | 0.00 | 45.60 | 0.06 | 1.34 | 0.00 | 0.00 | 0.01 | 98.73 | |
| AH-16 | 10.12 | 0.98 | 0.96 | 1.33 | 1.82 | 0.00 | 6.36 | 7.20 | 0.00 | 1.26 | 0.00 | 0.08 | 0.03 | 0.00 | 0.00 | 0.00 | 0.00 | 0.00 | 0.00 | 0.00 | 13.40 | 3.06 | 0.00 | 4.06 | 1.00 | 3.22 | 0.00 | 0.00 | 6.54 | 0.00 | 1.10 | 0.00 | 0.00 | 50.20 | 0.07 | 1.30 | 0.00 | 0.00 | 0.01 | 98.89 | |
| AH-17 | 10.09 | 0.96 | 0.99 | 1.26 | 1.85 | 0.00 | 5.72 | 8.12 | 0.00 | 0.65 | 0.00 | 0.09 | 0.06 | 0.00 | 0.00 | 0.00 | 0.00 | 0.00 | 0.00 | 0.00 | 11.40 | 3.06 | 0.00 | 4.69 | 0.58 | 2.71 | 0.00 | 0.00 | 6.61 | 0.00 | 0.92 | 0.00 | 0.00 | 52.50 | 0.03 | 1.30 | 0.00 | 0.00 | 0.66 | 99.10 | |
| AH-2 | 9.95 | 1.59 | 1.22 | 1.82 | 1.69 | 0.00 | 6.55 | 13.30 | 0.00 | 0.64 | 0.00 | 0.02 | 0.05 | 0.00 | 0.00 | 0.00 | 0.00 | 0.00 | 0.00 | 0.00 | 11.40 | 3.11 | 0.00 | 3.76 | 0.58 | 2.67 | 0.00 | 0.00 | 10.30 | 0.00 | 0.93 | 0.00 | 0.00 | 44.55 | 0.04 | 1.30 | 0.00 | 0.00 | 0.63 | 99.83 | |
| AH-4 | 10.43 | 1.07 | 1.07 | 1.66 | 1.97 | 0.00 | 4.69 | 7.06 | 0.00 | 1.00 | 0.00 | 0.05 | 0.06 | 0.00 | 0.00 | 0.00 | 0.00 | 0.00 | 0.00 | 0.00 | 11.00 | 3.16 | 0.00 | 4.10 | 0.73 | 2.12 | 0.00 | 0.00 | 9.89 | 0.00 | 0.97 | 0.00 | 0.00 | 53.48 | 0.05 | 1.30 | 0.00 | 0.00 | 0.01 | 99.67 | |
| AH-5 | 10.35 | 0.96 | 0.96 | 1.52 | 1.87 | 0.00 | 5.48 | 6.95 | 0.00 | 0.66 | 0.00 | 0.00 | 0.00 | 0.00 | 0.00 | 0.00 | 0.00 | 0.00 | 0.00 | 0.00 | 11.40 | 3.16 | 0.00 | 3.77 | 0.60 | 2.64 | 0.00 | 0.00 | 9.24 | 0.00 | 0.96 | 0.00 | 0.00 | 53.08 | 0.00 | 1.31 | 0.00 | 0.00 | 0.01 | 99.26 | |
| AH-6 | 10.61 | 1.30 | 1.19 | 1.74 | 1.93 | 0.00 | 5.56 | 9.33 | 0.00 | 0.68 | 0.00 | 0.00 | 0.06 | 0.00 | 0.00 | 0.00 | 0.00 | 0.00 | 0.00 | 0.00 | 11.80 | 3.14 | 0.00 | 4.59 | 0.60 | 2.72 | 0.00 | 0.00 | 10.50 | 0.00 | 0.94 | 0.00 | 0.00 | 47.30 | 0.04 | 1.40 | 0.00 | 0.00 | 0.67 | 99.33 | |
| AH-7 | 9.97 | 1.19 | 0.85 | 1.49 | 1.75 | 0.00 | 6.27 | 11.50 | 0.00 | 0.64 | 0.00 | 0.00 | 0.00 | 0.00 | 0.00 | 0.00 | 0.00 | 0.00 | 0.00 | 0.00 | 11.30 | 3.15 | 0.00 | 3.15 | 0.59 | 2.62 | 0.00 | 0.00 | 9.24 | 0.00 | 0.95 | 0.00 | 0.00 | 49.00 | 0.00 | 1.29 | 0.00 | 0.00 | 0.02 | 99.72 | |
| AH-8 | 10.06 | 1.20 | 0.91 | 1.55 | 1.83 | 0.00 | 5.88 | 10.10 | 0.00 | 0.69 | 0.00 | 0.02 | 0.04 | 0.00 | 0.00 | 0.00 | 0.00 | 0.00 | 0.00 | 0.00 | 11.60 | 3.08 | 0.00 | 3.17 | 1.20 | 2.68 | 0.00 | 0.00 | 9.76 | 0.00 | 0.97 | 0.00 | 0.00 | 49.00 | 0.05 | 1.32 | 0.00 | 0.00 | 0.01 | 99.57 | |
| AH-9 | 10.19 | 1.08 | 0.92 | 1.50 | 1.83 | 0.00 | 6.04 | 8.75 | 0.00 | 0.69 | 0.00 | 0.01 | 0.06 | 0.00 | 0.00 | 0.00 | 0.00 | 0.00 | 0.00 | 0.00 | 11.60 | 3.13 | 0.00 | 3.47 | 0.58 | 2.64 | 0.00 | 0.00 | 9.20 | 0.00 | 0.97 | 0.00 | 0.00 | 50.88 | 0.05 | 1.33 | 0.00 | 0.00 | 0.01 | 99.41 | |
| ARM-I | 2.75 | 10.33 | 1.25 | 1.15 | 1.58 | 1.79 | 0.00 | 5.59 | 11.30 | 0.66 | 2.23 | 1.44 | 0.00 | 1.16 | 0.00 | 0.00 | 0.00 | 0.00 | 0.00 | 0.00 | 5.08 | 0.00 | 0.00 | 0.00 | 0.00 | 1.67 | 9.67 | 5.96 | 0.00 | 0.65 | 0.00 | 46.50 | 0.45 | 3.21 | 0.00 | 1.46 | 1.80 | 98.83 | | | |
| ARM-I | 2.75 | 10.16 | 1.19 | 1.07 | 1.51 | 1.75 | 0.00 | 5.59 | 11.30 | 0.66 | 2.23 | 1.44 | 0.00 | 1.16 | 0.00 | 0.00 | 0.00 | 0.00 | 0.00 | 0.00 | 5.08 | 0.00 | 0.00 | 0.00 | 0.00 | 1.67 | 9.67 | 5.96 | 0.00 | 0.65 | 0.00 | 46.50 | 0.45 | 3.21 | 0.00 | 1.46 | 1.80 | 98.83 | | | |
| ARM-I | 2.75 | 10.52 | 1.24 | 1.14 | 1.57 | 1.79 | 0.00 | 5.59 | 11.30 | 0.66 | 2.23 | 1.44 | 0.00 | 1.16 | 0.00 | 0.00 | 0.00 | 0.00 | 0.00 | 0.00 | 5.08 | 0.00 | 0.00 | 0.00 | 0.00 | 1.67 | 9.67 | 5.96 | 0.00 | 0.65 | 0.00 | 46.50 | 0.45 | 3.21 | 0.00 | 1.46 | 1.80 | 98.83 | | | |
| ARM-I | 2.75 | 10.13 | 1.31 | 1.25 | 1.70 | 1.89 | 0.00 | 5.59 | 11.30 | 0.66 | 2.23 | 1.44 | 0.00 | 1.16 | 0.00 | 0.00 | 0.00 | 0.00 | 0.00 | 0.00 | 5.08 | 0.00 | 0.00 | 0.00 | 0.00 | 1.67 | 9.67 | 5.96 | 0.00 | 0.65 | 0.00 | 46.50 | 0.45 | 3.21 | 0.00 | 1.46 | 1.80 | 98.83 | | | |
| ARM-I | 2.75 | 9.90 | 1.23 | 1.13 | 1.56 | 1.76 | 0.00 | 5.59 | 11.30 | 0.66 | 2.23 | 1.44 | 0.00 | 1.16 | 0.00 | 0.00 | 0.00 | 0.00 | 0.00 | 0.00 | 5.08 | 0.00 | 0.00 | 0.00 | 0.00 | 1.67 | 9.67 | 5.96 | 0.00 | 0.65 | 0.00 | 46.50 | 0.45 | 3.21 | 0.00 | 1.46 | 1.80 | 98.83 | | | |
| ARM-I | 2.75 | 9.64 | 1.32 | 1.12 | 1.52 | 1.84 | 0.00 | 5.59 | 11.30 | 0.66 | 2.23 | 1.44 | 0.00 | 1.16 | 0.00 | 0.00 | 0.00 | 0.00 | 0.00 | 0.00 | 5.08 | 0.00 | 0.00 | 0.00 | 0.00 | 1.67 | 9.67 | 5.96 | 0.00 | 0.65 | 0.00 | 46.50 | 0.45 | 3.21 | 0.00 | 1.46 | 1.80 | 98.83 | | | |
| ARM-I | 2.75 | 10.42 | 1.28 | 1.17 | 1.59 | 1.80 | 0.00 | 5.59 | 11.30 | 0.66 | 2.23 | 1.44 | 0.00 | 1.16 | 0.00 | 0.00 | 0.00 | 0.00 | 0.00 | 0.00 | 5.08 | 0.00 | 0.00 | 0.00 | 0.00 | 1.67 | 9.67 | 5.96 | 0.00 | 0.65 | 0.00 | 46.50 | 0.45 | 3.21 | 0.00 | 1.46 | 1.80 | 98.83 | | | |
| ARM-I | 2.75 | 9.89 | 1.21 | 1.09 | 1.53 | 1.75 | 0.00 | 5.59 | 11.30 | 0.66 | 2.23 | 1.44 | 0.00 | 1.16 | 0.00 | 0.00 | 0.00 | 0.00 | 0.00 | 0.00 | 5.08 | 0.00 | 0.00 | 0.00 | 0.00 | 1.67 | 9.67 | 5.96 | 0.00 | 0.65 | 0.00 | 46.50 | 0.45 | 3.21 | 0.00 | 1.46 | 1.80 | 98.83 | | | |
| ARM-I | 2.75 | 10.22 | 1.23 | 1.13 | 1.57 | 1.78 | 0.00 | 5.59 | 11.30 | 0.66 | 2.23 | 1.44 | 0.00 | 1.16 | 0.00 | 0.00 | 0.00 | 0.00 | 0.00 | 0.00 | 5.08 | 0.00 | 0.00 | 0.00 | 0.00 | 1.67 | 9.67 | 5.96 | 0.00 | 0.65 | 0.00 | 46.50 | 0.45 | 3.21 | 0.00 | 1.46 | 1.80 | 98.83 | | | |
| ARM-I | 2.75 | 10.24 | 1.16 | 1.04 | 1.48 | 1.72 | 0.00 | 5.59 | 11.30 | 0.66 | 2.23 | 1.44 | 0.00 | 1.16 | 0.00 | 0.00 | 0.00 | 0.00 | 0.00 | 0.00 | 5.08 | 0.00 | 0.00 | 0.00 | 0.00 | 1.67 | 9.67 | 5.96 | 0.00 | 0.65 | 0.00 | 46.50 | 0.45 | 3.21 | 0.00 | 1.46 | 1.80 | 98.83 | | | |
| ARM-I | 2.75 | 9.38 | 1.25 | 1.15 | 1.57 | 1.77 | 0.00 | 5.59 | 11.30 | 0.66 | 2.23 | 1.44 | 0.00 | 1.16 | 0.00 | 0.00 | 0.00 | 0.00 | 0.00 | 0.00 | 5.08 | 0.00 | 0.00 | 0.00 | 0.00 | 1.67 | 9.67 | 5.96 | 0.00 | 0.65 | 0.00 | 46.50 | 0.45 | 3.21 | 0.00 | 1.46 | 1.80 | 98.83 | | | |
| ARM-I | 2.75 | 10.34 | 1.27 | 1.18 | 1.60 | 1.80 | 0.00 | 5.59 | 11.30 | 0.66 | 2.23 | 1.44 | 0.00 | 1.16 | 0.00 | 0.00 | 0.00 | 0.00 | 0.00 | 0.00 | 5.08 | 0.00 | 0.00 | 0.00 | 0.00 | 1.67 | 9.67 | 5.96 | 0.00 | 0.65 | 0.00 | 46.50 | 0.45 | 3.21 | 0.00 | 1.46 | 1.80 | 98.83 | | | |
| ARM-I | 2.75 | 10.32 | 1.24 | 1.15 | 1.58 | 1.78 | 0.00 | 5.59 | 11.30 | 0.66 | 2.23 | 1.44 | 0.00 | 1.16 | 0.00 | 0.00 | 0.00 | 0.00 | 0.00 | 0.00 | 5.08 | 0.00 | 0.00 | 0.00 | 0.00 | 1.67 | 9.67 | 5.96 | 0.00 | 0.65 | 0.00 | 46.50 | 0.45 | 3.21 | 0.00 | 1.46 | 1.80 | 98.83 | | | |
| DWPF STARTUP FRIT | 2.69 | 9.74 | 1.31 | 1.02 | 1.78 | 1.62 | 0.00 | 4.60 | 8.51 | 0.10 | 1.47 | 0.00 | 0.09 | 0.00 | 0.00 | 0.00 | 0.00 | 0.00 | 0.00 | 0.00 | 14.20 | 2.70 | 0.00 | 3.25 | 0.84 | 1.93 | 0.00 | 0.00 | 11.53 | 0.00 | 1.11 | 0.00 | 0.00 | 47.90 | 0.00 | 1.18 | 0.00 | 0.00 | 0.11 | 99.52 | |

SRNL-STI-2016-00372
Revision 0

| Sample ID | Measured Density (g/cc) | Mean(Measured pH) | Mean(log[B (ppm)]) | Mean(log[Li (ppm)]) | Mean(log[Na (ppm)]) | Mean(log[Si (ppm)]) | FeII/FeIII | Al2O3(v) | B2O3(v) | BaO(v) | CaO(v) | Ce2O3(v) | Cr2O3(v) | Cs2O(v) | CuO(v) | Cu2O(v) | Fe2O3(v) | K2O(v) | La2O3(v) | Li2O(v) | MgO(v) | MnO(v) | MnO2(v) | MoO3(v) | Na2O(v) | Nd2O3(v) | NiO(v) | P2O5(v) | PhO(v) | SiO2(v) | SrO(v) | TiO2(v) | Y2O3(v) | ZnO(v) | ZrO2(v) | *Oxides(v) | |
|-------------------|-------------------------|-------------------|--------------------|---------------------|---------------------|---------------------|------------|----------|---------|--------|--------|----------|----------|---------|--------|---------|----------|--------|----------|---------|--------|--------|---------|---------|---------|----------|--------|---------|--------|---------|--------|---------|---------|--------|---------|------------|--------|
| DWPF STARTUP FRIT | 2.69 | 10.09 | 1.29 | 1.03 | 1.78 | 1.89 | 0.00 | 4.60 | 8.51 | 0.10 | 1.47 | 0.00 | 0.09 | 0.00 | 0.00 | 0.00 | 14.20 | 2.70 | 0.00 | 3.25 | 0.84 | 1.93 | 0.00 | 0.00 | 11.53 | 0.00 | 1.11 | 0.00 | 0.00 | 47.90 | 0.00 | 1.18 | 0.00 | 0.00 | 0.11 | 99.52 | |
| DWPF STARTUP FRIT | 2.69 | 10.21 | 1.31 | 1.09 | 1.87 | 1.98 | 0.00 | 4.60 | 8.51 | 0.10 | 1.47 | 0.00 | 0.09 | 0.00 | 0.00 | 0.00 | 0.00 | 14.20 | 2.70 | 0.00 | 3.25 | 0.84 | 1.93 | 0.00 | 0.00 | 11.53 | 0.00 | 1.11 | 0.00 | 0.00 | 0.11 | 99.52 | | | | | |
| EA | 2.65 | 11.77 | 2.77 | 2.27 | 3.22 | 2.95 | 0.22 | 3.70 | 11.30 | 0.00 | 1.12 | 0.00 | 0.00 | 0.00 | 0.00 | 0.00 | 1.45 | 7.38 | 0.04 | 0.42 | 4.26 | 1.72 | 1.34 | 0.00 | 0.00 | 16.80 | 0.00 | 0.57 | 0.00 | 0.00 | 48.73 | 0.00 | 0.70 | 0.00 | 0.00 | 0.46 | 99.99 |
| EA | 2.65 | 11.80 | 2.77 | 2.33 | 3.26 | 3.03 | 0.22 | 3.70 | 11.30 | 0.00 | 1.12 | 0.00 | 0.00 | 0.00 | 0.00 | 0.00 | 1.45 | 7.38 | 0.04 | 0.42 | 4.26 | 1.72 | 1.34 | 0.00 | 0.00 | 16.80 | 0.00 | 0.57 | 0.00 | 0.00 | 48.73 | 0.00 | 0.70 | 0.00 | 0.00 | 0.46 | 99.99 |
| EA | 2.65 | 11.87 | 2.72 | 2.27 | 3.20 | 2.96 | 0.22 | 3.70 | 11.30 | 0.00 | 1.12 | 0.00 | 0.00 | 0.00 | 0.00 | 0.00 | 1.45 | 7.38 | 0.04 | 0.42 | 4.26 | 1.72 | 1.34 | 0.00 | 0.00 | 16.80 | 0.00 | 0.57 | 0.00 | 0.00 | 48.73 | 0.00 | 0.70 | 0.00 | 0.00 | 0.46 | 99.99 |
| EA | 2.65 | 11.59 | 2.79 | 2.29 | 3.24 | 2.97 | 0.22 | 3.70 | 11.30 | 0.00 | 1.12 | 0.00 | 0.00 | 0.00 | 0.00 | 0.00 | 1.45 | 7.38 | 0.04 | 0.42 | 4.26 | 1.72 | 1.34 | 0.00 | 0.00 | 16.80 | 0.00 | 0.57 | 0.00 | 0.00 | 48.73 | 0.00 | 0.70 | 0.00 | 0.00 | 0.46 | 99.99 |
| EA | 2.65 | 11.28 | 2.69 | 2.19 | 3.15 | 2.89 | 0.22 | 3.70 | 11.30 | 0.00 | 1.12 | 0.00 | 0.00 | 0.00 | 0.00 | 0.00 | 1.45 | 7.38 | 0.04 | 0.42 | 4.26 | 1.72 | 1.34 | 0.00 | 0.00 | 16.80 | 0.00 | 0.57 | 0.00 | 0.00 | 48.73 | 0.00 | 0.70 | 0.00 | 0.00 | 0.46 | 99.99 |
| EA | 2.65 | 11.78 | 2.77 | 2.26 | 3.22 | 2.94 | 0.22 | 3.70 | 11.30 | 0.00 | 1.12 | 0.00 | 0.00 | 0.00 | 0.00 | 0.00 | 1.45 | 7.38 | 0.04 | 0.42 | 4.26 | 1.72 | 1.34 | 0.00 | 0.00 | 16.80 | 0.00 | 0.57 | 0.00 | 0.00 | 48.73 | 0.00 | 0.70 | 0.00 | 0.00 | 0.46 | 99.99 |
| EA | 2.65 | 11.78 | 2.81 | 2.31 | 3.25 | 2.98 | 0.22 | 3.70 | 11.30 | 0.00 | 1.12 | 0.00 | 0.00 | 0.00 | 0.00 | 0.00 | 1.45 | 7.38 | 0.04 | 0.42 | 4.26 | 1.72 | 1.34 | 0.00 | 0.00 | 16.80 | 0.00 | 0.57 | 0.00 | 0.00 | 48.73 | 0.00 | 0.70 | 0.00 | 0.00 | 0.46 | 99.99 |
| EA | 2.65 | 11.95 | 2.77 | 2.29 | 3.22 | 2.93 | 0.22 | 3.70 | 11.30 | 0.00 | 1.12 | 0.00 | 0.00 | 0.00 | 0.00 | 0.00 | 1.45 | 7.38 | 0.04 | 0.42 | 4.26 | 1.72 | 1.34 | 0.00 | 0.00 | 16.80 | 0.00 | 0.57 | 0.00 | 0.00 | 48.73 | 0.00 | 0.70 | 0.00 | 0.00 | 0.46 | 99.99 |
| EA | 2.65 | 11.92 | 2.76 | 2.26 | 3.21 | 2.90 | 0.22 | 3.70 | 11.30 | 0.00 | 1.12 | 0.00 | 0.00 | 0.00 | 0.00 | 0.00 | 1.45 | 7.38 | 0.04 | 0.42 | 4.26 | 1.72 | 1.34 | 0.00 | 0.00 | 16.80 | 0.00 | 0.57 | 0.00 | 0.00 | 48.73 | 0.00 | 0.70 | 0.00 | 0.00 | 0.46 | 99.99 |
| EA | 2.65 | 11.75 | 2.79 | 2.29 | 3.23 | 2.96 | 0.22 | 3.70 | 11.30 | 0.00 | 1.12 | 0.00 | 0.00 | 0.00 | 0.00 | 0.00 | 1.45 | 7.38 | 0.04 | 0.42 | 4.26 | 1.72 | 1.34 | 0.00 | 0.00 | 16.80 | 0.00 | 0.57 | 0.00 | 0.00 | 48.73 | 0.00 | 0.70 | 0.00 | 0.00 | 0.46 | 99.99 |
| EA | 2.65 | 11.88 | 2.71 | 2.23 | 3.17 | 2.89 | 0.22 | 3.70 | 11.30 | 0.00 | 1.12 | 0.00 | 0.00 | 0.00 | 0.00 | 0.00 | 1.45 | 7.38 | 0.04 | 0.42 | 4.26 | 1.72 | 1.34 | 0.00 | 0.00 | 16.80 | 0.00 | 0.57 | 0.00 | 0.00 | 48.73 | 0.00 | 0.70 | 0.00 | 0.00 | 0.46 | 99.99 |
| HG-1-1 | | 10.43 | 1.17 | 1.13 | 1.66 | 1.97 | 0.00 | 5.44 | 7.02 | 0.11 | 1.32 | 0.00 | 0.35 | 0.07 | 0.16 | 0.14 | 0.04 | 12.94 | 2.67 | 0.00 | 4.42 | 1.54 | 2.17 | 0.00 | 0.00 | 9.18 | 0.00 | 0.86 | 0.01 | 0.11 | 52.24 | 0.01 | 0.46 | 0.00 | 0.31 | 0.16 | 101.73 |
| HG-1-2 | | 10.39 | 1.20 | 1.16 | 1.66 | 2.00 | 0.00 | 5.16 | 6.95 | 0.08 | 1.08 | 0.00 | 0.35 | 0.07 | 0.11 | 0.10 | 0.05 | 12.00 | 3.07 | 0.00 | 4.63 | 1.52 | 2.29 | 0.00 | 0.00 | 8.78 | 0.00 | 0.79 | 0.05 | 0.20 | 55.32 | 0.03 | 0.28 | 0.00 | 0.39 | 0.09 | 103.39 |
| HG-1-3 | | 10.39 | 1.17 | 1.15 | 1.63 | 1.98 | 0.01 | 5.01 | 6.97 | 0.07 | 1.11 | 0.00 | 0.28 | 0.07 | 0.11 | 0.10 | 0.15 | 11.75 | 2.60 | 0.00 | 4.64 | 1.51 | 2.25 | 0.00 | 0.00 | 8.86 | 0.00 | 0.75 | 0.05 | 0.18 | 55.20 | 0.03 | 0.26 | 0.00 | 0.37 | 0.00 | 102.32 |
| HG-2-1 | | 10.44 | 1.17 | 1.14 | 1.65 | 1.99 | 0.01 | 5.15 | 6.83 | 0.07 | 1.09 | 0.00 | 0.34 | 0.05 | 0.11 | 0.09 | 0.07 | 12.15 | 2.46 | 0.00 | 4.62 | 1.51 | 2.30 | 0.00 | 0.00 | 8.85 | 0.00 | 0.78 | 0.04 | 0.19 | 55.35 | 0.03 | 0.26 | 0.00 | 0.39 | 0.00 | 102.73 |
| HG-2-2 | | 10.73 | 1.17 | 1.18 | 1.80 | 2.02 | 0.01 | 5.59 | 6.19 | 0.09 | 1.13 | 0.00 | 0.30 | 0.04 | 0.08 | 0.07 | 0.07 | 13.08 | 1.85 | 0.00 | 4.51 | 1.40 | 2.49 | 0.00 | 0.00 | 10.59 | 0.00 | 0.79 | 0.06 | 0.25 | 54.82 | 0.03 | 0.23 | 0.00 | 0.42 | 0.21 | 104.28 |
| HG-2-3 | | 10.71 | 1.18 | 1.18 | 1.79 | 2.03 | 0.01 | 5.42 | 6.10 | 0.08 | 1.11 | 0.00 | 0.31 | 0.07 | 0.07 | 0.06 | 0.07 | 12.73 | 1.82 | 0.00 | 4.49 | 1.39 | 2.43 | 0.00 | 0.00 | 10.52 | 0.00 | 0.77 | 0.00 | 0.19 | 54.69 | 0.03 | 0.22 | 0.00 | 0.39 | 0.07 | 103.03 |
| HG-3-1 | | 10.73 | 1.16 | 1.16 | 1.76 | 2.00 | 0.05 | 5.62 | 6.15 | 0.08 | 1.14 | 0.00 | 0.33 | 0.03 | 0.09 | 0.08 | 0.52 | 12.54 | 2.02 | 0.00 | 4.36 | 1.37 | 2.48 | 0.00 | 0.00 | 10.10 | 0.00 | 0.80 | 0.04 | 0.23 | 53.39 | 0.03 | 0.23 | 0.00 | 0.44 | 0.18 | 102.24 |
| HG-3-2 | | 10.71 | 1.18 | 1.16 | 1.75 | 2.00 | 0.07 | 5.73 | 6.28 | 0.09 | 1.18 | 0.00 | 0.29 | 0.04 | 0.10 | 0.09 | 0.77 | 12.85 | 2.24 | 0.00 | 4.30 | 1.36 | 2.59 | 0.00 | 0.00 | 9.86 | 0.00 | 0.79 | 0.02 | 0.23 | 53.18 | 0.03 | 0.24 | 0.00 | 0.40 | 0.17 | 102.82 |
| HG-3-3 | | 10.68 | 1.17 | 1.14 | 1.72 | 1.98 | 0.09 | 5.79 | 6.43 | 0.09 | 1.24 | 0.00 | 0.25 | 0.01 | 0.10 | 0.09 | 1.05 | 12.48 | 2.35 | 0.00 | 4.35 | 1.38 | 2.50 | 0.00 | 0.00 | 9.70 | 0.00 | 0.79 | 0.02 | 0.22 | 53.45 | 0.03 | 0.25 | 0.00 | 0.43 | 0.16 | 103.15 |
| IDMS BLEND 1 3457 | | 10.22 | 1.10 | 1.11 | 1.67 | 1.94 | 0.01 | 5.18 | 6.76 | 0.09 | 1.08 | 0.00 | 0.23 | 0.00 | 0.11 | 0.09 | 0.06 | 12.41 | 2.47 | 0.00 | 4.12 | 1.26 | 2.07 | 0.00 | 0.00 | 9.87 | 0.00 | 0.81 | 0.00 | 0.00 | 49.35 | 0.00 | 0.24 | 0.00 | 0.00 | 0.00 | 96.20 |
| IDMS BLEND 1 3479 | | 10.26 | 1.08 | 1.09 | 1.66 | 1.93 | 0.01 | 5.15 | 6.78 | 0.10 | 1.04 | 0.00 | 0.22 | 0.00 | 0.09 | 0.08 | 0.16 | 12.16 | 2.51 | 0.00 | 4.13 | 1.24 | 2.11 | 0.00 | 0.00 | 9.74 | 0.00 | 0.83 | 0.00 | 0.00 | 49.25 | 0.00 | 0.22 | 0.00 | 0.00 | 0.00 | 95.81 |
| IDMS BLEND 1 3498 | | 10.31 | 1.13 | 1.12 | 1.72 | 1.94 | 0.01 | 5.16 | 6.82 | 0.10 | 1.07 | 0.00 | 0.23 | 0.00 | 0.10 | 0.09 | 0.08 | 12.43 | 2.65 | 0.00 | 4.06 | 1.22 | 2.19 | 0.00 | 0.00 | 10.54 | 0.00 | 0.89 | 0.00 | 0.00 | 48.06 | 0.00 | 0.19 | 0.00 | 0.00 | 0.00 | 95.87 |

SRNL-STI-2016-00372
Revision 0

| Sample ID | Measured Density (g/cc) | | | | | | | | | | | | | | | | | | | | | | | | | | | | | | | | | | | |
|-----------------------|-------------------------|--------------------|---------------------|---------------------|---------------------|-----------|----------|---------|--------|--------|----------|----------|---------|--------|---------|----------|--------|----------|---------|--------|--------|---------|---------|---------|----------|--------|---------|--------|---------|--------|---------|---------|--------|---------|------------|--------|
| | Mean(Measured pH) | Mean(log[B (ppm)]) | Mean(log[Li (ppm)]) | Mean(log[Na (ppm)]) | Mean(log[Si (ppm)]) | Fel/FelII | Al2O3(v) | B2O3(v) | BaO(v) | CaO(v) | Ce2O3(v) | Cr2O3(v) | Cs2O(v) | CuO(v) | Cu2O(v) | Fe2O3(v) | K2O(v) | La2O3(v) | Li2O(v) | MgO(v) | MnO(v) | MnO2(v) | MoO3(v) | Na2O(v) | Nd2O3(v) | NiO(v) | P2O5(v) | PhO(v) | SiO2(v) | SrO(v) | TiO2(v) | Y2O3(v) | ZnO(v) | ZrO2(v) | *Oxides(v) | |
| IDMS BLEND 1 3510 | 10.37 | 1.16 | 1.14 | 1.75 | 1.96 | 0.01 | 5.21 | 6.74 | 0.10 | 1.06 | 0.00 | 0.22 | 0.00 | 0.10 | 0.09 | 0.08 | 12.56 | 2.91 | 0.00 | 4.03 | 1.22 | 2.19 | 0.00 | 0.00 | 10.44 | 0.00 | 0.87 | 0.00 | 0.00 | 47.72 | 0.00 | 0.19 | 0.00 | 0.00 | 95.72 | |
| IDMS BLEND 2 3611 | 10.21 | 1.09 | 1.11 | 1.70 | 1.97 | 0.00 | 5.02 | 6.56 | 0.10 | 0.95 | 0.00 | 0.26 | 0.00 | 0.09 | 0.08 | 0.00 | 11.82 | 2.32 | 0.00 | 4.15 | 1.28 | 2.09 | 0.00 | 0.00 | 9.97 | 0.00 | 0.94 | 0.00 | 0.00 | 50.19 | 0.00 | 0.17 | 0.00 | 0.00 | 95.98 | |
| IDMS BLEND 2 3622 | 10.24 | 1.10 | 1.11 | 1.70 | 1.97 | 0.00 | 4.89 | 6.75 | 0.10 | 0.89 | 0.00 | 0.23 | 0.00 | 0.09 | 0.08 | 0.00 | 11.58 | 2.32 | 0.00 | 4.22 | 1.28 | 2.10 | 0.00 | 0.00 | 10.07 | 0.00 | 0.93 | 0.00 | 0.00 | 50.78 | 0.00 | 0.15 | 0.00 | 0.00 | 96.45 | |
| IDMS BLEND 2 3635 | 10.14 | 1.10 | 1.10 | 1.69 | 1.97 | 0.00 | 4.89 | 6.66 | 0.10 | 0.89 | 0.00 | 0.23 | 0.00 | 0.08 | 0.07 | 0.00 | 11.23 | 2.36 | 0.00 | 4.21 | 1.28 | 2.06 | 0.00 | 0.00 | 10.05 | 0.00 | 0.91 | 0.00 | 0.00 | 50.45 | 0.00 | 0.17 | 0.00 | 0.00 | 95.64 | |
| IDMS BLEND 2 3666 | 10.10 | 1.09 | 1.10 | 1.68 | 1.96 | 0.00 | 4.80 | 6.70 | 0.10 | 0.86 | 0.00 | 0.25 | 0.00 | 0.08 | 0.07 | 0.00 | 11.37 | 2.28 | 0.00 | 4.22 | 1.29 | 2.10 | 0.00 | 0.00 | 10.13 | 0.00 | 0.92 | 0.00 | 0.00 | 50.21 | 0.00 | 0.14 | 0.00 | 0.00 | 95.52 | |
| IDMS BLEND 2 3676 | 10.07 | 1.09 | 1.10 | 1.68 | 1.96 | 0.00 | 4.73 | 6.76 | 0.10 | 0.83 | 0.00 | 0.22 | 0.00 | 0.08 | 0.07 | 0.00 | 11.19 | 2.25 | 0.00 | 4.26 | 1.28 | 2.06 | 0.00 | 0.00 | 10.12 | 0.00 | 0.92 | 0.00 | 0.00 | 50.66 | 0.00 | 0.14 | 0.00 | 0.00 | 95.67 | |
| IDMS BLEND 3 3768 | 9.99 | 1.11 | 1.11 | 1.70 | 1.94 | 0.01 | 4.89 | 6.83 | 0.12 | 0.88 | 0.00 | 0.28 | 0.00 | 0.10 | 0.09 | 0.11 | 11.31 | 2.25 | 0.00 | 4.33 | 1.36 | 2.21 | 0.00 | 0.00 | 10.28 | 0.00 | 0.94 | 0.00 | 0.00 | 50.00 | 0.00 | 0.13 | 0.00 | 0.00 | 96.15 | |
| IDMS BLEND 3 3789 | 10.14 | 1.14 | 1.12 | 1.73 | 1.93 | 0.01 | 5.28 | 7.02 | 0.13 | 1.01 | 0.00 | 0.25 | 0.00 | 0.10 | 0.09 | 0.11 | 12.23 | 2.48 | 0.00 | 4.27 | 1.39 | 2.44 | 0.00 | 0.00 | 10.41 | 0.00 | 0.98 | 0.00 | 0.00 | 49.18 | 0.00 | 0.13 | 0.00 | 0.00 | 97.54 | |
| IDMS BLEND 3 3793 | 10.13 | 1.14 | 1.11 | 1.74 | 1.93 | 0.01 | 5.46 | 7.01 | 0.14 | 1.08 | 0.00 | 0.25 | 0.00 | 0.11 | 0.10 | 0.10 | 12.69 | 2.60 | 0.00 | 4.15 | 1.38 | 2.51 | 0.00 | 0.00 | 10.39 | 0.00 | 0.98 | 0.00 | 0.00 | 48.04 | 0.00 | 0.12 | 0.00 | 0.00 | 97.14 | |
| IDMS BLEND 3 3802B | 10.18 | 1.18 | 1.13 | 1.75 | 1.94 | 0.02 | 5.39 | 6.88 | 0.13 | 1.04 | 0.00 | 0.25 | 0.00 | 0.11 | 0.09 | 0.24 | 12.53 | 2.66 | 0.00 | 4.11 | 1.37 | 2.48 | 0.00 | 0.00 | 9.92 | 0.00 | 0.95 | 0.00 | 0.00 | 47.75 | 0.00 | 0.12 | 0.00 | 0.00 | 96.06 | |
| IDMS HM-1 3824B | 9.98 | 1.09 | 1.12 | 1.65 | 1.94 | 0.02 | 5.58 | 6.74 | 0.10 | 0.91 | 0.00 | 0.22 | 0.00 | 0.08 | 0.07 | 0.21 | 10.57 | 1.88 | 0.00 | 4.44 | 1.58 | 2.40 | 0.00 | 0.00 | 9.62 | 0.00 | 0.77 | 0.00 | 0.00 | 51.60 | 0.00 | 0.09 | 0.00 | 0.00 | 96.87 | |
| IDMS HM-1 3829A | 9.96 | 1.07 | 1.11 | 1.62 | 1.94 | 0.02 | 6.00 | 6.62 | 0.10 | 0.90 | 0.00 | 0.23 | 0.00 | 0.07 | 0.06 | 0.18 | 10.73 | 1.66 | 0.00 | 4.45 | 1.60 | 2.54 | 0.00 | 0.00 | 9.29 | 0.00 | 0.77 | 0.00 | 0.00 | 52.13 | 0.00 | 0.10 | 0.00 | 0.00 | 97.47 | |
| IDMS HM-1 3851B | 9.98 | 1.03 | 1.09 | 1.60 | 1.94 | 0.02 | 6.08 | 6.51 | 0.10 | 0.91 | 0.00 | 0.23 | 0.00 | 0.07 | 0.06 | 0.17 | 10.45 | 1.42 | 0.00 | 4.44 | 1.62 | 2.54 | 0.00 | 0.00 | 9.85 | 0.00 | 0.76 | 0.00 | 0.00 | 52.00 | 0.00 | 0.09 | 0.00 | 0.00 | 97.33 | |
| IDMS HM-1 3855A | 9.99 | 1.03 | 1.10 | 1.61 | 1.93 | 0.02 | 6.50 | 6.49 | 0.10 | 0.84 | 0.00 | 0.22 | 0.00 | 0.07 | 0.06 | 0.21 | 9.71 | 1.36 | 0.00 | 4.52 | 1.62 | 2.63 | 0.00 | 0.00 | 10.01 | 0.00 | 0.68 | 0.00 | 0.00 | 52.90 | 0.00 | 0.09 | 0.00 | 0.00 | 98.02 | |
| IDMS HM-2 3979C | 9.56 | 1.03 | 1.08 | 1.62 | 1.92 | 0.00 | 7.66 | 6.77 | 0.09 | 0.76 | 0.00 | 0.51 | 0.00 | 0.07 | 0.06 | 0.00 | 10.12 | 1.62 | 0.00 | 4.48 | 1.57 | 2.79 | 0.00 | 0.00 | 10.38 | 0.00 | 0.70 | 0.00 | 0.05 | 53.96 | 0.15 | 0.09 | 0.00 | 0.10 | 0.08 | 102.01 |
| IDMS HM-2 4099A | 9.60 | 1.04 | 1.09 | 1.64 | 1.92 | 0.00 | 7.82 | 6.78 | 0.09 | 0.73 | 0.00 | 0.47 | 0.00 | 0.08 | 0.07 | 0.00 | 10.08 | 1.85 | 0.00 | 4.43 | 1.54 | 2.80 | 0.00 | 0.00 | 10.56 | 0.00 | 0.67 | 0.00 | 0.06 | 53.28 | 0.16 | 0.12 | 0.00 | 0.10 | 0.06 | 101.74 |
| IDMS HM-2 4120B | 9.22 | 1.03 | 1.08 | 1.63 | 1.92 | 0.00 | 7.54 | 6.80 | 0.09 | 0.71 | 0.00 | 0.39 | 0.00 | 0.07 | 0.06 | 0.00 | 9.46 | 1.95 | 0.00 | 4.67 | 1.55 | 2.68 | 0.00 | 0.00 | 10.60 | 0.00 | 0.61 | 0.00 | 0.05 | 53.11 | 0.15 | 0.11 | 0.00 | 0.09 | 0.07 | 100.75 |
| IDMS HM-3 4176 | 9.22 | 1.02 | 1.06 | 1.61 | 1.90 | 0.00 | 7.49 | 6.25 | 0.08 | 0.66 | 0.00 | 0.38 | 0.00 | 0.07 | 0.06 | 0.00 | 9.20 | 2.11 | 0.00 | 4.02 | 1.44 | 2.48 | 0.00 | 0.00 | 10.48 | 0.00 | 0.56 | 0.00 | 0.04 | 51.11 | 0.14 | 0.10 | 0.00 | 0.08 | 0.05 | 96.80 |
| IDMS HM-3 4225 | 9.22 | 1.02 | 1.06 | 1.60 | 1.90 | 0.00 | 8.38 | 6.53 | 0.08 | 0.72 | 0.00 | 0.38 | 0.00 | 0.08 | 0.07 | 0.00 | 9.76 | 2.17 | 0.00 | 4.16 | 1.51 | 2.73 | 0.00 | 0.00 | 10.32 | 0.00 | 0.57 | 0.00 | 0.05 | 49.73 | 0.15 | 0.10 | 0.00 | 0.09 | 0.05 | 97.62 |
| IDMS HM-3 4357 | 9.20 | 1.00 | 1.03 | 1.59 | 1.87 | 0.00 | 8.96 | 6.61 | 0.09 | 0.77 | 0.00 | 0.41 | 0.00 | 0.08 | 0.07 | 0.00 | 10.27 | 2.23 | 0.00 | 4.15 | 1.55 | 2.90 | 0.00 | 0.00 | 9.95 | 0.00 | 0.59 | 0.00 | 0.04 | 49.60 | 0.15 | 0.10 | 0.00 | 0.08 | 0.07 | 98.67 |
| IDMS PX-14643 | 9.46 | 1.19 | 1.17 | 1.72 | 1.96 | 0.00 | 5.23 | 7.29 | 0.19 | 1.46 | 0.00 | 0.46 | 0.00 | 0.15 | 0.13 | 0.00 | 10.51 | 2.88 | 0.00 | 4.28 | 1.46 | 3.10 | 0.00 | 0.00 | 9.73 | 0.00 | 1.59 | 0.00 | 0.17 | 49.14 | 0.03 | 0.17 | 0.00 | 0.16 | 0.08 | 98.21 |
| IDMS PX-14726 | 9.36 | 1.19 | 1.16 | 1.73 | 1.97 | 0.00 | 4.96 | 7.36 | 0.20 | 1.50 | 0.00 | 0.55 | 0.00 | 0.17 | 0.15 | 0.00 | 11.17 | 3.03 | 0.00 | 4.34 | 1.44 | 3.26 | 0.00 | 0.00 | 10.02 | 0.00 | 1.71 | 0.00 | 0.19 | 50.58 | 0.03 | 0.37 | 0.00 | 0.17 | 0.07 | 101.26 |
| IDMS PX-14776 | 9.38 | 1.23 | 1.21 | 1.74 | 2.02 | 0.00 | 4.34 | 7.25 | 0.18 | 1.33 | 0.00 | 0.52 | 0.00 | 0.15 | 0.13 | 0.00 | 9.96 | 2.77 | 0.00 | 4.49 | 1.47 | 2.84 | 0.00 | 0.00 | 9.55 | 0.00 | 1.57 | 0.00 | 0.16 | 52.42 | 0.02 | 0.35 | 0.00 | 0.17 | 0.08 | 99.75 |
| IDMS PX-24455 | 9.32 | 0.99 | 1.03 | 1.57 | 1.88 | 0.00 | 8.52 | 6.87 | 0.09 | 0.79 | 0.00 | 0.39 | 0.00 | 0.08 | 0.07 | 0.00 | 9.52 | 2.15 | 0.00 | 4.33 | 1.59 | 2.84 | 0.00 | 0.00 | 10.45 | 0.00 | 0.64 | 0.00 | 0.03 | 51.86 | 0.14 | 0.10 | 0.00 | 0.10 | 0.06 | 100.62 |
| IDMS PX-24509 | 9.35 | 1.09 | 1.09 | 1.64 | 1.90 | 0.00 | 6.97 | 7.19 | 0.14 | 1.14 | 0.00 | 0.45 | 0.00 | 0.12 | 0.10 | 0.00 | 10.99 | 2.48 | 0.00 | 4.32 | 1.56 | 3.04 | 0.00 | 0.00 | 9.55 | 0.00 | 1.18 | 0.00 | 0.11 | 50.20 | 0.08 | 0.17 | 0.00 | 0.13 | 0.06 | 99.98 |

| Sample ID | Measured Density (g/cc) | | Mean(Measured pH) | | Mean(log[B (ppm)]) | | Mean(log[Li (ppm)]) | | Mean(log[Na (ppm)]) | | Mean(log[Si (ppm)]) | | FeII/FeIII | | Al2O3(v) | | B2O3(v) | | BaO(v) | | CaO(v) | | Ce2O3(v) | | Cr2O3(v) | | Cs2O(v) | | CuO(v) | | Cn2O(v) | | FeO(v) | | Fe2O3(v) | | K2O(v) | | La2O3(v) | | Li2O(v) | | MgO(v) | | MnO(v) | | MnO2(v) | | MoO3(v) | | Na2O(v) | | Nd2O3(v) | | NiO(v) | | P2O5(v) | | PbO(v) | | SiO2(v) | | SrO(v) | | TiO2(v) | | Y2O3(v) | | ZnO(v) | | ZrO2(v) | | ·Oxides(v) | |
|-----------------|-------------------------|-------|-------------------|------|--------------------|------|---------------------|------|---------------------|------|---------------------|------|------------|------|----------|------|---------|-------|--------|------|--------|------|----------|------|----------|-------|---------|------|--------|-------|---------|-------|--------|------|----------|-------|--------|-------|----------|--|---------|--|--------|--|--------|--|---------|--|---------|--|---------|--|----------|--|--------|--|---------|--|--------|--|---------|--|--------|--|---------|--|---------|--|--------|--|---------|--|------------|--|
| IDMS PX-24566 | 9.49 | 1.20 | 1.17 | 1.72 | 1.95 | 0.00 | 5.99 | 7.40 | 0.18 | 1.45 | 0.00 | 0.46 | 0.00 | 0.14 | 0.13 | 0.00 | 10.90 | 3.02 | 0.00 | 4.29 | 1.51 | 3.24 | 0.00 | 0.00 | 9.84 | 0.00 | 1.51 | 0.00 | 0.15 | 48.86 | 0.05 | 0.22 | 0.00 | 0.15 | 0.07 | 99.56 | | | | | | | | | | | | | | | | | | | | | | | | | | | | | | | | | | | | | | |
| SHUM-13 | 2.67 | 10.23 | 1.15 | 1.22 | 1.60 | 2.00 | 0.69 | 4.67 | 6.94 | 0.12 | 1.18 | 0.00 | 0.09 | 0.05 | 0.12 | 0.10 | 3.99 | 6.39 | 2.07 | 0.00 | 4.65 | 1.47 | 1.77 | 0.00 | 0.00 | 8.12 | 0.52 | 0.65 | 0.01 | 0.04 | 54.60 | 0.01 | 0.47 | 0.00 | 0.09 | 0.37 | 98.48 | | | | | | | | | | | | | | | | | | | | | | | | | | | | | | | | | | | | | |
| SHUM-14 | 2.60 | 10.03 | 1.36 | 1.38 | 1.71 | 2.14 | 0.61 | 3.60 | 7.48 | 0.11 | 0.87 | 0.00 | 0.07 | 0.05 | 0.11 | 0.10 | 2.57 | 4.66 | 2.17 | 0.00 | 5.16 | 1.59 | 1.24 | 0.00 | 0.00 | 7.66 | 0.37 | 0.46 | 0.03 | 0.12 | 59.80 | 0.03 | 0.48 | 0.01 | 0.07 | 0.28 | 99.06 | | | | | | | | | | | | | | | | | | | | | | | | | | | | | | | | | | | | | |
| SHUM-8 | 2.69 | 10.70 | 1.12 | 1.01 | 1.53 | 1.73 | 0.67 | 4.85 | 8.52 | 0.18 | 1.18 | 0.00 | 0.09 | 0.12 | 0.25 | 0.22 | 0.22 | 3.91 | 6.51 | 4.83 | 0.00 | 4.13 | 1.32 | 1.79 | 0.00 | 0.00 | 9.02 | 0.54 | 0.66 | 0.03 | 0.10 | 48.40 | 0.02 | 0.99 | 0.01 | 0.09 | 0.37 | 98.13 | | | | | | | | | | | | | | | | | | | | | | | | | | | | | | | | | | | | |
| SHUM-9 | 2.63 | 10.32 | 1.55 | 1.42 | 1.88 | 2.13 | 1.00 | 3.94 | 9.14 | 0.17 | 0.86 | 0.00 | 0.07 | 0.12 | 0.22 | 0.20 | 3.43 | 3.81 | 4.13 | 0.00 | 4.64 | 1.44 | 1.24 | 0.00 | 0.00 | 8.58 | 0.38 | 0.47 | 0.02 | 0.07 | 54.38 | 0.02 | 1.00 | 0.01 | 0.07 | 0.27 | 98.65 | | | | | | | | | | | | | | | | | | | | | | | | | | | | | | | | | | | | | |
| SHUM-T1 | 2.71 | 10.60 | 0.98 | 0.97 | 1.46 | 1.72 | 0.32 | 5.20 | 7.32 | 0.15 | 1.29 | 0.00 | 0.10 | 0.08 | 0.18 | 0.16 | 2.58 | 9.06 | 3.20 | 0.00 | 4.23 | 1.35 | 2.00 | 0.00 | 0.00 | 8.63 | 0.57 | 0.73 | 0.03 | 0.13 | 50.28 | 0.03 | 0.67 | 0.01 | 0.10 | 0.41 | 98.46 | | | | | | | | | | | | | | | | | | | | | | | | | | | | | | | | | | | | | |
| SHUM-T2 | 2.69 | 10.38 | 1.17 | 1.20 | 1.67 | 1.94 | 0.32 | 5.20 | 7.32 | 0.15 | 1.29 | 0.00 | 0.10 | 0.08 | 0.18 | 0.16 | 2.58 | 9.06 | 3.20 | 0.00 | 4.23 | 1.35 | 2.00 | 0.00 | 0.00 | 8.63 | 0.57 | 0.73 | 0.03 | 0.13 | 50.28 | 0.03 | 0.67 | 0.01 | 0.10 | 0.41 | 98.46 | | | | | | | | | | | | | | | | | | | | | | | | | | | | | | | | | | | | | |
| SHUM-T4 | 2.71 | 10.61 | 1.01 | 0.99 | 1.47 | 1.73 | 0.32 | 5.20 | 7.32 | 0.15 | 1.29 | 0.00 | 0.10 | 0.08 | 0.18 | 0.16 | 2.58 | 9.06 | 3.20 | 0.00 | 4.23 | 1.35 | 2.00 | 0.00 | 0.00 | 8.63 | 0.57 | 0.73 | 0.03 | 0.13 | 50.28 | 0.03 | 0.67 | 0.01 | 0.10 | 0.41 | 98.46 | | | | | | | | | | | | | | | | | | | | | | | | | | | | | | | | | | | | | |
| TDS 131 EA TYPE | 2.65 | 10.59 | 2.24 | 1.94 | 2.67 | 2.65 | 0.00 | 5.77 | 12.70 | 0.00 | 0.92 | 0.00 | 0.04 | 0.00 | 0.00 | 0.00 | 0.00 | 14.30 | 0.04 | 0.37 | 4.83 | 1.53 | 3.17 | 0.00 | 0.00 | 14.60 | 0.00 | 1.44 | 0.00 | 0.00 | 39.80 | 0.01 | 0.93 | 0.00 | 0.00 | 0.43 | 100.88 | | | | | | | | | | | | | | | | | | | | | | | | | | | | | | | | | | | | | |
| TDS 131 SOPER | 2.65 | 10.57 | 1.97 | 1.68 | 2.37 | 2.28 | 0.00 | 5.51 | 10.80 | 0.00 | 0.92 | 0.00 | 0.12 | 0.00 | 0.00 | 0.00 | 0.00 | 11.40 | 0.04 | 0.35 | 4.21 | 1.41 | 3.36 | 0.00 | 0.00 | 13.70 | 0.00 | 1.53 | 0.00 | 0.00 | 46.20 | 0.00 | 0.74 | 0.00 | 0.00 | 0.34 | 100.63 | | | | | | | | | | | | | | | | | | | | | | | | | | | | | | | | | | | | | |
| WCP BATCH 1 | 2.65 | 10.31 | 1.25 | 1.22 | 1.73 | 1.99 | 0.00 | 4.88 | 7.78 | 0.15 | 1.22 | 0.00 | 0.11 | 0.06 | 0.20 | 0.18 | 0.00 | 12.84 | 3.33 | 0.00 | 4.43 | 1.42 | 1.72 | 0.00 | 0.11 | 9.00 | 0.15 | 0.75 | 0.00 | 0.00 | 50.20 | 0.00 | 0.68 | 0.00 | 0.00 | 0.10 | 99.31 | | | | | | | | | | | | | | | | | | | | | | | | | | | | | | | | | | | | | |
| WCP BATCH 1 | 2.65 | 10.19 | 1.23 | 1.20 | 1.69 | 2.00 | 0.00 | 4.88 | 7.78 | 0.15 | 1.22 | 0.00 | 0.11 | 0.06 | 0.20 | 0.18 | 0.00 | 12.84 | 3.33 | 0.00 | 4.43 | 1.42 | 1.72 | 0.00 | 0.11 | 9.00 | 0.15 | 0.75 | 0.00 | 0.00 | 50.20 | 0.00 | 0.68 | 0.00 | 0.00 | 0.10 | 99.31 | | | | | | | | | | | | | | | | | | | | | | | | | | | | | | | | | | | | | |
| WCP BATCH 1 | 2.65 | 10.47 | 1.25 | 1.19 | 1.70 | 1.98 | 0.00 | 4.88 | 7.78 | 0.15 | 1.22 | 0.00 | 0.11 | 0.06 | 0.20 | 0.18 | 0.00 | 12.84 | 3.33 | 0.00 | 4.43 | 1.42 | 1.72 | 0.00 | 0.11 | 9.00 | 0.15 | 0.75 | 0.00 | 0.00 | 50.20 | 0.00 | 0.68 | 0.00 | 0.00 | 0.10 | 99.31 | | | | | | | | | | | | | | | | | | | | | | | | | | | | | | | | | | | | | |
| WCP BATCH 2 | 2.64 | 10.18 | 1.21 | 1.20 | 1.70 | 1.99 | 0.00 | 4.63 | 7.88 | 0.16 | 1.08 | 0.00 | 0.13 | 0.02 | 0.21 | 0.19 | 0.00 | 11.12 | 3.38 | 0.00 | 4.50 | 1.42 | 1.41 | 0.00 | 0.17 | 9.21 | 0.26 | 0.90 | 0.00 | 0.00 | 52.10 | 0.00 | 0.69 | 0.00 | 0.00 | 0.17 | 99.63 | | | | | | | | | | | | | | | | | | | | | | | | | | | | | | | | | | | | | |
| WCP BATCH 2 | 2.64 | 10.09 | 1.19 | 1.17 | 1.66 | 1.99 | 0.00 | 4.63 | 7.88 | 0.16 | 1.08 | 0.00 | 0.13 | 0.02 | 0.21 | 0.19 | 0.00 | 11.12 | 3.38 | 0.00 | 4.50 | 1.42 | 1.41 | 0.00 | 0.17 | 9.21 | 0.26 | 0.90 | 0.00 | 0.00 | 52.10 | 0.00 | 0.69 | 0.00 | 0.00 | 0.17 | 99.63 | | | | | | | | | | | | | | | | | | | | | | | | | | | | | | | | | | | | | |
| WCP BATCH 2 | 2.64 | 10.42 | 1.22 | 1.18 | 1.68 | 1.99 | 0.00 | 4.63 | 7.88 | 0.16 | 1.08 | 0.00 | 0.13 | 0.02 | 0.21 | 0.19 | 0.00 | 11.12 | 3.38 | 0.00 | 4.50 | 1.42 | 1.41 | 0.00 | 0.17 | 9.21 | 0.26 | 0.90 | 0.00 | 0.00 | 52.10 | 0.00 | 0.69 | 0.00 | 0.00 | 0.17 | 99.63 | | | | | | | | | | | | | | | | | | | | | | | | | | | | | | | | | | | | | |
| WCP BATCH 3 | 2.65 | 10.31 | 1.31 | 1.28 | 1.78 | 2.05 | 0.00 | 3.44 | 7.69 | 0.18 | 0.99 | 0.00 | 0.14 | 0.06 | 0.20 | 0.18 | 0.00 | 11.71 | 3.40 | 0.00 | 4.51 | 1.42 | 1.53 | 0.00 | 0.12 | 9.01 | 0.17 | 1.05 | 0.00 | 0.00 | 52.60 | 0.00 | 0.68 | 0.00 | 0.00 | 0.12 | 99.20 | | | | | | | | | | | | | | | | | | | | | | | | | | | | | | | | | | | | | |
| WCP BATCH 3 | 2.65 | 10.11 | 1.31 | 1.25 | 1.74 | 2.07 | 0.00 | 3.44 | 7.69 | 0.18 | 0.99 | 0.00 | 0.14 | 0.06 | 0.20 | 0.18 | 0.00 | 11.71 | 3.40 | 0.00 | 4.51 | 1.42 | 1.53 | 0.00 | 0.12 | 9.01 | 0.17 | 1.05 | 0.00 | 0.00 | 52.60 | 0.00 | 0.68 | 0.00 | 0.00 | 0.12 | 99.20 | | | | | | | | | | | | | | | | | | | | | | | | | | | | | | | | | | | | | |
| WCP BATCH 3 | 2.65 | 10.37 | 1.33 | 1.25 | 1.75 | 2.06 | 0.00 | 3.44 | 7.69 | 0.18 | 0.99 | 0.00 | 0.14 | 0.06 | 0.20 | 0.18 | 0.00 | 11.71 | 3.40 | 0.00 | 4.51 | 1.42 | 1.53 | 0.00 | 0.12 | 9.01 | 0.17 | 1.05 | 0.00 | 0.00 | 52.60 | 0.00 | 0.68 | 0.00 | 0.00 | 0.12 | 99.20 | | | | | | | | | | | | | | | | | | | | | | | | | | | | | | | | | | | | | |
| WCP BATCH 4 | 2.67 | 10.20 | 1.39 | 1.30 | 1.83 | 2.07 | 0.00 | 3.43 | 8.14 | 0.25 | 0.84 | 0.00 | 0.14 | 0.09 | 0.23 | 0.20 | 0.00 | 11.71 | 3.86 | 0.00 | 4.29 | 1.43 | 2.54 | 0.00 | 0.20 | 9.16 | 0.39 | 1.06 | 0.00 | 0.00 | 50.10 | 0.00 | 1.03 | 0.00 | 0.00 | 0.22 | 99.31 | | | | | | | | | | | | | | | | | | | | | | | | | | | | | | | | | | | | | |
| WCP BATCH 4 | 2.67 | 10.24 | 1.38 | 1.27 | 1.80 | 2.07 | 0.00 | 3.43 | 8.14 | 0.25 | 0.84 | 0.00 | 0.14 | 0.09 | 0.23 | 0.20 | 0.00 | 11.71 | 3.86 | 0.00 | 4.29 | 1.43 | 2.54 | 0.00 | 0.20 | 9.16 | 0.39 | 1.06 | 0.00 | 0.00 | 50.10 | 0.00 | 1.03 | 0.00 | 0.00 | 0.22 | 99.31 | | | | | | | | | | | | | | | | | | | | | | | | | | | | | | | | | | | | | |
| WCP BATCH 4 | 2.67 | 10.43 | 1.36 | 1.25 | 1.77 | 2.03 | 0.00 | 3.43 | 8.14 | 0.25 | 0.84 | 0.00 | 0.14 | 0.09 | 0.23 | 0.20 | 0.00 | 11.71 | 3.86 | 0.00 | 4.29 | 1.43 | 2.54 | 0.00 | 0.20 | 9.16 | 0.39 | 1.06 | 0.00 | 0.00 | 50.10 | 0.00 | 1.03 | 0.00 | 0.00 | 0.22 | 99.31 | | | | | | | | | | | | | | | | | | | | | | | | | | | | | | | | | | | | | |
| WCP BLEND 1 | 2.64 | 10.22 | 1.26 | 1.22 | 1.73 | 2.00 | 0.00 | 4.16 | 8.05 | 0.18 | 1.03 | 0.00 | 0.13 | 0.08 | 0.22 | 0.20 | 0.00 | 10.91 | 3.68 | 0.00 | 4.44 | 1.41 | 1.67 | 0.00 | 0.15 | 9.13 | 0.22 | 0.89 | 0.00 | 0.00 | 51.90 | 0.00 | 0.89 | 0.00 | 0.00 | 0.14 | 99.48 | | | | | | | | | | | | | | | | | | | | | | | | | | | | | | | | | | | | | |
| WCP BLEND 1 | 2.64 | 10.45 | 1.29 | 1.22 | 1.73 | 2.01 | 0.00 | 4.16 | 8.05 | 0.18 | 1.03 | 0.00 | 0.13 | 0.08 | 0.22 | 0.20 | 0.00 | 10.91 | 3.68 | 0.00 | 4.44 | 1.41 | 1.67 | 0.00 | 0.15 | 9.13 | 0.22 | 0.89 | 0.00 | 0.00 | 51.90 | 0.00 | 0.89 | 0.00 | 0.00 | 0.14 | 99.48 | | | | | | | | | | | | | | | | | | | | | | | | | | | | | | | | | | | | | |
| WCP BLEND 1 | 2.64 | 10.17 | 1.26 | 1.20 | 1.71 | 2.01 | 0.00 | 4.16 | 8.05 | 0.18 | 1.03 | 0.00 | 0.13 | 0.08 | 0.22 | 0.20 | 0.00 | 10.91 | 3.68 | 0.00 | 4.44 | 1.41 | 1.67 | 0.00 | 0.15 | 9.13 | 0.22 | 0.89 | 0.00 | 0.00 | 51.90 | 0.00 | 0.89 | 0.00 | 0.00 | 0.14 | 99.48 | | | | | | | | | | | | | | | | | | | | | | | | | | | | | | | | | | | | | |

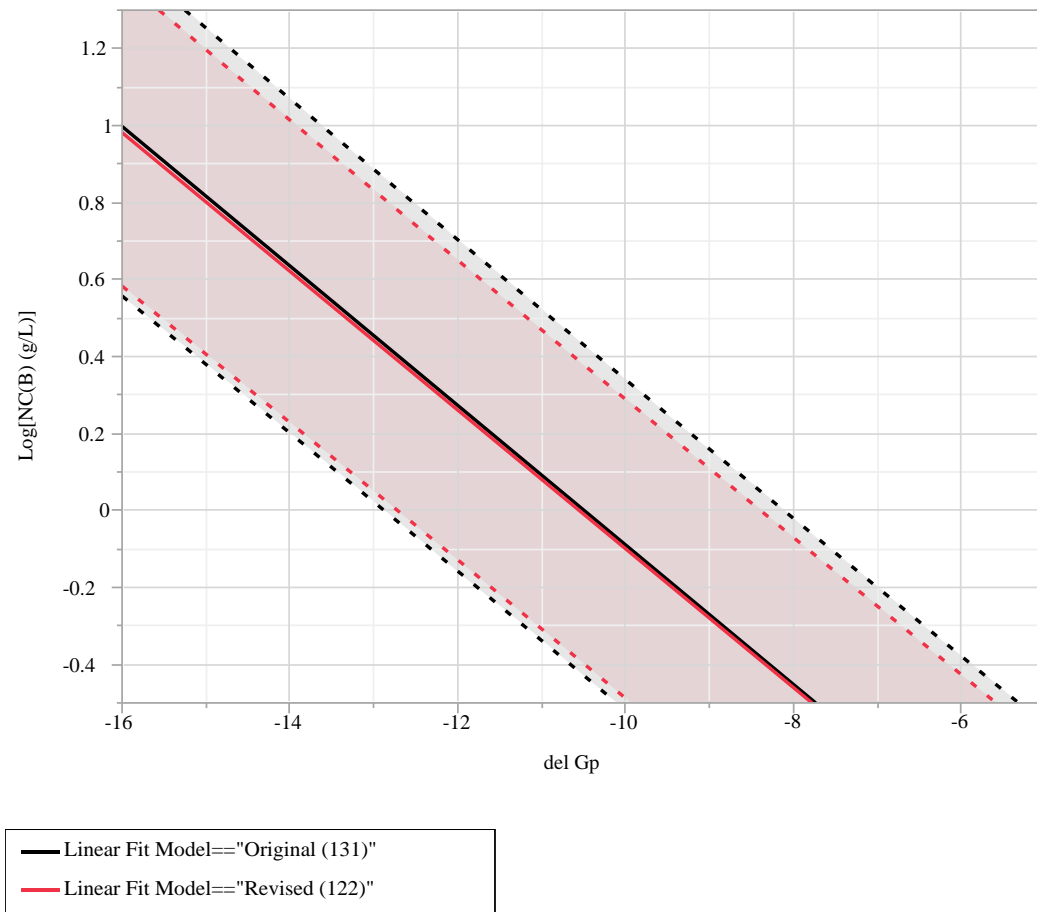
| Sample ID | Measured Density (g/cc) | Mean(Measured pH) | Mean(log[B (ppm)]) | Mean(log[Li (ppm)]) | Mean(log[Na (ppm)]) | Mean(log[Si (ppm)]) | FeII/FeIII | Al2O3(v) | B2O3(v) | BaO(v) | CaO(v) | Ce2O3(v) | Cr2O3(v) | Cs2O(v) | CuO(v) | Cn2O(v) | FeO(v) | Fe2O3(v) | K2O(v) | La2O3(v) | Li2O(v) | MgO(v) | MnO(v) | MnO2(v) | MoO3(v) | Na2O(v) | Nd2O3(v) | NiO(v) | P2O5(v) | PhO(v) | SiO2(v) | SrO(v) | TiO2(v) | Y2O3(v) | ZnO(v) | ZrO2(v) | *Oxides(v) |
|-----------|-------------------------|-------------------|--------------------|---------------------|---------------------|---------------------|------------|----------|---------|--------|--------|----------|----------|---------|--------|---------|--------|----------|--------|----------|---------|--------|--------|---------|---------|---------|----------|--------|---------|--------|---------|--------|---------|---------|--------|---------|------------|
| WCP HM | 2.59 | 10.13 | 1.00 | 1.13 | 1.49 | 1.90 | 0.00 | 7.15 | 7.03 | 0.11 | 1.01 | 0.00 | 0.09 | 0.06 | 0.13 | 0.11 | 0.00 | 7.78 | 2.21 | 0.00 | 4.62 | 1.49 | 1.75 | 0.00 | 0.22 | 8.56 | 0.55 | 0.41 | 0.00 | 0.00 | 55.80 | 0.00 | 0.56 | 0.00 | 0.00 | 0.33 | 99.97 |
| WCP HM | 2.59 | 9.87 | 0.98 | 1.08 | 1.45 | 1.91 | 0.00 | 7.15 | 7.03 | 0.11 | 1.01 | 0.00 | 0.09 | 0.06 | 0.13 | 0.11 | 0.00 | 7.78 | 2.21 | 0.00 | 4.62 | 1.49 | 1.75 | 0.00 | 0.22 | 8.56 | 0.55 | 0.41 | 0.00 | 0.00 | 55.80 | 0.00 | 0.56 | 0.00 | 0.00 | 0.33 | 99.97 |
| WCP HM | 2.59 | 10.28 | 1.01 | 1.09 | 1.47 | 1.90 | 0.00 | 7.15 | 7.03 | 0.11 | 1.01 | 0.00 | 0.09 | 0.06 | 0.13 | 0.11 | 0.00 | 7.78 | 2.21 | 0.00 | 4.62 | 1.49 | 1.75 | 0.00 | 0.22 | 8.56 | 0.55 | 0.41 | 0.00 | 0.00 | 55.80 | 0.00 | 0.56 | 0.00 | 0.00 | 0.33 | 99.97 |
| WCP PUREX | 2.68 | 10.75 | 1.96 | 1.55 | 2.35 | 2.26 | 0.00 | 2.99 | 10.33 | 0.20 | 1.09 | 0.00 | 0.15 | 0.06 | 0.21 | 0.19 | 0.00 | 13.25 | 3.41 | 0.00 | 3.22 | 1.41 | 1.69 | 0.00 | 0.08 | 12.62 | 0.06 | 1.19 | 0.00 | 0.00 | 46.50 | 0.00 | 0.68 | 0.00 | 0.00 | 0.05 | 99.38 |
| WCP PUREX | 2.68 | 10.60 | 1.85 | 1.44 | 2.29 | 2.25 | 0.00 | 2.99 | 10.33 | 0.20 | 1.09 | 0.00 | 0.15 | 0.06 | 0.21 | 0.19 | 0.00 | 13.25 | 3.41 | 0.00 | 3.22 | 1.41 | 1.69 | 0.00 | 0.08 | 12.62 | 0.06 | 1.19 | 0.00 | 0.00 | 46.50 | 0.00 | 0.68 | 0.00 | 0.00 | 0.05 | 99.38 |
| WCP PUREX | 2.68 | 10.66 | 1.92 | 1.50 | 2.45 | 2.29 | 0.00 | 2.99 | 10.33 | 0.20 | 1.09 | 0.00 | 0.15 | 0.06 | 0.21 | 0.19 | 0.00 | 13.25 | 3.41 | 0.00 | 3.22 | 1.41 | 1.69 | 0.00 | 0.08 | 12.62 | 0.06 | 1.19 | 0.00 | 0.00 | 46.50 | 0.00 | 0.68 | 0.00 | 0.00 | 0.05 | 99.38 |
| WCP PUREX | 2.68 | 10.64 | 1.80 | 1.39 | 2.22 | 2.20 | 0.00 | 2.99 | 10.33 | 0.20 | 1.09 | 0.00 | 0.15 | 0.06 | 0.21 | 0.19 | 0.00 | 13.25 | 3.41 | 0.00 | 3.22 | 1.41 | 1.69 | 0.00 | 0.08 | 12.62 | 0.06 | 1.19 | 0.00 | 0.00 | 46.50 | 0.00 | 0.68 | 0.00 | 0.00 | 0.05 | 99.38 |
| WCP PUREX | 2.68 | 10.63 | 1.87 | 1.48 | 2.28 | 2.27 | 0.00 | 2.99 | 10.33 | 0.20 | 1.09 | 0.00 | 0.15 | 0.06 | 0.21 | 0.19 | 0.00 | 13.25 | 3.41 | 0.00 | 3.22 | 1.41 | 1.69 | 0.00 | 0.08 | 12.62 | 0.06 | 1.19 | 0.00 | 0.00 | 46.50 | 0.00 | 0.68 | 0.00 | 0.00 | 0.05 | 99.38 |
| WCP PUREX | 2.68 | 10.62 | 1.85 | 1.47 | 2.27 | 2.32 | 0.00 | 2.99 | 10.33 | 0.20 | 1.09 | 0.00 | 0.15 | 0.06 | 0.21 | 0.19 | 0.00 | 13.25 | 3.41 | 0.00 | 3.22 | 1.41 | 1.69 | 0.00 | 0.08 | 12.62 | 0.06 | 1.19 | 0.00 | 0.00 | 46.50 | 0.00 | 0.68 | 0.00 | 0.00 | 0.05 | 99.38 |
| MAX* | 2.75 | 11.95 | 2.81 | 2.33 | 3.26 | 3.03 | 0.32 | 13.90 | 13.30 | 0.66 | 2.23 | 1.44 | 0.55 | 1.16 | 0.33 | 0.30 | 2.58 | 14.30 | 5.73 | 0.42 | 5.08 | 3.24 | 3.36 | 0.00 | 1.67 | 16.80 | 5.96 | 1.71 | 0.65 | 0.25 | 57.00 | 0.45 | 3.21 | 0.01 | 1.46 | 1.80 | 104.28 |
| MIN* | 2.52 | 9.20 | 0.87 | 0.79 | 1.20 | 1.62 | 0.00 | 2.99 | 6.10 | 0.00 | 0.38 | 0.00 | 0.00 | 0.00 | 0.00 | 0.00 | 0.00 | 0.00 | 0.00 | 0.00 | 0.00 | 0.00 | 0.00 | 0.00 | 0.00 | 39.80 | 0.00 | 0.00 | 0.00 | 0.00 | 0.00 | 95.52 | | | | | |

* maximum and minimum values are for the data actually used in modeling.

APPENDIX D. Uncertainties for THERMO™ Models

Exhibit E1. Summary of the Fitted Models (THERMO™ and Modified THERMO™) for Each Element of Interest

Bivariate Fit of Log[NC(B) (g/L)] By del Gp



Linear Fit Model=="Original (131)"

$$\text{Log}[NC(B) \text{ (g/L)}] = -1.901447 - 0.1812039 \cdot \text{del Gp}$$

Summary of Fit

| | |
|----------------------------|----------|
| RSquare | 0.767961 |
| RSquare Adj | 0.766163 |
| Root Mean Square Error | 0.216264 |
| Mean of Response | -0.02685 |
| Observations (or Sum Wgts) | 131 |

Analysis of Variance

| Source | DF | Sum of Squares | Mean Square | F Ratio |
|----------|-----|----------------|-------------|----------|
| Model | 1 | 19.968089 | 19.9681 | 426.9422 |
| Error | 129 | 6.033331 | 0.0468 | Prob > F |
| C. Total | 130 | 26.001420 | | <.0001* |

Parameter Estimates

| Term | Estimate | Std Error | t Ratio | Prob> t |
|-----------|-----------|-----------|---------|---------|
| Intercept | -1.901447 | 0.092671 | -20.52 | <.0001* |
| del Gp | -0.181204 | 0.00877 | -20.66 | <.0001* |

Linear Fit Model=="Revised (122)"

$$\text{Log}[NC(B) \text{ (g/L)}] = -1.901602 - 0.180215 \cdot \text{del Gp}$$

Summary of Fit

| | |
|----------------------------|----------|
| RSquare | 0.806193 |
| RSquare Adj | 0.804578 |
| Root Mean Square Error | 0.195316 |
| Mean of Response | -0.05128 |
| Observations (or Sum Wgts) | 122 |

Analysis of Variance

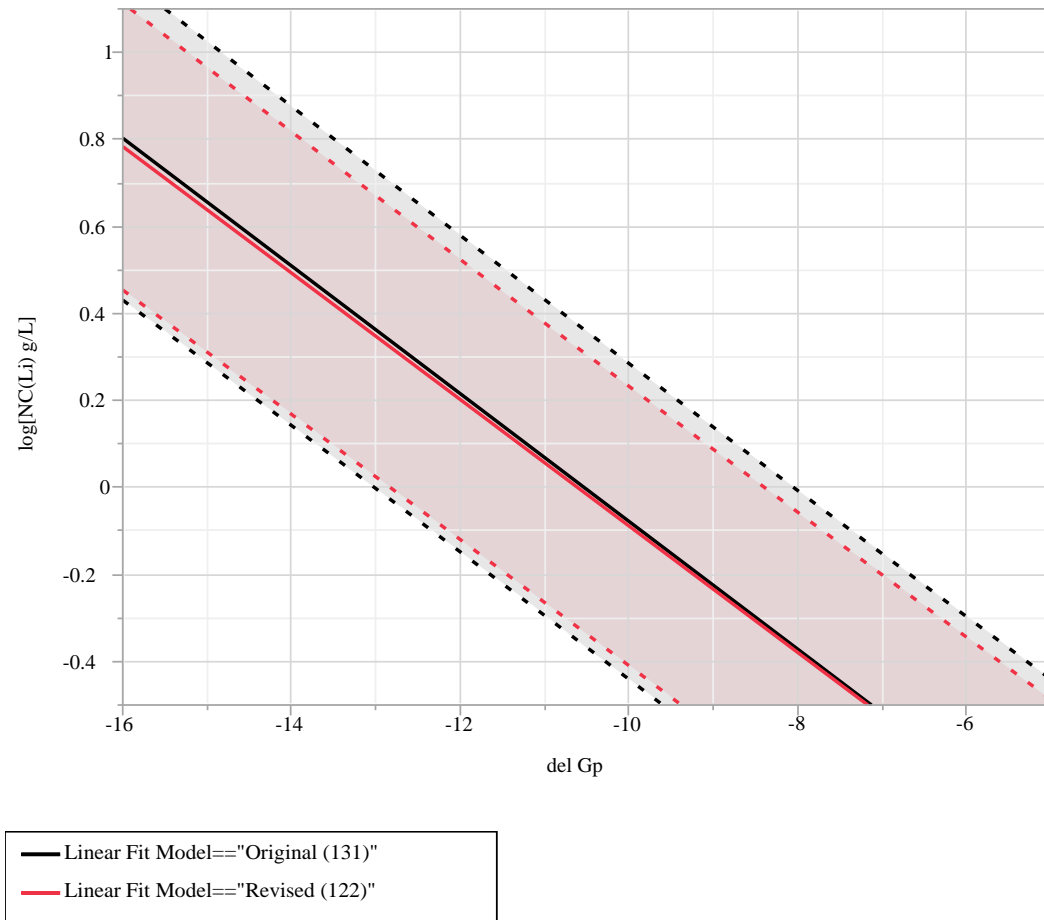
| Source | DF | Sum of Squares | Mean Square | F Ratio |
|----------|-----|----------------|-------------|----------|
| Model | 1 | 19.042657 | 19.0427 | 499.1722 |
| Error | 120 | 4.577817 | 0.0381 | Prob > F |
| C. Total | 121 | 23.620474 | | <.0001* |

Parameter Estimates

| Term | Estimate | Std Error | t Ratio | Prob> t |
|-----------|-----------|-----------|---------|---------|
| Intercept | -1.901602 | 0.084684 | -22.46 | <.0001* |
| del Gp | -0.180215 | 0.008066 | -22.34 | <.0001* |

Exhibit E1. Summary of the Fitted Models (THERMO™ and Modified THERMO™) for Each Element of Interest (continued)

Bivariate Fit of log[NC(Li) g/L] By del Gp



Linear Fit Model=="Original (131)"
 $\log[\text{NC}(\text{Li}) \text{ g/L}] = -1.545942 - 0.1468048 * \text{del Gp}$

Summary of Fit

| | |
|----------------------------|----------|
| RSquare | 0.752663 |
| RSquare Adj | 0.750746 |
| Root Mean Square Error | 0.182722 |
| Mean of Response | -0.02721 |
| Observations (or Sum Wgts) | 131 |

Analysis of Variance

| Source | DF | Sum of Squares | Mean Square | F Ratio |
|----------|-----|----------------|-------------|----------|
| Model | 1 | 13.106354 | 13.1064 | 392.5554 |
| Error | 129 | 4.306958 | 0.0334 | Prob > F |
| C. Total | 130 | 17.413312 | | <.0001* |

Parameter Estimates

| Term | Estimate | Std Error | t Ratio | Prob> t |
|-----------|-----------|-----------|---------|---------|
| Intercept | -1.545942 | 0.078298 | -19.74 | <.0001* |
| del Gp | -0.146805 | 0.00741 | -19.81 | <.0001* |

Linear Fit Model=="Revised (122)"

$\log[\text{NC}(\text{Li}) \text{ g/L}] = -1.541811 - 0.1453413 * \text{del Gp}$

Summary of Fit

| | |
|----------------------------|----------|
| RSquare | 0.79831 |
| RSquare Adj | 0.796629 |
| Root Mean Square Error | 0.161483 |
| Mean of Response | -0.04955 |
| Observations (or Sum Wgts) | 122 |

Analysis of Variance

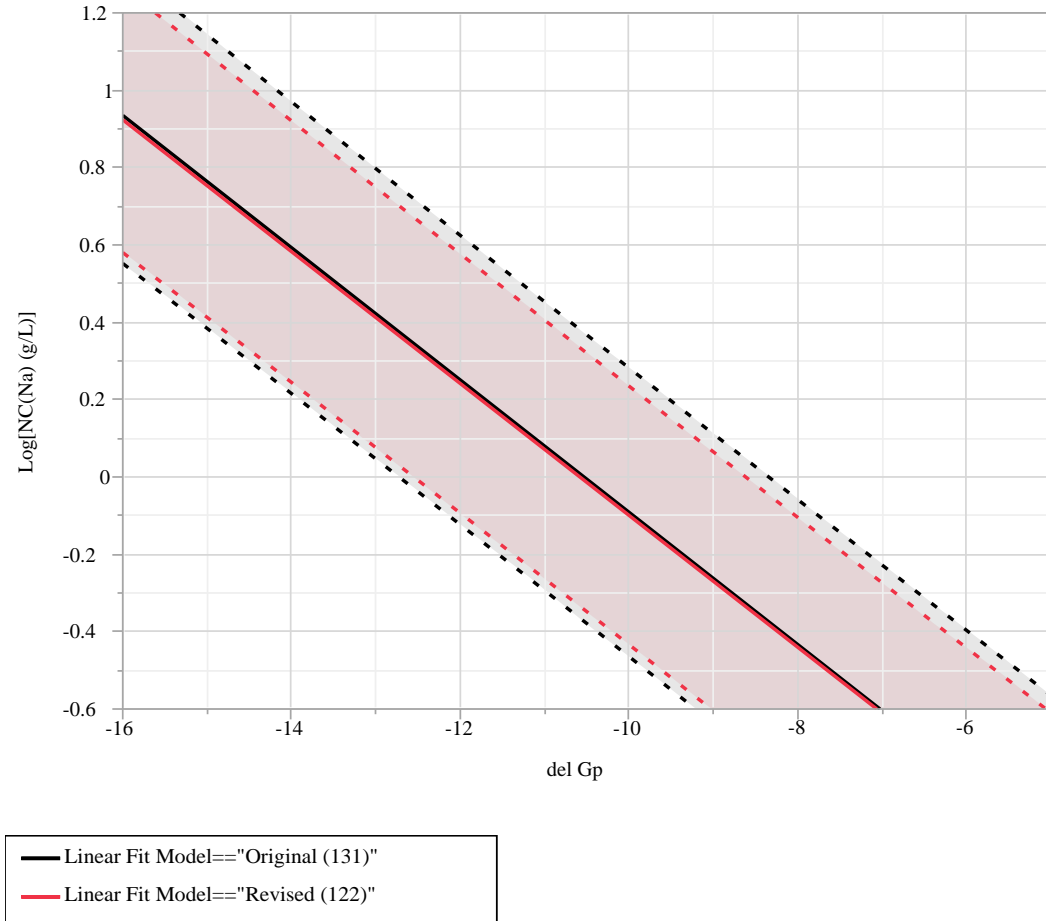
| Source | DF | Sum of Squares | Mean Square | F Ratio |
|----------|-----|----------------|-------------|----------|
| Model | 1 | 12.385791 | 12.3858 | 474.9715 |
| Error | 120 | 3.129230 | 0.0261 | Prob > F |
| C. Total | 121 | 15.515021 | | <.0001* |

Parameter Estimates

| Term | Estimate | Std Error | t Ratio | Prob> t |
|-----------|-----------|-----------|---------|---------|
| Intercept | -1.541811 | 0.070015 | -22.02 | <.0001* |
| del Gp | -0.145341 | 0.006669 | -21.79 | <.0001* |

Exhibit D1. Summary of the Fitted Models (THERMOTM and Modified THERMOTM) for Each Element of Interest (continued)

Bivariate Fit of Log[NC(Na) (g/L)] By del Gp



Linear Fit Model=="Original (131)"
 $\text{Log}[\text{NC}(\text{Na}) \text{ (g/L)}] = -1.801158 - 0.1710066 \text{del Gp}$

Summary of Fit

| | |
|----------------------------|----------|
| RSquare | 0.796146 |
| RSquare Adj | 0.794566 |
| Root Mean Square Error | 0.187881 |
| Mean of Response | -0.03205 |
| Observations (or Sum Wgts) | 131 |

Analysis of Variance

| Source | DF | Sum of Squares | Mean Square | F Ratio |
|----------|-----|----------------|-------------|--------------------|
| Model | 1 | 17.783905 | 17.7839 | 503.8055 |
| Error | 129 | 4.553590 | 0.0353 | Prob > F |
| C. Total | 130 | 22.337495 | | <.0001* |

Parameter Estimates

| Term | Estimate | Std Error | t Ratio | Prob> t |
|-----------|-----------|-----------|---------|---------|
| Intercept | -1.801158 | 0.080509 | -22.37 | <.0001* |
| del Gp | -0.171007 | 0.007619 | -22.45 | <.0001* |

Linear Fit Model=="Revised (122)"

$\text{Log}[\text{NC}(\text{Na}) \text{ (g/L)}] = -1.803846 - 0.1704731 \text{del Gp}$

Summary of Fit

| | |
|----------------------------|----------|
| RSquare | 0.833973 |
| RSquare Adj | 0.832589 |
| Root Mean Square Error | 0.168133 |
| Mean of Response | -0.05355 |
| Observations (or Sum Wgts) | 122 |

Analysis of Variance

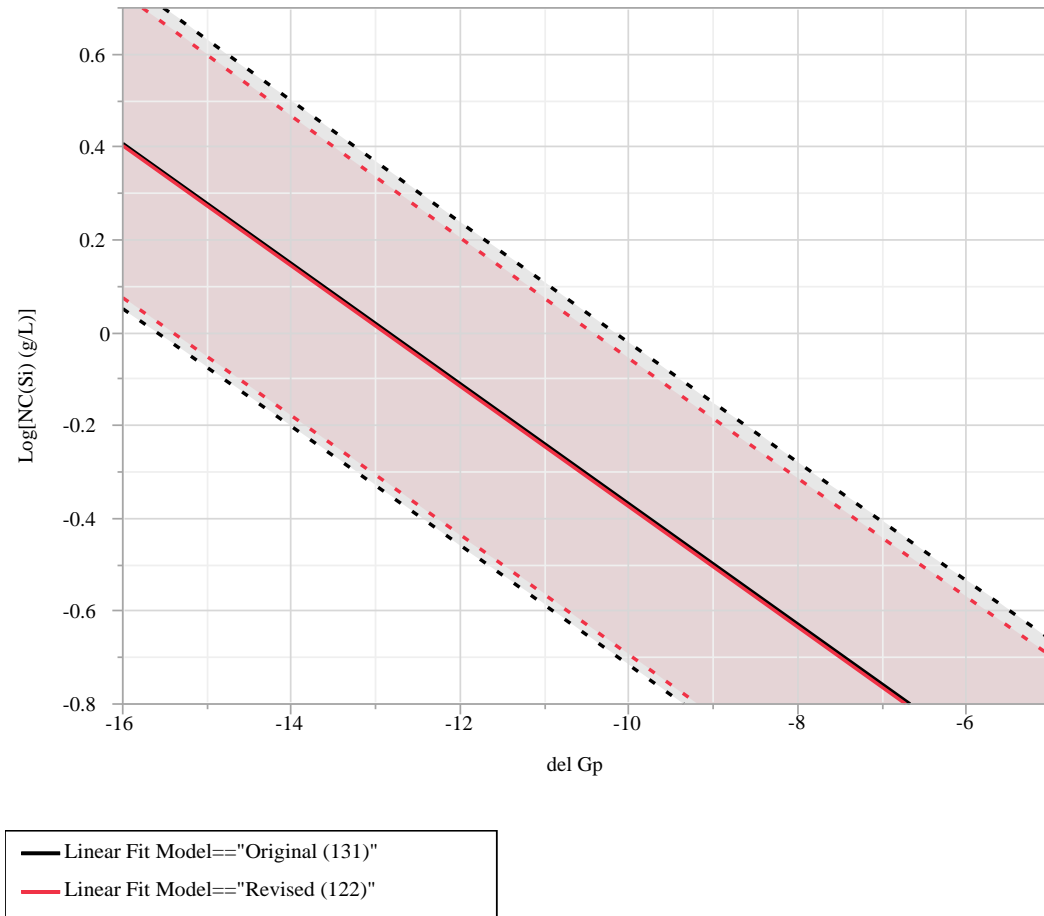
| Source | DF | Sum of Squares | Mean Square | F Ratio |
|----------|-----|----------------|-------------|--------------------|
| Model | 1 | 17.039533 | 17.0395 | 602.7731 |
| Error | 120 | 3.392228 | 0.0283 | Prob > F |
| C. Total | 121 | 20.431761 | | <.0001* |

Parameter Estimates

| Term | Estimate | Std Error | t Ratio | Prob> t |
|-----------|-----------|-----------|---------|---------|
| Intercept | -1.803846 | 0.072898 | -24.74 | <.0001* |
| del Gp | -0.170473 | 0.006944 | -24.55 | <.0001* |

Exhibit D1. Summary of the Fitted Models (THERMO™ and Modified THERMO™) for Each Element of Interest (continued)

Bivariate Fit of Log[NC(Si) (g/L)] By del Gp



Linear Fit Model=="Original (131)"
 $\text{Log}[\text{NC}(\text{Si}) \text{ (g/L)}] = -1.663012 - 0.1294282 \cdot \text{del Gp}$

Summary of Fit

| | |
|----------------------------|----------|
| RSquare | 0.721106 |
| RSquare Adj | 0.718944 |
| Root Mean Square Error | 0.174765 |
| Mean of Response | -0.32404 |
| Observations (or Sum Wgts) | 131 |

Analysis of Variance

| Source | DF | Sum of Squares | Mean Square | F Ratio |
|----------|-----|----------------|-------------|--------------------|
| Model | 1 | 10.187306 | 10.1873 | 333.5415 |
| Error | 129 | 3.940027 | 0.0305 | Prob > F |
| C. Total | 130 | 14.127333 | | <.0001* |

Parameter Estimates

| Term | Estimate | Std Error | t Ratio | Prob> t |
|-----------|-----------|-----------|---------|---------|
| Intercept | -1.663012 | 0.074889 | -22.21 | <.0001* |
| del Gp | -0.129428 | 0.007087 | -18.26 | <.0001* |

Linear Fit Model=="Revised (122)"

$\text{Log}[\text{NC}(\text{Si}) \text{ (g/L)}] = -1.671061 - 0.1296432 \cdot \text{del Gp}$

Summary of Fit

| | |
|----------------------------|----------|
| RSquare | 0.761252 |
| RSquare Adj | 0.759263 |
| Root Mean Square Error | 0.160486 |
| Mean of Response | -0.33998 |
| Observations (or Sum Wgts) | 122 |

Analysis of Variance

| Source | DF | Sum of Squares | Mean Square | F Ratio |
|----------|-----|----------------|-------------|--------------------|
| Model | 1 | 9.854737 | 9.85474 | 382.6225 |
| Error | 120 | 3.090693 | 0.02576 | Prob > F |
| C. Total | 121 | 12.945430 | | <.0001* |

Parameter Estimates

| Term | Estimate | Std Error | t Ratio | Prob> t |
|-----------|-----------|-----------|---------|---------|
| Intercept | -1.671061 | 0.069583 | -24.02 | <.0001* |
| del Gp | -0.129643 | 0.006628 | -19.56 | <.0001* |

Exhibit D2. THERMO™ Model with 131 points; Modified THERMO™ Model with 122 points

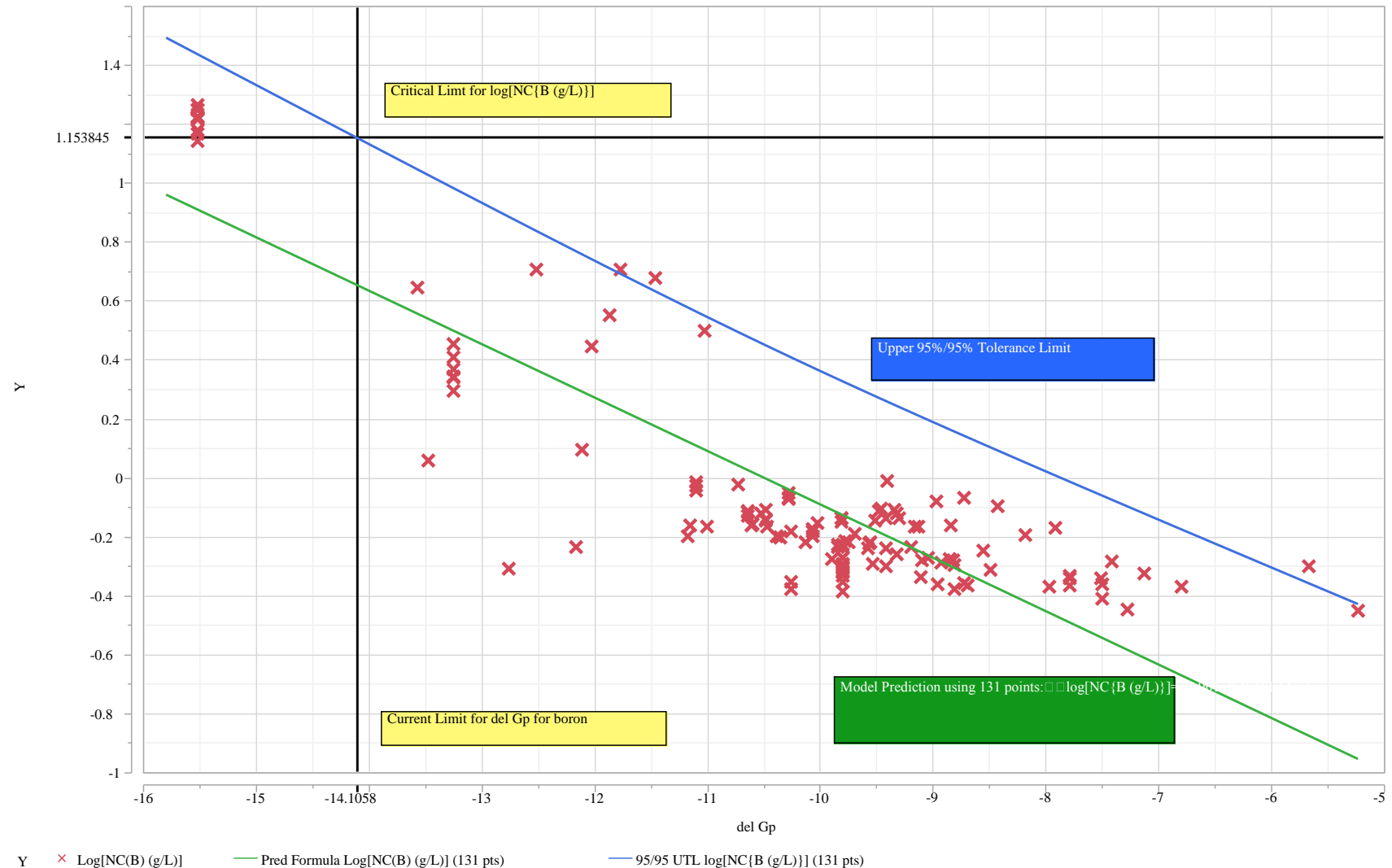


Exhibit D3. Summary of the Fitted Models (THERMO™ and Modified THERMO™) for Each Element of Interest THERMO™ Model with 131 points; Modified THERMO™ Model with 122 points

THERMO™ Model with 131 points; Modified THERMO™ Model with 122 points

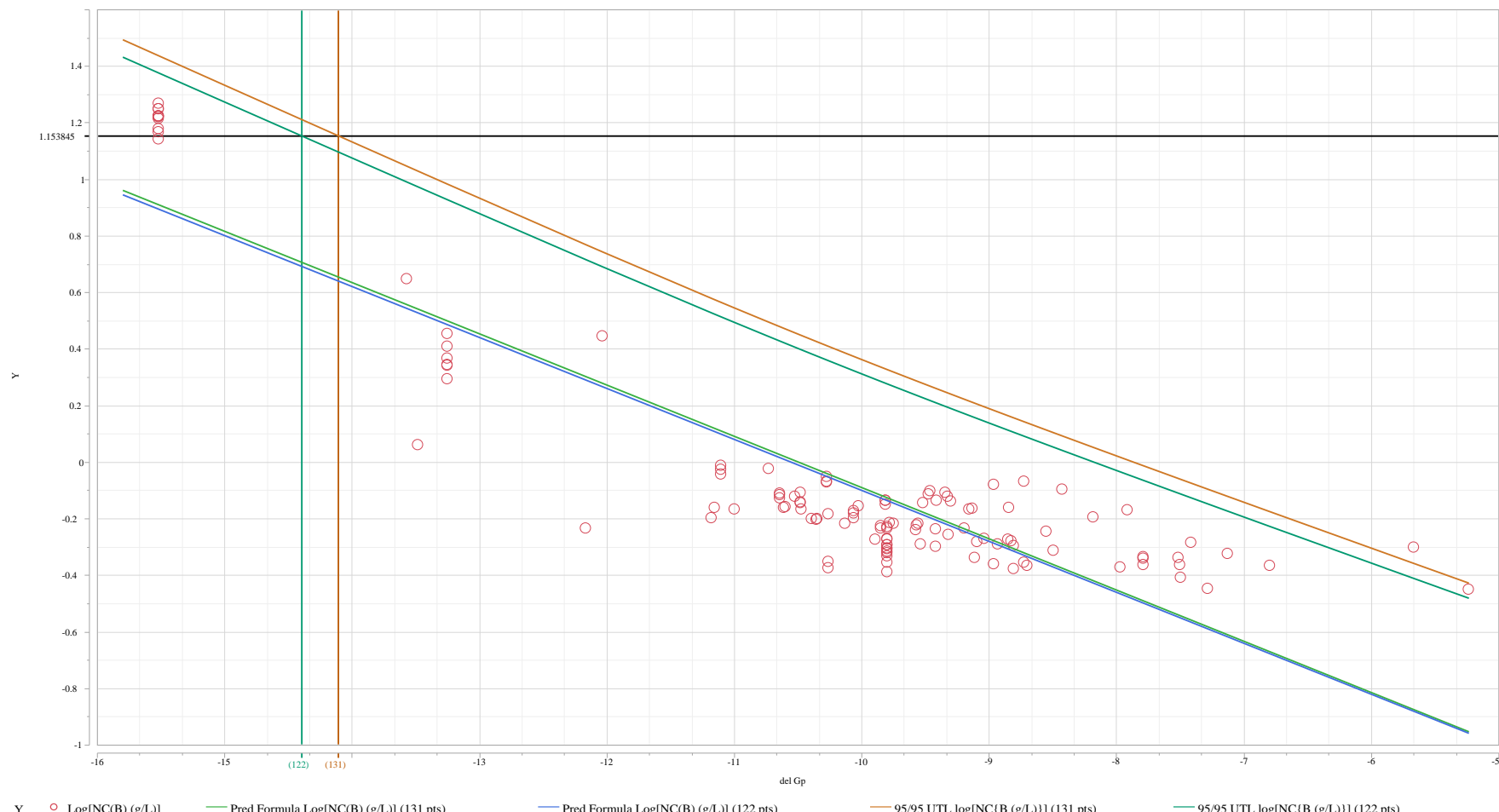


Exhibit D3. Summary of the Fitted Models (THERMOTM and Modified THERMOTM) for Each Element of Interest (continued)
THERMOTM Model with 131 points; Modified THERMOTM Model with 122 points

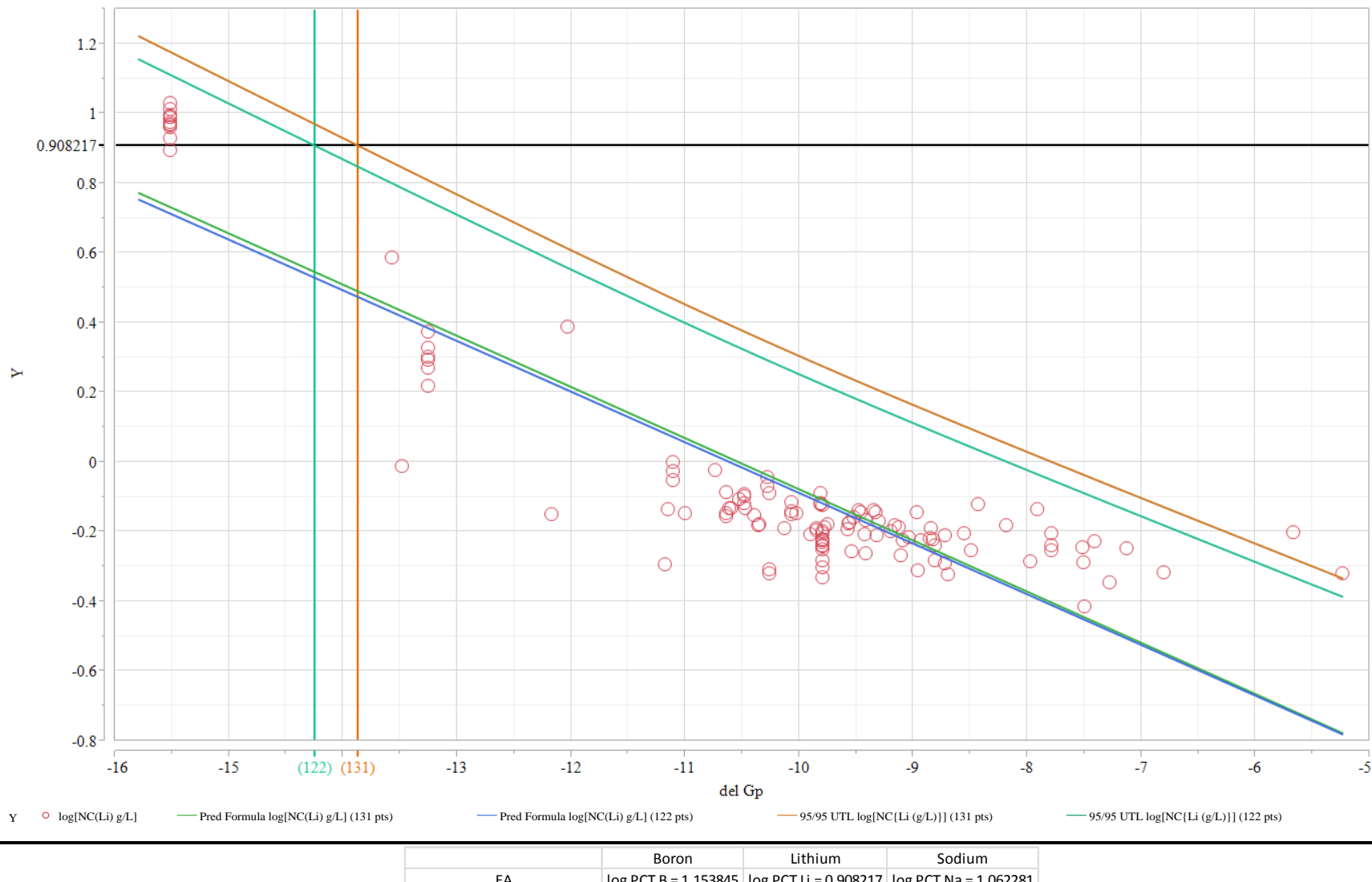
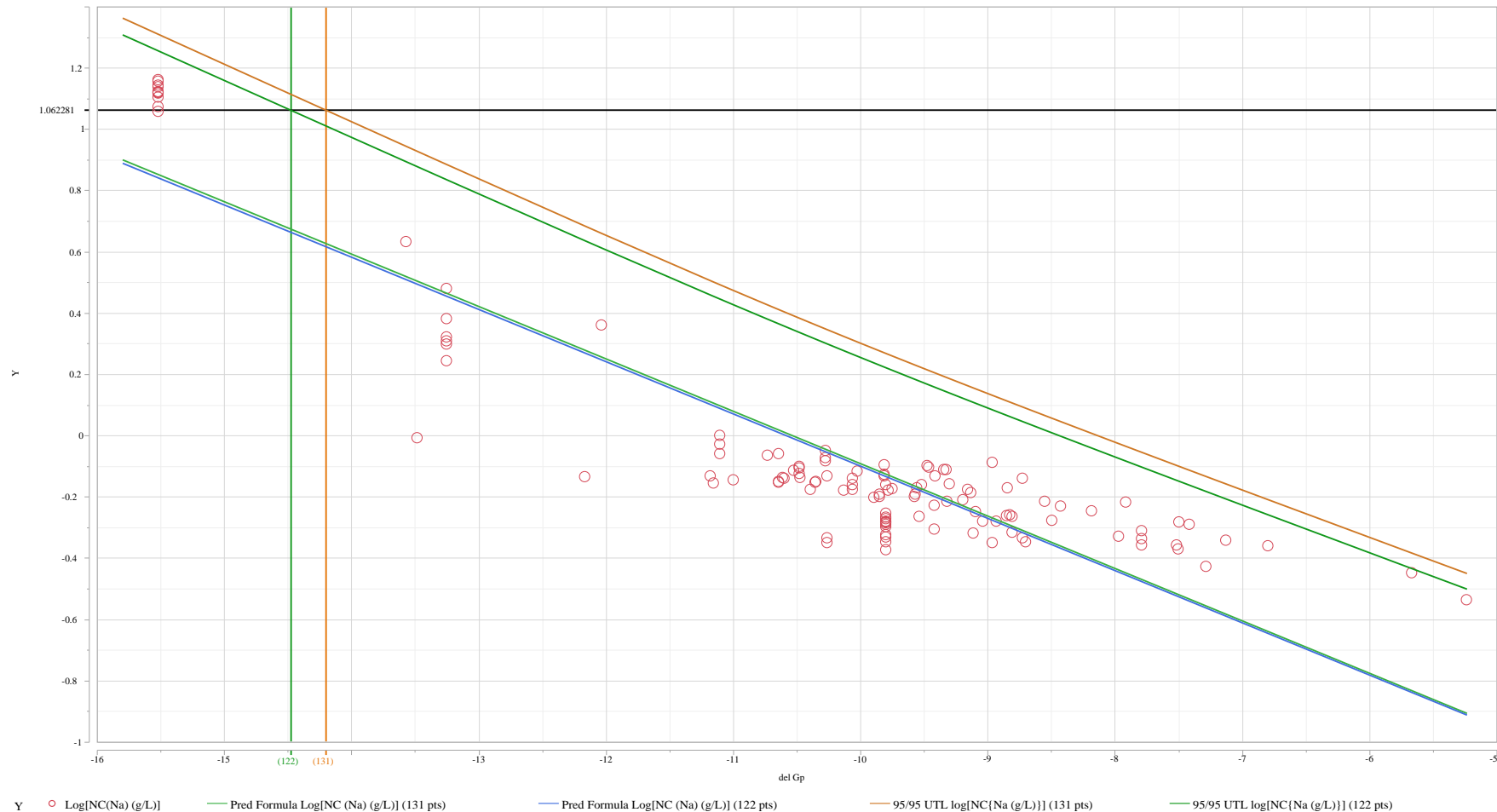


Exhibit D3. Summary of the Fitted Models (THERMO™ and Modified THERMO™) for Each Element of Interest (continued)

THERMO™ Model with 131 points; Modified THERMO™ Model with 122 points



| | Boron | Lithium | Sodium |
|-----------------------------|----------------------|-----------------------|-----------------------|
| EA | log PCT B = 1.153845 | log PCT Li = 0.908217 | log PCT Na = 1.062281 |
| Current PCCS Del Gp Limits: | -14.1058 | -13.8695 | -14.1991 |
| Revised PCCS Del Gp Limits: | -14.3952 | -14.2481 | -14.4765 |

Exhibit Z2. Summary of the Fitted Models (Historic and Modified Historic) for Each Element of Interest

Historic Model with 131 points; Modified Historic Model with 122 points

APPENDIX E. SRNL High TiO₂ Glass Validation Data (Measured Bias Corrected wt% on a vitrified oxide basis indicated by “v”).

| Sample ID | Glass Density (g/cc) | Mean(log[B (ppm)]) | Mean(log[Li (ppm)]) | Mean(log[Na (ppm)]) | Mean(log[Si (ppm)]) | Al2O3(v) | B2O3(v) | BaO(v) | CaO(v) | CdO (v) | Ce2O3(v) | Cr2O3(v) | Cs2O(v) | CuO(v) | Cu2O(v) | Fe2O3(v) | K2O(v) | La2O3(v) | Li2O(v) | MgO(v) | MnO(v) | Na2O(v) | NiO(v) | PbO(v) | SO4(v) | SiO2(v) | TiO2(v) | U3O8 (v) | ZnO(v) | ZrO2(v) | Oxide Sum (v) |
|---------------|----------------------|--------------------|---------------------|---------------------|---------------------|----------|---------|--------|--------|---------|----------|----------|---------|--------|---------|----------|--------|----------|---------|--------|--------|---------|--------|--------|--------|---------|---------|----------|--------|---------|---------------|
| HWL-01 | 2.68 | 1.19 | 1.22 | 1.55 | 1.89 | 10.90 | 7.84 | 0.09 | 1.22 | 0.00 | 0.23 | 0.10 | 0.00 | 0.02 | 0.02 | 13.74 | 0.10 | 0.08 | 5.26 | 0.19 | 1.51 | 10.16 | 0.45 | 0.10 | 0.00 | 44.12 | 1.42 | 0.00 | 0.05 | 0.22 | 97.82 |
| HWL-02 | 2.59 | 1.21 | 1.23 | 1.70 | 1.88 | 12.15 | 7.11 | 0.11 | 1.38 | 0.00 | 0.26 | 0.11 | 0.00 | 0.02 | 0.02 | 16.16 | 0.11 | 0.09 | 4.66 | 0.22 | 1.79 | 11.27 | 0.51 | 0.11 | 0.00 | 41.56 | 1.61 | 0.00 | 0.06 | 0.25 | 99.55 |
| HWL-03 | 2.68 | 1.27 | 1.16 | 1.52 | 1.84 | 10.83 | 9.92 | 0.10 | 1.21 | 0.00 | 0.24 | 0.10 | 0.00 | 0.02 | 0.02 | 13.53 | 0.09 | 0.09 | 4.37 | 0.20 | 1.49 | 10.15 | 0.48 | 0.10 | 0.00 | 42.09 | 1.47 | 0.00 | 0.06 | 0.23 | 96.79 |
| HWL-04 | 2.67 | 1.31 | 1.18 | 1.68 | 1.80 | 11.97 | 9.33 | 0.11 | 1.36 | 0.00 | 0.26 | 0.11 | 0.00 | 0.02 | 0.02 | 15.28 | 0.10 | 0.09 | 4.34 | 0.21 | 1.69 | 11.34 | 0.49 | 0.11 | 0.00 | 39.10 | 1.62 | 0.00 | 0.06 | 0.25 | 97.88 |
| HWL-05 | 2.73 | 1.29 | 1.29 | 1.72 | 1.96 | 7.03 | 7.57 | 0.12 | 1.58 | 0.00 | 0.25 | 0.13 | 0.00 | 0.03 | 0.02 | 16.05 | 0.12 | 0.09 | 5.14 | 0.22 | 2.03 | 10.77 | 0.49 | 0.11 | 0.00 | 45.46 | 1.23 | 0.00 | 0.07 | 0.27 | 98.78 |
| HWL-06 | 2.77 | 1.35 | 1.32 | 1.86 | 1.95 | 7.69 | 7.30 | 0.12 | 1.74 | 0.00 | 0.27 | 0.16 | 0.00 | 0.03 | 0.03 | 17.62 | 0.13 | 0.10 | 4.77 | 0.24 | 2.25 | 11.68 | 0.57 | 0.11 | 0.00 | 41.82 | 1.38 | 0.00 | 0.08 | 0.30 | 98.41 |
| HWL-07 | 2.73 | 1.16 | 1.32 | 1.97 | 2.03 | 6.92 | 4.90 | 0.11 | 1.53 | 0.00 | 0.25 | 0.15 | 0.00 | 0.03 | 0.02 | 16.01 | 0.11 | 0.09 | 5.10 | 0.22 | 2.02 | 12.17 | 0.54 | 0.11 | 0.00 | 46.37 | 1.25 | 0.00 | 0.07 | 0.27 | 98.24 |
| HWL-08 | 2.77 | 1.36 | 1.22 | 1.55 | 1.90 | 7.78 | 4.33 | 0.13 | 1.77 | 0.00 | 0.27 | 0.15 | 0.00 | 0.03 | 0.03 | 16.98 | 0.13 | 0.11 | 4.55 | 0.24 | 2.19 | 13.22 | 0.57 | 0.12 | 0.00 | 42.73 | 1.37 | 0.00 | 0.08 | 0.29 | 97.07 |
| HWL-09 | 2.66 | 1.07 | 1.31 | 1.87 | 2.09 | 4.53 | 11.91 | 0.07 | 0.84 | 0.00 | 0.18 | 0.08 | 0.00 | 0.02 | 0.02 | 10.37 | 0.06 | 0.06 | 5.42 | 0.13 | 2.84 | 8.00 | 0.60 | 0.10 | 0.00 | 49.36 | 2.25 | 0.00 | 0.03 | 0.72 | 97.58 |
| HWL-10 | 2.71 | 1.07 | 1.26 | 1.97 | 2.03 | 5.12 | 11.12 | 0.09 | 0.98 | 0.00 | 0.20 | 0.09 | 0.00 | 0.02 | 0.02 | 11.73 | 0.07 | 0.07 | 5.18 | 0.16 | 3.25 | 8.99 | 0.66 | 0.12 | 0.00 | 46.26 | 2.58 | 0.00 | 0.04 | 0.82 | 97.55 |
| HWL-11 | 2.77 | 1.29 | 1.07 | 1.40 | 1.87 | 5.70 | 10.14 | 0.10 | 1.12 | 0.00 | 0.23 | 0.08 | 0.00 | 0.02 | 0.02 | 12.85 | 0.08 | 0.08 | 4.77 | 0.18 | 3.68 | 9.86 | 0.72 | 0.12 | 0.00 | 43.16 | 2.89 | 0.00 | 0.04 | 0.86 | 96.70 |
| HWL-12 | 2.70 | 1.30 | 1.06 | 1.53 | 1.85 | 4.63 | 5.35 | 0.07 | 0.85 | 0.00 | 0.17 | 0.08 | 0.00 | 0.02 | 0.02 | 10.27 | 0.07 | 0.06 | 5.60 | 0.14 | 2.90 | 12.48 | 0.59 | 0.10 | 0.00 | 51.77 | 2.26 | 0.00 | 0.03 | 0.62 | 98.05 |
| HWL-13 | 2.74 | 1.09 | 1.33 | 1.86 | 2.11 | 5.17 | 4.85 | 0.10 | 0.99 | 0.00 | 0.20 | 0.08 | 0.00 | 0.02 | 0.02 | 11.50 | 0.08 | 0.07 | 5.15 | 0.16 | 3.22 | 13.27 | 0.66 | 0.12 | 0.00 | 47.07 | 2.62 | 0.00 | 0.04 | 0.72 | 96.10 |
| HWL-14 | 2.79 | 1.06 | 1.29 | 1.90 | 2.07 | 5.86 | 4.46 | 0.10 | 1.14 | 0.00 | 0.22 | 0.09 | 0.00 | 0.02 | 0.02 | 13.15 | 0.09 | 0.08 | 4.68 | 0.18 | 3.78 | 13.88 | 0.71 | 0.12 | 0.00 | 44.39 | 2.82 | 0.00 | 0.04 | 0.82 | 96.63 |
| HWL-15 | 2.62 | 1.08 | 1.27 | 1.94 | 2.04 | 3.91 | 12.52 | 0.07 | 0.87 | 0.00 | 0.21 | 0.06 | 0.00 | 0.01 | 0.01 | 10.53 | 0.06 | 0.07 | 4.37 | 0.14 | 1.94 | 7.59 | 0.27 | 0.10 | 0.00 | 51.83 | 2.57 | 0.00 | 0.01 | 0.53 | 97.65 |
| HWL-16 | 2.67 | 1.14 | 1.02 | 1.75 | 1.82 | 4.45 | 11.76 | 0.07 | 1.00 | 0.00 | 0.25 | 0.08 | 0.00 | 0.02 | 0.02 | 11.81 | 0.07 | 0.08 | 4.04 | 0.17 | 2.19 | 8.58 | 0.31 | 0.12 | 0.00 | 48.40 | 2.92 | 0.00 | 0.02 | 0.60 | 96.94 |
| HWL-17 | 2.72 | 1.15 | 1.00 | 1.87 | 1.80 | 5.05 | 10.57 | 0.09 | 1.15 | 0.00 | 0.28 | 0.08 | 0.00 | 0.02 | 0.02 | 13.61 | 0.07 | 0.09 | 3.66 | 0.19 | 2.54 | 9.46 | 0.36 | 0.14 | 0.00 | 45.73 | 3.35 | 0.00 | 0.02 | 0.70 | 97.18 |
| HWL-18 | 2.68 | 1.19 | 1.22 | 1.55 | 1.89 | 3.91 | 5.55 | 0.07 | 0.84 | 0.00 | 0.22 | 0.07 | 0.00 | 0.01 | 0.01 | 10.37 | 0.05 | 0.07 | 5.72 | 0.15 | 1.90 | 12.36 | 0.28 | 0.11 | 0.00 | 52.31 | 2.62 | 0.00 | 0.02 | 0.50 | 97.13 |
| HWL-19 | 2.72 | 1.21 | 1.23 | 1.70 | 1.88 | 4.48 | 5.14 | 0.08 | 1.01 | 0.00 | 0.24 | 0.09 | 0.00 | 0.02 | 0.01 | 11.67 | 0.07 | 0.08 | 5.27 | 0.16 | 2.23 | 13.14 | 0.32 | 0.12 | 0.00 | 49.95 | 2.93 | 0.00 | 0.02 | 0.62 | 97.64 |
| HWL-20 | 2.75 | 1.27 | 1.16 | 1.52 | 1.84 | 5.08 | 4.74 | 0.08 | 1.16 | 0.00 | 0.27 | 0.10 | 0.00 | 0.02 | 0.02 | 13.45 | 0.08 | 0.09 | 4.88 | 0.18 | 2.53 | 13.52 | 0.36 | 0.13 | 0.00 | 46.16 | 3.28 | 0.00 | 0.02 | 0.66 | 96.81 |
| HWL-21 | 2.60 | 1.31 | 1.18 | 1.68 | 1.80 | 17.21 | 8.80 | 0.09 | 1.44 | 0.00 | 0.09 | 0.13 | 0.00 | 0.02 | 0.02 | 8.77 | 0.12 | 0.05 | 4.03 | 0.19 | 0.70 | 14.53 | 0.14 | 0.03 | 0.00 | 40.22 | 1.47 | 0.00 | 0.04 | 0.22 | 98.29 |
| HWL-22 | 2.62 | 1.29 | 1.29 | 1.72 | 1.96 | 18.99 | 7.90 | 0.10 | 1.61 | 0.00 | 0.10 | 0.16 | 0.00 | 0.03 | 0.02 | 9.69 | 0.12 | 0.05 | 3.72 | 0.21 | 0.79 | 15.70 | 0.16 | 0.04 | 0.00 | 37.38 | 1.66 | 0.00 | 0.05 | 0.24 | 98.73 |
| FY09 EM21 -02 | 2.77 | 2.28 | 2.03 | 3.12 | 2.74 | 4.11 | 5.18 | 0.08 | 0.01 | 0.25 | 0.36 | 0.01 | 0.13 | 0.00 | 0.00 | 20.23 | 0.00 | 0.09 | 4.03 | 1.46 | 0.26 | 17.05 | 0.01 | 0.18 | 0.49 | 40.38 | 2.06 | 0.00 | 0.13 | 0.20 | 96.70 |

| Sample ID | Glass Density (α/α_c) | Mean(log[B (ppm)]) | Mean(log[Li (ppm)]) | Mean(log[Na (ppm)]) | Mean(log[Si (ppm)]) | Al2O3(v) | B2O3(v) | BaO(v) | CaO(v) | CdO (v) | Ce2O3(v) | Cr2O3(v) | Cs2O(v) | CuO(v) | Cu2O(v) | Fe2O3(v) | K2O(v) | La2O3(v) | Li2O(v) | MgO(v) | MnO(v) | Na2O(v) | NiO(v) | PbO(v) | SO4(v) | SiO2(v) | TiO2(v) | U3O8 (v) | ZnO(v) | ZrO2(v) | Oxide Sum (v) |
|---------------|-------------------------------------|--------------------|---------------------|---------------------|---------------------|----------|---------|--------|--------|---------|----------|----------|---------|--------|---------|----------|--------|----------|---------|--------|--------|---------|--------|--------|--------|---------|---------|----------|--------|---------|---------------|
| FY09 EM21 -03 | 2.77 | 1.58 | 1.86 | 2.37 | 2.37 | 6.93 | 4.63 | 0.01 | 0.02 | 0.01 | 0.01 | 0.02 | 0.01 | 0.00 | 0.00 | 13.22 | 0.00 | 0.01 | 6.74 | 1.42 | 4.58 | 14.58 | 0.01 | 0.01 | 0.07 | 40.11 | 4.98 | 0.00 | 0.01 | 0.01 | 97.36 |
| FY09 EM21 -05 | 2.76 | 1.18 | 1.24 | 1.80 | 2.08 | 3.69 | 4.33 | 0.01 | 4.11 | 0.01 | 0.01 | 0.02 | 0.01 | 0.00 | 0.00 | 13.35 | 0.00 | 0.01 | 3.95 | 0.01 | 0.25 | 9.95 | 2.29 | 0.01 | 0.07 | 49.74 | 5.83 | 0.00 | 0.01 | 0.01 | 97.64 |
| FY09 EM21 -06 | 2.74 | 2.28 | 1.89 | 2.61 | 2.45 | 4.44 | 11.48 | 0.07 | 0.03 | 0.25 | 0.34 | 0.19 | 0.13 | 0.00 | 0.00 | 5.19 | 0.00 | 0.09 | 3.85 | 1.37 | 4.43 | 12.83 | 0.06 | 0.01 | 0.07 | 33.16 | 1.99 | 0.00 | 0.01 | 0.01 | 97.25 |
| FY09 EM21 -07 | 2.82 | 2.77 | 2.28 | 2.98 | 2.24 | 4.81 | 13.70 | 0.01 | 3.97 | 0.01 | 0.01 | 0.01 | 0.01 | 0.00 | 0.00 | 16.84 | 0.00 | 0.01 | 3.87 | 1.37 | 4.43 | 14.80 | 2.39 | 0.19 | 0.43 | 42.95 | 5.90 | 0.00 | 0.01 | 0.01 | 97.16 |
| FY09 EM21 -08 | 2.82 | 1.90 | 2.05 | 2.41 | 2.55 | 3.26 | 4.83 | 0.01 | 0.52 | 0.01 | 0.01 | 0.16 | 0.01 | 0.00 | 0.00 | 20.16 | 0.00 | 0.01 | 6.73 | 1.38 | 1.16 | 9.66 | 0.02 | 0.01 | 0.07 | 42.73 | 5.95 | 0.00 | 0.01 | 0.01 | 96.67 |
| FY09 EM21 -09 | 2.66 | 1.40 | 1.45 | 1.73 | 1.94 | 12.97 | 9.54 | 0.01 | 3.01 | 0.01 | 0.01 | 0.14 | 0.01 | 0.00 | 0.00 | 10.53 | 0.00 | 0.01 | 6.79 | 0.01 | 1.68 | 10.08 | 0.59 | 0.01 | 0.07 | 40.43 | 2.49 | 0.00 | 0.01 | 0.01 | 98.38 |
| FY09 EM21 -11 | 2.75 | 1.53 | 1.74 | 2.30 | 2.43 | 3.23 | 4.28 | 0.07 | 4.03 | 0.25 | 0.33 | 0.02 | 0.12 | 0.00 | 0.00 | 5.99 | 0.00 | 0.08 | 5.49 | 1.35 | 4.41 | 12.29 | 0.01 | 0.18 | 0.45 | 47.71 | 6.76 | 0.00 | 0.13 | 0.19 | 97.37 |
| FY09 EM21 -12 | 2.77 | 1.36 | 1.61 | 1.95 | 2.26 | 4.57 | 5.23 | 0.01 | 0.01 | 0.01 | 0.01 | 0.02 | 0.01 | 0.00 | 0.00 | 15.37 | 0.00 | 0.01 | 6.62 | 0.01 | 3.81 | 9.81 | 1.69 | 0.01 | 0.07 | 46.26 | 1.99 | 0.00 | 0.01 | 0.01 | 95.50 |
| FY09 EM21 -14 | 2.75 | 1.67 | 1.31 | 1.74 | 1.93 | 3.22 | 14.97 | 0.08 | 0.04 | 0.25 | 0.34 | 0.14 | 0.13 | 0.00 | 0.00 | 19.62 | 0.00 | 0.09 | 4.34 | 0.01 | 0.24 | 9.77 | 0.01 | 0.19 | 0.43 | 39.42 | 5.60 | 0.00 | 0.13 | 0.19 | 99.20 |
| FY09 EM21 -15 | 2.76 | 1.21 | 1.48 | 1.90 | 2.13 | 5.55 | 4.60 | 0.10 | 3.33 | 0.21 | 0.35 | 0.14 | 0.13 | 0.00 | 0.00 | 7.92 | 0.00 | 0.09 | 5.89 | 1.34 | 4.35 | 9.94 | 2.27 | 0.18 | 0.44 | 49.35 | 1.86 | 0.00 | 0.13 | 0.19 | 98.35 |
| FY09 EM21 -16 | 2.71 | 1.76 | 1.64 | 2.51 | 2.45 | 3.74 | 6.62 | 0.08 | 3.84 | 0.23 | 0.35 | 0.15 | 0.13 | 0.00 | 0.00 | 8.74 | 0.00 | 0.09 | 3.99 | 1.41 | 0.25 | 15.27 | 2.34 | 0.19 | 0.43 | 48.08 | 1.97 | 0.00 | 0.14 | 0.20 | 98.21 |
| FY09 EM21 -17 | 2.73 | 1.22 | 1.60 | 2.26 | 2.25 | 7.67 | 4.80 | 0.09 | 0.11 | 0.27 | 0.37 | 0.01 | 0.14 | 0.00 | 0.00 | 13.81 | 0.00 | 0.10 | 7.00 | 0.01 | 0.48 | 15.03 | 0.01 | 0.21 | 0.49 | 41.29 | 6.13 | 0.00 | 0.14 | 0.21 | 98.35 |
| FY09 EM21 -18 | 2.60 | 0.97 | 1.27 | 2.15 | 2.12 | 11.07 | 4.86 | 0.08 | 0.40 | 0.20 | 0.35 | 0.02 | 0.12 | 0.00 | 0.00 | 6.67 | 0.00 | 0.09 | 5.33 | 0.01 | 0.65 | 16.11 | 0.01 | 0.19 | 0.43 | 49.74 | 1.96 | 0.00 | 0.12 | 0.20 | 98.61 |
| FY09 EM21 -19 | 2.65 | 0.99 | 1.29 | 2.28 | 2.13 | 5.84 | 4.58 | 0.01 | 4.07 | 0.01 | 0.01 | 0.02 | 0.01 | 0.00 | 0.00 | 4.98 | 0.00 | 0.01 | 3.97 | 0.01 | 0.25 | 16.72 | 0.90 | 0.01 | 0.07 | 51.45 | 5.85 | 0.00 | 0.01 | 0.01 | 98.74 |
| FY09 EM21 -20 | 2.67 | 1.27 | 1.26 | 2.30 | 2.29 | 6.16 | 5.41 | 0.01 | 0.01 | 0.01 | 0.01 | 0.16 | 0.01 | 0.00 | 0.00 | 11.39 | 0.00 | 0.01 | 4.02 | 1.18 | 0.24 | 16.95 | 2.31 | 0.01 | 0.07 | 47.87 | 1.98 | 0.00 | 0.01 | 0.01 | 97.79 |
| FY09 EM21 -21 | 2.75 | 2.92 | 2.66 | 3.37 | 2.84 | 4.86 | 8.95 | 0.08 | 0.01 | 0.28 | 0.36 | 0.19 | 0.13 | 0.00 | 0.00 | 18.84 | 0.00 | 0.09 | 6.88 | 0.01 | 0.82 | 14.42 | 0.01 | 0.21 | 0.47 | 39.15 | 1.98 | 0.00 | 0.13 | 0.20 | 98.07 |
| FY09 EM21 -25 | 2.70 | 1.18 | 1.35 | 2.17 | 2.15 | 6.41 | 4.98 | 0.01 | 4.14 | 0.01 | 0.01 | 0.16 | 0.01 | 0.00 | 0.00 | 7.53 | 0.00 | 0.01 | 4.01 | 0.01 | 4.61 | 15.40 | 0.01 | 0.01 | 0.07 | 48.83 | 2.01 | 0.00 | 0.01 | 0.01 | 98.22 |
| FY09 EM21 -27 | 2.75 | 1.37 | 1.39 | 2.00 | 2.08 | 7.29 | 6.87 | 0.04 | 1.79 | 0.14 | 0.18 | 0.09 | 0.07 | 0.00 | 0.00 | 12.69 | 0.00 | 0.05 | 4.95 | 0.67 | 2.20 | 12.63 | 1.13 | 0.10 | 0.25 | 43.05 | 3.89 | 0.00 | 0.07 | 0.11 | 98.25 |
| MAX* | 2.79 | 1.76 | 1.64 | 2.51 | 2.45 | 18.99 | 10.14 | 0.11 | 4.14 | 0.27 | 0.37 | 0.16 | 0.14 | 0.03 | 0.02 | 16.01 | 0.12 | 0.10 | 7.00 | 1.41 | 4.61 | 16.95 | 2.34 | 0.21 | 0.49 | 51.45 | 6.13 | 0.00 | 0.14 | 0.86 | 98.74 |
| MIN* | 2.60 | 0.97 | 1.07 | 1.40 | 1.80 | 3.74 | 4.46 | 0.01 | 0.01 | 0.00 | 0.01 | 0.01 | 0.00 | 0.00 | 0.00 | 4.98 | 0.00 | 0.01 | 3.72 | 0.01 | 0.24 | 9.81 | 0.01 | 0.01 | 0.00 | 37.38 | 1.25 | 0.00 | 0.01 | 0.01 | 95.50 |

* maximum and minimum values are for the data actually used in modeling.

Exhibit Z2. Summary of the Fitted Models (Historic and Modified Historic) for Each Element of Interest

Historic Model with 131 points; Modified Historic Model with 122 points

APPENDIX F. SRNL CST (TiO₂-Nb₂O₅-ZrO₂) Glass Validation Database (Measured Bias Corrected wt% on a vitrified oxide basis indicated by “v”).

| Sample ID | Mean(log[B (ppm)]) | Mean(log[Li (ppm)]) | Mean(log[Na (ppm)]) | Mean(log[Si (ppm)]) | Al2O3(v) | B2O3(v) | BaO(v) | CaO(v) | Ce2O3(v) | Cr2O3(v) | Cs2O(v) | CuO(v) | Cu2O(v) | Fe2O3(v) | K2O(v) | La2O3(v) | Li2O(v) | MgO(v) | MnO(v) | Na2O(v) | Nb2O5(v) | NiO(v) | PbO(v) | SO4(v) | SiO2(v) | ThO2(v) | TiO2(v) | U3O8 (v) | ZnO(v) | ZrO2(v) | Oxide Sum (v) |
|-----------|-----------------------|------------------------|------------------------|------------------------|----------|---------|--------|--------|----------|----------|---------|--------|---------|----------|--------|----------|---------|--------|--------|---------|----------|--------|--------|--------|---------|---------|---------|----------|--------|---------|------------------|
| KT04-01 | 1.00 | 1.05 | 1.81 | 1.96 | 6.03 | 5.91 | 0.07 | 0.98 | 0.27 | 0.07 | 0.00 | 0.03 | 0.03 | 11.71 | 0.04 | 0.09 | 3.52 | 0.15 | 1.93 | 13.03 | 0.95 | 0.33 | 0.13 | 0.00 | 47.90 | 0.00 | 4.48 | 0.00 | 0.01 | 0.83 | 98.50 |
| KT04-02 | 1.02 | 1.07 | 1.87 | 2.00 | 5.46 | 5.87 | 0.07 | 0.99 | 0.28 | 0.08 | 0.00 | 0.02 | 0.02 | 11.34 | 0.04 | 0.06 | 3.57 | 0.16 | 1.73 | 14.07 | 1.05 | 0.19 | 0.11 | 0.00 | 48.65 | 0.00 | 4.61 | 0.00 | 0.04 | 0.94 | 99.36 |
| KT04-03 | 1.05 | 1.08 | 1.92 | 2.01 | 4.79 | 5.93 | 0.07 | 1.03 | 0.24 | 0.08 | 0.00 | 0.02 | 0.02 | 11.60 | 0.05 | 0.06 | 3.55 | 0.15 | 1.84 | 14.44 | 1.04 | 0.29 | 0.11 | 0.00 | 48.90 | 0.00 | 4.47 | 0.00 | 0.04 | 0.92 | 99.66 |
| KT04-04 | 1.00 | 1.06 | 1.85 | 2.00 | 5.21 | 5.87 | 0.06 | 0.92 | 0.19 | 0.08 | 0.00 | 0.03 | 0.03 | 11.75 | 0.05 | 0.06 | 3.53 | 0.15 | 1.03 | 13.71 | 0.97 | 0.15 | 0.08 | 0.00 | 49.51 | 0.00 | 4.53 | 0.00 | 0.07 | 0.83 | 98.83 |
| KT04-05 | 0.94 | 1.04 | 1.81 | 1.99 | 7.19 | 6.00 | 0.07 | 0.96 | 0.14 | 0.15 | 0.00 | 0.03 | 0.03 | 9.44 | 0.09 | 0.06 | 3.53 | 0.16 | 1.00 | 13.42 | 1.02 | 0.12 | 0.06 | 0.00 | 49.99 | 0.00 | 4.58 | 0.00 | 0.04 | 0.94 | 99.01 |
| KT04-06 | 0.92 | 1.01 | 1.79 | 1.96 | 7.65 | 5.99 | 0.07 | 1.05 | 0.10 | 0.08 | 0.00 | 0.03 | 0.03 | 8.97 | 0.17 | 0.03 | 3.55 | 0.10 | 1.19 | 13.68 | 0.95 | 0.15 | 0.06 | 0.00 | 49.45 | 0.00 | 4.51 | 0.00 | 0.08 | 0.88 | 98.75 |
| KT04-07 | 0.95 | 1.02 | 1.86 | 1.99 | 5.96 | 5.93 | 0.07 | 0.93 | 0.08 | 0.11 | 0.00 | 0.02 | 0.02 | 9.40 | 0.11 | 0.03 | 3.55 | 0.11 | 0.71 | 14.28 | 1.12 | 0.62 | 0.06 | 0.00 | 49.28 | 0.00 | 5.00 | 0.00 | 0.08 | 0.99 | 98.48 |
| KT04-08 | 1.00 | 1.03 | 1.96 | 2.02 | 5.38 | 5.95 | 0.08 | 0.87 | 0.08 | 0.10 | 0.00 | 0.03 | 0.02 | 9.23 | 0.12 | 0.03 | 3.54 | 0.11 | 0.96 | 15.43 | 1.26 | 0.59 | 0.06 | 0.00 | 49.66 | 0.00 | 5.13 | 0.00 | 0.04 | 1.05 | 99.73 |
| KT04-09 | 1.04 | 1.07 | 1.89 | 2.01 | 5.96 | 5.99 | 0.07 | 1.04 | 0.19 | 0.07 | 0.00 | 0.04 | 0.03 | 12.35 | 0.13 | 0.07 | 3.52 | 0.11 | 0.55 | 14.21 | 0.82 | 0.48 | 0.12 | 0.00 | 48.30 | 0.00 | 5.03 | 0.00 | 0.05 | 0.74 | 99.86 |
| KT04-10 | 1.01 | 1.06 | 1.83 | 1.98 | 5.93 | 5.91 | 0.08 | 1.01 | 0.25 | 0.08 | 0.00 | 0.03 | 0.02 | 13.31 | 0.05 | 0.08 | 3.53 | 0.12 | 0.35 | 13.37 | 0.77 | 0.48 | 0.13 | 0.00 | 47.95 | 0.00 | 4.74 | 0.00 | 0.04 | 0.73 | 98.95 |
| KT06-01 | 1.09 | 1.03 | 1.75 | 1.95 | 5.81 | 8.27 | 0.04 | 1.22 | 0.20 | 0.10 | 0.00 | 0.02 | 0.02 | 8.94 | 0.13 | 0.06 | 3.55 | 0.10 | 1.33 | 12.56 | 0.59 | 0.59 | 0.10 | 0.15 | 47.57 | 0.00 | 6.05 | 0.00 | 0.05 | 0.61 | 98.04 |
| KT06-02 | 1.08 | 1.00 | 1.71 | 1.91 | 9.79 | 8.29 | 0.02 | 1.82 | 0.10 | 0.05 | 0.00 | 0.02 | 0.02 | 7.15 | 0.06 | 0.03 | 3.51 | 0.04 | 1.09 | 12.50 | 0.06 | 1.13 | 0.05 | 0.15 | 46.88 | 0.00 | 6.08 | 0.00 | 0.04 | 0.15 | 99.04 |
| KT06-03 | 0.91 | 1.23 | 1.87 | 2.07 | 5.70 | 4.76 | 0.05 | 1.23 | 0.20 | 0.10 | 0.00 | 0.02 | 0.02 | 9.15 | 0.13 | 0.06 | 4.74 | 0.10 | 1.33 | 12.48 | 0.58 | 0.59 | 0.10 | 0.15 | 50.68 | 0.00 | 6.14 | 0.00 | 0.05 | 0.73 | 99.09 |
| KT06-04 | 0.89 | 1.18 | 1.68 | 1.99 | 10.02 | 4.91 | 0.02 | 1.84 | 0.09 | 0.05 | 0.00 | 0.02 | 0.02 | 7.39 | 0.07 | 0.02 | 4.78 | 0.04 | 1.12 | 11.22 | 0.08 | 1.13 | 0.05 | 0.15 | 50.24 | 0.00 | 6.21 | 0.00 | 0.04 | 0.19 | 99.68 |
| KT06-05 | 1.06 | 1.12 | 1.47 | 1.93 | 7.46 | 8.44 | 0.02 | 1.18 | 0.11 | 0.06 | 0.00 | 0.01 | 0.01 | 11.46 | 0.07 | 0.03 | 4.22 | 0.07 | 1.21 | 9.99 | 0.51 | 0.40 | 0.05 | 0.15 | 47.68 | 0.00 | 6.06 | 0.00 | 0.03 | 0.59 | 99.81 |
| KT06-06 | 1.14 | 1.14 | 1.51 | 1.95 | 5.72 | 8.58 | 0.02 | 1.10 | 0.11 | 0.06 | 0.00 | 0.02 | 0.01 | 12.93 | 0.06 | 0.03 | 4.22 | 0.05 | 1.31 | 9.93 | 0.54 | 0.45 | 0.06 | 0.15 | 49.00 | 0.00 | 6.28 | 0.00 | 0.02 | 0.61 | 101.28 |
| KT06-07 | 1.02 | 1.10 | 1.41 | 1.88 | 9.77 | 8.14 | 0.05 | 0.74 | 0.23 | 0.10 | 0.00 | 0.02 | 0.02 | 6.93 | 0.11 | 0.07 | 4.17 | 0.12 | 3.53 | 10.02 | 0.09 | 0.12 | 0.11 | 0.15 | 47.05 | 0.00 | 6.18 | 0.00 | 0.05 | 1.54 | 99.30 |
| KT06-08 | 0.93 | 1.27 | 1.57 | 2.03 | 7.35 | 4.84 | 0.02 | 1.11 | 0.11 | 0.06 | 0.00 | 0.02 | 0.01 | 11.04 | 0.06 | 0.03 | 5.38 | 0.05 | 1.27 | 10.07 | 0.54 | 0.44 | 0.06 | 0.15 | 50.51 | 0.00 | 6.28 | 0.00 | 0.03 | 0.61 | 100.04 |
| KT06-09 | 0.93 | 1.32 | 1.71 | 2.09 | 5.71 | 4.86 | 0.02 | 1.11 | 0.11 | 0.05 | 0.00 | 0.01 | 0.01 | 12.28 | 0.07 | 0.03 | 5.42 | 0.05 | 1.24 | 10.54 | 0.51 | 0.40 | 0.05 | 0.15 | 49.96 | 0.00 | 6.17 | 0.00 | 0.02 | 0.58 | 99.35 |
| KT06-10 | 0.91 | 1.27 | 1.67 | 2.01 | 9.89 | 4.99 | 0.05 | 0.76 | 0.21 | 0.10 | 0.00 | 0.03 | 0.03 | 7.37 | 0.13 | 0.06 | 5.31 | 0.11 | 3.59 | 10.77 | 0.08 | 0.11 | 0.11 | 0.15 | 48.73 | 0.00 | 6.23 | 0.00 | 0.07 | 1.45 | 100.32 |
| KT06-11 | 1.15 | 1.18 | 1.49 | 1.96 | 5.57 | 8.39 | 0.02 | 1.09 | 0.10 | 0.05 | 0.00 | 0.02 | 0.02 | 14.62 | 0.07 | 0.03 | 4.16 | 0.05 | 1.24 | 9.14 | 0.48 | 0.39 | 0.05 | 0.15 | 47.54 | 0.00 | 6.20 | 0.00 | 0.03 | 0.55 | 99.97 |
| KT06-12 | 1.17 | 1.28 | 1.50 | 1.95 | 6.50 | 8.31 | 0.10 | 1.21 | 0.42 | 0.18 | 0.00 | 0.04 | 0.03 | 10.38 | 0.27 | 0.13 | 5.30 | 0.25 | 0.52 | 9.22 | 2.22 | 0.15 | 0.21 | 0.15 | 44.85 | 0.00 | 6.11 | 0.00 | 0.11 | 2.09 | 98.72 |
| KT06-13 | 1.07 | 1.22 | 1.44 | 1.96 | 9.98 | 8.56 | 0.07 | 0.74 | 0.29 | 0.14 | 0.00 | 0.02 | 0.02 | 7.44 | 0.17 | 0.09 | 5.36 | 0.15 | 3.47 | 9.08 | 0.03 | 0.11 | 0.14 | 0.15 | 49.00 | 0.00 | 6.08 | 0.00 | 0.07 | 0.11 | 101.27 |
| KT06-14 | 1.10 | 1.24 | 1.39 | 1.87 | 12.13 | 8.25 | 0.03 | 2.17 | 0.12 | 0.06 | 0.00 | 0.01 | 0.01 | 8.36 | 0.06 | 0.03 | 5.43 | 0.06 | 0.46 | 9.45 | 0.10 | 0.14 | 0.06 | 0.15 | 44.91 | 0.00 | 6.20 | 0.00 | 0.02 | 1.84 | 100.05 |

| Sample ID | Mean(log[B (ppm)]) | Mean(log[Li (ppm)]) | Mean(log[Na (ppm)]) | Mean(log[Si (ppm)]) | Al2O3(v) | B2O3(v) | BaO(v) | CaO(v) | Ce2O3(v) | Cr2O3(v) | Cs2O(v) | CuO(v) | Cu2O(v) | Fe2O3(v) | K2O(v) | La2O3(v) | Li2O(v) | MgO(v) | MnO(v) | Na2O(v) | Nb2O5(v) | NiO(v) | PbO(v) | SO4(v) | SiO2(v) | ThO2(v) | TiO2(v) | U3O8 (v) | ZnO(v) | ZrO2(v) | Oxide Sum (v) |
|-----------|--------------------|---------------------|---------------------|---------------------|----------|---------|--------|--------|----------|----------|---------|--------|---------|----------|--------|----------|---------|--------|--------|---------|----------|--------|--------|--------|---------|---------|---------|----------|--------|---------|---------------|
| KT06-15 | 0.88 | 1.39 | 1.55 | 2.01 | 6.56 | 4.77 | 0.11 | 1.07 | 0.43 | 0.17 | 0.00 | 0.04 | 0.04 | 10.54 | 0.24 | 0.13 | 6.57 | 0.23 | 0.53 | 9.76 | 2.30 | 0.16 | 0.22 | 0.15 | 47.45 | 0.00 | 5.95 | 0.00 | 0.12 | 2.06 | 99.62 |
| KT06-16 | 0.95 | 1.38 | 1.65 | 2.09 | 10.04 | 4.87 | 0.07 | 0.75 | 0.28 | 0.12 | 0.00 | 0.02 | 0.02 | 7.34 | 0.17 | 0.08 | 6.61 | 0.15 | 3.53 | 9.49 | 0.08 | 0.10 | 0.14 | 0.15 | 50.79 | 0.00 | 6.20 | 0.00 | 0.08 | 0.18 | 101.28 |
| KT06-17 | 0.82 | 1.32 | 1.46 | 1.92 | 12.05 | 4.80 | 0.02 | 2.28 | 0.11 | 0.06 | 0.00 | 0.01 | 0.01 | 8.64 | 0.08 | 0.03 | 6.60 | 0.08 | 0.43 | 9.43 | 0.07 | 0.13 | 0.06 | 0.15 | 47.40 | 0.00 | 6.06 | 0.00 | 0.02 | 1.71 | 100.23 |
| KT06-18 | 0.93 | 1.21 | 1.49 | 2.00 | 5.68 | 4.89 | 0.02 | 1.12 | 0.10 | 0.05 | 0.00 | 0.02 | 0.02 | 14.65 | 0.08 | 0.03 | 4.80 | 0.05 | 1.17 | 9.40 | 0.49 | 0.39 | 0.05 | 0.15 | 50.72 | 0.00 | 6.08 | 0.00 | 0.03 | 0.56 | 100.55 |
| KT07-01 | 1.02 | 1.07 | 1.78 | 1.97 | 5.77 | 5.97 | 0.06 | 1.01 | 0.28 | 0.10 | 0.00 | 0.03 | 0.02 | 11.68 | 0.03 | 0.09 | 3.47 | 0.15 | 1.93 | 13.01 | 0.90 | 0.33 | 0.15 | 0.37 | 45.99 | 0.00 | 4.17 | 0.00 | 0.01 | 0.83 | 96.37 |
| KT07-02 | 1.03 | 1.07 | 1.86 | 1.99 | 5.36 | 6.13 | 0.06 | 0.98 | 0.28 | 0.10 | 0.00 | 0.02 | 0.02 | 11.21 | 0.03 | 0.06 | 3.47 | 0.15 | 1.71 | 14.15 | 1.01 | 0.18 | 0.11 | 0.37 | 48.51 | 0.00 | 4.29 | 0.00 | 0.03 | 0.95 | 99.17 |
| KT07-03 | 1.04 | 1.07 | 1.89 | 2.00 | 4.53 | 6.00 | 0.06 | 1.02 | 0.25 | 0.12 | 0.00 | 0.02 | 0.02 | 11.21 | 0.03 | 0.06 | 3.45 | 0.15 | 1.81 | 13.85 | 1.04 | 0.31 | 0.12 | 0.38 | 48.29 | 0.00 | 4.20 | 0.00 | 0.03 | 0.97 | 97.94 |
| KT07-04 | 1.02 | 1.06 | 1.83 | 1.99 | 5.19 | 5.98 | 0.06 | 0.91 | 0.22 | 0.09 | 0.00 | 0.02 | 0.02 | 11.84 | 0.03 | 0.06 | 3.49 | 0.15 | 1.07 | 13.79 | 0.93 | 0.15 | 0.09 | 0.38 | 48.40 | 0.00 | 4.36 | 0.00 | 0.07 | 0.87 | 98.19 |
| KT07-05 | 0.92 | 1.02 | 1.77 | 1.96 | 7.02 | 6.14 | 0.06 | 1.10 | 0.15 | 0.14 | 0.00 | 0.03 | 0.02 | 9.56 | 0.07 | 0.06 | 3.47 | 0.16 | 1.03 | 13.62 | 1.04 | 0.11 | 0.06 | 0.37 | 49.95 | 0.00 | 4.32 | 0.00 | 0.06 | 0.99 | 99.54 |
| KT07-06 | 0.90 | 0.99 | 1.75 | 1.94 | 7.39 | 5.74 | 0.06 | 1.00 | 0.11 | 0.14 | 0.00 | 0.02 | 0.02 | 9.10 | 0.12 | 0.03 | 3.29 | 0.10 | 1.19 | 13.48 | 0.95 | 0.15 | 0.06 | 0.37 | 48.94 | 0.00 | 4.27 | 0.00 | 0.07 | 0.91 | 97.51 |
| KT07-07 | 0.98 | 1.03 | 1.87 | 2.00 | 5.67 | 5.87 | 0.07 | 0.93 | 0.08 | 0.15 | 0.00 | 0.03 | 0.02 | 9.32 | 0.08 | 0.03 | 3.40 | 0.11 | 0.72 | 14.02 | 1.13 | 0.62 | 0.07 | 0.39 | 48.94 | 0.00 | 4.77 | 0.00 | 0.08 | 1.03 | 97.52 |
| KT07-08 | 1.03 | 1.06 | 1.97 | 2.03 | 5.09 | 6.07 | 0.07 | 0.90 | 0.08 | 0.11 | 0.00 | 0.02 | 0.02 | 9.13 | 0.07 | 0.03 | 3.44 | 0.11 | 0.96 | 14.93 | 1.28 | 0.59 | 0.07 | 0.38 | 48.51 | 0.00 | 4.89 | 0.00 | 0.04 | 1.11 | 97.89 |
| KT07-09 | 1.06 | 1.08 | 1.88 | 2.01 | 5.51 | 5.98 | 0.07 | 1.00 | 0.19 | 0.11 | 0.00 | 0.02 | 0.02 | 12.05 | 0.08 | 0.06 | 3.41 | 0.11 | 0.56 | 13.67 | 0.72 | 0.49 | 0.12 | 0.36 | 46.90 | 0.00 | 4.75 | 0.00 | 0.04 | 0.74 | 96.97 |
| KT07-10 | 1.04 | 1.09 | 1.84 | 2.00 | 5.76 | 6.12 | 0.07 | 1.05 | 0.24 | 0.11 | 0.00 | 0.02 | 0.02 | 13.35 | 0.04 | 0.07 | 3.48 | 0.11 | 0.39 | 13.53 | 0.73 | 0.46 | 0.13 | 0.36 | 47.06 | 0.00 | 4.45 | 0.00 | 0.04 | 0.74 | 98.34 |
| KT08-01 | 1.01 | 1.04 | 1.78 | 1.97 | 6.06 | 6.01 | 0.07 | 0.98 | 0.29 | 0.09 | 0.00 | 0.04 | 0.04 | 11.82 | 0.21 | 0.09 | 3.53 | 0.15 | 1.88 | 13.32 | 0.86 | 0.34 | 0.21 | 0.26 | 45.92 | 0.17 | 4.12 | 0.60 | 0.01 | 0.82 | 97.89 |
| KT08-02 | 1.03 | 1.04 | 1.84 | 1.98 | 5.36 | 5.98 | 0.07 | 0.98 | 0.30 | 0.09 | 0.00 | 0.03 | 0.02 | 11.03 | 0.23 | 0.06 | 3.51 | 0.14 | 1.62 | 13.92 | 0.92 | 0.20 | 0.12 | 0.26 | 48.49 | 0.62 | 4.16 | 0.44 | 0.04 | 0.81 | 99.40 |
| KT08-03 | 1.08 | 1.07 | 1.89 | 2.01 | 4.66 | 6.01 | 0.07 | 0.96 | 0.27 | 0.08 | 0.00 | 0.02 | 0.02 | 10.85 | 0.23 | 0.06 | 3.47 | 0.15 | 1.74 | 14.19 | 0.97 | 0.32 | 0.12 | 0.26 | 52.09 | 0.89 | 4.13 | 0.63 | 0.04 | 0.82 | 103.08 |
| KT08-04 | 1.02 | 1.04 | 1.83 | 2.00 | 5.28 | 5.98 | 0.07 | 0.92 | 0.24 | 0.09 | 0.00 | 0.02 | 0.02 | 11.79 | 0.22 | 0.07 | 3.44 | 0.14 | 1.04 | 13.88 | 0.92 | 0.19 | 0.09 | 0.26 | 50.81 | 0.24 | 4.26 | 0.24 | 0.08 | 0.74 | 101.03 |
| KT08-05 | 0.94 | 0.99 | 1.76 | 1.98 | 7.22 | 6.01 | 0.07 | 0.98 | 0.17 | 0.13 | 0.00 | 0.03 | 0.02 | 9.65 | 0.24 | 0.07 | 3.46 | 0.15 | 1.02 | 13.99 | 0.98 | 0.14 | 0.12 | 0.26 | 51.93 | 0.02 | 4.35 | 0.49 | 0.04 | 0.91 | 102.45 |
| KT08-06 | 0.94 | 1.01 | 1.77 | 1.99 | 7.59 | 6.01 | 0.07 | 1.04 | 0.13 | 0.13 | 0.00 | 0.03 | 0.02 | 8.94 | 0.27 | 0.04 | 3.43 | 0.11 | 1.17 | 13.75 | 0.94 | 0.17 | 0.12 | 0.26 | 52.52 | 0.02 | 4.21 | 0.77 | 0.08 | 0.86 | 102.67 |
| KT08-07 | 1.00 | 1.04 | 1.79 | 2.02 | 5.35 | 6.06 | 0.07 | 0.84 | 0.11 | 0.13 | 0.00 | 0.02 | 0.02 | 8.32 | 0.27 | 0.04 | 3.55 | 0.10 | 0.65 | 13.75 | 0.89 | 0.57 | 0.06 | 0.26 | 47.21 | 0.02 | 4.27 | 3.73 | 0.07 | 0.77 | 97.13 |
| KT08-08 | 1.03 | 1.07 | 1.86 | 2.04 | 4.59 | 5.89 | 0.06 | 0.74 | 0.10 | 0.09 | 0.00 | 0.02 | 0.02 | 7.94 | 0.25 | 0.03 | 3.47 | 0.09 | 0.82 | 14.02 | 1.11 | 0.51 | 0.12 | 0.26 | 48.67 | 0.02 | 4.18 | 5.22 | 0.04 | 0.90 | 99.16 |
| KT08-09 | 1.03 | 1.06 | 1.77 | 2.01 | 5.21 | 6.02 | 0.07 | 0.92 | 0.20 | 0.09 | 0.00 | 0.02 | 0.02 | 10.73 | 0.28 | 0.07 | 3.51 | 0.10 | 0.50 | 13.01 | 0.65 | 0.45 | 0.13 | 0.26 | 45.67 | 0.02 | 4.20 | 4.86 | 0.04 | 0.57 | 97.59 |
| KT08-10 | 1.03 | 1.06 | 1.73 | 2.00 | 5.34 | 5.98 | 0.07 | 0.93 | 0.23 | 0.09 | 0.00 | 0.02 | 0.02 | 12.11 | 0.22 | 0.07 | 3.45 | 0.11 | 0.36 | 12.60 | 0.64 | 0.46 | 0.16 | 0.27 | 50.70 | 0.02 | 3.93 | 4.54 | 0.05 | 0.62 | 102.98 |
| KT10-01 | 1.05 | 1.34 | 1.77 | 2.07 | 5.50 | 4.98 | 0.06 | 0.88 | 0.25 | 0.09 | 0.00 | 0.02 | 0.02 | 10.91 | 0.04 | 0.08 | 5.39 | 0.14 | 1.78 | 11.29 | 1.35 | 0.30 | 0.13 | 0.00 | 48.24 | 0.00 | 5.98 | 0.00 | 0.01 | 1.17 | 98.59 |
| KT10-02 | 1.02 | 1.35 | 1.83 | 2.08 | 4.93 | 4.89 | 0.06 | 0.89 | 0.26 | 0.08 | 0.00 | 0.02 | 0.02 | 10.35 | 0.04 | 0.05 | 5.34 | 0.14 | 1.55 | 11.95 | 1.30 | 0.17 | 0.10 | 0.00 | 49.90 | 0.00 | 5.95 | 0.00 | 0.03 | 1.14 | 99.16 |
| KT10-03 | 1.02 | 1.34 | 1.83 | 2.08 | 4.25 | 4.82 | 0.06 | 0.85 | 0.23 | 0.09 | 0.00 | 0.02 | 0.02 | 10.40 | 0.04 | 0.06 | 5.39 | 0.14 | 1.67 | 12.28 | 1.51 | 0.27 | 0.11 | 0.00 | 49.31 | 0.00 | 6.06 | 0.00 | 0.04 | 1.28 | 98.89 |

SRNL-STI-2016-00372
Revision 0

| Sample ID | Mean(log[B (ppm)]) | Mean(log[Li (ppm)]) | Mean(log[Na (ppm)]) | Mean(log[Si (ppm)]) | Al2O3(v) | B2O3(v) | BaO(v) | CaO(v) | Ce2O3(v) | Cr2O3(v) | Cs2O(v) | CuO(v) | Cu2O(v) | Fe2O3(v) | K2O(v) | La2O3(v) | Li2O(v) | MgO(v) | MnO(v) | Na2O(v) | Nb2O5(v) | NiO(v) | PbO(v) | SO4(v) | SiO2(v) | ThO2(v) | TiO2(v) | U3O8 (v) | ZnO(v) | ZrO2(v) | Oxide Sum (v) |
|-------------|--------------------|---------------------|---------------------|---------------------|----------|---------|--------|--------|----------|----------|---------|--------|---------|----------|--------|----------|---------|--------|--------|---------|----------|--------|--------|--------|---------|---------|---------|----------|--------|---------|---------------|
| KT10-04 | 1.00 | 1.33 | 1.79 | 2.08 | 4.66 | 4.97 | 0.05 | 0.81 | 0.19 | 0.09 | 0.00 | 0.02 | 0.02 | 10.78 | 0.03 | 0.05 | 5.40 | 0.14 | 0.98 | 11.60 | 1.41 | 0.14 | 0.08 | 0.00 | 49.90 | 0.00 | 5.96 | 0.00 | 0.07 | 1.20 | 98.56 |
| KT10-05 | 0.91 | 1.29 | 1.73 | 2.04 | 6.44 | 4.81 | 0.05 | 0.87 | 0.13 | 0.13 | 0.00 | 0.02 | 0.02 | 8.74 | 0.07 | 0.05 | 5.39 | 0.14 | 0.92 | 11.70 | 1.47 | 0.10 | 0.05 | 0.00 | 50.27 | 0.00 | 6.10 | 0.00 | 0.03 | 1.30 | 98.79 |
| KT10-06 | 0.92 | 1.30 | 1.74 | 2.05 | 6.95 | 4.68 | 0.06 | 0.86 | 0.10 | 0.13 | 0.00 | 0.02 | 0.02 | 8.36 | 0.11 | 0.03 | 5.42 | 0.09 | 1.11 | 11.83 | 1.34 | 0.13 | 0.05 | 0.00 | 51.13 | 0.00 | 6.13 | 0.00 | 0.07 | 1.14 | 99.76 |
| KT10-07 | 0.97 | 1.32 | 1.84 | 2.08 | 5.37 | 4.83 | 0.06 | 0.83 | 0.07 | 0.14 | 0.00 | 0.02 | 0.02 | 8.59 | 0.08 | 0.03 | 5.34 | 0.11 | 0.67 | 12.43 | 1.60 | 0.54 | 0.06 | 0.00 | 50.06 | 0.00 | 6.53 | 0.00 | 0.08 | 1.32 | 98.79 |
| KT10-08 | 1.02 | 1.34 | 1.93 | 2.11 | 4.68 | 4.72 | 0.07 | 0.73 | 0.07 | 0.10 | 0.00 | 0.02 | 0.02 | 8.20 | 0.08 | 0.03 | 5.30 | 0.10 | 0.86 | 13.09 | 1.73 | 0.51 | 0.06 | 0.00 | 51.40 | 0.00 | 6.58 | 0.00 | 0.04 | 1.41 | 99.78 |
| KT10-09 | 0.99 | 1.32 | 1.80 | 2.06 | 5.21 | 4.68 | 0.07 | 0.85 | 0.18 | 0.10 | 0.00 | 0.02 | 0.02 | 11.25 | 0.08 | 0.06 | 5.36 | 0.10 | 0.52 | 12.09 | 1.17 | 0.44 | 0.12 | 0.00 | 49.95 | 0.00 | 6.62 | 0.00 | 0.04 | 1.02 | 99.96 |
| KT10-10 | 0.98 | 1.31 | 1.75 | 2.04 | 5.29 | 4.98 | 0.07 | 0.92 | 0.22 | 0.10 | 0.00 | 0.02 | 0.02 | 12.23 | 0.04 | 0.06 | 5.38 | 0.11 | 0.34 | 11.59 | 1.08 | 0.42 | 0.13 | 0.00 | 48.94 | 0.00 | 6.26 | 0.00 | 0.04 | 0.99 | 99.22 |
| cst01-FY99 | 1.29 | 1.30 | 1.59 | 2.09 | 2.74 | 8.25 | 0.00 | 0.91 | 0.00 | 0.14 | 0.00 | 0.04 | 0.04 | 9.723 | 0.19 | 0.00 | 4.71 | 0.06 | 1.83 | 8.87 | 0.66 | 0.85 | 0.00 | 0.00 | 55.40 | 0.00 | 2.03 | 2.02 | 0.00 | 0.41 | 98.85 |
| cst02-FY99 | 1.34 | 1.33 | 1.63 | 2.12 | 2.64 | 7.95 | 0.00 | 0.87 | 0.00 | 0.14 | 0.00 | 0.05 | 0.04 | 9.405 | 0.18 | 0.00 | 4.48 | 0.06 | 1.74 | 9.01 | 1.29 | 0.82 | 0.00 | 0.00 | 53.64 | 0.00 | 3.13 | 2.32 | 0.00 | 0.74 | 98.49 |
| cst03-FY99 | 1.21 | 1.26 | 1.48 | 2.06 | 2.46 | 7.68 | 0.00 | 0.84 | 0.00 | 0.15 | 0.00 | 0.04 | 0.04 | 10.605 | 0.19 | 0.00 | 4.31 | 0.06 | 1.48 | 8.51 | 1.96 | 0.78 | 0.00 | 0.00 | 52.80 | 0.00 | 4.19 | 2.55 | 0.00 | 1.04 | 99.67 |
| cst04-FY99 | 1.30 | 1.30 | 1.61 | 2.10 | 2.72 | 8.10 | 0.00 | 0.90 | 0.00 | 0.14 | 0.00 | 0.04 | 0.04 | 9.855 | 0.17 | 0.00 | 4.60 | 0.06 | 1.81 | 9.05 | 0.65 | 0.85 | 0.00 | 0.00 | 53.92 | 0.00 | 3.22 | 2.01 | 0.00 | 0.41 | 98.55 |
| cst05-FY99 | 1.22 | 1.26 | 1.53 | 2.06 | 2.70 | 7.86 | 0.00 | 0.91 | 0.00 | 0.16 | 0.00 | 0.05 | 0.04 | 9.692 | 0.22 | 0.00 | 4.44 | 0.07 | 1.77 | 8.92 | 1.31 | 0.85 | 0.00 | 0.00 | 53.05 | 0.00 | 4.16 | 2.38 | 0.00 | 0.74 | 99.30 |
| cst06-FY99 | 1.19 | 1.24 | 1.49 | 2.03 | 2.60 | 7.53 | 0.00 | 0.88 | 0.00 | 0.17 | 0.00 | 0.05 | 0.05 | 10.461 | 0.21 | 0.00 | 4.22 | 0.07 | 1.64 | 8.67 | 1.93 | 0.82 | 0.00 | 0.00 | 51.74 | 0.00 | 5.08 | 2.16 | 0.00 | 1.06 | 99.32 |
| cst07-FY99 | 1.30 | 1.27 | 1.62 | 2.10 | 2.94 | 7.79 | 0.00 | 0.98 | 0.00 | 0.13 | 0.00 | 0.03 | 0.03 | 11.249 | 0.09 | 0.00 | 4.05 | 0.09 | 1.93 | 8.97 | 0.70 | 0.88 | 0.00 | 0.00 | 53.44 | 0.00 | 1.81 | 2.86 | 0.00 | 0.65 | 98.61 |
| cst08-FY99 | 1.25 | 1.29 | 1.58 | 2.07 | 2.96 | 7.24 | 0.00 | 0.93 | 0.00 | 0.12 | 0.00 | 0.04 | 0.03 | 11.143 | 0.09 | 0.00 | 4.17 | 0.09 | 1.89 | 8.45 | 1.28 | 0.87 | 0.00 | 0.00 | 52.27 | 0.00 | 2.68 | 3.05 | 0.00 | 1.14 | 98.43 |
| cst09-FY99 | 1.22 | 1.21 | 1.56 | 2.03 | 2.83 | 7.10 | 0.00 | 0.99 | 0.00 | 0.13 | 0.00 | 0.04 | 0.04 | 11.981 | 0.12 | 0.00 | 3.72 | 0.09 | 1.91 | 8.73 | 1.92 | 0.89 | 0.00 | 0.00 | 50.40 | 0.00 | 3.81 | 2.51 | 0.00 | 1.66 | 98.88 |
| cst10-FY99 | 1.31 | 1.30 | 1.64 | 2.10 | 2.82 | 7.32 | 0.00 | 0.97 | 0.00 | 0.12 | 0.00 | 0.03 | 0.03 | 10.481 | 0.09 | 0.00 | 4.26 | 0.09 | 1.96 | 9.05 | 0.74 | 0.87 | 0.00 | 0.00 | 52.45 | 0.00 | 2.43 | 3.65 | 0.00 | 0.64 | 98.01 |
| cst11-FY99 | 1.30 | 1.27 | 1.62 | 2.09 | 2.89 | 7.71 | 0.00 | 1.01 | 0.00 | 0.12 | 0.00 | 0.03 | 0.03 | 11.911 | 0.09 | 0.00 | 3.98 | 0.09 | 2.00 | 9.05 | 1.41 | 0.93 | 0.00 | 0.00 | 52.50 | 0.00 | 3.53 | 2.50 | 0.00 | 1.17 | 100.94 |
| cst11c-FY99 | 1.19 | 1.23 | 1.56 | 2.02 | 3.01 | 7.88 | 0.00 | 0.96 | 0.00 | 0.17 | 0.00 | 0.05 | 0.04 | 11.192 | 0.21 | 0.00 | 4.13 | 0.07 | 2.09 | 8.94 | 1.27 | 0.95 | 0.00 | 0.00 | 49.68 | 0.00 | 4.22 | 2.55 | 0.00 | 0.94 | 98.35 |
| cst12-FY99 | 1.26 | 1.22 | 1.55 | 2.01 | 3.00 | 7.53 | 0.00 | 1.02 | 0.00 | 0.14 | 0.00 | 0.04 | 0.04 | 11.704 | 0.09 | 0.00 | 3.91 | 0.10 | 1.87 | 8.66 | 2.03 | 0.92 | 0.00 | 0.00 | 49.48 | 0.00 | 4.50 | 2.65 | 0.00 | 1.64 | 99.32 |
| cst12c-FY99 | 1.17 | 1.21 | 1.54 | 2.00 | 3.01 | 6.60 | 0.00 | 0.92 | 0.00 | 0.17 | 0.00 | 0.05 | 0.05 | 11.228 | 0.19 | 0.00 | 3.89 | 0.07 | 2.06 | 8.75 | 1.89 | 0.96 | 0.00 | 0.00 | 48.20 | 0.00 | 5.05 | 2.32 | 0.00 | 1.33 | 96.73 |
| cst13-FY99 | 1.30 | 1.29 | 1.65 | 2.03 | 3.77 | 7.51 | 0.00 | 1.10 | 0.00 | 0.15 | 0.00 | 0.04 | 0.03 | 13.769 | 0.18 | 0.00 | 4.37 | 0.09 | 2.26 | 9.30 | 0.66 | 1.07 | 0.00 | 0.00 | 51.55 | 0.00 | 1.77 | 2.77 | 0.00 | 0.70 | 101.08 |
| cst14-FY99 | 1.25 | 1.22 | 1.61 | 2.00 | 3.90 | 7.40 | 0.00 | 1.21 | 0.00 | 0.15 | 0.00 | 0.05 | 0.04 | 13.869 | 0.18 | 0.00 | 4.01 | 0.08 | 2.30 | 9.65 | 1.32 | 1.08 | 0.00 | 0.00 | 50.58 | 0.00 | 2.91 | 3.22 | 0.00 | 1.26 | 103.22 |
| cst15-FY99 | 1.12 | 1.19 | 1.54 | 1.97 | 4.00 | 6.58 | 0.00 | 1.22 | 0.00 | 0.15 | 0.00 | 0.05 | 0.04 | 13.191 | 0.17 | 0.00 | 3.97 | 0.07 | 2.49 | 9.53 | 1.96 | 1.13 | 0.00 | 0.00 | 49.60 | 0.00 | 3.94 | 2.84 | 0.00 | 1.78 | 102.70 |
| cst16-FY99 | 1.48 | 1.34 | 1.85 | 2.08 | 3.86 | 8.46 | 0.00 | 1.19 | 0.00 | 0.15 | 0.00 | 0.04 | 0.04 | 14.529 | 0.17 | 0.00 | 4.09 | 0.08 | 2.34 | 10.84 | 0.72 | 1.12 | 0.00 | 0.00 | 49.18 | 0.00 | 2.57 | 2.74 | 0.00 | 0.75 | 102.87 |
| cst17-FY99 | 1.17 | 1.21 | 1.55 | 1.99 | 3.86 | 7.05 | 0.00 | 1.19 | 0.00 | 0.15 | 0.00 | 0.04 | 0.04 | 14.131 | 0.18 | 0.00 | 4.10 | 0.07 | 2.30 | 9.30 | 1.32 | 1.08 | 0.00 | 0.00 | 50.81 | 0.00 | 3.63 | 2.77 | 0.00 | 1.27 | 103.30 |
| cst17c-FY99 | 1.18 | 1.21 | 1.59 | 1.99 | 3.40 | 6.82 | 0.00 | 1.06 | 0.00 | 0.21 | 0.00 | 0.06 | 0.05 | 12.759 | 0.20 | 0.00 | 3.95 | 0.09 | 2.45 | 9.16 | 1.30 | 1.12 | 0.00 | 0.00 | 48.39 | 0.00 | 4.22 | 3.05 | 0.00 | 0.98 | 99.27 |

| Sample ID | Mean(log[B (ppm)]) | Mean(log[Li (ppm)]) | Mean(log[Na (ppm)]) | Mean(log[Si (ppm)]) | Al2O3(v) | B2O3(v) | BaO(v) | CaO(v) | Ce2O3(v) | Cr2O3(v) | Cs2O(v) | CuO(v) | Cu2O(v) | Fe2O3(v) | K2O(v) | La2O3(v) | Li2O(v) | MgO(v) | MnO(v) | Na2O(v) | Nb2O5(v) | NiO(v) | PbO(v) | SO4(v) | SiO2(v) | TiO2(v) | U3O8 (v) | ZnO(v) | ZrO2(v) | Oxide Sum (v) | |
|-------------|--------------------|---------------------|---------------------|---------------------|----------|---------|--------|--------|----------|----------|---------|--------|---------|----------|--------|----------|---------|--------|--------|---------|----------|--------|--------|--------|---------|---------|----------|--------|---------|---------------|--------|
| cst18-FY99 | 1.17 | 1.20 | 1.60 | 1.95 | 3.97 | 7.00 | 0.00 | 1.23 | 0.00 | 0.15 | 0.00 | 0.06 | 0.05 | 13.141 | 0.21 | 0.00 | 3.88 | 0.08 | 2.50 | 9.79 | 1.97 | 1.11 | 0.00 | 0.00 | 47.87 | 0.00 | 4.69 | 2.99 | 0.00 | 1.78 | 102.45 |
| cst18c-FY99 | 1.17 | 1.18 | 1.59 | 1.96 | 3.15 | 6.75 | 0.00 | 1.04 | 0.00 | 0.17 | 0.00 | 0.05 | 0.05 | 13.014 | 0.20 | 0.00 | 3.73 | 0.08 | 2.19 | 9.15 | 1.93 | 1.05 | 0.00 | 0.00 | 46.61 | 0.00 | 5.26 | 2.75 | 0.00 | 1.38 | 98.55 |
| cst20-FY99 | 1.00 | 1.16 | 1.18 | 1.98 | 6.28 | 8.53 | 0.00 | 0.54 | 0.00 | 0.10 | 0.00 | 0.02 | 0.02 | 7.162 | 0.18 | 0.00 | 4.40 | 0.15 | 1.95 | 8.76 | 1.27 | 0.32 | 0.00 | 0.00 | 55.86 | 0.00 | 3.08 | 0.72 | 0.00 | 0.93 | 100.28 |
| cst26-FY99 | 0.99 | 1.15 | 1.21 | 1.98 | 6.82 | 7.68 | 0.00 | 0.52 | 0.00 | 0.12 | 0.00 | 0.02 | 0.02 | 7.84 | 0.18 | 0.00 | 4.19 | 0.15 | 2.16 | 8.64 | 1.27 | 0.35 | 0.00 | 0.00 | 54.77 | 0.00 | 3.03 | 0.61 | 0.00 | 0.94 | 99.29 |
| cst32-FY99 | 0.96 | 1.14 | 1.21 | 1.94 | 8.01 | 6.95 | 0.00 | 0.54 | 0.00 | 0.12 | 0.00 | 0.03 | 0.03 | 8.444 | 0.21 | 0.00 | 3.98 | 0.18 | 2.63 | 8.73 | 1.28 | 0.42 | 0.00 | 0.00 | 52.57 | 0.00 | 0.00 | | 0.00 | 0.97 | 95.08 |
| MAX* | 1.17 | 1.39 | 1.97 | 2.11 | 12.13 | 8.58 | 0.11 | 2.28 | 0.43 | 0.18 | 0.00 | 0.05 | 0.04 | 14.65 | 0.28 | 0.13 | 6.61 | 0.25 | 3.59 | 15.43 | 2.30 | 1.13 | 0.22 | 0.39 | 55.86 | 0.89 | 6.62 | 5.22 | 0.12 | 2.09 | 103.08 |
| MIN* | 0.82 | 0.99 | 1.18 | 1.87 | 4.00 | 4.68 | 0.00 | 0.52 | 0.00 | 0.05 | 0.00 | 0.01 | 0.01 | 6.93 | 0.03 | 0.00 | 3.29 | 0.04 | 0.34 | 8.64 | 0.03 | 0.10 | 0.00 | 0.00 | 44.85 | 0.00 | 0.00 | 0.00 | 0.11 | 95.08 | |

* maximum and minimum values are for the data actually used in modeling.

Exhibit Z2. Summary of the Fitted Models (Historic and Modified Historic) for Each Element of Interest

Historic Model with 131 points; Modified Historic Model with 122 points

10.0 References

- 1 C.M. Jantzen, "Systems Approach to Nuclear Waste Glass Development," J. Non-Cryst Solids, 84 [1-3], 215-225 (1986).
- 2 C.M. Jantzen, "Relationship of Glass Composition to Glass Viscosity, Resistivity, Liquidus Temperature, and Durability: First Principles Process-Product Models for Vitrification of Nuclear Waste," Proceedings of the 5th International Symposium on Ceramics in Nuclear Waste Management, G.G. Wicks, D.F. Bickford, and R. Bunnell (Eds.), American Ceramic Society, Westerville, OH, 37-51 (1991).
- 3 C.M. Jantzen and K.G. Brown, "Statistical Process Control of Glass Manufactured for the Disposal of Nuclear and Other Wastes," Am. Ceramic Society Bulletin, 72, 55-59 (May, 1993).
- 4 "Preliminary Technical Data Summary for the Defense Waste Processing Facility, Stage 1," U.S. DOE Report DPSTD-80-38, E.I. duPont deNemours & Co., Savannah River Plant, Aiken, SC (September, 1980).
- 5 A. Applewhite-Ramsey, K.Z. Wolf, and M.J. Plodinec, "EPA Tests of Simulated DWPF Waste Glass," Ceramic Transactions, V.29, A.K. Varshneya, D.F. Bickford, and P.P. Bihuniak (Eds.), Amer. Ceramic Society, Westerville, OH, 515-522 (1993).
- 6 C.M. Jantzen, J.B. Pickett, and I. Joseph, I., "Toxic Characteristic Leaching Procedure (TCLP) Testing of Waste Glass and K-3 Refractory: Revisited," Environmental Issues and Waste Management Technologies in the Ceramic and Nuclear Industries V, G. T. Chandler (Eds.), Ceramic Transactions, V. 107, 271-280 (2000).
- 7 M.M. Reigel, "Literature Review: Assessment of DWPF Melter and Melter Off-gas System Lifetime," SRNL-STI-2014-00134 (July 2015).
- 8 C.M. Jantzen, K.J. Imrich, K.G. Brown, and J.B. Pickett, "High Chrome Refractory Characterization: Part I. Impact of Melt REDuction/Oxidation (REDOX) on the Corrosion Mechanism in Radioactive Waste Glass Melters," International Journal of Applied Glass Science, 6[2], 137-157 (2015).
- 9 C.M. Jantzen, K.J. Imrich, K.G. Brown, and J.B. Pickett, "High Chrome Refractory Characterization: Part II. Accumulation of Spinel Corrosion Deposits in Radioactive Waste Glass Melters," International Journal of Applied Glass Science, 6[2], 158-171 (2015)
- 10 C.M. Jantzen and M.J. Plodinec, "Composition and Redox Control of Waste Glasses-Recommendation for Process Control Limit," U.S. DOE Report DPST-86-773 (1986).
- 11 H.D. Schreiber and A.L. Hockman, "Redox Chemistry in Candidate Glasses for Nuclear Waste Immobilization," J. Am. Ceram. Soc., 70[8], 591-594 (1987).
- 12 C.M. Jantzen, "Verification and Standardization of Glass Redox Measurement for DWPF," U.S. DOE Report DPST-89-222 (1989).
- 13 C.M. Jantzen, J.R. Zamecnik, D.C. Koopman, C.C. Herman, and J.B. Pickett, "Electron

-
- Equivalents Model for Controlling REDuction/OXidation (REDOX) Equilibrium During High Level Waste (HLW) Vitrification,” U.S. DOE Report WSRC-TR-2003-00126, Rev.0 (May 2003).**
- 14 C.M. Jantzen and F.C. Johnson, “**Impacts of Antifoam Additions and Argon Bubbling on Defense Waste Processing Facility (DWPF) REDuction/OXidation (REDOX),**” SRNL-STI-2011-00652 (April 2012).
- 15 Bickford, D.F., Applewhite-Ramsey, A., Jantzen, C.M., and Brown, K.G., “**Control of Radioactive Waste Glass Melters: I, Preliminary General Limits at Savannah River,**” J. Am. Ceram. Soc, 73 [10] 2896-2902 (1990).
- 16 R.L. Postles and K.G. Brown, “**The DWPF Product Composition Control System (PCCS) at Savannah River: Statistical Process Control Algorithm,**” Ceramic Transactions, 23, American Ceramic Society, Westerville, OH, 559-568 (1991).
- 17 C.M. Jantzen, “**Method for Controlling Glass Viscosity (VISCOMP™),**” U.S. Patent #5,102,439, (April, 1992).
- 18 C.M. Jantzen “**The Impacts of Uranium and Thorium on the Defense Waste Processing Facility (DWPF) Viscosity Model,**” U.S. DOE Report WSRC-TR-2004-00311 (2005).
- 19 C.M. Jantzen, K.G. Brown, T.B. Edwards, and J.B. Pickett, “**Method of Determining Glass Durability (THERMO™),**” U.S. Patent #5,846,278, (December 1998).
- 20 C.M. Jantzen, J.B. Pickett, K.G. Brown, T.B. Edwards, and D.C. Beam, “**Process/Product Models for the Defense Waste Processing Facility (DWPF): Part I. Predicting Glass Durability from Composition Using a Thermodynamic Hydration Energy Reaction Model (THERMO™),**” U.S. DOE Report WSRC-TR-93-0672, Westinghouse Savannah River Co., Savannah River Technology Center, Aiken, SC, 464p. (1995).
- 21 K.G. Brown, C.M. Jantzen, and G. Ritzhaupt, “**Relating Liquidus Temperature to Composition for Defense Waste Processing Facility (DWPF) Process Control,**” U.S. DOE Report WSRC-TR-2001-00520, Rev. 0, Westinghouse Savannah River Company, Aiken, SC (October 2001).
- 22 C.M. Jantzen and Brown, K.G. “**Predicting the Spinel-Nepheline Liquidus for Application to Nuclear Waste Glass Processing: Part I. Primary Phase Analysis, Liquidus Measurement, and Quasicrystalline Approach,**” J. Am. Ceramic Soc., 90 [6], 1866-1879 (2007).
- 23 C.M. Jantzen and Brown, K.G. “**Predicting the Spinel-Nepheline Liquidus for Application to Nuclear Waste Glass Processing: Part II. Quasicrystalline Freezing Point Depression Model,**” J. Am. Ceramic Soc. 90 [6], 1880-1891 (2007).
- 24 T.H. Lorier and C.M. Jantzen, “**Evaluation of the TiO₂ Limit for DWPF Glass,**” U.S. DOE Report WSRC-TR-2003-00396 (October 2003).
- 25 J.E. Miller and N.E. Brown, “**Development and Properties of Crystalline Silicotitanate (CST) Ion Exchangers for Radioactive Waste Applications,**” U.S. Govt. Report SAND97-0771, Sandia National Laboratory, Albuquerque, NM (April 1997).

-
- 26 J.L. Krumhansl, P.C. Zhang, C.Jove-Colon, H.L. Anderson, R.C. Moore, F.M. Salas, T.M. Nenoff, D.A. Lucero, “**A Preliminary Assessment of IE-911 Column Pretreatment Options,**” U.S. DOE Report SAND2001-1002, Sandia National Laboratory, Albuquerque, NM (April 2001).
- 27 C.M. Jantzen, “**Partial Molar Free Energy of Hydration of Niobium Oxide,**” U.S. DOE Report SRNL-TR-2010-00125, Rev. 0, Savannah River National Laboratory, Aiken, SC (October 2010).
- 28 Department of Energy, “**Civilian Radioactive Waste Management System Waste Acceptance System Requirements Document, Revision 5,**” U.S. DOE Report DOE/RW-0351 REV. 5 (March 2008).
- 29 C.M. Jantzen, N.E. Bibler, D.C. Beam, and M.A. Pickett, “**Characterization of the Defense Waste Processing Facility (DWPF) Environmental Assessment (EA) Glass Standard Reference Material,**” U.S. DOE Report WSRC-TR-92-346, Rev. 1, Westinghouse Savannah River Company, Aiken, SC (1993).
- 30 C.M. Jantzen, N.E. Bibler, D.C. Beam, and M.A. Pickett , “**Development and Characterization of the Defense Waste Processing Facility (DWPF) Environmental Assessment (EA) Glass Standard Reference Material,**” Environmental and Waste Management Issues in the Ceramic Industry, Ceramic Transactions, 39, American Ceramic Society, Westerville, OH, 313-322 (1994).
- 31 ASTM C1285. “**Standard Test Methods for Determining Chemical Durability of Nuclear, Hazardous, and Mixed Waste Glasses and Multiphase Glass Ceramics: The Product Consistency Test (PCT),**” Annual Book of ASTM Standards, Vol. 12.01 (2014).
- 32 W.B. White, "Theory of Corrosion of Glass and Ceramics," Corrosion of Glass, Ceramics, and Ceramic Superconductors, D.E. Clark and B.K. Ziohos, Noyes Publications, Park Ridge, NJ, 2-28 (1992).
- 33 W. Sinkler, T.P. O'Holleran, S.M. Frank, M.K. Richmann, S.G. Johnson, “**Characterization of A Glass-Bonded Ceramic Waste Form Loaded with U and Pu,**” Scientific Basis for Nuclear Waste Management, XXIII, R.W. Smith and D.W. Shoesmith (Eds.), Materials Research Society, Pittsburgh, PA, 423-429 (2000).
- 34 T. Moschetti, W. Sinkler, T. Disanto, M.H. Hois, A.R. Warren, D. Cummings, S.G. Johnson, K.M. Goff, K.J. Bateman, S.M. Frank, “**Characterization of a Ceramic Waste Form Encapsulating Radioactive Electrorefiner Salt,**” Scientific Basis for Nuclear Waste Management, XXIII, R.W. Smith and D.W. Shoesmith (Eds.), Materials Research Society, Pittsburgh, PA, 577-582 (2000).
- 35 N.E. Bibler and J.K. Bates, “**Product Consistency Leach Tests of Savannah River Site Radioactive Waste Glasses,**” *Scientific Basis for Nuclear Waste Management*, XIII, Oversby, V. M. and Brown, P. W., eds., Materials Research Society, Pittsburgh, PA, 327–338 (1990).
- 36 J.K. Bates, D.J. Lam, M.J. Steindler, “**Extended Leach Studies of Actinide-Doped SRL 131 Glass,**” *Scientific Basis for Nuclear Waste Management*, VI, D.G. Brookins (Ed.), North-Holland, New York, 183-190 (1983).
- 37 N.E. Bibler and A.R. Jurgensen, “**Leaching Tc-99 from SRP Glass in Simulated Tuff and Salt Groundwaters,**” *Scientific Basis for Nuclear Waste Management*, XI, M.J. Apted and R.E. Westerman (Eds.), Materials Research Society, Pittsburgh, PA, 585-593 (1988).

-
- 38 D.J. Bradley, C.O. Harvey, and R.P. Turcotte, “**Leaching of Actinides and Technetium from Simulated High-Level Waste Glass**,” Pacific Northwest Laboratory Report, PNL-3152, Richland, WA (1979).
- 39 S. Fillet, J. Nogues, E. Vernaz, and N. Jacquet-Francillon, “**Leaching of Actinides from the French LWR Reference Glass**,” Scientific Basis for Nuclear Waste Management, IX, L.O. Werme, Materials Research Society, Pittsburgh, PA, 211-218 (1985).
- 40 F. Bazan, J. Rego, and R.D. Aines, “**Leaching of Actinide-doped Nuclear Waste Glass in a Tuff-Dominated System**,” Scientific Basis for Nuclear Waste Management, X, J.K. Bates and W.B. Seefeldt (Eds.), Materials Research Society, Pittsburgh, PA, 447-458 (1987).
- 41 E.Y. Vernaz and N. Godon, “**Leaching of Actinides from Nuclear Waste Glass: French Experience**,” Scientific Basis for Nuclear Waste Management, XV, C.G. Sombret (Ed.), Materials Research Society, Pittsburgh, PA, 37-48 (1992).
- 42 W.L. Ebert, S.F. Wolf, and J.K. Bates, “**The Release of Technetium from Defense Waste Processing Facility Glasses**,” Scientific Basis for Nuclear Waste Management, XIX, W.M. Murphy and D.A. Knecht (Ed.), Materials Research Society, Pittsburgh, PA, 221-227 (1996).
- 43 B.P. McGrail, “**Waste Package Component Interactions with Savannah River Defense Waste Glass in a Low-Magnesium Salt Brine**,” Nuclear Technology, 168-186 (1986).
- 44 B.C. Bunker, G.W. Arnold, D.E. Day and P.J. Bray, “**The Effect of Molecular Structure on Borosilicate Glass Leaching**,” J. Non-Cryst. Solids, 87, 226-253 (1986).
- 45 C.M. Jantzen, K.G. Brown, and J.B. Pickett, “**Durable Glass for Thousands of Years**,” International Journal of Applied Glass Science, 1 [1], 38-62 (2010).
- 46 F.C. Johnson, T.B. Edwards, and K.M. Fox, “**The User Guide for the ComPro™ Database**,” SRNL-STI-2009-00093, Revision 1, (2013).
- 47 F.C. Johnson, T.B. Edwards, and K.M. Fox, “**Data Qualification Report: SRNL Glass Composition – Properties (ComPro™) Database**,” SRNL-STI-2009-00094, Revision 1, (2013).
- 48 J.W. Amoroso, D.K. Peeler, and T.B. Edwards, “**Elimination of the Characterization of DWPF Pour Stream Sample and the Glass Fabrication and Testing of the DWPF Sludge Batch Qualification Sample**,” U.S. DOE Report SRNL-STI-2012-00157, Savannah River National Laboratory, Aiken, SC (May 2012).
- 49 F.C. Johnson and J.M. Pareizs, “**Analysis of Sludge Batch 7a (Macrobatch 8) Pour Stream Samples**,” U.S. DOE Report SRNL-STI-2012-00017, Rev. 0 (May 2012).
- 50 F.C. Johnson, C.L. Crawford, and J.M. Pareizs, “**Analysis of Sludge Batch 7b (Macrobatch 9) Pour Stream Samples**,” U.S. DOE Report SRNL-STI-2013-00462, Rev. 0 (November 2013).
- 51 C.M. Jantzen and K.G. Brown, “**Impact of Phase Separation on Waste Glass Durability**,” Environmental Issues and Waste Management Technologies in the Ceramic and Nuclear Industries, V, G. T. Chandler (Eds.), Ceramic Transactions, V. 107, 289-300 (2000).

- 52 S.L. Marra, A.L. Applewhite-Ramsey, and C.M. Jantzen. “**DWPF Glass Transition Temperatures-What They Are and Why They Are Important,**” Proceedings of the 5th International Symposium on Ceramics in Nuclear Waste Management, G.G. Wicks, D.F. Bickford, and R. Bunnell (Eds.), American Ceramic Society, Westerville, OH, 465-473 (1991).
- 53 C.M. Jantzen, “**Partial Molar Free Energies of Hydration for XO_2 Species (UO_2 , PuO_2 , AmO_2 , ThO_2 , NpO_2) and Potential Non-radioactive Surrogates (HfO_2 , ZrO_2 , Nd_2O_3) for XO_2 and U_3O_8 ,**” U.S. DOE Report SRNL-TR-2009-00099, Rev. 0, Savannah River National Laboratory, Aiken, SC (June 2009).
- 54 C.M. Jantzen, “**Verification of Glass Composition and Strategy for SGM and DWPF Glass Composition Determination,**” U.S. DOE Report DPST-86-708, E.I. DuPont deNemours & Co., Aiken, SC (1986).
- 55 I. Tovena, T. Advocat, D. Ghaleb, E. Vernaz and F. Larche, “**Thermodynamic and Structural Models Compared with the Initial Dissolution Rates of SON Glass Samples,**” Sci. Basis for Nucl. Waste Mgt., XVII, A. Barkatt and R.A. Van Konynenburg (Eds.), Mat. Res. Soc., Pittsburgh, PA, 595-602 (1994).
- 56 M. Tomozawa and S. Sridharan, “**Viscosity Increase of Phase-Separated Borosilicate Glasses,**” J. Am. Ceram. Soc. 75[11], 3103-3110 (1992).
- 57 W. Zheng, M. Lin, J. Cheng, “**Effect of Phase Separation on the Crystallization and Properties of Lithium Aluminosilicate Glass-ceramics,**” Glass Physics and Chemistry, 39 [2], 142-149 (2013).
- 58 D.F. Bickford and C.M. Jantzen, “**Devitrification of Defense Nuclear Waste Glasses: Role of Melt Insolubles,**” J. Non-Crystalline Solids ,84 [1-3], 299-307 (1986).
- 59 D.K. Peeler and T.B. Edwards, “**Impact of REDOX on Glass Durability: The Glass Selection Process,**” U.S. DOE Report WSRC-TR-2004-00135, Rev.0, Westinghouse Savannah River Co., Aiken, SC (March 2004).
- 60 D.K. Peeler and T.B. Edwards, “**Impact of REDOX on Glass Durability: Experimental Results,**” U.S. DOE Report WSRC-TR-2004-00313, Rev. 0, Westinghouse Savannah River Co., Aiken, SC (June 2004).
- 61 A.D. Cozzi, T.B. Edwards, D.K. Peeler, and D.R. Best, “**The Impact of REDOX on Durability for Sludge Batch 2,**” U.S. DOE Report WSRC-TR-2003-00246, Rev. 0, Westinghouse Savannah River Co., Aiken, SC (May 2003).
- 62 K.G. Brown and T.B. Edwards, “**Definition of the DWPF Homogeneity Constraint,**” U.S. DOE Report WSRC-TR-95-0060, Westinghouse Savannah River Company, Aiken, SC (1995).
- 63 T.B. Edwards and K.G. Brown, “**Evaluating the Glasses Batched for the Tank 42 Variability Study,**” Westinghouse Savannah River Company, Aiken, SC, SRT-SCS-98-017, Revision 0 (1998).
- 64 D.K. Bailey and J.F. Schairer, “**The System $\text{Na}_2\text{O}\text{-}\text{Al}_2\text{O}_3\text{-}\text{Fe}_2\text{O}_3\text{-}\text{SiO}_2$ at 1 Atmosphere, and the Petrogenesis of Alkaline Rocks,**” Journal of Petrology, 7[1], 114-170 (1966).

-
- 65 I. M.H. Hager and W. Hinz, “**Beitrag zur Phasentrennung in Glasern der Systemme Na₂O-SiO₂-B₂O₃ and Na₂O-SiO₂-Al₂O₃,**” *Silikatechnik*, 18 [11], 360 (1967).
- 66 J.A. Topping and M.K. Murthy, “**Effect of Small Additions of Al₂O₃ and Ga₂O₃ on the Immiscibility Temperature of Na₂O-SiO₂ Glasses,**” *J. Am. Ceram. Soc.*, 56[5] 270-275 (1973).
- 67 C.M. Jantzen, C.L. Crawford, J.M. Pareizs, and J.B. Pickett, “**Accelerated Leach Testing of GLASS (ALTGLASS): I. The Database and Definition of High Level Waste (HLW) Glass Hydrogels**” (accepted to International Journal of Applied Glass Science SRNL-STI-2014-00274).
- 68 C.M. Jantzen, C.L. Crawford, J.M. Pareizs, and J.B. Pickett, “**Accelerated Leach Testing of GLASS (ALTGLASS): II. Mineralization of Hydrogels by Leachate Strong Bases**” (accepted to International Journal of Applied Glass Science SRNL-STI-2014-00381).
- 69 C.C. Herman, T.B. Edwards, D.M. Marsh, and R.J. Workman, “**Reduction of Constraints: Phase 2 Experimental Assessment for Sludge-Only Processing,**” U.S. DOE Report WSRC-TR-2002-00482, Revision 0, Savannah River National Laboratory, Aiken, SC (2002).
- 70 F.C. Raszewski and T.B. Edwards, “**Reduction of Constraints for Coupled Operations,**” U.S. DOE Report SRNL-STI-2009-00465, Revision 0, Savannah River National Laboratory, Aiken, SC, (2009).
- 71 C.M. Jantzen, “**Phosphate Additions to Borosilicate Waste Glass Cause Phase Separation,**” U.S. DOE Report DPST-86-389, E.I. DuPont deNemours & Co., Savannah River Laboratory, Aiken, SC (1986).
- 72 C.M. Jantzen, K.G. Brown, and J.B. Pickett, “**Impact of Phase Separation on Durability in Phosphate Containing Borosilicate Waste Glass for INEEL,**” Environmental Issues and Waste Management Technologies, D.R. Spearing, G.L. Smith, and R.L. Putnam (Eds.), Ceramic Transactions, V. 119, Amer. Ceram. Soc., Westerville, OH, VI, 271-280 (2001).
- 73 C.M. Jantzen, K.G. Brown, J.B. Pickett, and G.L. Ritzhaupt, “**Crystalline Phase Separation in Phosphate Containing Waste Glasses: Relevance to INEEL HAW,**” WSRC-TR-2000-00339 (September 2000).
- 74 W. Volf, **Glass Science and Technology, 7: Chemical Approach to Glass**, Elsevier Scientific Publishers, New York (1984).
- 75 C.M. Jantzen and D.F. Bickford, “**Leaching of Devitrified Glass Containing Simulated SRP Nuclear Waste,**” *Sci. Basis for Nuclear Waste Management*, VIII, C.M. Jantzen, J.A. Stone and R.C. Ewing (eds.), Materials Research Society, Pittsburgh, PA 135-146 (1985).
- 76 H. Li, B. Jones, P. Hrma, J.D. Vienna, “**Compositional Effects on Liquidus Temperature of Hanford Simulated High-Level Waste Glasses Precipitating Nepheline (NaAlSiO₄),**” Environmental Issues and Waste Management Technologies in the Ceramic and Nuclear Industries, III, D.K. Peeler and J.C. Marra (Eds.), Am. Ceram. Soc., Westerville, OH, 279-288 (1998).
- 77 H. Li, P. Hrma, J.D. Vienna, M. Qian, Y. Su, D.E. Smith, “**Effects of Al₂O₃, B₂O₃, Na₂O, and SiO₂ on Nepheline Formation in Borosilicate Glasses: Chemical and Physical Correlations,**” *J. Non-Crystalline Solids*, 331, 202-216 (2003).

-
- 78 T.B. Edwards, D.K. Peeler, and K.M. Fox, “**The Nepheline Discriminator: Reasons for and Details of its Implementation for DWPF’s PCCS,**” U.S. DOE Report WSRC-STI-2006-00014, Revision 0, Savannah River National Laboratory, Aiken, SC (2006).
- 79 D.K. Peeler and T.B. Edwards, “**Integration of SWPF into DWPF Flowsheet: Gap Analysis and Test Matrix Development,**” U.S. DOE Report SRNL-STI-2014-00578, Savannah River Nuclear Solutions, Aiken, SC (December 2014).
- 80 D.K. Peeler, T.B. Edwards, and C.M. Jantzen, “**Task Technical and Quality Assurance Plan for SWPF Integration into the DWPF – Glass Property / Model Impacts,**” U.S. DOE Report SRNL-RP-2014-00348, Savannah River National Laboratory, Aiken, South Carolina (2014).
- 81 D.K. Peeler and T.B. Edwards, “**SWPF Glass Test Matrix,**” U.S. DOE Memorandum SRNL-L3100-2014-00189, Savannah River National Laboratory, Aiken, SC (August 29, 2014).
- 82 W.K. Kot and I.L. Pegg, “**Letter Report Fabrication of High-Titanium Glasses to Support Salt Waste Processing Facility (SWPF) Gap Analysis Study,**” VSL-15L3500-1 (March 20, 2015).
- 83 T.B. Edwards and K.M. Fox, “**Evaluations of the Measurements of Chemical Composition, Viscosity, and Density of the SWPF Study Glasses with High Concentrations of Titanium,**” U.S. DOE Report SRNL-TR-2016-00094 (2016).
- 84 T.B. Edwards, and D.K. Peeler, “**Analytical Plans Supporting the SWPF Gap Analysis Being Conducted with Energy Solutions and the Vitreous State Laboratory at The CUA,**” SRNL-STI-2014-00494, Revision 0, Savannah River National Laboratory, Aiken, South Carolina, Revision 0, (2014).
- 85 W.K. Kot, and I.L. Pegg, “**Chemical Compositions and Durability Study of Salt Waste Processing Facility (SWPF) Gap Glasses,**” VSL-16L3500-1, Vitreous State Laboratory, The Catholic University of America Washington, DC (2016).
- 86 SAS Institute, Inc., JMP Pro Version 11.2.1, SAS Institute, Inc., Cary, NC (2014).
- 87 W.K. Kot, I.L. Pegg, D.K. Peeler and T.B. Edwards, “**Sludge Batch 8 Glass Variability Study with Frit 803,**” Vitreous State Laboratory, The Catholic University of America, VSL-13R2580-1, Revision 0, Washington, DC (2013).
- 88 V.A. Silva, M.L.F. Nascimento, P.C. Morais, and N.O. Dantas, “**The Structural Role of Ti in a Thermally-treated Li₂O-B₂O₃-Al₂O₃ Glass System,**” J. of Non-Crystalline Solids, 404, 104-108 (2014).
- 89 C. Romano, E. Paris, B.T. Poe, G. Giuli, D.B. Dingwell, and A. Montana, “**Effect of Aluminum on Ti-Coordination in Silicate Glasses: A XANES Study,**” Am. Mineralogist, 85, 108-117 (2000).
- 90 W.K. Kot, B. Bennett, and I.L. Pegg, “**Liquidus Temperature Measurements of Vitreous State Laboratory Salt Waste Processing Facility (SWPF) Gap Glasses Final Report,**” VSL-16R4080-1, Revision A (June 21, 2016).

-
- 91 Jantzen, C.M. and Edwards, T.B., “**Defense Waste Processing Facility (DWPF) Viscosity Model: Revisions for Processing High TiO₂ Containing Glasses**,” U.S. DOE Report SRNL-STI-2016-00115, Rev.0 (2016).
- 92 R.F. Schumacher, “Basic Data Report: Simulated New Batch 1 Glasses,” U.S. DOE Report WSRC-RP-95-0539, Rev. 0 (1995)
- 93 C.L. Trivelpiece, “**Composition-based Density Model for HLW Glass**,” SRNL-STI-2016-00378 (in preparation)
- 94 C.M. Jantzen, “**Evaluation of Experimental Factors that Influence the Application and Discrimination Capability of the Product Consistency Test**,” U.S. Department of Energy Report WSRC-TR-90-526, Westinghouse Savannah River Co. (1990).
- 95 K.G. Brown, R.L. Postles, and T.B. Edwards, “**SME Acceptability Determination for DWPF Process Control**,” WSRC-TR-95-0364, Revision 5, Westinghouse Savannah River Company, Aiken, South Carolina (2006).
- 96 T.B. Edwards, D.K. Peeler, and S.L. Marra. “**Revisiting the Prediction Limits for Acceptable Durability**”, WSRC-TR-2003-00510, Rev. 0, Westinghouse Savannah River Company, Aiken, South Carolina (2004).
- 97 F.C. Raszewski, T.B. Edwards, and D.K. Peeler, “**Matrix 2 Results of the FY07 Enhanced DOE High-Level Waste Melter Throughput Studies at SRNL**,” U.S. DOE Report SRNS-STI-2008-00055, Rev. 0, Savannah River National Laboratory, Aiken, SC (2008).
- 98 F.C. Raszewski and T.B. Edwards, “**Results of the FY09 Enhanced DOE High-Level Waste Melter Throughput Studies at SRNL**,” U.S. DOE Report, SRNL-STI-2009-00778, Rev. 0, Savannah River National Laboratory, Aiken, SC (2010).
- 99 T.B. Edwards, J.R. Harbour, and R.J. Workman, “**Summary of Results for CST Glass Study: Composition and Property Measurements**,” U.S. DOE WSRC-TR-99-00324, Westinghouse Savannah River Co., Aiken, SC (September 1999).
- 100 T.B. Edwards, J.R. Harbour, and R.J. Workman, “**Composition and Property Measurements for CST Phase 1 Glasses**,” U.S. DOE WSRC-TR-99-00245, Westinghouse Savannah River Co., Aiken, SC (July 1999).
- 101 T.B. Edwards, J.R. Harbour, and R.J. Workman, “**Composition and Property Measurements for CST Phase 2 Glasses**,” U.S. DOE WSRC-TR-99-00289, Westinghouse Savannah River Co., Aiken, SC (August 1999).
- 102 T.B. Edwards, J.R. Harbour, and R.J. Workman, “**Composition and Property Measurements for CST Phase 3 Glasses**,” U.S. DOE WSRC-TR-99-00291, Westinghouse Savannah River Co., Aiken, SC (August 1999).
- 103 T.B. Edwards, J.R. Harbour, and R.J. Workman, “**Composition and Property Measurements for CST Phase 4 Glasses**,” U.S. DOE WSRC-TR-99-00293, Westinghouse Savannah River Co., Aiken, SC (August 1999).

-
- 104 K.M. Fox and T.B. Edwards, "**Impacts of Small Column Ion Exchange Streams on DWPF Glass Formulation: KT01, KT02, KT03, and KT04-Series Glass Compositions**," U.S. DOE Report SRNL-STI-2010-00566, Savannah River National Laboratory, Aiken, SC (2010).
 - 105 K.M. Fox and T.B. Edwards, "**Impacts of Small Column Ion Exchange Streams on DWPF Glass Formulation: KT05 and KT06-Series Glass Compositions**," U.S. DOE Report SRNL-STI-2010-00687, Savannah River National Laboratory, Aiken, SC (2010).
 - 106 K.M. Fox and T.B. Edwards, "**Impacts of Small Column Ion Exchange Streams on DWPF Glass Formulation: KT07-Series Glass Compositions**," U.S. DOE Report SRNL-STI-2010-00759, Savannah River National Laboratory, Aiken, SC (2010).
 - 107 K.M. Fox and T.B. Edwards, "**Impacts of Small Column Ion Exchange Streams on DWPF Glass Formulation: KT08, KT09, and KT10-Series Glass Compositions**," U.S. DOE Report SRNL-STI-2011-00178, Savannah River National Laboratory, Aiken, SC (2011).

Distribution

Alexander Choi/SRNL/Srs
Amanda Shafer/SRR/Srs
Azadeh Samadi-Dezfouli/SRR/Srs
Bill Holtzscheiter/SRR/Srs
Carol Jantzen/SRNL/Srs
Celia Aponte/SRR/Srs
Charles Crawford/SRNL/Srs
Christopher Dandeneau/SRNL/Srs
Chris Martino/SRNL/Srs
Cj Bannochie/SRNL/Srs
Connie Herman/SRNL/Srs
Cory Trivelpiece/SRNL/Srs
Dan Lambert/SRNL/Srs
David Dooley/SRNL/Srs
David Newell/SRNL/Srs
David.Peeler@pnnl.gov
Devon McClane/SRNL/Srs
Earl Brass/SRR/Srs
Elizabeth Hoffman/SRNL/Srs
Eric Freed/SRR/Srs
Fabienne Johnson/SRNL/Srs
Frank Pennebaker/SRNL/Srs
Hasmukh Shah/SRR/Srs
Helen Boyd/SRR/Srs
Jack Zamecnik/SRNL/Srs
Jake Amoroso/SRNS/Srs
Jeff Ray/SRR/Srs
Jeffrey Gillam/SRR/Srs
John Contardi/SRR/Srs
John Iaukea/SRR/Srs
John Pareizs/SRNL/Srs
Jonathan Bricker/SRR/Srs
Kevin Fox/SRNL/Srs
Maria Rios-Armstrong/SRR/Srs
Michael Stone/SRNL/Srs
Richard Edwards/SRR/Srs
Ryan McNew/SRR/Srs
Terri Fellinger/SRR/Srs
Timothy Brown/SRNL/Srs
Tommy Edwards/SRNL/Srs
Vijay Jain/SRR/Srs